Natural Science in Archaeology

Manuel Álvarez-Martí-Aguilar
Francisco Machuca Prieto *Editors*

Historical Earthquakes, Tsunamis and Archaeology in the Iberian Peninsula

Springer

Natural Science in Archaeology

The last three decades have seen a steady growth of application of natural scientific methods to archaeology. The interdisciplinary approach of archaeometry has found increasing appreciation by the archaeologists and is now considered indispensable and an integral part of archaeological studies. Interdisciplinary collaboration requires a multidisciplinary background. It is becoming increasingly difficult for the individual to grasp the whole field of archaeometry with its rapid developments. The aim of the series *Natural Science in Archaeology* is to bridge this information gap at the interface between archaeology and science. The individual volumes cover a broad spectrum of physical, chemical, geological, and biological techniques applied to archaeology as well as to palaeoanthropology with the interested nonspecialist in mind.

The single monographs cover:

- large fields of research
- specific methods of general interest (archaeometric methods of dating, material analysis, environmental reconstruction, geophysical prospecting, remote sensing and data processing)
- materials of interest to the archaeologist, such as sediments, soils, metal and nonmetal artifacts, animal and plant remains and other organic residues
- practical aspects such as sampling and data interpretation
- case studies, to demonstrate the potential and limitations of the various techniques.

More information about this series at https://link.springer.com/bookseries/3703

Manuel Álvarez-Martí-Aguilar •
Francisco Machuca Prieto
Editors

Historical Earthquakes, Tsunamis and Archaeology in the Iberian Peninsula

Springer

Editors
Manuel Álvarez-Martí-Aguilar
Department of Historical Sciences
University of Malaga
Malaga, Spain

Francisco Machuca Prieto
Department of Historical Sciences
University of Malaga
Malaga, Spain

ISSN 1613-9712
Natural Science in Archaeology
ISBN 978-981-19-1978-7　　ISBN 978-981-19-1979-4 (eBook)
https://doi.org/10.1007/978-981-19-1979-4

This Springer imprint is published by the registered company Springer Nature Singapore Pte Ltd.
The registered company address is: 152 Beach Road, #21-01/04 Gateway East, Singapore 189721, Singapore

Acknowledgements

This book is the result of a line of research developed in two projects based at the University of Malaga, *The Tsunami in the Cultural Representations of the Ancient World: Gadir-Gades and the Gulf of Cádiz as a Case Study* (HAR2015-66011-P) and *Earthquakes and Tsunamis in the Iberian Peninsula: Social Responses in the Longue Durée* (PGC2018-093752-B-I00), funded by the Spanish Ministry of Science, Innovation and Universities (MCIU), the Spanish State Research Agency (AEI) and the European Regional Development Fund (ERDF).

In the framework of these projects, the International Congress entitled, "Historical Tsunamis in the Iberian Peninsula", was held in Malaga in February 2019, in collaboration with the Museum of Malaga and Malaga University. Since the Congress' keynotes and debates were the seed of this book, we, the editors, are deeply indebted to all the people and institutions that made this encounter possible: the Museum of Malaga and its director María Morente and staff; the Culture Department of Malaga City Council; and the International Campus of Excellence in Marine Science (CEI·MAR). Moreover, we would like to thank several departments and officials of the University of Malaga for their support: the Vice-Chancellor's Office for Research and the Vice-Chancellor's Office for Strategic Projects; the Dean and Vice-Dean of the Faculty of Philosophy and Literature, Juan Antonio Perles and Clelia Martínez Maza; the Director of the Strategic Chair of Leading-Edge Technologies in Humanities, José Luis Caro; the Head of the Department of Historical Sciences, Gonzalo Cruz Andreotti; and the Director of the Historiographical Studies Group, Fernando Wulff Alonso. Our heartfelt thanks also go to our colleague José Suárez Padilla, at the University of Malaga, for his invaluable collaboration in organisational tasks and, of course, to the keynote speakers and those attending the Congress.

We would also like to express our deep gratitude to the authors for their core contributions to this book. Similarly, we would like to thank the reviewers for their comments and suggestions and all those people who, in one way or another, have contributed to its production, especially Thomas MacFarlane who translated several of its chapters and revised the style of the work as a whole. Finally, thanks to Yosuke Nishida and Sridevi Purushothaman from Springer Nature for all their support in getting this book published.

Contents

About the Editors

Manuel Álvarez-Martí-Aguilar is a lecturer of Ancient History at the University of Malaga (Spain). His research interests include the historical process of Tartessos and Phoenician Iberia, as well as the modern historiography of the ancient world. In recent years, he has been leading a line of research on the impact of historical earthquakes and tsunamis on the coastal communities of the Iberian Peninsula, as the principal investigator of the projects *TSUNAMIGAD—The Tsunami in the Cultural Representations of the Ancient World: Gadir-Gades and the Gulf of Cádiz as a Case Study* (HAR2015-66011-P—MINECO/FEDER) and *TSUNIBER—Earthquakes and Tsunamis in the Iberian Peninsula: Social Responses in the Longue Durée* (PGC2018-093752-B-I00—MCI/AEI/FEDER, EU). In these projects, he has analysed the symbolic keys to the perception of tsunamis in the ancient world, studied the apotropaic responses to this type of phenomenon and reviewed the catalogue of historical earthquakes and tsunamis in the Iberian Peninsula.

Francisco Machuca Prieto is a postdoctoral fellow at the University of Malaga (Spain), where he obtained his PhD in 2017 with a dissertation focusing on the identity building of the Phoenician communities of the Iberian Peninsula in the context of their integration in the Roman world. His main research areas are as follows: identities and ethnic construction in the ancient world, the Phoenicians in the Western Mediterranean, the Roman presence in the south of the Iberian Peninsula and the historiography of Antiquity. He is a member of the *Historiography Studies Group* (PAIDI HUM-394) and a team member of the projects *TSUNAMIGAD—The Tsunami in the Cultural Representations of the Ancient World: Gadir-Gades and the Gulf of Cádiz as a Case Study* (HAR2015-66011-P—MINECO/FEDER, EU) and *TSUNIBER—Earthquakes and Tsunamis in the Iberian Peninsula: Social Responses in the Longue Durée* (PGC2018-093752-B-I00—MCI/AEI/FEDER).

1 Breaking the Waves: Earthquake and Tsunami Research in the Iberian Peninsula from a Historiographical Perspective

Manuel Álvarez-Martí-Aguilar and Francisco Machuca Prieto

Abstract

This chapter performs a historiographical overview for the purpose of describing the evolution of recent earthquake and tsunami research in the Iberian Peninsula, characterised by the convergence of information deriving from different scientific disciplines, such as historical seismology, geology and archaeology. From the early 1990s down to the present day, several stages of research are identified, while placing the spotlight on the boom years in geological research on paleotsunamis in Portugal and Spain, in the wake of the catastrophic tsunamis in the Indian Ocean in 2004 and in Japan in 2011, as well as addressing future perspectives for interdisciplinary collaboration. The final section describes the aim of this book, plus the organisation and content of its chapters, as well as reflects on the future challenges facing research in this field.

M. Álvarez-Martí-Aguilar (✉) · F. Machuca Prieto
Department of Historical Sciences, University of Malaga, Campus de Teatinos s/n. 29071, Malaga, Spain
e-mail: m_alvarez@uma.es

F. Machuca Prieto
e-mail: machucaprieto@uma.es

Keywords

Historical earthquakes · Historical tsunamis · Historical seismology · Paleotsunamis · Historiography · Iberian Peninsula

In the past decades, research on historical earthquakes and tsunamis in the Iberian Peninsula has gone from strength to strength in different scientific fields enquiring into these phenomena, above all geology, paleoseismology, stratigraphy, geochemistry, geomorphology, archaeology, geoarchaeology and historical seismology. This has made it possible to gain a much deeper understanding of the footprints of both well-known seismic and tsunamigenic events, such as the famous AD 1755 Lisbon earthquake and tsunami, and other events occurring in previous ages.

In the specific case of the historical tsunamis that struck the coasts of the Iberian Peninsula, the subject on which this book focuses, research is relatively recent, for it began in the 1990s, before coming into its own following the catastrophes in the Indian Ocean in 2004 and Japan in 2011. Be that as it may, the increase in knowledge of these phenomena and the growing body of literature in this regard have been constrained by a number of methodological problems arising in the intersection between different scientific disciplines at the forefront of this progress, such as geology and history, whose evolution will be approached in this introductory chapter from a diachronic perspective.

M. Álvarez-Martí-Aguilar and F. Machuca Prieto (eds.), *Historical Earthquakes, Tsunamis and Archaeology in the Iberian Peninsula*, Natural Science in Archaeology,
https://doi.org/10.1007/978-981-19-1979-4_1

In the first three sections of this chapter, a historiographical review is performed on the evolution of research on historical earthquakes and tsunamis in the Iberian Peninsula over time, stressing the interrelation between historiographical, historical seismological, geological and archaeological data. With this review, the aim is to identify some of the keys that define the present state of the question and to underline the need for closer interdisciplinary collaboration in order to make further progress. In the fourth section, the genesis of this book is described, and, lastly, in the fifth section, the structure and content of its chapters are presented.

1.1 The Written Sources

Earthquake and tsunami research in the Iberian Peninsula has been marked by the impact of the AD 1755 Lisbon cataclysm (Mendes-Victor et al. 2009). This event marked the advent of modern historical seismology, with compilations of accounts of ancient earthquakes and tsunamis as influential as Moreira de Mendonça's *Historia universal dos terremotos* (1758), published only three years after the catastrophe.

As shown in Chap. 3 of this book, before the Muslim conquest of the Iberian Peninsula in the eighth century AD, the written sources dealing with seismic events in the peninsula are very thin on the ground. In fact, they are limited to references to the cataclysm that caused Atlantis to sink into the sea, as described in the Platonic account—a literary myth written in the fourth century BC (see López-Ruiz, this volume)—, a succinct account of earthquakes in the Pyrenees at an unspecified date, appearing in the anonymous *De mirabilibus auscultationibus* (third century BC), a fleeting reference to an event occurring in Cordova between 79 and 72 BC, found in a fragment of Sallust's *Histories* (first century BC), the vague information contained in the *Chronicle* of Hydatius (fifth century AD) concerning the occurrence of earthquakes in *Gallaecia* in AD 451 and 454, and the description of an earthquake in Bordeaux—which would have been felt in the Pyrenees and Spain, in ca. AD 580—in Gregory of Tours' *History of the Franks* (sixth century AD).

From the beginning of Muslim rule in the Iberian Peninsula, the historians of Al Andalus and the Maghreb began to record contemporary seismic events, as was the case with the earthquakes occurring in Cordova in AD 971, 973 and 974, mentioned by the historian Isa ibn Ahmad al Razi (tenth century), and with those also affecting this city in AD 881, 944 and 955, which are known to us through the oeuvre of the Moroccan author Ibn Adhari (thirteenth–fourteenth century) and to which his compatriot Ibn Abi Zar (fourteenth century) also referred.

The AD 881 earthquake is a good example of the complications arising when using historical sources, a problem to which we shall return in this chapter. In diverse Arab and Christian sources, there are testimonies of a major earthquake on 26 May AD 881, which was felt in southern Spain and North Africa. The main sources are Ibn Adhari, who describes its effects on Cordova, and Ibn Abi Zar, who mentions the damage that it wrought in the Maghreb and Andalusia. The Spanish historian Juan de Mariana (1601) also mentions an earthquake in Spain in that year, but none of the aforementioned authors describe associated sea phenomena. Several centuries later, in his *Historia de la dominación de los árabes en España*, the historian Conde (1820) describes a receding ocean and the disappearance of islands and reefs associated with that earthquake, claiming that it also destroyed many localities in southern and western Spain. However, Conde does not specify the sources from which he drew this information on that possible tsunami (Udías 2015), about which we know practically nothing.

As of the end of the fourteenth century, the quantity of contemporary information on seismic events in the Iberian Peninsula increased, as evidenced by the greater number of accounts of earthquakes, which would be subsequently included in the most important seismic compilations and catalogues (e.g., Galbis 1932; 1940). In relation to earthquakes associated with possible tsunamis, noteworthy are those of Almeria in AD 1522 (López Marinas 1985; Reicherter and Becker-

Heidmann 2009), Lisbon in AD 1531 (Baptista et al. 2014), Malaga in AD 1680 (Goded 2006), the Algarve in AD 1722 (Baptista et al. 2007) and Cadiz in AD 1731 (see Gracia et al., this volume). Nevertheless, whether those earthquakes actually triggered tsunamis in some cases, such as that of Malaga in AD 1680, is a moot point (Goded 2006).

Indeed, no contemporary—or more or less contemporary—accounts of the vast majority of earthquakes and tsunamis occurring before AD 881, which have subsequently found their way into the most important Portuguese and Spanish seismic catalogues (Galbis 1932, 1940; Oliveira 1986), have come down to us. The sources in which the first news of these events appears include the works of the Spanish chronicler Florián de Ocampo and his Portuguese counterpart Bernardo de Brito, written between the sixteenth and seventeenth centuries, namely a long time after they had occurred. In Ocampo's *Crónica General de España* (1543, 1553), there is information about earthquakes and sea floods in Cadiz in 241, 216 and 210 BC; while in Brito's *Monarchia Lusytana* (1597, 1609), there is news about earthquakes and sea floods affecting the coasts of Portugal and Galicia in ca. 63 BC and the Portuguese seaboard in 47 BC, plus a description of the impact of the famous "universal earthquake" in AD 365 on the coasts of Portugal. The historicity of these accounts is highly questionable because, as already noted, both produced their works many centuries after the narrated events and, furthermore, resorted to spurious sources. Nonetheless, Ocampo's and Brito's reports were subsequently recuperated by historians like Esteban de Garibay (1571), Juan de Mariana (1601) and Manuel de Faria y Sousa (1678), to whom should be added others including Miguel Lafuente (1843), who described the impact of the AD 365 tsunami on the coasts of Malaga and Granada (see Álvarez-Martí-Aguilar, this volume).

1.2 The Seismic Catalogues

This information was gradually included in successive seismic compilations and catalogues, both with a global scope and covering Portugal and Spain, starting with the abovementioned work by Moreira de Mendonça (1758). The complex process of transmitting this information, thus, got underway, from the eighteenth century down to the present day, during which the dates of some events have been altered slightly, owing to typos or misunderstandings when transcribing them. This has resulted in the duplication of events in successive compilations, a tradition that has been followed by the most recent seismic catalogues (Udías 2015, 2020; Udías et al. 2020; Álvarez-Martí-Aguilar 2017a, b, 2020).

In the case of Spain, the current catalogue of earthquakes occurring before AD 1370, published by the Spanish National Geographic Institute (hereinafter IGN) (https://www.ign.es/web/ign/portal/sis-catalogo-terremotos; accessed 31/12/2020), fundamentally draws from the compilations appearing in the first half of the twentieth century, such as M. M.ª Sánchez Navarro-Neumann's (1921) and, above all, J. Galbis' *Catálogo sísmico* (1932, 1940). This last work has been a mandatory reference for several generations of geologists, archaeologists and historians interested in the Iberian Peninsula's seismological past. It is a meritorious compilation of an enormous quantity of data retrieved from previous historical works and seismic catalogues. However, no critical review was performed on the information contained in the catalogue in order to gauge its historicity, for which reason it includes, especially for the most ancient period, duplicated events and other nonexistent ones.

The evolution of seismic catalogues in Spain continued with works such as Munuera's (1963), which is based on the information contained in Galbis' *Catálogo*, although including magnitudes and geographical coordinates, even for events on which information is scarce or dubious (Muñiz Gómez 2001). The most recent compilations were performed by Mezcua and Martínez-Solares (1983), whose *Catálogo sísmico de la península Ibérica (880 a.C.–1900)* (Martínez-Solares and Mezcua 2002) served as the main source for the IGN's earthquake catalogue. Notwithstanding the fact that these recent catalogues contain more filtered and updated information, in Spanish tsunami research, the reference work has always been Galbis' *Catálogo*. There is a simple reason for this. Unlike the most recent ones, it includes descriptions of coastal phenomena and sea floods associated with earthquakes. This is the reason why it served as a fundamental reference for Campos (1991, 1992) in two works addressing the risk of tsunamis in Spain, which have been very influential in recent geological research. These works describe a series of earthquakes and tsunamis occurring before AD 1755: those of Cadiz in 218–216 and 210–209 BC; that of Portugal and Galicia in 60 BC; that of Malaga and Adra (Almeria) in AD 365; that of Cape St. Vincent in AD 382; that of Cadiz in AD 881; that of Lisbon and southern Portugal in AD 1531; that of Malaga in AD 1680 and that of the Algarve in AD 1722. For the period before AD 1755, the IGN's *Catálogo de Tsunamis en las Costas Españolas* records tsunamis in Cadiz in 218 and 210 BC (both with reliability = 0, very improbable), in south-western Portugal in 60 BC (reliability = 1, improbable), in southern Spain in AD 881 (reliability = 0, very improbable) and in Garachico (the Canary Isles) in AD 1706 (reliability = 3, probable).

Something similar has occurred in the tradition of Portuguese seismic catalogues. The influential work by Moreira de Mendonça (1758) includes brief descriptions of the events that it records and, as a result, has also been a permanent touchstone for tsunami research among Portuguese scholars. Nonetheless, the current reference works include the review of the seismic catalogue by Oliveira (1986) for the Portuguese National Laboratory for Civil Engineering (LNEC), the catalogue by Martins and Mendes-Victor (2001) and the review of the Portuguese tsunami catalogue by Baptista and Miranda (2009). Oliveira's review contains succinct descriptions of seismic events, including references to sea floods associated with earthquakes, for which reason it has been the major reference work for recent research in Portugal when linking geological and historical records of tsunamis. This work includes references to sea floods linked to earthquakes in 63 ("tsunami (?)") and 47 BC ("sismos variados i grandes marés"; *various earthquakes and great tides*) and AD 382 ("Desaparecimento de ilhas"; *Disappearance of islands*) (Oliveira 1986, p. 133). In reality, these accounts have been drawn from Bernardo de Brito (1597, 1609).

The compilations of Galbis (1932, 1940), Oliveira (1986) and Campos (1991, 1992), whose aim was not to determine the historicity of the recorded events, especially for the most ancient period, have made a powerful contribution to consolidating the perception that the earthquakes and tsunamis recorded in them are unquestionably historical events. Those teams that, as of the beginning of the 1990s, started to document the geological footprints of ancient extreme wave events (hereinafter EWEs) on the coasts of the Iberian Peninsula, based their research on that conviction.

1.3 The Historical Records and Geological Research

This section offers an overview of the process of reception of this historical information by those performing geological research on tsunamis in the Iberian Peninsula and the methodological problems to which it has given rise. The intention here is not to offer a comprehensive summary of the research and studies conducted during the past few decades, a task that exceeds the scope of this chapter, but to provide a number of keys to understand some of the most relevant questions posed by tsunami research in Portugal and Spain, in whose development it is possible to distinguish several stages.

In the 1990s, geomorphic and sedimentary evidence of the AD 1755 tsunami was first detected in Portugal, in places like Boca do Rio, Martinhal and Ria Formosa (Andrade 1992; Andrade et al. 1994, 1997, 1998; Dawson et al. 1995, 1996; Hindson et al. 1996; Hindson and Andrade 1999; Kortekaas et al. 1998a, b; see Costa et al. this volume). In the case of Spain, in the 1990s, geomorphological studies were performed in the estuaries of the rivers Tinto-Odiel, in Huelva (Lario 1996), in the marshlands of the river Guadalquivir, in the area of Doñana National Park (Lario et al. 1995, 2001; Lario 1996), at the mouth of the river Guadalete, in the Bay of Cadiz (Lario 1996; Dabrio et al. 1998; Luque et al. 2001, 2002) and in the south-easternmost coastal lowlands of the Gulf of Cadiz (Luque 2002; Whelan and Kelletat 2003, 2005; Alonso et al. 2004; Luque et al. 2004). These studies revealed an increasingly higher number of geomorphological footprints of EWEs, such as washover fans and *cheniers*, as well as a greater quantity of sedimentary records obtained from geological trenches and survey drilling.

The geological and sedimentary footprints of the tsunami of 1 November AD 1755 were the most evident and studied in this stage of research, particularly on the western seaboard of Portugal and the Algarve, although they were also documented on the coasts of Huelva and Cadiz (Dabrio et al. 1998; Luque et al. 2004). However, in research conducted on the coasts of the provinces of Huelva and Cadiz, the footprints of more ancient high-energy events also began to be documented.

Rodríguez Vidal (1987) and Zazo et al. (1994) had already detected an erosion event interrupting the progradation phase of the Punta Umbría and the Doñana spit bars, which they dated to ca. 2500 BP. But it was studies like those performed by Lario (1996), Lario et al. (2001), Rodríguez-Ramírez (1998) and Luque et al. (2001) in which sedimentary evidence of previous EWEs, datable to the prehistoric age or Antiquity, was discovered in the Doñana marshlands and at the mouth of the river Guadalquivir and to which a possible tsunamigenic origin was tentatively attributed.

Lario (1996) described two ancient erosive events in the southwest coasts of Spain dated to 4500–4200 BP and 2600–2350 BP, respectively. Rodríguez-Ramírez (1998) described three ancient erosive episodes in the Doñana and Algaida spit bars, at the end of the third millennium BC, ca. 2600 BP, and in the Roman imperial age, between the first and third centuries BC (Rodríguez-Ramírez 1998; Rodríguez-Ramírez et al., this volume). For their part, Lario et al. (2001) and Luque et al. (2001, 2002) described a series of washover fans in the Valdelagrana spit bar, in the Bay of Cadiz, some of which are attributed to a tsunami occurring during the late Roman Empire and others to the AD 1755 Lisbon tsunami. Later on, Luque et al. (2004) found geological evidence of the AD 1755 Lisbon tsunami in washover fans in Conil (Cadiz).

The growing suspicion that the high-energy marine events documented on the coasts of Huelva and Cadiz might have been tsunamis logically led research teams to contrast the radiocarbon dates obtained from geological surveys with the earthquakes and tsunamis recorded in the most important seismic catalogues. Thus, from the beginning of the 2000s up until the mid-2010s, there was a second stage of research on earthquakes and tsunamis in the southwest of the Iberian Peninsula characterised by a paradoxical drift.

On the one hand, in both Portugal and Spain, a greater number of more sophisticated studies were performed on paleotsunamis, driven by the growing interest aroused by the major catastrophes in the Indian Ocean in 2004, in Chile in 2010 and in Japan in 2011. The concern for determining the number, intensity and return periods of this type of phenomenon with such devastating consequences was reflected in scientific initiatives like TRANSFER (Tsunami risk and strategies for the European region, 2006–2009) and NEAREST (Integrated observation from NEAR shore sourcES of Tsunami: Towards an early warning system, 2006–2010), both funded by the European Commission, whose actions included updating European earthquake and tsunami catalogues. This was coupled with an upsurge in fieldwork in search of the footprints of ancient tsunamis. In both Portugal and Spain, there was an increase in the number of geomorphological and stratigraphic studies, accompanied by sets of mineralogical and paleofaunal analyses and radiocarbon dating, including studies of the off-shore earthquake record on the south-western seaboard of the Iberian Peninsula (Gràcia et al. 2010). Additionally, some of the key questions in recent research were posed, such as how to distinguish the footprints of tsunamis from those of violent storms (Kortekaas and Dawson 2007; Lario et al. 2010a) and how to determine the influence of the marine reservoir effect of coastal waters off the southern Atlantic coast of the Iberian Peninsula on radiocarbon dating (Lario et al. 2010b; Martins and Soares 2013; Monge 2015).

The 2000s and the beginning of the 2010s saw the publication of evidence of ancient EWEs, documented in areas like Cabo da Roca-Cascais, west of Lisbon (Scheffers and Kelletat 2005), the Alentejo (Ramos-Pereira et al. 2009), the Algarve (Schneider et al. 2010; Costa et al. 2010, 2012a, b), the Azores archipelago (Andrade, Borges and Freitas 2006), the Huelva estuary (Morales et al. 2008), the Bay of Cadiz (Gutiérrez-Mas et al. 2009a, b; Gutiérrez-Mas et al. 2011), the Atlantic coast of the Strait of Gibraltar (Alonso et al. 2004; 2007; Luque et al. 2004; Arteaga and Prados 2008; Koster and Reicherter 2014) and, in particular, the Doñana marshlands (Ruiz et al. 2004, 2005, 2008; Cáceres et al. 2006; Rodríguez-Vidal et al. 2008). While at the end of that decade and at the beginning of the 2010s, overviews of the results of the intense research activity during the previous decade, especially on the coasts of the Gulf of Cadiz (Luque 2008; Reicherter et al. 2010; Morales et al. 2011; Lario et al. 2010a, 2011; Ruiz et al. 2013), and reviews of Portuguese seismic catalogues (Baptista and Miranda 2009) saw the light of day. Lario et al. (2010a, 2011) concluded that at least seven very severe EWEs hit the southwest coast of the Iberian Peninsula in the last 7000 years, dated to ca. 7000 cal BP, ca. 5700–5300 cal BP, ca. 4500–4100 cal BP, ca. 3900–3700 cal BP, ca. 2700–2200 cal BP, ca. 2000 cal BP, ca. 1500 cal BP and AD 1755 (Lisbon earthquake).

On the other hand, despite this significant progress in the quantity and quality of geological research on EWEs in the Iberian Peninsula, during this stage, there was a tendency to employ insufficiently contrasted historical data of doubtful veracity. As of the beginning of the 2000s, the radiocarbon dates associated with these EWEs were compared with the dates recorded in the most important seismic catalogues, for the purpose of checking whether or not they coincided with the—allegedly—historical tsunamis recorded in them. Accordingly, recourse was had to the information appearing in Galbis' catalogue (1932, 1940), the summary of Spanish tsunamigenic events in a monograph published by Campos (1992) and, in the case of Portugal, Moreira de Mendonça's work (1758) and Oliveira's catalogue (1986), because, as already noted, they were the only ones that included descriptions of seismic events and sea phenomena compatible with tsunamis.

Throughout this stage, which got underway at the beginning of the 2000s, different pieces of evidence documented in the geological record of the peninsula were linked to the purported tsunamis in Cadiz in 218–209 BC, in Galicia and Portugal in 63 BC and in Cape St Vincent in AD 382, whose historicity was taken for granted (Luque et al. 2001, 2002; Ruiz et al. 2005, 2008; Cáceres et al. 2006; Morales et al. 2008; Rodríguez-Vidal et al. 2009; Gutiérrez-Más et al. 2009a; Baptista and Miranda 2009; Gràcia et al. 2010; Silva and Rodríguez-Pascua 2014, among others). Thus, the dates of those supposedly historical tsunamis had a powerful influence on the chronological contextualisation of events whose radiocarbon dates placed them in more or less close temporal horizons. The most explicit example was the linking of a body of evidence of EWEs documented in the Huelva estuary and the Doñana marshlands, with radiocarbon dates in the last three quarters of the first millennium BC, to the earthquakes and tsunamis that, according to Galbis (1932), occurred in Cadiz at the end of the third century BC, information that was ultimately drawn from Ocampo (Rodríguez-Vidal et al. 2011, 2015; Silva et al. 2015; Gómez et al. 2015).

An early critical assessment of the available information on allegedly historical tsunamis led researchers to place less faith in the entries appearing in seismic catalogues. This is the case of the research conducted on the ruins of the Roman city of *Baelo Claudia*, in the cove of Bolonia (Tarifa, Cadiz). The archaeological excavations carried out there since 1967 soon documented destruction layers attributable to seismic events (Le Roux 1973). Following the first comprehensive geological survey of the ruins and their surroundings (Menanteau et al. 1983), it was suggested that this evidence might be associated with the earthquakes and tsunamis, with epicentres in the Alboran Sea in AD 365 and in Cape St Vincent in AD 382, recorded in seismic catalogues such as that of Stahl (1971). However, the analyses performed by specialists on those historical sources containing references to the earthquake and tsunami occurring in the Eastern Mediterranean in AD 365 soon evinced that their impact on the far west was historically untenable (Jacques and Bousquet 1984; Lepelley 1984). In his seminal work on *Baelo Claudia*, Sillières (1997) rejects those events dated to the fourth century AD and, instead, claims that the city was struck by two major earthquakes in the mid-first century BC and in the second half of the third century AD. Sillières' thesis and the dates proposed by him have usually been taken very much into account by the research teams that have carried out pioneering archaeoseismological research work at the site of *Baelo Claudia* over the past few decades (Silva et al. 2005, 2009, 2015, 2016; Grützner 2011; Grützner et al. 2012). The recent discovery of EWE deposits at the site, dated to ca. AD 400 (Röth et al. 2015; see Reicherter et al., this volume) and possibly related to the tsunamigenic event that has been documented around the same time at sites on the coast of Huelva (see Bermejo Meléndez et al., this volume), does not allow us, by any means, to renew our trust in information like that provided by Brito on the impact of the AD 365 earthquake and tsunami in Portugal.

1.4 New Perspectives: The Need for Interdisciplinary Collaboration

Over the past few years, there has been growing evidence of possible tsunamigenic events affecting the coasts of the Iberian Peninsula in Antiquity, which are not mentioned in the ancient sources or in seismic catalogues. In the archaeological literature, there is a reference to evidence of a possible tsunami at the Phoenician site of Cerro del Villar, in the Bay of Malaga, between the eighth and seventh centuries BC (Aubet et al. 1999; see Álvarez-Martí-Aguilar et al., this volume), as well as at the site on Méndez Núñez Street, in the city of Huelva, in the first quarter of the sixth century BC (Osuna, Bedia and Domínguez 2000). A high-energy marine deposit, dated to ca. 2200–1800 cal. BP, has been documented in the vicinity of *Baelo Claudia* (Alonso et al. 2003, 2004), and indications of an EWE, dated to ca. AD 400–450, have been documented at the archaeological site (Röth et al. 2015), which are reviewed in this book (Reicherter et al., this volume). Similarly, evidence of a tsunami in the mid-first century AD has been discovered at the Roman archaeological site of Villa Victoria, in the Bay of Algeciras (Arteaga and Prados 2008; Arteaga, Blánquez and Roldán 2015). There are also further indications of an EWE, perhaps a tsunami, which would have affected the peninsula's southwestern seaboard between the second and third centuries AD, in both the geological and archaeological records. The footprints of events in that time horizon have been identified in the Guadalquivir estuary (Rodríguez-Vidal et al. 2008; Rodríguez-Ramírez et al. 2016), in the Bay of Cadiz (Luque et al. 2001; Gutiérrez-Mas 2011), at the site of Cerro da Vila in the Algarve (Teichner 2008, 2017) and even in the city of Seville, where a flood deposit has been documented in the port area of the ancient Roman city of *Hispalis* (Barral and Borja 2015), which is the object of study of one of the chapters of this book (Gutiérrez-Rodríguez et al., this volume). There has also been a steady accumulation of evidence of earthquakes at Roman sites in the south of the peninsula, including *Corduba*, *Munigua*, *Baelo Claudia* and *Carthago Nova* (for a recent summary, see Ruiz-Bueno 2017) in the third century AD, which are not mentioned either in the most important seismic catalogues.

On the other hand, studies casting doubt on the historical underpinnings of Spanish and Portuguese seismic catalogues and, specifically, the historicity of the information on earthquakes and tsunamis appearing in the works of Ocampo (Compatangelo-Soussignan 2013; Rodríguez Ramírez et al. 2016; Álvarez-Martí-Aguilar 2017a) and Brito (Ces Fernández 2015; Andrade et al. 2016; Álvarez-Martí-Aguilar 2017b) have begun to appear. In this vein, Udías (2015, 2020) has suggested reviewing the information on historical earthquakes in Spanish and Portuguese seismic catalogues, a task that has recently been undertaken by Álvarez-Martí-Aguilar (2020), who disputes the historicity of most of the information contained in them for the period before AD 881.

Thus, since the mid-2010s, it appears that a new research stage has commenced. This is based on the widespread belief that there is a need for fostering collaboration between the different disciplines—specifically, geology, archaeology and history—involved in research on historical earthquakes and tsunamis in the Iberian Peninsula, as highlighted in several contributions appearing in the 2015 monographic number of *The Spanish Journal of Quaternary and Geomorphology*, devoted to "Marine Events and Coastal Settlements in SW Iberia" (Rodríguez-Vidal, Campos and Cáceres 2015; see especially Campos et al. 2015; Bernal et al. 2015; Alonso et al. 2015; Gómez et al. 2015).

Imbued with that same spirit of interdisciplinary dialogue and with an eye to critically review the state of the research, the international congress *Historical Tsunamis in the Iberian Peninsula* was held in Malaga in February 2019, in collaboration with the Museum of Malaga and Malaga University. The congress was attended by a large number of specialists and research teams who have been at the forefront of the advances in the knowledge of this subject over the past few decades. The congress' keynotes and debates were the seed of this book. Both initiatives are framed in the activities of two research projects coordinated by the University of Malaga, *The Tsunami in the Cultural Representations of the Ancient World: Gadir-Gades and the Gulf of Cádiz as a case study* (HAR2015-66011-P) and *Earthquakes and Tsunamis in the Iberian Peninsula: Social Responses in the longue durée* (PGC2018-093752-B-I00), funded by the Spanish Ministry of Science, Innovation and Universities (MCIU), the Spanish State Research Agency (AEI) and the European Regional Development Fund (ERDF).

That scientific encounter placed special emphasis on the historical period in whose study there is a convergence between the historiographical tradition represented by the most important Portuguese and Spanish seismic catalogues, on the one hand, and by recent geological and archaeological research, on the other, namely between ca. 1000 BC and AD 1000. It was precisely in this period during which earthquakes and tsunamis purportedly occurred in Cadiz in 218–216 and 210–209 BC, in Portugal and Galicia in ca. 60 BC and in Cape St Vincent in AD 382—the available information on which has ultimately influenced recent geological research —and in which the most relevant progress in research on seismic and tsunamigenic events that are not recorded in seismic catalogues has been made.

1.5 Purpose and Organisation of the Book

This book has a dual purpose. On the one hand, the intention is to review the state of recent research on earthquakes and, in particular, tsunamis in the Iberian Peninsula, with special attention being paid to those events occurring between the first millennium BC and the first millennium AD. In its different chapters, this topic is approached from various perspectives: history and archaeology essays, geological overviews and case studies of specific sites and events.

Another of the book's aims is to deepen the necessary dialogue between the different scientific disciplines involved in research on this topic. Throughout this introduction, the emphasis has been placed on some of the methodological problems that have arisen in geological and geoarchaeological research on earthquakes and tsunamis in the Iberian Peninsula, resulting from the excessive trust that has been placed in historical information whose reliability is now being contended increasingly more. Accordingly, it offers excellent examples of a more updated and prudent use of the historiography on natural catastrophes in the Iberian Peninsula in Antiquity by those conducting geological and geoarchaeological research.

In the field of history, for its part, it is essential to pay greater attention to the role played by natural catastrophes in the evolution of historical processes affecting past societies, above all in periods before the Middle Ages, following the example of the work performed by Estévez (2005) on prehistoric cataclysms. In a world shaken by the COVID-19 pandemic, the capacity that phenomena of this type have for bringing about deep crises in many spheres of society and their role as catalysts or triggers of processes of structural change have been yet again evinced. As to the havoc wrought by major earthquakes and tsunamis, like that of AD 1755, their long return periods mean that societies—especially modern ones—tend to perceive them as extraordinary and distant phenomena, if at all, with the evident risk that this entails. So, it is essential that the results of geological and geoarchaeological research on ancient earthquakes and tsunamis in the Iberian Peninsula be taken into consideration in the field of history and that their implications for all facets of the social life of past communities be assessed.

With a view to meeting these objectives, this book includes a series of chapters written by some of the researchers and research teams who, in recent years, have been among the first to engage in the most interesting and relevant lines of enquiry into earthquakes and tsunamis in the Iberian Peninsula. Following this introduction, Chaps. 2 and 3, both of a historical and historiographical nature, comprising Part I of this book, focus on the study of accounts of cataclysms in the Iberian Peninsula in Antiquity appearing in the—ancient, mediaeval and modern—written sources.

Chapter 2 presents an updated analysis of Plato's account of Atlantis, whose catastrophic destruction has given rise to a distorted vision of the tsunami phenomenon in the field of pseudo-archaeology. In her essay, López-Ruiz highlights, on the one hand, the relationship of the story, invented by the Athenian philosopher, with images of marine or fluvial catastrophes in the mythical-religious traditions of the ancient Mediterranean and, on the other, the existence of a narrative language of cataclysms and ends of ages shared by the Middle East and Ancient Greece.

Chapter 3 delves into the origins of the accounts of earthquakes and tsunamis occurring in the Iberian Peninsula in ancient times, as well as analysing the historiographical context in which they emerged, for the purpose of assessing their historicity. It revolves around the Spanish historian Florián de Ocampo (sixteenth century) and the Portuguese chronicler Bernardo de Brito (sixteenth and seventeenth centuries), who are the sources for most of the information on ancient cataclysms in Spain and Portugal contained in modern seismic catalogues and whose historicity is very controversial.

Part II includes Chaps. 4–7 which offer overviews of the geological record of tsunamis in the Iberian Peninsula.

Chapter 4 offers a general description of the triggering mechanisms of tsunamis in the Gulf of Cadiz and the Alboran Sea, both areas characterised by noteworthy geological activity owing to the plate convergence between Eurasia and Africa. It briefly discusses the tsunamigenic faults and submarine landslides in both areas, stressing that both are likely to generate more destructive tsunamis in the Gulf of Cadiz than in the Alboran Sea. Moreover, the chapter also sets out the future challenges for research in order to gain a deeper understanding of seismogenic faults and landslides.

Chapter 5 presents a comprehensive summary of the state of the knowledge of storm and tsunami deposits on the Atlantic seaboard of the Iberian Peninsula, encapsulating three decades of research on the coasts of Portugal and Spain. This being the spirit of the book as a whole, the chapter discusses some of the sedimentological interpretations and dating of deposits associated with tsunamis appearing in the recent literature and, therefore, is a timely reassessment of reviews conducted in this regard at the beginning of the 2010s (Lario et al. 2010a, 2011; Ruiz et al. 2013).

Chapter 6 reviews the EWEs documented in the Guadalquivir estuary in the Late Holocene. This is a unique area due to the accumulation of geological evidence of events of this type and due to the fact that it was the geographical centre of one of the most relevant protohistoric phenomena in the Iberian Peninsula, namely the development of Tartessian culture, which coincided with the earliest Phoenician presence in Iberia. The chapter places special emphasis on the paleogeographic, cultural and historical implications of the EWEs documented in the area from a *longue durée* perspective.

Chapter 7 addresses the record of historical EWEs in the Bay of Cadiz, an area—as in the previous case—of special interest owing to the convergence between its geological record of tsunamis, its strong tradition of urban culture since the beginning of the first millennium BC and accounts of ancient cataclysms associated with the city of Cadiz. The chapter offers a detailed description of the characteristics of the Bay of Cadiz and a systematic review of the seven high-energy marine events documented in the area during the last 7,000 years, including the footprint of the AD 1755 Lisbon tsunami.

Lastly, Part III, comprising Chaps. 8–15, focuses on case studies of specific places where earthquakes and tsunamis have occurred, including important firsts, which are presented in chronological order in relation to the described event or the most significant among those addressed.

Chapter 8 provides an updated review of the evidence of an EWE documented at the archaeological site of Cerro del Villar, originally located on an island in the Guadalhorce estuary in Malaga, where the ruins of a Phoenician colony, which was struck by a high-energy marine event in about the last quarter of the seventh century BC, are to be found. Specifically, the chapter summarises the research carried out at the site, assessing the possibility that this EWE was of a tsunamigenic nature.

Chapter 9 re-examines extreme events documented in the Bay of Lagos (Portugal) by reviewing previous geological and archaeological research and new archaeological evidence. This revision allows for suggesting that the evolution of settlements in the area was affected by the impact of several earthquakes and EWEs from the first millennium BC, in Phoenician times, up until the beginning of the first millennium AD, in the Roman age. This evidence makes it possible to explore the relationship between them and more contemporary historical accounts of extreme events.

Chapter 10 enquires into the role played by EWEs in the decline of the salted fish industry in the western reaches of the Roman Empire between the second and third centuries AD, using as an example the case study of the archaeological site of Boca do Rio (Vila do Bispo, the Algarve). The geoarchaeological research conducted at the site in recent years has revealed that the profound changes detected in the Roman settlement in the second and third century AD were not brought about, in this case, by one extreme event, but by medium-term environmental changes. Additionally, it also offers a description of the sedimentary evidence of a hitherto unknown EWE in the late Middle Ages.

Chapter 11 examines the impact of high-energy marine events on the coastal communities of the province of Huelva in Roman times. The study addresses, on the one hand, the archaeological evidence of EWEs at sites such as El Eucaliptal, *Onoba* and El Terrón in the province of Huelva, while extending the analysis to the coasts of Portugal. On the other, this evidence is contrasted with the geological record of the Guadalquivir and Guadalete estuaries, plus Gibraltar. The chapter identifies two EWEs on the Atlantic seaboard in Roman times, in the third and fourth century AD, which had negative repercussions for the area's fishing industry.

Chapter 12 focuses on the flood deposit associated with a third-century-AD destruction layer at the archaeological site of the Patio de Banderas (Reales Alcázares, Seville), corresponding to the port suburbs of the Roman city of *Hispalis*. It offers a sedimentological analysis of this unique deposit and its archaeological context, exploring the possibility that it might have been caused by the combined action of an EWE and fluvial flooding. In addition, a critical review of the literature on the third-century-AD event affecting the SW of the Iberian Peninsula is performed.

Chapter 13 examines the archaeological deposits of marine high-energy events in the ancient Roman city of Baelo Claudia (Bolonia, Cadiz), one of the most important sites for the development of archaeoseismicity studies in Spain. In this contribution, resulting from a multi-disciplinary investigation, three tsunami deposits, dated to ca. 4000 cal. BP (2000 BC), ca. AD 400 and AD 1755, respectively, are described in the Bay of Bolonia. Special attention is paid to the ca. AD 400 event, associated with significant archaeoseismic damage identified in newly excavated buildings, which has been dated to the end of the fourth century AD.

Chapter 14 presents the results of the archaeological excavations carried out in the "Baluarte de la Bandera" in Ceuta—the Roman city of *Septem*—on the African coast of the Strait of Gibraltar, which have brought to light evidence of a powerful earthquake that damaged the city walls in the second half of the seventh century AD. This hitherto unknown seismic event serves as a starting point for a critical revision of the geoarchaeological evidence of earthquakes and tsunamis in the vicinity of the Strait of Gibraltar in Roman times and in the early Middle Ages, with special attention being paid to the city of *Baelo Claudia*.

Lastly, Chap. 15 focuses on the locality of El Palmar de Vejer (Cadiz), which was affected by the AD 1755 Lisbon tsunami, so as to present an example of the use of multi-proxy analyses for identifying tsunami deposits, with the accent being placed on geochemical applications. The results of this study underscore the usefulness of this type of approach when attempting to identify tsunami deposits.

The 15 chapters of this book reflect the trend towards the interdisciplinary integration between the different scientific fields involved in earthquake and tsunami research in the Iberian Peninsula. In turn, they also highlight a growing consensus on the existence of methodological problems arising in the intersection between these different disciplines, which should be ironed out in future research. From these chapters, it can also be deduced that research in this respect will have to meet other important challenges in the coming years, which include gaining a deeper understanding of the number, chronology and nature of the earthquakes and tsunamis affecting the Iberian Peninsula in the past. To undertake this task, it is essential to make progress in the distinction between the sedimentary evidence of tsunamis and violent storms, as well as establishing a more precise chronology for these events, something that will be possible thanks to more radiocarbon dating, a correct assessment of the marine reservoir effect and a better contrast between these dates and those provided by archaeology and the written sources.

All this is crucial for defining return periods of these phenomena with potentially catastrophic consequences for human beings and infrastructures and, therefore, for assessing the risk factors and vulnerability of coastal communities in the Iberian Peninsula. From a historical point of view, all these developments have opened up a fascinating field of research for gaining further insights into the impact that these earthquakes and tsunamis had on the lives of people in the past and come as a necessary reminder that these phenomena will certainly repeat themselves in the more or less distant future.

Acknowledgements This research has been conducted as part of the projects *The Tsunami in the Cultural Representations of the Ancient World: Gadir-Gades and the Gulf of Cádiz as a case study* (HAR2015-66011-P MINECO-FEDER), and *Earthquakes and Tsunamis in the Iberian Peninsula: Social Responses in the longue durée* (PGC2018-093752-B-I00), funded by the Spanish Ministry of Science, Innovation and Universities (MCIU), the Spanish State Research Agency (AEI) and the European Regional Development Fund of the European Union (ERDF, EU).

References

Alonso C, Gracia FJ, Ménanteau L et al (2003) Paléogéographie de l'anse de Bolonia (Tarifa, Espagne) à l'époque romaine. The Mediterranean World. Environ Hist Elsevier, Amsterdam, pp 407–417

Alonso C, Gracia FJ, Del Río L et al (2004) Registro morfosedimentario de eventos históricos de alta energía en el litoral atlántico del Estrecho de Gibraltar (Trafalgar-Tarifa). In: Benito G, Díez Herrero A (eds) Contribuciones recientes sobre Geomorfología. SEG-CSIC, Madrid, pp 263–271

Alonso C, Ménanteau L, Gracia FJ, Ojeda R (2007) Geoarqueología y paleomorfología litoral de la ensenada de Bolonia: primeros resultados y nuevas propuestas. In: Arévalo A, Bernal D (eds) Las "Cetariae" de "Baelo Claudia": avance de las investigaciones arqueológicas en el barrio meridional (2000–2004). Universidad de Cádiz – Junta de Andalucía, Cádiz, pp 521–538

Alonso C, Gracia FJ, Rodríguez-Polo S et al (2015) El registro de eventos energéticos marinos en la bahía de Cádiz durante épocas históricas. Cuaternario y Geomorfología 29(1–2):95–117

Álvarez-Martí-Aguilar M (2017a) La tradición historiográfica sobre catástrofes naturales en la Península Ibérica durante la Antigüedad y el supuesto tsunami del Golfo de Cádiz de 218–209 a.C. Dialogues d'histoire ancienne 43(2):117–145

Álvarez-Martí-Aguilar M (2017b) Terremotos y tsunamis en Portugal en época antigua: el legado de Bernardo de Brito y su Monarchia Lusytana (1597–1609). Euphrosyne 45:183–204

Álvarez-Martí-Aguilar M (2020) The Historicity of the Earthquakes Occurring in the Iberian Peninsula before A.D. 881 Recorded in Spanish and Portuguese Seismic Catalogs. Seismol Res Lett 91(6):3585–3594. https://doi.org/10.1785/0220200168

Andrade C (1992) Tsunami generated forms in the Algarve barrier islands. Sci Tsunami Haz 10:21–33

Andrade C, Munhá JM, Paulino J (1998) Geochemical signature of extreme marine flooding in the Boca do Rio lowland (Algarve, Portugal). Actas, V Congresso Nacional de Geologia, Lisboa 84(1):51–54

Andrade C, Hindson R, Freitas C et al (1994) Sedimentary evidence of tsunami flooding in Algarve coastal lowlands. Littoral 94:26–29

Andrade C, Andrade AM, Kortekaas S et al (1997) Sedimentological traces of tsunamigenic overwash of the Martinhal lowland (Western Algarve - Portugal). Proceedings Sem. Zona Costeira do Algarve, Faro, Eurocoast-Portugal, pp 11–18

Andrade C, Borges P, Freitas MC (2006) Historical tsunami in the Azores archipelago (Portugal). J Volcanol Geoth Res 156:172–185

Andrade C, Freitas MC, Oliveira MA et al (2016) On the Sedimentological and Historical Evidences of Seismic Triggered Tsunamis on the Algarve Coast of Portugal. In: Duarte JC, Schellart WP (eds) Plate Boundaries and Natural Hazards. Am Geophys Union, Washington, pp 219–232

Arteaga C, Prados F (2008) Aplicaciones geomorfológicas en el alfar romano de Villa Victoria (San Roque, Cádiz). Apuntes sobre un modelo de investigación arqueológica interdisciplinar. In: González S, Pérez M, Bango CI (coords) Una nueva mirada sobre el Patrimonio Histórico. Líneas de investigación arqueológica en la UAM. UAM Ediciones, Madrid, pp 169–184

Arteaga C, Blánquez J, Roldán, L (2015) Consideraciones paleogeográficas en la bahía de Algeciras. Acerca de un posible tsunami en la Carteia romana (San Roque, Cádiz). Cuaternario y Geomorfología 29(1–2):137–156

Aubet ME, Carmona P, Curià E, Delgado A et al (1999) Cerro del Villar. I, El asentamiento fenicio en la desembocadura del río Guadalhorce y su interacción con el hinterland. Consejería de Cultura de la Junta de Andalucía, Sevilla

Baptista MA, Miranda JM, Lopes FC et al (2007) The source of the 1722 Algarve earthquake: evidence from MCS and Tsunami data. J Seismol 11:371–380

Baptista MA, Miranda JM (2009) Revision of the Portuguese catalog of tsunamis. Nat Hazards Earth Syst Sci 9:25–42

Baptista MA, Miranda JM, Batlló J (2014) The 1531 Lisbon Earthquake: A Tsunami in the Tagus Estuary? Bull Seismol Soc Am 104:2149–2161

Bernal D, Expósito JA, Díaz JJ et al (2015) Evidencias arqueológicas de desplomes paramentales traumáticos en las Termas Marítimas de Baelo Claudia. Reflexiones Arqueosismológicas. Cuaternario y Geomorfología 29(1–2):119–136

Barral MÁ, Borja F (2015) Análisis geoarqueológico. In: Tabales Rodríguez MA (ed) Excavaciones Arqueológicas en el Patio de Banderas, Alcázar de Sevilla. Memoria de Investigación 2009–2014. Sevilla, Patronato del Real Alcázar y Casa Consistorial de Sevilla, pp 40–51

Brito B de (1597) Monarchia Lusytana. Composta por Frey Bernardo de Brito, Chronista geral & Religioso da ordem de s. Bernardo, professo no Real mosteiro de Alcobaça. Parte Primeira… Mosteiro de Alcobaça

Brito B de (1609) Segunda parte da Monarchia Lusytana em que se continuão as historias de Portugal desde o nacimento de nosso Salvador Iesu Christo até ser dado em dote ao Conde dom Henrique. Pedro Crasbeeck, Lisboa

Cáceres LM, Rodríguez-Vidal J, Ruiz F et al (2006) El registro geológico Holoceno como instrumento para establecer periodos de recurrencia de tsunamis: el caso de la costa de Huelva. Paper presented at the V Asamblea Hispano Portuguesa de Geodesia y Geofísica, Sevilla pp 1–4

Campos JM, Bermejo J, Rodríguez-Vidal J (2015) La ocupación del litoral onubense en época romana y su relación con eventos marinos de alta energía. Cuaternario y Geomorfología 29(1–2):75–93

Campos ML (1991) Tsunami hazard on the Spanish coasts of the Iberian peninsula. Sci Tsunami Haz 9:83–90
Campos ML (1992) El riesgo de tsunamis en España: análisis y valoración geográfica. Instituto Geográfico Nacional, Madrid
Ces Fernández B (2015) Los efectos del seísmo de Lisboa de 1755 sobre el patrimonio monumental de Galicia. Dissertation, Universidade da Coruña
Compatangelo-Soussignan R (2013) Un tsunami antique à l'embouchure du Guadalquivir? Sources documentaires et archives paléoenvironnementales. In: Marie-Yvane D. et al. (eds) Anciens peuplements littoraux et relations homme/milieu sur les côtes de l'Europe Atlantique = Ancient maritime communities and the relationship between people and environment along the European Atlantic coasts. Colloque International HOMER (2011: Vannes, France). Archaeopress, Oxford, pp 595–603
Conde JA (1820) Historia de la dominación de los árabes en España, sacada de varios manuscritos y memorias arábigas. Imprenta que fue de García, Madrid
Costa PJM, Andrade C, Freitas MC et al (2010) Reconhecimento de um depósito de tsunami na Lagoa dos Salgados (Algarve, Portugal). Revista e-Terra 12. Resumos VIII Congresso Nacional de Geologia(10), 4 pp
Costa PJM, Andrade C, Dawson AG et al (2012a) Microtextural characteristics of quartz grains transported and deposited by tsunamis and storms. Sed Geol 275–276:55–69
Costa PJM, Andrade C, Freitas MC et al (2012b) A tsunami record in the sedimentary archive of the central Algarve coast, Portugal: characterizing sediment, reconstructing sources and inundation paths. The Holocene 22(8):899–914
Dabrio CJ, Goy JL, Zazo C (1998) The record of the tsunami produced by the 1755 Lisbon earthquake in Valdelagrana spit (Gulf of Cadiz, southern Spain). Geogaceta 23:31–34
Dawson AG, Hindson R, Andrade C et al (1995) Tsunami sedimentation associated with the Lisbon earthquake of 1 November AD 1755: Boca do Rio, Algarve. Portugal. the Holocene 5(2):209–215
Dawson AG, Smith DE, Ruffman A et al (1996) The diatom biostratigraphy of tsunami sediments: examples from recent and middle Holocene events. Phys Chem Earth 21:87–92
Estévez J (2005) Catástrofes en la prehistoria. Bellaterra, Barcelona
Faria y Sousa M (1678) Europa Portuguesa. Segunda edicion correta, ilustrada y añadida ... Tomo I. Antonio Craesbeeck de Mello, Lisboa
Galbis J (1932) Catálogo Sísmico de la Zona comprendida entre los meridianos 5° E. y 20° W. de Greenwich y los paralelos 45° y 25° N. Tomo I. Instituto Geográfico, Catastral y de Estadística, Madrid
Galbis J (1940) Catálogo Sísmico de la Zona comprendida entre los meridianos 5° E. y 20° W. de Greenwich y los paralelos 45° y 25° N. Tomo II. Instituto Geográfico y Catastral, Madrid
Garibay E (1571) Los Quarenta libros del Compendio Historial de las Chronicas y Universal Historia de todos los Reynos de España. Christophoro Plantino, Amberes
Goded T (2006) Reevaluación de daños de los terremotos de Málaga de 1494 y 1680. Dissertation, Universidad Complutense de Madrid
Gómez F, Arruda AM, Rodríguez-Vidal J et al (2015) Eventos marinos de alta energía y cambios traumáticos en los asentamientos costeros del Suroeste de la Península Ibérica. Cuaternario y Geomorfología 29(1–2):57–74
Gràcia E, Vizcaino A, Escutia C et al (2010) Holocene earthquake record offshore Portugal (SW Iberia): testing turbidite paleoseismology in a slow-convergence margin. Quatern Sci Rev 29(9–10):1156–1172
Grützner C (2011) The *Baelo Claudia* earthquake problem. Dissertation, RWTH Aachen
Grützner C, Reicherter K, Hübscher C et al (2012) Active faulting and neotectonics in the Baelo Claudia area, Campo de Gibraltar (Southern Spain). Tectonophysics 554–557:127–142. https://doi.org/10.1016/j.tecto.2012.05.025
Gutiérrez-Mas JM, Juan C, Morales JA (2009a) Evidence of high-energy events in shelly layers interbedded in coastal Holocene sands in Cadiz Bay (south-west Spain). Earth Surf Process Landforms 34:810–823
Gutiérrez-Mas JM, López-Arroyo J, Morales JA (2009b) Recent marine lithofacies in Cadiz Bay (SW Spain) Sequences, processes and control factors. Sed Geol 218:31–47
Gutierrez-Mas JM (2011) Glycymeris shell accumulations as indicators of recent sea-level changes and high-energy events in Cadiz Bay (SW Spain). Estuar Coast Shelf Sci 92(4):546–554
Hindson RA, Andrade C (1999) Sedimentation and hydrodynamic processes associated with the tsunami generated by the 1755 Lisbon earthquake. Quatern Int 56(1):27–38
Hindson RA, Andrade C, Dawson AG (1996) Sedimentary processes associated with the tsunami generated by the 1755 Lisbon earthquake on the Algarve coast, Portugal. Phys Chem Earth 21(1–2):57–63
Jacques F, Bousquet B (1984) Le cataclysme du 21 juillet 365: Phénomène régional ou catastrophe cosmique? In: Tremblements de terre, histoire et archéologie. IVèmes Rencontres internationales d'archéologie et d'histoire d'Antibes,2, 3, 4, novembre 1983. Valbonne, pp 183–198
Kortekaas S, Andrade C, Andrade AM (1998a) Litoestratigrafia e foraminíferos do enchimento sedimentar da baixa do Martinhal - Algarve (Portugal) - dados preliminares. In: V Congresso Nacional de Geologia, Lisboa, Instituto Geológico e Mineiro, 84(1):C-55-C-58
Kortekaas S, Andrade C, Dawson A (1998b) Palaeotsunami deposits at Martinhal, South West Portugal,

associated with the earthquake of November 1st, 1755 AD. In: SC Stiros, PA Pirazzoli (conv) Meeting on Rapid Coastal Changes in the Late Quaternary, INQUA, Greece, 29
Kortekaas S, Dawson AG (2007) Distinguishing tsunami and storm deposits: an example from Martinhal. SW Portugal. Sediment Geol 200(3–4):208–221
Koster B, Reicherter K (2014) Sedimentological and geophysical properties of a ca. 4000 year old tsunami deposit in southern Spain. Sed Geol 314:1–16
Lafuente Alcántara M (1843) Historia de Granada, comprendiendo las de sus cuatro provincias Almería, Jaén, Granada y Málaga. Desde remotos tiempos a nuestros días… Imprenta y Librería de Sanz, Granada
Lario J (1996) Ultimo y Presente Interglacial en el área de conexión Atlántico-Mediterráneo: Variaciones del nivel del mar, paleoclima y paleoambientes. Dissertation, Universidad Complutense de Madrid
Lario J, Zazo C, Dabrio CJ et al (1995) Record of Recent Holocene Sediment Input on Spit Bars and Deltas of south Spain. In: Core B (ed) Holocene cycles: clímate, sea levels, and sedimentation. J Coast Res 17:241–245
Lario J, Zazo C, Plater AJ et al (2001) Particle size and magnetic properties of Holocene estuarine deposits from the Doñana National Park (SW Iberia): evidence of gradual and abrupt coastal sedimentation. Z Geomorphol 45(1):33–54
Lario J, Luque L, Law C et al (2010a) Tsunami vs. Storm surge deposits: a review of the sedimentological and geomorphological records of extreme wave events (EWE) during the Holocene in the gulf of Cádiz, Spain. Zeitschrift für Geomorphologie 54(3):301–316
Lario J, Dabrio CJ, Zazo C et al (2010b). Comment on “Formation of chenier plain of the Doñana marshland (SW Spain): Observations and geomorphic model” by A. Rodríguez-Ramírez and C.M. Yáñez-Camacho [Marine Geology 254 (2008) 187–196]. Marine Geology 275(1–4):283–286
Lario J, Zazo C, Goy JL et al (2011) Holocene palaeotsunami catalogue of SW Iberia. Quatern Int 242:196–200. https://doi.org/10.1016/j.quaint.2011.01.036
Lepelley C (1984) L’Afrique du Nord et le séisme du 21 juillet 365: remarques méthodologiques et critiques. In: Tremblements de terre, histoire et archéologie. IVèmes Rencontres internationales d'archéologie et d'histoire d'Antibes, 2,3,4, novembre 1983. Valbonne, pp 199–206
Le Roux P (1973) La VIIe campagne de fouilles à Belo (Bolonia, province de Cadix). Mélanges De La Casa De Velázquez 9:755–770
López Marinas JL (1985) El terremoto catastrófico de 22 de septiembre de 1522, en Almería. Seminario sobre Sismicidad y Riesgo Sísmico del área ibero-Magrebí. Instituto Geográfico Nacional, Madrid, pp 51–60
Luque L (2002) Cambios en los palaeoambientes costeros del sur de la Península Ibérica (España) durante el Holoceno. Dissertation, Universidad Complutense de Madrid
Luque L (2008) El impacto de eventos catastróficos costeros en el litoral del Golfo de Cádiz. Revista Atlántica-Mediterránea de Prehistoria y Arqueología Social 10:131–153
Luque L, Lario J, Zazo G et al (2001) Tsunami deposits as paleoseismic indicators: examples from the Spanish coast. Acta Geologica Hispanica 36(3–4):197–211
Luque L, Lario J, Civis J et al (2002) Sedimentary Record of a Tsunami during Roman Times, Bay of Cádiz. Spain. J Quart Sci 17(5–6):623–631
Luque L, Zazo C, Lario J et al (2004) El efecto del tsunami de 1755 en el litoral de Conil de la Frontera (Cádiz). In: Baquedano E, Rubio S (eds) Miscelánea en Homenaje a Emiliano Aguirre. Geología, Volumen I. Museo Arqueológico Regional, Alcalá de Henares, pp 72–82
Mariana J (1601) Historia general de España. Tomo primero. Pedro Rodríguez, Toledo
Mezcua J, Martínez-Solares JM (1983) Sismicidad del área Ibero Mogrebí. Instituto Geográfico Nacional, Madrid
Martínez-Solares JM, Mezcua J (2002) Catálogo sísmico de la Península Ibérica (880 a.C.-1900). Instituto Geográfico Nacional, Madrid
Martins I, Mendes Victor LA (2001) Contribuição para o estudo da sismicidade da região oeste da península Ibérica. Universidade de Lisboa, Instituto Geofísico do Infante D. Luís. Publicação Nº 25:1–56
Martins J, Soares A (2013) Marine Radiocarbon Reservoir Effect in Southern Atlantic Iberian Coast. Radiocarbon 55(3):1123–1134. https://doi.org/10.1017/S0033822200048037
Menanteau L, Vanney JR, Zazo C (1983) Belo et son environment (Détroit de Gibraltar). Etude physique d’un site Antique. In Belo II. Broccard, Publications de la Casa de Velázquez, Paris, pp 39–221
Mendes-Victor L, Oliveira CS, Azevedo J et al (eds) (2009) The 1755 Lisbon earthquake: revisited. Springer, Berlin
Monge Soares AM (2015) Radiocarbon dating of marine shells from the Gulf of Cadiz: the marine radiocarbon reservoir effect, its variability during the Holocene and palaeoenvironmental inferences. Cuaternario y Geomorfología 29(1–2):19–29
Morales JA, Borrego J, San Miguel EG et al (2008) Sedimentary record of recent tsunamis in the Huelva Estuary (southwestern Spain). Quatern Sci Rev 27:734–746. https://doi.org/10.1016/j.quascirev.2007.12.002
Morales JA, Gutiérrez JM, Borrego J, Rodríguez-Ramírez A (2011) Sedimentary Characteristics of the Holocene Tsunamigenic Deposits in the Coastal Systems of the Cadiz Gulf (Spain). In: Mörner NA (ed) The tsunami threat – research and technology. IntechOpen, Rijeka, pp 237–258
Moreira de Mendonça JJ (1758) Historia universal dos terremotos, que tem havido no mundo, de que ha noticia, desde a sua creaçaõ até o seculo presente. Com huma narraçam individual do terremoto do

primeiro de novembro de 1755, e noticia verdadeira dos seus effeitos em Lisboa, todo Portugal, Algarves, e mais partes da Europa, Africa, e América, aonde se estendeu: E huma dissertaçaõ phisica sobre as causas geraes dos Terremotos, seus effeitos, differenças, e Prognosticos; e as particulares do ultimo. Antonio Vicente da Silva, Lisboa

Munuera JM (1963) Datos básicos para un estudio de sismicidad en el área de la península Ibérica (Seismic Data). Memorias del Instituto Geográfico y Estadístico XXXII:1–47

Muñiz Gómez S (2001) Revisión del catálogo sísmico gallego. T. I. Dissertation. ETSA, Universidad de A Coruña

Ocampo F de (1543) Los quatro libros primeros de la Cronica general de España que recopila el maestro Florian do Campo criado y cronista del Emperador Rey nuestro señor por mandado de su magestad Çesarea. Juan Picardo, Zamora

Ocampo F de (1553) Los cinco libros primeros de la Cronica general de España, que recopila el maestro Florian do Campo, Cronista del Rey nuestro señor, por mandado de su Magestad, en Zamora, Guillermo de Millis, Medina del Campo

Oliveira CS (1986) A sismicidade histórica e a revisão do catálogo sísmico. Laboratório Nacional de Engenharia Civil, Lisboa

Osuna M, Bedia J, Domínguez AM (2000) El santuario protohistórico hallado en la calle Méndez Núñez (Huelva). In: Cabrera P, Santos M (coords) Ceràmiques jònies d'època arcaica: centres de producció i comercialització al Mediterrani occidental. Actes de la taula rodona celebrada a Empúries, els dies 26 al 28 de maig de 1999. Museu d'Arqueologia de Catalunya-Empúries, Barcelona, pp 177–188

Ramos-Pereira AR, Trindade J, Neves M et al (2009) Indicadores geomorfológicos de tsunami no Parque Natural do SW Alentejano e Costa Vicentina (Malhão). In: Publicações da Associação Portuguesa de Geomorfólogos, vol. VI, APGEOM, Braga, pp 51–56

Reicherter K, Becker-Heidmann P (2009) Tsunami deposits in the western Mediterranean: remains of the 1522 Almería earthquake? In: Reicherter K, Michetti AA, Silva PG (eds) Palaeoseismology: historical and prehistorical records of earthquake ground effects for seismic hazard assessment. The Geological Society, Special Publications, 316, London, pp 217–235

Reicherter K, Vonberg D, Koster B et al (2010) The sedimentary inventory of tsunamis along the southern Gulf of Cadiz (southwestern Spain). Z Geomorphol 54 (Suppl. 3):147–173

Rodríguez-Ramírez A (1998) Geomorfología del Parque Nacional de Doñana y su entorno. Organismo Autónomo Parques Nacionales del Ministerio de Medio Ambiente, Madrid

Rodríguez-Ramírez A, Villarías-Robles JJR, Pérez-Asensio JN et al (2016) Geomorphological record of extreme wave events during Roman times in the Guadalquivir estuary (Gulf of Cadiz, SW Spain): an archaeological and paleogeographical approach. Geomorphology 261:103–118. https://doi.org/10.1016/j.geomorph.2016.02.030

Rodríguez-Vidal J (1987) Modelo de evolución geomorfológica de la flecha litoral de Punta Umbría, Huelva, España. Cuaternario y Geomorfología 1:247–256

Rodríguez-Vidal J, Ruiz F, Cáceres LM et al (2008) Morphosedimentary features of historical tsunamis in the Guadalquivir estuary (SW of Spain). In: 2nd International Tsunami Field Symposium IGCP Project 495 Quaternary Land-Ocean Interactions: Driving Mechanisms and Coastal Responses. Ostuni (Italy) and Ionian Islands (Greece) 22–28 September 2008, pp 139–141

Rodríguez-Vidal J, Ruiz F, Cáceres LM et al (2011) Geomarkers of the 218–209 BC Atlantic tsunami in the Roman Lacus Ligustinus (SW Spain): a palaeogeographical approach. Quatern Int 242:201–212

Rodríguez-Vidal J, Campos JM, Cáceres LM (2015) Eventos marinos y asentamientos costeros en el suroeste de Iberia. Cuaternario y Geomorfología 29 (1–2):5–18

Rodríguez-Vidal J, Ruiz F, Cáceres LM et al (2009) Geoindicadores del tsunami de finales del s. III a.C. en el estuario del Guadalquivir (SW de España), VII Reuniao do Quaternario Ibérico. Livro de Resumos, Faro, Portugal, 5–9 de Outubro de 2009, Faro, CIMA, pp 272–276

Röth J, Mathes-Schmidt M, García Jíménez I et al (2015) The Baelo Claudia tsunami hypothesis - results from a multi-method sediment analysis of late-Roman deposits (Gibraltar Strait, Southern Spain), 6th International INQUA Meeting on Paleoseismology, Active Tectonics and Archaeoseismology, 19–24 April 2015, Pescina, Fucino Basin, Italy, pp 50–53

Ruiz-Bueno MD (2017) Actividad sísmica en el mediodía ibérico durante el siglo III d.C. La incidencia arqueológica en Corduba (Córdoba). Pyrenae 48 (2):29–51

Ruiz F, Rodríguez-Ramírez A, Cáceres LM et al (2004) Late Holocene evolution of the southwestern Doñana National Park (Guadalquivir Estuary, SW Spain): a multivariate approach. Palaeogeogr Palaeoclimatol Palaeoecol 204(1–2):47–64

Ruiz F, Rodríguez-Ramírez A, Cáceres LM et al (2005) Evidence of high-energy events in the geological record: mid-holocene evolution of the southwestern Doñana National Park (SW Spain). Palaeogeogr Palaeoclimatol Palaeoecol 229(3):212–229

Ruiz F, Abad M, Rodríguez-Vidal J et al (2008) The geological record of the oldest historical tsunamis in Southwestern Spain. Riv Ital Paleontol Stratigr 114 (1):145–154

Ruiz F, Rodríguez-Vidal J, Abad M et al (2013) Sedimentological and geomorphological imprints of Holocene tsunamis in southwestern Spain: an approach to establish the recurrence period. Geomorphology 203:97–104

Sánchez-Navarro Neumann MM (1921) Lista de los terremotos más notables sentidos en la Península Ibérica

desde los tiempos más remotos, hasta 1917, inclusive, con ensayo de agrupación en regiones y periodos sísmicos. La Estación Sismológica y el Observatorio Astronómico y Meteorológico de Cartuja (Granada). Granada, Observatorio de Cartuja, pp 11–51
Scheffers A, Kelletat D (2005) Tsunami relics on the coastal landscape west of Lisbon. Portugal. Sci Tsunami Hazards 23(1):3–16
Schneider H, Höfer D, Trog C et al (2010) Holocene estuary development in the Algarve Region (Southern Portugal)—a reconstruction of sedimentological and ecological evolution. Quat Int 221:141–158
Sillières P (1997) Baelo Claudia: una ciudad romana de la Bética. Casa de Velázquez, Madrid; Junta de Andalucía, Sevilla
Silva PG, Rodríguez-Pascua MA (eds) (2014) Catálogo de los efectos geológicos de los terremotos en España (Grupo de trabajo español de la escala macrosísmica ESI-07). Instituto Geológico y Minero de España, Madrid
Silva PG, Borja F, Zazo C et al (2005) Archaeoseismic record at the ancient Roman city of Baelo Claudia (Cádiz, south Spain). Tectonophysics 408:129–146
Silva PG, Reicherter K, Grützner C et al (2009) Surface and subsurface palaeoseismic records at the ancient Roman city of Baelo Claudia and the Bolonia Bay area, Cádiz (south Spain). In: Reicherter K, Michetti AA, Silva PG (eds) Palaeoseismology: historical and prehistorical records of earthquake ground effects for seismic hazard assessment. Geol Soc Special Publ 316:93–121
Silva PG, Bardají T, Roquero E et al (2015) Seismic palaeogeography of coastal zones in the Iberian Peninsula: Understanding ancient and historic earthquakes in Spain. Cuaternario y Geomorfología 29(1–2):31–56
Silva PG, Giner-Robles JL, Reicherter K et al (2016) Los terremotos antiguos del conjunto arqueológico romano de Baelo Claudia (Cádiz, Sur de España): Quince años de investigación arqueosismológica. Estud Geol 72(1):1–24
Stahl P (1971) La séismicité de Tanger et de sa región. In: Mémoire explicatif de la Carte géotechnique de Tanger au 1/25 000. Contribution à la connaissance du Tangérois. Notes et Memoires du Service Geologique du Maroc. Rabat, Ed. Serv. Géol. Maroc, 222 bis:101–109
Teichner F (2008) Zwischen Land und Meer – Entre tierra y mar. Studien zur Architektur und Wirtschaftsweise ländlicher Siedlungen im Süden der römischen Provinz Lusitanien. Museo Nacional de Arte Romano, Mérida
Teichner F (2017) Cerro da Vila: a rural commercial harbour beyond the Pillars of Hercules. In: Campos Carrasco JM (ed) Los puertos romanos Atlánticos Béticos y Lusitanos y su relación comercial con el Mediterráneo. L'Erma di Bretschneider, Roma, pp 403–435
Udías A (2015) Historical earthquakes (before 1755) of the Iberian Peninsula in early catalogs (Electronic Supplement: Critical Revision of Earthquakes in the Iberian Peninsula before Year 1000). Seismol Res Lett 86(3):999–1005
Udías A (2020) Large Earthquakes and Tsunamis at Saint Vincent Cape before the Lisbon 1755 earthquake: a historical review. Pure Appl Geophys 177:1739–1745. https://doi.org/10.1007/s00024-019-02323-z
Udías A, Buforn E, Martínez-Solares JM et al (2020) Historical sources for Earthquakes before 1900 on the Iberian Peninsula and in the offshore region. Seismol Res Lett XX:1–10. https://doi.org/10.1785/0220200038
Whelan F, Kelletat D (2003) Analysis of tsunami deposits at cabo de Trafalgar, Spain, using GIS and GPS technology. Essener Geographische Arbeiten 35:11–25
Whelan F, Kelletat D (2005) Boulder deposits on the Southern Spanish Atlantic Coast: possible evidence for the 1755 AD Lisbon Tsunami? Sci Tsunami Haz 23:25–38
Zazo C, Goy JL, Somoza L et al (1994) Holocene sequence of sea-level fluctuations in relation to climatic trends in the Atlantic-Mediterranean linkage coast. J Coast Res 10(4):933–945

Part I

Introduction: History and Historiography

Not Exactly Atlantis: Some Lessons from Ancient Mediterranean Myths

2

Carolina López-Ruiz

Abstract

This chapter starts by briefly discussing the methodological pitfalls of the "Where is Atlantis" question, including the identification of Tartessos with the fantastic sea empire in Plato's dialogs. It then examines the myth of Atlantis in its own terms, as a tool in Plato's philosophical teachings particularly related to the discussion of ideal and corrupt state models, while also highlighting their connection with widely held ideas about maritime or fluvial catastrophes in the ancient Mediterranean. And, lastly, an overview is provided of other Near Eastern and Greek narratives about cataclysms and ends of ages. These narratives doubtless channeled the accumulated experience and fear of "high-energy events", which entered the mythical imagination as catalysts of the end of ages or of the world. At the same time, they do not necessarily allude to real events or places, but are part and parcel of culture-specific views of the human position in relation to the gods and are of particular relevance today in more than one way.

C. López-Ruiz (✉)
Divinity School, The University of Chicago, Chicago, IL, USA
e-mail: lopezruiz.academic@gmail.com

Keywords

Atlantis · Tartessos · Plato · Cataclysms · Flood stories · Near Eastern mythology

2.1 Tartessos and Atlantis: Comparing Apples and Oranges?

Notwithstanding the obvious methodological hurdles, amateurs and not a few scholars since the Renaissance and even in the twentieth century have insisted on finding a historical precedent for the myth of sunken Atlantis. Some pointed to the volcanic eruption that sunk part of the island of Thera (modern Santorini) in about the sixteenth century BC, and others fantasized about an Atlantian past for the Americas—there is really no limit to the associations of Atlantis with fantasies relating to ancient and modern nations (Fritze 2009, pp. 19–62; cf. Vidal-Naquet 1992), but one of the most productive theories was the one which sought it in Tartessos (e.g., Schulten 1927; García y Bellido 1953, 1963; discussion in Álvarez-Martí-Aguilar 2019). Even recently, the publication of satellite images of Doñana National park (Kühne 2004) and the subsequent geomorphological and archeological prospections in its marshlands (Celestino et al. 2016) have inevitably revived the enthusiasm for this pseudo-archeological hypothesis in various

M. Álvarez-Martí-Aguilar and F. Machuca Prieto (eds.), *Historical Earthquakes, Tsunamis and Archaeology in the Iberian Peninsula*, Natural Science in Archaeology,
https://doi.org/10.1007/978-981-19-1979-4_2

media, whose problems Rodríguez González (2017) has effectively dealt with, not without backlash from the pseudo-scientific (or rather para-scientific) "Atlantology" front.

The above-mentioned geo-morphological study suggested that some seismic and maritime cataclysm hit a vast area of the lower Guadalquivir region in the first part of the sixth century BC, which may have contributed to the crisis that seems to have affected the area of Tartessos at the time (Osuna et al 2000; Celestino 2014, p. 105; Celestino and López-Ruiz 2016, pp. 206, 306; 2020, pp. 264–267; see Rodríguez-Ramírez et al., this volume). Evidence for this event and its date are still far from conclusive (Celestino and López-Ruiz 2020, pp. 264–66), and the effect of other possible tsunamis on the Iberian coasts and in the Mediterranean at large (Papadopoulos et al 2014) during the Iron Age have barely begun to be explored (see the chapter by Álvarez-Martí-Aguilar et al. on Cerro del Villar, Malaga, in this volume). Ultimately, the historicity of this event and its consequences for Tartessos is beyond the point when it comes to discussing the Atlantis story. Instead, I will focus on what Tartessos and Plato's Atlantis share for certain: the fascination with lost civilizations, real and imagined. Both are also said to have possessed incredible wealth in metals, to have thrived on maritime trade, and to have been located beyond the Pillars of Herakles in the Atlantic. The key lies in the distinction between "real and imaginary". The story of Atlantis as he wrote it was a figment of Plato's imagination, one of the several myths that he elaborated to convey a philosophical message. No other Greek source mentions it as a myth, let alone as a historical event. Plato's Atlantis is not a fixed point on a map, not even on a mythological one. Far from giving us specific geographical coordinates, Plato intentionally placed his Atlantis out in the "Atlantic sea", from where it launched an attack against "all of Europe and Asia" (*Ti.* 24e; translations from Plato follow Anderson 2018, with minor modifications). The Titan Atlas lent his name to both the "outer sea", first attested as "Atlantic" in Herodotus's *Histories* (Hdt. 1.202.4–203.1, 4.152.2) and the North African mountain range that extends as far as the ocean (Hdt. 4.184.3–185.1). In Plato's story, this is a fitting realm in which to imagine the god Poseidon breeding his own race and founding his failed empire, a titanic entity full of *hybris*. In other words, Plato's Atlantis existed in the imagined *eschaton* of the known world and it conveniently disappeared without a trace, as it "sank beneath the sea and vanished, wherefore even now the sea in that area is unnavigable and unexplored" (*Ti.* 25d).

A different matter is whether the mythology associated with the far west and the region of Tartessos might have served as inspiration for the imaginary location of the lost civilization there. Knowledge of Tartessos was within reach of sixth century Greeks (e.g., Hecataeus of Miletus), and a particular channel seems to have been the Phocaeans, as these Ionians from Asia Minor settled in Marseille and northwest Iberia, and their extraordinary dealings with the Tartessian king Arganthonios reached Herodotus' ears (Hdt. 1.163.1–165.2; cf. also 4.152.2–5, referring to the merchant Colaeus of Samos). And the same lore is in all likelihood behind the quip made by the poet Anacreon (sixth century BC) that neither did he crave for a rich life nor "for a hundred and fifty years to be king of Tartessos" (Anacreon PMG fr. 361; fr. 4 Gentili-Prato, Teubner [= Strabo 3.2.14]) (see discussion in Celestino and López-Ruiz 2016, pp. 26–42). More to the point, news of seismic and maritime catastrophes along the Atlantic seaboard, especially in the Bay of Cadiz, are well attested since Antiquity, although dating these events is often a challenge (Álvarez-Martí-Aguilar 2017a, 2019, this volume). Plato may be drawing from traditions about western oceanic cataclysms as he explicitly refers to the Pillars and the realm of Gadir (Gadeira): after all, his Atlantis is "an island before the mouth that your people call the Pillars of Herakles, an island larger than Libya and Asia combined" (*Ti.* 24e); and the first-born twins of Poseidon were named Atlas and Gadeiros, who inherited the central part of the island and "the headland of the island by the Pillars of Herakles over against the region now named Gadeira" (*Criti.* 114b), respectively. But, as others have suggested, there were events closer to his time that could have also made an impression on him, like the tsunami in the Gulf of Corinth in 373/72 BC, which according to ancient historians submerged the sites of Helike and Boura (Álvarez-Martí-Aguilar 2019, p. 125; cf. Giovannini 1985). But none of these geographical cues can be taken out of the context of Plato's storytelling, as will be discussed below.

The discussion of Atlantis as a real place is a methodological catastrophe (no pun intended). Anyone trained in history, archeology or philology knows that we cannot expect the same kinds of answers from mythological and historical sources or from their archeological counterparts, nor should we put the same questions to them. The question "Where was Atlantis?" or "Was Tartessos Atlantis?" is in itself a trap, in the sense that it obliges us to compare the incomparable and to confuse ontological and epistemological categories. As Rodríguez puts it, "Until we stop feeling the need to justify the lack of connection between Tartessos and Atlantis, we will neither free the former from its mythological context, nor accept that the latter is solely a myth" (Rodríguez González 2017, p. 16, my translation). The point she brings home is that both positions in the debate ultimately engage with the issue of the ontological reality or lack of reality of Atlantis and its presumed location in Tartessos or elsewhere. Just as importantly, they both leave Plato outside the discussion. They either take the story in search of an actual place waiting to be discovered at face value or they discard it altogether as an irrelevant, pointless falsehood. But this is where the classics step in to remind us that neither is a myth a lie, nor a reality. The ancient Greeks, Plato included, knew as much. The alliance between the fictional and the real was already expressed by Hesiod in his *Theogony* as precisely a skill of the Muses: "We know how to tell many fantasies that seem real, and we know, if we want, how to sing of real things" (Hesiod, *Theog*. 27–28; see Heiden 2007. Translations of ancient Greek texts are mine).

In its broadest definition, a myth is a traditional narrative with cultural relevance, which transcends any particular text (e.g., Graf 1993, pp. 1–8). Myths are preserved and passed down because they are relevant to a specific community, and sometimes they also become meaningful for a broader audience (e.g., Panhellenic culture, Christianity, the Western world). One indication that a narrative is what the Greeks regarded as "a myth" (which they called *logos* or *mythos*, both meaning "story") is the involvement of supernatural and extraordinary elements: gods, monsters, and heroes, some of them demigods. Their functions are infinite (ritual, ethical, genealogical, etc.), but in all cases, they are perpetuated because they are effective *as narratives* in capturing and transmitting essential ideas about the place of humans in the universe vis-à-vis other humans, nature, and the gods. (e.g., Edmunds 2014; sources in López-Ruiz 2018; a narratological approach in Johnston 2018).

With the conclusion (at least in academia) of the misconceived debate on the location of Atlantis, its myth can be revisited and explored in its own terms as a Platonic story, something that is rarely done, in part due to the shadow of popular "Atlantology" hanging over it. It is also interesting to determine how the myth connects with widely held ideas about maritime or fluvial catastrophes in the ancient Mediterranean. Accordingly, after reviewing the myth of Atlantis as a tool in Plato's philosophical teachings, a brief overview of other Near Eastern and Greek narratives about maritime cataclysms or sea floods will be provided in the following pages. These narratives doubtless channeled the accumulated experience and fear of "high-energy events", which entered the mythical imagination as catalysts of the end of ages or of the world. At the same time, they do not necessarily allude to real events or places, but form part of a culture-specific "worldview" of the human position in relation to the gods and their power over natural forces.

2.2 Some Lessons From Plato's Atlantis

Plato tells the story of Atlantis in two parts in his inter-linked dialogs *Timaeus* and *Critias* (Pl. *Ti.* 20d-25d, *Criti.* 108e-121c). Despite all the details that he offers in both dialogs, the philosopher, true to form, leaves it up to the reader to deduce the story's relevance and message.

Plato never makes himself the speaker in his dialogs (Socrates, his teacher, is often the main interlocutor). Moreover, he often introduces several degrees of separation between his interlocutors and the stories that they narrate, which they claim to have heard from someone else and so on and so forth. The most familiar example is the account of what was said at a banquet (*symposium*) hosted by the playwright Agathon; what happened at the gathering and the speeches improvised there about Love (Eros) are "recalled" by someone who heard them from someone else some 30 years before (Plato, *Symposium*). Plato deceives us by making his speaker seem confident of the account's veracity, despite the fact that it has been indirectly transmitted and deals with events occurring in the distant past. This intentional ambiguity allows him to elaborate on the whole narrative to suit his purposes.

Another example is the "Myth of Er" (*Resp.* 614b-621d), which comes somewhat as a surprise at the end of a dialog devoted to the question of what makes the ideal state. At the end of the dialog, Socrates tells the unlikely story of a youth who, after dying in battle, experienced the afterlife before resuscitating 12 days later, just before he was going to be buried. This "Lazarus" brought back with him a detailed vision of the process that souls went through after death. This fascinating narrative contains not only a model of judgment, with punishments and rewards for souls according to their deeds in life, but also the idea of reincarnation (*metempsychosis*), whereby, after a variable period of cleansing, they pass into another living body (of a human or an animal) and experience another "type of life" (e.g., that of a king, a hero, a laborer, a swan, etc.) through a process combining chance and choice. This allows souls to somehow leverage the wisdom that they acquired in their previous lives. After the choice is made, their memory is erased before being reincarnated. The lesson? (or one of them): what you do in your life can harm or improve your chances of being happier in future lives. Through the story of Er, Plato articulates ideas about virtue and the importance of improving the soul through philosophy.

Much scholarship has scrutinized the myth of Er for its connections with Pythagorean and Orphic beliefs (e.g., Edmonds 2004), and we will never know whether Plato or Socrates endorsed such eschatological views. What matters is that this story, as with others in Plato, is presented as such, rather than a doctrine (altogether absent from Plato's writing). The philosopher's myths, which are few and carefully crafted, are didactical tools. In fact, he seems to have been harshly critical of traditional myths, like those to be found in Hesiod and Homer, which portray the gods as immoral beings, setting the wrong ethical examples. Hence, in the ideal state, there would be no room for traditional poetry or myths in the education of children (*Resp.* 377d-378e). What should take their place? Plato leads by example, occasionally creating his own myths and allegories, but only those serving as useful tools for philosophical learning, for which he selectively draws from characters or ideas familiar to his audience (Clay 2000; Collobert et al. 2012). In a society, in which traditional myths about Olympian gods and Homeric heroes had a huge influence, the action of presenting different, invented myths, conveyed a clear underlying message: Since the general public learns through the power of stories, is it not best that they should learn from the sort of stories that convey a philosophically useful message? Similarly, in Plato's free account of the creation of animals and humans by Prometheus (*Prt.* 320c-324d), the Titan endows the otherwise naturally unarmed humans with intelligence and political wisdom, which reminds us of our responsibility to put our inherent "socio-political" skills to good use.

In his account of Atlantis, Plato resorts to the same kind of storytelling. Firstly, the story is told by Critias, one of Socrates' interlocutors, who swears by its truthfulness and offers a genealogy of the account to support it, which for us only makes it sound even more remote and dubious: Critias himself heard this story from his grandfather, who had heard it from *his* father, who had heard it from Solon (the sixth century Athenian lawgiver and poet), who had been told it by an

Egyptian priest in Egypt. Firstly, neither is there any mention of Atlantis in Solon's writings or in any other Greek source before Plato, nor is there any evidence of such a story in Egyptian texts. Secondly, like the myth of Er and others in Plato's dialogs, the account of Atlantis seems somewhat detached from its immediate context; its connection with the dialog in which it is embedded is not stated, being up to the listener or reader to draw conclusions. In the case of Atlantis, Socrates is asking his interlocutors to provide examples of how the ideal state that they had been discussing on a previous occasion (cf. the topic of the *Republic*) would work in practice. To this question, Critias comes up with the exemplary story of Atlantis, which he repeats in both dialogs. In the first (*Ti.* 20d-25d), he dwells on the transmission of the story and how the Egyptians had come by this valuable information about Athens' prehistory; in the second, he elaborates on different details regarding Atlantis' geography and socio-political organization (*Criti.* 108e-121c). At first sight, this is no less puzzling as an example than Timaeus' answer, in which he recounts the creation of the universe by an all-intelligent demiurge god (*Ti.* 29d-34b), instead of tackling the topics of human societies and political organization.

But everything has a purpose in Plato's writings. He wants us to tone our philosophical muscles at every step. For instance, it is no coincidence that Critias is most probably one of the 30 tyrants who came to power in a weakened Athens at the end of the Peloponnesian War. As Critias personifies the arrogance of Atlantis, he should sink as well; this is perhaps why Plato interrupts Critias' speech mid-sentence in the second dialog (at the end of the *Critias*), just when he is about to repeat the words that Zeus pronounced to the council of the gods ("and after gathering them all together, he said …"). We know that this unfinished ending was no coincidence. One way of interpreting this is that Plato is preventing Critias from speaking for Zeus, which would be too much *hybris* to bear. The temporal remoteness of the story is also remarkable and makes its historicity inconceivable, irrespective of the claims of the pretentious Critias. By establishing this cataclysm 9000 years before Socrates' and Critias' time, that is, way back in prehistory, Plato is indicating that it is a myth. Reminding us of our ignorance of the remote past, he also alludes to the superiority of Egyptian culture in this respect: the Egyptians are represented as the keepers of knowledge of other civilizations, versus the Greeks who were ignorant of their own remote past. Not only the early custom of putting knowledge down in writing, but also the more stable geology and drier climate of the Nile Valley (no earthquakes or sea floods), helped these Egyptian accounts to survive the passing of time. This was not the case with the Greeks and other peoples who, in addition to natural catastrophes, were also prone to cyclic civilizational collapses.

So, what is the philosophical lesson of Atlantis' rise and destruction? Once we appreciate it as a fictional myth, everyone can draw their own conclusions. Only a few aspects of the story, which are often neglected in the popular reception of the myth, will be highlighted here. First and foremost, Atlantis is not only a story about a great sunken civilization (indeed a continent), but one about war and the clash of civilizations, in which Atlantians are actually the "villains" (more on this below). In a nutshell, Atlantis was a society founded by the children of Poseidon, overwhelmed by corruption and *hybris* as their divine blood slowly thinned out; their imperialist ambitions, with their incursions into North Africa (which the Greeks called "Libya") and Europe, endangered the entire known world (i.e., the Mediterranean regions):

> *Now, on this Atlantic island a great and wondrous power of kings was formed by alliance, which dominated the entire island as well as many other islands and regions on the mainland; and in addition to these, of the places within the straits they ruled Libya as far as Egypt and Europe as far as Tyrrhenia* (cf. *Ti.* 25b; cf. *Criti.* 114c).

Eventually, an allied force defeated Atlantis and Zeus ordered that the island-continent be sunk by a great cataclysm (*kataklysmos* in Greek literally means "inundation, deluge"), thus forcing Poseidon to be the tool of destruction of his own descendants. This is the end of Atlantis' manic imperialism and of an imagined prehistoric age.

Secondly, Atlantis's morally superior adversary in the story is usually left out. It was Athens, presented as an equally ahistorical and remote place, which we can call "proto-Athens," that defeated Atlantis and hence saved the civilized world in that mythical age. The Athenians did not achieve victory due to their natural wealth or resources but thanks to their discipline and leadership, having chosen an austere way of life, prospering from their industry and intellect under the auspices of Hephaistos and Athena. Atlantis is the antithesis of proto-Athens. Atlantis is an aggressive sea empire, represented by Poseidon, built on the exploitation of natural resources. But this remote proto-Athens is no more real than Atlantis. Besides the temporal abyss, Plato makes this clear when describing a strange topography, almost unrecognizable due to the erosion caused by deluges and other elements, and a socio-political organization reminiscent of his utopian *Republic*. The stark hills marking the Athens of Critias' (and Socrates') time, such as the Lykavittos and the Akropolis, are pale remainders of that past (Fig. 2.1).

Instead of *where*, the question should be *what* was this Athens, this Atlantis? This issue—also interpreted by others before him (Giovannini 1985)—has probably been most comprehensively addressed by Pierre Vidal-Naquet (1986, pp. 263–284) who, following a structuralist approach, suggests that Plato's "proto-Athens" and Atlantis represented the ideal Platonic state of the *Republic* and its opposite, namely, a tyrannical and morally corrupt one, respectively. But there is more to it than meets the eye. With this dichotomy, Plato would be alluding to the Athenian military and political disaster in the Peloponnesian Wars, which directly affected Socrates' and Plato's lives. It was Pericles' Athens that adopted an imperialist policy based on its naval power, "selling out", as it were, to Poseidon and thus betraying in a way its debt to Athena and Hephaistos, its traditional gods; and it was this Athens that sank (not literally) at the end of the war with Sparta and its allies. Moreover, Plato makes his imagined "proto-Athens" disappear in very much the same way as Atlantis, so as to make both equally unreal (impossible to find) and perhaps to allude to the physical destruction of Athens' walls and its mighty navy in the wake of the war. As Solon was told:

> *But at a later time with the outbreak of intense earthquakes and cataclysmic floods, and under harsh assault day and night, the whole of your military body sank beneath the earth* (*Ti.* 25d).

In turn, following its logic, the "real-life" antagonist of this Atlantis-like Athens would be its rival Sparta, which led the coalition against its empire and whose socio-political organization was much admired by Plato, providing the model for part of his ideal polity and, according to this interpretation, for the idealized "proto-Athens".

In conclusion, the myth of Atlantis was a story about moral and immoral state models and the exemplary punishment that the gods meted out to men for their arrogance. Regardless of whether or not Plato was inspired by the Athens/Sparta dichotomy, readers are supposed to draw their own historical or ethical lessons from the myth. Yet another allusion to Atlantian maritime power will be discussed at the end of this chapter.

2.3 The Theme of the "Great Flood" as a Universal Cataclysm

The theme of a disaster that brings a civilization or an age to an end had been around long before Plato wrote his myth of Atlantis. The story of the Great Flood appears in the earliest known literature, which comes from Mesopotamia. The Universal Flood appears first in Old Babylonian texts written ca. 1700 BC, and subsequently in versions contained in *The Epic of Atrahasis* and, with some variation, in *The Epic of Gilgamesh* (Tablet XI) (translations in Dalley 2000, pp. 9–35 and 109–120), composed in the early first millennium. As is known from fragments of other versions (e.g., in Berossos *Babiloniaka*, third century BC: *BNJ* [= *FGrH*] 680 F4; Dalley 2000, pp. 5–8), the myth had a far greater reach.

The story's socio-economic and geological backdrop is clear: urban culture in Mesopotamia was sustained by its irrigation system fed by the

Fig. 2.1 The Acropolis of Athens with classical-period remains (Photo by Carolina López-Ruiz)

Tigris and the Euphrates, with canalization being essential to prevent flooding after the extreme deluges characterizing desert/semi-desert climates. In the "land between rivers," floods could reach catastrophic proportions (they still occur in present-day Iraq), unlike in other parts of the Levant or Greece. It is generally accepted that the myth originated in a Sumerian tradition that transformed a series of historical inundations into a universal, mythical catastrophe: silt deposits from flooding in the late fourth millennium have been found at Early Dynastic sites, such as Ur. Moreover, a great flood is mentioned in Sumerian king lists, where the figure of Atrahasis (the survivor of the flood in the Old Babylonian epic) is listed as a king of Shuruppak before the flood (Dalley 2000, pp. 4–8). In other words, "the Flood" was mythologized early on as a single event and a chronological marker at the dawn of the region's history.

In both the *Atrahasis* and *Gilgamesh* epics, the plot follows a familiar pattern: the gods send a flood to destroy humankind; a pious man favored by one of the gods (Ea/Enki) is chosen to survive; he is called Atrahasis, "exceedingly wise," and Ut-napishtim, "he who found life" in the respective stories; the man receives instructions from his god and survives along with his family and a group of people and animals. After the Flood, the gods accept his offering of a sacrifice, allow humanity to continue to exist, and grant him and his wife immortality. Gilgamesh learns this story from the

Flood survivor himself, whom he finds at the end of the world while searching for an answer to mortality after the death of his friend Enkidu. Utnapishtim tells Gilgamesh the story as a clear lesson that this was a "one-off" event; that the Flood marked the end of the time when true "sages" and culture-bringers walked the earth and gods could grant immortality (Dalley 2000, p. 5).

The story had a huge impact on surrounding cultures. The best-known adaptation is the story of Noah in Genesis (Gen. 6–9). Some details (the boat's construction, the animals, the birds sent to find dry land) are astonishingly similar. It may come as a surprise, however, that in Mesopotamia, the Universal Flood was not a punishment for impiety, but a "demographic-control" measure on the part of the gods, and only then as a last resort, meted out by the head of their pantheon, Enlil, who was disturbed by the excessive noise and tumult caused by the growing number of humans below. Other disasters unleashed by him included plagues and famines, each sent by the appropriate god under Enlil's orders, and each averted thanks to Atrahasis' protector god Ea/Enki (a sort of Prometheus figure), who each time instructed him and his community to pray to the correct god. For example, the Deluge was specifically the storm god Adad's doing:

> *The face of the weather changed. Adad bellowed from the clouds.* […] *The winds were raging even as he went us [and] cut through the rope, he released the boat* […]. *The kashushu-weapon went against the people like an army. No one could see anyone else, they could not recognize the catastrophe. The Flood roared like a bull, like a wild ass screaming the winds [howled]. The darkness was total, there was no sun* (*Atrahasis*, OBV, Tablet III, ii; transl. from Dalley 2000).

Once the flood gates had opened, "torrent, storm, and flood came on", and even the gods (other than Enlil) "wept for the country". Nintu, a mother goddess, was especially distressed by the annihilation of her offspring as a result of Enlil's "wicked order" (Tablet III, iii–iv):

> *Even the gods were afraid of the flood-weapon. They withdrew; they went up to the heaven with Anu [the upper-sky god]. The gods cowered, like dogs couched by an outside wall. Ishtar screamed like a woman giving birth; the Mistress of the Gods [i.e., Nintu] sweet of voice, was wailing: '[…] I myself gave birth [to them], they are my own people, yet they fill the sea like fish spawn!* (*Epic of Gilgamesh*, Tablet XI, iii).

When the Israelites adapted the theme to a monotheistic mythology, the motivations and agents changed drastically. Yahweh is both the instigator of the Flood and the savior of pious Noah. The Israelite god acts as the storm god and sends the Flood as a punishment for moral corruption and impiety, but he allows them to survive through Noah's descendants.

In cosmogonic thinking, the storm and water are perfect tools of destruction, since the primordial waters open the creation narratives of both Mesopotamian and biblical traditions. In Mesopotamia (*Enuma Elish*, Tablet I), the first divine couple Apsu and Tiamat represent the sweet and salty waters, from whom all the generations of gods descend. In the Hebrew tradition, the waters are also central to the creation:

> […] *the earth was a formless void and darkness covered the face of the deep, while a wind from God swept over the face of the waters* (Gen. 1:2, New Revised Standard Version [NRSV]).

The waters can both spawn and destroy the creation. Principal gods like Enlil, Adad, Teshub, Yahweh, and Baal are thus represented as dominating the waters, whereby becoming the sustainers or potential destroyers of the world (Fig. 2.2).

This cataclysmic story has a Greek version, albeit much less elaborate, in the extant sources. Its main characters are Deucalion and his wife Pyrrha, who survive the flood sent by Zeus (the Greek sky and storm god), with the help of Prometheus, a double-dealing Titan who helps people in various stories. Deucalion and Pyrrha become the (re)creators of humanity when they are instructed through a prophecy to throw rocks over their shoulders so that men and women should spring from the earth. The details are fragmentary and there are only brief allusions to Deucalion in Hesiod's *Catalogue of Women* (*Cat*. fr. 1, 3, 5) and in Pindar (*Olympian Ode* 9.42–46), who links him to the flood; versions of the myth were later compiled by Apollodorus

Fig. 2.2 Mesopotamian depiction of Ea residing in the waters of Apsu, receiving another god, on cylinder seal from Ur (Akkadian period, c. 2350–2150 BC) (Drawing by Esther Rodríguez González)

(*Library* 1.7.2–3), among other mythographers. None of them, however, offers a reason for the flood sent by Zeus, and in the Greek story, the emphasis seems to be placed on the genealogies initiated by Deucalion and Pyrrha (Darshan 2013; West 1997, pp. 489–493; Finkelberg 2005, pp. 33–35).

But literary adaptations are timeless, with the Roman poet Ovid (first century BC-AD) leaving us a beautiful description of the flood in his *Metamorphoses*. The "biblical" moral overtones are present here since Zeus sent the deluge to punish human beings for their impious ways (this is the story of Lycaon, *Met*. 1.163–239), although pious Deucalion and Pyrrha survive (by chance?) and are allowed to repopulate the earth (Ovid, *Met.* 1.240-451; cf. *Met*. 7.353). The philosophical ideas of Epicureanism make their way into Ovid's creation and flood narratives: his flood is also a temporary return to that primeval time before the elements were separated from the initial random chaos, while the cataclysm also reminds us of the underlying tension (strife) between air, water, and earth (cf. Álvarez-Martí-Aguilar 2017b, pp. 979–980, with references therein). Moreover, Ovid vividly depicts the pathetic attempts of the people to survive, the absurd effect of land turned into the sea and the famine that is as deadly as the waters:

> *Now the sea and land have no distinction. All is sea, but a sea without a shore. Here one man seeks a hill-top in his flight; another sits in his curved skiff, plying the oars where lately he has plowed; one sails over his fields of terrain or the roof of his buried farmhouse, and one takes fish caught in the elm-tree's top.* […] *And where recently the slender goats had browsed, the ugly seals rested their bulk.* […] *The dolphins invade the woods, brushing against the high branches, and shake the oak-trees as they knock against them in their course. The wolf swims among the sheep, while tawny lions and tigers are borne along by the waves.* […] *The sea in unchecked liberty has now buried all the hills, and strange waves now beat upon the mountain peaks. Most living things are drowned outright. Those who have escaped the water slow starvation at last overcomes through lack of food* (Ovid, *Met*. 1.290–312, transl. Miller 1921, with minor modifications).

A similar scenario is conjured up by Horace when recalling a violent storm in Rome. He believed that Jupiter wanted to threaten the city dwellers with another great flood, and he imagined the Tiber overflowing, with fish, instead of pigeons, crawling over the branches of the trees, and terrified deer floating in the new sea (Horace, *Odes* 1.2.5–12).

But the punishment has consequences for the gods too since they need the people's offerings:

> *[The gods] all grieved over the threatened loss of the human race, and asked what would be the state of the world bereft of mortals. Who would bring incense to their altars?* (Ovid, *Met.* 1.246–249, transl. after Miller 1921).

In *The Epic of Atrahasis*, "the gods smelled the fragrance, gathered like flies over the offering" (*Atrahasis*, Tablet III, v), and in Genesis, "Yahweh smelled the pleasing odor" of the burnt offering made by Noah as soon as he had reached dry land (Gen. 8:20) and only then promised not to attempt to destroy humankind again. The same concern also appears when Demeter inflicts drought on the earth as she grieves her daughter Persephone's disappearance (*Hymn to Demeter* 310–312). In other words, humans share the product of their exploitation of the earth with the gods, and the gods hold sway over the earth's viability, in a circle of mutual dependency that makes utter universal destruction an unlikely outcome.

2.4 The Final Ordeal, With or Without Water

The cataclysmic destruction by flood is one of the most popular themes marking the end of ages in Eastern Mediterranean lore, but not the only one. The most widespread idea among the Greeks was that past ages had been brought to a close by war.

Hesiod represents this idea in his *Myth of the Five Races*, composed in the late-eighth-early seventh century BC (*Op.* 106–201). According to the poet, there had been five human "races" (*genê*) or ages, the last of which, the Race of Iron corresponded with his own historical time (i.e., the Iron Age). The first three were the Races of Gold, Silver, and Bronze, each of which, as the metal metaphor evinces, deteriorated morally and drifted away from the gods. Yet, before the Race of Iron, Hesiod breaks the neat sequence and introduces the Race of Heroes. This sort of interlude can be seen as a second act or expansion of the Race of Bronze (hence Gold, Silver, Bronze-Heroes, and Iron). The Bronze people were "terrible and powerful", but excessively violent, as a result of which they destroyed each other. Zeus sent them "nameless" to the Underworld, that is, without fame or glory, the worse punishment for the *kleos*-seeking Greek heroes. Hesiod, we think, inserted the Race of Demigods as a hinge between the legendary and historical pasts, in order to bring the curtain down on the "Bronze Age," in which the Greeks situated the Trojan War and other famous episodes at the dawn of their collective history—he does not need to mention them all, since they are remembered and celebrated in the Greek epics. Summarizing them, Hesiod mentions only the two greatest war sagas, those of Thebes and Troy:

> *Evil war and terrible combat also destroyed these ones, some under seven-gated Thebes, in the land of Kadmos, fighting for Oedipus' flocks, and others when war carried them in ships, over the deep abyss of the sea, for the sake of Helen of the beautiful mane* (Hes. *Op.* 161–165).

In *The Epic Cycle* (*Cypria*, Fr. 1; West 2003), the relationship between the Trojan War and the intentional destruction of the Race of Heroes is made explicit: it was Zeus' plan (*boulê*) to make the host of heroes die in the Trojan War to relieve the earth of the burden of mankind. But echoes of the Flood tradition can also be detected in passages of the Homeric epics, most clearly in the theme of the destruction of the Achaean Wall by Poseidon (Hom. *Il.* 12.6–26; Scodel 1982; cf. Burkert 1992, p. 103; West 1997, pp. 377–380; Doak 2012, pp. 119–152).

For the ancient Greeks, these epic wars were historical events, albeit distorted and mythologized, as observed by historians like Herodotus and Thucydides (Hdt. 2.112–120, Thucyd. 1.11).

It is also worth noting that they based the progression from the prehistoric past to their own "age" on that of the Bronze Age–Iron Age transition, which has become a technological convention in modern archeology of the Eastern Mediterranean for the end of the Bronze Age to the beginning of the Iron Age ca. 1200 BC. Hesiod describes his "Race of Bronze" precisely in those terms: "Bronze was their armor, and of bronze their houses, and they worked with bronze; for there used to be no black iron" (Hes. *Op.* 150–151), and it is clear that there was a certain collective social memory of the wars, migrations, and disruptions marking this period (e.g., Finkelberg 2004, 2005, pp. 167–176).

Neither ancient writers nor modern scholars really know what factors or chain of factors triggered the crisis in which whole empires, city-states, international commercial networks, and an entire elite way of life disappeared in the Near East and the Aegean. According to several theories, the economic collapse of an entire international system was caused by social unrest, invasion, natural disasters or probably the combination of all or several of these factors (e.g., Drews 1993; Cline 2014). But Hesiod's story, like that of Atlantis, is a reminder that human societies can collapse, and the more far-reaching and ambitious they are, the harder the fall will be.

Returning to the Near Eastern world, it is perhaps surprising that the Canaanites of the Late Bronze Age did not adopt the Mesopotamian narrative of the Great Deluge, unlike their relatives, the later Hebrews (they might have acquired this mythology in the first millennium, maybe even during their exile in Babylon). Instead, the Canaanites from Ugarit focused their main epic poem on the struggles between their gods, and on the figure of Baal, the storm god. In the *Baal Cycle* or *Baal Epic* (*CAT* 1.1–1.6), composed ca. thirteenth century BC, Baal is struggling to claim his rightful place as the king of the gods, and to that end, he confronts his rivals Mot (Death) and Yam (Sea). The sea, also called "Judge River", is described as a monstrous snake-like creature, "the Serpent, the twisting one, the tyrant with seven heads" (*Baal Cycle*, 3. III, transl. Meier 2018: 181). In other words, Yam is destructive water, typhoons and hurricanes, and flooding rivers, while Baal is the weather god of rain and thunder and tied to the earth (called "Prince, Lord of the Earth"); he needs to defeat the disorderly sea waters in order to consolidate his power (see Ayali-Darshan 2020). In Ugaritic iconography, Baal is represented standing over the waters, represented by two wavy lines, the thicker one perhaps also alluding to the serpentine body of Yam (Wyatt 2018) (Fig. 2.3), much like Ea in Mesopotamia (Fig. 2.2).

Baal's final ordeal, however, even after overpowering Yam/sea, is to defeat death itself, which means dying at the hands of Mot (death) and resuscitating. This reinforces his condition as a fertility divinity of the "dying-and-rising" or the seasonal type who disappears only to return (Mettinger 2001). While myths are not "ancient science" or limited by geographical or meteorological conditions, the *Baal Epic* and other such myths about the victory of storm gods (Marduk, Teshub/Tarhun, Haddad/Adad, Zeus) do transfer to a mythical dimension the acknowledgment of a natural order characterized by the dry and rainy seasons on which the prosperity of urban societies depended in the Levant. This is not a universal theme, but one linked to particular geographies/climates and cultures. Treating Baal or any of these weather gods as being the embodiment of thunder or rain should also be avoided: the Baal Cycle has a lot more to do with the fragility of political order, the consequences of the death of a king, and perhaps also with the disruptions caused by a catastrophe (Wyatt 2017a). It is not uncommon for particular political or geological events to be woven into mythical-cosmic traditions, because of their significance for the identity and cultural memory of a community (e.g., Barber and Barber 2004). In the case of Ugarit, an earthquake and likely tsunami documented archeologically for ca. 1250 BC, and the attested partial reconstruction of Baal's temple at Ugarit at this time by the city's king, may lie behind the particular rendition of the *Baal Cycle* that has come down to us,

Fig. 2.3 Stela from Ugarit (fifteenth–thirteenth centuries BC) with Baal with a mace and a thunderbolt, standing over the waters (drawing by Esther Rodríguez González)

in which Baal is first defeated and humiliated by Yam, and only then is his power restored and his "house" (temple) rebuilt (Wyatt 2017b).

At the same time, these storm gods, after vanquishing the destructive waters, can also be destructive (his enemies' weapons become his own). So in *Enuma Elish*, Marduk grasps "the flood-weapon" and mounts "the frightful, unfaceable storm-chariot" to fight against Tiamat, the ancestral salty water that is trying to destroy him. When challenging her, he reveals the deceitful nature of the sea: "Why are you so friendly on the surface when your depths conspire to muster a battle force?" (*Enuma Elish*, Tablet IV). Even the Hebrew god Yahweh confronts his own marine enemy, Leviathan, who seems to be a version of Yam (Isa 27:1, Ps 74:14, Job 3:8, 4:25), as well as acquiring the qualities of the Canaanite storm god in the Psalms, asserting his power over the sea (Yam) (Ps 74:13–14, Job 7:12, 26:12, 38:8; Ps 29), e.g.:

> *The voice of the Lord is over the waters,*
> *the God of glory thunders,*
> *the Lord, over the mighty waters* (Ps. 29.3, transl. NRSV).

The motif of divine struggle is of course widespread, but this particular version had an influence on how Zeus' last cosmic battle was represented by the Greeks, namely, that between the god and the monster Typhoeus (Typhon) (Fig 2.4), who is depicted as a watery dragon. The clash between these "Titans" is described as a "high-energy event" in which the effects of earthquakes, volcanos, and tsunamis apparently converge:

> *For a fire took hold of the dark-blue sea under the thunder and lightning, under the fire from such a monstrosity of hurricanes and winds and flaming thunderbolt. The entire earth boiled, as did the sky*

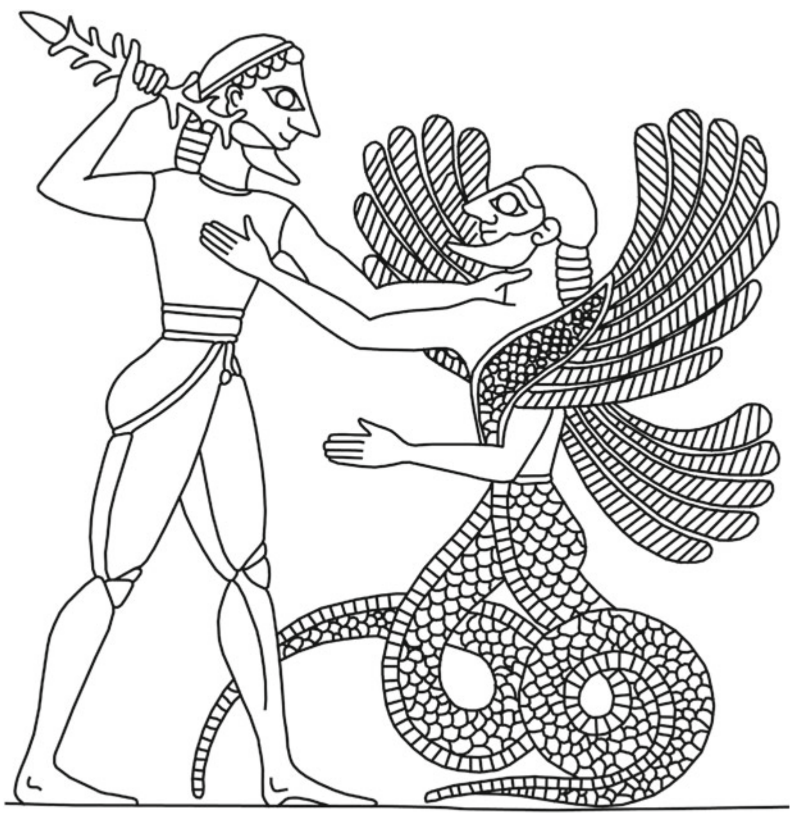

Fig. 2.4 Zeus fighting Typhon, archaic relief on bronze shield from Olympia (Drawing by Esther Rodríguez González)

> *and the sea; tall waves then swelled on both sides of the coast, and all around, under the impetus of the gods, and a ceaseless commotion arose* (Hes. *Theog*. 844–849).

In fact, the Canaanite genealogy of the Greek monster Typhon is practically self-evident: the name Typhon might be a Greek adaptation of Saphon/Zaphon, and the ancient sources establish his abode on Mount Kasios, which is the Mount Saphon (Zaphon/Sapan) of the Ugaritic epic, where Baal established his palace after defeating his enemies. In other sources, the episode occurred to the west, in the volcanic areas of the Gulf of Naples and Sicily (López-Ruiz 2010, pp. 109–113, 2014; Lane Fox 2008, pp. 242–258). Within their own logic and following the tropes of their literary genres, all these stories express anxieties about the natural catastrophes (seismic, maritime, fluvial, volcanic) that marked the lives of ancient Mediterranean peoples.

2.5 Back to Atlantis and the West

Typhon did not apparently reach the far Western Mediterranean, but this *eschaton* of the known world certainly formed part of the mythological imaginary of the ancient Greeks. The Strait of Gibraltar or Pillars of Herakles marked the beginning of "the unknown" for the majority and the perils awaiting them beyond. Thanks to a wide range of testimonies, from Stesichorus and Hesiod to Herodotus and Strabo, among others, we know the far west was a favorite hiding place for epic monsters and dangerously close to the abyss of the Underworld (e.g., for the mythical traditions, Gómez Espelosín 2009; Celestino and López-Ruiz 2016, pp. 96–104; for Atlantic explorations, Roller 2006).

Returning to Plato's Atlantis, we can now better appreciate its multi-layered mythical dimensions: its location at the end of the world in the outer sea; the theme of earthquakes and maritime destruction; the rivalry between gods; and the issue of human hubris and moral corruption. It should also be noted that, at first sight, the Platonic story is more in keeping with the Near Eastern motif of destruction by inundation (cataclysm) than with that of ages brought to an end by war, although, as has been seen, Plato combines both in his myth of Atlantis. The philosopher also resorts to the *topos* of the fantastically rich island, which breeds envy and because of its ambition deserves its comeuppance. Homer made Scheria, the island of the Phaeacians, a utopian place far removed from real geography and forever isolated by the gods (as a punishment for helping Odysseus, Poseidon turned their ship into stone and threw up a mountain around the city: *Od*. 13.130–179). Indeed, ancient historians speculated that, for Homer, the mysterious island was located in the Atlantic (e.g., Strabo, 1.2.18). The idea of a utopian island-kingdom is also the inspiration for Euhemerus of Messene's imagined island (Euhemerus' *Sacred History*, written in the Hellenistic period, of which only fragments are preserved: Winiarczyk 2013). This island, Panchaia, seemingly inspired by Crete, and the utopian island motif are also the basis of Francis Bacon's *New Atlantis* (for these island-utopias, Clay and Purvis 1999). All in all, in this and other of his myths, Plato purposely leverages and fashions a varied universe of themes that do not fit our "Eastern-Western" division of cultures.

Also looking westward, the Israelite prophets decried the Phoenicians' maritime and commercial network and its expansion to Tarshish—which most take as an allusion to Tartessos—in the far west, calling for the island of Tyre's destruction at the hands of the Assyrians (cf. Fig 2.5) (see López-Ruiz 2009; Celestino and López-Ruiz 2016, pp. 110–121; also discussion in Rodríguez-Ramírez et al., this volume):

> Cross over to Tarshish—
> wail, O inhabitants of the coast!
> Is this your exultant city
> whose origin is from days of old,
> whose feet carried her to settle far away? (Isaiah 23: 6–7, NRSV)

Jumping from Tyre to Gadir, its western counterpart (where the story places Atlas' brother), I am of the mind that Plato's Atlantis might not only be alluding to the Athenian empire. Contemporary to it and during Plato's

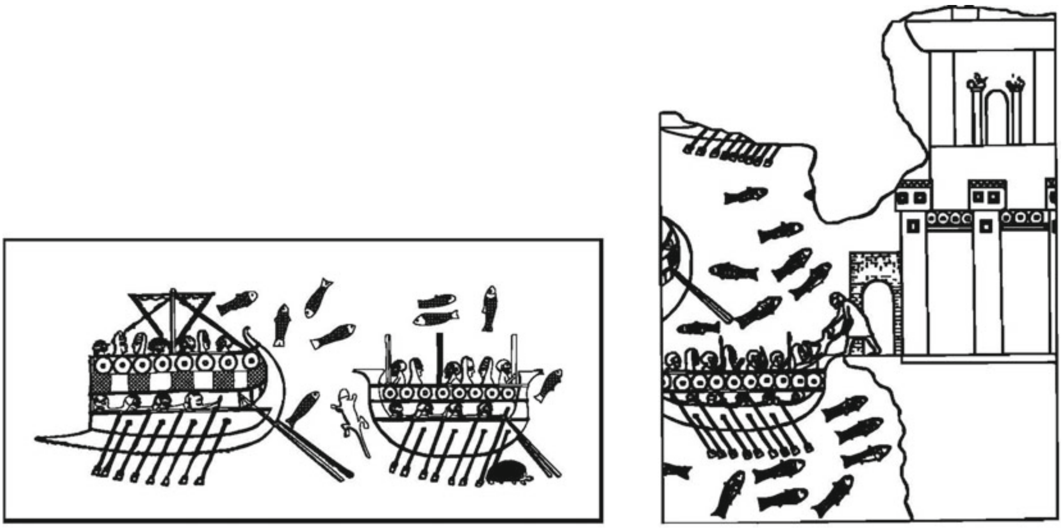

Fig. 2.5 Phoenician ships in flight from Tire, Assyrian relief from the palace of Sennacherib (705-681 BC) (Drawing by Esther Rodríguez González)

lifetime, the Phoenicians' commercial network was tantamount to a mercantile thalassocracy, revolving around the axis formed by Tyre and its colonies, such as Carthage, Gadir/Gadeira, and multiple islands and headlands from east to west. Carthage in particular was a force to be reckoned with. It was in full expansion at the turn of the fourth century BC, in Plato's time, when it was the military rival of the Greek city-states of Sicily, led by Syracuse. To single out a few dates during Plato's life, in 409 BC, the Carthaginians destroyed Selinus; in 405 BC, they retook Himera (a milestone in the Greek victory over the Carthaginians in 480 BC); and also in 405 BC, Dionysius I of Syracuse had to recognize the Carthaginian protectorate in western Sicily; although they lost some political ground in the 390s–80s, they remained strong on the island until the First Punic War (264–241 BC). To contextualize this, it should be recalled that Socrates was sentenced to death and executed in 399 BC and that Plato visited and mentored two rulers of Syracuse (Dion and Dionysus II) in the first half of the fourth century BC (Plutarch's *Lives: Life of Dion*). Carthage's wealth was proverbial among the Greeks (e.g., the Sicilians thought that Carthage had the greatest store of gold and silver in the world: Thuc. 6.34; Hoyos 2019, p. 155). Not only did Plato know a thing or two about the Phoenicians and Carthaginians (e.g., *Resp*. 3.414c, *Leg*. 1.637d, 2.674a–b), but his student Aristotle was also familiar with the constitution of Carthage, which was regarded as one of the most effective at the time, along with that of Sparta (Arist. *Pol*. 2.11 [1272b24–1273b26]). As Carthage absorbed the western Tyrian network after the sixth century BC, its power extended throughout "Libya" (North Africa), east toward Cyrenaica, and west to Atlantic Morocco, with a growing involvement in metal trade with Sardinia and the Etruscans on the Tyrrhenian Sea (for Carthage's expansion and the conflicts in Sicily, Miles 2010, pp. 112–138; Hoyos 2019). Greek historians saw the Carthaginians as rulers over the "Libyans" (Xenophon, *Memorabilia* 2.1.10; cf. Dio Chrysostom, *Orat*. 25.7), while in the ethnographic-geographical tradition of Herodotus those who inhabited Libya/North Africa in the Atlas mountain range were referred to as "Atlantes" (4.184.3–185.1, cf. 3.115). Did Carthage color Plato's Atlantis too?

This suggestion does not by any means bring us back to the issue of the historicity of Atlantis. Not even popular culture has been overly enthusiastic about a Carthaginian "Atlantis," notwithstanding the popularity of the equally fantastic association of the Carthaginians with the early colonization of the Americas in early-modern literature (Fritze 2009, pp. 33, 84–88). Always remaining within the realm of the allegorical, I would like to elaborate on Vidal-Naquet's dichotomic interpretation of the myth (Athens/Atlantis versus Sparta/proto-Athens). By adding the Carthaginian *emporia* as a third element (while others should probably be considered, perhaps even Syracuse itself), I am merely suggesting that other contemporary factors may have had an influence on how Plato represented various types of polities, whose virtues and flaws could turn them into heroic leaders or destructive tyrants.

2.6 Final Remarks

Cataclysmic events formed part of the mythologies of ancient Mediterranean peoples, who lived "around the sea, like ants and frogs around a pond" (Pl. *Phd.* 109B) and who thrived on the opportunities and resources provided by the sea. Myths, however, are not ciphers for real, sporadic events, but form part of belief systems that nourish group identities and transmit cultural capital; sometimes they perpetuate traditions, sometimes they create new messages or lead to new ways of thinking.

The Atlantian cataclysm capturing so much of our attention distracts us from asking why Atlantis sank in the story. Plato barely dedicates a few sentences to the sinking of the Atlantians under the sea and of the "proto-Athenians" under the earth. Instead, he elaborates on the origins and transformation of Atlantian society. At first, "they disdained everything except virtue […], nor did their wealth cause them to lose control of themselves and stumble from being drunk with wantonness…", but as the divine streak in their blood thinned out, and while they still seemed on the surface to be "all-beautiful and blessed", they became corrupt and truly "full of unjust greed and power" (*Criti.* 121a–b).

In the end, Tartessos is not Atlantis, nor can it be. But the two are not totally dissimilar in some ways: each one in its own ontological realm evokes the loss of wealth, the undoing of civilizations; their stories make us think of the fragility of socio-economic systems and the inevitability of historical change. Writing in the spring of 2020, with a viral pandemic coming on the heels of a vertiginous technological boom and the effects of climate change, it is not divine punishment but human behavior we should worry about. The lesson has never been to emulate the lost Atlantis or look for it on a map, but to search for that dangerous "Atlantian" streak in our societies before it is too late.

Acknowledgments This research has been conducted as part of the projects *The Tsunami in the Cultural Representations of the Ancient World: Gadir-Gades and the Gulf of Cádiz as a case study* (HAR2015-66011-P MINECO-FEDER), and *Earthquakes and Tsunamis in the Iberian Peninsula: Social Responses in the longue durée* (PGC2018-093752-B-I00), funded by the Spanish Ministry of Science, Innovation and Universities (MCIU), the Spanish State Research Agency (AEI) and the European Regional Development Fund of the European Union (ERDF, EU). I would like to thank the audience at the conference "Tsunamis históricos en la Península Ibérica" (February 14–15, 2019) for their comments and suggestions, especially Maria Eugenia Aubet and Gonzalo Cruz Andreotti. My thanks also go to Dannu Hutwohl for offering feedback on my draft and Esther Rodríguez González for drawing my figures.

References

Álvarez-Martí-Aguilar M (2017a) La tradición historiográfica sobre catástrofes naturales en la Península Ibérica durante la Antigüedad y el supuesto tsunami del Golfo de Cádiz de 218-209 a.C. Dialogues d'Histoire Ancienne 43(2):117–145

Álvarez-Martí-Aguilar M (2017b) Talismans against Tsunamis: Apollonius of Tyana and the *stelai* of the Herakleion in Gades (*VA* 5.5). Greek Rom Byz Stud 57:968–993

Álvarez-Martí-Aguilar M (2019) El retorno del cataclismo: de la Atlántida a Tarteso. Sánchez Moreno E (coord) Veinticinco estampas de la España antigua cincuenta años después (1967–2017). En torno a la obra de Antonio García y Bellido y su actualización científica. Editorial Universidad de Sevilla, Sevilla, pp 115–129

Anderson M (2018) Athens and Atlantis, from Plato's Timaeus and Kritias. In: López-Ruiz C (ed) Gods, heroes, and monsters: a sourcebook of Greek, Roman, and Near Eastern Myths in Translation. Oxford University Press, Oxford, pp 333–334

Ayali-Darshan N (2020) The storm-god and the sea: the origin, versions, and diffusion of a myth throughout the ancient near east. Mohr Siebeck, Tübingen

Barber EW, Barber PT (2004) When they severed earth from sky. How the Human Mind Shapes Myth. Princeton University Press, Princeton NJ

BNJ Brill's New Jacoby (fragments of ancient historians, editor in chief: Ian Worthington). Brill Online http://referenceworks.brillonline.com/entries/brill-s-new-jacoby

Burkert W (1992) The orientalizing revolution. Near Eastern influence on Greek culture in the early archaic age. Harvard University Press, Cambridge MA

Celestino S, López-Ruiz C (2016) Tartessos and the Phoenicians in Iberia. Oxford University Press, Oxford

Celestino S, Cerrillo E, León A et al (2016) Razones geológicas, arqueológicas y antropológicas para la conservación de Doñana: el Proyecto Hinojos (2005–2013). In: Ferrer M (ed) Doñana: 50 años de investigaciones científicas (Arbor Anejos 11). CSIC, Madrid, pp 81–100

Celestino S, López-Ruiz C (2020) Tarteso y los fenicios de occidente. Almuzara, Córdoba

Celestino S (2014) Tarteso. Viaje a los confines del Mundo Antiguo. Trébede, Madrid

Clay D (2000) Platonic questions: dialogues with the silent philosopher. Pennsylvania State University Press, University Park

Clay D, Purvis A (1999) Four Island Utopias: Being Plato's Atlantis, Euhemeros of Messene's Panchaia, Iamboulos' Island of the Sun, Sir Francis Bacon's New Atlantis. Focus, Newburyport MA

Cline E (2014) 1177 B.C. The year civilization collapsed. Princeton University Press, Princeton and Oxford

Collobert C, Destrée P, Gonzalez FJ (2012) Plato and myths: studies on the use and status of platonic myths. Brill, Leiden

Dalley S (2000) (2nd rev ed) Myths from Mesopotamia: creation, the flood, Gilgamesh, and others. Oxford University Press, Oxford

Darshan G (2013) The Biblical account of the post-diluvian generation (Gen. 9:20–10:32) in the light of the Greek Genealogical literature. Vetus Testamentum 63:515–535

Doak BR (2012) The last of the Rephaim: conquest and cataclysm in the heroic ages of ancient Israel. Ilex Foundation-Center for Hellenic Studies, Cambridge MA

Drews R (1993) The end of the bronze age: changes in warfare and the Catastrophe ca. 1200 BC. Princeton University Press, Princeton

Edmonds RIII (2004) Myths of the underworld journey: Plato, Aristophanes, and the "Orphic" gold tablets. Cambridge University Press, Cambridge

Edmunds L (ed) (2014) (2nd rev ed) Approaches to Greek myth. Johns Hopkins University Press, Baltimore

Finkelberg M (2004) The end of the heroic age in Homer, Hesiod, and the Cycle. Ordia Prima 3:11–24

Finkelberg M (2005) Greeks and pre-Greeks: Aegean prehistory and Greek heroic tradition. Cambridge University Press, Cambridge

Fritze RH (2009) Invented knowledge: false history, fake science and pseudo-religions. Reaktion Books, London

García y Bellido A (1953) La Península Ibérica en los comienzos de su historia. Una invitación al estudio de nuestra Edad Antigua. Instituto "Rodrigo Caro". CSIC, Madrid

García y Bellido A (1963) La Atlántida. Atlántida: Revista del pensamiento actual 1(5):461–475

Giovannini A (1985) Peut-on démythifier l'Atlantide? Mus Helv 42(2):151–156

Gómez Espelosín J (2009) Iberia in the Greek geographical imagination. In: Dietler M, López-Ruiz C (eds) Colonial encounters in ancient Iberia: Phoenician, Greek, and indigenous relations. University of Chicago Press, Chicago, pp 281–29

Graf F (1993) Greek mythology: an introduction. Johns Hopkins University Press, Baltimore

Heiden B (2007) The Muses' uncanny lies: Hesiod, Theogony 27 and its translators. Am J Philol 128:153–175

Hoyos D (2019) Classical-Hellenistic Carthage before the Punic Wars (479–265 BC). In: López-Ruiz C, Doak BR (eds) Oxford handbook of the Phoenician and Punic Mediterranean. Oxford University Press, Oxford and New York, pp 155–168

Johnston SI (2018) The story of myth. Harvard University Press, Cambridge MA

Kühne RW (2004) A location for 'Atlantis? Antiquity online 78(300) http://antiquity.ac.uk/projgall/kuhne/

Lane Fox R (2008) Travelling heroes: Greeks and their myths in the epic age of Homer. Alfred A. Knopf, London

López-Ruiz C (2009) Tarshish and Tartessos revisited: textual problems and historical implications. In: Dietler M, López-Ruiz C (eds) Colonial encounters in ancient Iberia: Phoenician, Greek, and indigenous relations. The University of Chicago Press, Chicago, pp 255–280

López-Ruiz C (2010) When the gods were born: Greek cosmogonies and the Near East. Harvard University Press, Cambridge MA

López-Ruiz C (2014) Greek and Canaanite mythologies: Zeus, Baal, and their rivals. Relig Compass 8(1):1–10

López-Ruiz C (2018) Gods, heroes, and monsters: a sourcebook of Greek, Roman, and Near Eastern Myths in translation, 2nd rev edn. Oxford University Press, Oxford

Meier S (2018) Ugaritic epic poems. In: López-Ruiz C (ed) Gods, heroes, and monsters: a sourcebook of Greek, Roman, and Near Eastern Myths in Translation. Oxford University Press, Oxford, pp 176–199

Mettinger T (2001) The riddle of resurrection: dying and rising gods in the Ancient Near East. Coniectanea Biblica, Almqvist and Wiksell, Stockholm

Miles R (2010) Carthage must be destroyed: the rise and fall of an ancient civilization. Penguin, London and New York

Miller FJ (1921) Ovid, Metamorphoses. Loeb Classical Library, Harvard University Press, Cambridge MA and London

Osuna M, Bedia J and Domínguez AM (2000) El santuario protohistórico hallado en la calle Méndez Núñez (Huelva). In: P Cabrera P and Santos M (eds) Ceràmiques jònies d'època arcaica: centres de producció i comercialització al Mediterrani occidental. Museu d'Arqueologia de Catalunya, Barcelona, pp 177–188

Papadopoulos GA, Gràcia E, Urgeles R et al (2014) Historical and pre-historical tsunamis in the Mediterranean and its connected seas: geological signatures, generation mechanisms and coastal impacts. Marine Geol 354:81–109

PMG Page DL (ed) (1962) Poetae melici graeci. Oxford University Press, Oxford

Rodríguez González E (2017) Tarteso versus la Atlántida: un debate que trasciende al mito. ArqueoWeb 18:15–30

Roller DR (2006) Through the Pillars of Herakles: Greco-Roman exploration of the Atlantic. Routledge, New York and London

Schulten A (1927) Tartessos und Atlantis. Petermanns Geograph Mitteilungen 73:284–288

Scodel R (1982) The Achaean wall and the myth of destruction. Harv Stud Class Philol 86:33–50

Vidal-Naquet P (1986) The black hunter: forms of thought and forms of society in the Greek world. Johns Hopkins University Press, Baltimore

Vidal-Naquet P (1992) Atlantis and the nations. Crit Inq 18(2):300–326

West ML (1997) The east face of Helicon: West Asiatic elements in Greek poetry and myth. Oxford University Press, Oxford

West ML (2003) Greek Epic Fragments. Harvard University Press, Cambridge MA, Loeb Classical Library

Winiarczyk M (2013) The "Sacred History" of Euhemerus of Messene. De Gruyter, Munich and Leipzig

Wyatt N (2017a) The Problem of "Dying and Rising" Gods: The Case of Baal. Ugarit-Forschungen 48:819–845

Wyatt N (2017b) National memory, seismic activity at Ras Shamra and the composition of the Ugaritic Baal Cycle. Ugarit-Forschungen 48:551–591

Wyatt N (2018) The Baal au Foudre stela and its Historical Context. Ugarit-Forschungen 49:429–437

3 Earthquakes and Tsunamis in Ancient Iberia: The Historical Sources

Manuel Álvarez-Martí-Aguilar

Abstract

According to recent Portuguese and Spanish seismic catalogues, a remarkable number of earthquakes and tsunamis were recorded in the Iberian Peninsula during Antiquity. They list earthquakes and tsunamis in 218–209 BC (Gulf of Cadiz); 60 BC (Galicia and Portugal); 365 AD (Southern Spain); and 382 AD (Cape St. Vincent, Portugal). In this chapter, the origin of these and other references to ancient earthquakes and tsunamis in the Iberian Peninsula is identified and their literary and historiographical contexts are analysed in order to assess their historicity. Most of this information is provided by two chroniclers: the Spanish historian Florián de Ocampo (ca. 1495–ca. 1558) and the Portuguese chronicler Bernardo de Brito (1569–1617). The historicity of most of the literature on ancient earthquakes and tsunamis in the Iberian Peninsula is very dubious, when not totally lacking credibility. However, sometimes, and especially in the case of Ocampo's references to the ancient city of Cadiz, the information may reflect the collective memory of catastrophic events that occurred at a still undetermined moment in the past.

Keywords

Florián de Ocampo · Bernardo de Brito · Spain · Portugal · Earthquakes · Tsunamis

3.1 Introduction

Research on the nature and reliability of the historical sources on earthquakes and tsunamis in the Iberian Peninsula before 1755 has progressed by leaps and bounds in recent years (Udías 2015, 2020; Ces 2015; Álvarez-Martí-Aguilar 2017a, b, 2020; Silva 2019). However, it has primarily focused on assessing the soundness of the data recorded in the foremost earthquake catalogues in Portugal (Oliveira 1986; Martins and Mendes 2001) and Spain (Galbis 1932, 1940; Martínez-Solares and Mezcua 2002). This approach has neither allowed for an adequate understanding of the context in which these accounts originated over time, nor of the authors or works from which this information ultimately recorded in such catalogues was retrieved.

This calls for a comprehensive review of the historical accounts of seismic events, identifying their provenance and evaluating their historicity in the context of the period in question and the circumstances in which they were produced,

M. Álvarez-Martí-Aguilar (✉)
Department of Historical Sciences, University of Malaga, Campus de Teatinos s/n. 29071, Malaga, Spain
e-mail: m_alvarez@uma.es

M. Álvarez-Martí-Aguilar and F. Machuca Prieto (eds.), *Historical Earthquakes, Tsunamis and Archaeology in the Iberian Peninsula*, Natural Science in Archaeology,
https://doi.org/10.1007/978-981-19-1979-4_3

something of capital importance, as will be seen, in the case of Renaissance and modern accounts. The aim of this chapter is, therefore, to examine the historical reports on earthquakes and tsunamis occurring in ancient Iberia. Antiquity is a period especially in need of review, due to the fact that some of the historical tsunamis purportedly affecting the Iberian Peninsula before 1755, such as that of Cadiz in 218–209 BC or those on the Portuguese coasts in 60 BC and 382 AD, have been precisely dated to that historical period (Galbis 1932; Campos 1992; Rodríguez-Vidal et al. 2011; Silva et al. 2015).

3.2 The Ancient and Mediaeval Literary Sources

The references to earthquakes and tsunamis in ancient Iberia in classical sources are very scarce and, in some cases, particularly problematic. The first of the few testimonies that have come down to us are the Athenian philosopher Plato's (ca. 427–347 BC) famous references to Atlantis sinking deep into the ocean after an earthquake in his dialogues *Timaeus* and *Critias*.

Few ancient themes have produced such a tremendous amount of literature as Plato's Atlantis, a subject specifically broached by Carolina-López Ruiz in Chap. 2 of this book. Nonetheless, it should be recalled that the legend of Atlantis—which is only mentioned by Plato in the classical literature—is essentially just that: a myth with a philosophical and political purpose. Notwithstanding the fact that it contains references to geographical features characteristic of the far west, the Platonic account is not a faithful rendering of a specific historical reality. Plato located his imaginary island/continent beyond the Pillars of Heracles, in the outer ocean, facing the region of *Gadeira*. The two passages of the dialogues *Timaeus* and *Critias* in which Gadir and the seismic events that put an end to Atlantis are mentioned, read as follows:

> *But at a later time there occurred portentous earthquakes and floods, and one grievous day and night befell them, when the whole body of your warriors was swallowed up by the earth, and the island of Atlantis in like manner was swallowed up by the sea and vanished; wherefore also the ocean at that spot has now become impassable and unsearchable, being blocked up by the shoal mud which the island created as it settled down* (Pl. *Ti.*, 24e–25d; transl. Lamb 1925).
>
> *It was stated that this city of ours was in command of the one side and fought through the whole of the war, and in command of the other side were the kings of the island of Atlantis, which we said was an island larger than Libya and Asia once upon a time, but now lies sunk by earthquakes and has created a barrier of impassable mud which prevents those who are sailing out from here to the ocean beyond from proceeding further […]. And the name of his younger twin-brother, who had for his portion the extremity of the island near the pillars of Heracles up to the part of the country now called Gadeira after the name of that region, was Eumelus in Greek, but in the native tongue Gadeirus,—which fact may have given its title to the country* (Pl. *Criti.*, 108e–114b; transl. Lamb 1925).

The reference to the ancient Phoenician city of Gadir—in Greek, Gadeira—founded by Tyrian colonists in the ninth century BC, forms part of a small kernel of historical elements around which Plato elaborated his literary fiction. As Udías (2020) has recently proposed, these elements may also refer to a cataclysmic event on the Atlantic coast of the Iberian Peninsula, in the vicinity of Gadir. The context in which this event is framed only allows for considering the possibility that Plato received, in a more or less direct fashion, information relating to the collective memory of some type of marine seismic event occurring in the vicinity of the Straits of Gibraltar and Gadir, before the mid-fourth century BC, when he wrote his dialogues.

The next account of an earthquake in ancient Iberia is a brief reference in a text transmitted as part of Aristotle's oeuvre and known, in its Latin translation, as the *De mirabilibus auscultationibus*. This work, the author of which definitely was not Aristotle, is a compilation divided into 178 sections devoted to diverse topics, pertaining by and large to the natural world and whose common denominator is their wondrous character, thus being a good example of paradoxography (Pajón 2008). Section 87 contains one of the scant references to earthquakes in ancient Iberia:

> *In Iberia they say that, when the coppices were set on fire by certain shepherds, and the earth was heated by the wood, the country visibly flowed with silver; and when, after some time, earthquakes succeeded, and the ground in different places burst asunder, a large quantity of silver was collected, which brought in no ordinary revenue to the Massilians* (*Mir. ausc*., 87; transl. Dowdall 1909).

The main core of the *De mirabilibus auscultationibus* has been dated to the mid- or late third century BC (Pajón 2008), while the presence of Greeks from the city of Massalia (present-day Marseille) in the northeast of the Iberian Peninsula, has been documented as from the beginning of the sixth century BC. In turn, the mention of the enrichment of the Massilians might refer to their most direct scope of influence on the Iberian Peninsula, namely, the area surrounding the Greek city of Emporion (present-day Ampurias), founded in the first quarter of the sixth century BC. As this account is shrouded in myth, however, it is currently impossible to pinpoint either the place or the date.

To assess the historical value of this account, it should be seen in conjunction with the description of the fire breaking out before the earthquake and which, unlike the latter, is indeed recorded in other ancient sources. One such source is Poseidonius of Apamea (ca. 135–51 BC), who visited southern Iberia at the end of the second century BC. The Syrian polymath mentions this legendary fire in an excursus on the rich mines of Turdetania, the area to the south and southwest of ancient Iberia (Posid., fr. 239 Edelstein-Kidd; *apud* Strabo 3.2.9). On the other hand, it has been suggested that Poseidonius might have borrowed this information from the Sicilian historian Timaeus of Tauromenium (ca. 356–260 BC), of whose work only fragments have survived. Then again, the fire raging in certain Iberian forests is mentioned by Diodorus Siculus (ca. 90–30 BC) who, unlike Poseidonius, places it in the Pyrenees, while also associating it with the arrival—in this case—of the Phoenicians in Spain:

> *And since they [the Pyrenees] contain many thick and deep forests, in Ancient times, we are told, certain herdsmen left a fire and the whole area of the mountains was entirely consumed; and due to this fire, since it raged continuously day after day, the surface of the earth was also burned and the mountains, because of what had taken place, were called the Pyrenees; furthermore, the surface of the burned land ran with much silver and, since the elementary substance out of which the silver is worked was melted down, there were formed many streams of pure silver. Now the natives were ignorant of the use of the silver, and the Phoenicians, as they pursued their commercial enterprises and learned of what had taken place, purchased the silver in exchange for other wares of little if any worth* (Diod. Sic., 5.35; transl. Oldfather 1939).

The fire's location in the Pyrenees is owing to the similarity of the root of the place name—Greek Πυρήνη or Πυρηναῖα, Latin *Pyrenaei*—to the Greek word for fire—Greek πῦρ, Latin *pyr*. This homonymy is the reason why in his account Diodorus sets a legendary event in this Iberian mountain chain, which, nonetheless, for other classical authors occurred elsewhere. The legend of burning forests that produced rivers of molten silver is, for instance, documented in the work of Athenaeus (6.233 E), for whom the legendary event occurred in the Alps. All these different traditions are adaptations of a theory put forward by Lucretius (5.1251–1261) (99–44 BC), but perhaps ultimately attributable to Democritus (ca. 460–370 BC), who attempts to find an explanation for the presence of precious metals in the foothills of the mountains, attributing this to the effect of a fire (Gómez Espelosín 2007, p. 184).

Notwithstanding the imaginative attempts to relate the legendary fire in the Pyrenees to the volcanic eruptions occurring in the area 9000 years before (Silva 2019), Diodorus' account should be taken as a legend. While establishing the exact place and date of the earthquakes mentioned in the *De mirabilibus auscultationibus*, beyond relating them to the initial stages of the Massalian presence on the peninsula's northeast coast, as from the end of the sixth century BC, should be recognised as an impossible task.

The information contained in one of the extant fragments of Sallust's *Histories* (86–ca. 35 BC), refers to a catastrophic event in *Corduba* (Cordova) during Quintus Caecilius Metellus Pius' governorship of the *provincia* of *Hispania Ulterior*, coinciding with the Sertorian War (79–72 BC):

> *But, while Metellus wintered with two legions, due to coincidence or, as the wise hold, to the winds blowing inside the earth's cavities, some mountains and hills crumbled and fell* (Sall. *Hist*., 2.28).

Despite the passage's succinctness, this information deserves credit and, even more so, when relating it to a poem that Lucius Annaeus Seneca (4 BC–65 AD) dedicated to his hometown of Corduba. The philosopher bewails the tragedies befalling the city, including an event that caused 300 casualties in one night:

> *Not even at that time when, O!, three hundred funerals*
> *you suffered in one night which was the most dire for you* (Sen. *De se ad patriam*, 8–9).

It can be reasonably assumed that Seneca is describing the effects of an earthquake and, consequently, there might be a connection here with Sallust's account (Knapp 1983, p. 17).

Plato's dialogues, the *De mirabilibus auscultationibus*, and Sallust's *Histories* contain the only explicit information on seismic events in ancient Iberia deriving from the classical literature, prior to the news contained in the *Chronicle* of Hydatius (ca. 400–ca. 469 AD), concerning the occurrence of earthquakes in *Gallaecia* in 451 and 454 AD (Hydat. *Chron*., 149, 159). In recent research, however, it has been suggested that a certain passage in the epic poem *Punica* by Silius Italicus (25/26–101 AD) might refer to a tsunami. It describes the Carthaginian general Hannibal's visit to the temple of the Phoenician god Melqart—associated with the Greek Heracles and the Roman Hercules—in Gadir in 219 BC, for the purpose of fulfilling his vows after conquering the Iberian city of Saguntum and before setting out for Italy to wage the Second Punic War:

> *When Hannibal's eyes were sated with the picture of all that valour, he saw next a marvellous sight the sea suddenly flung upon the land with the mass of the rising deep, and no encircling shores, and the fields inundated by the invading waters. For, where Nereus rolls forth from his blue caverns and churns up the waters of Neptune from the bottom, the sea rushes forward in flood, and Ocean, opening his hidden springs, rushes on with furious waves. Then the water, as if stirred to the depths by the fierce trident, strives to cover the land with the swollen sea. But soon the water turns and glides back with ebbing tide; and then the ships, robbed of the sea, are stranded, and the sailors, lying on their benches, await the waters' return. It is the Moon that stirs this realm of wandering Cymothoe and troubles the deep; the Moon, driving her chariot through the sky, draws the sea this way and that, and Tethys follows with ebb and flow* (Sil. *Pun*., 3.45–60; transl. Duff 1927).

Gómez et al. (2015, pp. 69–70) and Arruda (this volume) have suggested that this passage might be referring to a tsunami, the same event that, as will be seen further on, the chronicler Florián de Ocampo establishes in Cadiz at around the same time. Nevertheless, Silius' description seems to refer clearly to a king tide, a phenomenon for which Gadir was famous in Antiquity (Manolaraki 2010), and which attracted the curiosity of people such as Poseidonius of Apamea himself at the end of the second century BC.

Explicit accounts of earthquakes associated with tsunamis in ancient Iberia do not reappear in the literature until many centuries later, with the publication of Ocampo's work. However, in the Arab literature, there are two accounts of sea floods in Cadiz, which just might stem from the collective memory of ancient seismic events.

The first of these accounts is to be found in the work of the Arab geographer Mohammed Ibn Abu Bakr Al-Zuhri (fl. 1130 s–1150 s), the author of the *Kitab al-Jaghrafiyya* (*Book of Geography*). Al-Zuhri came from Granada, in Al-Andalus, a city close to Cadiz, the place in which the narrated events take place:

> *Let us return to Cadiz and how it was levelled: in the city there was the 'house of the Tunas' [Dar al-Tunn], on the banks of the great cistern, with a gate through which a branch of the river passed. It was under an enchantment [tilasm] that attracted the tunas during the month of May. But the wife of King Sant Batar told her husband, 'If you opened a gate at the foot of this hill, two branches would enter the river from the sea; our river would be even larger and fish and tunas would enter it from the sea.' To this he replied, 'I will do no such thing because I do not want our country to be divided.' She then ordered engineers and workers to open the entrance through which ships and vessels [qawarib] now pass between Rota and Cadiz; but*

> *when the waters entered and joined the river called 'Guadalete', they rose until practically covering the bridge, engulfing the city of Cadiz and submerging it. For this reason, only a small island remained*. (Bramon 1991, pp. 162–163, my translation from original in Spanish).

The end of this passage might point to an ancient seismic marine event in Cadiz, whose scale and date are impossible to establish. Sant Batar, the name of the king featuring in the account, is apparently related to the name of the place Sancti Petri, which gives its name to a stream located to the south of the archipelago of Cadiz and to the small island in whose vicinity it is believed that the aforementioned Temple of Heracles-Melqart in Gadir must have been located.

Information similar to that provided by Al-Zuhri can be found in a passage of the work by the Egyptian Ibn Zanbal, who served at the court of the Mamluk sultan of Egypt (r. 906–922/1501–16). In a brief reference, recorded by E. Fagnan, Ibn Zanbal also alludes to a sea flood that engulfed Cadiz:

> *Located to the south of Seville, the city of Cadiz, where there was a famous lighthouse, was engulfed, along with its farms, by the sea. This flood was caused by the invasion of salty waves* (Fagnan 1924, pp. 138–139, my translation from original in French).

Although lacking a chronological context, this information, in addition to Al-Zuhri's reference, reveals that the collective memory of a sea flood of catastrophic proportions still prevailed in the city of Cadiz during the Islamic period, at least since the twelfth century. This is especially telling owing to the relevance that, as will be seen in the following section, Cadiz has in the accounts of natural catastrophes that Ocampo includes in his work.

3.3 Florián de Ocampo and the *Crónica General de España*

Florián de Ocampo (ca. 1499–ca. 1558) is the original source for most of the accounts of earthquakes and tsunamis in ancient Iberia. He was the official chronicler of Charles V and the author of an ambitious national history entitled, *Crónica General de España*, of which he only managed to complete the part dedicated to the country's origins up until the time of the Second Punic War (218–206 BC). The first four books of this work were published in 1543 (Fig. 3.1), before being republished with the fifth book in 1553 (Fig. 3.2). Before publishing his own *Crónica*, Ocampo (1541) had supervised an edition of the *Estoria de España* written between 1270–1274 at the behest of Alfonso X the Wise, from which he would draw much of his material.

In his *Crónica General de España*, Ocampo attempts to offer a continuous account of the country's origins, the most complicated to address because of the dearth of sources. To this end, he not only resorts to classical and mediaeval sources—such as the abovementioned *Estoria de España*—but also to notorious fabulists. This is the case of the Italian Dominican Giovanni Nanni—known as Annius of Viterbo—who in his *Commentaria super opera auctorum diversorum de antiquitatibus loquentium* (Nanni 1498) attributes a veritable string of bogus works to the Babylonian priest Berossus, an author living in the third century BC whose original oeuvre has been lost. These feature a mythical genealogy of ancient Spanish kings, starting with Tubal, the son of Japheth and grandson of Noah, which Ocampo includes in his *Crónica*.

In order to understand the role played by natural catastrophes in Ocampo's work, it is worth starting its analysis with a passage in which an attempt has been made to identify the collective memory of ancient earthquakes (Silva 2019), but actually reveals the mythical nature of the descriptions of ancient cataclysms contained therein. The passage in question is to be found in the chapter dealing with the peninsula's alleged depopulation, due to a calamitous 26-year-long drought occurring after the death of King Abidis, the last of the primitive Hispanic monarchs, in 1071 BC:

> *And it came to pass that it started to become very hot and dry, without a drop of rain for twenty-six years. This is recalled by our Spanish historians […] claiming that, due to such a long period without any rain, it became uncommonly hot, to the point that there was not a fountain or river in*

LOs quatro libros primeros de la Cro=
nica general de España que recopila el mae=
stro Florian do canpo criado y cronista del
Emperador Rey nuestro señor por man=
dado de su magestad çesarea.

En çamora. Año. M.D.xliii.

Fig. 3.1 Title page of Florián de Ocampo, *Los quatro libros primeros de la Cronica General de España* (1543) (*Source* Biblioteca Nacional de España—Biblioteca Digital Hispánica, BDH)

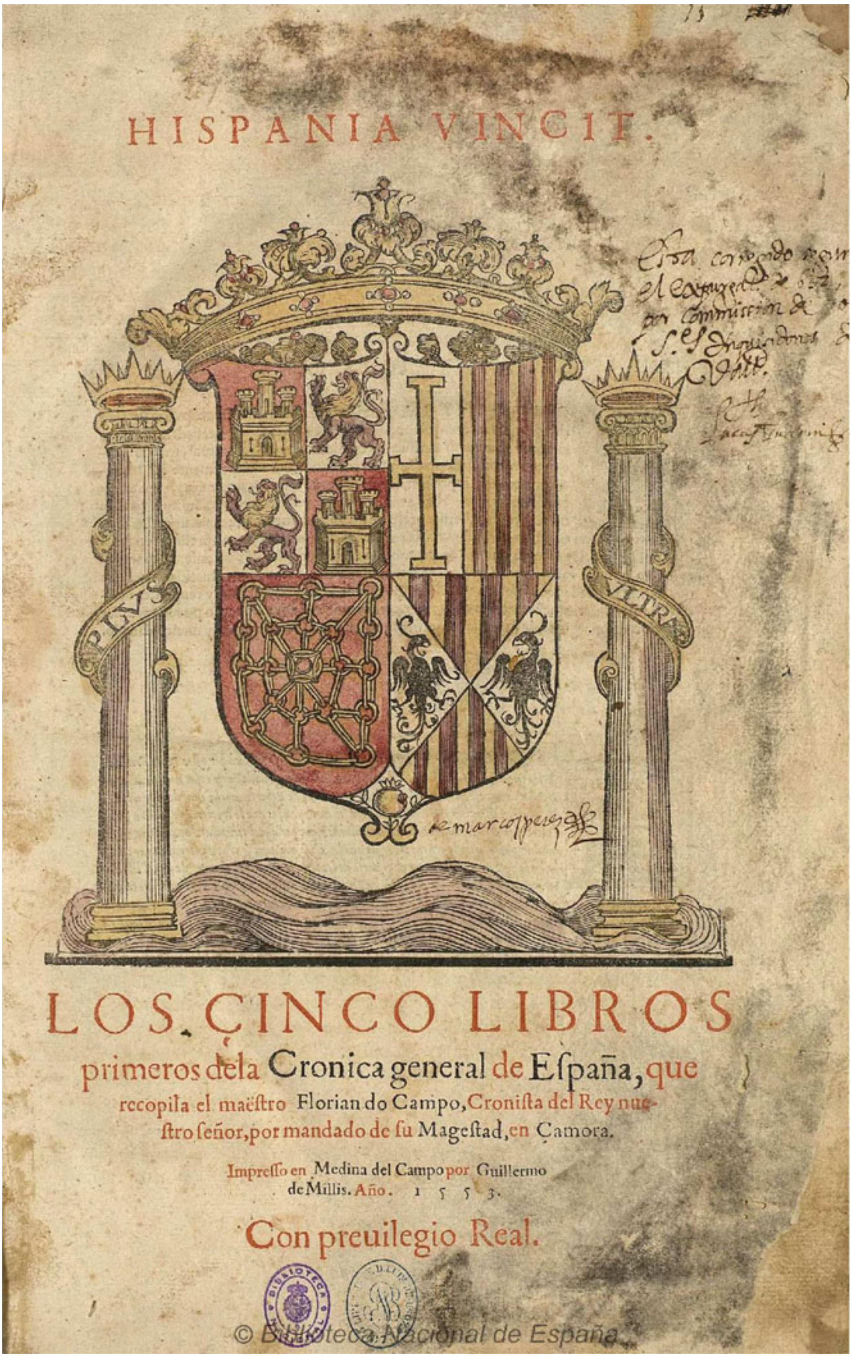

Fig. 3.2 Title page of Florián de Ocampo, *Los cinco libros primeros de la Cronica general de España* (1553) (*Source* Biblioteca Nacional de España—Biblioteca Digital Hispánica, BDH)

Spain that did not dry up, except for the Ebro and the Guadalquivir, whose waters were very low. In addition, the earth was split asunder in many places, resulting in huge crevices and fissures, which caused very many people much misery. Consequently, it was impossible to walk and men were unable to escape or find refuge … (Ocampo 1553, pp. 78r–78v, my translation from original in Spanish; see Álvarez-Martí-Aguilar 2020 for the original texts of Ocampo).

This passage plays an important role in the *Crónica*, for the 'great drought' in Spain is associated with the extinction of the primitive Hispanic monarchy and, as a consequence, the peninsula's virtual depopulation. The precedent of Ocampo's account is to be found in the *Estoria de España* commissioned by Alfonso X, which describes a 26-year-long drought that forced the population to flee beyond the Pyrenees. This period of drought culminated in extraordinarily strong winds that swept away the dry trees, reducing them to dust, followed by a three-year deluge, 'to the point that the land was covered with water, as if it were the sea' (*de guisa que toda la tierra era cubierta de agua que semeiaua mar*). In the wake of this string of catastrophes, the Iberian Peninsula was repopulated by the emigrants (Ocampo 1541, p. 11; Menéndez Pidal 1906, p. 14).

For his account, Ocampo clearly drew inspiration from the *Estoria de España*, while introducing new elements, products of his own imagination, such as the appearance of 'crevices and fissures' which prevented the people living inland far from the sea from fleeing from the devastation. All these factors leading to the peninsula's depopulation are evidently the stuff of myth and, at any rate, cannot be reasonably interpreted as the result of a specific seismic event (cf. Silva 2019).

Ocampo dates the first explicit reference to an earthquake in Iberia to 500 BC. His source—which he does not cite—is the passage in the *De mirabilibus auscultationibus* (87) describing the wildfires, the earthquakes producing rivers of molten silver and their exploitation by the Massilians. On the basis of this concise information, Ocampo weaves a baroque narrative:

During that age, there were arduous and painful times in Spain, with death and famine, because the land produced little food owing to the lack of rain. Particularly during the last years of this period, five hundred years before the birth of the Lord our God, when in addition to the aforementioned adversities, major earthquakes affected all of the seacoast, where they tend to be more frequent than in other places, as asserted by the natural philosophers. And those tremors were so terrible that many houses and walls collapsed in the villages, and many rivers changed their course. Towering mountains and hills were displaced by the force of the movement that flung them from their original place. Large crevices appeared in the earth close to the coast, from some of which flowed new fountains and streams of asphalt and much water never seen before. These crevices featured a mouth that appeared close to the place where, centuries before, the famous fires of the Pyrenees mountains had raged, when because of their intensity large torrents of silver and metals flowed abundantly. It is said that these torrents engulfed much of the land, while others seeped into the interior veins and channels, for which reason it seems that part of the molten silver pooled in a certain cavity in one of these mountains. Once the fires had ceased, this silver solidified in the deepest recesses of the mountains, covered with earth. But, as the earthquakes of that year were, as it was alleged, terrible and continuous, they opened up certain areas of those mountains and, thus exposed, revealed huge mounds of silver (…). At that time, the ships of Massalia frequented the Spanish coasts, doing business to which the peoples living in seaports are accustomed and trading in merchandise. And as a result, they found themselves close to where this silver had been discovered, approached the place and, after performing their verifications and taking samples of the metal, understood that it was silver in great quantities. Thus, they collected much of it […]. Apparently, all this was supposed to have happened in the direction of the Cape of Creus, the Cape of Crosses, in our Mediterranean sea, where the Pyrenees Mountains terminate, the place in which the majority of historians say that the ancient fires raged. This might also have happened towards the mountains of Denia or of Muxácra, which many cosmographers and chroniclers call the Pyrenees and which we know are abundant in metals. In contrast, we do not believe that this occurred in more distant lands, in Andalusia, since the Carthaginians were so well established there that no one could visit that region or carry away anything for their own profit … (Ocampo 1553, p. 137r–137v, my translation from original in Spanish).

Ocampo's mystification is clever, combining two different information sources. On the one hand, he employs the information on fires and earthquakes—without any precise location—appearing in the *De mirabilibus auscultationibus*, while mentioning how the Massilians benefited most from the rivers of solidified silver. On the other hand, he resorts to information on the great fire in the Pyrenees narrated by Diodorus Siculus, in which it is the Phoenicians who exploit the windfall. This combination allows him to suggest that the earthquakes not only occurred on the eastern edge of the Pyrenees, in Creus (Girona)—but, stretching the imagination, also in Denia (Alicante). The date—500 BC—and the place that, according to Ocampo, the earthquakes occurred are speculations that depend on when the Massilians first arrived on the peninsula (Álvarez-Martí-Aguilar 2020).

The next news of natural disasters in Ocampo's Crónica encompasses a three-year period, starting in 349 BC, with floods in the first year, earthquakes in the second and sea storms in the third:

> *The following three years* [after 350 BC] *are better known in the Spanish chronicles. The first* [349 BC] *was notable for its heavy rains, which terrified men since they were so abundant and continuous. The rivers swelled in all of our regions, drowning livestock and people and wreaking havoc in the countryside and the villages that the floodwaters reached. In the second year* [348 BC] *there were terrible earthquakes in most of the coastal areas of our Mediterranean sea, where these tremors occur naturally and more frequently than in other places in Spain. In particular, they affected primarily the city of Saguntum or Monvedre, damage to which, as it was the most powerful and richest coastal city at the time, had graver consequences than that to any other city. The following year* [347 BC] *the seas were so rough and tempestuous that many ships, both Spanish and those of other foreign nations, sank off the coast due to tempests never seen before, while other ships were driven ashore between the stretch of coast between the Pyrenees mountains and the Straits of Gibraltar. And the storms drove ships from very safe ports and wrecked them, the people being powerless to avoid it …* (Ocampo 1553, p. 182r, my translation from original in Spanish).

Ocampo does not mention the sources from which this amazing description of a chain of natural disasters might have derived and, unlike in the previous case, the ancient sources remain silent on this point. The improbability of three consecutive years marked by remarkable catastrophes of such a distinct nature only underscores its fictitiousness.

With the cataclysm that struck Cadiz in 241 BC, Ocampo recounts a sequence of four events relating to natural catastrophes, all occurring in the second half of the third century BC, whose common denominator is the Phoenician city or its vicinity. The chronicler offers a description of the first of these events in the chapter devoted to the end of the First Punic War (264–241 BC):

> *There are also some chronicles which indicate that it was a year* [241 BC] *characterised by the lack of rain in different regions of Spain. Because of this, the pastures dried up and many cattle and people perished. Sea storms were more frequent and violent than in previous years; and close to Cadiz the earth roared and part of the inland was flooded, while there were terrible manifestations and portents that struck terror into the hearts of the people living in all the neighbouring lands ...* (Ocampo 1553, p. 216r, my translation from original in Spanish).

Ocampo does not identify those chronicles (*memorias*) in which these catastrophic events were supposedly narrated, and there are no references in this regard in the classical literature. The allusion to an earthquake in the vicinity of Cadiz and to the flooding of part of the island vaguely recalls the Platonic account of Atlantis, while bearing some resemblance to Al-Zuhri's description of the legendary flood engulfing Cadiz—although the Andalusi author does not record any earthquake.

The next cataclysm in Ocampo's *Crónica* also occurred in Cadiz, where there would have been an earthquake and a sea flood in the year that Hannibal's expedition set out for Italy, which the chronicler dates—erroneously—to 216 BC:

> *As to conditions that year* [216 BC], *the two Julians claim that, judging by the accounts to be found in certain Spanish chronicles, it is known that there was an abundance of food and products*

> *of the land, but not so as regards people's health, with plagues and diverse maladies in some Spanish provinces. The island of Cadiz and the entire coast of Andalusia were shaken by major earthquakes or tremors that destroyed buildings and killed people, and wreaked terrible havoc there. The sea flooded many areas that were first exposed and expelled many fish, both common and known and those never seen before. Armed hosts were heard in the air, without knowing from where the din came, all being signs and portents of the dismay and woes that came to pass shortly afterwards, with the wars and savagery that commenced there …* (Ocampo 1553, p. 262v, my translation from original in Spanish).

As observed above, Hannibal's expedition set out for Italy in 218 BC. It should be noted that Ocampo is always two or three years out with respect to the real chronology of developments during the Second Punic War. In any case, the description of the earthquake and, above all, the effects of the tsunami are extraordinarily plausible. This is so because they feature elements included time and again in ancient and modern descriptions of cataclysms of this sort, such as the retreating sea and the subsequent flooding, the expulsion of known and unknown species of fish and strange sounds, like cannon fire or the din of a battle (Martínez–Solares 2001, pp. 55–56).

Nor does Ocampo explicitly refer to his sources on this occasion, and those that he does mention at the beginning of the passage, the 'two Julians', should be given little credence (Rodríguez-Ramírez et al. 2016; Álvarez-Martí-Aguilar 2017a, 2020). These two authors are cited in the prologue to his *Crónica*, among other sources, which include several authors, both Graeco-Latin and mediaeval. Specifically, these dubious authors receive a mention following the reference to the *Crónica* of Isidore of Seville (ca. 560–636):

> *A certain Julian, who some identify with the archbishop of Toledo, and who was known by the alias of 'Pomerio', continued writing an excellent history of Spain from the time of King Wamba* [630–688] *onwards. But when listing the books written by Julian, along with their titles and topics, Don Felix, who was also the bishop of Toledo, does not include that volume, or chronicle, but only that describing the rebellion of certain knights, instigated by another of their number called Paul, against Wamba, the king of the Goths, as will be seen in book seventeen of the second part.* (Ocampo 1553, p. 4v, my translation from original in Spanish).

Ocampo refers to a 'chronicle of Spain' supposedly written by a certain Julian, who some have identified with his namesake, the archbishop of Toledo (644–690), who indeed authored the *Historia rebellionis Pauli adversus Wambam Gothorum regem*, which records Paul's attempted rebellion against King Wamba in 673 AD. However, on the list of works by Julian that his successor and biographer the bishop Felix of Toledo includes in his *Vita sancti Iuliani*, the other reputed chronicle is not mentioned, as Ocampo himself admits.

Ocampo's reference to Julian of Toledo's sobriquet of 'Pomerio' only complicates matters even further. For Julian Pomerio was a presbyter in Gaul, who died in around 490 AD, and the author of two books—the dialogue *De animæ natura* and the treatise *De vita contemplativa*—who was occasionally mistaken for Julian of Toledo, living two centuries later, a blunder that Ocampo also makes. Either way, nor is Julian Pomerio known to have produced a history of Spain.

The information that Ocampo provides is confusing and seemingly implies that the 'chronicle of Spain', covering events from the time of King Wamba, was the work of a certain Julian, who was not his namesake, the archbishop of Toledo, but, nonetheless, is sometimes held to be one and the same. Be that as it may, nothing is known about this alleged chronicle. The second of the 'two Julians' cited by Ocampo is even more vexing:

> *After the aforesaid Julian, another Julian, a deacon also of Toledo, a resident of that same city, but of Greek provenance, as he himself appears to admit at the beginning of his chronicle, resumed the account of the history of Spain. In this work, before addressing contemporary matters, he offers a brief summary of many ancient events occurring in Spain, being apparently well-versed in this subject and an expert in the writings and knowledge of his Greek compatriots. Following this, he recounts the endeavours and victories of the saintly king Don Pelayo* [reigning from 718 to 737], *in whose time he alleges to have lived, when those African Arabs and Moors arrived, which we have already noted above*. (Ocampo 1553, pp. 4v–5r, my translation from original in Spanish).

In his chronicle, Ocampo draws repeatedly from the purportedly bona fide information provided by this author. Nevertheless, there is not a single mention of this Julian the Deacon in the Spanish historiographical tradition that does not depend on Ocampo's account. Very early on, it was considered that this spurious author had been invented by the chronicler. Ambrosio de Morales, who was commissioned to resume the *Crónica General de España* after Ocampo's death, expresses in the work's prologue the conviction that the chronicle of Julian the Deacon never existed:

> *In the prologue* [to his *Crónica*], *Florián de Ocampo says that he possessed a history of these times, the work of a certain Julian of Thessalonica, who prospered in Toledo at the time, and who was the deacon of its holy church. All that I can say about this matter is that many of Florián's friends asked him to show them that book, which he never did, nor has it appeared afterwards and, in contrast, I found many indications in his documents that the book had never existed* (Morales 1586, p. 14v, my translation from original in Spanish).

The testimony of Ambrosio de Morales confirms that Julian the Deacon was a figment of Ocampo's imagination. Inventing fake sources was not infrequent in the historiography of the period. Proof of this is Annius of Viterbo's Berosus Chaldaeus or, as will be seen in the following section, the brace of fictitious authors invented by the Portuguese chronicler Bernardo de Brito. Returning to the Cadiz earthquake and tsunami, even though Ocampo does not explicitly claim that the information comes from 'the two Julians', the narrative suggests that the account is endorsed by the authority of these sources, which casts plenty of doubt on its historicity.

As observed in the previous section, there are no ancient sources from which Ocampo could have obtained his information. Nevertheless, there are two literary passages from which he might have drawn inspiration. On the one hand, the passage in Silius' *Punica* describing the king tide observed by Hannibal in the Heracleion of Gades in 219 BC. And, on the other hand, the earthquake in 217 BC, which, according to ancient tradition, occurred during the Battle of Lake Trasimene, in Italy (Guidoboni 1994: 143–145). In both cases, they can only be indirect references, and everything seems to indicate that the description of the cataclysm that struck Cadiz in 218 BC is also a product of Ocampo's fancy.

Regarding the events that Ocampo dates to 211 BC, he yet again alludes to extraordinary occurrences, including strange sounds, earthquakes and perturbations at sea. Under the heading 'wonders in Spain' (*prodigios en España*), he has the following to say:

> *The army's rank and file spoke of ghosts and signs, which, according to them, they had heard in the air, similar to the sounds made by armed people and battles, in different place for days on end. Some said that they* [those sounds] *had been heard in the Pyrenees mountains, while others said in Andalusia, and there were people who claimed to have seen and felt them, recounting these things in detail and as they saw fit. There was also news of earthquakes and perturbations in Africa, great movements in the sky and sea tempests, in forms and manners never seen or known before* (Ocampo 1553, p. 306r, my translation from original in Spanish).

This episode resembles the description of the event in 218 BC in relation to the 'signs' and sounds of armed people and battles, heard in the Pyrenees and Andalusia, which implicitly refers to seismic events. However, Ocampo only explicitly mentions earthquakes in Africa. In the part of his *Crónica* including this episode, he directly follows the account offered by Livy (59 BC–17 AD) in his *Ab Urbe Condita*. The subsequent occurrences are based on events described by Livy (24.41.7–11), which correspond to 214 BC, and not to 211 BC (Álvarez-Martí-Aguilar 2017a), although the Roman historian does not mention any earthquakes in Iberia or Africa in those years.

The last of the cataclysms described by Ocampo would have come to pass yet again in Cadiz in around 210 BC:

> *We know that those were prosperous times, the land produced food in abundance, the people and cattle enjoyed good health, except for the inhabitants of Cadiz, who suffered several earthquakes, and the sea was tempestuous for many days on end, with strong storm surges and currents, penetrating beyond their customary limits. In the air,*

> *there were signs just as terrible as in previous years. Flaming comets were seen in the western confines of the sky: dangerous lightning bolts struck inhabited places. Some mare mules foaled and two howling wolves approached the chamber of the Scipios and, after biting people and beasts and other things in their way, departed unscathed by the men assembled there* … (Ocampo 1553, p. 323r, my translation from original in Spanish).

Immediately before this passage there is a reference to events based as before on Livy (24.49.7–8) and which actually correspond to 213 BC, and not to 210 BC (Álvarez-Martí-Aguilar 2017a). Nor in this case, does Livy mention a similar episode in Gades. To recreate this passage, Ocampo borrows different portents from the Roman historian and combines them in an original way. Comets, lightning bolts and foaling mare mules are commonplace in the Roman author's oeuvre, but the episode involving the wolves, in particular, is inspired by a scene relating to the run-up to the Battle of Ticinus, which took place precisely in 218 BCE:

> *On the Roman side there was far less alacrity, for, besides other things, they were also frightened by some recent portents: a wolf had entered the camp and after rending those whom it met, had itself escaped unharmed* (Liv., 21.46.1–3; transl. Foster 1929).

Livy, drawing from the ancient priestly annals, often documents the yearly tally of prodigies—*prodigia*—occurrences regarded as extraordinary or ominous, occurring in Rome and Italy, which were supposed to be expiated through the performance of adequate rites at the beginning of the year (Rasmussen 2003). It should come as no surprise that the examples provided by Livy were especially abundant during the Hannibalic War, a period that caused much collective anxiety in Rome. Wolves frequently feature in these *prodigia* in Livy's oeuvre, the case in which one such animal enters a city or a military camp having been documented on twenty occasions (Trinquier 2004, p. 94; Lewis and Llewellyn-Jones 2018, p. 360).

The news of the cataclysm in Cadiz is a good example of how Ocampo puts together fictitious accounts, freely combining portents appearing in Livy with news of earthquakes and sea floods in Iberia, specifically in Cadiz, which are not mentioned by the Roman historian. Livy's huge influence on Ocampo's work could explain why the chronicler establishes most of the cataclysms to which he refers in the Second Punic War (Álvarez-Martí-Aguilar 2017a).

The seismic events narrated by Ocampo are not addressed independently by any other subsequent author. All the references to these episodes are taken—explicitly or implicitly—from his *Crónica*. This is the case of Esteban de Garibay's *Los Quarenta libros del Compendio Historial* (1571) and Juan de Mariana's *Historia General de España* (1601), whose information, which was considered to be original, subsequently found its way into modern seismic catalogues (Álvarez-Martí-Aguilar 2020). The account of a cataclysm in Cadiz at the end of the First Punic War, offered by Mariana, serves as an example:

> *This year* [in which the war ended] *was unfortunate for Spain, owing to the drought and the lack of water and because of the earth tremors, as a result of which it is held that the island of Cadiz was split asunder and sank into the sea* (Mariana 1601, p. 79, my translation from original in Spanish).

The absence of independent references to the catastrophic events described by Ocampo in the country's historiographic tradition is the ultimate proof of their more than questionable historicity. In any event, it is convenient to assess Ocampo's information in relation to that of the Portuguese chronicler Bernardo de Brito.

3.4 Bernardo de Brito and the *Monarchia Lusytana*

Bernardo de Brito (1569–1617) is, together with Ocampo, the source from which the historical literature on earthquakes and tsunamis in ancient Iberia draws most. Brito, a Cistercian monk belonging to the Alcobaça Monastery, was the chronicler of the Cistercian Order as of 1606 and of the kingdom of Portugal as of 1614. Unlike Ocampo, he managed to complete a history of Portugal up until the time of Henry Count of

Portugal (Henry of Burgundy 1066–1112), which was published in two volumes under the title of *Monarchia Lusytana* (Brito 1597, 1609; Da Silva 1973) (Figs. 3.3 and 3.4).

As with Ocampo, Brito was faced with the difficult challenge of fleshing out the historical origins of a country, in this case, Portugal. When undertaking this task, he resorted to a host of spurious sources, but, nonetheless, broached the subject in a singular fashion. In his *Monarchia*, he constantly refers to a number of hitherto unheard of works, which he claims to have discovered in the library of the Alcobaça Monastery. Aware of the suspicions that this would raise, he requested two authorities—including the monastery's abbot—to bear witness to their existence in the library (Brito 1597, pp. 5v–6v). Thanks to these reports, we have a description of those dubious sources, prominent among which, because of their relationship with natural catastrophes occurring in Portugal, are Laymundo Ortega and Pedro Aladio.

Laymundo is doubtless Brito's most relevant source in the work as a whole. According to Brito's witnesses, he would be the author of a work written in 878 AD, entitled, *De antiquitatibus Lusytanorum*, containing 11 books. In the prologue to his *Monarchia Lusytana*, the Cistercian records how he discovered this manuscript:

> *… among other things, I discovered a notable antiquity, which my diligence and work recovered from oblivion. It was a very ancient book, written in Gothic script on thick and rough parchment, by a Portuguese man called Laymundo Ortega: in which he describes Lusitania in ancient times and addresses very clearly the truth of things that were known in the times in which he lived …* (Brito 1597, p. 4v, my translation from original in Portuguese; see Álvarez-Martí-Aguilar 2020 for the original texts of Brito).

Besides Laymundo's work, another of the main sources that Brito employs is Pedro Aladio, the alleged author of two treatises on the way of life of the ancient Portuguese people, written in 1234. To these should be added characters such as a certain Mestre Menegaldo, the author of a general history of the world, written in 1236, a certain 'Jew Zacuto', the author of a book on the climate of Portugal, and Mendo Gómez, the author of a 'memoire of ancient things' of the kingdom (Álvarez-Martí-Aguilar 2017b, p. 189).

Later on, in the seventeenth century, critical scholars like Nicolás Antonio, in his posthumous *Bibliotheca Hispana Vetus* (Antonio 1696, pp. 331–336), brought to light the apocryphal character of authors like Julian the Deacon and Laymundo Ortega. As already observed, the use of fake historical sources was not unusual in the Renaissance historiography of the peninsula, a phenomenon that would become more pronounced in the Baroque period, with the proliferation of specious works, known as 'falsos cronicones' ('false cronicons') (Godoy Alcántara 1868). Nonetheless, Brito's work is exceptional due to the quantity of spurious sources that it contains. It is no coincidence that in both Ocampo's and Brito's works, the accounts of ancient cataclysms in the Iberian Peninsula are systematically associated with such sources.

As noted above, Brito does not mention any of the natural catastrophes appearing in Ocampo's *Crónica*, despite the fact that it would not have been difficult to associate the alleged cataclysms affecting the island of Cadiz—datable to 241, 216 and 210 BC—with the Portuguese coast. In contrast, he documents an earthquake in Portugal, also in 216 BC, but in relation to the one occurring during the Battle of Lake Trasimene—which actually took place the year before.

This earthquake is included in an account of several consecutive calamities. The first was the 'most terrible plague that swept across Spain', as a result of which Hannibal's wife and son perished. The second catastrophe, in the following year, commenced with widespread fog that resulted in a devastating famine in the coastal areas of Portugal, from which only those living in the mountains escaped (Brito 1597, pp. 166r–166v). The source that Brito cites before recounting this string of natural disasters is none other than Laymundo Ortega, on whose testimony he apparently bases his account of the third consecutive disaster:

MONARCHIA LVSYTANA

Composta por Frey Bernardo de Brito, Chronista geral & Religioso da ordem de S. Bernardo, professo no Real mosteiro de Alcobaça.

PARTE PRIMEIRA

que contem as histotias de Portugal desde a criação do mundo te o nacimento de nosso snõr IESV CHRISTO

DONEC IMPLEAT

BERNARDVS DOCTOR INCLITVS

DIRIGIDA AO CATHOLICO REI DO PHILIPPE II DO NOME REI DE ESPANHA EMPERADOR DO NOVO MVNDO

Impressa no Insigne mosteiro de Alcobaca por mandado do R.mo Padre Geral Frey Francisco de S. clara com licenca & priuilegio Real

Anno de 1597

Fig. 3.3 Title page of Bernardo de Brito, *Monarchia Lusytana* (1597) (*Source* Biblioteca Nacional de Portugal—Biblioteca Nacional Digital, BND)

SEGVNDA
PARTE
DA MONARCHIA
LVSYTANA.

Em que ſe continuão as hiſtorias de Portugal deſde o nacimento de noſſo Saluador IESV Chriſto, ate ſer dado em dote ao Conde dom Henrique.

Dirigida ao Catholico Rey dom Phelippe, ſegundo do nome em Portugal, & terceiro em Caſtella, ſenhor d'Eſpanha, Emperador do nouo mundo.

E compoſta por ſeu mandado, pello Doutor Frey Bernardo de Britto Chroniſta gèral, & monge da Ordem de São Bernardo.

Impreſſa em Lisboa no Moſteiro de São Bernardo, com licença & Priuilegio Real. Por Pedro Crasbeeck. Anno Dñi 1609.

Fig. 3.4 Title page of Bernardo de Brito, *Segunda parte da Monarchia Lusytana* … (1609) (*Source* Biblioteca Nacional de Portugal—Biblioteca Nacional Digital, BND)

> *Those exhalations were followed by powerful earth tremors, not only in Portugal but also in most of Europe. As a result of being drawn into the depths of the earth, and being followed by a great calm and heat—as Aristotle teaches—it caused the earth tremor which was felt in Italy, where it destroyed many cities on the same day as Hannibal won the Battle of Trasimene, as Titus Livy recorded …* (Brito 1597, p. 166v, my translation from original in Portuguese).

Brito is referring to the earthquake that, according to Livy and Pliny, among other authors, occurred during the Battle of Lake Trasimene in 217 BC (Guidoboni 1994, pp. 143–145). The chronicler resorts to the earthquake theory proposed by Aristotle (*Mete*. 365a–369a) in order to point to certain pervasive sea fogs and exhalations on the Portuguese coast as the cause of the earthquake in the western reaches of the Iberian Peninsula, whose effect was also felt as far away as the area around Lake Trasimene in Central Italy. The 'Portuguese version' of this earthquake is the first of many attempts that Brito makes to 'universalise' historical earthquakes with epicentres far from the Iberian Peninsula in order to relate them to Portugal. Despite the closeness of the dates of Ocampo's cataclysm in Cadiz in 216 BC [218 BC] and Brito's earthquake in 216 BC [217 BC], there does not seem to be any connection between the two, beyond the influence of Livius' work.

The first of the accounts in which Brito explicitly describes an earthquake associated with sea floods in Portugal refers to events that he dates to around 63 BC:

> *At around that time, or a few years before, there was a notable earth tremor on the coasts of Portugal and Galicia, which destroyed many places and killed so many people that the rest (as if beside themselves) fled from the villages to the hills, parents leaving behind their children and husbands abandoning their wives, all believing that they had been very fortunate to save their own lives, without having preserved those of others. And the sea, surpassing its ordinary limits in some places, covered much of the land where it had never shown signs of reaching, while leaving it exposed in other parts. Aladio refers to many other freak occurrences during those years, which I will not go into because they seem to me to be very special for such an ancient time, given that otherwise everything that this author writes adds up and appears to me to be very true …* (Brito 1597, 316r–316v, my translation from original in Portuguese).

Brito's account, based on the purported testimony of Pedro Aladio, continues with the birth of a monstrous hybrid creature off Cape St. Vincent, a tall story that vaguely recalls the Roman narrative of prodigies or portents. Neither is there any ancient source from which Brito could have borrowed this account, nor is it possible to draw parallels between this alleged earthquake and tsunami on the Atlantic coasts of Portugal and Galicia in around 63 BC and the information that Sallust provides on an earthquake in Cordova in the 70 s BC (Knapp 1983, p. 17).

The next earthquake appearing in Brito's *Monarchia Lusytana* occurred when Publius Cornelius Lentulus Spinther was governor of Hispania Citerior in 59 BC, which the chronicler dates erroneously to 55 BC (Brito 1597, p. 334r):

> *Laimundo states that, around the same time, the inhabitants of the Luna mountains suffered major earth tremors, which were so sudden and intense that, abandoning the places in which they lived, they travelled abroad, where they were neither in danger nor feared that the mountains and hills, collapsing with the tremor, would harm them …* (Brito 1597, 334v, my translation from original in Portuguese).

Brito is apparently referring to the Luna Mountain mentioned by the Greek geographer Claudius Ptolemy (100–ca. 170 AD) (*Geogr*., 2.5.4), located in the vicinity of the mouth of the river Tagus, but as before there is no such news of this seismic event in the ancient sources. As could not be otherwise, his source is Laymundo Ortega, implying that this episode's historicity should also be ruled out.

Brito includes a new catastrophic event in the chapter devoted to Caesar's victory over Pompey's legates in Hispania and to the activities of Marcus Varro in Lusitania, which he also dates incorrectly to 47 BC (Brito 1597, p. 345r). In this same year, according to Pedro Aladio, the Portuguese coast would have been hit by sea floods:

> *Aladio says that, at around this time, the coast of Portugal was hit by such extraordinary and adverse sea floods that many coastal villages were levelled. And the people, as if lost, fled to the hills*

to save their lives. There followed heavy rains and earth tremors, to the point that the world seemed to collapse under the weight of summer (Brito 1597, p. 351v, my translation from original in Portuguese).

In Brito's account, the events running up to these catastrophes actually correspond to 49 BC, the year in which the civil war between Caesar and Pompey broke out, when, according to Cassius Dio (41.14.3), there were frequent earthquakes, among other portents. But the description of the event, attributed to Pedro Aladio, is clearly different and is not inspired by Dio. Moreover, Brito's account is striking because of the strange succession of catastrophes: the sea floods are followed by heavy rain and earth tremors. Nor in this case is there any news of this cataclysm in the ancient sources, for which reason this episode is clearly a fabrication.

Brito includes a vague reference to an earthquake in Portugal and Spain in 33 AD or, better said, the effects of the famous earthquake that, according to tradition, occurred in Judea at the death of Christ in the Iberian Peninsula:

So, returning to the Empire and the life of Tiberius Caesar, Paulus Orosius and Eutropius record that in the sixteenth year of his reign, in March, the world was shaken by a universal earthquake, accompanied by such an extraordinary eclipse of the sun that there was not one sage (there being many great ones at the time) who could explain such a new form of opposition, such as that between the sun and the moon at that moment. It was all due to the general sentiment that nature showed when its creator and our Saviour Jesus Christ died, as narrated in the Holy Gospel. I thought it proper to recall this here because it was such a remarkable thing that it was even perceived in these parts of Portugal and Spain (where, according to Laymundus, there were rocks that had been split asunder by this earthquake), as well as in Asia and Judea, where its cause was to be found ... (Brito 1609, p. 8r, my translation from original in Portuguese).

The provenance of this news of the earthquake occurring when Christ died is to be found, as Brito himself records, in Matthew (27.51–52.). Besides this biblical source, Brito mentions Orosius, who includes this episode in his *Historiae adversus paganos* (7.4.13). However, there is no such mention in Eutropius. Brito exploits the references to the 'universal' character of the earthquake in Orosius' work to introduce the testimony of Laymundo as regards the existence of evidence—'rocks that had been split asunder'—of that earthquake. Indeed, Brito had a penchant for associating famous earthquakes in distant places with Portugal. As with the earthquake in Lake Trasimene in 217 BC, he also does this with the earthquake and tsunami in 365 AD. All this reveals that, as before, the information that he provides has no historical basis whatsoever.

Brito's last description of the impact of an extreme marine event on the coasts of the Iberian Peninsula appears in a convoluted passage, whose interpretation has given rise to confusion owing, among other things, to the year to which he dates it. After recounting the death of the Roman Emperor Valens, which he mistakenly establishes in 382 AD—four years later than the correct date of 378 AD—Brito reviews the historical facts known in Portugal with respect to the reigns of the Emperors Valentinian and Valens, concluding his account with a 'universal earthquake':

The things that happened in Portugal in the time of those two emperors [Valentinian I and Valens] *have been buried by the silence of authors who, occupied with the developments in the Empire, disregarded everything else. The only thing that can be read is that a certain captain called Venusto was the vicarius of the Empire in Spain in the time of Julian, and through Paulus Orosius and others we know that there was a universal earthquake that destroyed many cities; and the sea, abandoning its natural flow, flooded some formerly inhabited lands and left others hitherto navigable exposed* (Brito 1609, p. 124v, my translation from original in Portuguese).

Brito alleges that the earthquake and sea flood occurred during the reigns of Valentinian I and Valens—namely, between 364 and 375/378 AD. The context allows us to conjecture that the chronicler is referring to the famous earthquake in the Central and Eastern Mediterranean in 365 AD (Jacques and Bousquet 1984; Guidoboni 1994, pp. 267–274). However, the date 382 AD appears in the margin of the page, in reference to the year to which Brito wrongly dates the death of the Emperor Valens (Brito 1609, p. 124v). Many subsequent authors have believed that 382 AD is the year to which Brito dates the earthquake (Moreira de Mendonça 1758, p. 26; Galbis 1932, p. 7; Oliveira 1986, p. 133; Baptista and Miranda 2009, p. 26), when in fact he does not mention any specific date for this event.

In spite of the fact that Ammianus Marcellinus (26.10.15–19) is the source offering the most comprehensive description of the effects of the earthquake and tsunami in 365 AD, Brito does not mention this historian in relation to the cataclysm, but to certain facts pertaining to the history of Portugal at the time, specifically, the appointment of Venusto as the vicarius in Hispania during the reign of the Emperor Julian (Amm. Marc. 23.1.4.). Paulus Orosius is the only ancient source that Brito mentions when referring to the 'universal earthquake', but he does not seem to rely on this author (Oros. *Hist*., 7.32.5) for his description of the effects of the cataclysm in 365 AD. In order to address the repercussions of this 'universal earthquake' for Portugal, Brito resorts yet again to the testimony of Laymundo Ortega who, according to him, elaborates on the words of a certain 'monk Eutropius':

> *Laymundo pays considerable attention to this sea flood, practically reproducing, word for word, the description provided by the monk Eutropius and elaborating on it:* Non solum id per Siciliam, Græciam, et Palestinam, sed per multas Hispaniæ oras continentem subuertit, antiquas insulas sub egit, nouas rupes monstrauit diruta vndique terra, quæ visuntur vel iuxta, vel intra Occeanum, præcipuè ad sacrum Promontorium, quo antiquæ insulæ parua vestigia remansere, et discurrente Occeano in septentrionem. *Practically saying that the earthquake not only caused damage in Sicily, Greece and Palestine, but also on the coasts of Spain the sea floods also submerged some parts of the mainland and covered some islands that had been inhabited in ancient times. Only a few rocks, exposed by the sea, remained of these islands, which can be seen close to land or in the ocean, principally off Cape St Vincent, where there are a few small indications of a certain ancient island, plus others on the same coast of the ocean further to the north ...* (Brito 1609, p. 124v, my translation from original in Portuguese).

Contrary to what has been assumed (cf. Andrade et al. 2016), the 'monk Eutropius', mentioned by Brito, whose words were supposedly elaborated on by Laymundo Ortega, is not Flavius Eutropius, a pagan historian who appeared in around 360 AD and whose *Breviarium Historiae Romanae* covers Roman history only up until the accession of the Emperor Valens in 364 AD. Brito is actually referring to Paulus Diaconus, known as Paul the Deacon (ca. 720–ca. 799 AD), the author of the *Historia Romana*, in which he resumes the narrative of Eutropius' *Breviarium*, extending it to 522 AD. During the Middle Ages, both works, Eutropius' and Paulus', were published together, which led to the latter being known as the 'monk' Eutropius to distinguish him from the former.

Paul the Deacon, drawing inspiration from the *Chronicon* of Jerome (244c), refers briefly to the terrible consequences that the 'universal' earthquake in 365 AD had for the cities of Sicily and other islands:

> *Around this time, an earthquake occurred all over the earth, the sea came out of the coast to the point that the cities of Sicily and many islands, shaken and collapsed, killed countless people with the ruins* (Paul. Diac. *HR*, 11.2; Guidoboni et al. 2008, p. 508).

Brito inserts the words of Laymundo into those of Paul the Deacon for a purpose that becomes clearer as he develops his argument: to explain the disappearance of a certain island called 'Erytheia' off the Portuguese coast. The passage continues as follows:

> *From whose words we can surmise that in this destruction the ancient and noted island of Erytheia, of which we have already spoken in the first part of this work and which, according to Pomponius Mela, was located off the coast of Lusitania, disappeared* (Brito 1609, p. 124v, my translation from original in Portuguese).

Erytheia or Eritia is an ancient place name deriving from the Greek mythical-geographical tradition, associated with the tenth labour of Heracles, viz. the theft of Geryon's cattle. It was located in the legendary far west and was gradually associated with the island of Gades (Cadiz) and, more specifically, with one of the islands of its ancient archipelago, the smallest, according to Pliny (*HN*, 4.120). However, Pliny himself (*HN*, 4.120) and other authors, such as Pomponius Mela (*Chor*. 3.47.), mention the existence of an island going by the same name off the coast of Lusitania.

In the first part of his *Monarchia Lusytana*, Brito (1597, pp. 19v–20r) capitalises on these testimonies to assert that this Portuguese Erytheia is older than its Spanish counterpart, located in Cadiz. Faced with the problem of the ancient island's uncertain location, Brito resorts to the reefs off Cape St Vincent and the 'universal earthquake' in 365 AD to explain the disappearance of the Portuguese Erytheia. As a whole, Brito's speculations are based on the testimony of the bogus Laymundo, for which reason the possibility that the famous cataclysm occurring in the Eastern Mediterranean in 365 AD affected the Portuguese coasts either in this year or in 382 AD should be completely dismissed.

The diagnosis of the historical value of Brito's accounts of natural catastrophes in ancient Iberia is as adverse as that of Ocampo's, although in the case of the Portuguese chronicler, the invention of sources and fictitious episodes is even more bizarre. As in the case of five of the six accounts of natural catastrophes in Ocampo's work, nor are those mentioned by Brito addressed individually by subsequent authors, among other reasons because no one else made use of Laymundo Ortega's or Pedro Aladio's alleged works.

3.5 Some Subsequent Accounts

The information provided by Ocampo and Brito forms the greater part of the historical literature on earthquakes and tsunamis in ancient Iberia, which subsequently made its way into the foremost Spanish and Portuguese earthquake catalogues in the twentieth century, including those compiled by Galbis (1932, 1940), Oliveira (1986) and Martínez-Solares and Mezcua-Rodríguez (2002) (Álvarez-Martí-Aguilar 2020). Nevertheless, there are a number of independent accounts of catastrophic events in ancient Iberia in the works of subsequent authors, also with no historical value whatsoever.

This is the case of the information provided by the Portuguese author Manuel de Faria y Sousa (1590–1649) in his *Europa Portuguesa*, which was published posthumously in Lisbon between 1678 and 1680 (Fig. 3.5). On the one hand, Faria reproduces Brito's account of the earthquake on the Portuguese and Galician coasts in 63 BC (Faria 1678, p. 203), but without citing him—which has led Udías (2015, 2020) to believe that Faria was the original source.

On the other hand, Faria, who does not refer to any other natural disaster described by Brito, comes up with one of his own inventions. This reference is to be found in the account of the building of a temple on the Sacred Promontory, to wit, in Cape St. Vincent, by Hercules. As in the case of Brito, it is an attempt to transfer legendary elements associated with ancient Gades to Portugal. This temple of Hercules in Portuguese territory would presumably have been destroyed by an earthquake in around 1299 BC, if Faria is to be believed:

> *They* [the Portuguese] *were satisfied with their resolve and way of life when something that produced much sorrow came to pass* […]. *This was the unexpected destruction of Libyan Hercules' celebrated temple. For with the shattering of the harmony of the earth and the subsequent major earthquake, it completely collapsed* … (Faria 1678, p. 63, my translation from original in Portuguese).

Faria's account finds no echo in the ancient sources and is, therefore, a blatant invention that fortunately has not been included in modern seismic catalogues. In contrast, some catalogues do indeed record a unique piece of information that is just as implausible. In 1810, Francisco Tavares published a work on the characteristics and properties of the mineral waters of Portugal, paying special attention to the locality of Caldas. When referring to the lack of information on the earthquakes devastating Lisbon over the ages, he includes a footnote that reads as follows:

> *Besides the two most ancient general earthquakes which can be remembered, in 377 and 370 BC, as well as similar ones occurring in 1009, 1117, 1146, 1183 and 1290 AD, Lisbon has suffered many earthquakes, some of which reduced it to*

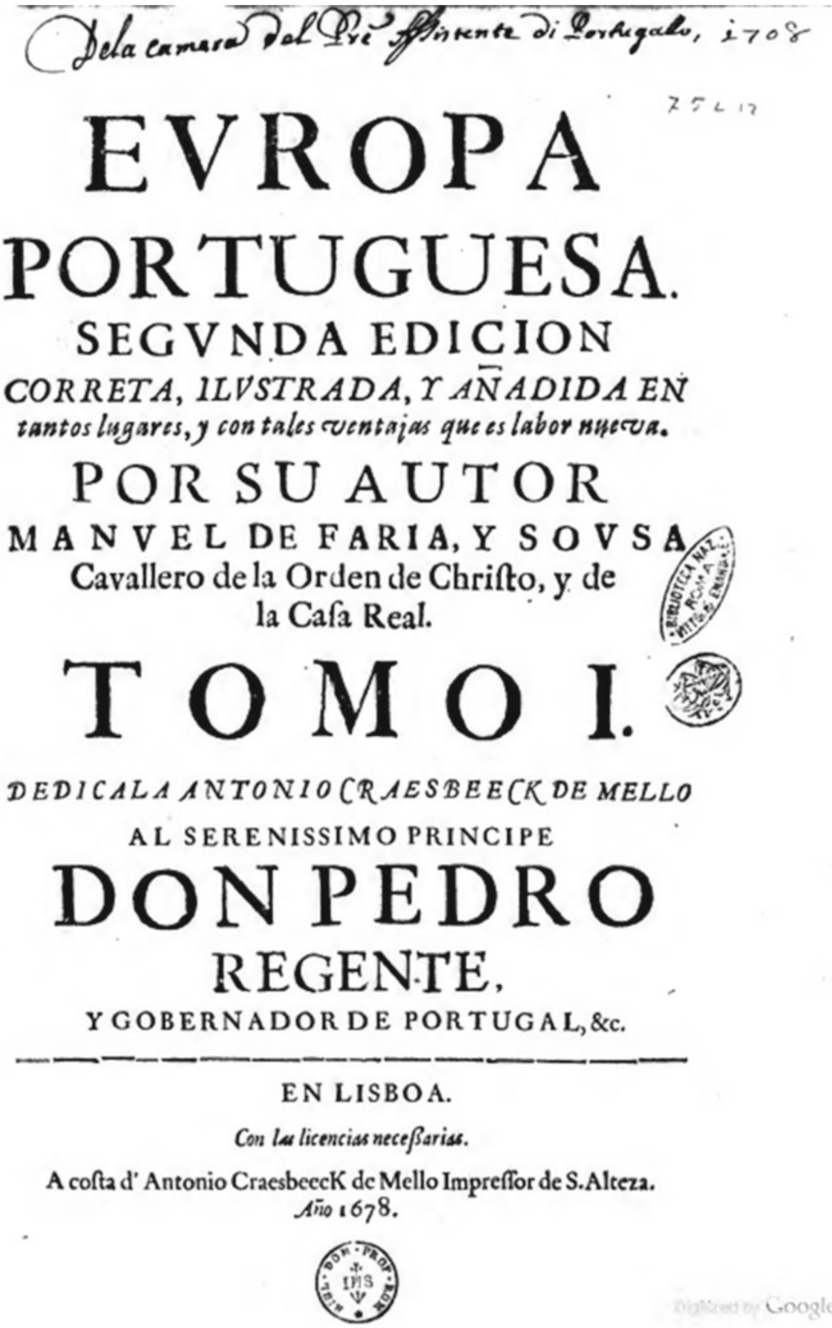
Dela camara del Pre Assistente di Portugalo, 1708

EVROPA
PORTUGUESA.
SEGVNDA EDICION
CORRETA, ILVSTRADA, Y AÑADIDA EN
tantos lugares, y con tales ventajas que es labor nueva.
POR SU AUTOR
MANVEL DE FARIA, Y SOVSA
Cavallero de la Orden de Christo, y de
la Casa Real.
TOMO I.
DEDICALA ANTONIO CRAESBEECK DE MELLO
AL SERENISSIMO PRINCIPE
DON PEDRO
REGENTE,
Y GOBERNADOR DE PORTUGAL, &c.

EN LISBOA.
Con las licencias necessarias.
A costa d' Antonio CraesbeecK de Mello Impressor de S. Alteza.
Año 1678.

Fig. 3.5 Title page of Manuel de Faria y Sousa, *Europa Portuguesa. Tomo I* (1678) (*Source* National Central Library of Rome)

> *rubble* … (Tavares 1810, p. 126, my translation from original in Portuguese).

Neither does Tavares offer any information on the source of the news of purported earthquakes in Lisbon in 377 and 370 BC, nor is there any reason to consider them as historical. Nonetheless, they both appear in modern seismic catalogues (Martínez–Solares and Mezcua 2002, p. 23; cf. Álvarez-Martí-Aguilar 2020).

The same can be said of the interpolation that the Spanish historian Miguel Lafuente Alcántara (1817–1850) makes in his *Historia de Granada* … (*History of Granada*; Lafuente 1843) (Fig. 3.6). Lafuente avails himself of the famous testimony of Ammianus Marcellinus (26.10.15–19), probably borrowed from the 1842 Spanish edition of Gibbon's *The History of the Decline and Fall of the Roman Empire* (Gibbon 1842, p. 273), before slipping in a fraudulent reference to the southern coasts of the Iberian Peninsula:

> *At dawn on 21 July 365, in the second year of the reign of Valentinian and Valens, a violent earthquake was felt in the provinces of Granada and in others of the Empire. The waves of the Mediterranean churned as in the most furious of tempests. The beaches, which had always been lapped by the sea, were left dry many yards from Malaca, Exi and Abdera: the fish, outside their natural element, were picked off the sand without the need for nets or hooks. With rapt attention, the inhabitants of the coast saw the depths of the abysms that, full of water perhaps from the beginnings of the world, had allowed them to navigate with ease. After several hours, the sea returned with furious impetus* … (Lafuente 1843, pp. 235–236, my translation from original in Spanish).

In Ammianus' (26.10.15–19) famous text, there is no mention of those localities—*Malaca* (present-day Malaga), *Exi* (present-day Almuñécar, Granada) and *Abdera* (present-day Adra, Almeria)—in the southern reaches of the peninsula. The inclusion of these geographical references in his account is clearly an interpolation that, as in the previous case, has made its way into the most important seismic catalogues, as well as leading some authors to believe that the tsunami in 365 AD struck the Mediterranean coast of Southern Spain (Galbis 1932, p. 6; Espinar 1994, pp. 124–126; cf. Udías 1983; Álvarez-Martí-Aguilar 2020).

3.6 Conclusions

The ancient and early mediaeval historical sources on earthquakes and tsunamis in ancient Iberia are, as has been seen, very few and far between and tend to lack chronological and geographical context. The reference to the cataclysm that led to the disappearance of the island/continent of Atlantis could be one of the very few vaguely inspired by real events, occurring beyond the Pillars of Heracles, in the vicinity of the Phoenician city of Gadir, before the middle of the fourth century BC, when Plato wrote his dialogues (Udías 2020). Little more can be said about this possible event, taking into account the moralistic fictional character of the Platonic account (see López-Ruiz, this volume). The reference to certain earthquakes in ancient Iberia in the *De mirabilibus auscultationibus* lacks a reliable chronological context, beyond the date of the work per se (usually the third century BC), and the description of the activities of the Massalians in the area, which commenced at the beginning of the sixth century BC.

Another matter is the information contained in Sallust's *Histories* regarding a natural catastrophe in the Roman city of Corduba (Cordova), which must have taken place between 79 and 72 BC, and which is plausibly endorsed by Seneca's reference in the poem that he dedicated to his hometown. Both elements make it possible to claim that this information has a high degree of historicity, the only reasonably tenable account that has come down to us from before ca. 450 AD.

The news of a sea flood in the city of Cadiz, recorded by the Andalusi author Al-Zuhri and the Egyptian Ibn Zanbal, also lacks chronological context, although Al-Zuhri's account seems to be set in a historical period before the Islamic domination of Al-Andalus, commencing in the eighth century. The prominence of Cadiz in the

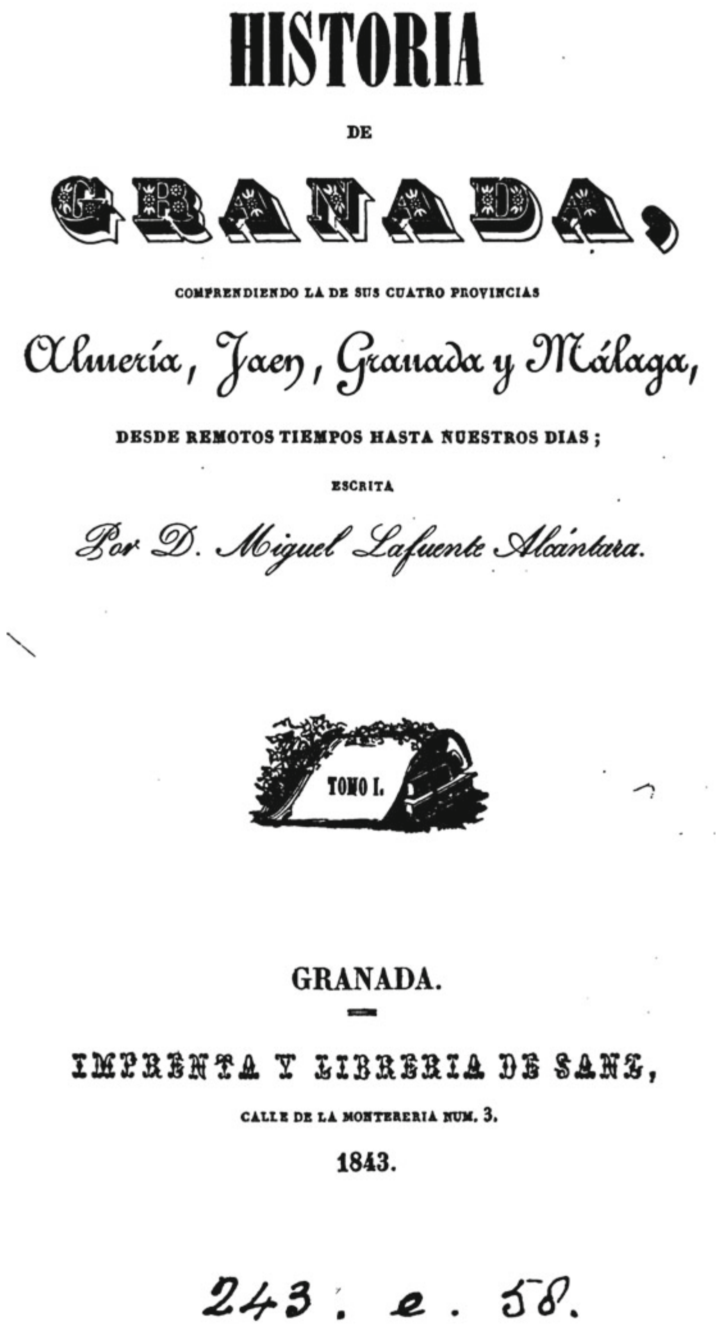

HISTORIA

DE

GRANADA,

COMPRENDIENDO LA DE SUS CUATRO PROVINCIAS

Almería, Jaen, Granada y Málaga,

DESDE REMOTOS TIEMPOS HASTA NUESTROS DIAS;

ESCRITA

Por D. Miguel Lafuente Alcántara.

TOMO I.

GRANADA.

IMPRENTA Y LIBRERIA DE SANZ,

CALLE DE LA MONTERERIA NUM. 3.

1843.

Fig. 3.6 Title page of Miguel Lafuente Alcántara, *Historia de Granada, comprendiendo las de sus cuatro provincias Almería, Jaén, Granada y Málaga*… (1843) (*Source* Oxford University—Google Books) news of cataclysmic events in the remote past links to the Platonic account and would also characterise the information provided by Ocampo.

We have seen that Ocampo's and Brito's works form the backbone of the literature on earthquakes and tsunamis in ancient Iberia. The overall assessment of Ocampo's descriptions of seismic events of this sort in the Iberian Peninsula varies. In the first accounts of the earthquakes in the Pyrenees in 500 BC, Ocampo demonstrates that he is well-versed in the classical literature when speculating about the chronology and location of the earthquake mentioned in the *De mirabilibus auscultationibus*. He subsequently includes a series of descriptions of natural catastrophes that lack specific ancient precedents, like the calamitous triennial affecting the east coasts of the peninsula and the city of Saguntum, between 349 and 347 BC, and the cataclysms in Cadiz in 241 BC, 216 BC and 210 BC, plus the earthquakes in Africa in 211 BC. The Spanish chronicler's reference to the 'two Julians' in relation to the event in 216 BC, one of whom being Julian the Deacon of Toledo, a blatantly spurious source, completely undermines their credibility.

However, the prominence that Cadiz has as the setting of natural catastrophes in Ocampo's work should be related to the information provided by Arab authors such as al-Zuhri and Ibn Zanbal. It is possible that Ocampo is echoing the local traditions of Cadiz, in which ancient cataclysms occurring in the city might have survived in the collective memory, albeit without any chronological context. Based on this vague information, he would have written his descriptions of ancient cataclysms in Cadiz, placing them in the part of his account with which they dovetailed best, namely, at the time of the Second Punic War. As has been observed, for this period, the chronicler draws from Livy, whose oeuvre abounds with portents occurring precisely during the Hannibalic War.

The case of Brito is different, for the characteristics of his information and the sources that he claims to have employed, principally Laymundo Ortega and Pedro Aladio, both admittedly bogus, means that his accounts should be completely disregarded. On occasion, he asserts that the effects of historical seismic events occurring in faraway places, such as Judea and the Central and Eastern Mediterranean in 33 AD and 365 AD, respectively, were felt in Portugal. On others, as with Ocampo, he conjures up catastrophic events of which no news is to be found in ancient or modern sources.

What Brito and Ocampo have in common is the fact that their interest in natural catastrophes might have been inspired by the collective memory, in Portugal and in Spain, of cataclysms occurring in the not-so-distant past. The realism with which Ocampo depicts the alleged earthquake and tsunami in Cadiz in 216 BC [218 BC] and the drama with which Brito describes the reactions of the population to the purported disaster affecting the Portuguese and Galician coasts in 63 BC point to contemporary examples as sources for recreating these events. It has been rightly remarked that contemporary experiences of earthquakes in the Iberian Peninsula during the first decades of the sixteenth century must have influenced Ocampo's account (Compatangelo–Soussignan 2013, p. 598). In that period, there were several earthquakes of considerable magnitude: in Carmona (Seville) in 1504; in Vera (Almeria) in 1518; in Almería in 1522, which may have been affected by a tsunami (Reicherter and Becker-Heidmann 2009); and in Lisbon in 1531, which was struck by a tsunami affecting the mouth of the river Tagus (Baptista et al. 2014). The accounts and recollections of this last catastrophe must have been important examples for Ocampo and Brito, alike.

As a closing thought, it should be noted that the information analysed throughout this review should be treated with caution when undertaking the task of identifying the number, location and date of seismic events in ancient Iberia. The historicity of most of the literature on earthquakes and tsunamis in the Iberian Peninsula is, as has been observed, very dubious, when not totally lacking credibility (Álvarez-Martí-Aguilar 2020). This obliges us to be especially rigorous and critical when attempting to link the natural disasters recorded in the historical literature, particularly in Ocampo's and Brito's works, to the seismic events that, in recent decades, have been documented in the geological record and which have been dated—employing radiocarbon, stratigraphic and archaeological dating methods—to horizons coinciding with the dates supplied by Renaissance historians, for example, to the third century BC or the fourth century AD, some of which are dealt with in several chapters of this book. These new techniques for identifying earthquakes and tsunamis occurring in ancient Iberia in a more chronologically precise fashion have ultimately allowed us to overcome our dependence on the information provided by these historians, so far removed in time from the narrated events.

Acknowledgements This research has been conducted as part of the projects *The Tsunami in the Cultural Representations of the Ancient World: Gadir-Gades and the Gulf of Cádiz as a case study* (HAR2015-66011-P MINECO-FEDER), and *Earthquakes and Tsunamis in the Iberian Peninsula: Social Responses in the longue durée* (PGC2018-093752-B-I00), funded by the Spanish Ministry of Science, Innovation and Universities (MCIU), the Spanish State Research Agency (AEI) and the European Regional Development Fund of the European Union (ERDF, EU).

References

Álvarez-Martí-Aguilar M (2017a) La tradición historiográfica sobre catástrofes naturales en la Península Ibérica durante la Antigüedad y el supuesto tsunami del Golfo de Cádiz de 218–209 a.C. Dialogues d'histoire ancienne 43(2):117–145

Álvarez-Martí-Aguilar M (2017b) Terremotos y tsunamis en Portugal en época antigua: el legado de Bernardo de Brito y su Monarchia Lusytana (1597–1609). Euphrosyne 45:183–204

Álvarez-Martí-Aguilar M (2020) The Historicity of the earthquakes occurring in the Iberian Peninsula Before A.D. 881 Recorded in Spanish and Portuguese Seismic Catalogs. Seismolo Res Lett 91(6):3585–3594. https://doi.org/10.1785/0220200168

Andrade C, Freitas MC, Oliveira MA et al (2016) On the sedimentological and historical evidences of seismic triggered tsunamis on the algarve coast of Portugal. In: Duarte JC, Schellart WP (eds) Plate boundaries and natural hazards. American Geophysical Union, Washington, pp 219–232

Antonio N (1696) Bibliotheca Hispana Vetus, sive Hispanorum, qui usquam unquamve scripto aliquid consignaverunt, notitia. Completens scriptores omnes qui ab Octaviani Augusti imperio usque ad annum M. Floruerunt. Tomus Primus. Ex typographia Antonii de Rubeis, Roma

Baptista MA, Miranda JM (2009) Revision of the Portuguese catalog of tsunamis. Nat Hazard 9:25–42

Baptista MA, Miranda JM, Batlló J (2014) The 1531 Lisbon earthquake: a tsunami in the tagus estuary? Bull Seismol Soc Am 104:2149–2161

Bramon D (1991) El mundo en el siglo XII: estudio de la versión castellana y del "Original" árabe de una geografía universal, "El tratado de al-Zuhri". AUSA, Sabadell

Brito B de (1597) Monarchia Lusytana. Composta por Frey Bernardo de Brito, Chronista geral & Religioso da ordem de s. Bernardo, professo no Real mosteiro de Alcobaça. Parte Primeira… Mosteiro de Alcobaça

Brito B de (1609) Segunda parte da Monarchia Lusytana em que se continuão as historias de Portugal desde o nacimento de nosso Salvador Iesu Christo até ser dado em dote ao Conde dom Henrique. Pedro Crasbeeck, Lisboa

Campos ML (1992) El riesgo de tsunamis en España: análisis y valoración geográfica. Instituto Geográfico Nacional, Madrid

Ces Fernández B (2015) Los efectos del seísmo de Lisboa de 1755 sobre el patrimonio monumental de Galicia. Dissertation, Universidade da Coruña

Compatangelo-Soussignan R (2013) Un tsunami antique à l'embouchure du Guadalquivir? Sources documentaires et archives paléoenvironnementales. In: Marie-Yvane D et al (eds) Anciens peuplements littoraux et relations homme/milieu sur les côtes de l'Europe Atlantique. Colloque International HOMER (2011, Vannes, France). Archaeopress, Oxford, pp 595–603

Dowdall LD (1909) The works of Aristotle, translated into English. Clarendon Press, Oxford, De mirabilibus auscultationibus

Duff JD (1927) Silius Italicus. Punica, Vol. I: Books 1–8. William Heinemann Ltd, London; Harvard University Press, Cambridge, MA

Guidoboni E (ed) (1994) Catalogue of ancient earthquakes in the Mediterranean area up to the 10th century; with the collaboration of A. Comastri and G. Traina. Istituto Nazionale di Geofisica, Rome

Espinar M (1994) Los estudios de sismicidad histórica en Andalucía: los terremotos históricos de la provincia de Almería. In: Posadas A, Vidal F (eds) El estudio de los terremotos en Almería. Instituto de Estudios Almerienses - Diputación de Almería, Almería, pp 115–122

Fagnan E (1924) Extraits inédits relatifs au Maghreb (géographie et histoire); traduits de l'arabe et annotés. J. Carbonell, Alger

Faria y Sousa M (1678) Europa Portuguesa. Tomo I. Antonio Craesbeeck de Mello, Lisboa

Foster BO (1929) Livy, vol V. Harvard University Press, Cambridge, MA, William Heinemann Ltd, London

Galbis J (1932) Catálogo Sísmico de la Zona comprendida entre los meridianos 5° E. y 20° W. de Greenwich y los paralelos 45° y 25° N. Tomo I. Instituto Geográfico, Catastral y de Estadística, Madrid

Galbis J (1940) Catálogo Sísmico de la Zona comprendida entre los meridianos 5° E. y 20° W. de Greenwich y los paralelos 45° y 25° N. Tomo II. Instituto Geográfico y Catastral, Madrid

Garibay E de (1571) Los Quarenta libros del Compendio Historial de las Chronicas y Universal Historia de todos los Reynos de España. Christophoro Plantino, Amberes

Gibbon E (1842) Historia de la decadencia y ruina del Imperio Romano …, traducida del inglés de la reciente de H.H. Milman con todas las notas del autor y las de aquel y Guizot por Don José Mor de Fuentes. Tomo III. Antonio Bergnes y compañía, Barcelona

Godoy Alcántara J (1868) Historia crítica de los Falsos Cronicones. M. Rivadenyra, Madrid

Gómez F, Arruda AM, Rodríguez-Vidal J et al (2015) Eventos marinos de alta energía y cambios traumáticos en los asentamientos costeros del Suroeste de la Península Ibérica. Cuaternario y Geomorfología 29(1–2):57–74

Gómez Espelosín F (2007) Estrabón. Geografía de Iberia. Presentaciones, notas y comentarios de G Cruz Andreotti, MV García Quintela and FJ Gómez Espelosín. Alianza, Madrid

Guidoboni E, Muggia A, Comastri A et al (2008) Ipotesi sul 'predecessore' del terremoto del 1908: archeologia, storia, geologia. In: Bertolaso G et al (eds) Il terremoto e il maremoto del 28 dicembre 1908: analisi sismologica, impatto, prospettive. DPC–INGV, Roma–Bologna, pp 483–516

Jacques F, Bousquet, B (1984) Le raz de marée du 21 juillet 365. Mélanges de l'Ecole française de Rome. Antiquité 96(1):423–461

Knapp RC (1983) Roman Córdoba. University of California Press, Berkeley

Lafuente M (1843) Historia de Granada, comprendiendo las de sus cuatro provincias Almería, Jaén, Granada y Málaga. Desde remotos tiempos a nuestros días... Imprenta y Librería de Sanz, Granada

Lamb WRM (1925) Plato in twelve volumes: with an English translation, vol 9. Harvard University Press, Cambridge, MA, William Heinemann Ltd, London

Lewis S, Llewellyn-Jones L (2018) The culture of animals in antiquity. A sourcebook with commentaries. Routledge, London & New York

Manolaraki E (2010) Silius' natural history: tides in the Punica. In: Augoustakis A (ed) Brill's companion to Silius Italicus. Brill, Leiden – Boston, pp 293–321

Mariana J de (1601) Historia general de España. Tomo primero. Pedro Rodríguez, Toledo

Martínez-Solares JM (2001) Los efectos en España del terremoto de Lisboa (1 de noviembre de 1755). Instituto Geográfico Nacional, Madrid

Martínez-Solares JM, Mezcua J (2002) Catálogo sísmico de la Península Ibérica (880 a.C.-1900). Instituto Geográfico Nacional, Madrid

Martins I, Mendes Victor LA (2001) Contribuição para o estudo da sismicidade da região oeste da península Ibérica. Universidade de Lisboa, Lisboa

Menéndez Pidal R (ed) (1906) Primera Crónica General de España. Estoria de España que mandó componer Alfonso el Sabio y se continuaba bajo Sancho IV en 1289, publicada por Ramón Menéndez Pidal. Bailly-Bailliere é Hijos, Madrid

Morales A (1586) Los Cinco libros postreros de la Coronica general de España que continuaua Ambrosio de Morales natural de Cordoua, Coronista del Rey Cathlico nuestro señor don Philipe segundo deste nombre prossiguiendo adelante la restauracion de España desde que se començo a ganar de los Moros, hasta el rey don Bermudo el tercero deste nombre. Gabriel Ramos Bejarano, Córdoba

Moreira de Mendonça JJ (1758) Historia universal dos terremotos, que tem havido no mundo, de que ha noticia, desde a sua creaçaõ até o seculo presente. Com huma narraçam individual do terremoto do primeiro de novembro de 1755, e noticia verdadeira dos seus effeitos em Lisboa, todo Portugal, Algarves, e mais partes da Europa, Africa, e América, aonde se estendeu: E huma dissertaçaõ phisica sobre as causas geraes dos Terremotos, seus effeitos, differenças, e Prognosticos; e as particulares do ultimo. Antonio Vicente da Silva, Lisboa

Nanni G (1498) Commentaria super opera diversorum auctorum de antiquitatibus loquentium; eiusdem chronographia etrusca et italica. E. Silber, Roma

Ocampo F (1541) Las quatro partes enteras de la Cronica de España que mando componer el Serenissimo rey don Alonso llamado el Sabio: donde se contienen los acontescimientos y hazañas mayores y mas señaladas que suçedieron en España desde su primera poblaçion hasta casi los tiempos del dicho señor rey, vista y emendada mucha parte de su impression por el maestro Florian Doca[m]po. Agustin de Paz y Juan Picardo, Zamora

Ocampo F de (1543) Los quatro libros primeros de la Cronica general de España que recopila el maestro Florian do Campo criado y cronista del Emperador Rey nuestro señor por mandado de su magestad Çesarea. Juan Picardo, Zamora

Ocampo F de (1553) Los cinco libros primeros de la Cronica general de España, que recopila el maestro Florian do Campo, Cronista del Rey nuestro señor, por mandado de su Magestad, en Zamora, Guillermo de Millis, Medina del Campo

Oldfather ChH (1939) The library of history of diodorus of sicily, vol III. Harvard University Press, Cambridge, MA, William Heinemann Ltd, London

Oliveira CS (1986) A sismicidade histórica e a revisão do catálogo sísmico. Laboratório Nacional de Engenharia Civil, Lisboa

Pajón I (2008) Paradoxografía griega: estudio de un género literario. Dissertation, Universidad Complutense de Madrid

Rasmussen SW (2003) Public portents in republican Rome. L'Erma di Bretschneider, Koebenhavn

Reicherter K, Becker-Heidmann P (2009) Tsunami deposits in the western Mediterranean: remains of the 1522 Almería earthquake? In: Reicherter K, Michetti AA, Silva PG (eds) Palaeoseismology: historical and prehistorical records of earthquake ground effects for seismic hazard assessment. The Geological Society, London, Special Publications 316, pp 217–235

Rodríguez-Ramírez A, Villarías-Robles JJR, Pérez-Asensio JN et al (2016) Geomorphological record of extreme wave events during Roman times in the Guadalquivir estuary (Gulf of Cadiz, SW Spain): an archaeological and paleogeographical approach. Geomorphology 261:103–118

Rodríguez-Vidal J, Ruiz F, Cáceres LM et al (2011) Geomarkers of the 218–209 BC Atlantic tsunami in the Roman Lacus Ligustinus (SW Spain): a palaeogeographical approach. Quatern Int 242:201–212

Silva PG (2019) Fuentes históricas y geológicas de los terremotos antiguos en la Península Ibérica. Revista De La Sociedad Geológica De España 32(2):43–64

Silva PG, Bardají T, Roquero E et al (2015) Seismic palaeogeography of coastal zones in the Iberian Peninsula: Understanding ancient and historic earthquakes in Spain. Cuaternario y Geomorfología 29(1–2):31–56

Da Silva, A (1973) Introdução. In: Bernardo de Brito, Monarquia Lusitana, Parte Primeira. Introdução de A. da Silva Rego e notas de A. A. Banha de Andrade e M. dos Santos Alves. Imprenta Nacional, Lisboa, pp ix–xxx

Tavares F (1810) Instrucções e cautelas practicas sobre a natureza, differentes especies, virtudes em geral, e uso legitimo das aguas mineraes, principalmente de Caldas; como a noticia daquellas, que sao conhecidas em cada huma das Provincias do Reino de Portugal, e o methodo de preparar as aguas artificiaes. Real Imprensa da Universidade, Coimbra

Trinquier A (2004) Les loups sont entrés dans la ville: de la peur du loup à la hantise de la cité ensauvagée. In: Charpentier MC (ed) Les espaces du sauvage dans le monde antique: approaches et définitions. Actes du colloque (Besançon, 4–5 mai 2000). Institut des Sciences et Techniques de l'Antiquité, Besançon, pp 85–118

Udías A (1983) El terremoto del 21 de Julio 365, erróneamente atribuido a la costa de Málaga. Sismicidad Histórica de la Región de la península Ibérica. Asociación Española de Ingeniería Sísmica, Madrid, pp 53–55

Udías A (2015) Historical earthquakes (before 1755) of the Iberian Peninsula in early catalogs (electronic supplement: critical revision of earthquakes in the Iberian Peninsula before year 1000). Seismol Res Lett 86(3):999–1005

Udías A (2020) Large earthquakes and tsunamis at saint vincent cape before the Lisbon 1755 earthquake: a historical review. Pure Appl Geophys 177:1739–1745. https://doi.org/10.1007/s00024-019-02323-z

Part II

The Geological Record of Tsunamis in the Iberian Peninsula: An Overview

4

Triggering Mechanisms of Tsunamis in the Gulf of Cadiz and the Alboran Sea: An Overview

Juan-Tomás Vázquez, Gemma Ercilla, Belén Alonso, José Antonio Peláez, Desirée Palomino, Ricardo León, Patricia Bárcenas, David Casas, Ferran Estrada, Mª Carmen Fernández-Puga, Jesús Galindo-Zaldívar, Jesús Henares, Miguel Llorente, Olga Sánchez-Guillamón, Elia d'Acremont, Abdellah Ammar, Mimoun Chourak, Luis Miguel Fernández-Salas, Nieves López-González, and Sara Lafuerza

Abstract

The Gulf of Cadiz and the Alboran Sea are characterized by tectonic activity due to oblique convergence at the boundary between the Eurasian and Nubian plates. This activity has favored a variety of tsunamigenic sources: basically, seismogenic faults and submarine landslides. The main tsunamigenic faults in the Gulf of Cadiz would comprise the thrust systems of Gorringe Ridge, Marquês de Pombal, São Vicente Canyon, and Horseshoe faults with a high susceptibility; meanwhile in the Alboran Sea would be the thrust system of the northern Alboran Ridge with high susceptibility, and the thrust systems of north Xauen and Adra margin, the transpressive segment of Al Idrissi fault, and the Yusuf-Habibas and Averroes faults, with moderate to high susceptibility. The areas with the greatest potential to generate tsunamigenic submarine landslides are in the Gulf of Cadiz, the São Vicente Canyon, Hirondelle Seamount, and Gorringe Ridge; and in the Alboran Sea are the southern and northern flanks of Alboran Ridge. Both sources are likely to generate destructive tsunamis in the Gulf of Cadiz, given its history of bigger earthquakes (>7

J.-T. Vázquez (✉) · D. Palomino · P. Bárcenas · O. Sánchez-Guillamón · L. M. Fernández-Salas · N. López-González
Instituto Español de Oceanografía (IEO, CSIC), Centro Oceanográfico de Málaga, 29640 Fuengirola, Spain
e-mail: juantomas.vazquez@ieo.es

D. Palomino
e-mail: desiree.palomino@ieo.es

P. Bárcenas
e-mail: patricia.barcenas@ieo.es

O. Sánchez-Guillamón
e-mail: olga.sanchez@ieo.es

L. M. Fernández-Salas
e-mail: luismi.fernandez@ieo.es

N. López-González
e-mail: nieves.lopez@ieo.es

G. Ercilla · B. Alonso · D. Casas · F. Estrada
Instituto de Ciencias del Mar, ICM-CSIC, GMC, Barcelona, Spain
e-mail: gemma@icm.csic.es

B. Alonso
e-mail: belen@icm.csic.es

D. Casas
e-mail: davidcasas@icm.csic.es

M. Álvarez-Martí-Aguilar and F. Machuca Prieto (eds.), *Historical Earthquakes, Tsunamis and Archaeology in the Iberian Peninsula*, Natural Science in Archaeology,
https://doi.org/10.1007/978-981-19-1979-4_4

Mw) and larger landslides. To fully assess tsunamigenic sources, further work needs to be performed. In the case of seismogenic faults, research focus on geometry, offsets, timing, paleoearthquakes, and recurrence, and in landslides on early post-failure evolution, age, events, and recurrence. In situ measurements, paleotsunami records, and long-term monitoring, in addition to major modeling developments, will be also necessary.

Keywords

Seismicity · Active tectonics · Faults · Landslides · Potential tsunamigenic sources

4.1 Introduction

4.1.1 Gulf of Cadiz and the Alboran Sea: A Region Affected by Tsunamis

Tsunami wave generation is a geological hazard posing an enormous threat to society and the economy, given urban development and infrastructure trends that have led to the settlement of a large proportion of the world's population in coastal areas. The region between southern Iberia and North Africa, which includes the Gulf of Cadiz and the nearby Atlantic (hereinafter Gulf of Cadiz) and the Alboran Sea, linked by the Strait of Gibraltar, is no exception to this geohazard. The economic activity on the seaboard of the northern region—southern Spain and Portugal—based largely on tourism, is intense, a factor that doubles and even triples the usual population in high seasons. Likewise, the coastline shared by Algeria and Morocco is also characterized by its high population and important economic development, where tourism is an emerging activity. Tsunami events have been described for this region, above all for the Gulf of Cadiz sector, particularly the 1755 event (Mendes-Victor et al. 2009). The geodynamics of Gulf of Cadiz has certain characteristics that magnify tsunami action, such as the occurrence of major earthquakes (>7 Mw) and an open deep-sea configuration (Medialdea et al. 2004; Buforn et al. 2014; Custódio et al. 2016). In comparison, the Alboran Sea, whose instrumentally recorded earthquakes would have a maximum magnitude of around 6.5 Mw, has a semi-enclosed configuration with maximum depths of 1500–2000 m (Álvarez-Gómez et al. 2011a, b; Ercilla et al. 2021). Historically, there have been significant

F. Estrada
e-mail: festrada@icm.csic.es

J. A. Peláez
Departamento de Física, Universidad de Jaén, Jaén, Spain
e-mail: japelaez@ujaen.es

R. León · M. Llorente
Instituto Geológico Y Minero de España (IGME CSIC), Madrid, Spain
e-mail: r.leon@igme.es

M. Llorente
e-mail: m.llorente@igme.es

M. C. Fernández-Puga
Departamento de Ciencias de La Tierra, Universidad de Cádiz, Cádiz, Spain
e-mail: mcarmen.fernandez@uca.es

J. Galindo-Zaldívar
Departamento de Geodinámica, Universidad de Granada—Instituto Andaluz de Ciencias de la Tierra, CSIC, Granada, Spain
e-mail: jgalindo@ugr.es

J. Henares
Universidad Internacional de La Rioja, Logroño, Spain
e-mail: jesus.henares@unir.net

E. d'Acremont · S. Lafuerza
CNRS-INSU, Institut Des Sciences de La Terre Paris, Sorbonne Université, Paris, Spain
e-mail: elia.dacremont@sorbonne-universite.fr

S. Lafuerza
e-mail: sara.lafuerza@sorbonne-universite.fr

A. Ammar
Department of Earth Sciences, Faculty of Sciences, Mohammed V-Agdal University, Agdal, Morocco
e-mail: siadamammar@yahoo.fr

M. Chourak
Université Mohammed Premier, Oujda, Morocco

L. M. Fernández-Salas
Instituto Español de Oceanografía (IEO, CSIC), Centro Oceanográfico de Cádiz, Cádiz, Spain

earthquakes in the Alboran region that have also been related to tsunami waves (Raji et al. 2015), such as the 1522 earthquake of Almeria (Reicherter and Hübscher 2007; Reicherter and Becker-Heidmann, 2009) in the northern Alboran Sea and the 1790 earthquake of Oran in the southern area (Buforn et al. 2019). The maximum estimated magnitude increases up to Mw 6.9 in the Algerian area (Buforn et al. 2015).

Because of the higher risk of tsunamis in the Gulf of Cadiz (García-Mayordomo 2015), the scientific community has made significant efforts to determine possible sources (Gjevik et al. 1997; Batista et al. 2003; Gràcia et al. 2003b; Terrinha et al. 2003; Gutscher et al. 2006; Stich et al. 2007; Bartolome et al. 2012; Matias et al. 2013; Rosas et al. 2016). In the framework of this international endeavor, up to nine zones of seismotectonic sources with the potential for generating tsunami waves have been defined (Matias et al. 2013). The role of submarine landslides as potential sources of tsunamis in this region was also assessed, especially when they involve mass movements on the flanks of major submarine reliefs (Lo Iacono et al. 2012; Omira et al. 2016).

In the Alboran Sea, studies of tsunamis triggered by seismic-tectonic activity have been published by several authors in recent years (Reicherter and Hübscher 2007; Reicherter and Becker-Heidmann 2009; González et al. 2010; Álvarez-Gómez et al. 2011a, b). They have identified 12 probable tsunamigenic seismic sources in geological studies of the seafloor. Accordingly, earthquakes located on the Alboran Ridge have the greatest potential for generating destructive tsunamis, with a calculated wave elevation on the coast exceeding 1.5 m (Álvarez-Gómez et al. 2011a, b). Although landslide mechanisms in the Alboran Sea have hardly been explored hitherto, a few models have been proposed (Macías et al. 2015; Rodriguez et al. 2017). Based on the sedimentary and geomorphological record of landslides, these authors have modeled tsunami waves generated by submarine landslides along the southern slope of the Alboran Ridge and the northern slope of the Xauen Bank, respectively, obtaining waves that would impact the coasts of the basin with a maximum height of roughly 1.5 m.

4.1.2 Tsunamigenic Sources

Assessing tsunami hazards in a region entails considering the most probable tsunamigenic sources. Several mechanisms causing tsunami waves have been proposed in the literature (Röbke and Vött 2017: Ercilla et al. 2021). Earthquakes are identified as the main triggering factor (82.3% of the total), yet submarine and locally subaerial landslides (8.8%), volcanic activity (4%), large volumes of gas suddenly released from the seafloor, atmospheric disturbances (meteotsunamis), and even cosmic impacts may also generate tsunamis.

Seismotectonically induced tsunami waves are usually triggered by the sudden coseismic vertical displacement of the seafloor along faults due to the release of elastic deformation during an earthquake and the transmission of this rapid movement to the water column (Murty 1977; Geist 1997). A sinking movement of the underwater fault causes the water masses to rush toward the newly formed depression, generating an initial large sine wave on the water mass surface (Klug 1986); when faults move the seafloor upwards, the water column is pushed toward the top, forming an initial large crest wave on the sea surface. In addition, Rayleigh seismic waves cause a temporary vertical displacement of the seafloor by several decimeters (Murty 1977; Bryant 2014), which can cause moderate tsunami waves in shallow water areas, or can intensify tsunami waves originally generated by seafloor faults in deeper areas.

Not all earthquakes in marine areas generate tsunami waves. Most tsunamigenic earthquakes are produced by shallow-focus earthquakes at depths of less than 60 km (Bryant 2014; Sorensen 2010). This is because the transfer of coseismic deformation to the overlying water column is more effective at shallow crustal depths. This is the case of earthquakes along dip-slip and oblique-slip faults owing to tectonic compression or extension. In contrast, pure strike-slip faults have no vertical component and generally do not favor tsunamigenic earthquakes, even if the earthquake's magnitude is high (Klug 1986).

Earthquakes along shallow-dipping thrust faults (dip values of 20–30°) in compressive belts are the most efficient for generating tsunami waves, as their geometry favors large vertical movements of the crust (Kopp and Weinreibe 2009). Two good examples would be the 2004 Indian Ocean tsunami (Lauterjung et al. 2009) and the 2011 Tōhoku tsunami (Lin et al. 2012; Hwang 2014). This type of fault is common in subduction zones, where most tsunamis are generated worldwide (Kopp and Weinreibe 2009).

The generation of tsunami waves by seismotectonic processes also depends on the rupture velocity, the average vertical displacement, and the length of the rupture zone on the seafloor (Bryant 2014). The rupture velocity is usually very fast, but in such cases the movement transmission to the water column may not be effective (Todorovska and Trifunac 2001). Indeed, earthquakes with a slower rupture velocity (0.1–1 km s^{1}) and long duration (>100 s) have the greatest tsunamigenic effect, with the higher effective transmission of the seismic moment to the water mass (Kanamori 1972). The mean vertical displacement of the seafloor affected by the fault is directly correlated with the initial height of the tsunami wave (Dawson and Stewart 2007), and the same correlation is maintained for the length of the rupture zone (Todorovska and Trifunac 2001).

In recent decades, there has been a growing interest in researching submarine landslides and their role in triggering tsunamis. Technological improvements in seafloor exploration have led to a better knowledge of the geomorphological characteristics of the bottom surface and the identification of numerous underwater landslides on the seafloor (e.g., Locat et al. 1999; Lee et al. 2003). These observations have led to the evaluation of the role that underwater landslides may play as tsunamigenic sources and allow for confirming the high impact that tsunami waves of this type, producing important run-up heights, can have on the coast from a local or regional point of view (Harbitz 1992; Harbitz et al. 2006, 2014; Haugen et al. 2005; Løvholt et al. 2005; Masson et al. 2006; Tappin 2010, 2017). Subaerial rock falls, or coastal landslides, and submarine mass wasting processes may trigger tsunami waves along the coast (Dawson and Stewart 2007). Submarine landslides are more likely to generate major tsunami waves, implying better energy transfer to the water column due to the large volume involved, up to 1000 km^3 (Bryant 2014).

The triggering of submarine landslides can be multifactorial (Locat and Lee 2002), even though the most important single cause would be tectonic-related earthquakes (Grotzinger et al. 2008). In addition, seismic surface waves temporarily increase the sediment pore water pressure, thereby favoring slope instabilities (Niedoroda et al. 2007). Other factors are sediment overload due to high sedimentation rates; the alongslope and downslope erosion of continental slopes (Costa et al. 2005); differential stress linked to high-amplitude sea-level changes (Neves et al. 2016); storm surges that can magnify the effect of pore water pressure in sediments (Bryant 2014); and the presence of fluids in sediments that may generate abnormally high interstitial pore pressures, weaken sediment cohesion, and lead to a loss of underwater mass (Max 2003; Tinivella et al. 2008).

Volcanic eruptions can also induce vast subaerial and submarine landslides or debris avalanches on the flanks of volcanoes, or even cause the complete collapse of the edifice as evidenced by the giant slide masses—exceeding several 1000 km^3—located at the base of volcanic islands, including the Canary Islands, Cape Verde, and the Hawaiian Islands (Lipman et al. 1988; Moore et al. 1994; Masson 1996; Urgeles et al. 1999; Keating and McGuire 2000; Krastel et al. 2001; Kopp and Weinreibe 2009; León et al. 2019).

Finally, anthropogenically induced submarine and coastal landslides, attributable to engineering works, have been known to generate tsunami waves. An example is the one caused by recharge produced by the expansion work at the French airport of Nice, which caused 3 m high waves on the Antibes coast, about 10 km away (Assier-Rzadkiewic et al. 2000).

4.1.3 Aim of the Study

In the Gulf of Cadiz-Alboran Sea region, where no active magmatic volcanoes exist, the two major geological mechanisms generating tsunami waves that should be considered are seismotectonic activity and submarine landslides affecting the seafloor. The aim of this work is to compile and review the seismicity, active tectonic structures, and areas with landslides that could potentially trigger tsunami waves, and to assess their susceptibility.

This work is based on a compilation of seismicity catalogs (Peláez et al. 2007; Hamdache et al. 2010; IGN 2020) and a vast geophysical dataset, featuring multibeam bathymetry and high- to very high-resolution seismic profiles, from IEO, ICM-CSIC, IGME, and Sorbonne and Mohammed V-Agdal Universities. In addition, regional bathymetric data were obtained from the EMODnet Bathymetric Consortium (2018).

4.2 Geodynamic Setting

The Gulf of Cadiz-Alboran Sea region is located at the current plate boundary between Eurasia and Nubia (West Africa), for which reason there is significant seismotectonic activity there; it generated important reliefs during the Pliocene–Quaternary, as well as slope instabilities (Comas et al. 1992; Medialdea et al. 2004; Terrinha et al. 2009; Martínez-García et al. 2013; Omira et al. 2016; Ramos et al. 2017; Juan et al. 2016). The region extends from the Gorringe Ridge and the Horseshoe Abyssal Plain in the west to the beginning of the Algerian Compressional Belt in the east (Fig. 4.1), and includes the Gibraltar Arc, the deformation front of the Betic-Rif Orogenic Belt, and related structures (Vázquez and Vegas 2000).

Geodynamic models indicate oblique convergence between the plates of Eurasia and Nubia in a NW–SE to WNW-ESE trend (Dewey et al. 1989; Reilly et al. 1992; Herraiz et al. 2000) at a rate of 2–5 mm/y (Nocquet 2012). Geodetic data obtained from continuously recording GPS stations (CGPS) and non-permanent GPS stations show a general NW-WNW displacement in the western Betic Ranges with respect to the Iberian Massif (Koulali et al. 2011; Palano et al. 2013; Gonzalez del Castillo et al. 2015), demonstrating that the structures that make up the Gibraltar Arc are still active today (Fig. 4.1). Regional deformation has a diffuse pattern, corresponding to distributed tectonics ranging from the Gorringe Ridge to the Betic-Rif Belt (Vázquez and Vegas 2000; Serpelloni et al. 2007; De Vicente et al. 2008; Custódio et al. 2016).

In the Gulf of Cadiz, contemporary WNW-ESE convergence has produced the South Western Iberian Margin (SWIM) right-lateral transfer zone, as well as NE-SW to E-W thrusting structures (Medialdea et al. 2004; Zitellini et al. 2009; Terrinha et al. 2009; Rosas et al. 2009, 2012; Duarte et al. 2011; Cunha et al. 2012; Neres et al. 2016; Hensen et al. 2019) (Fig. 4.1). The SWIM zone continues toward the Josephine Bank and connects with the Gloria transform fault zone (Argus et al. 1989; Custódio et al. 2016; Neres et al. 2016; Hensen et al. 2019; Omira et al. 2019; Sanchez et al. 2019). In the Alboran Sea, the SWIM zone connects eastward to compressive structures at the southern limit of the Rif Belt (Jimenez-Munt et al. 2003; Chalouan et al. 2006, 2014; Pedrera et al. 2011). The main tectonic boundary extends eastward to the Algerian compressive belt by means of the Al Idrissi left-lateral transfer fault, the northern reverse flank of the Alboran Ridge, and the Yusuf-Habibas right-lateral transfer fault (Estrada et al. 2018a; Galindo-Zaldívar et al. 2018; Vázquez et al. 2021) (Fig. 4.1).

Two different geodynamic models have been proposed in relation to the relevance of the currently active subduction of the Atlantic oceanic lithosphere in the Gulf of Cadiz, geodynamic models suggesting (i) slow subduction of the Atlantic oceanic lithosphere under the Gibraltar Arc in relation to the Betic-Rif Orogenic Belt (Gutscher et al. 2002; Gutscher et al. 2012; Spakman et al. 2004, 2018); or (ii) incipient subduction processes associated with the Gorringe Ridge, the Horseshoe fault, or the continental-oceanic lithosphere boundary (Maldonado et al. 1999; Duarte et al. 2013). Other geodynamic models consider that subduction

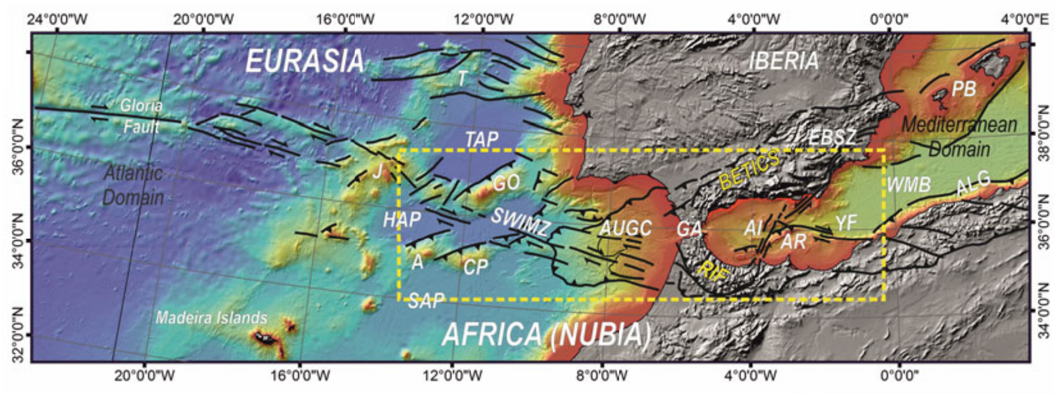

Fig. 4.1 Geodynamic framework of the Gulf of Cadiz (Atlantic Domain) and the Alboran Sea (Western Mediterranean Basin). Yellow box: Study area. Legend: A—Ampere Seamount; AUGC—Allochthonous Unit of the Gulf of Cadiz; CP—Coral Patch Seamount; GO—Gorringe Ridge; HAP—Horseshoe Abyssal Plain; J—Josephine Bank; SAP—Seine Abyssal Plain; SWIMZ—Southwest Iberian Margin fault zone; T—Tore Seamount; TAP—Tagus Abyssal Plain; AI—Al-Idrissi Seismic Zone; ALG—Algerian Margin Subduction Zone; AR—Alboran Ridge Indenter; EBSZ—Eastern Betic Seismic Zone; GA—Gibraltar Arc; BP—Balearic Promontory; WMB—Western Mediterranean Basin; YF—Yusuf-Habibas fault zone (modified from Vázquez et al. 2021. Reprinted with permission from Springer Nature)

under the Gibraltar Arc is no longer active or blocked (Medialdea et al. 2004; Terrinha et al. 2009; Zitellini et al. 2009). It was also proposed that the current plate boundary structures in the Gulf of Cadiz correspond to the SWIM dextral transfer fault zone. This zone would accommodate much of the slow oblique convergence between the Eurasian and Nubian plates, although part of the deformation is possibly assumed by NE-SW to ENE-WSW thrust faults systems (Vegas et al. 2008; Sallares et al. 2013; Martínez-Loriente et al. 2014).

Two main factors condition the most superficial regional tectonic activity in the Gulf of Cadiz (Vázquez et al. 2008) (Figs. 4.1 and 4.2): (i) the dynamics of the Eurasia and Nubia plates across their boundary; and ii) the emplacement of the Allochthonous Unit of the Gulf of Cadiz (AUGC) in the western front of the Gibraltar Arc upon the African and Iberian continental margins and the Atlantic oceanic domains, by means of a tectonic-gravitational mechanism (Medialdea et al. 2004). Pliocene–Quaternary plate dynamics gave rise to the proposal of the SWIM transfer system (Zitellini et al. 2009) and the reactivation of the AUGC (Medialdea et al. 2004) (Figs. 4.1 and 4.3).

The Alboran Sea Basin, located in the backarc region of the Betic-Rif Belt, was generated by means of extensional tectonics from the Late Oligocene-Early Miocene to the Tortonian. This orogenic system was generated by the westward migration of the Alboran Domain in relation to the westward retreat of a subduction slab in a N-S convergence setting between the main plates (Platt et al. 2013 and references therein). Since the Late Tortonian, a regional change of the convergence regime has established a compressive scenario that has led to the inversion of the basin. This inversion has created a large transcurrent deformation zone known as the Trans-Alboran shear zone (TASZ), which extends from the eastern Betics crossing the Alboran Sea to the Rif. The uplift affects both the surrounding Betic-Rif ranges and internal reliefs of the basin, namely the Alboran Ridge system, with tilting of the margins (Comas et al. 1999; Vázquez 2001; Soto et al. 2008, 2012; Martínez-García et al. 2013, 2017; Do Couto et al. 2016; D'Acremont et al. 2020). Throughout the Pliocene and Quaternary, an indentation of the crustal block of the Alboran Ridge occurred in the central part of the basin, producing a system of conjugated left-lateral NE-SW to NNE-SSW and right-lateral

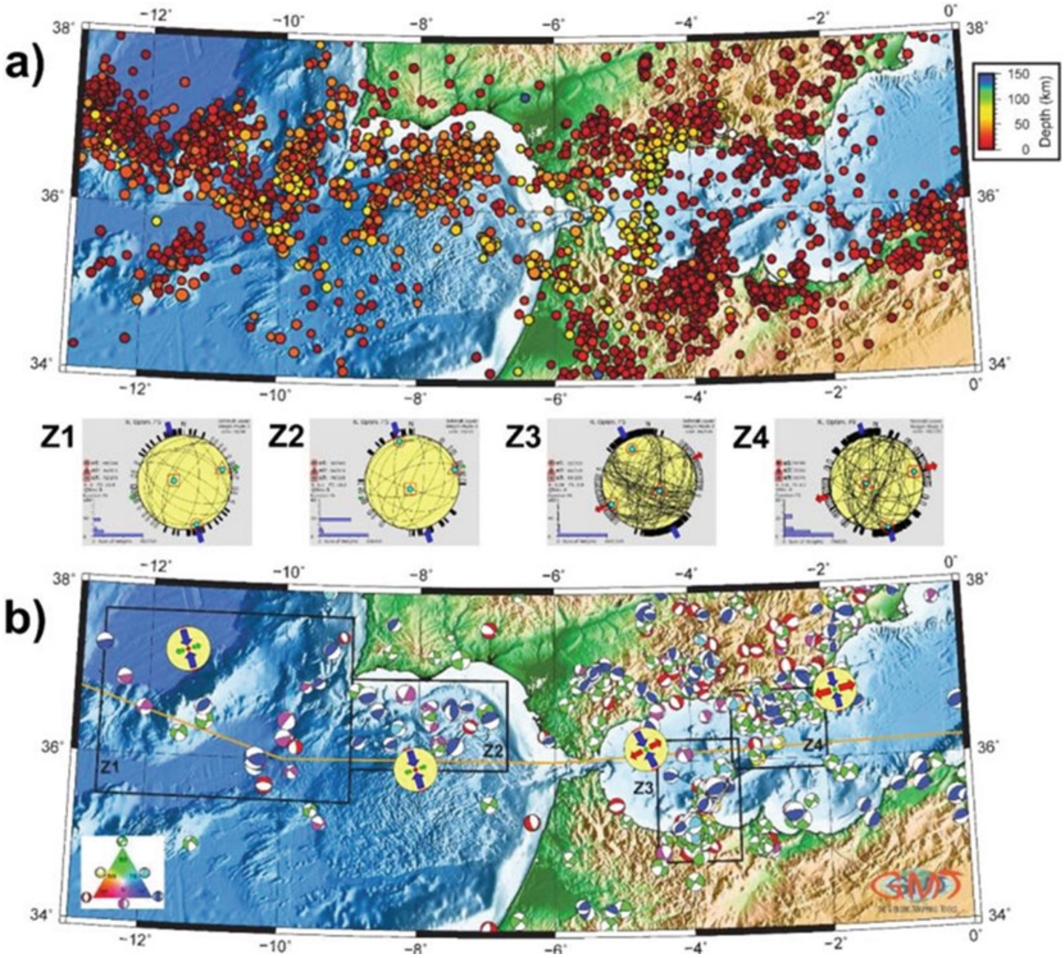

Fig. 4.2 Seismicity and focal mechanisms in the Gulf of Cadiz-Alboran Sea region. **a** Recorded seismicity from 1970 to 2020 with a magnitude equal to or higher than m_b 3.5 (IGN 2020). **b** Compiled focal mechanism solutions as of 1970 with a magnitude of above Mw 3.0 for the study region. For the selected areas (Z1–Z4), the stress regime was computed and depicted using the Win-Tensor™ code (Delvaux and Sperner 2003). The orange line marks the NUVEL-1A plate model boundary (DeMets et al. 1994) as a reference. A ternary diagram for classifying focal mechanism solutions is shown

WNW-ESE faults propagating northward (Estrada et al. 2018a; D'Acremont et al. 2020; Lafosse et al. 2020).

4.3 Seismicity of the Gulf of Cadiz-Alboran Sea Region

Seismicity in this region is considered to be moderate or low to moderate on the global scale, depending on the authors, even though some damaging earthquakes occurred (Peláez et al. 2007; Hamdache et al. 2010; IGN 2020). A description of the main characteristics of earthquakes and the computed focal mechanism solutions affecting the region of study is presented. These data were used to explain the present-day stress regime.

4.3.1 Seismicity Distribution

The seismicity with a magnitude higher than m_b 3.5 from 1970 onwards is shown in Fig. 4.2. The

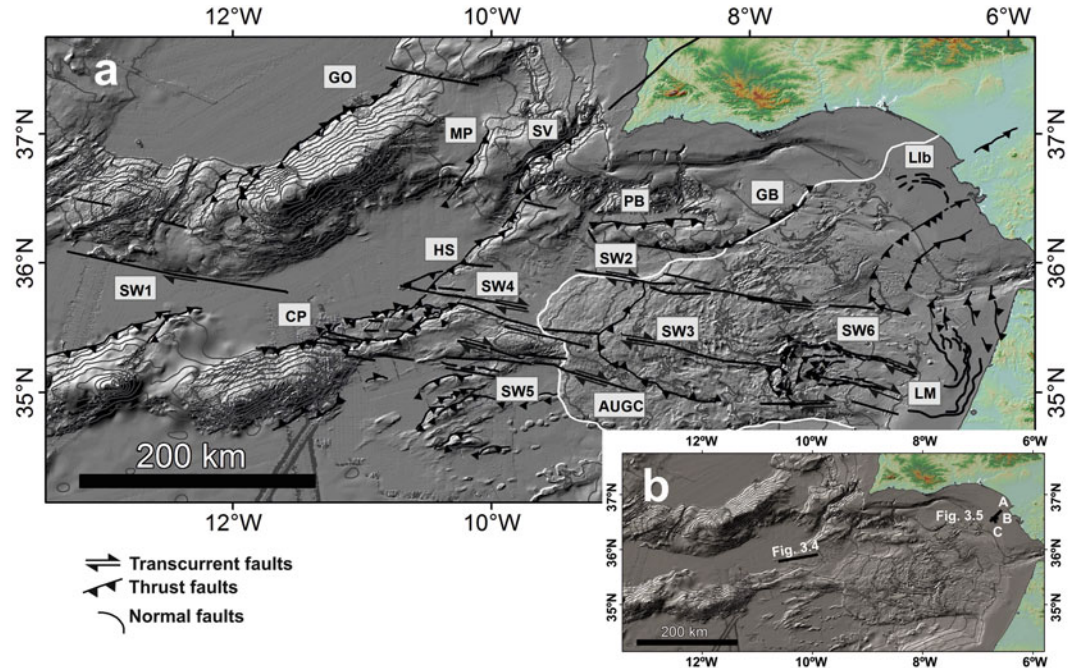

Fig. 4.3 **a** Main tectonic structures developed in the Gulf of Cadiz from the Tortonian. The faults showing activity in the Quaternary are highlighted. GO: Gorringe Ridge thrust; MP: Marquês de Pombal thrust; SV: São Vicente Canyon thrust; HS: Horseshoe thrust; CP: Coral Patch Ridge thrust; PB: Portimão Bank thrust; GB: Guadalquivir Bank thrust; SW: SWIM system (SW1–SW6, SWIM segments in Table 4.1); LIb: listric normal fault system of the Iberian margin; LM: listric normal Moroccan margin; AUGC: Morphostructural expression of the Allochthonous Unit of the Gulf of Cadiz (white line). **b** Location of seismic profiles of Figs. 4.4 and 4.5

starting year and the threshold magnitude represent a compromise between the thoroughness and precision of the catalog used. According to González (2017) and later studies, seismicity in the Gulf of Cadiz-Alboran Sea region has been fully recorded in the m_b 3.5–4.0 magnitude range only since 1995–2000, approximately. In addition, seismicity in the m_b 4.0–4.5 range has been complete for the Gulf of Cadiz-Atlantic and Alboran Sea-North Africa regions since 1975 and 1940, respectively. In other words, not all earthquakes taking place in these areas are included in the catalog (Fig. 4.2), especially those with a magnitude in the m_b 3.5–4.0 range.

In this region, seismicity is related to the boundary between the Eurasian and Nubian plates, although this limit corresponds to a wide deformation zone (e.g., Peláez et al. 2018; Stich et al. 2020). For instance, in areas such as the Alboran Sea, the recorded seismicity covers a width of over 300 km. Yet although seismicity is spread over a wide zone, it is not a diffuse distribution. Manifold alignments, clearly related to more or less active tectonic features, can be seen in both the Gulf of Cadiz and the Alboran Sea—that is, by and large seismicity tends to be related to known active faults or structures.

The hypocentral depths in the Spanish catalog are very uncertain before 1980. Even in the last decades, offshore events near the coast have depth uncertainties of the order of 5 km for a confidence level of 90%, but uncertainties above 50 km, for the same confidence level, over 150 km from the coast (González 2017). At any rate, mean depth values of recorded events can be used to describe the depth of the seismicity in the different areas (Fig. 4.2). In the Gulf of Cadiz and nearby areas to the west, earthquakes are mainly located within the crust. Distributed seismicity occurs up to a depth of 100 km; and about 90% of the observed seismicity has approximate depths of up to 55–60 km. Throughout the Alboran Sea, with a thinned continental crust, there is also significant shallow seismicity, especially in the eastern part of this area, at the Algerian margin, the Moroccan coast, and the trans-Alboran shear zone. In addition, intermediate-depth earthquakes (40–150 km), with low magnitude values (below m_b 4.5), depict a well-known "C"-shape structure (e.g., López-Casado et al. 2001) in the western part of the Alboran Sea (Fig. 4.2). Different hypotheses have been put forward to explain this seismicity, including delamination processes (e.g., Seber et al. 1996; Mezcua and Rueda 1997), subducted slab processes (e.g., Royden 1993; Morales et al. 1999), or a combination of both (e.g., Buforn et al. 1991; López-Casado et al. 2001).

The maximum magnitude known for the Gulf of Cadiz would be the historic December 12, 1722, earthquake, with a perceived intensity equal to VIII on the EMS-98 scale. Using macroseismic data and the Bakun and Wentworth (1997) approach, Mezcua et al. (2004) assign this event a magnitude equal to Mw 6.9. To the west, in the Gorringe Ridge and the Horseshoe Abyssal Plain, the likely source of the November 1, 1755, Lisbon earthquake, magnitudes of higher values have been recorded. Different magnitudes in the range of 8.5–9.0 have been assigned to this historical event—the largest earthquake to have ever taken place in the vicinity of the Iberian Peninsula and affecting Western Europe. On the basis of macroseismic data, Mezcua et al. (2004) assigned the event a magnitude equal to Mw 8.7. The more recent 1969 earthquake of M_S 8.0 also occurred in this area (Buforn et al. 1988; Cabieces et al. 2020).

Maximum recorded magnitudes in the Alboran Sea have lower values. The most energetic events were the Mw 6.1, 1910 Adra earthquake (Stich et al. 2003), and the Mw 6.4, 1994 (e.g., El Alami et al. 1998), Mw 6.3, 2004 (e.g., Galindo-Zaldívar et al. 2009), and the Mw 6.4, 2016 (e.g., Buforn et al. 2017) Al Hoceima earthquakes, all followed by noteworthy seismic sequences. The 1910 Adra earthquake was most likely related to a system of faults along the northern edge of the Alboran Basin striking 120° N–130° E (Stich et al. 2003). The Mw 6.4, 1994 Al Hoceima earthquake epicenter was located just off the coast, suggesting the continuation of an onshore fracture zone trending NNE-SSW (Alami et al. 1998). The Mw 6.3, 2004 Al Hoceima event occurred onshore, hosted in a fault with no surface signature, and striking NNW-SSE or NNE-SSW (Galindo-Zaldívar et al. 2009; Van der Woerd et al. 2014). The epicenter of the Mw 6.4, 2016 Al Hoceima (or south Alboran) event was located offshore, probably associated with new structures west of the Al Idrissi fault zone, striking NNE-SSW (Buforn et al. 2017; Galindo-Zaldívar et al. 2018). When comparing seismic and geodetic moment rates in the Alboran Sea, a significant contribution to the measured crustal deformation is attributed to aseismic mechanisms, like afterslip and viscoelastic relaxation (Sparacino et al. 2020).

In sum, in recent decades the Alboran Sea has hosted shallow earthquakes in the Mw 6.0–6.5 range (moderate magnitude) in tectonically and seismically active areas. In addition, the Gulf of Cadiz area was the source of moderate- to high-magnitude tsunamigenic events in the Mw 7.0–9.0 range in historical times, as well as moderate- to high-magnitude events in the instrumental period: the M_S 8.0, 1969 Cape St Vincent and the M_S 6.4, 1964 Gulf of Cadiz earthquakes. Because most seismicity is located near the crust in both areas, future moderate- to high-magnitude earthquakes could generate significant deformation on the seafloor.

4.3.2 Focal Mechanism Solutions

A database of focal mechanism solutions was specially created for this study. It includes data from national and international agencies and dozens of specific scientific works. The catalogs making the largest contribution were those of Henares and López Casado (2001) and Custódio et al. (2016). The focal mechanisms of post-1970 events, with a magnitude of above Mw 3.0 and a depth of up to 30 km, were retrieved from the database (Fig. 4.2). At first glance, what is remarkable is that in the Gulf of Cadiz area pure normal faulting (NF), normal to strike-slip (NS), and thrust to strike-slip type (TS) solutions are unusual.

Four specific zones (Z1–Z4) were chosen from the Gulf of Cadiz-Alboran region as a whole in order to compute and define specific stress regimes in view of the focal mechanism solutions (Fig. 4.2). The inversion approach developed by Delvaux and Sperner (2003) and Delvaux and Barth (2010) was applied, and Win-Tensor™ software was used. As previously mentioned, only earthquakes with a magnitude greater than Mw 3.0 were considered. Lower magnitude events, often related to aftershocks, could display very local stresses. The software runs in an iterative way, first using the Right Dihedron method to obtain an initial estimation of the reduced stress tensor parameters and a preliminary focal mechanism dataset, removing nodal planes incompatible with the computed initial average stress. Then, the Rotational Optimization technique is used to minimize the so-called misfit function, inverting the two nodal planes for each solution. Finally, the excluded focal planes are reconsidered, incorporating them into the database and re-optimizing the stress tensor. This process is replicated as many times as necessary. In addition to the directions of the principal stress axes, σ_1, σ_2, and σ_3, the stress ratio $R = (\sigma_2 - \sigma_3)/(\sigma_1 - \sigma_3)$ is obtained.

The results indicate the following behavior (Fig. 4.2): Z1 and Z2 show a clear NNW-SSE almost horizontal compression. Both σ_1 and σ_2 are near horizontal (<15°). In both cases, the obtained stress ratio is very low, 0.0 and 0.1 for Z1 and Z2, respectively, supporting a prolate stress ellipsoid. With these values, the stress regime can be defined as a strike-slip compressional regime for both areas. Z3 and Z4 also show similar, although not identical, behavior. In this case, the nearly horizontal NNW-SSE compression is combined with perpendicular extension. Both σ_1 and σ_3 are near horizontal (< 20°), and the obtained stress ratios are 0.29 and 0.61 for Z3 and Z4, respectively. In light of these values, the stress regime of Z3 can be considered as a pure strike-slip/strike-slip compressional regime, and in the case of Z4 a pure strike-slip regime, according to the criteria established by Delvaux et al. (1997).

The most significant conclusion is that all four areas (Z1–Z4) show a maximum horizontal stress ratio (SH_{max}) in the range of 150–165°. The main difference is that in the Alboran Sea (Z3–Z4), σ_3 is nearly horizontal, thus favoring perpendicular extension to the horizontal compression trend. These findings, deriving from a newer and larger database, are in line with previous results (e.g., Henares et al. 2003; De Vicente et al. 2008; Peláez et al. 2018; Sparacino et al. 2020).

4.4 Quaternary Faults

4.4.1 General Considerations

When assessing the potential behavior of a fault as a tsunamigenic source, it is necessary to establish its activity and capability (orientation to stress field). Several fault features are considered in conjunction: (i) the fault type and slip displacement; (ii) the relation between vertical and lateral components; (iii) geometric parameters such as the length and width of the fault zone, the length of the rupture zone on the seafloor, and the segmentation of the fault; and (iv) its correlation with seismological data (Bryant 2014).

A fault is considered to be seismically active when it has a relationship with current seismicity, as well as a paleoseismicity register confirming its activity. Here, a fault is considered to be potentially active if seismicity has affected the Quaternary units or generated a morphological signature on the seafloor surface (Keller and Pinter 2002; Trifonov and Kozhurin 2010). During the past decade, great efforts have been made in the Iberian Peninsula, both offshore and onshore, to define the faults potentially active in the Quaternary. They are compiled in the QAFI database (García Mayordomo et al. 2012, 2017).

4.4.2 The Gulf of Cadiz

Several tectonic structures active during the Quaternary affect and/or control the seabed morphology, locally generating morphological elements on the seafloor such as scarps, depressions, ridges, or bulges (Flinch 1996; Flinch and Soto 2017; Gràcia et al. 2003a, b; Terrinha et al. 2003, 2009; Medialdea et al. 2004; Vázquez et al. 2004, 2008, 2010a, b; Hernández-Molina et al. 2006; Rosas et al. 2009, 2016; Duarte et al. 2011; Bartolomé et al. 2012; Fernández-Puga et al. 2014) (Fig. 4.3). These active tectonic structures comprise transcurrent faults, reverse faults, and normal faults, and explain the main seismic activity.

Multibeam bathymetric models allowed for mapping a system of WNW-ESE trending faults, interpreted as dextral transform faults and the possible boundary between the Eurasia and Nubia plates, called the southwest Iberian margin (SWIM) system (Rosas et al. 2009; Terrinha et al. 2009; Zitellini et al. 2009). However, only the western segments evince significant seismicity; the easternmost segments reflect slow motion, creeping, or even being locked (Fig. 4.3). At least six segments of this transform fault system connect the northern part of the Josephine Bank (Sanchez et al. 2019) with the southern part of the Gorringe Ridge, extending eastward to the southern part of the Rif Belt (Zitellini et al. 2009). The fault zone is roughly 200 km wide and 600 km long (Hensen et al. 2019) (Table 4.1). The faults comprising this zone constrain the emplacement of the AUGC into the Horseshoe Abyssal Plain (Fig. 4.1), dislocating and displacing arched structures located on the slope, or connecting the displacement of two of these structures as transfer faults. Morphologically, traces produce seafloor scarps, depressions, and elongated discontinuous ridges, in response to the different transtensive or transpressive structures along their fault traces (Bartolomé et al. 2012; Hensen et al. 2015).

Table 4.1 Characteristic and tsunamigenic evaluation of Quaternary faults, by fault type (SS: strike-slip; R: reverse; N: normal), SC: secondary component (SS, R, N as in fault type), segmentation (yes or no), fault length, vertical slip occurrence (VS, yes or no), seismicity hazard from IGME (2015) (http://info.igme.es/eventos/zesis) (SH-VH: very high; H: high; L: low), and inferred magnitude (Mw) from Wells and Coppersmith (1994) equations. Tsunami Potential (TP) is shown as a relative parameter (H: high; M: moderate; L: low)

Fault name		Type	SC	Segments	Length	VS	SH	Magnitude	TP
Gulf of Cadiz									
SWIM		SS		YES	600	NO	L	8.27	M
	SW1			W	160	NO	L	7.63	L
	SW2			E1	295	NO	L	7.93	L
	SW3			E2	360	NO	L	8.02	M
	SW4			E3	23	NO	L	6.68	L
	SW5			E4	180	NO	L	7.68	L
	SW6			E5	80	NO	L	7.29	L
Gorringe	GO	R		YES	120	YES	VH	7.54	H
Coral Patch	CP	R		YES	150	YES	L	7.65	M-H
		R		W	61	YES	L	7.18	M-H
		R		E1	100	YES	L	7.44	M-H
		R		E2	88	YES	L	7.37	M-H
Horseshoe	HS	R		YES	140	YES	VH	7.68	H
		R		SW	38	YES	VH	6.93	H
		R		C	49	YES	VH	7.06	H
		R		NE	44	YES	VH	7.00	H

(continued)

Table 4.1 (continued)

Fault name		Type	SC	Segments	Length	VS	SH	Magnitude	TP
Gulf of Cadiz									
Marquês de Pombal	MP	R		?	70	YES	VH	7.25	H
S. Vicente Canyon	SV	R		?	74	YES	VH	7.28	H
Portimão B	PB	R	?	?	55	YES	VH	7.12	H
Guadalquivir B	GB	R	?	?	100	NO	VH	7.44	M
Listric—Morocco	LM	N		YES	110	YES	H	7.55	M
Listric—Iberia	Lib	N		YES	50	YES	VH	7.10	M
Alboran Sea									
La Herradura Sound	HS	SS	N	YES	40	YES	VH	6.95	M
				SW	22	YES	VH	6.66	M
				NE	18	YES	VH	6.56	M
Calahonda Sound	CS	SS	N	YES	79	YES/NO	VH	7.28	M
				SW	32,6	NO	VH	6.85	L
			N	C	16	YES	VH	6.51	M
			N	NE	30,4	YES	VH	6.82	M
Djibouti Ville Seamount	DVS	SS	N	YES	68	YES/NO	VH	7.21	M
				SW	19	NO	VH	6.59	L
			N	C	20	YES	VH	6.62	M
			N	NE	29	YES	VH	6.80	M
Djibouti Passage	DP	SS	N	YES	45	YES	VH	7.01	M
Al Idrissi	AI	SS	N-R	YES	125	YES/NO	VH	7.50	M
				SW	32	YES	VH	6.84	M
				C	48,4	YES	VH	7.05	H
				NE	44,7	NO	VH	7.01	M
La Serrata-Carboneras	SC	SS	R	YES	90	YES	VH	7.35	M
			R	SW	42	YES	VH	6.98	M
				NE	48	NO	VH	7.04	L
Yusuf-Habbibas	Yu	SS	N	YES	175	YES	VH	7.67	H
				NW	85	YES	VH	7.32	H
				SE	90	YES	VH	7.35	H
Averroes	Av	SS	N	YES	38	YES	VH	6.93	H
			N	NW	22	YES	VH	6.66	H
				SE	16	NO	VH	6.51	L
Adra	Ad	SS	N	YES	16	YES	VH	6.51	M
		SS	N	NW	8	YES	VH	6.17	M
		SS	N	SE	8	YES	VH	6.17	M
North Alboran Ridge	ARI	R	SS	YES	75	YES	VH	7.29	H
				W	39,5	YES	VH	6.95	M
				E	40,5	YES	VH	6.96	H
North Xauen	NX	R		YES	60	YES	VH	7.17	H
Adra margin thrust	AdT	R		YES	11	YES	VH	6.27	H

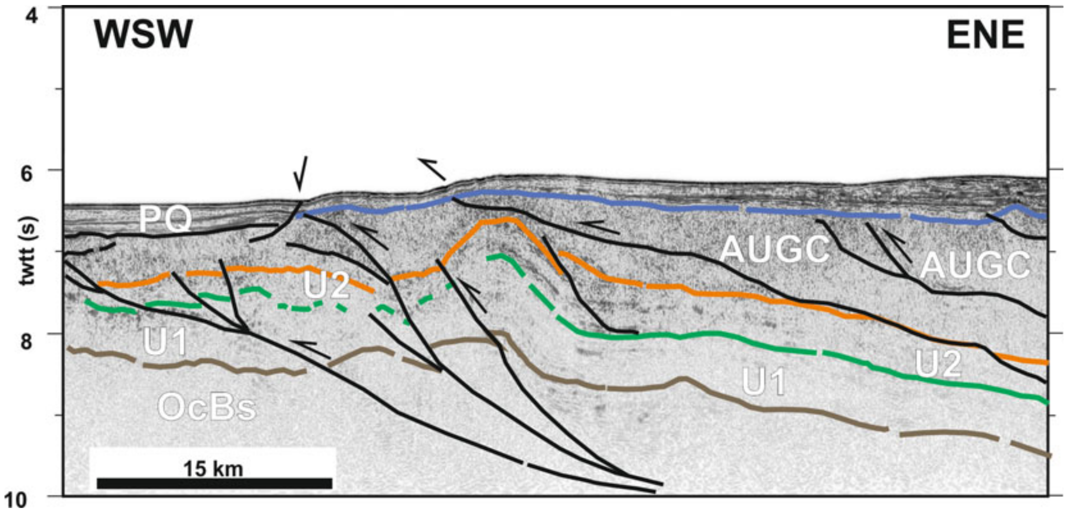

Fig. 4.4 Horseshoe thrust fault. Main thrust system located on the lower continental slope-abyssal plain boundary. The main thrust does not apparently affect the upper units, but this is a consequence of gravitational faults that dismantle the active front scarp. PQ: Pliocene–Quaternary Unit; AUGC: Allochthonous Unit of the Gulf of Cadiz; U1: Upper Jurassic-Lower Aptian Unit; U2: Upper Cretaceous-Lower Eocene Unit; OcBs: Oceanic basement (units from Medialdea et al. 2004 and Vázquez et al. 2004). See profile location in Fig. 4.3b

Several structures interpreted as large reverse faults are depicted in Figs. 4.3 and 4.4. They trend from NE-SW to E-W, and a concentration of seismic events indicates their substantial activity at present. From west to east, this group includes the following structures:

- The *Gorringe Ridge fault* (120 km long) is located on the northwest flank of this ridge. It is considered to be part of a pop-up structure with a second thrust fault affecting the southern flank (Rosas et al. 2009, 2016; Terrinha et al. 2009).
- The *Coral Patch Ridge fault*, extending from the northern flank of the Coral Patch Ridge (Martínez-Loriente et al. 2013) to the northern flank of the Coral Patch Seamount (Rosas et al. 2016), has an approximate length of 150 km and three different segments. This fault could be the WSW prolongation of the Horseshoe fault with a slight shift in trend from NE-SW to ENE-WSW.
- The *Horseshoe fault* (Fig. 4.4), located practically on the boundary between the lower continental slope and the Horseshoe Abyssal Plain (Medialdea et al. 2004; Martínez-Loriente et al. 2018). It has a marked scarp with an approximate length of 140 km, and comprises at least two segments, owing to the interaction of strike-slip faults belonging to the SWIM system.
- The *Marquês de Pombal fault* is located on the western boundary of the Alentejo continental margin (Terrinha et al. 2003; Zitellini et al. 2004) and has a length of about 70 km.
- The *São Vicente Canyon fault*, located in the southwestern extension of Cape St. Vincent (Rosas et al. 2009; Serra et al. 2020), runs approximately 74 km along the continental margin.
- The *Portimão Bank fault*, located on the northern flank of the Portim*ã*o Bank (Fig. 4.3), characterized by an E-W trend, has a length of 55 km. This fault system appears to be related to reverse faults on both the northern and southern flanks. They are closely associated with salt diapiric mobility without basement involvement (Terrinha et al. 2009; Ramos et al. 2017) during Pliocene–Quaternary.
- The *Guadalquivir Bank fault* was proposed recently as a blinded thrust related to the

inversion of the necking domain of the previous continental margin rifting phase (Ramos et al. 2017). This thrust has produced the uplift of the Guadalquivir Bank area, where previous extensional normal faults were folded from the Neogene until the present day.

In addition, thrust faults with an arched geometry were identified within the AUGC in relation to several morphostructural elements on the Seine Abyssal Plain (Fig. 4.3). The first group of faults affects the Moroccan continental slope in particular, with scarps and ridges. The orientation of the arc secant varies from N-S to NW–SE, showing a convexity toward the west. These structures mainly control the morphology of the lower slope, and locally the middle Moroccan continental slope. They are interpreted as thin-skinned reverse fault structures affecting the AUGC. The second group comprises ENE-WSW trending thrust faults relating to salt mobility which condition the uplift of several elongated seamounts on the Seine Abyssal Plain (Martínez-Loriente et al. 2013).

Finally, normal faults have been described in various physiographic domains of the Gulf of Cadiz. Within the study setting, the most significant ones are two listric faults located on the continental shelf and upper slope, respectively, of the Moroccan and Spanish margins. They produce seafloor scarps of up to 6 m height (Vazquez et al. 2010a, b; Sanchez Guillamon et al. 2014). These faults are generated by decollement surfaces favored by plastic units in the AUGC (Fig. 4.5) (Flinch and Soto 2017). In this group, other types are gravitational faults and half-graben fault-bounded mini-basins, developed in the middle and lower slope of the AUGC. Finally, crestal-type normal faults and collapse structures are frequently related to diapirism (Fernández-Puga et al. 2010; Leon et al. 2010; Vázquez et al. 2015c) (Fig. 4.5).

Comparing the activity of the described faults in the Gulf of Cadiz, the WNW-ESE transcurrent faults have a remarkable influence on morphology. Notwithstanding this, their segments are not linked to substantial seismic activity, given the low magnitude of plate convergence in this region.

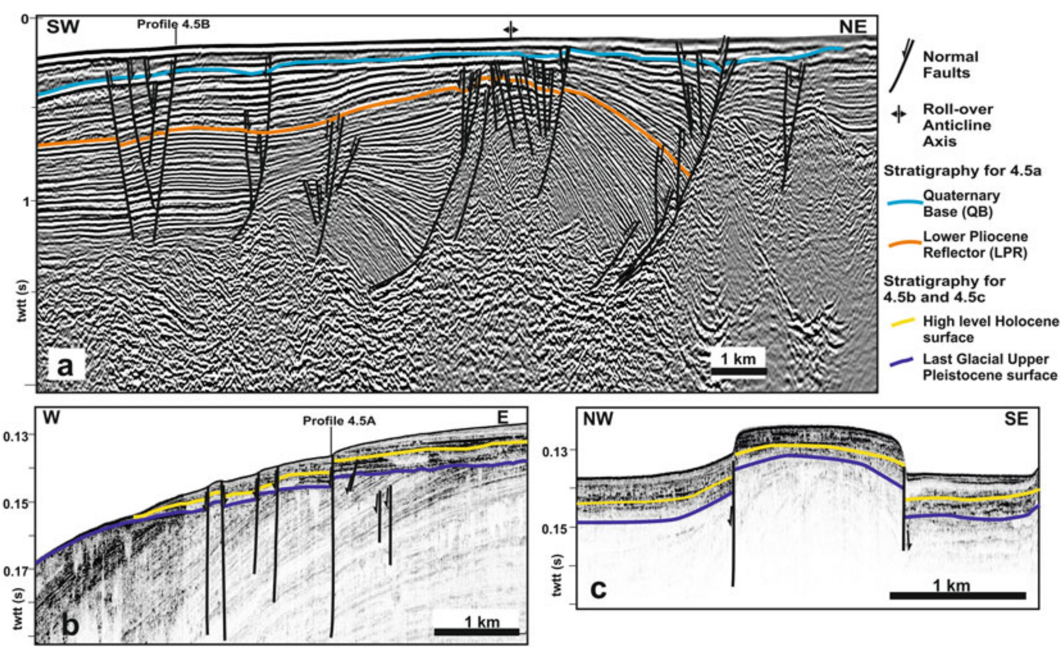

Fig. 4.5 Listric normal fault system of Cadiz (Iberian margin). **a** Multichannel seismic profile showing the listric normal fault system; **b** and **c** High-resolution seismic profiles showing the deformation associated with the listric fault affecting the last postglacial units. See profile location in Fig. 4.3b

The fact that reverse faults have developed obliquely to perpendicular with respect to the regional stresses would point to the accommodation of an intense deformation. In the main, seismicity is concentrated in the structures that best assume plate convergence, namely the reverse faults and, especially, the areas of interference between the reverse and transcurrent faults (Rosas et al. 2016).

4.4.3 The Alboran Sea

The main active tectonic structures during the Quaternary comprise left-lateral transcurrent faults (NE-SW to NNE-SSW), right-lateral transcurrent to normal faults (WNW-ESE), compressive faults and folds (ENE-WSW), and minor N-S to NNW-SSE normal faults. These faults explain the main seismic activity in the Alboran Sea (Fig. 4.2). They have affected the seafloor morphology (Gràcia et al. 2006; Estrada et al. 2018a; Galindo-Zaldívar et al. 2018; Perea et al. 2018) creating morphotectonic features such as linear scarps, elongated pressure ridges, and longitudinal or rhombus-shaped depressions that evince the contemporary variety of Quaternary tectonics (Ballesteros et al. 2008; Vázquez et al. 2008, 2016) (Fig. 4.6).

In the central sector of the basin, at least five NNE-SSW trending fault zones were identified with seafloor deformation. They are characterized as left-lateral strike-slip faults with an intense brittle deformation and a transtensive character, located north of the La Herradura and Djibouti Ville Seamounts (Vázquez et al. 2018). The seismic profiles point to intense faulting of the subsurface, although the faults do not always reach the seafloor. In addition, the main NE-SW fault lies in the northeastern margin of the Alboran Basin-La Serrata fault zone, also known as La Serrata-Carboneras (Estrada et al. 1997; Gracia et al. 2006) (Fig. 4.6).

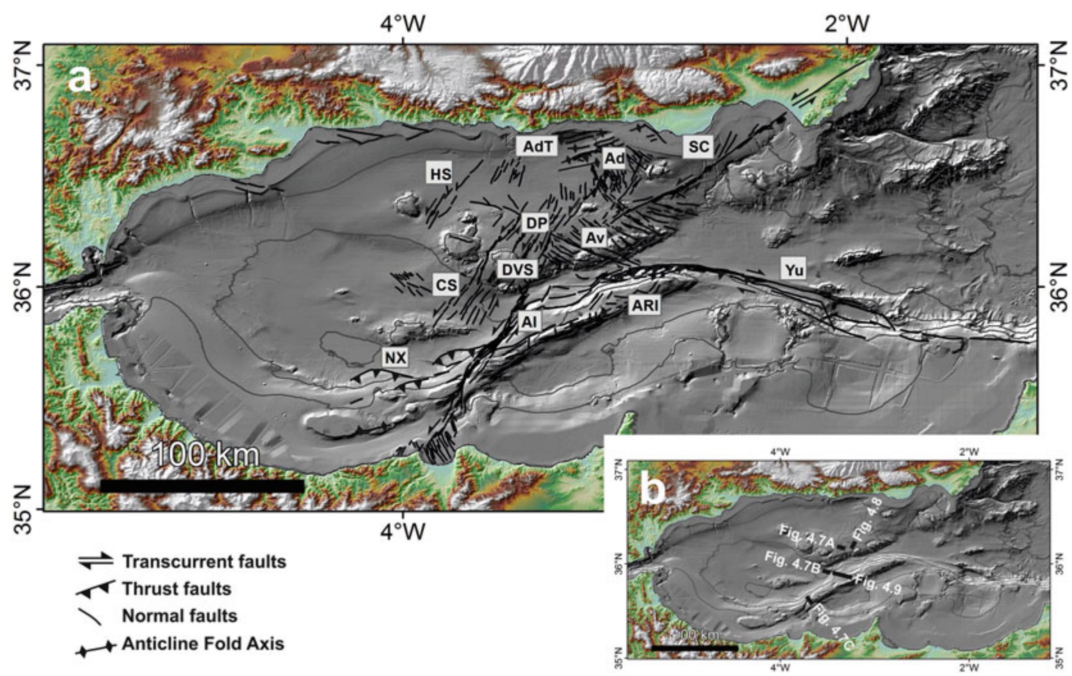

Fig. 4.6 **a** Main tectonic structures in the Alboran Sea region active in the Quaternary. HS: La Herradura Sound fault; CS: Calahonda Sound fault; DVS: Djibouti Ville Seamount fault; DP: Djibouti Passage fault; AI: Al Idrissi fault; SC: La Serrata-Carboneras fault; Av: Averroes fault; Yu: Yusuf-Habibas fault; Ad: Adra fault; NX: Northern Xauen thrust; ARI: Northern Alboran Ridge indenter fault; AdT: Adra margin thrust. **b** Seismic profile location of Figs. 4.7, 4.8, and 4.9

- The *La Herradura Sound fault zone*, including the main NNE-SSW left-lateral strike-slip faults, has a length of 40 km and is divided into two segments (Table 4.1). The SW segment has a width of 1.4 km and features a transtensional graben geometry bounded by high-angle faults with a normal component, while the NE segment is characterized by a normal fault scarp.
- The *Calahonda Sound fault zone*, lying between the La Herradura and Djibouti Ville Seamounts, is 79 km long and can be divided into three segments: the SW segment affects the Ibn Batouta Seamount and is characterized by several high-angle faults; the central segment is a narrow corridor (0.7 km) of high-angle normal fault scarps with a rhombus-shaped transtensional depression (3 km long by 1.2 km wide); and the NE segment has a maximum width of 4 km on the seafloor, characterized by a transtensional depression bounded by high-angle normal faults and a depression corridor of pull-apart mini-basins.
- The *Djibouti Ville Seamount fault zone* has a length of 68 km and three segments showing slight changes in direction when crossing the Djibouti Ville Seamount. The surficial structure of the SW segment is characterized by a high-angle normal fault scarp, the central one features two transtensional relays, and the surficial structure of the NE segment corresponds to a fairly symmetrical corridor (1.7 km wide) of fault scarps and depressions.
- The *Djibouti Passage fault zone*, 1 km wide, affects the Ibn Gabirol Seamount and extends 45 km to the NNE. The main fault has a normal component dipping to the SE, and on the surface it is reflected by a corridor of fault scarps and transtensional asymmetric depressions.
- The *Al Idrissi fault zone* has a length of 125 km divided into at least three segments. The SW segment extends from Al-Hoceima Bay to the Alboran Ridge and has an extensional horsetail splay. The central segment extends from the Alboran Ridge to the Alboran Trough and marks the western boundary of the Alboran Ridge indenter (Fig. 4.6). It has a transpressive configuration, constituted by elongated pressure ridges and restraining bends with a set of high-angle reverse faults. The NE segment extends NNE of the Alboran Trough and has a transtensive character. On the seafloor, it conforms to a narrow corridor (1.4 km wide) of tectonic depressions and linear normal fault scarps, which generate a negative flower structure (Fig. 4.7).
- The *La Serrata-Carboneras fault zone* contains a NE-SW left-lateral strike-slip fault, with land-sea continuation—approximately 50 km inland and 90 km on the continental margin. It has been widely described in the emerged area as part of the eastern Betics shear zone. There, it affects sedimentary units and the Miocene Cabo de Gata volcanic complex during the last 133 ka (Silva et al. 1993; Bell et al. 1997; Moreno et al. 2015; Masana et al. 2018). Its trace is imaged by bathymetry and seismic profiles in the marginal platform of Motril-Djibouti (Estrada et al. 1997; Gracia et al. 2006; Moreno et al. 2016). Its seafloor expression includes linear scarps, pressure ridges bounded by high-angle reverse faults, and several aligned dislocations (Vázquez et al. 2016).

A right-lateral transcurrent system with NW–SE to WNW-ESE trends and secondary normal component are predominating in the eastern part of the Alboran Basin. They correspond to the main Yusuf-Habibas fault zone and a set of structures on the northeastern continental margin of the basin, represented by the Averroes fault zone (Fig. 4.6).

- The *Yusuf-Habbibas fault zone*, which corresponds to the eastern boundary of the Alboran Ridge indenter (Estrada et al. 2018a), features a 175 km-long right-lateral strike-slip fault with a transtensional component, divided into two segments. Its morphology is marked by the main rectilinear escarpment with a relief ranging from 800 to 2000 m, plus a pull-apart basin in the relay zone of the two segments (Mauffret et al. 1992, 2007; Gómez de la Peña et al. 2018).

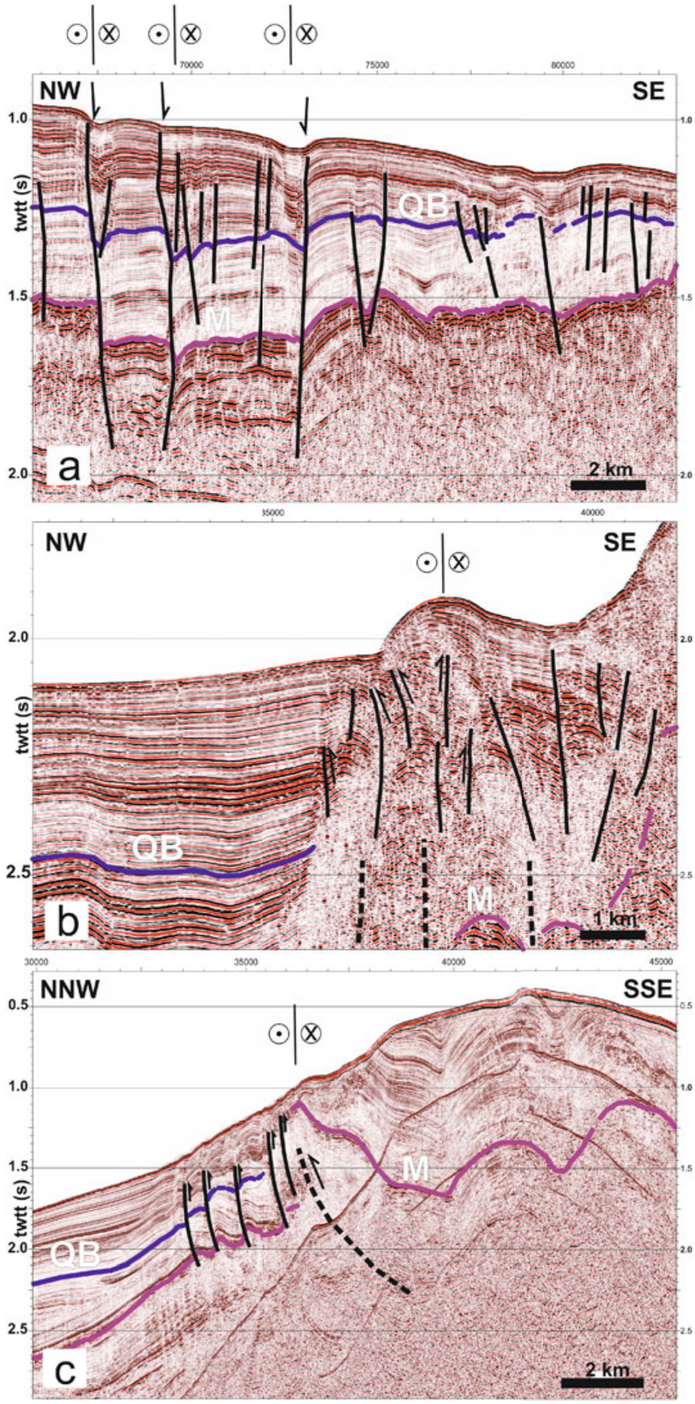

Fig. 4.7 Al Idrissi fault zone, from north to south: **a** Northern transtensive segment; **b** and **c** Central transpressive segment. *Legend*: M—Top Messinian (purple line); QB—Quaternary base (blue line). See profile location in Fig. 4.6b

- The *Averroes fault zone* is a high-angle fault (38 km long) made up of at least two fault surfaces. One of its two segments, the SE one, laterally displaces the seafloor. While its NW segment has a vertical offset of up to 470 m, with a downthrown block to the NE and a half-graben structure on the surface (Estrada et al. 2018b) (Fig. 4.8).
- The *Adra fault*, located on the upper continental slope in front of Adra region, is interpreted as a dextral strike-slip fault (Gràcia et al. 2012). Three faults are discerned on the seafloor (16, 12, and 10 km long). They have produced changes in the slope gradient and minor scarps, interpreted as normal component (Vázquez et al. 2014).

In the third place, a compressive set of ENE-WSW structures are located in the Alboran Sea. They include antiformal folding relating to the main elongated ENE-WSW ridges and banks, as well as thrust faults. Two main structures can be highlighted: the northern Alboran Ridge fault and the Xauen compressive system.

- The *northern Alboran Ridge fault*, which controls the northeastern segment of the Alboran Ridge chain, follows an ENE-WSW trend. It is located between the Yusuf-Habbibas fault escarpments to the east, and the Al Idrissi fault to the west, tracing approximately 75 km (Fig. 4.6). This structure and its southwestward prolongation are regarded as a mainly left-lateral strike-slip fault zone, 165 km in length, with a compressive component that was active in the Late Miocene (Bourgois et al. 1992; Woodside and Maldonado 1992; Watts et al. 1993; Comas et al. 1999). However, the uplift—through folding and thrust faults—of the Alboran Ridge as a tectonic relief (Martínez-García et al. 2013; Estrada et al. 2018a) and the arched geometry in the eastern segment highlighting its reverse component in the

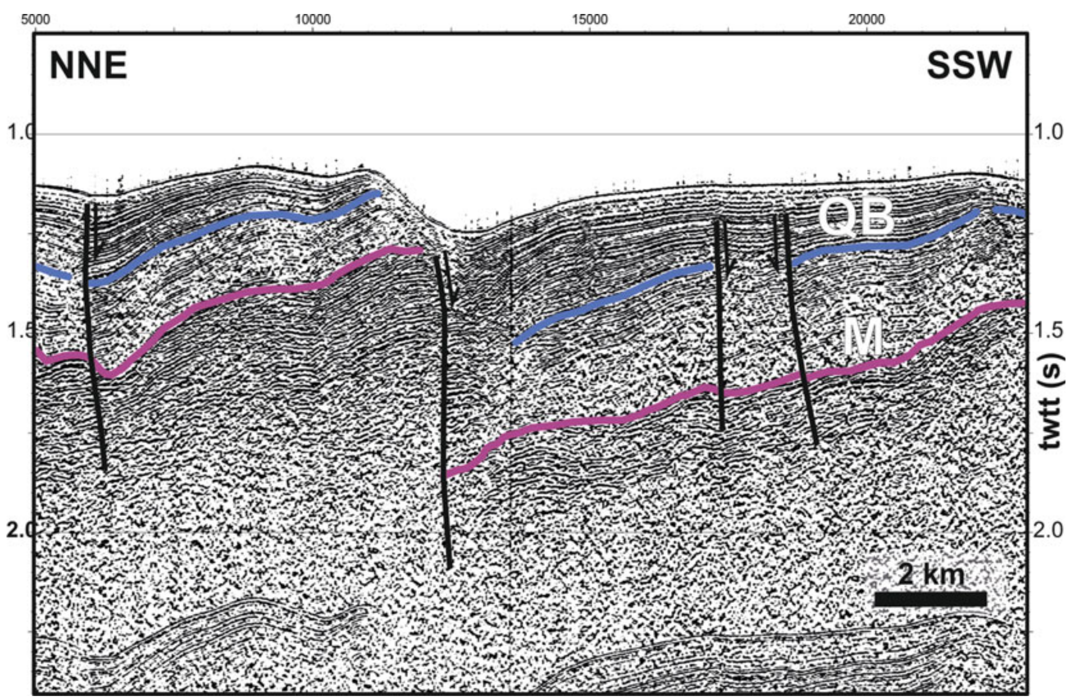

Fig. 4.8 Normal segment of the Averroes fault zone. *Legend*: M—Top Messinian (purple line); QB—Quaternary base (blue line). See profile location in Fig. 4.6b

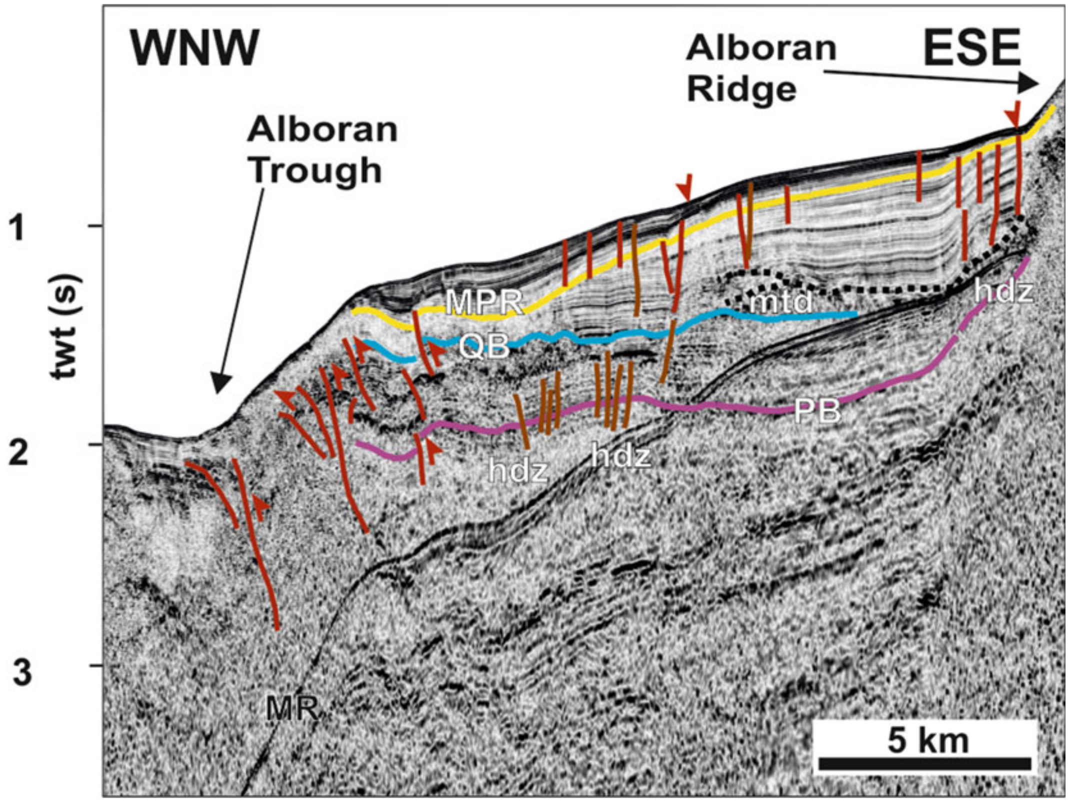

Fig. 4.9 Northern Alboran Ridge thrust system. Reverse faults have affected different Pliocene and Quaternary units and generated the main scarp on the relief. *Legend*: PB—Pliocene Base (purple line); QB—Quaternary base (blue line); MPR—Mid-Pleistocene Reflector (yellow line); mtd—Buried mass transport deposits; hdz—high deformed zone; and MR—Multiple reflector. See profile location in Fig. 4.6b

Pliocene–Quaternary, verging northwards (Woodside and Maldonado 1992; Martínez-García et al. 2013, 2017; Vázquez et al. 2015a) (Fig. 4.9), suggest that it may be the northern front of the Alboran Ridge indenter (Estrada et al. 2018a). The observed thrust fault has a length of between 40 and 75 km and a maximum width close to 6 km.

- The *Xauen compressive system* is responsible for the Xauen Seamount morphology and the southwestern termination of the Alboran Ridge, left-laterally displaced by the Al Idrissi fault (Figs. 4.6 and 4.7). The Xauen Seamount is interpreted as a pop-up structure, controlled by at least four thrusts that are gently arched and largely verge toward the north (Bourgois et al. 1992; D'Acremont et al. 2020). The two main thrusts limit the seamount and reach the seafloor surface, while the northern one corresponds to a blind thrust comprising the deformation front (D'Acremont et al. 2020).

In addition, three smooth asymmetric ridges, trending 50–60 N, are located in front of the Adra coast. They are roughly 17–22 km long, and 30–80 m high. The most prominent feature—offsets of up to 7 m in the Upper Pleistocene-Holocene units at the top of the ridge—is controlled by two high-angle inverse faults some 11 km long (Vázquez et al. 2014, 2016) (Fig. 4.6). They are interpreted as anticline folds associated with blind thrusts verging to the NW, affecting the Quaternary units and deforming the seafloor (Comas et al. 1992; Vázquez et al. 2008).

The earthquake epicenter distribution indicates that most of the current regional deformation is due to the NNE-SSW left-lateral strike-slip fault system. It comprises the Al Idrissi fault that connects the Al Hoceima and Adra seismic areas on its southern and northern margins, respectively. Hence, the Al Idrissi fault zone can be proposed as the current TASZ. In its southern area, a newly developing fault zone of similar characteristics has recently been defined at crustal levels, which could explain the three main earthquake series between 1994 and 2016 (Galindo-Zaldívar et al. 2018). Secondarily, seismic activity is concentrated in the NW–SE right-lateral conjugate fault system and in ENE-WSW structures, such as the compressive zone of the northern Alboran Ridge. In contrast, there are no high seismic NE-SW swarms along the La Serrata-Carboneras fault.

4.4.4 An Approach to Tsunami Potential

When an appropriate fault geometry occurs, the minimum earthquake magnitude required to generate tsunami waves is generally believed to be Ms = 6.5 (Sorensen 2010). To assess the potential of the aforementioned faults as tsunamigenic sources, it is necessary to consider the geometry, behavior, and deformation history. Parameters such as fault length allow us to infer the maximum earthquake magnitude that might be generated, using the Wells and Coppersmith (1994) or Stirling et al. (2002) equations. Fault segmentation allows an evaluation of the possible seafloor rupture length. The rake of the fault sheds light on vertical displacement, and paleoseismic analysis helps to study the recurrence of the fault movement. Other useful parameters are the type of fault and any possible vertical slip in its movement, or whether or not the fault affects the seafloor. Having gathered and analyzed these data, we offer a relative appraisal of the potential of faults active in the Quaternary, although a better knowledge of every single fault is needed to offer a more complete evaluation (Table 4.1).

In the Gulf of Cadiz, the tsunamigenic sources with the highest potential correspond to the NE-SW thrust faults, even though their seafloor rupture is not always clear. In contrast, the listric normal faults have a moderate potential, while the transform faults have a comparatively low one. For the Alboran Sea, we arrived at similar results: the ENE-WSW thrust faults have the highest potential. Several WNW-ESE to NW–SE right-lateral-normal strike-slips likewise have high potential, conditioned by a length in the case of the Yusuf-Habbibas fault zone, or by the well-known characteristics of the Averroes fault zone (Estrada et al. 2018b). Exceptionally, a transpressive segment of the Al Idrissi fault zone containing reverse faults is classified as having a high potential (Table 4.1).

4.4.5 Recommendations for Future Actions

The assessment of tsunami potential presented here, specifically regarding faults in the Gulf of Cadiz-Alboran Sea region, can be understood as an important scientific contribution. The faults are described in terms of their tectonic style, dynamics, and present-day activity. Yet, a full appraisal of their tsunami potential calls for further work in the future. To this end, the dataset should include.

(i) the geometry of both the fault zone and the fault surface, with an emphasis on fault offsets involving different sedimentary units;
(ii) the geomorphology of the fault on the seafloor, so as to predict possible areas of rupture;
(iii) dating and timing of fault movements by means of sediment core logging;
(iv) identification of paleoearthquakes and paleotsunamis, determining the recurrence intervals; and
(v) the application of *in situ* measurements, plus long-term monitoring, to ensure a sound approach to assessing current tectonic activity.

To address these concerns longer sediment cores, high- and ultra-high-resolution geophysical data, in situ seismicity measurements and observations, long-term monitoring, and major modeling efforts are necessary.

4.5 Submarine Landslides

4.5.1 General Considerations

There are still many uncertainties surrounding the tsunamigenic character of submarine landslides, especially regarding flows, implying high deformation and long run-outs. A wide range of flow types (mudflow, debris flow, grain flow, debris/rock avalanche) can occur because of the interplay of rheology, grain size composition, and concentration (Mulder and Alexander 2001; Masson et al. 2002). Depending on the sediment's capacity to be partially or totally remolded, a given event may evolve into a flow or may develop directly when the remolded, undrained shear strength of the sediment is surpassed. A review of critical landslide parameters confirms that landslide acceleration determines tsunami wave elevation in the case of submarine translational landslides, whereas landslide velocity is key for slumps (Løvholt et al. 2015). Because such parameters can rarely be recorded (except in laboratory experiments), the main approach to assessing the tsunamigenesis of sedimentary instabilities takes into account their water depth distribution, the sediment volume, and the type of process involved. In this sense, we hold that the areas prone to produce tsunamigenic landslides are those that have registered landslide activity at least since the Late Quaternary.

4.5.2 Landslides in the Gulf of Cadiz-Alboran Sea Region: Distribution, Types, and Recurrence

Although many authors have provided detailed mapping and morphology of a single landslide phenomenon by means of geophysical studies in the Gulf of Cadiz (e.g., Baraza et al. 1999; Mulder et al. 2006, 2009; Sayago-Gil et al., 2008; Hanquiez et al. 2010; León and Somoza 2011; Lo Iacono et al. 2012; García et al. 2016; Omira et al. 2016; León et al. 2020), and the Alboran Sea (e.g., Reicherter and Hübscher, 2007; Martínez-García et al. 2010; Casas et al. 2011, 2015; Alonso et al. 2012, 2014; Vázquez et al. 2013, 2015a, b; Macías et al. 2015; Rodriguez et al. 2017; Galindo-Zaldívar et al. 2018; Ercilla et al. 2019; d'Acremont et al 2022), a compilation of landslides has yet to be performed. In this study, the landslide data were uploaded to a geographic information system (ArcGIS desktop) in order to analyze their distribution (regional and water depth location) and morpho-seismic characteristics. The distribution of landslides is a key factor for (i) identifying the different types of slope failure processes, and (ii) obtaining essential morphostructure parameters for assessing landslide susceptibility and ensuing tsunami generation (Sect. 4.5.3).

The landslides mapped in Figs. 4.10 and 4.11 can be divided into three main groups, associated with (i) morphostructural highs, (ii) submarine canyons, and (iii) open slopes. The landslides linked to structural highs (i) tend to occur on the oversteepened (up to 20º) flanks of seamounts in the Gulf of Cadiz and the Alboran Sea. They display varied dimensions, anywhere from 1 to 427 km^2 (Fig. 4.10). Landslides are defined by headwall slide scars easily identifiable by collapse features produced on the seafloor. The scar slides appearing downslope are related to slide, debris flow, and avalanche deposits, stacked within the Quaternary and Holocene sedimentary record and interrupting the lateral continuity of the surrounding stratified deposits. In the Gulf of Cadiz, the best examples of landslides are found along the flanks of the Portimão (Fig. 4.12) and Guadalquivir Banks in the northern part of the Gulf of Cadiz, and the Gorringe Ridge and Hirondelle Seamount located SW of the Gulf of Cadiz (Fig. 4.10; Maestro et al. 2003; García et al. 2016; Mulder et al. 2009; León and Somoza, 2011; Lo Iacono et al. 2012; Omira et al. 2016; Vázquez et al. 2015a; Silva et al. 2020). In the Alboran Sea (Fig. 4.11), landslides are identified by flanks of the Alboran Ridge (central sector of the Alboran Sea, Fig. 4.13a, b), north of the Tres Forcas Promontory (SE Alboran Sea, Fig. 4.13c, d), the Xauen and Tofiño

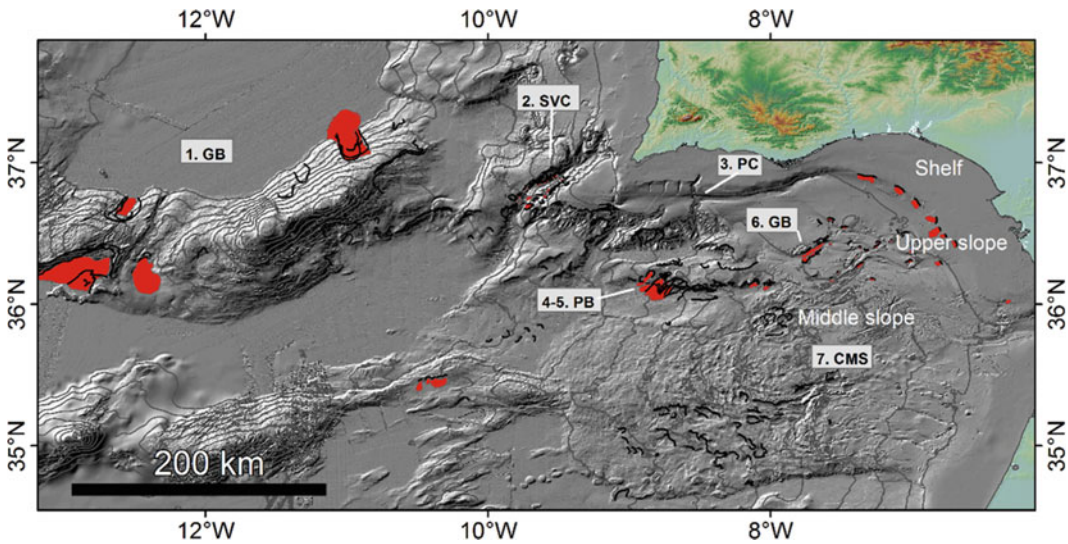

Fig. 4.10 Submarine landslides in the Gulf of Cadiz. Black line, headwall escarpments; red polygon, sliding mass. Taken from Baraza et al. (1999); Maldonado et al. (1999); Mulder et al. (2006, 2009); Hanquiez et al. (2010); León and Somoza (2011); Lo Iacono et al. (2012); Urgeles and Camerlenghi (2013); Omira et al. (2016); León et al. (2020); Serra et al. (2020); Silva et al. (2020). Numbers 1–7 refer to selected landslides to evaluate their tsunamigenic potential (Table 4.2). 1, GO Gorringe Ridge; 2, SVC São Vicente Canyon; 3, PC Portimão Canyon; 4–5, PB Portimão Bank (north and south); 6, GB Guadalquivir Bank; and 7, CMS, contourite middle slope

Banks (SW sector of the Alboran Sea), the Adra Ridge (NE sector of the Alboran Sea; Fig. 4.14 a), the Pollux Bank, the Sabinar Platform, the Western Sabinar, and the Maimonides Ridge (Fig. 4.14b) (e.g., Martínez-García et al. 2010; Vázquez et al. 2015a; Alonso et al. 2014; Galindo-Zaldívar et al. 2018).

The landslides linked to submarine canyons (ii) are identifiable by their heads and flanks in both regions (Figs. 4.10 and 4.11). They feature arcuate slide scars and slumps and provoke a retrogressive erosion. Several landslides are found on the flanks of six submarine canyons on the upper slope of the Gulf of Cadiz: Fado, Salema, Lagos Superior, Portimão, Meninas, and São Vicente (Sayago-Gil et al. 2008; Roque et al. 2012; Serra et al. 2020). In the Alboran Sea, similar landslide features are identifiable in the canyons located on the Spanish margin: La Linea, Guadiaro, Fuengirola, Motril, and Almeria (Estrada et al. 1997; Alonso and Ercilla 2003; Vázquez et al. 2015b; Ercilla et al. 2019); and on the Moroccan margin, with the Nekor and Ceuta Canyons (Ercilla et al. 2002, 2019; Juan et al. 2016).

The landslides linked to open slopes (iii), with lesser density and scattered occurrence (Figs. 4.10 and 4.11), comprise slides and mass flow deposits and affect contourite deposits and features. In the Gulf of Cadiz, they are mainly located on the flanks of contourite channels (e.g., Cadiz and Diego Cao channels; García et al. 2016), inside circular crater-like depressions, and close to diapiric ridges (Mulder et al. 2003, 2009; León and Somoza 2011; León et al. 2020). In the Alboran region, the best example of this category would be the Baraza Slide. It represents an isolated complex landslide, involving debris flow deposits and slumps, which affects the slope's plastered drift along the Spanish margin (Figs. 4.11 and 4.14d, e; Casas et al. 2011; Ercilla et al. 2016; Juan et al. 2016).

The recurrence of landslide events was only quantified for those located in the NW Sector of the Alboran Sea. There, where 53 events were identified, accurate age determinations led us to establish a recurrence interval ranging from 40 to 473 kyr (Alonso et al. 2014), which could be classified as low to moderate in view of the

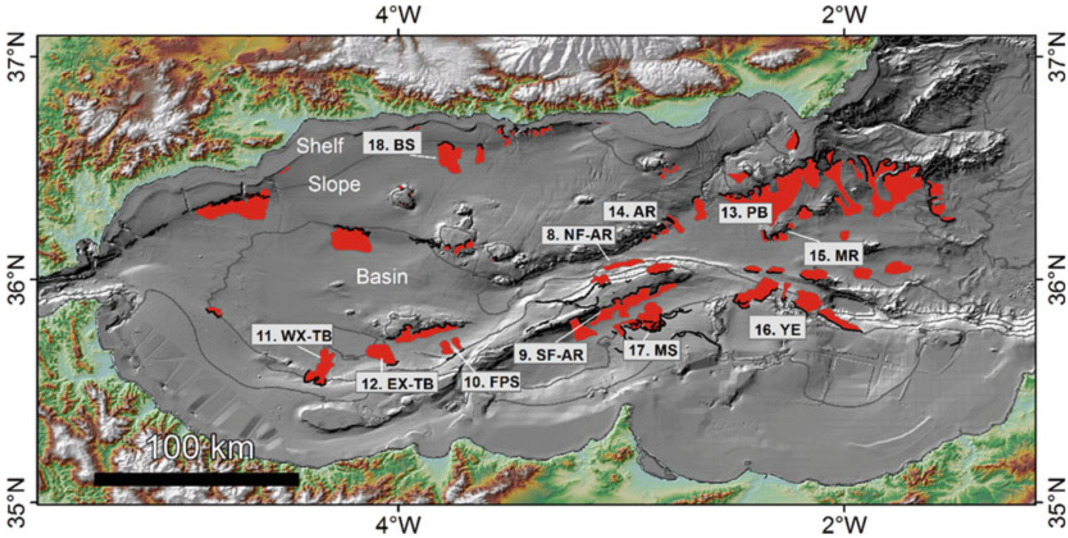

Fig. 4.11 Submarine landslides in the Alboran Sea. Black line, headwall escarpments; red polygon, sliding mass. Taken from Martínez-García et al. (2010); Vázquez et al. (2010a, b, 2015a, b, c); Casas et al. (2011); Alonso et al. (2012; 2014); Rodriguez et al. (2017); Galindo-Zaldívar et al. (2018). Numbers 8–18 refer to selected landslides to evaluate their tsunamigenic potential. 8. NF-AR northern flank of the Alboran Ridge; 9. SF-AR southern flank of the Alboran Ridge; 10. FPS Francesc Pagès Seamount; 11. WX-T western sector of the Xauen and Tofiño Banks; 12. EX-TB eastern sector of the Xauen and Tofiño Banks; 13. PB Pollux Bank; 14.AR Adra Ridge; 15. MR Maimonides Ridge; 16. YE Yusuf Escarpment; 17. MS Montera Slide; and 18. BS Baraza Slide

frequency values obtained in other areas (Piper et al. 2003; Ratzov et al. 2010; Strozyk et al. 2010).

4.5.3 Defining Tsunamigenic Potential

Not unlike coastal landslides, the tsunami amplitude generated often depends on the frontal area and impact velocity; a further key parameter for submerged landslides would be their time evolution (Løvholt et al. 2015). Obviously, no direct data on velocity for the different landslides studied is available, for which reason secondary/deduced parameters had to be used. The set of morphostructural parameters shown in Table 4.2 provided one means of assessing tsunamigenic potential, as a hierarchy, in the study region. The concept behind each parameter relies on the following assumption: potential tsunamigenic submarine landslides in an area can be qualitatively estimated or ranked after a normalized aggregation of all known values that could possibly contribute to triggering tsunami waves.

The median of the slope of the headwall scar was selected in order to correlate a hierarchy related to the velocity of the process. The highest values of the slope were correlated with a possibly high value for the velocity of the landslide process. This is known to be correct if all the other parameters remain equal, providing that the force acting parallel to the rupture plane increases with a greater angle of the rupture plane.

Four parameters were adopted to consider the tsunamigenic potential in terms of the size-magnitude of the landslide event: evacuated height, volume of the deposit, headwall scar depth, and retrogressive character. The (i) evacuated height is correlated with the vertical movement of the landslide and subsequent motion transferred to the water column, (ii) the volume with the magnitude (energy) of the event, (iii) the headwall scar depth with the frequency dispersion, the attenuation of the movement, or

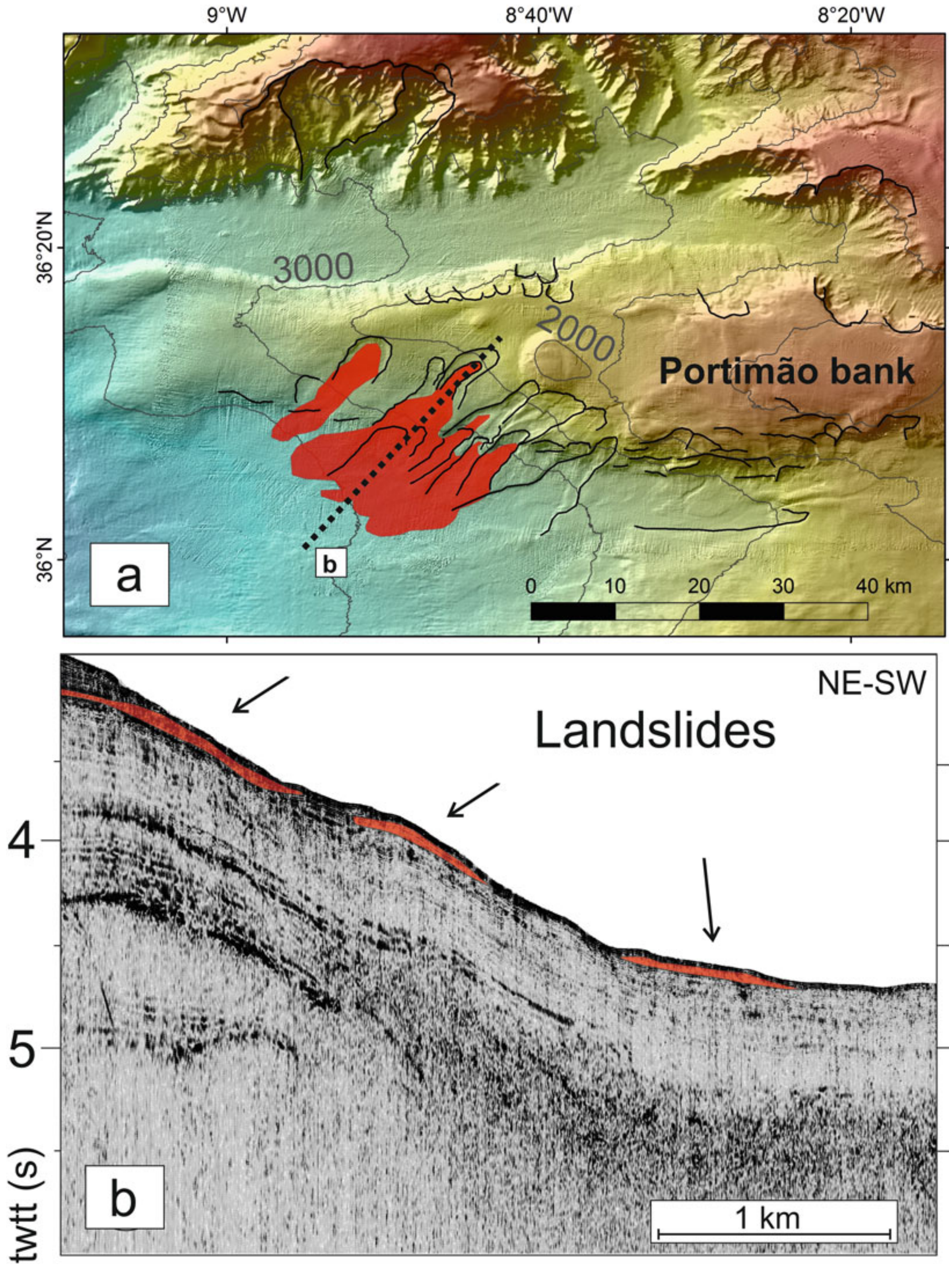

Fig. 4.12 Selected examples of submarine landslides in the Gulf of Cadiz: **a** Bathymetric map of Portimão Bank indicating headwall escarpments (black lines) and landslide deposits (red polygon); **b** Seismic profile crossing the landslides of the Portimão Bank. Bathymetric contours every 500 m. Bathymetric data obtained from MONTERA (IEO; ICM-CSIC) project and EMODnet Bathymetry Consortium (2018)

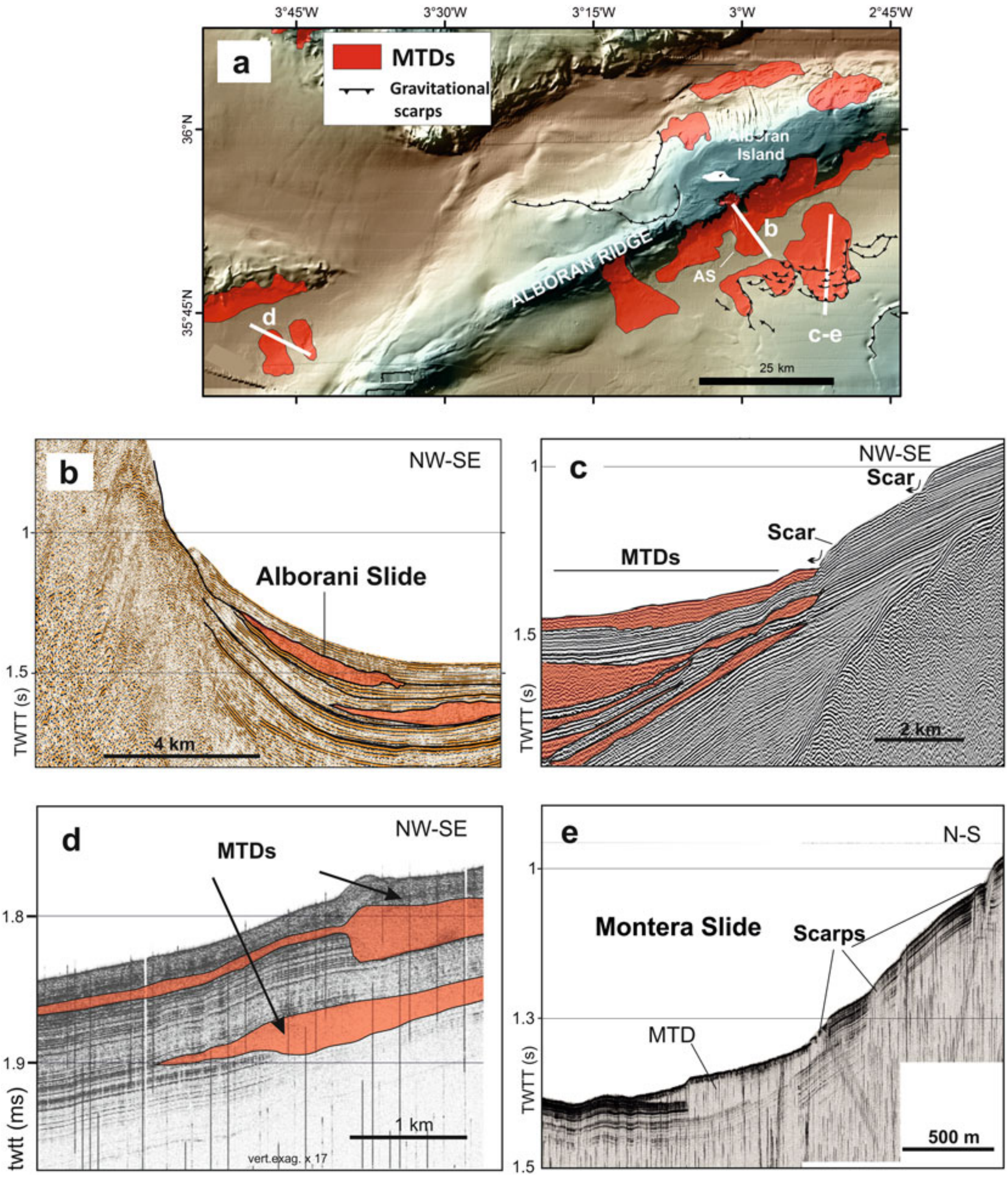

Fig. 4.13 Selected examples of landslides linked to seamounts in the central and SW sectors of the Alboran Sea. **a** Bathymetric map showing landslides on the Alboran Ridge; **b** Seismic profile crossing the southern Alboran Ridge showing stacked debris flows within the Quaternary record (modified from Macías et al. 2015. Reprinted with permission from Elsevier); **c** Parametric high-resolution profile showing landslides on the northern flank of the Alboran Ridge (modified from Galindo-Zaldívar et al. 2018. Reprinted with permission from John Wiley and Sons). **d** and **e** Parametric high-resolution profile and seismic profile of the Montera Slide at the Tres Forcas Promontory

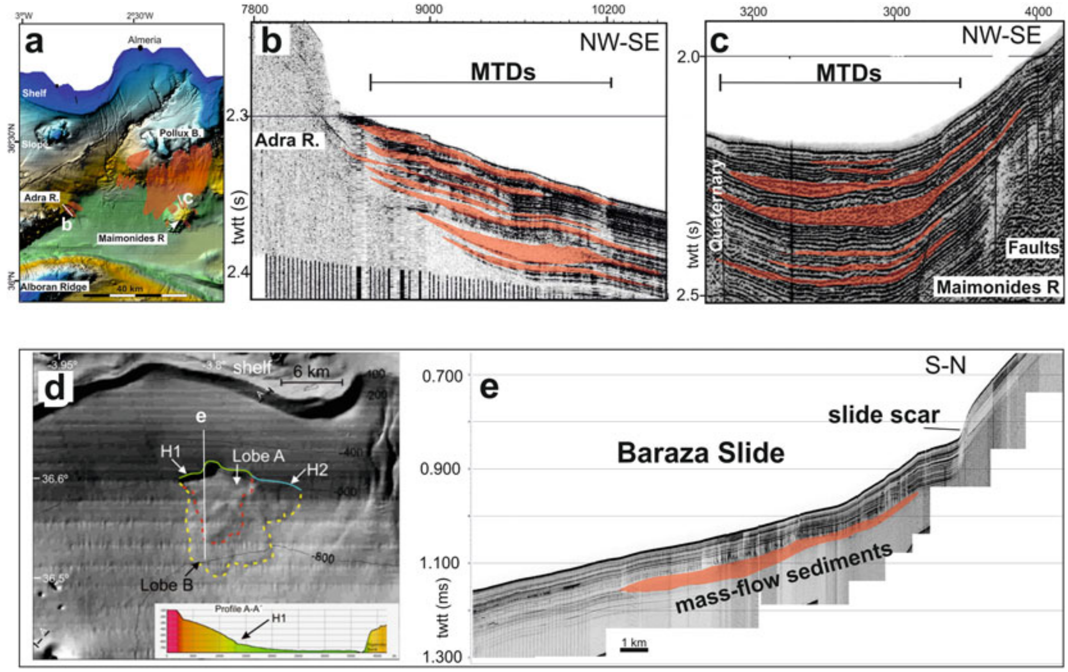

Fig. 4.14 Selected examples of submarine landslides linked to seamounts in the NW sector and to open slopes in the NE sector of the Alboran Sea. **a** Bathymetric map showing landslides linked to seamounts; **b** Topas profile crossing the landslides of the Adra Ridge; **c** Seismic profile across the landslides of the Maimonides Ridge (a, b, and c modified from Alonso et al. 2014. Reprinted with permission from Springer Nature); **d** and **e** Bathymetric map and topas profile of the Baraza Slide (modified from Casas et al. 2011. Reprinted with permission from Springer Nature)

the energy along the water column (landslides in shallow waters are more critical), and (iv) the presence of retrogressive and multi-event structures with a decrease in tsunamigenic potential (Harbitz et al. 2006).

The landslide dynamics were established as a geological/seismic proxy of released energy and velocity of the gravitational process. The velocity and coherence of the movement were correlated with a possible transference of the seafloor deformation and associated morphological changes to the water column. In this way, a tsunamigenic potential hierarchy could be established for the landslide process. Debris avalanches are cataloged as the most tsunamigenic process due to their inferred velocity (Masson et al. 2006). Slides are catalogued with moderate and high tsunamigenic potential, due to their coherent dynamics in the block, whereby their potential for transferring deformation to the water column. Rotational slides (i.e., slumps), where a thick slide block with a steep headwall can move rapidly downwards, may be particularly effective in generating tsunami waves, even when the area covered is minor and little effect is seen on the seafloor downslope of the immediate landslide site (Masson et al. 2006). Mass flows have limited tsunamigenic potential. Internal facies can be used as a proxy of sediment disaggregation and, subsequently, the energy released in the process. Finally, two ratios, maximum width of the MTDs *versus* runout and height of the evacuation zone versus runout, were used to measure the tsunamigenic potential of landslides based on the dynamics of mass transport (Masson et al. 2006) and the correlation between slumps and disintegrative movements (McAdoo et al. 2000), respectively.

The total area of the tsunamigenic landslide zone identified can be inversely correlated with

Table 4.2 Morphostructural parameters used to organize the 18 selected examples of submarine landslides with tsunamigenic potential and to discuss the tsunamigenesis of sedimentary instabilities in the Gulf of Cadiz-Alboran Sea region

	Size-magnitude							Velocity	MMDyn: size-magn			Other	T-Value	
	PTZ		Head-scarp height (m)	Area (km^2)	Vol (km^3)	H-Scar depth (mwd)	Retro & ME Stru	Scar slope (°)	Dynamic type	Internal facies	Deposit elongation (Wd/Ld)	Seismicity hazard (ZESIS)		
	Nº events	Area of PTZ (km^2)												
Gulf of Cadiz														
1 Gorringe Bank	29	29,139	684	427.50	242	2462	Yes	14.5	A/S	Ch	0.63	Very high	0.835	High
2 São Vicente Canyon	71	2956	277	0.89	0.03	1826	Yes	21	SI	ND	0.59	Very high	1	High
3 Portimão Canyon	3	430	46	5.5	0.04	276	ND	18	S	Ch	0.13	Very high	0.386	Middle
4 Sf Portimão Bank	56	2703	77	16.3	2.12	1995	Yes	14.5	MF	Ch	0.24	Very high	0	Low
5 Nf Portimão Bank	20	1317	94	4.9	0.37	2244	Yes	19.5	S	ND	0.63	Very high	0.624	High
6 Guadalquivir Bank	5	109	163	1.50	0.06	475	Low	18.5	SI	Ch	0.51	Very high	0.627	High
7 Contourite M Slope	43	3744	41	3.95	0.27	640	Low	17	S	HS	0.25	Very high	0.533	Middle
Alboran Sea														
8 Nf-Alboran Ridge	1	110	80	10	1.04	230	Yes/yes	15	MF	ND	0.99	Very high	0.557	Middle
9 Sf-Alboran Ridge	9	190	90	27	4.42	174	Yes/yes	14.5	S/MF	StD	2.99	Very high	1	High
10 Francesc Pages Seamount	2	40	40	21	3.06	1202	No/no	6	MF	StD HS	0.72	Very high	0.167	Low

(continued)

Table 4.2 (continued)

	Size-magnitude							Velocity	MMDyn: size-magn			Other	T-Value	
	PTZ		Head-scarp height (m)	Area (km^2)	Vol (km^3)	H-Scar depth (mwd)	Retro & ME Stru	Scar slope (°)	Dynamic type	Internal facies	Deposit elongation (Wd/Ld)	Seismicity hazard (ZESIS)		
	Nº events	Area of PTZ (km^2)												
11 W Xauen-Tofiño banks	2	108	45	108	32.93	816	Yes/yes	6	MF	Ch-Tr	2.50	Very high	0.371	Middle
12 E Xauen-Tofino banks	4	86	20	86	23.67	958	Yes/yes	5	MF	Ch-Tr HS	0.75	Very high	0.179	Low
13 Pollux Bank	6	418	3	418	234.38	687	Yes/yes	6	MF	Ch-Tr	0.29	High	0	Low
14 Adra Ridge	2	28.4	30	28	4.65	1500	No/no	5	MF	Ch-Tr HS	0.46	Very high	0.065	Low
15 Maimonides Ridge	4	129	25	129	42.61	1511	Yes	12	MF	StD	0.77	High	0.044	Low
16 Yusuf Escarpment	3	89	85	89	24.87	1810	Yes	10	SI	ND	0.42	Very high	0.359	Middle
17 Montera Slide	2	107	55	107	32.49	734	Yes	5	MF	Ch-Tr HS	1.50	Very high	0.302	Middle
18 Baraza Slide	2	116	53	116	36.53	590	Yes	6.5	MF	Ch-Tr HS	1.69	Very high	0.365	Middle

the tsunamigenic potential, particularly if the number of landslides identified within that area correlates directly. The idea is to approach a density factor, where a denser area (in terms of landslides) would have greater potential than a less dense area. Therefore, the larger the area, the lower the tsunamigenic potential; and the larger the number of landslides identified, the greater the tsunamigenic potential. The final equation can be written as follows:

$$T = \sum\nolimits_j^t \frac{\left(\sum_i^n \left(\frac{P_i - P_i^{\min}}{P_i^{\max} - P_i^{\min}}\right)\right)_j - \left(\sum_i^n \left(\frac{P_i - P_i^{\min}}{P_i^{\max} - P_i^{\min}}\right)\right)_j^{\min}}{\left(\sum_i^n \left(\frac{P_i - P_i^{\min}}{P_i^{\max} - P_i^{\min}}\right)\right)_j^{\max} - \left(\sum_i^n \left(\frac{P_i - P_i^{\min}}{P_i^{\max} - P_i^{\min}}\right)\right)_j^{\min}};$$

$$\begin{cases} if \quad T \geq 0.6 \rightarrow high \\ if \quad 0.6 \quad < T \leq 0.3 \rightarrow medium \\ if \quad T < 0.3 \rightarrow low \end{cases}$$

where T is tsunamigenic potential and Pi is any of the aforementioned parameters. Each parameter is normalized (from 0, the minimum value of P, to 1, the maximum value of P) and then areas (each j) are again normalized.

The interpretation of the results is therefore consistent with a qualitative or hierarchical classification, with little room for doubt: any given tsunamigenic potential is related to the database's domain and, hence, incomparable with other databases or domains.

In the Gulf of Cadiz, volume and head-scarp height are the two parameters showing the highest degree of asymmetry, yet they are not at all predominant. Sharp changes in any single parameter indexed (max–min alteration) do not significantly vary the output of the hierarchy, meaning that the method is very robust and consistent. Moreover, a log-distributed version of the proposed classification method would not alter the hierarchy for the two highest ranked ones, and would drop just one category for the rest. Even though the selection criteria of the parameters were oriented toward independency, in order that each parameter should be equally weighted, a simple Pearson independency test shows a very poor overall correlation between the parameters. The highest Pearson coefficients are an artifact of asymmetry, and even so, the overall internal correlation is lower than 0.3. Therefore, despite the scant information, it can safely be claimed that in the Gulf of Cadiz, the Hirondelle Seamount, the Gorringe Ridge, and São Vicente Canyon are the areas with the highest tsunamigenic potential. The tsunamigenic potential of the Portimão (north) and Guadalquivir Banks are somewhere between high and medium (Table 4.2).

In the Alboran Sea, the southern flank of the Alboran Ridge clearly represents the area with the highest potential to generate landslides which could in turn trigger tsunamis (Table 4.2). This is followed by the northern flank within the limits of medium tsunamigenic potential, mainly due to its elongation ratio and dynamic type. The areas of the western Xauen-Tofiño Banks, Yusuf Escarpment, and Montera and Baraza Slides are all near the limit between medium and low potential, leaving the remainder well within the lowest hierarchy. Given the methodology used, the exclusion of any single type of data leads to a very slight variation to no change, whereas if a category is discarded for only two items, the data would be at the limit of the category. This criterion is a good indicator, suggesting that the hierarchy method is very robust. Again, the Pearson coefficients are extremely low, below 0.2, with only one exception: the ratio of the area of the tsunamigenic potential and the number of events, which increases to around 0.4 in a direct relationship. Even if the correlation is very low, the poor direct relationship seems reasonable, resulting in a greater number of events recorded in larger areas, which means in this case that the average density of events is around 35 × 10–3 per km^2 (Table 4.2).

Although the proposed method evaluates each area internally, meaning that each one has its own non-comparable hierarchy, a further test involved the full-range indexing of the parameters, as if the Gulf of Cadiz and the Alboran Sea were integrated into the same area. Only three hierarchies were seen to change, namely those closer to a class limit within less than a 10% variation. This contributed to confirming that the Gulf of Cadiz is clearly the most tsunamigenic area.

4.5.4 Recommendations for Future Actions

A full appraisal of the areas with tsunamigenic landslides calls for further work, because there are still important gaps in knowledge. To this end, the dataset should include the following:

(i) the identification of sediment core sites, as events may be missing or under-represented depending on the depositional location;
(ii) the recurrence of landslide events, especially near highly populated areas;
(iii) the dating and timing of slope failure processes; and
(iv) an understanding of the early post-failure evolution of submarine slopes, which is critical for assessing the potential of submarine landslides for generating tsunami waves.

As in the case of the study of active faults, this would imply longer sediment core recovery, high- and ultra-high-resolution geophysical data acquisition, *in situ* geotechnical measurements and observations, long-term monitoring, and major modeling efforts.

4.6 Discussion and Conclusions

Of all the possible mechanisms proposed in the literature as tsunamigenic sources, the two with the greatest potential in the Gulf of Cadiz-Alboran Sea region are associated with seismotectonic faults and submarine landslides. The most important mechanism would be seismotectonic fault activity which, in conjunction with the seafloor overstepping process and the mechanical properties of sediments, could trigger sediment landslides. The recent geological history of this region provides examples of significant seismic activity and Quaternary-to-contemporary fault activity, which have generated structural reliefs of varying importance and associated landslides. Both sources are clearly expressed by the seafloor landscape. By analyzing the susceptibility of two potential tsunamigenic sources—seismotectonic activity and submarine landslides—we have been able to establish a qualitative series of considerations regarding the relative importance of these two processes.

4.6.1 Seismotectonic Sources

In the Gulf of Cadiz, seismic activity mainly derives from areas trending NE-SW, where the concentration of events at crustal levels is high, both in number and magnitude (Fig. 4.2). These areas correlate well with the main tectonic relief features of the region, characterized by steep slopes. In this sense, noteworthy activity is observed in association with the Hirondelle Seamount and the Gorringe Ridge. A second focal point (Fig. 4.2) would correspond to the western Portuguese continental margin and its continuation along the border between the lower continental slope and the Horseshoe Abyssal Plain. Two other foci showing a high density of events correspond to the Coral Patch Seamount-Ridge system and to the Portimão and Guadalquivir Banks chain, the latter located on the southern Portuguese continental margin. Hence, there is a direct correlation between seismic activity and the main thrust systems described in the region (Fig. 4.3), from NE-SW to ENE-WSW (Rosas et al. 2016), which implies that the regional stress is in turn responsible for the main positive underwater reliefs in the physiography (Terrinha et al. 2003, 2009; Rosas et al. 2009). Regional listric normal fault systems are a secondary cause, both systems being located in proximal sectors of the Iberian and Moroccan continental margins; they have associated earthquake accumulations of less density, characterized by lower magnitudes (Fig. 4.2), while the vertical movement relating to fault activity would not generate such significant offset on the seafloor surface. Consequently, these faults have a moderate potential. In contrast, the SWIM fault system (Fig. 4.2) appears to be associated with relatively low seismic activity (Hensen et al. 2019). This low activity mainly affects its eastern segments, while the western segment, at the eastern sector of the Horseshoe Abyssal Plain (between the lower continental slope and the Gorringe Ridge), exhibits higher activity, given its intersections with the Horseshoe and Gorringe Ridge thrusts (Rosas et al. 2016; Silva et al. 2017). Notwithstanding this, the SWIM fault system has been proposed as a possible transform plate boundary between the Eurasia and Nubia plates (Zitellini et al. 2009), and its trace is followed in a very marked way on the seafloor in some of its segments (Terrinha et al. 2009). The general seismic activity of the SWIM system can be attributed to low deformation velocity or even blocked behavior (Cunha et al. 2012; Hensen et al. 2019).

In the Alboran Sea, earthquakes of an intermediate depth (>60 km) are not taken into account for this purpose. Shallow seismic activity corresponds to the indentation model of the Alboran Ridge (Estrada et al. 2018a). The main deformation is assumed along the transverse Alboran shear zone (Fig. 4.2), which partly corresponds to the western boundary of the indenter block and consists of NNE-SSE left-lateral strike-slip faults, such as those of the Al-Idrissi and the Motril-Djibouti marginal platform fault systems (Vázquez et al. 2018), the former characterized by transpressive features in one of its segments (Figs. 4.6 and 4.7). Throughout that zone, two higher seismicity accumulations can be distinguished on the Moroccan (Al Hoceima area) and Spanish (Adra area) margins. Less markedly, another two seismic concentrations are associated with the northern front of the Alboran Ridge, which corresponds to an ENE-WSW thrust system verging toward the north; and with the Yusuf-Habibas Escarpment, triggered by a WNW-ESE right-lateral strike-slip fault system. In the Alboran Sea, the relationship between submarine reliefs and seismicity is not always so evident. The fault activity of the northern flank of the Alboran and Xauen Seamounts is clear, as is that of the minor Adra margin fault anticline. A vertical secondary transpressive component has been identified in the central segment of Al Idrissi fault, while a transtensive component characterizes the Yusuf-Habibas fault, with an associated pull-apart basin (Mauffret et al. 2007). Faults of this WNW-ESE family include the Averroes fault zone (Estrada et al. 2018a). The La Serrata-Carboneras left-lateral NE-SW strike-slip fault, easily imaged on the seafloor and active along its entire trace during the Late Quaternary (Silva et al. 1993; Bell et al. 1997; Masana et al. 2018), has no associated seismic activity. This lack of seismic events could indicate that the La Serrata-Carboneras fault is blocked. Its direction (Fig. 4.6) with respect to the regional stress (Fig. 4.2) does not favor the action of a strike-slip fault, although it may favor its reactivation as a compressive fault.

From a seismotectonic point of view, the Gulf of Cadiz is the area in Spain with the highest potential for triggering tsunami waves as a result of fault activity (Table 4.1). The thrust systems of the Gorringe Ridge and the Marquês de Pombal, the São Vicente Canyon, and the Horseshoe faults have a high potential. For their part, the thrust systems of the Coral-Patch and Guadalquivir Ridges and the listric fault system of the Iberian margin have a moderate potential, while the transform SWIM system has a low potential (Table 4.1). In the Alboran Sea, the ENE-WSW thrusts have the highest potential of all: the north flank of the Alboran Ridge has a high potential, while the North Xauen thrust system (D'Acremont et al. 2020), in the south-western prolongation of the Alboran Ridge, and the Adra margin thrust (Vázquez et al. 2016) have a moderate to high one. The NNE-SSW transpressive segment of the Al Idrissi fault also displays a moderate to high potential, as with the WNW-ESE Yusuf-Habibas and Averroes faults. The rest of the strike-slip faults in the Gulf of Cadiz have a low potential (Table 4.1).

4.6.2 Submarine Landslide Area Sources

There are many areas affected by landslides throughout the Gulf of Cadiz and the Alboran Sea, probably as a consequence of the important seismic and tectonic activity in the region as a whole during the Quaternary (Figs. 4.10 and 4.11). Landslides are located on both the continental slope of the margins and on the flanks of seamounts. When comparing the landslides of the two areas, however, there are few differences in their distribution and size. In the Gulf of Cadiz, landslides are larger in volume (Table 4.2) and affect the flanks of main seamounts as well as canyon walls. This fact clearly evinces the correlation between active seismotectonic processes, relief generation, and oversteeping with large-scale slope failures. In the Alboran Sea, landslides are of a comparatively minor scale (Table 4.2), affecting not only the flanks of the seismic and uplifting seamounts (Alboran Ridge and Xauen-Tofiño-Pagès Seamount chains) related not only to the intersection with the trans-Alboran shear zone but also to the open continental slope of both the Spanish and Moroccan margins. In the latter case, this is probably due to the interplay between the tilting of the margins—in turn, owing to the important regional Quaternary compression (Vázquez 2001; Martínez-Garcia et al. 2013; Estrada et al. 2018a)—and the activity of the surrounding seismic faults.

These results suggest that the Gulf of Cadiz is the area with the highest potential for triggering tsunamigenic landslides (Table 4.2), especially the Hirondelle Seamount and the Gorringe Ridge, which form a chain of up to 5000 m in relief, the Portimão and Guadalquivir Banks, and the margins of the São Vicente Canyon. In the Alboran Sea, the most outstanding areas are the Alboran Ridge, with a high potential on its southern flank and a moderate one on its northern counterpart, and the western Xauen-Tofiño Seamount chain and the Yusuf Escarpment, both with a moderate potential (Table 4.2).

4.6.3 Interplay Between Different Factors in the Region

Throughout this discussion, seismotectonic structures and related landslide zones have been identified as the main potential tsunamigenic sources. Clear examples of this relationship are to be found in the Gorringe Ridge and the Portimão Bank in the Gulf of Cadiz, and the Alboran Ridge in the Alboran Sea. These three major underwater ridges, with linear flanks and steep slopes, are characterized by active thrust systems showing significant seismic activity, and landslide systems developed on their flanks. Therefore, in this scenario, the interplay between the two sources may facilitate the generation of tsunami waves. High-magnitude seismotectonic events displace the seafloor, and subsequently trigger submarine landslides on seamount flanks. In such cases, the theoretically generated tsunami would have a dual component, meaning it could either modulate or produce a second successive wave that could increase its impact.

Acknowledgements This work was supported by the Spanish projects INCRISIS, DAMAGE (CGL2016-80687-R AEI/FEDER), FAUCES (CTM2015-65461-C2-1-R) and INPULSE (CTM2016-75129-C3-1-R), RIGEL (*Instituto Español de Oceanografía*), PAPEL (B-RNM-301-UGR18), AGORA (P18-RT-3275), RNM 148 and RNM 328 (*Junta de Andalucía*), as well as by the French program Actions Marges, the Marlboro cruise, and the EUROFLEETS program-SARAS cruise (FP7/2007-2013; 228344). The *Secretaría General de Pesca* (Spain) provided the bathymetric data from the northern part of the Alboran Sea. The IHS-Kingdom Geoscience educational license is also acknowledged.

References

Alonso B, Ercilla G (2003) Small turbidite systems in a complex tectonic setting (SW Mediterranean Sea): morphology and growth patterns. Mar Pet Geol 19 (10):1225–1240

Alonso B, Ercilla G, Vázquez JT et al (2012) Caracterización morfo-sísmica de las inestabilidades sedimentarias del sector oriental del Mar de Alborán durante el Cuaternario (SO Mediterráneo). Geo-Temas 13:561–564

Alonso B, Ercilla G, Garcia M et al (2014) Quaternary mass-transport deposits on the North-Eastern Alboran Seamounts (SW Mediterranean Sea). In: Krastel S et al (eds) Submarine mass movements and their consequences: 6th international symposium. Advances in natural and technological hazards research, vol 37. Springer, Cham, pp 561−570

Álvarez-Gómez JA, Aniel-Quiroga Í, González M et al (2011a) Scenarios for earthquake-generated tsunamis on a complex tectonic area of diffuse deformation and low velocity: the Alboran Sea, Western Mediterranean. Marine Geol 284(1–4):55–73

Álvarez-Gómez JA, Aniel-Quiroga Í, González M et al (2011b) Tsunami hazard at the Western Mediterranean Spanish coast from seismic sources. Nat Hazards Earth Syst Sci 11:227–240. https://doi.org/10.5194/nhess-11-227-2011

Argus DF, Gordon RG, DeMets C, Stein S (1989) Closure of the Africa-Eurasia-North America plate motion circuit and tectonics of the gloria fault. J Geophys Res 94(B5):5585–5602

Assier-Rzadkiewic S, Heinrich P, Sabatier PC et al (2000) numerical modelling of a landslide-generated Tsunami: the 1979 nice event. Pure Appl Geophys 157:1707–1727. https://doi.org/10.1007/PL00001057

Bakun WH, Wentworth CM (1997) Estimating earthquake location and magnitude from seismic intensity data. Bull Seismol Soc Am 87:1502–1521

Ballesteros M, Rivera J, Muñoz A et al (2008) Alboran Basin, southern Spain—Part II: neogene tectonic implications for the orogenic float model. Mar Pet Geol 25:75–101

Baraza J, Ercilla G, Nelson CH (1999) Potential geologic hazards on the eastern Gulf of Cadiz slope (SW Spain). Mar Geol 155(1–2):191–215

Bartolomé R, Gràcia E, Stich D et al (2012) Evidence for active strike-slip faulting along the Eurasia-Africa convergence zone: implications for seismic hazard in the southwest Iberian margin. Geology 40(6):495–498

Batista MA, Miranda J, Chierici F et al (2003) New study of the 1755 earthquake source based on multichannel seismic survey data and tsunami modeling. Nat Hazards Earth Syst Sci 3:330–340

Bell JW, Amelung F, King GCP (1997) Preliminary late quaternary slip history of the Carboneras fault, southeastern Spain. J Geodyn 24:51–66

Bourgois J, Mauffret A, Ammar A et al (1992) Multichannel seismic data imaging of inversion tectonics of the Alboran Ridge (Western Mediterranean Sea). Geo-Marines Lett 12(2–3):117–122

Bryant EA (2014) Tsunami: The Underrated Hazard, 3rd edn. Springer, Berlin-Heidelberg

Buforn E, Udías A, Colombás MA (1988) Seismicity, source mechanism and tectonics of the Azores-Gibraltar plate boundary. Tectonophysics 152:89–118

Buforn E, Udías A, Madariaga R (1991) Intermediate and deep earthquakes in Spain. Pure Appl Geophys 136:375–393

Buforn E, Pro C, Sanz de Galdeano C, Cantavella JV et al (2017) The 2016 south Alboran earthquake (Mw = 6.4): a reactivation of the Ibero-Maghrebian región? Tectonophysics 712–713:704–715

Buforn E, Coca P, Bezzeghoud M, Udías A et al (2019) The destructive 1790 Oran (NW Algeria) earthquake in a region of low seismicity. Tectonophysics 759:1–14

Buforn E, Udías A, Pro C (2015) Large earthquakes at the Ibero-Maghrebian region: basis for an EEWS. Pure Appl Geophys 172(9):2387–2396

Cabieces R, Buforn E, Cesca S et al (2020) Focal parameters of earthquakes offshore Cape St. Vincent using an amphibious network. Pure Appl Geophys 177:1781–1800

Casas D, Ercilla G, Yenes F et al (2011) The Baraza slide: model and dynamics. Marine Geophys Res 32:245–256

Casas D, Casalbore D, Yenes M et al (2015) Submarine mass movements around the Iberian Peninsula. The building of continental margins through hazardous processes. Boletín Geológico y Minero 126(2–3):257–278

Chalouan A, Galindo-Zaldívar J, Akil M et al (2006) Tectonic wedge escape in the southwestern front of the Rif Cordillera (Morocco). Geol Soc Lond 262:101–118

Chalouan A, Gil AJ, Galindo-Zaldívar J et al (2014) Active faulting in the frontal Rif Cordillera (Fes region, Morocco): constraints from GPS data. J Geodyn 77:110–122

Comas MC, García-Dueñas V, Jurado MJ (1992) Neogene tectonic evolution of the Alboran Sea from MCS data. Geo-Marines Lett 12(2–3):157–164

Comas, MC, Platt JP, Soto JI et al (1999) The origin and tectonic history of the Alboran Basin: insights from Leg 161 results. In: Zahn R, Comas MC, Klaus A (eds) Proceedings of the ocean drilling program scientific results 161. Ocean Drilling Program, College Station, pp 555–580

Costa PJM, Leroy SAG, Kershaw S et al (2005) Tsunamis: causes, behaviour and sedimentary signature. Studies on the AD 1755 (Portugal). In: Martínez-Frías J, Madero J (eds) Meteoritos y Geología Planetaria. Museo de la Ciencia de Castilla-La Mancha, Cuenca, pp 151–171

Cunha TA, Matias LM, Terrinha P et al (2012) Neotectonics of the SW Iberia margin, Gulf of Cadiz and Alboran Sea: a reassessment including recent structural, seismic and geodetic data. Geophys J Int 188:850–872

Custódio S, Lima V, Vales D et al (2016) Imaging active faulting in a region of distributed deformation from the joint clustering of focal mechanisms and hypocentres: application to the Azores-western Mediterranean region. Tectonophysics 676:70–89

d'Acremont E, Lafosse M, Rabaute A et al (2020) Polyphase tectonic evolution of fore-arc basin related to STEP fault as revealed by seismic reflection data from the Alboran Sea (W-Mediterranean). Tectonics 39:e2019TC005885. https://doi.org/10.1029/2019TC005885

d'Acremont E, Lafuerza S, Rabaute A et al (2022) Distribution and origin of submarine landslides in the active margin 2 of thesouthern Alboran Sea (Western Mediterranean Sea) Mar Geol 445:106739

Dawson AG, Stewart I (2007) Tsunami deposits in the geological record. Sed Geol 200:166–183

Delvaux D, Barth A (2010) African stress pattern from formal inversion of focal mechanism data. Tectonophysics 482:105–128

Delvaux D, Sperner B (2003) New aspects of tectonic stress inversion with reference to the TENSOR program. Geol Soc Lond 212:75–100

Delvaux D, Moeys R, Stapel G et al (1997) Paleostress reconstructions and geodynamics of the Baikal region, Central Asia. Part II: cenozoic rifting. Tectonophysics 282:1–38

DeMets C, Gordon R, Argus DF et al (1994) Effect of recent revisions to the geomagnetic reversal time scale on estimates of current plate motions. Geophys Res Lett 21:2191–2194

Dewey JF, Helman ML, Turco E et al (1989) Kinematics of the western Mediterranean. In: Coward MP, Dietric D, Park RG (eds) Alpine tectonics, vol 45. Geological Society of London, Special Publication, pp 265–283

Do Couto D, Gorini C, Jolivet L et al (2016) Tectonic and stratigraphic evolution of the western Alboran Sea basin in the last 25Myrs. Tectonophysics 677:280–311

Duarte JC, Rosas FM, Terrinha P et al (2011) Thrust-wrench interference tectonics in the Gulf of Cadiz (Africa-Iberia plate boundary in the North-East Atlantic): insights from analog models. Mar Geol 289(1–4):135–149

Duarte JC, Rosas FM, Terrinha P et al (2013) Are subduction zones invading the Atlantic? Evidence from the southwest Iberia margin. Geology 41:839–842

El Alami SO, Tadili BA, Cherkaoui TE et al (1998) The Al Hoceima earthquake of May 26, 1994 and its aftershocks: a seismotectonic study. Ann Geophys 41:519–537

EMODnet Bathymetry Consortium (2018) Digital terrain model. https://www.emodnet-bathymetry.eu/home. Accessed 30 Apr 2020

Ercilla G, Juan C, Hernández-Molina FJ et al (2016) Significance of bottom currents in deep-sea morphodynamics: an example from the Alboran Sea. Mar Geol 378:157–170

Ercilla G, Juan C, Periáñez R et al (2019) Influence of alongslope processes on modern turbidite systems and canyons in the Alboran Sea (southwestern Mediterranean). Deep Sea Res Part I 144:1–16

Ercilla G, Baraza J, Alonso B et al (2002) The Ceuta Drift, Alboran Sea, southwestern Mediterranean. In: Stow DAV Stow et al (eds) Deep-water contourite systems: modern drifts and ancient series, seismic and sedimentary characteristics. Geol Soc Lond Memoirs 22(1):155–170

Ercilla G, Vázquez JT, Alonso B et al (2021) Seafloor morphology and processes in the Alboran Sea. In: Baéz JC et al (eds) Alboran sea and its marine resources, Ch. 6. Springer Nature Switzerland AG, pp 157–205

Ercilla G, Casas D, Alonso B et al (2021) Offshore Geological Hazards: Charting the Course of Progress and Future Directions.Oceans 2:393–428

Estrada F, Ercilla G, Alonso B (1997) Pliocene-quaternary tectonic-sedimentary evolution of the NE Alboran Sea (SW Mediterranean Sea). Tectonophysics 282(1–4):423–442

Estrada F, Galindo-Zaldívar J, Vázquez JT et al (2018a) Tectonic indentation in the central Alboran Sea (westernmost Mediterranean). Terra Nova 30(1):24–33. https://doi.org/10.1111/ter.12304

Estrada F, Galindo-Zaldívar J, González-Vida JM et al (2018b) Indentación Tectónica en la Zona Central del Mar de Alboran. In: Canora C et al (eds) Avances en el estudio de Fallas Activas, Terremotos y Peligrosidad Sísmica de Iberia. III Reunión Ibérica sobre Fallas Activas y Paleosismología, Alicante, pp 121–124

Fernández-Puga MC, Vázquez JT, Medialdea T et al (2010) Morphological and geophysical evidences of tectonic activity in the Gulf of Cadiz northern continental slope sector. In: Insua-Arévalo JM, Martín-González F (eds) Contribución de la Geología al Análisis de la Peligrosidad Sísmica. I Reunión Ibérica sobre Fallas Activas y Paleosismología, Sigüenza, pp 159–162

Fernández-Puga MC, Vázquez JT, Sánchez-Guillamón O et al (2014) Evidences of contemporary tectonic activity along the eastern Gulf of Cadiz continental shelf and upper slope (SW Iberian Peninsula). In: Álvarez-Gómez JA, Martín-González F (eds) Una aproximación multidisciplinar al estudio de las fallas activas, los terremotos y el riesgo sísmico. II Reunión Ibérica sobre Fallas Activas y Paleosismología, Lorca, pp 85–88

Flinch JF, Soto JI (2017) Allochthonous triassic and salt tectonic processes in the Betic-Rif orogenic arc. In: Soto JI, Flinch JF, Tari G (eds) Permo-triassic salt provinces of Europe, North Africa and the atlantic margins. Tectonics and hydrocarbon potential. Elsevier, Amsterdam, pp 417–446

Flinch JF (1996) Accretion and extensional collapse of the external Western Rif (Northern Morocco). In: Ziegler PA, Horvath F (eds) Peri-Tethys Memoir 2: structure and prospects of Alpine basins and forelands. Mémoires du Muséum national d'histoire naturelle 170:61–85

Galindo-Zaldívar J, Chalouan A, Azzouz O et al (2009) Are seismological and geological observations of the Al Hoceima (Morocco Rif) 2004 earthquake (M = 6.3) contradictory? Tectonophysics 475:59–67

Galindo-Zaldívar J, Ercilla G, Estrada F et al (2018) Imaging the growth of recent faults: the case of 2016–2017 seismic sequence sea bottom deformation in the Alboran Sea (Western Mediterranean). Tectonics 37:2513–2530. https://doi.org/10.1029/2017TC004941

García M, Hernández-Molina FJ, Alonso B et al (2016) Erosive sub-circular depressions on the Guadalquivir Bank (Gulf of Cadiz): interaction between bottom current, mass-wasting and tectonic processes. Mar Geol 378:5–19

García-Mayordomo J (2015) Creación de un modelo de zonas sismogénicas para el cálculo del mapa de peligrosidad sísmica de España. IGME, Madrid

García-Mayordomo J, Martín-Banda R, Insua-Arévalo JM et al (2017) Active fault databases: building a bridge between earthquake geologists and seismic hazard practitioners, the case of the QAFI vol 3 database. Nat Hazards Earth Syst Sci 17:1447–1459. https://doi.org/10.5194/nhess-17-1447-2017

García-Mayordomo J, Insua-Arévalo JM, Martínez-Díaz JJ et al (2012) The Quaternary active faults database of Iberia (QAFI v.2.0). J Iberian Geol 38(1):285–302. https://doi.org/10.5209/rev_JIGE.2012.v38.n1.39219

Geist EL (1997) Local tsunamis and earthquake source parameters. Adv Geophys 39:117–209. https://doi.org/10.1016/S0065-2687(08)60276-9

Gjevik B, Pedersen G, Dybesland E et al (1997) Modeling tsunamis from earthquake sources near Gorringe Bank southwest of Portugal. J Geophys Res 102 (C13):27,931–27,949

Goméz de la Peña L, Ranero CR, Gràcia E (2018) The crustal domains of the Alboran Basin (Western Mediterranean). Tectonics 37(10):3352–3377

González A (2017) The Spanish national earthquake catalogue: evolution, precision and completeness. J Seismolog 21:435–471

González M, Medina R, Olabarrieta M et al (2010) Tsunami hazard assessment on the southern coast of Spain. Turk J Earth Sci 19:351–366

González del Castillo L, Galindo-Zaldivar J, Pedrera A et al (2015) Shallow frontal deformation related to active continental subduction: structure and recent stresses in the westernmost Betic Cordillera. Terranova 27(2):114–121

Gràcia E, Dañobeitia J, Vergés J et al (2003a) Crustal architecture and tectonic evolution of the Gulf of Cadiz (SW Iberian margin) at the convergence of the Eurasian and African plates. Tectonics 22(4):1033. https://doi.org/10.1029/2001TC901045

Gràcia E, Dañobeitia J, Vergés J et al (2003b) Mapping active faults offshore Portugal (36°N–38°N): implications for seismic hazard assessment along the southwest Iberian margin. Geology 31(1):83–86

Gràcia E, Pallàs R, Soto JI et al (2006) Active faulting offshore SE Spain (Alboran Sea): implications for earthquake hazard assessment in the Southern Iberian Margin. Earth Planet Sci Lett 241(3–4):734–749

Gràcia E, Bartolomé de la Peña R, Lo Iacono C et al (2012) Acoustic and seismic imaging of the active Adra Fault (NE Alboran Sea): in search for the source of the 1910 Adra Earthquake. Nat Hazards Earth Syst Sci 12(11):3255–3268

Grotzinger J, Jordan TH, Press F et al (2008) Allgemeine Geologie, 5th edn. Springer, Berlin

Gutscher MA, Malod J, Réhault JP et al (2002) Evidence for active subduction beneath Gibraltar. Geology 30:1071–1074

Gutscher MA, Baptista MA, Miranda JM (2006) The Gibraltar Arc seismogenic zone (part 2): constraints on a shallow east dipping fault plane source for the 1755 Lisbon earthquake provided by tsunami modeling and seismic intensity. Tectonophysics 426:153–166

Gutscher MA, Dominguez S, Westbrook GK et al (2012) The Gibraltar subduction: a decade of new geophysical data. Tectonophysics 574–575:72–91

Hamdache M, Peláez JA, Talbi A et al (2010) A unified catalog of main earthquakes for Northern Algeria from A.D. 856 to 2008. Seismol Res Lett 81:732–739

Hanquiez V, Mulder T, Toucanne S et al (2010) The sandy channel–lobe depositional systems in the Gulf of Cadiz: gravity processes forced by contour current processes. Sed Geol 229(3):110–123

Harbitz CB (1992) Model simulation of tsunamis generated by the Storegga Slides. Mar Geol 105:1–21

Harbitz CB, Lovholt F, Pedersen G et al (2006) Mechanisms of tsunami generation by submarine landslides a short review. Norw J Geol 86:255–264

Harbitz CB, Løvholt F, Bungum H (2014) Submarine landslide tsunamis: how extreme and how likely? Nat Hazards 72:1341–1374

Haugen KB, Lovholt F, Harbitz CB (2005) Fundamental mechanisms for tsunami generation by submarine mass flows in idealized geometries. Mar Pet Geol 22:195–202

Henares J, López-Casado C (2001) Catálogo de mecanismos focales del área Ibero-Mogrebí. University of Granada, Granada

Henares J, López-Casado C, Sanz de Galdeano C et al (2003) Stress fields in the Iberian-Maghrebi región. J Seismol 7:65–78

Hensen C, Scholz F, Nuzzo M et al (2015) Strike-slip faults mediate the rise of crustal-derived fluids and mud volcanism in the deep sea. Geology 43(4):339–342. https://doi.org/10.1130/G36359.1

Hensen C, Duarte JC, Vannucchi (2019) Marine transform faults and fracture zones: a joint perspective integrating seismicity, fluid flow and life. Front Earth Sci 7:39. https://doi.org/10.3389/feart.2019.00039

Hernández-Molina FJ, Llave E, Stow DAV et al (2006) The contourite depositional system of the Gulf of Cadiz: a sedimentary model related to the bottom current activity of the Mediterranean outflow water and its interaction with the continental margin. Deep Sea Res Part II 53(11–13):1420–1463

Herraiz M, De Vicente G, Lindo-Ñaupari R et al (2000) The recent (upper Miocene to Quaternary) and present tectonic stress distributions in the Iberian Peninsula. Tectonics 19(4):762–786

Hwang RD (2014) First-order rupture features of the 2011 MW 9.0 Tohoku (Japan) earthquake from surface waves. J Asian Earth Sci 81(25):20–27

IGME (2015) ZESIS: Bases de Datos de Zonas Sismogénicas de la Península Ibérica y territorios de influencia para el cálculo de la peligrosidad sísmica en España. http://info.igme.es/zesis. Accessed 30 Apr 2020

IGN (2020) Earthquake catalog. https://www.ign.es/web/ign/portal/sis-catalogo-terremotos. Accessed 30 Apr 2020

Jimenez-Munt I, Sabadini R, Gardi A et al (2003) Active deformation in the Mediterranean from Gibraltar to Anatolia inferred from numerical modeling and geodetic and seismological data. J Geophys Res Solid Earth 108(B1):2006. https://doi.org/10.1029/2001JB001544

Juan G, Ercilla G, Hernández-Molina FJ et al (2016) Seismic evidence of current-controlled sedimentation in the Alboran Sea during the pliocene and quaternary: palaeoceanographic implications. Marine Geol 378:292–311. https://doi.org/10.1016/jmargeo.2016.01.006.

Kanamori H (1972) Mechanism of tsunami earthquakes. Phys Earth Planet Inter 6(5):346–359

Keating B, McGuire W (2000) Island edifice failures and associated tsunami hazards. Pure Appl Geophys 157:899–955

Keller EA, Pinter N (2002) Active tectonics, earthquakes, uplift and landscape, 2nd edn. Prentice Hall, Upper Saddle River

Klug H (1986) Flutwellen und Risiken der Küste. Franz Steiner Verlag, Stuttgart

Kopp H, Weinreibe W (2009) Ursachen von Tsunamis: ein Überblick. Geogr Rundsch 61:20–27

Koulali A, Ouazar D, Tahayt A et al (2011) New GPS constraints on active deformation along the Africa-Iberia plate boundary. Earth Planet Sci Lett 308(1–2):211–217

Krastel S, Schmincke HS, Jacobs CL et al (2001) Submarine landslides around the Canary Islands. J Geophys Res Solid Earth 106(B3):3977–3997

Lafosse M, D'Acremont E, Rabaute A et al (2020) Plio-quaternary tectonic evolution of the southern margin of the Alboran Basin (Western Mediterranean). Solid Earth 11:714–765. https://doi.org/10.5194/se-11-741-2020

Lauterjung J, Münch U, Rudloff A (2009) Geotechnik im Dienst der Menschheit. Geogr Rundsch 61:36–41

Lee HJ, Kayen RE, Gardner JV et al (2003) Characteristics of several tsunamigenic submarine landslides. In: Locat J, Mienert J, Boisvert L (eds) Submarine mass movements and their consequences: 1st international symposium. Advances in natural and technological hazards, vol 19. Springer, Dordrecht, pp 357–366

León R, Somoza L (2011) GIS-based mapping for marine geohazards in seabed fluid leakage areas (Gulf of Cadiz, Spain). Marine Geophys Res 32(1–2):207–223

León R, Somoza L, Medialdea T et al (2019) A new scenario for the mass transport deposits west Canary volcanic province. Earth Planet Sci Lett 509:27–37

León R, Urgeles R, Pérez-López R et al (2020) Geological and tectonic controls on morphometrics of submarine landslides of the Spanish margins. Geol Soc Lond 500:495–513. https://doi.org/10.1144/SP500-2019-153

Lin A, Ikuta R, Rao G (2012) Tsunami run-up associated with co-seismic thrust slip produced by the 2011 Mw 9.0 Off Pacific Coast of Tohoku earthquake, Japan. Earth Planetary Sci Lett 337–338:121–132

Lipman PW, Normark WR, Moore JG et al (1988) The giant submarine Alika Debris Slide, Mauna Loa, Hawaii. J Geophys Res Solid Earth 93(B5):4279–4299

Lo Iacono C, Gràcia E, Zaniboni F et al (2012) Large, deepwater slope failures: implications for landslide-generated tsunamis. Geology 40(10):931–934

Locat J, Gardner JV, Lee H et al (1999) Using multibeam sonar surveys for submarine landslide investigations. In: Slope stability engineering. Proceedings of the international symposium, IS-Shikiku '99, Matsuyama, Shikoku, Japan, 8–11 November 1999, pp 127–134

Locat J, Lee HJ (2002) Submarine landslides: advances and challenges. Can Geotech J 39(1):193–212

López-Casado C, Sanz de Galdeano C, Molina-Palacios S et al (2001) The structure of the Alboran Sea: an interpretation from seismological and geological data. Tectonophysics 338:79–95

Løvholt F, Harbitz CB, Haugen KB (2005) A parametric study of tsunamis generated by submarine slides in the Ormen Lange/Storegga area off western Norway. Mar Pet Geol 22:219–231

Løvholt F, Pedersen G, Harbitz B et al (2015) On the characteristics of landslide tsunamis. Phil Trans R Soc A 373:20140376. https://doi.org/10.1098/rsta.2014.0376

Macías J, Vázquez JT, Fernández-Salas LM et al (2015) The Al-Borani submarine landslide and associated tsunami. A modelling approach. Mar Geol 361:79–95

Maestro A, Somoza L, Medialdea T (2003) Large-scale slope failure involving Triassic and Middle Miocene salt and shale in the Gulf of Cadiz (Atlantic Iberian Margin). Terranova 15:380–391

Maldonado A, Somoza L, Pallarés L (1999) The Betic orogen and the Iberian-African boundary in the Gulf of Cadiz: geological evolution (Central North Atlantic). Mar Geol 155:9–43

Martínez-García P, Soto JI, Comas JI (2010) Recent structures in the Alboran Ridge and Yusuf fault zones based on swath bathymetry and sub-bottom profiling: evidence of active tectonics. Geo-Mar Lett 31:19–36

Martínez-García P, Comas M, Soto JI et al (2013) Strike-slip tectonics and basin inversion in the Western Mediterranean: the Post-Messinian evolution of the Alboran Sea. Basin Res 25(4):361–387

Martínez-García P, Comas M, Lonergan L et al (2017) From extension to shortening: tectonic inversion distributed in time and space in the Alboran Sea, western mediterranean. Tectonics 36(12):2777–2805

Martínez-Loriente S, Gràcia E, Bartolomé R et al (2013) Active deformation in old oceanic lithosphere and significance for earthquake hazard: Seismic imaging of the Coral Patch Ridge area and neighboring abyssal plains (SW Iberian Margin). Geochem Geophys Geosyst 14(7):2206–2231

Martínez-Loriente S, Sallarès V, Gràcia E et al (2014) Seismic and gravity constraints on the nature of the basement in the Africa-Eurasia plate boundary: new insights for the geodynamic evolution of the SW Iberian margin. J Geophys Res Solid Earth 119(1):127–149

Martínez-Loriente S, Gràcia E, Bartolomé R et al (2018) Morphostructure, tectono-sedimentary evolution and seismic potential of the Horseshoe Fault, SW Iberian margin. Basin Res 30(S1):382–400

Masana E, Moreno X, Gràcia E et al (2018) First evidence of paleoearthquakes along the Carboneras Fault Zone (SE Iberian Peninsula): Los Trances site. Geol Acta 16(4):461–476. https://doi.org/10.1344/GeologicaActa2018.16.4.8

Masson DG (1996) Catastrophic collapse of the flank of El Hierro about 15,000 years ago, and the history of

large flank collapses in the Canary Islands. Geology 24:231–234
Masson DG, Watts AB, Gee MJR et al (2002) Slope failures on the flanks of the western Canary Islands. Earth Sci Rev 57(1–2):1–35
Masson DG, Harbitz CB, Wynn RB et al (2006) Submarine landslides: processes, triggers and hazard prediction. Phil Trans R Soc A 364:2009–2039. https://doi.org/10.1098/rsta.2006.1810
Matias LM, Cunha T, Annunziato A et al (2013) Tsunamigenic earthquakes in the Gulf of Cadiz: fault model and recurrence. Nat Hazards Earth Syst Sci 13:1–13
Mauffret A, Maldonado A, Campillo AC (1992) Tectonic framework of the Eastern Alboran and Western Algerian Basins, Western Mediterranean. Geo-Mar Lett 12:104–110
Mauffret A, Ammar A, Gorini C et al (2007) The Alboran Sea (Western Mediterranean) revisited with a view from the Moroccan margin. Terranova 19:195–203
Max MD (2003) Natual gas hydrate in oceanic and permafrost environments. Springer, Dordrecht
McAdoo BG, Pratson LF, Orange DL (2000) Submarine landslide geomorphology, US continental slope. Mar Geol 169:103–136. https://doi.org/10.1016/S0025-3227(00)00050-5
Medialdea T, Vegas R, Somoza L et al (2004) Structure and evolution of the “Olistostrome” complex of the Gibraltar Arc in the Gulf of Cadiz (Eastern Central Atlantic): evidence from two long seismic cross-sections. Mar Geol 209:173–198
Mendes-Victor LA, Sousa Olivera C, Azevedo J et al (eds) (2009) The 1755 Lisbon earthquake: revisited. Geotechnical, geological and earthquake engineering, vol 7. Springer, Dordrecht
Mezcua J, Rueda J (1997) Seismological evidence for a delamination process in the lithosphere under the Alboran Sea. Geophys J Int 129(1):F1–F8
Mezcua J, Rueda J, García-Blanco RM (2004) Reevaluation of historic earthquakes in Spain. Seismol Res Lett 75:75–81
Moore JG, Normark WR, Holcomb RT (1994) Giant Hawaiian Landslides. Annu Rev Earth Planet Sci 22:119–144
Morales J, Serrano I, Jabaloy A et al (1999) Active continental subduction beneath the Betic Cordillera and the Alborán Sea. Geology 27:735–738
Moreno X, Masana E, Pallàs R et al (2015) Quaternary tectonic activity of the Carboneras Fault in the La Serrata range (SE Iberia): geomorphological and chronological constraints. Tectonophysics 663:78–94
Moreno X, Gràcia E, Bartolomé R et al (2016) Seismostratigraphy and tectonic architecture of the Carboneras fault offshore based on multiscale seismic imaging: implications for the Neogene evolution of the NE Alboran Sea. Tectonophysics 689:115–132
Mulder T, Alexander J (2001) The physical character of subaqueous sedimentary density flows and their deposits. Sedimentology 48:269–299
Mulder T, Voisset M, Lecroart P et al (2003) The Gulf of Cadiz: an unstable giant contouritic levee. Geo-Mar Lett 23:7–18
Mulder T, Lecroart P, Hanquiez V et al (2006) The western part of the Gulf of Cadiz: contour currents and turbidity currents interactions. Geo-Mar Lett 26(1):31–41
Mulder T, Gonthier E, Lecroart P et al (2009) Sediment failures and flows in the Gulf of Cadiz (eastern Atlantic). Mar Pet Geol 26(5):660–672
Murty TS (1977) Seismic sea waves, tsunamis. Department of Fisheries and the Environment Fisheries and Marine Service, Ottawa
Neres M, Carafa MMC, Fernandes RMS et al (2016) Lithospheric deformation in the Africa-Iberia plate boundary: improved neotectonic modeling testing a basal driven Alboran plate. J Geophys Res Solid Earth 121:6566–6596
Neves MC, Roque C, Luttrell KM et al (2016) Impact of sea-level rise on earthquake and landslide triggering offshore the Alentejo margin (SW Iberia). Geo-Mar Lett 36:415–424
Niedoroda AW, Reed CW, Das H, Hatchett L (2007) The general behavior of mass gravity flows in the marine environment. In: Lykousis V, Sakellariou D, Locat J (eds) Submarine mass movements and their consequences: 3rd international symposium. Advances in natural and technological hazards research, vol 27. Springer, Dordrecht, pp 111–118
Nocquet JM (2012) Present-day kinematics of the Mediterranean: a comprehensive overviewof GPS results. Tectonophysics 579:220–242
Omira R, Ramalho I, Terrinha P et al (2016) Deep-water seamounts, a potential source of tsunami generated by landslides? The Hirondelle Seamount, NE Atlantic. Mar Geol 379:267–280
Omira R, Dogan GG, Hidayat R et al (2019) The september 28th, 2018, Tsunami in Palu-Sulawesi, Indonesia: a post-event field survey. Pure Appl Geophys 176:1379–1395
Palano M, González PJ, Fernández J (2013) Strain and stress fields along the Gibraltar Orogenic Arc: constraints on active geodynamics. Gondwana Res 23:1071–1088
Pedrera A, Ruiz-Constán A, Galindo-Zaldívar J et al (2011) Is there an active subduction beneath the Gibraltar orogenic arc? Constraints from Pliocene to present-day stress field. J Geodyn 52(2):83–96
Peláez JA, Chourak M, Tadili BA et al (2007) A catalog of main Moroccan earthquakes from 1045 to 2005. Seismol Res Lett 78:614–621
Peláez JA, Henares J, Hamdache M et al (2018) A seismogenic zone model for seismic hazard studies in Northwestern Africa. In: D'Amico S (ed) Moment tensor solutions. A useful tool for seismotectonics. Springer, Cham, pp 643–680
Perea H, Gràcia E, Martínez-Loriente S et al (2018) Kinematic analysis of secondary faults within a distributed shear-zone reveals fault linkage and increased seismic hazard. Mar Geol 399:23–33

Piper DJW, Mosher DC, Gauley BJ, Kenner K (2003) The chronology and recurrence of submarine mass movements on the continental slope off southern Canada. In: Locat J, Mienert J, Boisvert L (eds) Submarine mass movements and their consequences: 1st international symposium. Advances in natural and technological hazards, vol 19. Springer, Dordrecht, pp 299–306

Platt JP, Behr WM, Johanesen KWJR (2013) The Betic-Rif arc and its orogenic hinterland: a review. Annu Rev Earth Planet Sci 41:313–357

Raji O, Dezileau L, Von Grafenstein U et al (2015) Extreme sea events during the last millennium in the northeast of Morocco. Nat Hazard 15(2):203–211

Ramos A, Fernández O, Terrinha P et al (2017) Neogene to recent contraction and basin inversion along the Nubia-Iberia boundary in SW Iberia. Tectonics 36:257–286

Ratzov G, Collot JY, Sosson M et al (2010) Mass-transport deposits in the northern Ecuador subduction trench: Result of frontal erosion over multiple seismic cycles. Earth Planet Sci Lett 296:80–102

Reicherter K, Becker-Heidmann P (2009) Tsunami deposits in the western mediterranean: remains of the 1522 Almería earthquake? In: Reicherter K, Michetti AA, Silva PG (eds) Palaeoseismology: historical and prehistorical records of earthquake ground effects for seismic hazard assessment, vol 316. The Geological Society, London, Special Publications, pp 217–235

Reicherter K, Hübscher C (2007) Evidence for a seafloor rupture of the Carboneras Fault Zone (southern Spain): relation to the 1522 Almería earthquake? J Seismolog 11(1):15–26

Reilly WI, Fredrich G, Hein GW et al (1992) Geodetic determination of crustal deformation across the Strait of Gibraltar. Geophys J Int 111(2):391–398

Röbke BR, Vött A (2017) Tsunami phenomenon. Prog Oceanogr 159:296–322. https://doi.org/10.1016/j.pocean.2017.09.003

Rodriguez M, Cl M, Jollivet-Castelot M et al (2017) Tsunamigenic submarine landslides along the Xauen-Tofiño banks in the Alboran Sea (Western Mediterranean Sea). Geophys J Int 209:266–281

Roque C, Duarte H, Terrinha P, Valadares V, Noiva J, Cachão M, Ferreira J, Legoinha P, Zitellini N (2012) Pliocene and quaternary depositional model of the Algarve margin contourite drifts (Gulf of Cadiz, SW Iberia): seismic architecture, tectonic control and paleoceanographic insights. Mar Geol 303–306:42–62

Rosas FM, Duarte JC, Terrinha P et al (2009) Morphotectonic characterization of major bathymetric lineaments in Gulf of Cadiz (Africa-Iberia plate boundary): insights from analogue modelling experiments. Mar Geol 261(1–4):33–47

Rosas F, Duarte J, Neves M et al (2012) Thrust–wrench interference between major active faults in the Gulf of Cadiz (Africa–Eurasia plate boundary, offshore SW Iberia): tectonic implications from coupled analog and numerical modelling. Tectonophysics 548:1–21

Rosas F, Duarte J, Schellart WP et al (2016) Seismic potential of thrust-wrench tectonic interference between major active faults offshore SW Iberia. A new explanation for the 1755 great lisbon earthquake? In: Duarte JC, Schellart WP (eds) Plate boundaries and natural hazards. Wiley, Hoboken, pp 193–217

Royden L (1993) Evolution of retreating subduction boundaries formed during continental collision. Tectonics 12:629–638

Sallares V, Martínez-Loriente S, Prada M et al (2013) Seismic evidence of exhumed mantle rock basement at the Gorringe Bank and the adjacent Horseshoe and Tagus abyssal plains (SW Iberia). Earth Planet Sci Lett 365:120–131

Sanchez G, Merleb R, Hinschbergerc F et al (2019) Post-spreading deformation and associated magmatism along the Iberia Morocco Atlantic margins: Insight from submarine volcanoes of the Tore Madeira Rise. Mar Geol 407:76–93

Sánchez-Guillamón O, Vázquez-Garrido JT, Fernández-Puga MC et al (2014) Caracterización de fallas normales recientes en la plataforma continental del Golfo de Cádiz (SO de la Península Ibérica). In: Álvarez-Gómez JA, Martín-González F (eds) Una aproximación multidisciplinar al estudio de las fallas activas, los terremotos y el riesgo sísmico. II Reunión Ibérica sobre Fallas Activas y Paleosismología, Lorca, pp 129–132

Sayago-Gil M, Pérez-García C, Vázquez JT et al (2008) Slides on the flanks of submarine canyons in the Upper Slope of the Algarve. Thalassas 24(1):65–72

Seber D, Barazangi M, Ibenbrahim A et al (1996) Geophysical evidence for lithospheric delamination beneath the Alboran Sea and Rif-Betic mountains. Nature 379:785–790

Serpelloni E, Vannucci G, Pondrelli S et al (2007) Kinematics of the Western Africa-Eurasia plate boundary from focal mechanisms and GPS data. Geophys J Int 169:1180–1200

Serra CS, Martínez-Loriente S, Gràcia E et al (2020) Tectonic evolution, geomorphology and influence of bottom currents along a large submarine canyon system: the São Vicente Canyon (SW Iberian margin). Mar Geol 426:106219

Silva PG, Goy JL, Somoza L et al (1993) Landscape response to strike-slip faulting linked to collisional settings: quaternary tectonics and basin formation in the Eastern Betics, southeastern Spain. Tectonophysics 224(4):289–303

Silva S, Terrinha P, Matias L et al (2017) Micro-seismicity in the Gulf of Cadiz: is there a link between micro-seismicity, high magnitude earthquakes and active faults? Tectonophysics 717:226–241

Silva PF, Roque C, Drago T et al (2020) Multidisciplinary characterization of quaternary mass movement deposits in the Portimão Bank (Gulf of Cadiz, SW Iberia). Mar Geol 420:106086

Sorensen RM (2010) Basic coastal engineering, 3rd edn. Springer, New York

Soto JI, Fernández-Ibáñez F, Fernández M et al (2008) Thermal structure of the crust in the GibraltarArc: influence on active tectonics in the western mediterranean. Geochem Geophys Geosyst 9:Q10011
Soto JI, Fernández-Ibáñez F, Talukder AR (2012) Recent shale tectonics and basin evolution of the NW Alboran Sea. Lead Edge 31(7):768–775
Spakman W, Wortel R (2004) A tomographic view on western mediterranean geodynamics. In: Cavazza W et al (eds) The TRANSMED Atlas: the mediterranean region from crust to mantle. Springer, Berlin, pp 31–52
Spakman W, Chertova MV, Van Den Berg A et al (2018) Puzzling features of western Mediterranean tectonics explained by slab dragging. Nat Geosci 11(3):211–216
Sparacino F, Palano M, Peláez JA (2020) Geodetic deformation versus seismic crustal moment-rates: insights from the Ibero-Maghrebian region. Remote Sensing 12:952
Stich D, Batlló J, Morales J et al (2003) Source parameters of the Mw = 6.1 1910 Adra earthquake (southern Spain). Geophys J Int 155:539–546
Stich D, Martínez Solares JM, Custódio S et al (2020) Seismicity of the Iberian Peninsula. In: Quesada C, Oliveira JT (eds) The geology of Iberia: a geodynamic approach. Springer, Cham, pp 11–32
Stich D, Mancilla FdeL, Pondrelli S et al (2007) Source analysis of the February 12th 2007, Mw6.0 Horseshoe earthquake: implications for the 1755 Lisbon earthquake. Geophys Res Lett 34(12):L12308
Stirling M, McVerry G, Berryman K (2002) A new seismic hazard model for New Zealand. Bull Seismol Soc Am 92(5):1878–1903
Strozyk F, Strasser M, Föster A et al (2010) Slope failure in active margin environment: constraints from submarine landslide in the Hellenic arc. J Geophys Res Solid Earth 115:B08103. https://doi.org/10.1029/2009JB006841
Tappin DR (2017) Tsunamis from submarine landslides. Geol Today 33(5):190–200. https://doi.org/10.1111/gto.12200
Tappin DR (2010) Mass transport events and their tsunami hazard. In: Mosher DC et al (eds) Submarine mass movements and their consequences: 4th international symposium. Advances in natural and technological hazards research, vol 48. Springer, Dordrecht, pp 667–684
Terrinha P, Pinheiro LM, Henrie JP et al (2003) Tsunamigenic-seismogenic structures, neotectonics, sedimentary processes and slope instability on the southwest Portuguese Margin. Mar Geol 195:55–73
Terrinha P, Matias L, Vicente J et al (2009) Morphotectonics and strain partitioning at the Iberia-Africa plate boundary from multibeam and seismic reflection data. Mar Geol 267(3):156–174
Tinivella U, Accaino F, Della Vedova B (2008) Gas hydrates and active mud volcanism on the South Shetland continental margin, Antarctic Peninsula. Geo-Mar Lett 28:97–106
Todorovska MI, Trifunac MD (2001) Generation of tsunamis by a slowly spreading uplift of the sea floor. Soil Dyn Earthq Eng 21:151–167
Trifonov VG, Kozhurin A (2010) Study of active faults: theoretical and applied implications. Geotectonics 44 (6):510–528
Urgeles R, Camerlenghi A (2013) Submarine landslides of the Mediterranean Sea: trigger mechanisms, dynamics, and frequency magnitude distribution. J Geophys Res Earth Surf 118(4):2600–2618
Urgeles R, Masson DG, Canals M et al (1999) Recurrent giant landslides on the west flank of LaPalma, Canary Islands. J Geophys Res 104:25331–25348
Van der Woerd J, Dorbath C, Ousadou F et al (2014) The Al Hoceima Mw 6.4 earthquake of 24 February 2004 and its aftershocks sequence. J Geodyn 77:89–109
Vázquez JT, Vegas R (2000) Acomodación de la convergencia entre África y la Península Ibérica, Golfo de Cádiz y Mar de Alborán, a partir del análisis de terremotos. Geogaceta 27:171–174
Vázquez JT, Medialdea T, Hernández-Molina FJ et al (2004) Morfología y tectónica del talud inferior del Golfo de Cádiz. Geo-Temas 6(4):211–214
Vázquez JT, Medialdea T, Somoza L et al (2008) Revisión de las estructuras neotectónicas en la región del Golfo de Cádiz. Margen continental y Llanuras abisales adyacentes. Geo-Temas 10:592–594
Vázquez JT, Alonso B, Fernández-Puga MC et al (2015a) Seamounts along the Iberian continental margins: a key morphological feature. Bol Geol Min 126(2–3):483–514
Vázquez JT, Ercilla G, Alonso B et al (2015b) Submarine canyons and related features in the Alboran Sea: continental margins and major isolated reliefs. CIESM Workshop Monogr 47:183–196
Vázquez JT, Fernández-Puga MC, Medialdea T et al (2010a) Fracturación normal durante el Cuaternario Superior en la Plataforma Continental Septentrional del Golfo de Cádiz (SO de Iberia). In: Insua-Arévalo JM, Martín-González F (eds) Contribución de la Geología al Análisis de la Peligrosidad Sísmica. I Reunión Ibérica sobre Fallas Activas y Paleosismología, Sigüenza, pp 179–182
Vázquez JT, López-González N, Fernández-Salas LM et al (2010b) Nuevos datos de actividad tectónica durante el Pleistoceno Superior – Holoceno en el Sector Oriental de la Plataforma Continental del Golfo de Cádiz (SO de Iberia). In: Insua-Arévalo JM, Martín-González F (eds) Contribución de la Geología al Análisis de la Peligrosidad Sísmica. I Reunión Ibérica sobre Fallas Activas y Paleosismología, Sigüenza, pp 183–186
Vázquez JT, Alonso B, Palomino D et al (2013) Mass movement deposits and tectonics relation as a main factor to control the stratigraphical architecture of the South Alboran Basin (Alboran Sea, Western Mediterranean). V Regional Committee on Atlantic Neogene Stratigraphy (RCANS) Congress: Two decades of Atlantic Neogene study, Huelva, pp 46–47

Vázquez JT, Estrada F, Vegas R et al (2014) Quaternary tectonics influence on the Adra continental slope morphology (Northern Alboran Sea). In: Álvarez-Gómez JA, Martín-González F (eds) Una aproximación multidisciplinar al estudio de las fallas activas, los terremotos y el riesgo sísmico. II Reunión Ibérica sobre Fallas Activas y Paleosismología, Lorca, pp 89–92

Vázquez JT, Fernández-Puga MC, Palomino D et al (2015c) Shallow tectonics on the middle continental slope of the northeastern Gulf of Cadiz continental margin (SW Iberia). In: Díaz del Río V et al (eds) Resúmenes sobre el VIII Simposio MIA15, Málaga del 21 al 23 de septiembre de 2015c, Instituto Español de Oceanografía, pp 149–152

Vázquez JT, Estrada F, Vegas R et al (2016) Geomorfología submarina en relación con la actividad tectónica Cuaternaria en la Cuenca del Mar de Alborán. In: Durán Valsero JJ et al (eds) Comprendiendo el relieve: del pasado al futuro. Actas de la XIV Reunión Nacional de Geomorfología, Málaga. Publicaciones IGME Geología y Geofísica 5:587–595

Vázquez JT, Estrada F, Ercilla G et al (2018) Geomorfología y deformaciones cuaternarias en zonas de falla de la plataforma marginal de Motril-Djibouti. In: Canora C et al (eds) Avances en el estudio de Fallas Activas, Terremotos y Peligrosidad Sísmica de Iberia. III Reunión Ibérica sobre Fallas Activas y Paleosismología, Alicante, pp 137–140

Vázquez JT, Ercilla G, Catalán M et al (2021) A geological history for the alboran sea region. In: Baéz JC et al (eds) Alboran sea and its marine resources, Ch. 5, Springer Nature Switzerland AG, pp 111–156

Vázquez JT (2001) Estructura del margen septentrional del Mar de Alborán. Dissertation, Univ. Complutense

Vegas R, Medialdea T, Vázquez JT (2008) Sobre la naturaleza del límite de placas actual entre la Península Ibérica y el norte de África. Geo-Temas 10:1535–1538

De Vicente G, Cloetingh S, Muñoz-Martín A et al (2008) Inversion of moment tensor focal mechanisms for active stresses around the microcontinent Iberia: Tectonic implications. Tectonics 27:TC1009

Watts AB, Platt JP, Buhl P (1993) Tectonic evolution of the Alboran Sea basin. Basin Res 5:153–177

Wells DL, Coppersmith KJ (1994) New empirical relationships among magnitude, rupture length, rupture width, rupture area, and surface displacement. Bull Seismol Soc Am 84(4):974–1002

Woodside MJ, Maldonado A (1992) Styles of compressional neotectonics in the eastern Alboran Sea. Geo-Mar Lett 12:111–116

Zitellini N, Rovere M, Terrinha P (2004) Neogene through quaternary tectonic teractivation of SW Iberian passive margin. Pure Appl Geophys 161:565–587

Zitellini N, Gràcia E, Matias L et al (2009) The quest for the Africa-Eurasia plate boundary west of the Strait of Gibraltar. Earth Planet Sci Lett 280(1–4):13–50

5 Tsunami Deposits in Atlantic Iberia: A Succinct Review

Pedro J. M. Costa, Javier Lario, and Klaus Reicherter

Abstract

This chapter offers an overview of the current knowledge of the southwest Iberian tsunami geological record. Specifically, this chapter summarizes three decades of research on tsunami and storm deposit recognition, differentiation and establishing chronologies of past events. The impact and signature of the CE 1755 within coastal stratigraphic units are impressive, and its study in such a wide spatial area has provided very useful insights into tsunami dynamics. Another peculiarity addressed in this chapter is the contrast between the diverse record of tsunami or storm imprints on the Spanish part of the Gulf of Cadiz when compared with the Portuguese area. This discrepancy essentially relates to the dominance of aggrading or eroding processes favouring the preservation of deposits and also with different sediment availability during the Holocene. This allowed for a better correlation between the Spanish tsunami onshore record and its turbidite data. However, some of the deposits previously described are controversial not only sedimentologically but also because of constraints on the dates obtained. Therefore, further work is necessary on both sides of the border to establish indisputably return periods and to define a catalogue of past tsunami events affecting the southwest Iberian Peninsula during the Holocene.

Keywords

Sediments · Tsunami · Portugal · Spain · Extreme wave events

5.1 Introduction

Tsunami geoscience has evolved considerably since its seminal works in the late 1980s. Initially, tsunami deposits were merely identified in

P. J. M. Costa (✉)
Departamento de Ciências da Terra, Faculdade de Ciências E Tecnologia, Universidade de Coimbra, Rua Sílvio Lima, Pólo II, 3030-790 Coimbra, Portugal
e-mail: ppcosta@dct.uc.pt

P. J. M. Costa
Instituto Dom Luiz, Faculdade de Ciências, Universidade de Lisboa, Edifício C6, 1749-016 Lisbon, Portugal

J. Lario
Facultad de Ciencias, Universidad Nacional de Educación a Distancia (UNED), Avda. Esparta s/n, 28232 Las Rozas – Madrid, Spain
e-mail: javier.lario@ccia.uned.es

K. Reicherter
Institute for Neotectonics and Natural Hazards, RWTH Aachen University, Lochnerstr. 4-20, 52056 Aachen, Germany
e-mail: k.reicherter@nug.rwth-aachen.de

M. Álvarez-Martí-Aguilar and F. Machuca Prieto (eds.), *Historical Earthquakes, Tsunamis and Archaeology in the Iberian Peninsula*, Natural Science in Archaeology,
https://doi.org/10.1007/978-981-19-1979-4_5

the stratigraphic record on the basis of their singularity and deposition further inland. Subsequently, especially after the 2004 and 2011 tsunami events, the recognition of tsunami deposits progressed due to the interpretation of sediment dynamics and inundation phases based on the progressive application of different sedimentological, geochemical, palaeontological and geophysical analytical techniques.

In the Iberian Peninsula tsunamis are uncommon; therefore, it is essential to use the geological record to study them and establish their return periods. The study of sediments deposited by tsunamis is crucial because it increases our knowledge and understanding of the frequency and intensity of past events. In areas with a low frequency of tsunamis, such as the Iberian Atlantic and Mediterranean coasts, the accurate estimation of coastal risk involves a high-resolution analysis that can also help to reconstruct the physical parameters, run-ups and inundation limits, and to quantify sediment transported both inland and offshore. However, identifying tsunami deposits is a difficult task. Tsunamis are high energy events that often deposit a coarser sedimentary unit in coastal stratigraphic sequences. Their sedimentary imprints tend to differ from background sedimentation. However, other events such as channel migrations, river floods and storms have the ability to generate similar sedimentological signatures.

Lario et al. (2011) suggested the use of extreme wave events (hereinafter EWEs) to mitigate the problems in differentiating these (tsunami and storm) units. After the 2004 Indian Ocean and the 2011 Japanese tsunamis, there were many scientific developments in the geological differentiation between tsunami and storm imprints (e.g., Morton et al. 2007; Chagué-Goff et al. 2011; Costa et al. 2012a, 2018). Nevertheless, classifying a sedimentary unit as tsunami-related is a challenge. In regions with a low frequency of tsunami events, this is further complicated by natural post-depositional processes and changes (e.g., Szczuciński 2012) and anthropogenic modifications. Furthermore, seismic sources are important, such as earthquake recurrence rates, expected maximum magnitudes, kinematics (thrust vs. strike-slip vs. normal fault) and the distance from the coast, as are the processes generating tsunamis (faults and landslides).

Tsunami depositional and erosional imprints have been widely discussed in the literature over the past three decades. Commonly these deposits are peculiar in the lithostratigraphic sequence, display an erosional or abrupt basal contact, tend to be coarser and exhibit geochemical and micropalaeontological features correlating their association with a diversity of coastal environments affected by tsunami inundations and backwash. This diversity is also observed in the minerogenic components, despite the shared provenance of beach, dune and shallow offshore sediments and tsunami deposits. Following the destructive landfall of a tsunami, the sedimentary signature in the archive after the event may also display significant changes (opening/closure of lagoons, spits, river inlets, marshlands, open marine beaches, etc.).

Their preservation is also a key issue. This is usually favoured in coastal low-energy sedimentation environments, while it is important to bear in mind that geological records tend to be biased towards the most extreme events, precisely because of their enhanced preservation and erosion potential obliterating older and weaker event layers in the geological record. Therefore, in the Iberian Peninsula caution must be used when interpreting the geological data of tsunami events.

Based on previous works (Lario et al. 2010a, 2011; Andrade et al. 2016), it is possible to observe that the Spanish coasts have recorded more events than their Portuguese counterparts (Fig. 5.1). This is mainly due to the different geomorphological conditions of the two coastal sectors. The southern coast of Portugal is essentially under pressure from erosion, whilst the southwest coast of Spain is often characterized by aggradation or tectonic uplift, thus favouring the preservation of deposits.

Although some coastal regions of the Mediterranean and the Atlantic have been affected by such events, tsunamis are infrequent in

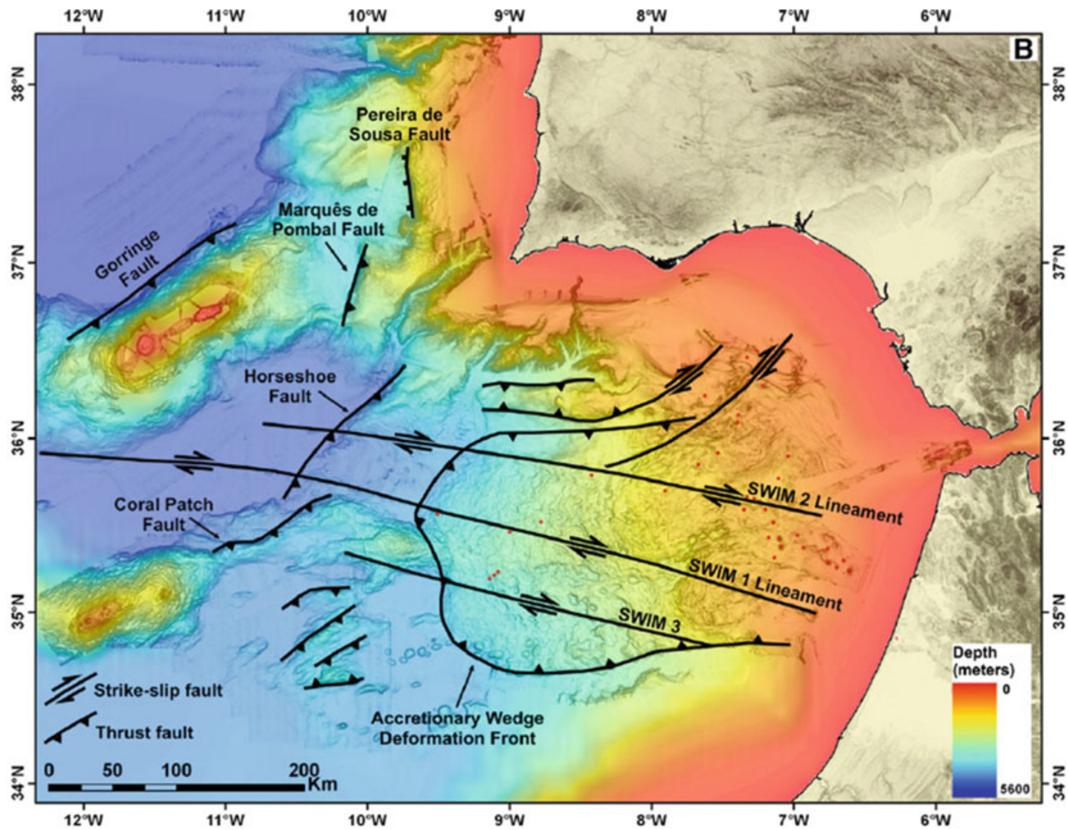

Fig. 5.1 Main geomorphologic features and detailed tectonic characterization of the Gulf of Cadiz (*Source* Adapted from Duarte et al. (2010), Fig. 2). SWIM (SW Iberian Margin) lineaments are several major WNW-ESE trending lineaments, interpreted as aligned arrays of also deep-seated, sub-vertical dextral strike-slip faults. The small red dots, in the vicinity of SWIM lineaments, mark seismic or sound velocity acquisition locations

Europe. The most prominent regions struck by tsunamis in the European area include the seaboard of insular Greece, in the Eastern Mediterranean, and the coast of southern Italy, in the Central Mediterranean (Moreira 1988; Cita and Rimoldi 1997). Although in terms of magnitude, the most important tsunamigenic zone of Europe, besides the Hellenic trench, is the Gorringe Bank located 200 km southwest of Cape St. Vincent (the south-westernmost point of the Iberian Peninsula).

The southern Iberian Peninsula is located within the diffuse Eurasian-African tectonic boundary which contributes decisively to its tsunami risk (Fig. 5.1). Nearby, the Gorringe Bank is also the main tsunamigenic zone affecting the peninsula. This continental upthrust (or pop-up) is located on the eastern part of the Azores-Gibraltar Fracture Zone (hereinafter AGFZ), the western boundary between the African and Eurasian Plates, which runs roughly east–west connecting the Azores triple junction to the Strait of Gibraltar (Zitellini et al. 2001).

According to Campos (1991), three main seismotectonic areas are considered on the Iberian Atlantic coasts and, consequently, three main tsunamigenic zones:

1. Zone A: From the mid-Atlantic ridge to 25° W. It is an area of extension and the formation of oceanic crust because of spreading. It is unlikely that it would generate tsunamis because extensional earthquakes are of small to medium magnitudes with a maximum of ca. M 6.5 and minor vertical displacement.

2. Zone B: From 24° W to 18° W where the Gloria Fault forms a large transform segment of the AGFZ. It is an area of friction where large magnitude earthquakes may occur (Omira et al. 2019), which are however associated with dextral horizontal displacements along an E-W orientated fault (Udías et al. 1985). This kind of displacement generates small tsunamis that are not generally observed on the south-western coast of the Iberian Peninsula. An exception to the rule was the earthquake and associated tsunami on 25 November 1941, with peak amplitudes of 40 cm in the Azores and Madeira (Baptista et al. 2016).
3. Zone C: The Cadiz Gulf is the main source of tsunamis. This is a zone of intense collision between the African and the Eurasian plates that are undergoing strong and localized contractional deformation and thrusting. The most important tsunamis were generated in this area, located from 12° to 6° W along the 36° N parallel (e.g., Gutscher et al. 2002, 2006).

Nevertheless, there is still much scientific debate on the possibility of subduction initiation in this region and on the epicentral mechanisms of large earthquakes affecting it (e.g., Duarte et al. 2013).

Figure 5.2 is based on Lario et al. (2011) and the tsunami deposit database of the OnOff project (http://tsunami.campus.ciencias.ulisboa.pt/). It shows the locations where tsunami deposits have been described in the Iberian Peninsula. In this chapter, all these sites are reviewed, briefly

Fig. 5.2 Locations where tsunami deposits have been described along the southwest Atlantic Iberian coastline: 1. Aveiro, 2. Cabo Raso, 3. Cascais, 4. Tagus estuary, 5. Alfeite, 6. Pancas (Benavente), 7. Tróia, 8. Praia do Malhão, 9. Martinhal, 10. Furnas, 11. Barranco, 12. Boca do Rio, 13–14. Alcantarilha and Salgados, 15. Quarteira-Almargem-Carcavai, 16. Ria Formosa, 17. Guadiana estuary, 18. Rio Piedras estuary, 19. Tinto Odiel estuary and Punta Umbría spit bar, 20. Guadalquivir estuary and Doñana spit bar, 21. Guadalete estuary and Valdelagrana spit bar, 22–23. Conil-Trafalgar-Barbate area, 24. Los Lances-Tarifa, 25. Algeciras-Gibraltar

discussing their geological features and their overall contribution to establishing tsunami return periods for the south-western Iberian seaboard.

The Iberian coastline is, fortunately, rarely affected by tsunamis. Despite the huge tsunami of 1755 CE and its consequences in terms of human casualties, the historical literature on tsunami risk on both the Atlantic and the Mediterranean coasts is rare. In this chapter, the depositional tsunami imprints along the Iberian coastline are reviewed. The sites are grouped regionally (Fig. 5.2) and their deposits and geomorphological settings are briefly summarized. The aim here is also to stress the importance of performing further high-resolution geological studies on the Iberian shores so as to reconstruct and to date at least the Holocene tsunami record in this region, as best we can.

5.2 Iberian Tsunami Deposits

In this connection, over the past decade, multiproxy analyses have been performed and new sites studied (Salgados, Alcantarilha, Furnas, Barranco, Almargem, etc.), thus contributing to gain further insights into the 1755 CE tsunami and other extreme events occurring on the Portuguese coasts. For example, cobble and boulder analyses and the erosional signature in dune fields were used to model wave flow characteristics, like run-up, flow velocity and flow depth (Costa et al. 2011, 2016). On the other hand, grain-size data and microtextural and heavy mineral composition established a robust source-to-sink relationship between the 1755 CE tsunami deposits and dune sediments (Costa et al. 2012a, b, c, 2015, 2018). The application of geochemistry and high-resolution micropalaeontological analysis contributed to estimating the inundation extent and differentiating inundation phases (Font et al. 2010; Moreira et al. 2017). All those analyses helped to gain a better understanding of the 1755 CE tsunami dynamics and its onshore sedimentological imprint. Very recently, state-of-the-art hydrodynamic and morphodynamic modelling has been conducted using this unique geological database yet to be validated (Dourado et al. 2020), which has contributed to exclude potential tsunami generation zones and narrow down the search for the 1755 CE epicentre. The RV METEOR cruise M152 in 2018 was short but extremely successful; the preliminary results allowed for the offshore identification of the CE 1755 Lisbon tsunami deposits in cores. Moreover, at least one preceding tsunami backwash deposit dating back to ca. 3.5 kyr BP was identified. Although this has not been described before in the onshore sedimentary record of the Algarve (Reicherter et al. 2019), it has indeed been detected in the Gulf of Cadiz (Lario et al. 2010a, 2011). This pioneering study opened the offshore archives on shelves for tsunami deposit studies along the Algarve coast at least for the time span since the Holocene, post-glacial sea-level rise.

As in other locations worldwide, tsunami deposits in Portugal were originally identified during the early 1990s, thanks to their geomorphological imprint or coarser sandy nature in muddy low-lying basins within the Holocene stratigraphic sequences of coastal sectors along the southern coast of Portugal. Many of these deposits were first studied in detail in terms of their spatial distribution, texture and micropalaeontological composition (e.g., Hindson et al. 1996; Kortekaas and Dawson 2007; Cunha et al. 2010, etc.). One aspect noted was the uniqueness of the 1755 CE event deposits on top of the Holocene sequence (Costa et al. 2015; Andrade et al. 2016). Exceptions included remains of a 7 kyr-old event in Cascais-Cabo Raso (location 2 in Fig. 5.2; Scheffers and Kelletat 2005), a possible first millennium CE event detected in the Boca do Rio-Algarve (Feist et al. 2019), and the tsunami deposits related to the 1531 CE and 1969 CE events described in the inner Tagus estuary (locations 4, 5 and 6 in Fig. 5.2; Andrade et al. 2003; Abrantes et al. 2005).

This is in contrast with the more extensive and diverse sedimentological catalogue of tsunami events in the Gulf of Cadiz. In this region, several tsunami deposits have been detected both onshore (e.g., Lario et al. 2010a, 2011) and offshore (e.g., Gràcia et al. 2010). The former focused on the onshore record of tsunami events and also attempted to describe the different features produced by tsunamis and other EWEs, such as severe storm surges (Lario et al. 2010a, 2011). Most surveys of EWEs in the area have concentrated on its main estuaries: the Guadiana (Lario 1996; Ruiz et al. 2013; Klein et al. 2016), the Piedras (Lario et al. 2015, 2016), the Tinto-Odiel (Lario 1996; Ruiz et al. 2007; Morales et al. 2008; González-Regalado et al. 2019a, b), the Guadalquivir (Lario et al. 1995, 2001a, b; Lario 1996; Rodriguez-Ramírez et al. 1996, 2015, 2016; Ruiz et al. 2004, 2005; Cáceres et al. 2006; Rodriguez Vidal et al. 2011; Silva et al. 2015) and the Guadalete (Lario et al. 1995; Lario 1996; Dabrio et al. 1999a, b; Luque et al. 2001, 2002; Gutiérrez-Mas et al. 2009; Gutiérrez-Mas, 2011), plus the littoral lowlands on the south-eastern coast of the Gulf of Cadiz (Luque 2002; Whelan and Kelletat 2003, 2005; Alonso et al. 2004; Luque et al. 2004; Gracia et al. 2006; Reicherter et al. 2010; Rodriguez Vidal et al. 2011; Cuven et al. 2013; Koster et al. 2013; Koster and Reicherter 2014; Alonso et al. 2015; Gutiérrez-Mas et al. 2016; Reicherter et al., this volume). These studies, which described the sedimentary record of high energy events in the Gulf of Cadiz, concluded that most of them were tsunami-related in origin.

The main problem when trying to correlate the diverse episodes identified by different authors is the dispersion of dates, probably around the same event. Lario et al. (2010a, b, 2011) suggest that all these likely tsunami deposits of a specific date (previously related to EWE) in the vicinity may correspond to a sole event. The discrepancy in the reported numerical ages is the result of the use of different biological taxa for radiocarbon dating, the limited amount of radiocarbon samples analysed and the use of the same reservoir effect for differently affected coastal environments. Most of the events have been dated by radiocarbon analyses in marine or estuarine shells, but using different reservoir effect values to calibrate the raw data obtained. Seminally, Lario (1996) proposed a reservoir effect of 440 ± 85 yr on the strength of two radiocarbon samples retrieved from exactly the same level (marine shell and twig fragments). Data from the southwest Iberian Peninsula suggest that the value of ΔR varies with time because it is affected by changes in upwelling (Soares and Dias 2006). According to Soares and Dias (2006), the ΔR values range from +940 ± 50 yr to −160 ± 40 yr, while suggesting that the only realistic values were those determined by Soares (1989, in Stuiver and Braziunas 1993) for historical samples (250 ± 25 yr) and the mean of another 30 ΔR values, covering the interval 3000–600 BP with an average ΔR = 95 ± 15 yr. Subsequently, Lario et al. (2010b) proposed a more reliable ΔR value in the Gulf of Cadiz for the mid-late Holocene, ranging from ΔR = 35 ± 85 yr to ΔR = 95 ± 15 yr. Soares (2015) found that during the last 3000 yr, the ΔR values on the southern Atlantic coast of the Iberian Peninsula have followed the fluctuations of oceanographic conditions of each sector, thus the average value is +69 ± 17 yr ^{14}C on the windward south coast of Portugal, −26 ± 14 yr on the leeward south coast of Portugal and −108 ± 31 yr on the west coast of Andalusia. Previous values proposed for ΔR were 95 ± 15 yr (Soares and Martins 2009); −160 ± 80 yr (Soares and Martins 2009) and −135 ± 31 (Soares and Martins 2010). In a worldwide study, Alves et al. (2018) conclude that, despite the high variability in the data, most of the ΔR values are between −100 and +100 ^{14}C yr. In order to compare and correlate all the published data, the modelled ocean average of ΔR = 0 used in the Marine13 radiocarbon age calibration curve (Reimer et al. 2013) has been applied and all the data have been recalibrated with Calib v.7.1 (Stuiver et al. 2020).

5.2.1 EWEs Ca. 8000–6400 cal BP

The oldest EWE is recorded in the Valdelagrana spit barrier system (Lario 1996; Dabrio et al. 2000, location 21 in Fig. 5.2). Data such as the input of coarse sediments, the presence of marine shell fragments and increased magnetic susceptibility suggest the occurrence of an EWE, but it has not been validated by other supplementary onshore data. This event has an age of ca. 7900–7600 cal BP and can be reasonably correlated with the E9-turbidite event described offshore (Gràcia et al. 2010). Therefore, a tsunami-related origin for the onshore deposits is possible. Also, in Valdelagrana a comparable deposit was found in cores (Lario 1996) and dated between 6700–6400 cal BP has been observed. In this case, it may be correlated either with the E8 or E7-turbidite event described by Gràcia et al. (2010).

5.2.2 EWEs Ca. 5000–4000 cal BP

An EWE in the Valdelagrana and Punta Umbría spit barrier systems has been dated to ca. 4900–4700 cal BP and interpreted in two studies as storm-generated (Lario 1996; Ruiz et al. 2007). Data in Ruiz et al. (2007) from Punta Umbría have not been recalibrated because the original ^{14}C (5705 yr BP) data are missing. Comparable deposits that were observed in the Doñana marshlands (Ruiz et al. 2005; Cáceres et al. 2006) could be related to an event between 4880 (4740) and 4560 cal BP. These authors attributed the event to a tsunami but there is no other record (e.g., a palaeoseismic event) supporting this claim. These data indicate that major palaeo-EWEs struck broad areas of the southwest Iberian coast, causing relevant geomorphological changes and leaving deposits in the stratigraphic record of particularly vulnerable coastal environments.

Between ca. 4500 and 4100 cal BP, a large EWE has been recorded in the Doñana marshlands as an interbedded marine layer within the inner marsh deposits of the Guadalquivir estuary (location 20 in Fig. 5.2). This event caused major geomorphological changes, leading to the breaching and sudden erosion of the Doñana spit barrier. However, in light of the sedimentary record, it is impossible to know whether this EWE was caused by a tsunami or a severe storm (Lario et al. 1995, 2010a; Lario 1996; Rodriguez-Ramírez et al. 2015; Ruiz et al. 2005; Cáceres et al. 2006).

In the Barbate-Zahara de los Atunes coastal sector, Koster and Reicherter (2014) described (location 23 in Fig. 5.2) an event associated with a tsunami ca. 4000 BP (OSL), as the deposits are characteristic of a tsunami backwash. Radiocarbon dating was unsuccessful as huge reworked Cerastoderma shells in the layer turned out to be older than 30,000 years (Koster and Reicherter 2014). The OSL dating from sand layers above the coarse clastic shell and pebble layer yielded results of between 3.88 ± 0.56 and 4.32 ± 0.90 kyr. Further south, in the Bay of Bolonia (*Baelo Claudia*) north of Tarifa, an excavation detected an EWE dated to ca. 4900 ± 0.2 BP (OSL, ka), characterized by coarse gravels with medium sands. The layer led to significant landscape changes in the bay, including the formation of a beach berm and lagoon at the back, blocking the Arroyo del Alpariate from the sea. The lagoon, which persisted until late Roman/early Medieval times (Reicherter et al., this volume), contains the eastern necropolis. These data pointing to abrupt changes in the coastal landscape have been corroborated by data obtained by Reicherter et al. (this volume) when the estuary of Zahara de los Atunes (Rio Cachón) was transformed from marine (sublittoral) into limnic (coastal lake). Because of the uncertain dating, this EWE tends to be classified as an extraordinary powerful tsunami associated with E6 or E5/6 (Fig. 5.4).

5.2.3 EWEs Ca. 4000–3000 cal BP

A later (ca. 3900–3700 cal BP) EWE has also been identified in Doñana, relating to marine fauna input in the estuary (Ruiz et al. 2005) and chenier formation (Lario 1996; Rodriguez-Ramírez et al. 1996, 2015, 2016). Events with similar features—an erosive phase in the spit barrier, chenier development and input of marine fauna in the Doñana estuary—have been described by the same authors in ca. 3500 cal BP and ca. 3000 cal BP. Between 3400 and 3300 cal BP, Gutiérrez-Mas et al. (2009) and Gutierrez-Mas (2011) identified shell layers in the Guadalete estuary (location 21 in Fig. 5.2), attributing them to a tsunami deposit. An event around 3100 cal BP has been described in the same estuary with spit barrier breaching and the reorganization of the back-barrier drainage system (Lario et al. 1995; Lario 1996; Dabrio et al. 2000). Further south, in the "Cachón" estuary in Zahara de los Atunes, drilling discovered an EWE dated to 3125 cal BP, tentatively interpreted as a tsunami layer (Koster and Reicherter 2014). However, the layer is below a sheet of white sand which would pre-date the event. Furthermore, the back-barrier of the inlet changed completely from limnic to alluvial (terrestrial). Rodriguez Vidal et al. (2015) dated an event ca. 3000 cal BP in a deposit filling cliff cracks in Gibraltar. Lastly, Lario et al. (2015, 2016) have dated an EWE in the Piedras estuary to around 3000 cal BP (3180—2685 cal BP).

In Portugal, where descriptions of offshore depositional signatures of tsunamis have been hitherto thin on the ground, offshore studies have recently revealed a broader picture of tsunami events in this region.

Reicherter et al. (2019) describe a geophysical survey and coring campaign along the Algarve continental shelf (for the upper 500 m of the water column, conducted on board the RV METEOR in November 2018). The retrieved sedimentary archive covers the last 11,000 years (representing the post-LGM transgression of the Algarve shelf) down to the bedrock (bioclastic sandstone), representing a former coastal cliff. Sub-bottom profiles obtained in the shallower area (up to 75 m deep) revealed a strong reflector, caused by a coarser sediment layer, at a depth of approximately 1.25–1.60 m in the sediment column above the Jurassic-Cretaceous bedrock. This layer shares similarities with high-density flows, displaying a distinctive poorly sorted coarse bioclastic basal layer, followed by inversely graded sand and a massive matrix-poor siliciclastic sandy unit (Reicherter et al. 2019). Radiocarbon dating of marine shells indicated that the massive sand layer was formed between 3656 and 3721 cal. BP (Reicherter et al. 2019), this being tentatively associated with a yet unreported (onshore and offshore) tsunami that might be correlated with the E5-E6 events in the eastern region of the Gulf of Cadiz (Fig. 5.4).

In the upper parts of the retrieved cores, a few thin coarser layers have been detected and analysed. With their contrasting sedimentary and geochemical features, they show indications of being tsunami-related. In particular, the radiocarbon ages of two layers at a depth of 12–14 cm and 22–25 cm correlate with the 1969 and 1755 tsunamis (Reicherter et al. 2019). However, the layer detected in ca. 3700 cal. BP is traceable in the sub-bottom profiles and the sediment cores for at least a 2000 m downslope in water depths of up to 75 m, displaying a broad lateral distribution on the shelf (Reicherter et al. 2019). An abrupt sedimentological distinction of the deposit from its surrounding background stratum is displayed in a complex structure (four sub-units), coarser texture (medium sand) and compositional singularity (diverse siliciclastic and bioclastic content).

Reicherter et al. (2019) have gathered extensive and unique sedimentological data from the shallow offshore area of the western Algarve which, once this multidisciplinary study covering the LGM time window has been completed, should help to gain a deeper understanding of tsunami events and to define return periods more precisely for this region.

Deeper offshore geological studies have mostly relied on geophysical data and have focused on the search for tsunami generation mechanisms, namely earthquake or landslide sources. A study similar to that of Gràcia et al. (2010) has yet to be performed in the areas closer to the southern coast of Portugal. On the western coast, the poor preservation of tsunami deposits is likely due to its highly hydrodynamic character (deeper closure depth and strong offshore currents), its major incised canyons (e.g., Douro, Nazaré, Tejo, Sado, etc.) and stronger fluvial and human interference.

5.2.4 EWEs Ca. 3000–2500 cal BP

Between 3000 and 2500 cal BP (depending on the area) there was an EWE that affected all the area's estuaries (Guadiana, Rio Piedras, Tinto-Odiel and Guadalquivir), pointing to an erosional event resulting in the breaching of the spit barrier system, the reorganization of the back-barrier drainage system and marine sediment input inside the estuaries, as well as chenier development (Lario 1996; Dabrio et al. 2000; Lario et al. 1995, 2001a, b, 2010a, 2015, 2016; Rodriguez-Ramírez et al. 2015, 2016).

5.2.5 EWEs Ca. 2200–1600 CalBP: The "Roman" Event and "sibling" Events

This event is the most controversial of all due to the broad range of dates and the lack of sedimentary evidence. In the Rio Piedras estuary (location 18 in Fig. 5.2), an erosional gap between 2100 and 1900 cal BP has been detected in the spit barrier (Lario 1996). In the Tinto-Odiel estuary (location 19 in Fig. 5.1), this erosional gap in the Punta Umbría spit barrier and other high energy marine event features appear at 2100 cal BP and between 1900 and 1650 cal BP (Lario 1996; Dabrio et al. 1999a, 2000). The last one has also been described associated with a tsunami or storms by González-Regalado et al. (2019a, b a and b), using the dates proposed by Lario (1996) and Dabrio et al. (2000) and a new radiocarbon date suggesting that the event occurred around 1990–1690 cal BP (recalibrating the proposed data).

In drill cores, this event is dated to around 2000 cal BP and characterized by shell accumulation in the sand and muddy-sand deposits (Morales et al. 2008). The first evidence of a high energy marine event at this time was found by Lario (1996) in the Doñana area, where in cores a sandy layer with marine fauna is sandwiched between estuarine deposits. With a distinctive erosional base and high magnetic susceptibility, it has been dated to around 2200–2000 cal BP. This event has also been described as an erosional and breaching phase of the spit barrier between progradational episodes (Zazo et al. 1994; Lario 1996; Rodriguez-Ramírez et al. 1996; Cáceres et al. 2006) and chenier development (Ruiz et al. 2004; Rodriguez-Ramírez et al. 2015). A recalibration of all radiocarbon dates of the spit barrier system (Lario 1996; Rodriguez-Ramírez et al. 1996, 2016) has situated this event between 2050 and 1900 cal BP. Another event of spit barrier erosion and breaching has been detected by the same authors in ca. 1700–1600 cal BP. For their part, Rodriguez-Vidal et al. (2008) also reported a tsunamigenic layer in Doñana in 1700 cal BP, but have not mentioned it again in subsequent papers. In the Valdelagrana-Guadalete estuary, an episode with spit barrier breaching and the reorganization of the back-barrier drainage system has been identified in ca. 2100 cal BP (Lario et al. 1995; Lario 1996; Dabrio et al. 2000). Luque et al. (2001, 2002) studied some washover fans and found repeated fining upward sequences (two to three times), marine shell fragments, armed mounted clasts and an erosional lower limit, attributing it to a tsunami occurring between 2250 and 1710 cal BP.

Further tsunami deposits have been found along the coast between Cadiz and Gibraltar. In the Bay of Bolonia (Tarifa), Alonso et al. (2003) were the first to describe and interpret some coarse sediments and bioclasts, discovered in the Arroyo del Alpariate, as a result of a tsunami occurring between 2200 and 1850 cal BP. Specifically, they describe an isolated "sand lens" on the western bank of the Arroyo del Alpariate, near its mouth, interpreting it as "washover" deposits. As the beach is full of bioclasts, which might have been reworked, and because the age was subsequently modified to 2150–1825 cal BP (Alonso et al. 2004), without providing dated material, a ΔR or an exact location, this finding should be interpreted very cautiously, as it reflects a "*terminus ante quem*" age, namely, a maximum age for the deposit. Until now, this is the only vague sedimentary evidence in the bay for the E5 and sibling events, as well as a tsunami associated eventually with the 40–60 CE earthquake (Silva et al. 2005).

A blackish layer within the eastern necropolis of *Baelo Claudia* was dated to 2120–1945 cal BP, but not interpreted as a tsunami layer (Reicherter et al., this volume). Most probably, the 40–60 CE seismic event was not accompanied by a tsunami. In the Roman settlement of Carteia (Algeciras, location 25 in Fig. 5.2), a coarse sandy layer, with a fining upward sequence, mounted clast, bioclasts, calcareous rhodolites and an erosional base, has been described and interpreted as "backwash" deposits resulting from a high energy event (Arteaga and Gonzalez 2004; Arteaga et al. 2015). From this, the authors inferred that an inundation of >170 m had occurred in Carteia and, based on archaeological remains, dated the tsunami layer to ca. 50 CE.

Clear evidence of tsunami landfall in *Baelo Claudia* is to be found in the Roman baths outside the city walls and along the eastern necropolis/Decumanus (Reicherter et al., this volume). Röth et al. (2015) described sedimentary evidence of a tsunami in the pool of the Roman baths. Charcoal dates between 255 and 263 CE were tentatively linked to the 260–290 CE earthquake (Silva et al. 2009; Grützner et al. 2010). Bernal et al. (2015) dated the abandonment of the bath complex to the late third/early fourth century CE (the Diocletian or Constantine period), but a wall collapsed ca. 500 CE. Röth et al. (2015) also discussed an earlier event associated with a tsunami in ca. 400–450 CE and correlated it with the earthquake occurring around 350–395 CE, first described by Menanteau et al. (1983). In all likelihood, these two observations are related to tsunami landfall in Baelo Claudia but constitute only one deposit and so confirm only one event, the most probable date of late fourth century CE being discussed in Reicherter et al. (this volume).

Rodriguez Vidal et al. (2015) used an innovative approach and identified crevices infilling deposits on the Gibraltar coast as a tsunamite record, recording events at 218–209 BC, 60 CE and 365 CE.

5.2.6 Last 1500 years

Several rare EWEs have been described in the last 1500-year time interval. In the Piedras River estuary, Lario (1996) identified an erosional event with breaching of the spit barrier around 1300–1200 cal BP. In the Tinto-Odiel estuary, almost two EWEs with spit barrier breaching and the reorganization of the back-barrier drainage system have been described in the Punta Umbria-Saltés spit system, both occurring around 1050 cal BP (Lario 1996; Lario et al. 2010a). The erosional gaps detected in spit-bar units H3 and H4 between 1700 and 1600 cal BP and between 1250 cal BP and 1000 cal BP provided the first evidence of high energy events in the Doñana spit-Guadalquivir estuary (Zazo et al. 1994; Lario et al. 1995), which were subsequently confirmed as spit breaching episodes with a complete radiocarbon dataset of the spit barrier system (Lario 1996; Rodríguez-Ramírez et al. 1996). With similar ages, several chenier structures also linked to high energy events have been described by the same authors (Lario 1996; Rodríguez-Ramírez et al. 1996, 2015, 2016). In the Valdelagrana spit-Guadalete estuary, episodes of spit barrier breaching and the reorganization of the back-barrier drainage system have been dated to ca. 1500–1300 cal BP and 1000 cal BP (Lario et al. 1995; Lario 1996; Dabrio et al. 2000), matching the new dates proposed by Rodríguez Polo et al. (2009). Some shell layers dated to between 1600 and 900 cal BP have been interpreted as the result of EWEs, specifically tsunamis correlating with seismic catalogue (Gutiérrez Mas et al. 2009; Gutierrez Mas 2011). For the SW Iberian coast as a whole, Ruiz et al. (2008) positioned a tsunami in 1568 BP, but without offering further details. In the southern coastal sector, Becker-Heidmann et al. (2007) described an EWE deposit near Cape Camarinal (Bolonia), dating it to around 500 cal BP and suggesting that it was formed by a tsunami. However, this radiocarbon dating of charcoal is a “terminus ante quem” due to house- or wildfires close-by and may involve considerable “burial” time and reworking. The possibility that the deposits were the result of the 1755 Lisbon event has not been ruled out and is favoured by Reicherter et al. (this volume).

In the Portuguese coast and the Greater Lisbon area, some deposits associated with the 1531 CE, the 1969 CE and also the 1755 CE tsunamis were identified. Andrade et al. (2003) found evidence in sediment cored from the Tagus marshes that was correlated with the 1755 CE and 1531 CE events. The techniques used included magnetic susceptibility, geochemistry, nannoplankton abundance and diversity, and a range of sedimentological proxies. The evidence was provided by slight increases in SiO_2 and $CaCO_3$ and abrupt changes in magnetic susceptibility values suggesting the temporary disturbance of sediment sources, together with greater amounts of calcareous nannoplankton. On the other hand, in the Tagus pro-delta Abrantes et al. (2005, 2008) were able to identify an “instantaneous deposit” of coarser material, including broken shells, on the south-southwest coring site on the shelf area just offshore from Lisbon; and a 1.5 m thick “instantaneous deposit” of fine material on the west site in their box cores. Magnetic susceptibility, grain size and Fe data by XRF, as well as ^{210}Pb and AMS ^{14}C age estimations, were used to characterize the material and constrain the time of deposition. By considering the ages of the undisturbed underlying unit, a hiatus was recognised on both sites, roughly corresponding to 355 years of sedimentation. Both the hiatus and instantaneous deposit were considered to be of tsunamigenic origin, the former corresponding to an erosive episode and the latter to sedimentation, both in association with the backwash of the same tsunami event.

In the shallow offshore areas of the Algarve, just south of Faro, Quintela et al. (2016) studied a sediment core retrieved at 98 m below mean sea level. Their identification of the CE 1969 and CE 1755 tsunami deposits was based on coastal foraminifera species in coarse silt layers within a fine silt sequence. Furthermore, the textural and palaeontological changes were slight and those deposits that were macroscopically indistinguishable could only be identified through a high-resolution analysis. The age estimation of layers was obtained through indirect radiocarbon dates and ^{210}Pb and ^{137}Cs sedimentation rates. Nevertheless, the thinness of the 1969 CE deposit and, in contrast, the very notable thickness (>35 cm of coarse silt) of the 1755 CE deposit raises questions regarding the hydrodynamic conditions capable of leaving such imprints.

5.2.7 The 1755 Lisbon Earthquake and Tsunami

The 1755 Lisbon earthquake and associated tsunami are the best documented historical events of this type in the western Iberian Peninsula. Despite the extensive historical data on the impact of the 1755 CE event on the western coast of Portugal, namely on the city of Lisbon, there are only a handful of records for this extensive >500 km long coastal stretch. Corrochano et al. (2000) described washover fans in the Aveiro ria (location 1 in Fig. 5.2), associating their distribution and the erosion of the dune ridges with the 1755 CE tsunami, albeit without providing age assignments for their geomorphological observations.

Costa et al. (2012c) and Tudor et al. (2020) discussed the possibility of the presence of deposits associated with the 1755 CE tsunami in the lagoonal area of Óbidos and on the alluvial plain of the Alcabrichel river (both on the west-central coast of Portugal, approximately 50 and 80 km northwest of Lisbon). However, both were cautious and unable to establish a conclusive link between the coarser sandy units and a tsunami event. Nevertheless, the ages obtained for these deposits, using different methodologies (OSL and radiocarbon), point to their association with a major marine inundation affecting these two coastal areas of central Portugal during the eighteenth century. Similarly, as for the Aveiro deposit, further sedimentological studies are needed before ascribing these deposits to a tsunami.

On the sandy Troia spit (location 7 in Fig. 5.2) just south of Lisbon, Rebêlo et al. (2013) described the evolution of a sand barrier and suggested the association of levels observed in the georadar profiles with the 1755 CE tsunami. Again, insufficient and low-resolution dating of these layers makes it difficult to certain associate these features with the 1755 CE tsunami. Finally, boulder deposits in the Cascais (location 3 in Fig. 5.2) and Malhão regions (location 8 in Fig. 5.2) have been related to tsunami transport and deposition (Scheffers and Kelletat 2005; Ramos-Pereira et al. 2009). Complications like poor stratigraphic framework and difficulties in precise age estimation in limestone environments led to simple numerical approaches for wave-related sediment transport. The results suggested that only rare and high-magnitude wave heights would have been able to move boulders upward weighing up to 120 tons, up to approx. 20 m above the sea level and inland <150 m from the current coastline.

In alluvial plains, lagoons and estuaries, deposits associated with the 1755 CE tsunami have been described along the Algarve coast in southern Portugal (Fig. 5.3). Kortekaas and Dawson (2007) described and interpreted the lithostratigraphy of the Martinhal estuary infill (location 9 in Fig. 5.2) that includes the 1755 CE tsunami deposit between the pre- and post-event sedimentation pattern that extends across most of the lowland, but is more evident in the seaward sector of the estuary. There is also evidence of storm activity in the eighteenth century resulting in thin sandy overwash layers barely extending inland. In all likelihood, this can be associated with the barrier destruction by tsunami waves during the 1755 CE event, which then never fully recovered in a sediment-starved coastal depression.

In the Barranco and Furnas lowlands (location 10 in Fig. 5.2), Costa et al. (2011) observed scattered cobbles and boulders (0.3–1 m a-axis length) evincing marine bioerosion and colonization by endolithic fauna indicative of an origin at a minimum water depth of 5 m. Boulders were transported a few hundred meters inland into the alluvial plain located 2.5 m above mean sea level. Radiocarbon dates obtained from in situ endolithic bivalve shells of *Petricola lithophaga* (240 ± 40 yr BP and 360 ± 40 yr BP) suggest that boulder transport and deposition are compatible with the 1755 CE tsunami (Costa et al. 2011). Furthermore, in Barranco (location 11 in Fig. 5.2) a thin marine sand layer with shells, embedded in alluvial mud about 0.25 m below the surface and extending more than 300 m inland, has been associated with the boulder deposit. Radiocarbon dating of 340 ± 30 yr BP obtained from a gastropod shell (*Cabestana* sp.) from the sand is compatible with the dating results and with the same inundation.

Dawson et al. (1995), Hindson et al. (1996), Hindson and Andrade (1999), Allen (2003), Cunha et al. (2010), Font et al. (2010, 2013), Costa et al. (2012a, 2015, 2018) and Feist et al. (2019) identified a coarse clastic layer, attributed to the 1755 CE tsunami, in the Holocene infilling of the Boca do Rio river inlet, in alluvial muds approximately 0.8 m below the surface. Eyewitness reports described this inundation and the destruction of a coastal dune at the back of the beach (Lopes 1841, p. 222): “On the day of the earthquake, the sea invaded the freshwater creek that gives into the sea. It inundated the land for more than ½ of a league, with a water height of 10–12 varas [11–13 m], destroying some large sand mounds [dunes] and dragging 50 of the heaviest anchors for more than ¼ of a league inland. On the beach, the backwash uncovered great and noble buildings [i.e., Roman ruins] of which no memory existed.”

The unit marks a distinct sedimentary and micropalaeontological break from the deposits enclosing it. In the seaward section of the alluvial plain, the lowermost section of the layer appears to have been deposited from a highly turbulent water mass, which was able to transport gravel-sized limestone clasts, as well as rip-up mud clasts eroded from the underlying estuarine clayish material. The water mass rapidly lost energy as it progressed inland, leading to the

Fig. 5.3 Sedimentary evidence of the 1755 CE tsunami in the Algarve lowlands: **a** Boca do Rio, **b** Martinhal, **c** Alcantarilha, **d** Salgados, and **e** box core from Salgados (Reprinted from Costa and Dawson (2015) Copyright 2015). The vertical scale is approx. 1 m for (**a**), 0.30 m for (**e**) and ca. 0.5 m for all the other images. Note the contrasting texture of the sandy deposits and the low-energy framing (muddy) sediments and that only in Martinhal the top sequence has more than one sandy layer

deposition of predominantly shell-rich sand, silt and clay particles up to about 1 km inland. The provenance study performed by Costa et al. (2012b) points to dune sands, and to a lesser extent to the beach sands, as the most likely sediment sources of this tsunami layer.

Schneider et al. (2010) analysed cores from the Carcavai valley (location 15 in Fig. 5.2) near Quarteira, east of Salgados in the central Algarve, detecting a prominent sand layer interrupting the fine-grained sedimentation. Based on radiocarbon dating, the authors suggested that this peculiar unit might have been deposited by the 1755 CE tsunami, although further sedimentary details are lacking.

The inundation of the Alcantarilha lowlands (location 13 in Fig. 5.2) by the 1755 CE tsunami is described in historical records (Lopes 1841, p. 290): "In Armação [the Alcantarilha lowlands], located ¼ of a league from another village named Pera, the sea left only one house standing on the day of the earthquake; it rushed more than

½ of a league inland, flooding everything, forming saltwater lakes in the lowlands, creating islands and drowning 84 people […].”

The imprints in this alluvial plain/lagoonal area are compiled in Costa et al. (2016), in which both the erosional imprint on the dune barrier and the depositional signatures on top of the lithostratigraphic sequence are described. Radiocarbon and OSL dates confirmed the association of an erosional structure in the dune barrier and a unique sandy unit in the lowlands with the 1755 CE event.

Costa et al. (2012b, 2018) also characterized a tsunami deposit in late Holocene lagoonal sediments of Lagoa dos Salgados (location 14 in Fig. 5.2), using stratigraphical, textural, palaeoecological and compositional diagnostic criteria commonly used to distinguish these tsunami deposits. Furthermore, age constraining using ^{210}Pb, ^{137}Cs and ^{14}C methods yielded results that were mutually consistent with the 1755 CE event (details in Costa et al. 2012a). Microtextural studies revealed a strong similarity between the dune sand and the tsunami deposit grains, suggesting the latter as the likely source of the tsunami deposit (Costa et al. 2012b). Moreira et al. (2017) subsequently demonstrated the usefulness of geochemical data and high-resolution grain size based on digital image analysis for establishing inundation limits and inundation phases. Finally, following a regressive approach to tsunami deposits Dourado et al. (2020) discuss the use of sediment-based data from Salgados to identify earthquake epicentres. This work exemplifies the progress made in the study of tsunami deposits in the Iberian Peninsula, where contributions have been made to the ongoing debate on the 1755 CE epicentre based on tsunami deposit data.

On the coasts of Huelva and Cadiz, there are many accounts of the number of waves, their time of arrival, run-up and inundation extension, the number of casualties and the damage caused to large communities, but the geological record of coastal damage is still insufficient (Campos 1991; Luque et al. 2001, 2004; Martínez Solares 2001; Luque 2002; Alonso et al. 2015).

In the Guadiana estuary (location 17 in Fig. 5.2), Lario (1996) identified an erosional event in the spit barrier system at approximately 1750 CE. Furthermore, Klein et al. (2016, p. 120) found a “layer of coarse gravel, brick fragments and broken shell material between 1.32 and 1.40 m b.s., which intercalates abruptly with a sharp erosional contact into deposits of a low energy environment” in a drill core from the Guadiana estuary. The layer has been dated to 1750 CE by radiocarbon. In the Rio Piedras estuary, Lario et al. (2015, 2016) described the input of marine fauna in a tidal channel during an EWE dated to around 1755 CE from drill cores, correlating it with the Lisbon tsunami. Similarly, Lario (1996) noted the absence of new crests in the spit barrier after an erosional event occurring 250 years ago. In the Tinto-Odiel estuary, Morales et al. (2008) identified high energy levels characterized by an erosional base, shell accumulation and sand and muddy-sand deposits, dated high energy level HEL-2 to 250 yr BP and correlated it with the Lisbon tsunami. In Valdelagrana within the Guadalete estuary, Dabrio et al. (1999a) reported the breaching of the spit barrier and the generation of washover fans. When these washover fans were sampled by Luque et al. (2001), repeated fining upward sequences (three to four times), with marine shell fragments, armed mud clasts and an erosional base, were detected. These sedimentary characteristics fit in with three to four waves in this area during the 1755 CE Lisbon tsunami and confirm descriptions in historical reports and documents.

Along the coast between Cadiz and Gibraltar there is plenty of evidence of deposits resulting from the 1755 CE Lisbon tsunami, and other geological indications of this event. Near the Castilnovo Tower/Conil (locations 22 and 23 in Fig. 5.2), the tsunami destroyed the fishing village of Conilete and the tuna factory “La Chança” (Gutiérrez-Mas et al. 2016). Some washover fans with remains of this event were found in drill cores by Luque et al. (2004) and, later on, Gutiérrez-Mas et al. (2016) performed more in-depth studies on the sedimentary record of the tsunami in this area. Further south in the

Conilete creek and marshland (El Palmar) the organics of the 1755 CE tsunami deposits have been studied (Frenken et al., this volume). The tsunami boulders of Cape Trafalgar (locations 22 and 23 in Fig. 5.2) were first described by Whelan and Kelletat (2003, 2005) and subsequently characterized by Gracia et al. (2006), but the specific age has not been established (Lario et al. 2009). From Barbate to Tarifa there are also some descriptions of tsunami deposits related to the Lisbon event (Gracia et al. 2006; Reicherter et al. 2010). However, the preservation of those deposits is problematic, there being only some coarse-grained and shell hash remains on the beach between Barbate and Zahara de los Atunes. Coarse clastic sediment accumulations at beaches in the Bay of Bolonia have also been ascribed to the Lisbon event (Gracia et al. 2006). The Los Lances Beach (location 14 in Fig. 5.2) northwest of Tarifa and the Roman *Mellaria* have been studied by different authors (Alonso et al. 2004; Gracia et al. 2006; Reicherter et al. 2010) who briefly describe some deposits associated with the Lisbon tsunami. Cuven et al. (2013) published a detailed and innovative sedimentological study of washover fans using drill cores and trenches, which confirmed the sedimentological record of this tsunami. A destroyed bridge over the Rio de la Jara, parts of which have drifted southward along the beach, parallel to the coast, can still be observed today (Reicherter et al. 2010). In Gibraltar, Rodríguez-Vidal et al. (2011, 2015) found evidence of this tsunami as a sandy level in a lagoon core, shelly sediments filling open crevices and sandy subaqueous tsunami deposits.

5.3 EWEs: Tsunamis or Large Storms?

There is a long record of EWEs in the Gulf of Cadiz, but the interpretation of their origin is still a thorny issue. Many recent studies have attempted to characterize the sedimentological features of tsunami and palaeotsunami events (Dawson et al. 1996; Goff et al. 1998; Dawson and Shi 2000; Nott 2003; Scheffers and Kelletat 2003; Dominey-Howes et al. 2006) or to identify the distinguishing features of tsunamis and deposits of other high energy events (EWEs), such as severe storms or storm surges (Foster et al. 1991; Nanayama et al. 2000; Lario et al. 2010a, 2011; Kortekaas 2002; Kortekaas and Dawson 2007; Morton et al. 2007; Switzer and Jones 2008). Most of them have concluded that the deposits generated by both types of events display similar textural, structural and sedimentary features. Therefore, no clear-cut criterion can be established for the conclusive identification of tsunami deposits based on sedimentological studies and differentiating between the high energy coastal deposits generated by tsunamis and large storms is still a challenge (Kortekaas and Dawson 2007; Bridge 2008; Jaffe et al. 2008; Switzer and Jones 2008). This is why other recent studies have focused on the geochemical variation and anthropogenic markers in tsunami deposits (e.g., Bellanova et al. 2020) or have searched for other offshore archives, for example, in sediments below the storm base in backwash deposits (e.g., Reicherter et al. 2019).

Lario et al. (2011) proposed correlating the record of earthquake-triggered turbidites offshore in this area (Gràcia et al. 2010) with the onshore evidence of EWEs so as to assign, or not, a tsunamigenic origin to the latter. Gràcia et al. (2010) recognized eight turbidite events during the last 7000 yr (E1–E9, ages in Fig. 5.4). E1, E3, E5, E6, E8 and E9 are super-regional events associated with widespread turbidites triggered by Mw > 8.0 earthquakes; E2, E4 and E7 are local turbidite events generated not only by low to moderate earthquakes, but also by other non-seismic events. The correlation of these with the described EWEs allows for identifying almost six tsunamis, triggered by Mw > 8.0 earthquakes, along the coast, plus other ones for which there is less evidence in the geological record. Furthermore, there are no onshore geological records of the 1969 Horseshoe, except within the Tagus estuary, earthquake (Mw > 8.0, albeit with a

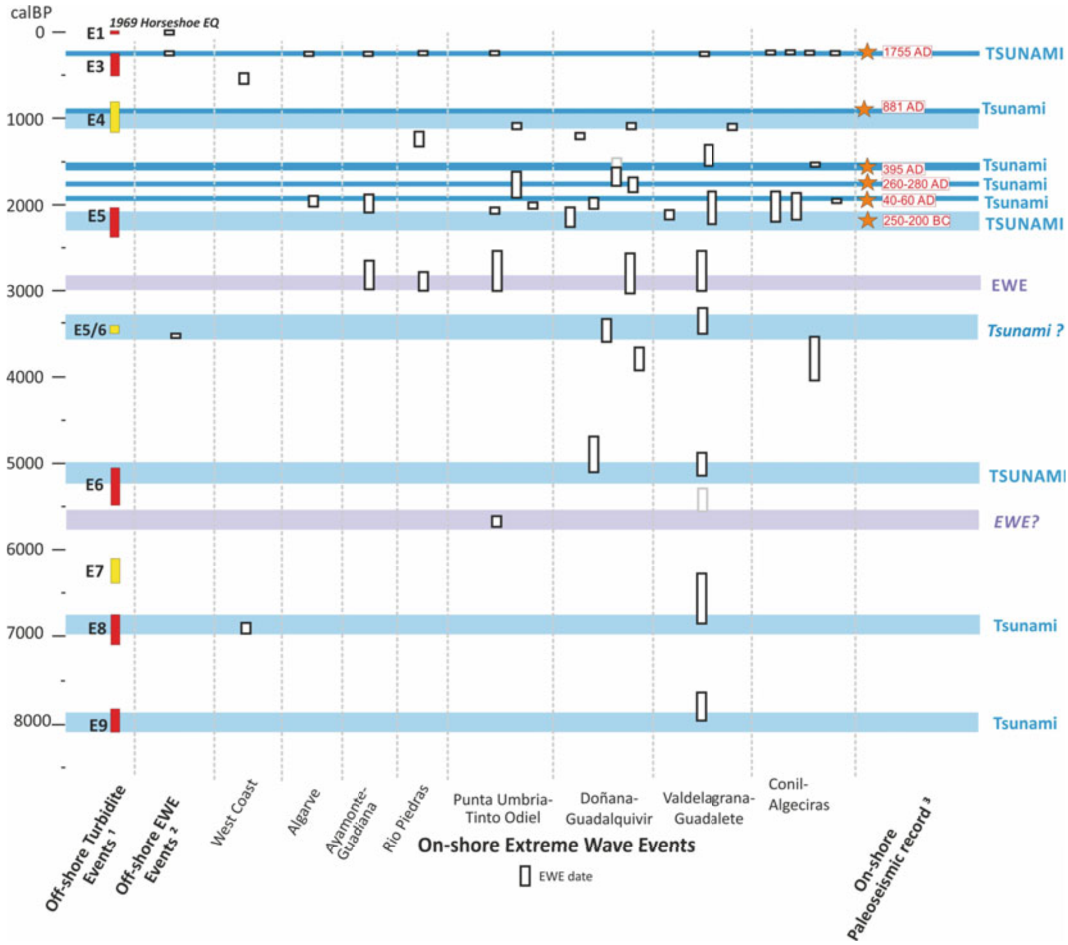

Fig. 5.4 Correlation between turbidites (E1–E9) described in the offshore region of the Gulf of Cadiz and onshore evidence of similar age-related EWEs presented by areas (x-axis) and age (y-axis). Although there is widespread evidence of the 1755 CE tsunami, other events are less identifiable along the Atlantic coast of the Iberian Peninsula, despite some relevant ones (affecting more than one location). 1. Data from Gràcia et al. (2010). Widespread events generated by EQs Mw > 8.0 in red and local events in yellow. 2. Offshore EWEs on the Portuguese coast, data from Quintela et al. (2016); Reicherter et al. (2019, this volume). 3. Data from Silva et al. (2009, 2014, 2019). Stars show documented EQs with geological effects. Letter mark archaeological sites: ***B***: *Baelo Claudia,* ***C***: *Carteia*. All data recalibrated to ΔR = 0 (modified from Lario et al. 2011)

minor associated tsunami), while there are other EWEs with no seismic evidence which can be attributed to large storms or which require further evidence to be interpreted as tsunamis. Another crucial point is that regional or even local active faults (Portimão fault in the Algarve, off the Portuguese coast, Terrinha et al. 1999; Cabo de Gracia fault in the Bay of Bolonia, off the Spanish coast, Grützner et al. 2012) may also trigger tsunamis with a local impact.

5.4 Concluding Remarks

This chapter summarizes the state of the knowledge on tsunamis and other EWEs and their geological signatures on the Portuguese and Spanish coasts along the Gulf of Cadiz. The number of identified events is very limited on the Portuguese side, presumably because of their specific geomorphological and sedimentological context and preservation. On the other hand, the Spanish onshore Holocene tsunami and EWE stratigraphy present a good correlation with the deep-sea turbidite record thought to have been generated by strong earthquakes, thus allowing for more accurate inferences on return periods in this region.

Sedimentological and geomorphological settings where imprints of EWEs have been described in the Iberian Peninsula share many similarities. The deposits tend to be coarser sandy layers sandwiched between muddy sediments in estuarine, alluvial or lagoonal environments. These deposits are also characterized by their palaeontological peculiarity which has been widely used as an EWE diagnostic criterion. Other common textural, compositional, geochemical and geophysical features have also been described in a similar way to other tsunami and storm deposits elsewhere in the world.

A common problem in distinguishing between tsunami and storm deposits is accurately narrowing down the period in which they occurred. This is particularly crucial for such high-intensity events and, in the Iberian Peninsula, raises doubts about the exact number of events described hitherto. The second problem in dating them is the sample material (e.g., reservoir effects of marine organisms, reworking of charcoal) and the fact that these radiocarbon analyses have been performed over ca. 25 years, applying different calibration and interpretation techniques (e.g., dating the event directly, bracketing the event by sampling the top and base of the tsunami deposit, considering sediment erosion at the base of the event and so on). Due to uncertainty about estimating intervals, some geological evidence discovered on the Iberian seaboard overlaps the dates of different offshore events, thus raising doubts about its association with specific events (although the offshore record may be incomplete). Nevertheless, the widespread impact of the 1755 CE tsunami and its strong presence in the stratigraphy of the various locations studied are inquestionable. This event is unique in its regional imprint and probably in its intensity. Other events reported on the Spanish coast seem to suggest a return period for catastrophic EWEs of approximately a millennium (i.e., 1000 years).

The need for further studies is obvious, as are the integration of onshore and offshore records and the incorporation of landscape and past sea level changes, so as to reconstruct past events in this region more precisely. Furthermore, the present and future developments of age estimation methodologies, coupled with high-resolution sedimentological studies, will yield even more reliable data. Nevertheless, in the European context, the southwest Iberian Peninsula provides the best and most detailed sedimentological examples of tsunami and storm deposits, thus converting it into an invaluable natural laboratory for geological records of EWEs.

Acknowledgements The authors acknowledge the financial support of FCT through projects UIDB/50019/2020-IDL and OnOff—PTDC/CTAGEO/28941/2017 to PJMC; and DFG-project Re 1361/28-1 to KR.

References

Abrantes F, Lebreiro S, Rodrigues T et al (2005) Shallow-marine sediment cores record climate variability and earthquake activity off Lisbon (Portugal) for the last 2000 years. Quatern Sci Rev 24(23–24):2477–2494

Abrantes F, Alt-Epping U, Lebreiro S et al (2008) Sedimentological record of tsunamis on shallow-shelf areas: the case of the 1969 AD and 1755 AD tsunamis on the Portuguese Shelf off Lisbon. Mar Geol 249(3–4):283–293

Allen HD (2003) A transient coastal wetland: from estuarine to supratidal conditions in less than 200 years—Boca do Rio, Algarve, Portugal. Land Degrad Dev 14:265–283

Alonso C, Gracia FJ, Anfuso G et al (2004) Registro morfosedimentario de eventos históricos de alta energía en el litoral atlántico del Estrecho de Gibraltar (Trafalgar—Tarifa). In: Benito G, Díez Herrero A (eds) Contribuciones recientes sobre Geomorfología. SEG-CSIC, Madrid, pp 263–271

Alonso C, Gracia FJ, Manenteau L et al (2003) Paléogéographie de l´anse de Bolonia (Tarifa, Espagne) à l´époque romaine. In: Fouache E (ed) The mediterranean world environment and history. Environmental dynamics and history in Mediterranean areas, Paris, Université de Paris-Sorbonne, 24–26 avril 2002. Swamp areas and seashores dynamics/Dynamiques des zones humides et mobilite des lignes de rivage. Elsevier, Paris, pp 405–417

Alves EQ, Macario K, Ascough P et al (2018) The worldwide marine radiocarbon reservoir effect:

definitions, mechanisms, and prospects. Rev Geophys 56:278–305

Andrade C, Freitas MC, Oliveira MA et al (2016) On the sedimentological and historical evidences of seismic-triggered tsunamis on the algarve coast of Portugal. In: Duarte JC, Schellart WP (eds) Plate boundaries and natural hazards. Wiley & Sons, Hoboken, pp 219–238

Andrade C, Freitas MC, Miranda JM et al (2003) Recognizing possible tsunami sediments in the ultra-dissipative environment of the Tagus estuary (Portugal). In: Davis RA (ed) Coastal sediments'03—The 5th international symposium on coastal engineering and science of coastal sediment processes, Clearwater Beach, Florida, 18–23 May

Arteaga C, González JA (2004) Presencia de materiales marinos y dunares sobre un alfar romano en la Bahía de Algeciras (Cádiz, España). In: Benito G, Díez Herrero A (eds) Contribuciones recientes sobre Geomorfología. SEG-CSIC, Madrid, pp 393–400

Arteaga C, Blánquez J, Roldán L (2015) Consideraciones paleogeográficas en la bahía de Algeciras. Acerca de un possible tsunami en la *Carteia* romana. Cuaternario y Geomorfología 29:137–156

Baptista MA, Miranda J, Batlló J et al (2016) New study on the 1941 gloria fault earthquake and tsunami. Nat Hazards Earth Syst Sci 16:1967–1977

Becker-Heidmann P, Reicherter K, Silva PG (2007) 14C dated charcoal and sediment drilling cores as first evidence of Holocene tsunamis at the Southern Spanish coast. Radiocarbon 49(2):827–835

Bellanova P, Frenken M, Reicherter K et al (2020) Anthropogenic pollutants and biomarkers for the identification of 2011 Tohoku-oki tsunami deposits (Japan). Mar Geol 422:106–117

Bernal D, Expósito JA, Díaz JJ, Bustamante M et al (2015) Evidencias arquelogicas de desplomes paramentales traumáticos en las termas marítimas de Baelo Claudia: reflexiones arqueosismológicas. Cuaternario y Geomorfología 29:119–136

Bridge JS (2008) Discussion of articles in "Sedimentary features of tsunami deposits." Sed Geol 211:94

Cáceres LM, Rodríguez-Vidal J, Ruiz F et al (2006) El registro geológico Holoceno como instrumento para establecer periodos de recurrencia de tsunamis. El caso de la costa de Huelva. In: V Asamblea Hispano Portuguesa de Geodesia y Geofísica, Sevilla, pp 1–4

Campos ML (1991) Tsunami on the Spanish coasts of the Iberian Peninsula. Sci Tsunami Haz 9:83–90

Chagué-Goff C, Schneider JL, Goff JR et al (2011) Expanding the proxy toolkit to help identify past events—lessons from the 2004 Indian Ocean Tsunami and the 2009 South Pacific Tsunami. Earth Sci Rev 107(1–2):107–122

Cita MB, Rimoldi B (1997) Geological and geophysical evidence for a holocene tsunami deposit in the eastern Mediterranean deep-sea record. J Geodyn 24(1–4):293–304

Corrochano A, Merino SG, Barba P et al (2000) Los sedimentos del canalmareal de Mira (Aveiro, Portugal): propriedades texturales, procedencia y modelo paleogeográfico. Stvdia Geologica Salmanticensia 36:143–160

Costa PJM, Dawson S (2015) Tsunami sedimentology. In: Meyers RA (ed) Encyclopedia of complexity and systems science. Springer Science - Business Media, New York, pp 1–17

Costa PJM, Andrade C, Freitas MC et al (2011) Boulder deposition during major tsunami events. Earth Surf Proc Land 36:2054–2068

Costa PJM, Andrade C, Dawson AG et al (2012a) Microtextural characteristics of quartz grains transported and deposited by tsunamis and storms. Sed Geol 275–276:55–69

Costa PJM, Andrade C, Freitas MC et al (2012b) A tsunami record in the sedimentary archive of the central Algarve coast, Portugal: characterizing sediment, reconstructing sources and inundation paths. The Holocene 22(8):899–914

Costa PJM, Leroy SAG, Dinis JL et al (2012c) Recent high-energy marine events in the sediments of Lagoa de Óbidos and Martinhal (Portugal): recognition, age and likely causes. Nat Hazards Earth Syst Sci 12:1367–1380

Costa PJM, Andrade C, Cascalho J et al (2015) Onshore tsunami sediment transport mechanisms inferred from heavy mineral assemblages. The Holocene 25:795–809

Costa PJM, Costas S, Oliveira MA (2016) How did the AD 1755 tsunami impact on sand barriers across the southern coast of Portugal? Geomorphology 268:296–311

Costa PJM, Gelfenbaum G, Dawson S et al (2018) The application of microtextural and heavy mineral analysis to discriminate between storm and tsunami deposits. In: Scourse EM et al (ed) Tsunamis: geology, hazards and risk. Geol Soc Lond 456:167–190

Cunha PP, Buylaert JP, Murray AS et al (2010) Optical dating of clastic deposits generated by an extreme marine coastal flood: the 1755 tsunami deposits in the Algarve (Portugal). Quat Geochronol 5(2–3):329–335

Cuven S, Paris R, Falvard S et al (2013) High-resolution analysis of a tsunami deposit: case-study from the 1755 Lisbon tsunami in southwestern Spain. Mar Geol 337:98–111

Dabrio CJ, Goy JL, Zazo C (1999a) The record of the tsunami produced by the 1755 Lisbon earthquake in Valdelagrana spit (Gulf of Cadiz, southern Spain). Geogaceta 23:31–34

Dabrio CJ, Zazo C, Lario J et al (1999b) Sequence stratigraphy of Holocene incised-valley fills and coastal evolution in the Gulf of Cadiz (southern Spain). Geologie En Minjbow 77:263–281

Dabrio CJ, Zazo C, Goy JL et al (2000) Depositional history of estuarine infill during the Late Pleistocene-Holocene postglacial transgression. Mar Geol 162:381–404

Dawson AG, Shi S (2000) Tsunami deposits. Pure Appl Geophys 157:875–897

Dawson AG, Hindson R, Andrade C et al (1995) Tsunami sedimentation associated with the Lisbon earthquake of 1 November AD 1755: Boca do Rio, Algarve, Portugal. The Holocene 5(2):209–215

Dawson AG, Smith DE, Ruffman A et al (1996) The diatom biostratigraphy of tsunami sediments: examples from Recent and Middle Holocene events. Phys Chem Earth 21:87–92

Dominey-Howes DT, Humphreys GS, Hesse PP (2006) Tsunami and palaeotsunami depositional signatures and their potential value in understanding the late-Holocenetsunami record. The Holocene 16:1095–1107

Dourado F, Costa PJM, La Selle S, et al (2020) Can the tsunami geological record contribute to constrain the tectonic source of the 1755 AD earthquake? The Earth and Space Science Open Archive (ESSOAr)

Duarte JC, Terrinha P, Rosas FM et al. (2010) Crescent-shaped morphotectonic features in the Gulf of Cadiz (offshore SW Iberia). Mar Geol 271:236–249

Duarte JC, Rosas FM, Terrinha P et al (2013) Are subduction zones invading the Atlantic? Evidence from the southwest Iberia margin. Geology 41(8):839–842

Feist L, Frank S, Bellanova P et al (2019) The sedimentological and environmental footprint of extreme wave events in Boca do Rio, Algarve coast, Portugal. Sed Geol 389:147–160

Font E, Nascimento C, Omira R et al (2010) Identification of tsunami-induced deposits using numerical modeling and rock magnetism techniques: a study case of the 1755 Lisbon tsunami in Algarve, Portugal. Phys Earth Planet Inter 182(3–4):187–198

Font E, Veiga-Pires C, Pozo M et al (2013) Benchmarks and sediment source(s) of the 1755 Lisbon tsunami deposit at Boca do Rio Estuary. Mar Geol 343:1–14

Foster ID, Albon AJ, Bardell KM et al (1991) High energy coastal sedimentary deposits; an evaluation of depositional processes in southwest England. Earth Surf Process Landforms 16:341–356

Goff JR, Crozier M, Sutherland V et al (1998) Possible tsunami deposits from the 1855 earthquake, North Island, New Zealand. Geol Soc Lond 133:353–374

González-Regalado ML, Gómez P, Ruiz F et al (2019a) Holocene palaeoenvironmental evolution of Saltés Island (Tinto and Odiel estuary, SW Spain) during the Roman period (1st century BC–5th century AD). J Iber Geol 45:129–145

González-Regalado ML, Gómez P, Ruiz F et al (2019b) Facies analysis, foraminiferal record and chronostratigraphy of Holocene sequences from Saltés Island (Tinto-Odiel estuary, SW Spain): the origin of high-energy deposits. Estuar Coast Shelf Sci 218:95–105

Gracia FJ, Alonso C, Benavente J et al (2006) The different coastal records of the 1755 tsunami waves along the south Atlantic Spanish Coast. Zeit f Geomorph 146:195–220

Gràcia E, Vizcaino A, Escutia C et al (2010) Holocene earthquake record offshore Portugal (SW Iberia): testing turbidite palaeoseismology in a slow-convergence margin. Quat Sci Rev 29(9–10):1156–1172

Grützner C, Reicherter K, Hübscher C, Silva PG (2012) Active faulting and neotectonics in the Baelo Claudia area, Campo de Gibraltar (southern Spain). Tectonophysics 554–557:127–142

Grützner C, Reicherter K, Silva PG (2010) Comparing semiquantitative logic trees for archaeoseismology and palaeoseismology: The Baelo Claudia (southern Spain) case study. In: Sintubin M et al (eds) Ancient earthquakes. Geol Soc Am 471:129–144

Gutiérrez-Mas JM (2011) Glycymeris shell accumulations as indicators of recent sea-level changes and high-energy events in Cadiz Bay (SW Spain). Estuar Coast Shelf Sci 92:546–554

Gutiérrez-Mas JM, Juan C, Morales JA (2009) Evidence of high energy events in shelly layers interbedded in coastal Holocene sands in Cadiz Bay (south-west Spain). Earth Surf Proc Land 34:810–823

Gutiérrez-Mas JM, Gómez Fernández V, García-López S et al (2016) Comparative analysis of the deposits left by the tsunami that followed the Lisbon earthquake (1755 AD), on the Castilnovo beach and the old tuna factory of la Chança (Conil de la Frontera, SW Spain). Revista De La Sociedad Geologica De España 29 (1):21–33

Gutscher MA, Malod J, Rehault JP et al (2002) Evidence for active subduction beneath Gibraltar. Geology 30 (12):1071–1074

Gutscher MA, Baptista MA, Miranda JM (2006) The Gibraltar Arc seismogenic zone (part 2): constraints on a shallow east dipping fault plane source for the 1755 Lisbon earthquake provided by tsunami modeling and seismic intensity. Tectonophysics 426(1–2):153–166

Hindson RA, Andrade C (1999) Sedimentation and hydrodynamic processes associated with the tsunami generated by the 1755 Lisbon earthquake. Quatern Int 56(1):27–38

Hindson RA, Andrade C, Dawson AG (1996) Sedimentary processes associated with the tsunami generated by the 1755 Lisbon earthquake on the Algarve coast, Portugal. Phys Chem Earth 21(1–2):57–63

Jaffe BE, Morton RA, Kortekaas S et al (2008) Reply to Bridge (2008) Discussion of articles in “Sedimentary features of tsunami deposits.” Sed Geol 211:95–97

Klein T, Bebermeier W, Krause J et al (2016) Sedimentological evidence of an assumed ancient anchorage in the hinterland of a Phoenician settlement (Guadiana estuary/SW-Spain). Quatern Int 407:110–125

Kortekaas S, Dawson AG (2007) Distinguishing tsunami and storm deposits: an example from Martinhal. SW Portugal. Sedimentary Geology 200(3–4):208–221

Kortekaas S (2002) Tsunamis, storms, and earthquakes: distinguishing coastal flooding events. Dissertation, Converty University

Koster B, Reicherter K (2014) Sedimentological and geophysical properties of a ca. 4000 year old tsunami deposit in southern Spain. Sed Geol 314:1–16

Koster B, Hadler H, Vött A et al (2013) Application of GPR for visualising spatial distribution and internal structures of tsunami deposits—case studies from Spain and Greece. Zeit f Geomorph 57(suppl. 4):29–45

Lario J, Zazo C, Plater AJ et al (2001a) Particle size and magnetic properties of Holocene estuarine deposits

from the Doñana National Park (SW Iberia): evidence of gradual and abrupt coastal sedimentation. Zeit f Geomorph 45(1):33–54
Lario J, Spencer C, Plater AJ et al (2001b) Particle size characterisation of Holocene back-barrier sequences from North Atlantic coasts (SW Spain and SE England). Geomorphology 42:25–42
Lario J, Zazo C, Goy JL et al (2011) Holocene palaeotsunami catalogue of SW Iberia. Quatern Int 242:196–200
Lario J, Alonso-Azcarate J, Spencer C et al (2016) Evolution of the pollution in the Piedras River Natural Site (Gulf of Cadiz, southern Spain) during the Holocene. Environ Earth Sci 75:481–496
Lario J, Zazo C, Dabrio CJ et al (1995) Record of recent holocene sediment input on spit bars and deltas of South Spain. In: Ocre B (ed) Holocene cycles: climate, sea levels, and sedimentation. J Coastal Res 17:241–245
Lario J, Luque L, Zazo C et al (2009) Tsunami deposits at Torre de Castilnovo, Conil de la Frontera. In: Lario et al (eds) Palaeoseismicity and active tectonics during the Quaternary in the Gibraltar Strait (Betic Cordillera, South Spain). IGME, Madrid, pp 85–96
Lario J, Luque L, Zazo C et al (2010a) Tsunami vs. storm surge deposits: a review of the sedimentological and geomorphological records of extreme wave events (EWE) during the Holocene in the Gulf of Cadiz, Spain. Zeit f Geomorph 54(suppl. 3):301–316
Lario J, Dabrio CJ, Zazo C et al (2010b) Comment on "Formation of chenier plain of the Doñana marshland (SW Spain): Observations and geomorphic model" by A. Rodríguez-Ramírez and C. M. Yáñez-Camacho [Marine Geology 254 (2008) 187–196]. Mar Geol 275 (1–4):283–286
Lario J, Spencer C, Zazo C et al (2015) Evolución del estuario del rio Piedras (Huelva) durante el Holoceno. In: Galve JP et al (eds) Una visión global del Cuaternario. El hombre como condicionante de procesos geológicos. XIV Reunión Nacional de Cuaternario, Granada (España):28–30
Lario J (1996) Último y presente Interglacial en el área de conexión Atlántico-Mediterráneo: Variaciones del nivel del mar, paleoclima y paleoambientes. Dissertation, Univ. Complutense
Luque L, Lario J, Zazo C et al (2001) Tsunami deposits as paleoseismic indicators: examples from the Spanish coast. Acta Geológica Hispánica 36(3–4):197–211
Luque L, Lario J, Civis J et al (2002) Sedimentary record of a tsunami during Roman times, Bay of Cadiz, Spain. J Quat Sci 17:623–631
Luque L, Zazo C, Lario J et al (2004) El efecto del tsunami de 1755 en el litoral de Conil de la Frontera (Cádiz). In: Baquedano E, Rubio S (eds) Miscelánea en Homenaje a Emiliano Aguirre, vol I. Geología. Museo Arqueológico Regional, Alcalá de Henares, pp 72–82
Luque L (2002) Cambios en los palaeoambientes costeros del sur de la Península Ibérica (España) durante el Holoceno. Dissertation, Univ. Complutense
Martínez Solares JM (2001) Los efectos en España del terremoto de Lisboa (1 de noviembre de 1755). Instituto Geográfico Nacional, Madrid
Menanteau L, Vanney JR, Zazo C (1983) Belo II: Belo et son environment (Detroit de Gibraltar, Etude physique d´un site antique. Pub. Casa de Velázquez, Serie Archeologie 4., Ed. Broccard, Paris
Morales JA, Borrego J, San Miguel EG et al (2008) Sedimentary record of recent tsunamis in the Huelva Estuary (southwestern Spain). Quat Sci Rev 27:734–746
Moreira VS (1988) Historical and recent tsunamis in the European area. Sci Tsunami Haz 6:37–42
Moreira S, Costa PJM, Andrade C et al (2017) High resolution geochemical and grain-size analysis of the AD 1755 tsunami deposit: insights into the inland extent and inundation phases. Mar Geol 390:94–105
Morton RA, Gelfenbaum G, Jaffe BE (2007) Physical criteria for distinguishing sandy tsunami and storm deposits using modern examples. Sed Geol 200:184–207
Nanayama F, Shigeno K, Satake K et al (2000) Sedimentary differences between the 1993 Hokkaido-nansei-oki tsunami and the 1959 Miyakojima typhoon at Taisei, southwestern Hokkaido, northern Japan. Sed Geol 135:255–264
Nott J (2003) Waves, coastal boulder deposits and the importance of the pre-transport setting. Earth Planet Sci Lett 210:269–276
Omira R, Neres M, Batista L (2019) The gloria transform fault—NE Atlantic: seismogenic and tsunamigenic potential. In: Duarte E (ed) Transform plate boundaries and fracture zones. Elsevier, Amsterdam, pp 157–167
Quintela M, Costa PJM, Fatela F (2016) The AD 1755 tsunami deposits onshore and offshore of Algarve (south Portugal): sediment transport interpretatons based on the study of Foraminifera assemblages. Quatern Int 408(Part A):123–138
Ramos-Pereira AR, Trindade J, Neves M et al (2009) Indicadores geomorfológicos de tsunami no Parque Natural do SW Alentejano e Costa Vicentina (Malhão). In: Publicações da Associação Portuguesa de Geomorfólogos, vol VI, APGEOM, Braga, pp 51–56
Rebêlo L, Costas S, Brito P et al (2013) Imprints of the 1755 tsunami in the Tróia Peninsula shoreline, Portugal. In: Conley DC et al (eds) Proceedings 12th international coastal symposium (Plymouth, England). J Coastal Res 65:814–819
Reicherter K, Vonberg D, Koster B et al (2010) The sedimentary inventory of tsunamis along the southern Gulf of Cádiz (southwestern Spain). Zeit f Geomorph 54(suppl. 3):147–173
Reicherter K, Vött A, Feist L et al (2019) Lisbon 1755, Cruise No. M152/1, 02.11.-14.11.2018, Funchal (Portugal) - Hamburg (Germany). METEOR-Berichte. https://doi.org/10.2312/cr_m152
Reimer PJ, Bard E, Bayliss A et al (2013) IntCal13 and MARINE13 radiocarbon age calibration curves, 0–50,000 Years cal BP. Radiocarbon 55(4):1869–1887

Rodríguez Polo S, Gracia, FJ, Benavente J, et al. (2009). Geometry and recent evolution of the Holocene beach ridges of the Valdelagrana littoral spit (Cádiz Bay, SW Spain). J Coastal Res 56:20–23
Rodríguez-Ramírez A, Rodríguez-Vidal J, Cáceres LM et al (1996) Recent coastal evolution of the Doñana national park (SW Spain). Quat Sci Rev 15:803–809
Rodríguez-Ramírez A, Pérez-Asensio JN, Santos A et al (2015) Atlantic extreme wave events during the last four millennia in the Guadalquivir estuary, SW Spain. Quatern Res 83:24–40
Rodríguez-Ramírez A, Villarías-Robles J, Pérez-Asensio J et al (2016) Geomorphological record of extreme wave events during Roman times in the Guadalquivir estuary (Gulf of Cadiz, SW Spain): An archaeological and paleogeographical approach. Geomorphology 261:103–118
Rodríguez-Vidal J, Ruiz F, Cáceres LM et al (2011) Geomarkers of the 218–209 BC Atlantic tsunami in the Roman Lacus Ligustinus (SW Spain): a palaegeographical approach. Quatern Int 242:201–212
Rodríguez-Vidal J, Cáceres LM, González-Regalado ML et al (2015) Las grietas de acantilado como un nuevo tipo de registro de tsunamitas: ejemplo en la costa de Gibraltar. Granada, XIV Reunión Nacional del Cuaternario, pp 31–32
Rodríguez-Vidal J, Ruiz F, Cáceres LM et al (2008) Morphosedimentary features of historical tsunamis in the Guadalquivir estuary (SW of Spain). In: 2nd international tsunami field symposium IGCP project 495 quaternary land-ocean interactions: driving mechanisms and coastal responses. Ostuni (Italy) and Ionian Islands (Greece) 22–28 September 2008, pp 139–141
Röth J, Mathes-Schmidt M, García Jiménez I et al (2015) The Baelo Claudia tsunami hypothesis: results from a multi-method sediment analysis of late-Roman deposits (Gibraltar Strait, Southern Spain). In: Blumetti AM et al (eds) 6th international inqua meeting on paleoseismology, active tectonics and archaeoseismology, 19–24 April 2015, Pescina, Fucino Basin, Italy. Miscellanea INGV 27:418–422
Ruiz F, Rodríguez-Ramírez A, Cáceres LM et al (2004) Late Holocene evolution of the southwestern Doñana Nacional Park (Guadalquivir estuary, SW Spain): a multivariate approach. Palaeogeogr Palaeoclimatol Palaeoecol 204:47–64
Ruiz F, Rodríguez-Ramírez A, Cáceres LM et al (2005) Evidence of high energy events in the geological records: mid-holocene evolution of the southwestern Doñana National Park (SW Spain). Palaeogeogr Palaeoclimatol Palaeoecol 229:212–229
Ruiz F, Borrego J, López-González N et al (2007) The geological record of a mid-Holocene marine storm in southwestern Spain. Geobios 40(5):689–699
Ruiz F, Rodríguez-Vidal J, Abad M et al (2013) Sedimentological and geomorphological imprints of Holocene tsunamis in southwestern Spain: an approach to establish the recurrence period. Geomorphology 203:97–104
Ruiz F, Abad M, Rodríguez-Vidal J et al (2008) The Holocene record of tsunamis in the Southwestern Iberian Margin: date and consequences of the next tsunami. 6ª Assembleia Luso Espanhola de Geodesia e Geofisica. Tomar, Portugal, febrero 2008, 2 pp
Scheffers A, Kelletat D (2003) Sedimentologic and geomorphologic tsunami imprints worldwide—a review. Earth Sci Rev 63(1–2):83–92
Scheffers A, Kelletat D (2005) Tsunami relics on the coastal landscape west of Lisbon, Portugal. Sci Tsunami Haz 23(1):3–16
Schneider H, Höfer D, Trog C et al (2010) Holocene estuary development in the Algarve Region (Southern Portugal)—a reconstruction of sedimentological and ecological evolution. Quatern Int 221(1–2):141–158
Silva PG, Borja F, Zazo C et al (2005) Archaeoseismic record at the ancient Roman city of Baelo Claudia (Cádiz, South Spain). Tectonophysics 408:129–146
Silva PG, Reicherter K, Grützner C et al (2009) Surface and subsurface palaeoseismic records at the ancient Roman city of Baelo Claudia and the Bolonia Bay area, Cádiz (south Spain). Geol Soc Lond 316:93–121
Silva PG, Rodríguez Pascua MA, Giner JL et al (2014) Catálogo de Efectos Geológicos de los terremotos en España. IGME, Madrid
Silva PG, Bardají T, Roquero E et al (2015) Seismic palaeogeography of coastal zones in the Iberian Peninsula: understanding ancient and historic earthquakes in Spain. Cuaternario y Geomorfología 29(1–2):31–56
Silva PG, Rodríguez Pascua MA, Giner JL et al (2019) Catálogo de Efectos Geológicos de los terremotos en España. 2ª edición corregida y ampliada. IGME, Madrid
Lopes JB da Silva (1841) Corografia ou Memória Económica, Estatística e Topográfica do Reino do Algarve. Academia Real das Sciencias de Lisboa, Lisboa
Soares AMM (2015) Radiocarbon dating of marine shells from the Gulf of Cadiz: the marine radiocarbon reservoir effect, its variability during the Holocene and palaeoenvironmental inferences. Cuaternario y Geomorfología 29:19–29
Soares AMM, Dias JMA (2006) Coastal upwelling and radiocarbon-evidence for temporal fluctuations in ocean reservoir effect off Portugal during the Holocene. Radiocarbon 48:45–60
Soares AMM, Martins JMM (2010) Radiocarbon dating of marine samples from Gulf of Cadiz: the reservoir effect. Quatern Int 221(1–2):9–12
Soares AMM, Martins JMM (2009) Radiocarbon dating of marine shell samples. The marine radiocarbon reservoir effect of coastal waters off Atlantic Iberia during Late Neolithic and Chalcolithic periods. J Archaeol Sci 36(12):2875–2881
Soares AMM (1989) O efeito de reservatório oceânico nas águas costeiras de Portugal continental. ICEN-LNETI, Dept. de Quimica
Stuiver M, Braziunas P (1993) Modelling atmospheric ^{14}C influences and ^{14}C ages of marine samples to 10,000 BC yr BP. Radiocarbon 35(1):137–189

Stuiver M, Reimer PJ, Reimer RW (2020) CALIB 7.1. WWW Program. http://calib.org
Switzer AD, Jones BG (2008) Large-scale washover sedimentation in a freshwater lagoon from the southeast Australian coast: sea-Ievel change, tsunami or exceptionally large storm? The Holocene 18(5):787–803
Szczuciński W (2012) The post-depositional changes of the onshore 2004 tsunami deposits on the Andaman Sea coast of Thailand. Nat Hazards 60(1):115–133
Terrinha P, Dias RP, Ribeiro A et al (1999) The Portimão Fault, Algarve Basin, South Portugal. Comun Inst Geol e Mineiro 86:107–120
Tudor M, Ramos-Pereira A, Costa PJM (2020) A possible tsunami deposit associated to the CE 1755 Lisbon earthquake on the Western Coast of Portugal. Geosciences 10(7):257
Udías A, Buforn E, Muñoz D (1985) Mecanismo de los terremotos y téctonica. Universidad Complutense de Madrid, Madrid
Whelan F, Kelletat D (2003) Analysis of tsunami deposits at cabo de Trafalgar, Spain, using GIS and GPS technology. Essener Geographische Arbeiten 35:11–25
Whelan F, Kelletat D (2005) Boulder deposits on the Southern Spanish Atlantic Coast: possible evidence for the 1755 AD Lisbon Tsunami? Sci Tsunami Haz 23:25–38
Zazo C, Goy JL, Somoza L et al (1994) Holocene sequence of sea-level fluctuations in relation to climatic trends in the Atlantic-Mediterranean linkage coast. J Coastal Res 10(4):933–945
Zitellini N, Mendes LA, Cordoba D et al (2001) Source of 1755 Lisbon earthquake and tsunami investigated. Eos: Trans Am Geophys Union 26(285):290–291

6 Extreme-Wave Events in the Guadalquivir Estuary in the Late Holocene: Paleogeographical and Cultural Implications

Antonio Rodríguez-Ramírez,
Juan J. R. Villarías-Robles, Sebastián Celestino-Pérez,
José-Antonio López-Sáez,
José N. Pérez-Asensio, and Ángel León

Abstract

Research in the Guadalquivir estuary and its environs has revealed evidence of a periodic succession of extreme-wave events in the area from the third millennium BC to the third century AD. Return periods range from 400 to 800 years. Some of these extreme-wave events may have had a magnitude comparable with that of the so-called "Lisbon earthquake" of 1755. Contrary to the tenets of the uniformitarian paradigm in geology—still influential in the archeological literature—these events had short-, mid-, and long-term geomorphological and paleo-environmental, as well as immediately destructive and demographic, effects. Attention should also be called to the reverberations of these events in the cultural development of southwestern Iberia, which is independently known for puzzling interruptions, recommencements, and transformations every few centuries from the Neolithic to the Roman period. The two records, natural and cultural, might be connected. In study areas with a compelling historical and archeological heritage, such as western Andalusia, there is a need for multidisciplinary projects that, by bringing geology and biology to bear on archeology and history, aim to accurately establish the succession of geographical and

A. Rodríguez-Ramírez
Departamento de Geodinámica y Paleontología, Universidad de Huelva, Huelva, Spain
e-mail: arodri@uhu.es

J. J. R. Villarías-Robles (✉)
Instituto de Lengua, Literatura y Antropología, Centro de Ciencias Humanas y Sociales(CCHS), Consejo Superior de Investigaciones Científicas (CSIC), Madrid, Spain
e-mail: juanjose.villarias@cchs.csic.es

S. Celestino-Pérez
Instituto de Arqueología de Mérida, Consejo Superior de Investigaciones Científicas (CSIC), Mérida, Spain
e-mail: scelestino@iam.csic.es

J.-A. López-Sáez
Instituto de Historia, Centro de Ciencias Humanas y Sociales (CCHS), Consejo Superior deInvestigaciones Científicas (CSIC), Madrid, Spain
e-mail: joseantonio.lopez@cchs.csic.es

J. N. Pérez-Asensio
CEREGE UM34, Aix Marseille Université, CNRS, IRD, INRAE, Coll France, 13545 Aix-en-Provence, France
e-mail: perez@cerege.fr

Á. León
Fundación del Hogar del Empleado (FUHEM), Madrid, Spain
e-mail: angelzah@hotmail.com

M. Álvarez-Martí-Aguilar and F. Machuca Prieto (eds.), *Historical Earthquakes, Tsunamis and Archaeology in the Iberian Peninsula*, Natural Science in Archaeology,
https://doi.org/10.1007/978-981-19-1979-4_6

environmental transformations, the impact of these transformations on the area's cultural history, and the chronology of the events.

Keywords

Guadalquivir estuary · Late Holocene · Extreme-wave event · EWE recurrence · Geographical transformations · Cultural impact

6.1 Introduction: The Illustrative Case of the Short-, Mid-, and Long-Term Effects of the So-Called "Lisbon Earthquake" of 1755

Historical extreme-wave events (hereinafter EWEs) are not only interesting because of their short-, mid-, and long-term destructive, demographic, geomorphological, and geographical impact, but also because of their aftereffects in many realms of culture, such as the economy, social and political organization, social dynamics, and ideological and religious concepts, beliefs, and values.

To give an idea of this complexity of manifestations and repercussions, in both time and space, in 2005 geologists Jelle Zeilinga de Boer and Donald Th. Sanders used the metaphor of the inversely proportional relation that exists between amplitude and wavelength in an earthquake. The higher the amplitude of a quake is, the shorter its wavelength will be; and vice versa. The first vibrations of a quake, they wrote, "will be powerful, but each will last only a moment. Farther along […], with the passage of time, the amplitudes will decrease and the wavelengths increase. That is to say, the aftereffects will become less intense, and they will last longer" (Zeilinga de Boer and Sanders 2005, pp. x–xi). While high amplitudes bring immediate destruction and have clearly perceptible demographic, geomorphological, and geographic consequences in relatively small areas within a few days, weeks, or months, progressively longer wavelengths will propagate for longer periods of time—years, even centuries—as they reach increasingly larger areas—regions, countries, and even continents. These longer wavelengths are those of the lasting economic, social, political, and ideological impact of the event.

In a number of regions of the planet, a series of events recurring at regular intervals—each event with its short-, mid-, and long-term repercussions—further compound the problem of reconstructing specific natural and cultural moments, as well as the complete sequence of punctuations and transformations. The general public is perfectly aware of the terrifying regularity with which earthquakes and tsunamis strike the coasts of Japan, California, Peru, and Chile. Not so well known is the regularity with which they have devastated the coasts of the Gulf of Cadiz, possibly because—we might presume—the return period is significantly longer.

The so-called "Lisbon earthquake" in November 1755, also known as the "Maremoto de Cádiz," is a model example of the complexity and different durations of the effects of an EWE, as illustrated by Zeilinga de Boer and Sanders. It may be sufficiently revealing in this regard that this event made Voltaire, the great eighteenth-century French philosopher, infer that human society did not really live in a perfect world, created and supervised by an infinitely wise, well-meaning, and mighty god (Voltaire 1877 [original in 1756], 1999 [1758]), as other philosophers and poets—e.g., Gottfried Leibniz and Alexander Pope—had written and ministers of the Roman Catholic Church had preached. None of these authors could accept the idea of a Divine Providence that could also be responsible for the misfortune and injustice that afflicted humankind often, unless they were calamities and penances that God had meted out to the man as a punishment for his moral weakness and evil deeds. Moreover—as many of these authors also assumed—the trials and tribulations suffered by some people were compensated by the happiness and fortune enjoyed by others; in the end, the positive and negative aspects of the life of a person canceled each other out. In sum, man lived in the best of all possible worlds, a fact that he was supposed to accept.

In writing about the 1755 earthquake, Voltaire must have learned that its destructive force had affected a large part of the Iberian Peninsula—first and foremost, the southwest, from Cape Roca to the Strait of Gibraltar—as well as Morocco, ravaging the cities of Fes and Casablanca. While the intensity of the quake has been estimated to have been as high as IX on the Mercalli scale (the maximum being XII) its magnitude on the Richter scale might have been as high as 8.5 (Zeilinga de Boer and Sanders 2005, pp. 88–101).

It is not, however, the seismological features, geological context, or demographic calamity caused by the event which interest us here; colleagues more authoritative than us address these aspects in this book. Instead, it is the more inclusive historical and anthropological aspects to which we wish to call attention. The quake shook Lisbon on November 1, All Saints' Day, taking many citizens attending church by surprise. Many churches and other buildings soon collapsed and caught fire. In the harbor of Lisbon, as in other Portuguese harbors, the waves ripped vessels from their moorings and engulfed the people who had fled to piers and beaches. Those who survived the destruction soon fell into a sort of religious frenzy, fueled by priests, self-styled preachers, or simply honest, well-intentioned people who had been seized by panic. One J. Chase, an eyewitness, later wrote that he had seen in Lisbon swarms of desperate people joining impromptu processions behind all sorts of images of saints, including those that had been badly damaged by the quake. The larger the image of the saint was—no matter how much damage it had sustained—the higher the number of people in the procession was. Autos-da-fe were also held, followed by the execution of sentences against people deemed responsible for the tragedy, which was perceived as God's punishment for society's sins (Voltaire 1999, pp. 21–22; Zeilinga de Boer and Sanders 2005, pp. 92–93, 99–100).

The king of Portugal, Joseph I, gave his minister for War and Foreign Affairs, Sebastiao José de Carvalho e Mello, later the Marquis of Pombal, effective power to bury the dead, succor the injured, restore public order, rebuild Lisbon, and restart the country's economy. Carvalho e Mello's administration brought the Jesuits' political influence and the nobility's social preeminence to an end. The Jesuits and the nobility represented those parts of Portugal's social and political structures in which the doctrine of Divine Providence and punishment as an explanation for the country's sudden plight was most accepted. Such a doctrine called for no other redress for the terrible destruction than purging sinners and begging for God's forgiveness (Zeilinga de Boer and Sanders 2005, pp. 98–101).

6.2 The Recurrence of EWEs in Southwestern Iberia

Interesting though the event is for the forms of religious fanaticism and political change to which it gave rise, the "Lisbon earthquake" is also noteworthy because it was the object of scientific curiosity and scrutiny. Indeed, it was the first quake in history to be thus approached. This reaction should come as no surprise, as the event occurred in a historical context that included the intellectual and political movement of the Enlightenment—of which Voltaire's writings are among the most brilliant expressions. For example, the Real Academia de la Historia drafted a report on the EWE for the king of Spain, Ferdinand VI, the year after the event (Campos 1992, pp. 118–123). While in England, John Mitchell's seminal *Conjectures concerning the Cause, and Observations upon the Phaenomena of Earthquakes*, proposing a method for ascertaining the epicenter of earthquakes generating large waves in the sea, was published in 1760. With this method, Mitchell determined that the epicenter of the Lisbon earthquake had been in the Eastern Atlantic, not on the mainland. A professor of geology at Cambridge University at the time, Mitchell is currently regarded as the founder of seismology. In 1793, the US scientist and statesman Benjamin Franklin sketched out what in the twentieth century would be known as "plate tectonics theory." He hypothesized that the crust of the earth rested on "a fluid more dense, and of greater specific gravity than any of the solids we are acquainted with," albeit unstable (Zeilinga de Boer and Sanders 2005, pp. 3, 95).

As other contributors to this book point out, it was not the first time that a destructive event of the presumed intensity and magnitude of that of 1755 hit the coasts of the Gulf of Cadiz and southwestern Iberia. Other events had devastated the region before, as the Portuguese historian Joachim Joseph Moreira de Mendonça recollected soon enough in his influential *Historia universal dos terremotos* (1758). Moreira built upon a tradition that had begun at least in the sixteenth century (de Ocampo 1543, 1553; de Brito 1597, 1609; de Mariana 1601; Udías 2015; Álvarez-Martí-Aguilar 2020). In the long list of earlier events drawn up by the Portuguese scholar (1758, pp. 13–111), there are as many as six EWEs of power and manifestations that are comparable with those of the "Maremoto de Cádiz," specifically in 245 and 60 BC and AD 382, 1356, 1531, and 1722. Subsequent authors, such as Perrey (1847), Sánchez Navarro-Neumann (1921), and Galbis (1932, 1940) would elaborate on, or amend, that list. Galbis' catalog, for instance, lists 12 EWEs, the first of which, according to this Spanish geographer and military officer, had occurred in the time of Tubal, Noah's grandson (*Gen*. 10:1–5). He borrowed this piece of information from the *Crónica General de España*, by the king of Castile, Alfonso X "the Wise" (1252–1284). Galbis observed that this first event "broke the spit of land bridging Africa and Spain and thereby opened communication between the Atlantic and the Mediterranean" (Galbis 1932, p. 3). Other EWEs that Galbis listed, but Moreira did not, were those in 218, 216, 210, and 209 BC, and AD 881.

Geological, archeological, and historical evidence to support some of these EWEs is currently scant or nonexistent, in part because physical signs of these events have eluded scientists, and in part because the information about them is not contemporary but is provided by authors writing many years, even centuries or millennia, after those cataclysms had supposedly occurred—as is the case of King Alfonso X's account of the event in the time of Tubal or the information provided by the sixteenth-century Spanish historian Florián de Ocampo on EWEs in 241, 216, and 210 BC (Rodríguez-Ramírez et al. 2016; Álvarez-Martí-Aguilar 2017a, b, 2020, this volume).

There is, however, unquestionable evidence of other cataclysms, such as that in AD 881—described in reliable Arabic sources (Campos 1992, p. 102; Guidoboni et al. 1994, p. 388)—and possibly that in 1356, an earthquake reported by the contemporary Villani (1729 [1364], XIV, p. 404) and López de Ayala (1779 [ca. 1395], I, p. 215).

Regardless of the correct number of EWEs prior to 1755 about which there is trustworthy information, the fact remains that there existed at the time, if not earlier, a clear awareness among the learned that EWEs had occurred in the region before and that these events had had a significant impact on the coastal landscape and the people living there. In this vein, it should be recalled that, in the eighteenth century, the first archeological excavations worthy of the name were carried out at the large sites of Pompeii and Herculaneum (Italy) and at Palenque (Mexico), which were promoted and sponsored by the king of the Two Sicilies, Charles of Bourbon, subsequently known as Charles III of Spain (Magnusson 1973, p. 20; Willey and Sabloff 1980, p. 13).

From the perspective of a series of transformations in a study area in the course of several millennia, the significant impact of those events on landscapes and peoples may have been rather complex, in accordance with Zeilinga de Boer and Sanders's long-term model. The full impact of each EWE would have ranged from the high, destructive, localized amplitude of the first vibrations to the ever more subtle, yet lasting, aftereffects of the progressively longer wavelengths in increasingly large territories and cultural spheres: modes of subsistence, social and political organization, manners and customs, religion, and ideology. We propose that this complex chain of mutually interacting effects of different duration after an EWE, let alone a cyclic series of EWEs, ought to be factored into any model of the geomorphological evolution and cultural development of the coastal areas of the Gulf of Cadiz from at least the end of the last Ice Age to 1755, especially in the late Holocene.

The content of this book shows that we are not alone in opting for this multidisciplinary approach to the problem of understanding such an evolution and development. With these and other colleagues, as well as readers who are interested but not specialists on the subject, we would like to share the conclusions that we have arrived at during the course of such a dialogically conceived project, the Hinojos Project, in the marshes of the lower basin of the rivers Guadalquivir and Guadiamar, which got underway in 2005 (see Fig. 6.1).

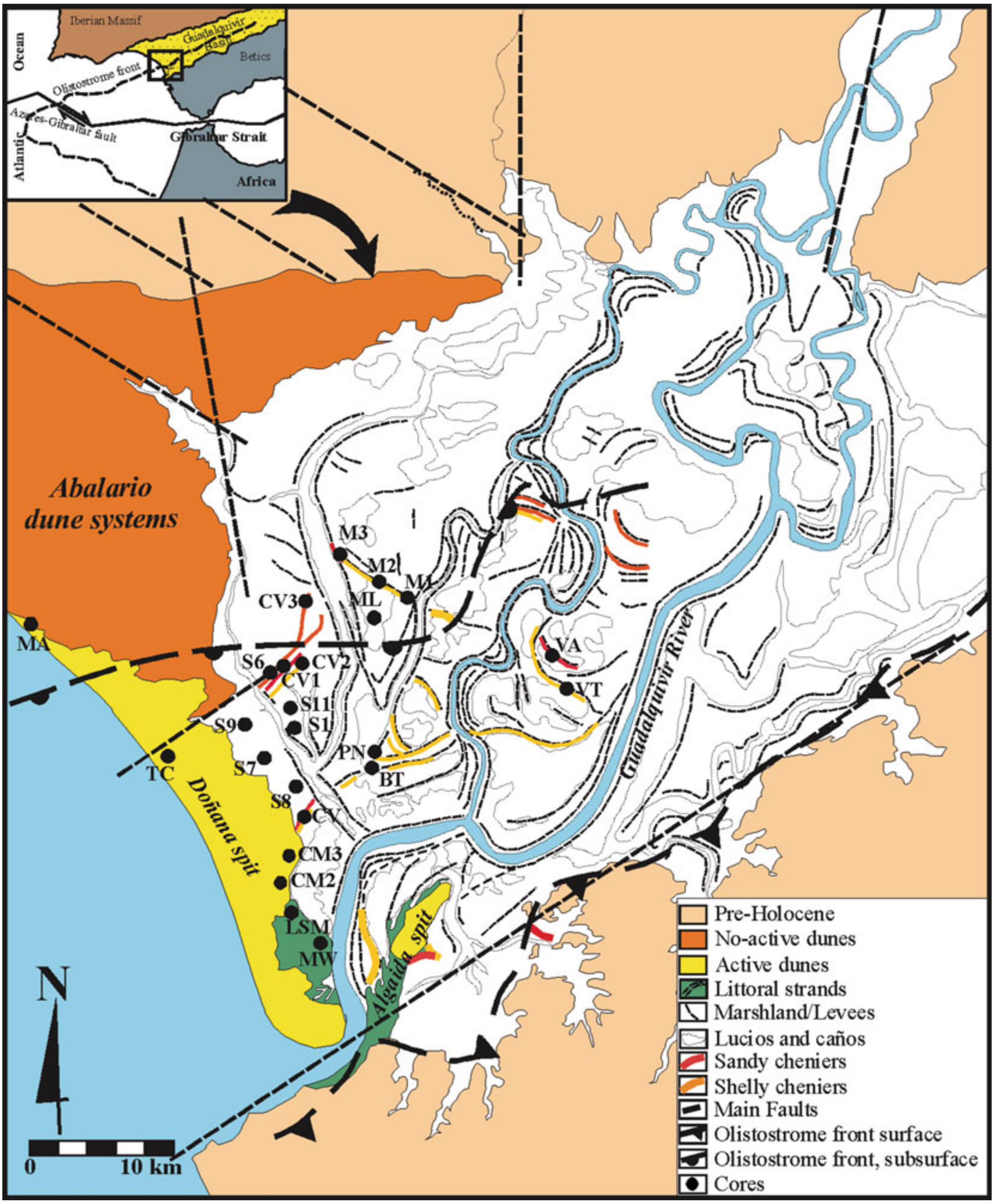

Fig. 6.1 Geomorphological outline of the Guadalquivir estuary and location of probing points

The results of the Hinojos Project confirm the recurrence of EWEs on the coasts of the Gulf of Cadiz in the late Holocene, which colleagues such as Morales et al. (2008) and Lario et al. (2010, 2011) have also inferred. From the perspective of Zeilinga de Boer and Sanders (2005), we submit that at least some of these EWEs may serve as hypotheses with which to help explain a number of interruptions, recommencements, and transformations in the prehistory, early history, and ancient history of southwestern Iberia. Although these discontinuities in the archeological and historical records have been widely discussed in the literature, we hold that there is still room for contributions of the kind presented here. We are referring specifically to issues such as the succession of the Bronze Age after the Copper Age (García-Sanjuán and Odriozola 2012; Lillios et al. 2016; Blanco-González et al. 2018), the scarcity of the material record of the Bronze Age versus that of the Copper Age (Fernández-Castro 2007; Escacena 2018), the passage to the Iron Age (López-Sáez et al. 2002; Celestino-Pérez et al. 2008), the transformation in the core area of the polity of Tartessos in the sixth century BC (Celestino-Pérez 2014, pp. 217–222; Celestino-Pérez and López-Ruiz 2016, pp. 202–213), and the crisis in the Roman province of *Baetica* in the second and third centuries AD (Sánchez-León 1978; Fernández-Ubiña 1981; Tsirkin 1987; Remesal 2011, pp. 142–157; Campos et al. 2015).

Below, we will present the data that we have obtained regarding a succession of EWEs occurring in the third and second millennia BC (Rodríguez-Ramírez et al. 2014, 2015; Celestino-Pérez et al. 2016; López-Sáez et al. 2018), as well as data concerning an EWE sometime in the early Roman Imperial era, between the first and third centuries AD (Rodríguez-Ramírez et al. 2016). In addition, we will provide evidence that points to at least one EWE taking place sometime between the eighth and the fourth centuries BC which might have severely affected the economic, social, and political core of the realm of Tartessos and, presumably, other aspects of Tartessian culture in lower Andalusia.

6.3 The Rise and Fall of the Uniformitarian Paradigm in the Geology of Southwestern Iberia

Let us return first, however, to the time when Moreira's influential treatise and Mitchell's revolutionary method were published. These works foreshadowed the emergence of geology as a scientific and academic discipline through the efforts of scholars such as Hutton (1785) and Lyell (1850 [1830–1833]). Ironically, this scientific progress spawned a—natural and human—historical concept according to which sudden, unexpected major disasters—including earthquakes, tsunamis, and volcanic eruptions—had little effect. Hutton and Lyell proposed, in opposition to the literal reading of the Bible, a "uniformitarian" paradigm with which to approach and account scientifically for the geological dynamics of the planet. Up until then, the Bible had been the main source of knowledge of humankind's past. It taught that the world had been created only a few thousand years ago and that humankind had had an eventful history replete with prodigies, such as the flood, the destruction of Sodom and Gomorrah, and the Israelite nation's passing through the Red Sea. The uniformitarian paradigm, in contrast, enabled geologists and geographers to assume that the planet had an age of at least hundreds of thousands of years, that major changes in it were gradual and slow—most of them imperceptible—and that present-day developments were the same as those that had taken place in the past (Renfrew 2007, p. 7). Such geological assumptions with respect to the earth's dynamics had parallels in biology with the theory of the evolution of the species proposed by Wallace (1855) and Darwin (1859) and, not long thereafter, in sociology and anthropology with the theory of cultural evolution (Tylor 1871; Spencer 1876; Morgan 1877).

In studies of the southwest of the Iberian Peninsula, the uniformitarian paradigm was expressed in the inquiries of and models produced by the geologists Otto Jessen in the 1920s (in Schulten 1945, pp. 270–273, map II) and Juan Gavala y Laborde from the 1920s to the 1950s (Gavala 1927, 1936, 1959). Jessen participated in the philologist Adolf Schulten and the archeologist George Bonsor's quest for the capital of the kingdom of Tartessos. Gavala was a distinguished member of Spain's Real Academia de Ciencias Exactas, Físicas y Naturales and became President of the Instituto Geológico y Minero. He had been born in the town of Lebrija and lived at one time in that of Puerto de Santa María, both in the province of Cadiz. As a result, he must have learned about the "Lisbon earthquake" of 1755; but, if so, in no way did it affect his model of the evolution of the Spanish coast of the Gulf of Cadiz in the Holocene.

According to this model, the maximum transgression of the Atlantic after the end of the last Ice Age opened up a wide estuary in the lower Guadalquivir basin that extended as far inland as Coria del Río, some 15 km south of Seville. Thereafter, a slow, regular process of sedimentation in and filling of the estuary began, fed by the deposit-carrying Guadalquivir, Guadiamar, Arroyo de la Rocina, Salado de Morón, and other tributaries, as well as the tidal flows of the ocean. After many millennia, this resulted in the formation of coastal barriers and, thereby, of an inland lake ("*Lacus Ligustinus*" mentioned by the Roman author Rufus Festus Avienus in his poem *Ora maritima*), which in turn resulted eventually in the landscape of marshes, shallows, relict channels, and dunes that can be seen nowadays in Doñana National Park. Consequently, the area of the erstwhile vast, open estuary could never have sustained any large, permanent human settlement before the Middle Ages.

This model has been accepted by many an archeologist inquiring into the prehistory and early history of southwestern Iberia until relatively recently. "Proyecto Marismas," designed and carried out by O. Arteaga, H. D. Schulz, and A. M. Roos in the 1990s is a clear case in point (Arteaga et al. 1995). In addressing the geomorphological configuration of the lower Guadalquivir river basin during the Holocene, these authors neglected to consider the role played by neo-tectonics and a number of significant dynamic processes in that evolution.

Research by geographers and especially geologists on the coasts and in the hinterland of southwestern Iberia since the 1970s (e.g., Menanteau 1981; Zazo et al. 1994; Flores-Hurtado 1995; Lario et al. 1995; Rodríguez-Ramírez et al. 1996; Lario 1996; Goy et al. 1996; Zazo et al. 1999; Borja et al. 1999; Ruiz et al. 2004, 2005; Rodríguez-Ramírez and Yáñez 2008) has rendered Jesssen's and Gavala's models obsolete, eliciting in substitution a novel, more complex understanding of such a configuration and its transformations over the past 7,000 years. There is currently an emerging consensus on long-term cyclic processes of erosion and sedimentation combined with more rapid developments generated by climate changes, sea-level fluctuations resulting from these changes, and more rapid disruptions of beaches and estuaries by EWEs.

Covering 185,000 ha, the estuary into which the rivers Guadalquivir, Guadiamar, Arroyo de la Rocina, and Salado de Morón run (hereinafter "the Guadalquivir estuary" or simply "the estuary") is the largest in the Gulf of Cadiz. Two coastal barriers or spit bars, "Doñana" and "Algaida," mark the estuary's boundaries to the west and the east, respectively, protecting it from the ocean. This enclosed, extensive area features a marshland plain with a number of *cheniers* (Rodríguez-Ramírez and Yáñez 2008); these are sandy estuarine ridges, with shelly deposits, overlying the clayey infilling of the marshland (Fig. 6.2). With a littoral strand morphology, these ridges are many kilometers long but just a few dozen meters wide. They indicate the location of successive ancient shorelines in the punctuated process of estuary infilling, from the transgressive maximum in the Holocene up until the present day. *Cheniers* formed within the complex dynamics of wave and current movement that the varying degree of connection of the estuary with the open sea imposed. Nonetheless, *cheniers* per se are not immediate, unequivocal evidence of tsunamis or cyclonic storms, or both (Rodríguez-Ramírez and Yáñez 2008; Rodríguez-Ramírez et al. 2016).

Fig. 6.2 Shelly *chenier* of Vetalengua, generated by drift currents and storm waves as part of the general dynamics in the Guadalquivir estuary. Though excellent markers of geo-dynamics at work in the estuary, *cheniers* are not by themselves unmistakable evidence of tsunamis

The first geomorphological studies of the estuary, in the 1980s and 1990s, enabled scientists to identify and date a succession of phases of progradation and erosion in the spit bars. Climate changes had been responsible for this periodic dynamic, after the transgressive maximum in the Holocene, dated by ^{14}C to ca. 6500 cal yr BP (Zazo et al. 1994). In the context of this progress in inferring the geology, paleo-geography, and paleo-climatology of the area, in the late 1990s clear signs of at least two historical EWEs were discovered: one EWE in the late third millennium BC and another in the early Roman Imperial era, between the first and the third centuries AD (Rodríguez-Ramírez 1998; Lario et al. 2001).

Since then, further geomorphological research and analysis of long cores extracted from the sedimentation have confirmed the existence of rather complex neotectonics in the estuary and its environs. Every formation in the Holocene is equally complex, insofar as the area extends over two very different tectonic domains: the Hercynian domain and that of the Baetic system. The lower Guadalquivir river basin is crisscrossed by countless faults which affect the formations of the Plio-Quaternary, including those of the Holocene. These faults have left clear manifestations in the orography which guide river beds and shorelines. A number of sets of these faults have been related to a presumed extensional phase of the Pliocene: first, a main set, with a N–S orientation, which includes the Lower Guadalquivir faults (BGF) and the Guadiamar-Matalascañas faults (GMF); and, secondly, a subsidiary set, in the westernmost sector of the basin, with an E–W orientation, which comprises the Torre del Loro faults (TLF) and the Hato

Blanco faults (HBF). During the Pleistocene, these subsidiary sets controlled the sedimentation on the coast of the province of Huelva (Armijo et al. 1977; Viguier 1977; Salvany and Custodio 1995; Goy et al. 1994, 1996; Zazo et al. 2005). In addition, there is a system of alignments with NW–SE or NE-SW orientations, as well as a tilt toward the S-SE which structurally constrains sedimentation in the basin (Flores-Hurtado 1995; Salvany 2004). Finally, on the underwater platform of the gulf, there is an additional system of alignments, most of which have NE–SW or NW–SE orientations. This system is the source of emerging and developing mud volcanoes, as well as structures of diapirism (Medialdea et al. 2009).

6.4 EWEs in the Guadalquivir Estuary: The Hinojos Project

The sedimentological, paleontological, geomorphological, palynological, archeological, and chronological analysis of deep and surface probing cores drilled in the ground, in the framework of the multidisciplinary Hinojos Project, has revealed evidence of five EWEs in the Guadalquivir estuary from the third millennium BC to the Roman Imperial period (Rodríguez-Ramírez et al. 2014, 2015, 2016; Jiménez-Moreno et al. 2015; López-Sáez et al. 2018). We shall refer to these events with the letters A to E of the Latin alphabet: EWE A, ca. 2555 cal yr BC; EWE B, ca. 2000 cal yr BC; EWE C, ca. 1550 cal yr BC; EWE D, ca. 1150 cal yr BC; and EWE E, sometime between AD 100 and 300. Radiocarbon data were calibrated by using CALIB 7.0 (Stuiver and Reimer 1993) and the Reimer et al. (2013) calibration dataset. The final results correspond to calibrated ages (cal.) with a 2σ uncertainty, corrected for the reservoir effect in this area as recommended by Soares (2015).

While nearly all of these events may have included tsunamis with a magnitude as high as that of 1755 (EWEs B, C, D, and E), EWE A may have consisted of no more than violent storm surges and, therefore, have had a significantly lower magnitude (Rodríguez-Ramírez et al. 2015, 2016; López-Sáez et al. 2018). All five EWEs, however, generated clearly diagnostic facies in the sedimentation. These facies consist of a layer of sand on an erosive base that contains foraminifera and a massive accumulation of shells and shell fragments of a high diversity of species—open marine species as well as protected low-energy environment species—in a sandy-muddy matrix that also includes gravel and lithoclasts. The longer the distance of the probing locations from the seashore, as far as 10 km, if not farther, the more these facies turn into sediments made up of a muddy-sandy layer containing lower percentages of open marine species and higher percentages of species of confined estuarine environments. EWEs A, B, C, and D also resulted in noticeable changes in the record of pollen, non-pollen palynomorphs, charcoal particles, and other microorganisms that are accepted signs of anthropic activity (Fig. 6.3).

6.4.1 EWE A, ca. 2555 cal yr BC

We were able to infer the first EWE in the middle of the present-day Marsh of Hinojos, within a chronological range of ca. 2610–2500 cal yr BC, from the sedimentation of significantly new amounts of anomalous sand content (15–20% sand) and remains of diverse marine macrofauna: a mixture of disarticulated valves, shell fragments, and whole bivalves of species characteristic of both a marine environment and an inner estuary. In an increasingly confined estuary during the postglacial transgressive maximum, low marsh dominated the environment. Conspicuous in the vegetation would have been Cyperaceae grasslands (15.6–22.6% of the pollen record), with species able to withstand seasonal salinity and relatively brackish waters. Agriculture was practiced, as indicated by the high values (1–2.5%) of *Cerealia* pollen; as was husbandry, judging by notable amounts of coprophilous fungi (18–20%). Therefore, there must have been one or more human settlements in the area (López-Sáez et al. 2018).

As anticipated above, this first EWE record could be explained by a storm surge or a series of

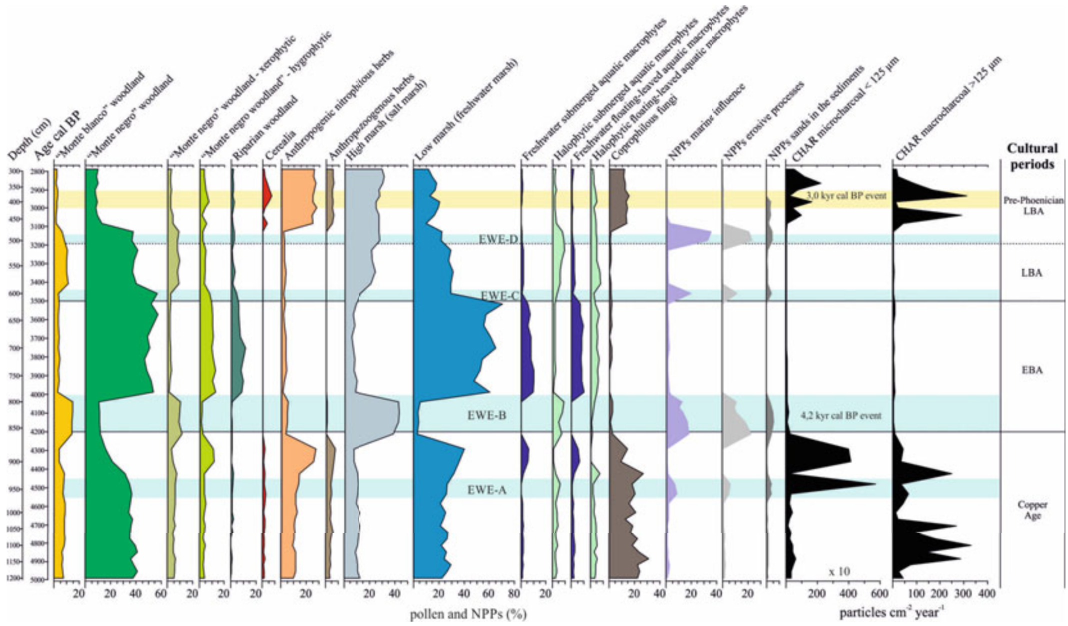

Fig. 6.3 Fluctuation of paleo-environmental indicators in the Guadalquivir marshland plain from ca. 3000 to 800 BC, modified from López-Sáez et al. (2018)

them, rather than by a tsunami. If so, EWE A would have had no more than a local character—the sediment accumulation rate (3.63 mm/yr) being lower than for the deposits below—and, consequently, would not have affected much the prehistoric, Copper Age settlement of the marsh environment; in fact, the sedimentary record shows a continuity of high values of *Cerealia* pollen and coprophilous fungi. The relative stability of both "monte negro" and "monte blanco" woodland pollen assemblages reinforces this interpretation (see Fig. 6.3). "Monte negro" is moisture-thriving scrubland comprising *Rubus ulmifolius*, *Ulex minor*, *U. australis*, and *Calluna vulgaris*; in particularly humid areas, it also includes hygrophytic species such as *Erica scoparia*, *E. ciliaris*, *E. umbellata*, *Saccharum ravennae*, and *Imperata cylindrica*. "Monte blanco" is scrubland of dry, xerophytic enclaves; it consists of *Cistus salvifolius*, *C. libatonis*, *Osyris quadripartita*, *Rosmarinus officinalis*, *Stauracanthus genistoides*, *Thymus mastichina*, *Lavandula stoechas*, *Helichrysum angustifolium*, *Halimium commutatum*, and *H. halimifolium* (López-Sáez et al. 2018).

6.4.2 EWE B, ca. cal yr 2000 BC

The second event, in contrast, was likely the most cataclysmic and destructive of the series, as it must have dramatically altered the geography and environment of the estuary. At the time the estuary was no longer under much marine influence and had permanent fresh water inputs, because it was partially protected in its westernmost boundary by aeolian units of the Abalario Sand Formation and to the south and southeast by the prograding Doñana spit bar. Before EWE B, the extension of the estuary may have been less than half of what it had been at the time of the postglacial transgressive maximum, making it a brackish lagoon landscape in practice. Low percentages of *Quercus suber* suggest "dehesa-type" vegetation (open savannah-like woodlands) as well. North of this landscape, the original estuary had turned into marshes, the oldest formed in the lower Guadalquivir river valley during the Holocene (López-Sáez et al. 2018).

At the most proximal locations to the shoreline, a geomorphological analysis of the sedimentation revealed morpho-stratigraphic evidence that is characteristic of a washover fan generated by the overwash resulting from the rupture of a sandy coastal barrier. As concluded in a number of studies (see, for instance, Switzer et al. 2004), washover features are the product of high-energy events, either tsunamis or violent storm surges; however, washover facies generated by the latter are found at sites adjacent to former barrier islands rather than in inner sectors of estuaries (Morton et al. 2007). In the case of EWE B, the sand layer distinguishing it has been identified at very long distances—as far as approximately 10 km—away from the coastline, in the middle of the marshland plain; this formation extends, both laterally and longitudinally, over many kilometers. Due to these morpho-stratigraphic dimensions, as well as the facies, that it exhibits, it can safely be attributed to an energy event of a very large magnitude. In addition, such facies fit in well with the typology of tsunamitic facies described by Fujiwara et al. (2000).

The event ushered in a long erosive phase in the sandy barriers of the estuary (Zazo et al. 1994; Lario et al. 1995; Lario 1996; Rodríguez-Ramírez et al. 1996), which has been ascribed to an interbedded marine layer found within the inner marsh deposits (Zazo et al. 1999). On the westernmost side of the estuary, sedimentation produced by this EWE rests upon eroded aeolian sands of the Abalario Sand Formation (Fig. 6.4).

Sands deposited in the estuary were subsequently reworked by the dynamics of the rivers and the ocean into the sandy *cheniers* of Carrizosa, Vetalarena, and Veta de Ali. This also affected cultural debris from settlements of the Copper or Early Bronze Age, or both, in the area which had been destroyed and their remains, dispersed (Celestino-Pérez et al. 2016). Before the event, at least in what is at present the Marsh of Hinojos and its environs, significant frequencies of anthropogenic nitrophilous herbs (*Aster*, Boraginaceae undiff., Cardueae, Cichorioideae, *Heliotropium*, *Malva sylvestris*, *Rumex acetosa*, *R. acetosella*) and anthropozoogenous types like

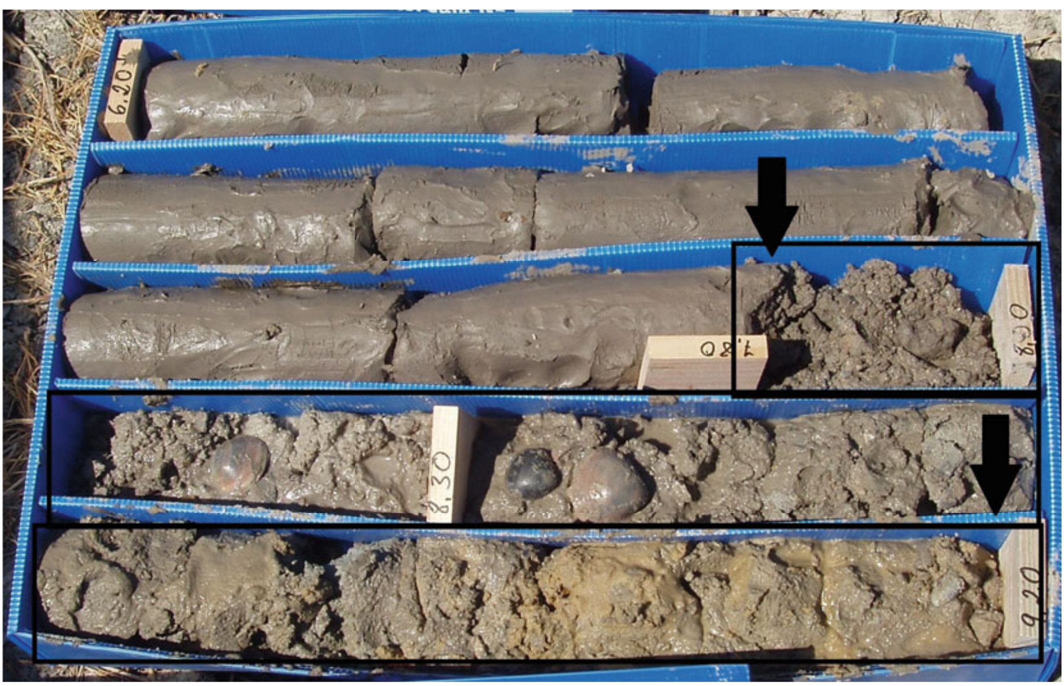

Fig. 6.4 Facies of the washover fan, including Glycimeris shells, of EWE B below the clayey facies of the marshland plain

Plantago lanceolata, *P. major/media*, and *Urtica dioica* (1.5–4%), as well as the continuous presence of coprophilous fungi such as *Chaetomium*, *Sordaria*, *Cercophora*, *Sporormiella*, *Coniochaeta*, and *Podospora*, suggest seasonal grazing activities and high human pressure in the second half of the third millennium. The presence of pollen of *Cerealia* at the same time suggests again that agriculture was practiced as well (López-Sáez et al. 2018).

Calibrated ^{14}C dates obtained for the anomalous sedimentation range from roughly 2200 to 1800 BC, the average date approximating 2000 BC. A long period characterized by a submerged, arid, and bleak environment followed. The sedimentary record revealed a significant rise of halophytic herbaceous (high marsh) pollen taxa such as *Chenopodiaceae*, *Artemisia*, *Apiaceae*, *Armeria/Limonium*, and *Frankenia*, as well as submerged-aquatic macrophytes typical of saline or brackish waters, including *Ruppia*, *Lemna*, and *Zannichellia*. Such an environmental change must have been favored by new climate conditions, as well as by a relative rise of the level of the ocean within a regime of local subsidence (Rodríguez-Ramírez et al. 2014; López-Sáez et al. 2018).

Research elsewhere on the European side of the Gulf of Cadiz has produced evidence of a large EWE in the gulf within a chronological range comparable with that of EWE B in the present-day marshes of Doñana National Park. Off-shore studies of the turbidite record as a marine paleo-seismic indicator of active tectonics in southwestern Iberia have made it possible to infer that a tsunami struck the littoral in ca. 1900–1600 cal yr BC (Gràcia et al. 2010). On-shore, anomalous high-energy deposits of approximately the same age as evidence of a possible tsunami have been found on all the coasts of SW Spain (see Costa et al., this volume), particularly in the Guadiana estuary (Camacho et al. 2016), in the Tinto-Odiel estuary (Morales et al. 2008), and on the coasts of the province of Cadiz, specifically at Barbate (Koster and Reicherter 2014), as well as in the Guadalquivir estuary before the Hinojos Project (Lario 1996; Zazo et al. 1999; Pozo et al. 2010). Researchers of the "Proyecto Marismas" in the Guadalquivir estuary may have inadvertently come across sedimentary evidence of the same tsunami at a site some 10 km southwest of Puebla del Río (Arteaga et al. 1995, pp. 114–115).

Set in a broader environmental context, the date of EWE B is about the same as that of a change to a warmer, drier climate worldwide, or shortly thereafter. The shift to the new climatic period is known as "the 4.2 ky BP aridification event." For many a researcher, this date represents the inception of the late Holocene in the Northern Hemisphere.

Whether inaugurated by EWE B or by the 4.2 ky BP event, or both, in the Guadalquivir estuary a new, more arid, but open-to-the-ocean natural environment ensued, which lasted about 1,000 years. This was a long period of demographic and cultural depression. The sedimentary record registers a dramatic drop in pollen of *Cerealia*, anthropogenic nitrophilous herbs, anthropozoogenous herbs, coprophilous fungi, and charcoal particles, among other signs; all of which indicates a significant diminution or outright abandonment of agricultural and animal husbandry activities, as well as human depopulation (López-Sáez et al. 2018).

Such a long demographic and cultural depression has also been inferred from the stratigraphic record at archeological sites in the vicinity of the estuary, including San Bartolomé de Almonte (García-Sanz and Fernández-Jurado 1999), Cerro de San Juan (in Coria del Río, Seville) (Escacena 2018), and Lebrija (Tejera-Gaspar 1985; Caro-Bellido 1995). Colleagues such as Lario et al. (2011) have called attention to the correlation between EWE B and the material decline registered at the large Copper Age site of Valencina de la Concepción-Castilleja de Guzmán, in the neighboring district of Aljarafe. This correlation may arguably be tied in with the puzzling end of the Copper Age or that of the Early Bronze Age in southwestern Iberia and possibly beyond; the change of scenario, cultural as well as natural, abrupt in the short term and more subtle, insidious in the mid and long terms, would square well with Zeilinga de Boer and Sanders's model of different durations for the effects of an event of such a cataclysmic, catastrophic magnitude as that of 1755. As is known, however, correlation does not mean necessarily causality. Whether or not there was indeed a cause-effect relationship between the two facts—EWE B and the beginning of a long, 1,000-year depression in the cultural history of southwestern Iberia—there can be no doubt that the dates for both coincide approximately.

6.4.3 EWE C, ca. cal yr 1550 BC

Within this long period, in ca. 1550 cal yr BC a third event occurred. The sedimentary and faunal evidence for this EWE in the probing cores is consistent with both a tsunami and a storm surge. Cases of such a typological uncertainty are not infrequent in the literature: in a number of geographical and geomorphological contexts, the sedimentological features left by tsunamis and storm surges exhibit similar textural, structural, and sedimentary properties, rendering definite ascription difficult (Morton et al. 2007). As earthquake-related turbidite deposits in the southwest Portuguese margin have been reported for ca. 1600 cal yr BC by Vizcaíno et al. (2006), we find it tempting, with Lario et al. (2011), to attribute the evidence found in the Guadalquivir estuary to the same EWE, probably a moderate seismic event (Mw <8.0) that generated a local tsunami in the gulf. Since this same coastal area had been affected by a previous EWE with stronger seismic effects (Mw ≥ 8.0), the magnitude of the tsunami of EWE C might have been lower, yet its apparent effects over-magnified because the coast had already suffered much damage.

6.4.4 EWE D, ca. cal yr 1150 BC

Some 400 years later, a fourth EWE struck. As in the case of EWE B, facies distinguishing this fourth event have been widely encountered across the estuary, notwithstanding the fact that at the time it was more confined because of the development of the sandy coastal barriers. The anomalous layers of EWE D have been found as far as 10–15 km away from the paleo-coastline. In addition, the morpho-stratigraphic and paleontological traits in the facies resemble those reported for signs of other EWEs elsewhere on the planet (Fujiwara et al. 2000). All of these are sound premises for suggesting as a source for the traits a tsunamitic event that extensively affected the estuary. It is hard to imagine for the Gulf of Cadiz storm surges that generate facies so far inland as those encountered in connection with EWE D. Furthermore, the content of the facies varies in terms of the distance from the paleo-coastline—from the most proximal locations to the most distal and restricted—as predicted in the model of Fujiwara et al. (2000) and identified in certain tsunamites described by Morales et al. (2008) for the Tinto-Odiel estuary. Evidence of EWE D also includes large block deposits attached to a paleo-cliff and drawn from lithologies in the submerged rock outcrops that extend in front of the coastal system (Fig. 6.5), as recognized and described for other areas (Whelan and Kelletat 2005; Gracia et al. 2006).

EWE D may have destroyed a Bronze II, or Middle Bronze Age, site found in the marsh of Rajaldabas, near Trebujena, in the eastern sector of the estuary. This site was described by geographer Loïc Menanteau in his doctoral dissertation after a chronological appraisal by archeologist Manuel Pellicer (Menanteau 1981, pp. 115–117, Figs. 70 and 92). EWE D affected the estuaries of Río Piedras (Lario et al. 2015, 2016) and Tinto-Odiel (Morales et al. 2008) and may have had an impact on the Bay of Cadiz and the Guadalete paleo-estuary as well (Lario et al. 1995; Luque et al. 2001; perhaps also Alonso et al. 2015, p. 106).

After the event, the low-energy marine dynamics resumed their action in the Guadalquivir estuary: the Doñana spit bar started to grow again, even further towards the southeast than before, while fluvial inputs within the estuary brought stability again to the marshland ecosystems. The aridification process resumed, too: high marsh increased, whereas low marsh, *Isoetes* (a fern that lives in seasonally flooded soils), and aquatic freshwater macrophytes

Fig. 6.5 Large sandstone block from the Paleogene moved by EWE D amid the marshland clay deposits and left at the foot of the cliff of the southern sector of the estuary

decreased. Aquatic vegetation capable of withstanding a certain degree of salinity underwent a small increase or remained at values of the preceding pollen period (López-Sáez et al. 2018).

The resulting landscape at these and other locations in southwestern Iberia is that of the archeological period known as Bronze III or Late Bronze Age, which corresponds to the early history of the region. It was the period of the first contacts with Phoenician explorers, merchants, and colonists and the formation of the culture of Tartessos. The Guadalquivir estuary was peopled again and saw agriculture and animal husbandry practiced anew, as implied by a clear increase in such indicators in the sedimentary record as pollen of *Cerealia*, anthropogenic nitrophilous and anthropozoogenous herbs, coprophilous fungi, and charcoal particles (López-Sáez et al. 2018). These demographic and cultural developments have been remarked on elsewhere in the Guadalquivir river valley and western Andalusia (Belén and Escacena 1992).

6.4.5 Ewe E, 100–300 AD

The present-day mouth of the river Guadalquivir exhibits a number of geomorphological and sedimentary formations that suggest EWEs in the Roman period as well, whether storm surges or tsunamis. Features in these formations are diverse and include washover fans, paleo-cliffs or erosional scarps, beach rocks, crevasse splays, and sedimentary lags of sand, shells, and coarse deposits with different facies types. The most significant evidence thereof dates to the second or third century AD and consists of an extensive geomorphological and sedimentological record left in the estuary. The event interrupted the progradation of littoral strands in the spit bars and carved striking paleo-cliffs or erosional scarps; at some locations, it even generated washover fans and produced beach rocks. However, it failed to breach the spit bar of Doñana and the tombolo of Algaida by means of inlets. Inside the estuary, it did break a number of *cheniers* and levees, which resulted in crevasse splays and sedimentary formations such as lags of sand, shells, and coarse stratified deposits showing facies types that indicate a return to greater marine influence in the estuary (Rodríguez-Ramírez et al. 2016). These facies types have been reported for the same chronological range in the Tinto-Odiel estuary (Morales et al. 2008) and Bay of Cadiz (Gutiérrez-Mas 2011).

As Campos et al. (2015; Bermejo Meléndez et al., this volume) have done, it is tempting to add this EWE in the Roman Imperial period to other factors proposed by other colleagues (Sánchez-León 1978; Fernández-Ubiña 1981; Tsirkin 1987; Remesal 2011, pp. 142–157) to explain the crisis in the Roman province of *Baetica* in the second and third centuries AD: factors of a political, economic, social, and military nature. The accumulated archeological evidence is compelling: a number of gaps in the record dated to the span between the late first and the mid-third centuries AD have been recognized on the coasts of the Gulf of Cadiz (Campos et al. 2002; Mayet and Tavares da Silva 2002; Sillières 2006; Fabião 2008); in Cordova, archeologists have found clear signs of "a devastating earthquake" before AD 270–280 which destroyed the theater (Ventura and Monterroso 2003, pp. 439–444); in Malaga and other cities and *villae* of Hispania, researchers have identified destruction at approximately the same time (Tsirkin 1987, pp. 264–266). When correlated with this archeological evidence, the geomorphological and sedimentary traces of the event in the Guadalquivir estuary and the interruption of the archeological record on the coasts of the gulf almost emphatically point to an earthquake-cum-tsunami in the second or third century AD.

Throughout the history of geomorphological transformations in the outlet of the river Guadalquivir—even more so in the Roman period—the diverse human communities in the area were strongly influenced by a number of different geodynamic processes. The location of these communities, in particular, depended upon rapid, convenient communication with the ocean and, more importantly, adequate protection from EWEs by lying on the leeward side of the sandy barriers. The rapid process of progradation of the spit bars and the even more rapid process of infilling of the estuary made navigation to and from the ocean increasingly difficult. Such a geodynamic development was the driving force behind the eventual abandonment of these settlements during the early centuries of the Christian era.

6.5 A Possible EWE Between the Eighth and the Fourth Centuries BC

As some evidence suggests, sometime between ca. 1150 BC and the second century AD an additional EWE occurred. This event may have significantly affected the cultural core of the polity of Tartessos.

The relevant evidence is of a geological, archeological, and philological nature. The geological evidence has been recently collected by Álvarez-Martí-Aguilar (2019) in the following areas: the district of Quarteira in the Portuguese Algarve (Schneider et al. 2010); in the spit bar of Punta Umbría, by the outlet of the Tinto-Odiel estuary (Lario 1996); in the Guadalquivir estuary, some 18 km away from the coast (Lario et al. 2001; Luque et al. 2001); and in the spit bar of Valdelagrana, in the Guadalete paleo-estuary (Alonso et al. 2015). The evidence for this last area suggests two EWEs rather than one: the first around the middle of the first millennium BC ("between 2700 and 2300 BP") and the second in the fourth or third century BC ("between 2300 and 2200 BP").

The archeological evidence, also gathered by Álvarez-Martí-Aguilar, points to an EWE around the middle of the first millennium BC. This evidence appeared in the course of archeological excavations conducted in downtown Huelva, a key Tartessian site, specifically in building lots nos. 7 and 9 on Méndez Núñez Street, where archeologists found remains of a hypothetical sanctuary destroyed by "an earthquake" and "a tsunami." This event would have occurred "approximately in the first quarter" of the sixth century BC (Osuna et al. 2000).

In order to assess the importance of this evidence properly, it should be taken into account that archeological excavations in the city of Huelva have often been prompted by urgent, salvage projects stemming from urban planning and building necessities. Because these circumstances make it difficult to study the site in detail and excavate extensively across it and neighboring areas, archeologists have had little choice but to compare the findings from two or more—ideally neighboring—locations in the city and then draw inferences from such a comparison. The conclusion of a possible earthquake-cum-tsunami in the sixth century BC that could help explain the crisis in the core of Tartessos in the same century was arrived at by this method.

The remains of the presumed sanctuary across some building lots on Méndez Núñez Street surfaced during an extensive excavation carried out in 1998. These remains consisted of structures belonging to three different phases of building and occupation, the first phase being that of a hypothetical sanctuary that had a trapezoidal floor plan and included a *témenos* in front. The archeologists soon noticed the collapse or displacement of a number of walls which, paradoxically, appeared to be very solid. They interpreted this incongruity as the direct effect of an earthquake; indeed, they christened the main wall, coded "E. T. 311," "the earthquake wall" (Rey 2011). In addition, they identified in the layers associated with this first sanctuary three kinds of marine shells by source: (1) the shells in the alluvial deposits on which the city stands, transported from the hillocks outside the city which had formed in the Pliocene; (2) the shells that resulted from the residents' eating habits; and (3) the shells accumulated in large deposits below ground which are native to sea bottoms and rather infrequent on coasts. These anomalous deposits suggested that a tsunami after the earthquake had caused destruction in the city. Additional finds reinforcing this inference included, among other things, a metallurgical oven that had been abandoned before the copper ore inside it had fused.

The razed sanctuary would not be rebuilt until the second half of the sixth century BC, in the area's second phase of occupation. Although this phase is considered to form part of the Turdetanian period in the cultural history of Huelva, it can be conceived as a revival of Tartessian culture instead, in stark contrast to contemporary developments in the Guadalquivir river valley, where Tartessian culture had disappeared and failed to return.

Additional, but less conclusive, evidence of an earthquake followed by a tsunami in Huelva dated to the sixth century BC surfaced in building lots no. 10 and no. 12 on Puerto Street (García-Sanz 1988–1989, pp. 162–166; Garrido and Orta 1994, pp. 117–140; 182–183, 344–345; Rufete 2002, pp. 99, 111–116). There, the archeologists came across remains of a large enclosure, apparently with a religious function, which they dated to between the seventh and fifth centuries BC. Like the sanctuary on Méndez Núñez Street, this enclosure had undergone three phases of construction, the second phase being that which interests us here: rebuilt early in the sixth century BC, the structure functioned during a period of ostensible economic diversity and material growth in at least that sector of the city; in relation to the structure, the archaeologists found large amounts of sherds of Phoenician and Greek pottery, fragments of bone, shells, chunks of slag, turtle shells (seemingly parts of musical instruments), the paw of a lion, and a representation of a fertility goddess. The archaeologists also discovered that later in the same century the upper parts of the walls of the building collapsed for some or other reason (Garrido and Orta 1994, pp. 117–118; Rufete 2002, p. 109).

Nearby, in building lot no. 9 on Puerto Street, archeologists led by Fernández-Jurado (1988–1989, I, pp. 149–151, 163–171) singled out the thick flood-related deposits of gravel and sand covering level III or stratum VIII in the lot.

However, the precise chronology of this stratum is unclear. Judging by the Greek pottery retrieved, the stratum would have formed between 570 and 530 BC (Fernández-Jurado 1988–1989, I, pp. 253–264).

Be that as it may, the vitality of Tartessian culture in Huelva throughout the first half of the sixth century remains clear enough, as the massive imports from Greece at the time suggest (Fernández-Jurado 1988–1989, I, pp. 163–171; Rufete 2002, pp. 159–160). Consequently, whatever happened then could not have been a decline in the economic organization and other realms of the culture, but more likely an abrupt turning point, such as that brought about by a major cataclysm. Tartessian culture continued to thrive elsewhere in western Andalusia; for instance, at Tejada La Vieja, by the upper Tinto River, where it experienced a moment of splendor (García-Sanz 1988–1989, pp. 170–171).

The aforementioned archeological and geological evidence would give substance to a suggestion from the field of biblical studies; in particular, a passage in the Old Testament where reference is made to the place name *Tarshish*—provided, as Koch (2003) noted, that this name from Old Hebrew is semantically analogous to the Greek *Tartêssós* in the work of Herodotus (I, 163; IV, 152) and Strabo (III, 2, 11–12). The passage is to be found in verses 10 to 12 of Chapter 23 of the Book of Isaiah, in the context of prophecies *post eventu* leveled at the city-state of Tyre; these prophecies have been attributed to the prophet "Second Isaiah" and dated to the fourth century BC (O. Eissfeldt in Cantera-Burgos and Iglesias-González 1975, p. 387, note 23). In consequence, the event referred to in the passage would have taken place sometime between the eighth (the time of prophet "First Isaiah") and the fourth centuries BC.

For the interpretation of this passage, we are indebted to Rainer W. Kühne,[1] later confirmed by the biblical scholar Natalio Fernández-Marcos after examining the traditional Masoretic Hebrew text of the Book of Prophets in the Jewish Holy Scriptures.[2]

To cite the critical English edition of the Hebrew text, published by The Jewish Publication Society of America (1978, pp. 400–401), after a comparison with the critical Spanish edition of Cantera-Burgos and Iglesias-González (1975, p. 387) and Fernández-Marcos's commentary, the passage reads as follows:

> [23, 10] Traverse[3] your land like the Nile,
> Fair Tarshish;
> This is a harbor[4] no more,
>
> [23, 11] The Lord poised His arm o'er the sea
> And made kingdoms quake;
> It was He decreed destruction
> For Phoenicia's strongholds,
> [23, 12] And said,
> "You shall be gay no more,
> O plundered one, Fair Maiden Sidon.
> Up, cross over to Kittim—
> Even there you shall have no rest.

The phrase "Fair Tarshish" in verse 10 parallels the phrase "Fair Maiden Sidon" in verse 12, of whom the prophet predicts that she will no longer feel happy because she will be robbed and will have to migrate and settle among the *Kittim*, the inhabitants of the island of Cyprus, the capital city of which was "Kition" (Cantera-Burgos and Iglesias-González 1975, p. 387, note 23). The place name "Tarshish," in consequence, would be no metaphor or metonymy for the city of Tyre or the land of Phoenicia—contrary to what the name would appear to mean—but the name of a different city instead, the women of which are ordered to make a living out of agriculture because there will be no commerce any more to live off, as "The Lord poised His arm o'er the sea and made kingdoms quake"; that is, He will unleash an earthquake and a tsunami, destroying such a city, namely, Tarshish, or at least its harbor or its walls.

[1] Personal communication by e-mail to co-author J. J. R. Villarías-Robles on 10 August 2015.

[2] Personal communication to co-author Villarías-Robles on 20 November 2015.

[3] Or "till".

[4] Or "fortification" or "fortress," according to Fernández-Marcos, in possibly parallel construction with verse 14: "Your stronghold is destroyed"; the Old Hebrew name is "*mezaḥ*".

Should this philological evidence be accepted, it would imply the only passage in the Old Testament in which the place name “Tarshish” refers to a city; which, furthermore, as also suggested in the passage, was destroyed by an earthquake and a tsunami.

6.6 Conclusions

As Moreira de Mendonça contended in 1758, like other authors before him, the Gulf of Cadiz has been repeatedly struck by catastrophic events like the earthquake and tsunami of 1755 since time immemorial. In the Guadalquivir estuary and neighboring areas, there is evidence of such events from the third millennium BC up until Roman Imperial times, recurring in cycles of 400–800 years (Fig. 6.6). If the effects of most of these events in the geomorphology and the landscape, as well as the fluvial, marine, and tectonic dynamics, of these areas were compared with the effects of the 1755 event in southwestern Iberia, then it is reasonable to propose that their cultural repercussions—on the economy, social and political organization, beliefs, rituals, and values—besides their immediate physical and demographic impact, must have been, for different durations, just as powerful as those of the 1755 event.

After the first, non-tsunamitic event took place in ca. 2555 BC, a second, tsunamitic event in ca. 2000 BC occurred about the time of the onset of a new—a warmer, drier—climate phase in the Holocene which, therefore, most likely exacerbated the natural conditions for the continuity of the materially rich Copper Age into the Early Bronze Age in the estuary and its environs. At least in the Marsh of Hinojos and its vicinity, this event ushered in a markedly different, practically depopulated landscape which changed little for about 1,000 years. In ca. 1550 BC, a third EWE, perhaps the same as the event which has been identified in southern Portugal for about the same time, and probably of a lesser magnitude than that of the second event, would have strengthened the mid- and long-term effects of this second event. Some 400 years further later, in ca. 1150 BC, a fourth event, in all likelihood as large as the second event, brought to an end the weak development of a Middle Bronze Age culture in the Guadalquivir estuary, the Guadalete estuary, and the Bay of Cadiz, clearly marking it off from that of the Late Bronze Age and Iron Age in these areas. A fifth, and perhaps a sixth, event in the following 400–800 years may help explain the disappearance of Tartessian culture in the Guadalquivir river valley. Finally, another event between AD 100 and 300 might have exacerbated the economic, social, political, and military problems in the Roman province of *Baetica* in the second and third centuries AD.

In study areas with such a rich historical and archeological record as the Guadalquivir estuary and western Andalusia as a whole, we feel that the research results presented here teach all interested parties, as well as ourselves, that there is a need for multidisciplinary projects that by bringing geology and biology to bear on archeology and history aim to offer a precise explanation for the succession of the geographical and environmental transformations occurring during such a long period, the complex effects of these transformations on its interesting cultural history, and the chronology of the turning events.

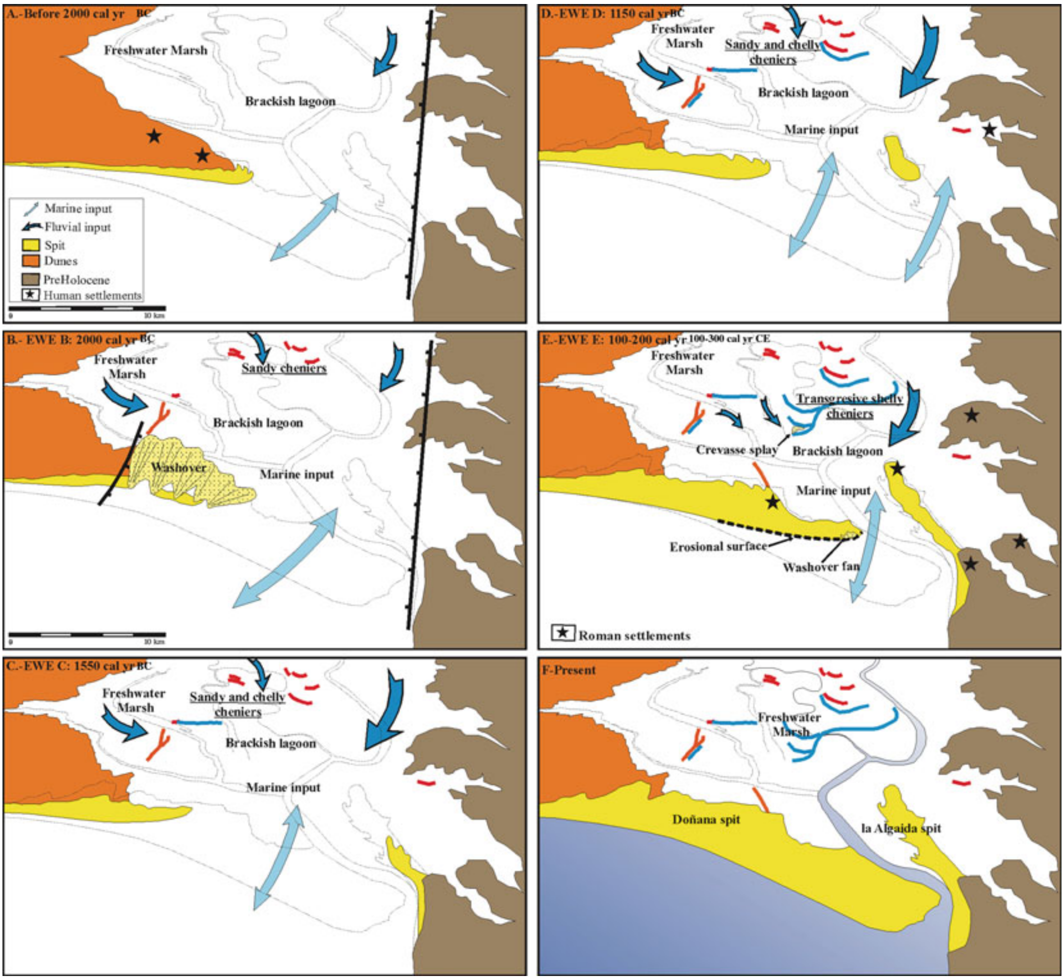

Fig. 6.6 Paleo-geographical reconstruction of the impact of the large EWEs, modified from Rodríguez-Ramírez et al. (2014, 2015, 2016). The *cheniers* represented always formed after EWEs. The sandy *cheniers* were formed by deposits of sand carried into the estuary by way of the inlets opened in the spit bars, while the shelly *cheniers* formed in periods of confinement of the estuary. Neither the morphology of the sandy *cheniers* nor that of the shelly *cheniers* is direct evidence of tsunamis

Acknowledgements This contribution to the book *Historical Earthquakes, Tsunamis and Archaeology in the Iberian Peninsula* is a result of both the project Relictflora-P11-RNM-7033 (Excellence Research Projects Program of Junta de Andalucía) and the Hinojos Project of the Universidad de Huelva, Consejo Superior de Investigaciones Científicas (CSIC), and Fundación FUHEM. We are indebted for funding and other forms of encouragement to the Ayuntamiento de Hinojos, Fundación Caja de Madrid, Fundación Doñana 21, Estación Biológica de Doñana (EBD), Espacio Natural de Doñana (END), Instituto Andaluz del Patrimonio Histórico (IAPH), Delegación de Cultura of Junta de Andalucía in Huelva, and Organismo Autónomo Parques Nacionales of Ministerio de Medio Ambiente y Medio Rural y Marino de España. This chapter is also a contribution of IGCP Project 639, "Sea Level Change from Minutes to Millennia" and IGCP 588, "Preparing for coastal change," as well as to the INQUA Coastal and Marine Processes Commission. The co-author J. N. Pérez-Asensio participated in the preparation of the chapter as member of the research groups RNM-190 (Junta de Andalucía) and GRC Geociències Marines (2017 SGR 315, Generalitat de Catalunya). Additional support from Junta de Andalucía to the Research Group RNM276 is also acknowledged.

References

Alonso C, Gracia, FJ, Rodríguez-Polo S et al (2015) El registro de eventos energéticos marinos en la bahía de Cádiz durante épocas históricas. Cuaternario y Geomorfología 29(1–2):95–117. https://doi.org/10.17735/cyg.v29i1-2.29935

Álvarez-Martí-Aguilar M (2017a) La tradición historiográfica sobre catástrofes naturales en la Península Ibérica durante la Antigüedad y el supuesto tsunami del Golfo de Cádiz de 218–209 a.C. Dialogues d'histoire ancienne 43(2):117–145

Álvarez-Martí-Aguilar M (2017b) Terremotos y tsunamis en Portugal en época antigua: el legado de Bernardo de Brito y su *Monarchia Lusytana* (1597–1609). Euphrosyne 45:183–204

Álvarez-Martí-Aguilar M (2019) El retorno del cataclismo: de la Atlántida a Tarteso. In: Sánchez Moreno E (ed) Veinticinco estampas de la España Antigua. Cincuenta años después (1967–2017). En torno a la obra de Antonio García y Bellido y su actualización científica. Universidad de Sevilla, Sevilla, pp 115–130

Álvarez-Martí-Aguilar M (2020) The historicity of the earthquakes occurring in the Iberian Peninsula before A.D. 881 recorded in Spanish and Portuguese seismic catalogs. Seismol Res Lett 91(6):3585–3594. https://doi.org/10.1785/0220200168

Armijo R, Benkhelil J, Bousquet JC et al (1977) L'histoire tectonique récent (Tortonien à Quaternaire) de l'Arc de Gibraltar et des bordures de la mer d'Alboran. Bulletin de laSociété Géologique de France 7–19:575–614

Arteaga O, Schulz HD, Roos AM (1995) El problema del "Lacus ligustinus": investigaciones geo-arqueológicas en torno a las marismas del Bajo Guadalquivir. In: Tartessos 25 años después, 1968–1993. Actas del Congreso Conmemorativo del V Symposium Internacional de Prehistoria Peninsular, Jerez de La Frontera, 9–12 November 1993. Ayuntamiento de Jerez de La Frontera, Jerez de La Frontera, pp 99–133

Belén M, Escacena JL (1992) Las comunidades prerromanas de Andalucía Occidental. Complutum 2–3:65–88

Blanco-González A, Lillios KT, López-Sáez JA et al (2018) Cultural, demographic and environmental dynamics of the Copper and Early Bronze Age in Iberia (3300–1500 BC): towards an interregional multiproxy comparison at the time of the 4.2 ky BP event. J World Prehist 31:1–79. https://doi.org/10.1007/s10963-018-9113-3

Borja F, Zazo C, Dabrio CJ et al (1999) Holocene aeolian phases and human settlements along the Atlantic coast of southern Spain. The Holocene 9(3):333–339. https://doi.org/10.1191/095968399668924476

Camacho S, Boski T, Moura D et al (2016) Paleoenvironmental evolution of the Guadiana Estuary, Portugal, during the Holocene: a modern foraminifera analog approach. The Holocene 27(2):1–39

Campos JM, Gómez-Toscano A, Vidal NO et al (2002) La factoría romana de El Cerro del Trigo (Doñana, Almonte, Huelva). Anuario Arqueológico de Andalucía 1999(III–1):330–348

Campos JM, Bermejo-Meléndez J, Rodríguez-Vidal J (2015) La ocupación del litoral onubense en época romana y su relación con eventos marinos de alta energía. Cuaternario y geomorfología 29(1–2):75–93. https://doi.org/10.17735/cyg.v29i1-2.31570

Campos ML (1992) El riesgo de tsunamis en España: análisis y valoración geográfica. Instituto Geográfico Nacional, Madrid

Cantera-Burgos F, Iglesias-González M (1975) Sagrada Biblia: versión crítica sobre los textos hebreo, arameo y griego. BAC, Madrid

Caro-Bellido A (1995) Contribución a la protohistoria del Bajo Guadalquivir: el área de Lebrija (Sevilla): In: Tartessos 25 años después, 1968–1993. Actas del Congreso Conmemorativo del V Symposium Internacional de Prehistoria Peninsular, Jerez de La Frontera, 9–12 November 1993. Ayuntamiento de Jerez de La Frontera, Jerez de La Frontera, pp 333–358

Celestino-Pérez S (2014) Tarteso: viaje a los confines del Mundo Antiguo. Trébede, Madrid

Celestino-Pérez S, López-Ruiz C (2016) Tartessos and the Phoenicians in Iberia. Oxford University Press, Oxford

Celestino-Pérez S, Rafel N, Armada XL (eds) (2008) Contacto cultural entre el Mediterráneo y el Atlántico (siglos XII–VIII ane). La precolonización a debate. CSIC, Madrid

Celestino-Pérez S, Cerrillo-Cuenca E, León A et al (2016) Razones geológicas, arqueológicas y antropológicas de la conservación de Doñana: El Proyecto Hinojos (2005–2013). In: Ferrer M (ed) Doñana: 50 años de investigaciones científicas. CSIC, Madrid, pp 81–100

Darwin C (1859) On the origin of species by means of natural selection. John Murray, London

de Brito B (1597) Monarchia Lusytana. Composta por Frey Bernardo de Brito, Chronista geral & Religioso da ordem de s. Bernardo, professo no Real mosteiro de Alcobaça. Parte Primeira… Mosteiro de Alcobaça

de Brito B (1609) Segunda parte da Monarchia Lusytana em que se continuão as historias de Portugal desde o nacimento de nosso Salvador Iesu Christo até ser dado em dote ao Conde dom Henrique. Pedro Crasbeeck, Lisboa

de Mariana J (1601) Historia general de España. Tomo primero. Pedro Rodríguez, Toledo

de Ocampo F (1543) Los quatro libros primeros de la Cronica general de España que recopila el maestro Florian do Campo criado y cronista del Emperador Rey nuestro señor por mandado de su magestad Çesarea. Juan Picardo, Zamora

de Ocampo F (1553) Los cinco libros primeros de la Cronica general de España, que recopila el maestro Florian do Campo, Cronista del Rey nuestro señor, por mandado de su Magestad, en Zamora, Guillermo de Millis, Medina del Campo

Escacena JL (2018) Vivir junto al río grande. Sobre la Prehistoria Reciente en el paleoestuario bético. In: Escacena JL, Gómez-Peña A, Pérez-Aguilar LG (eds) Caura: arqueología en el estuario del Guadalquivir. Universidad de Sevilla, Sevilla, pp 47–71

Fabião C (2008) Las ánforas de Lusitania. In: Bernal Casasola D, Ribera i Lacomba A (eds) Cerámicas hispanorromanas: un estado de la cuestión. Actas del XXVI Congreso Internacional de la Asociación Rei Cretariae Romanae Fautores, Universidad de Cádiz, Cádiz, 29 September–5 October 2008. Universidad de Cádiz, Cádiz, pp 725–748

Fernández-Castro MC (2007) Las necrópolis del Suroeste. In: Lynch J (ed) Historia de España,vol 1: La Prehistoria. El País, Madrid, pp 405–415

Fernández-Jurado J (1988–1989) Tartessos y Huelva. Huelva Arqueológica 10–11. Diputación Provincial de Huelva, Huelva

Fernández-Ubiña J (1981) La crisis del siglo III en la Bética. Universidad de Granada, Granada

Flores-Hurtado E (1995) Tectónica reciente en el Margen Ibérico Suroccidental. Dissertation, Universidad de Huelva

Fujiwara O, Masuda F, Sakai T et al (2000) Tsunami deposits in Holocene bay mud in southern Kanto region, Pacific coast of central Japan. Sed Geol 135:219–223

Galbis J (1932) Catálogo Sísmico de la Zona comprendida entre los meridianos 5° E. y 20° W. de Greenwich y los paralelos 45° y 25° N. Tomo I. Instituto Geográfico, Catastral y de Estadística, Madrid

Galbis J (1940) Catálogo Sísmico de la Zona comprendida entre los meridianos 5° E. y 20° W. de Greenwich y los paralelos 45° y 25° N. Tomo II. Instituto Geográfico y Catastral, Madrid

García-Sanjuán L, Odriozola C (2012) La cronología radiocarbónica de la Edad del Bronce (c. 2200–850 cal ANE) en el Suroeste de la Península Ibérica. Anejos De AEspA 62:363–387

García-Sanz C (1988–1989) El urbanismo protohistórico de Huelva. Huelva Arqueológica 10–11(3):143–175

García-Sanz C, Fernández-Jurado J (1999) La época calcolítica de San Bartolomé de Almonte. Huelva Arqueológica 15:7–132

Garrido JP, Orta EM (1994) El hábitat antiguo de Huelva (períodos orientalizante y arcaico). La primera excavación arqueológica en la calle del Puerto. Excavaciones Arqueológicas en España 171. Ministerio de Cultura, Madrid

Gavala J (1927) Cádiz y su bahía en el transcurso de los tiempos geológicos. Boletín del Instituto Geológico y Minero de España 3ª serie 49(9):1–29

Gavala J (1936) Memoria explicativa de la Hoja 1017: El Asperillo, del Mapa Geológico de España, escala 1:50.000. Instituto Geológico y Minero de España, Madrid

Gavala J (1959) Geología de la costa y bahía de Cádiz y el poema "Ora maritima" de Avieno. Coullaut, Madrid

Goy JL, Zazo C, Dabrio CJ et al (1994) Fault-controlled shifting shorelines in the Gulf of Cadiz since 20 Ky BP. In: Abstracts of the 1st symposium on the Atlantic Iberian Continental Margin, Lisbon, 28–30 November 1994, p 24

Goy JL, Zazo C, Dabrio CJ et al (1996) Global and regional factors controlling changes of coastlines in Southern Iberia (Spain) during the Holocene. Quatern Sci Rev 15(8–9):773–780

Gracia FJ, Alonso C, Benavente J et al (2006) The different coastal records of the 1755 tsunami waves along the South Atlantic Spanish coast. Zeitschrift für Geomorphologie, Supplement 146:195–220

Gràcia E, Vizcaíno A, Escutia C et al (2010) Holocene earthquake record offshore Portugal (SW Iberia): testing turbidite palaeoseismology in a slow-convergence margin. Quatern Sci Rev 29(9–10):1156–1172

Guidoboni E, Comastri A, Traina G (1994) Catalogue of ancient earthquakes in the Mediterranean Area up to the 10th century. Istituto Nazionale di Geofisica, Roma

Gutiérrez-Mas JM (2011) Glycymeris shell accumulations as indicators of recent sea-level changes and high-energy events in Cadiz Bay (SW Spain). Estuar Coast Shelf Sci 92(4):546–554. https://doi.org/10.1016/j.ecss.2011.02.010

Hutton J (1785) Theory of the Earth; or an investigation of the laws observable in the composition, dissolution, and restoration of land upon the Globe. Royal Society of Edinburgh, Edinburgh

Jiménez-Moreno G, Rodríguez-Ramírez A, Pérez-Asensio JN et al (2015) Impact of late-Holocene aridification trend, climate variability and geodynamic control on the environment from a coastal area in SW Spain. The Holocene 25(4):607–617

Koch M (2003) Taršiš e Hispania. Estudios histórico-geográficos y etimológicos sobre la colonización fenicia de la Península Ibérica (trans. M Prieto-Vilas). Centro de Estudios Fenicios y Púnicos, Madrid

Koster B, Reicherter K (2014) Sedimentological and geophysical properties of a ca. 4000 year old tsunami deposit in southern Spain. Sed Geol 314:1–16

Lario J (1996) Último y presente interglacial en el área de conexión Atlántico-Mediterráneo (Sur de España): variaciones del nivel del mar, paleoclima y paleoambientes. Dissertation, Universidad Complutense de Madrid

Lario J, Zazo C, Dabrio CJ et al (1995) Record of Recent Holocene sediment input on spit bars and deltas of south Spain. J Coastal Res 17:241–245

Lario J, Zazo C, Plater AJ et al (2001) Particle size and magnetic properties of Holocene estuarine deposits from the Doñana National Park (SW Iberia): evidence of gradual and abrupt coastal sedimentation. Z Geomorphol 45(1):33–54

Lario J, Luque L, Zazo C et al (2010) Tsunami vs. storm surge deposits: a review of the sedimentological and geomorphological records of extreme wave events (EWE) during the Holocene in the Gulf of Cadiz, Spain. Zeitschrift für Geomorphologie 54(suppl. 3):301–316

Lario J, Zazo C, Goy JL et al (2011) Holocene palaeotsunami catalogue of SW Iberia. Quatern Int 242:196–200. https://doi.org/10.1016/j.quaint.2011.01.036
Lario J, Spencer C, Zazo C et al (2015) Evolución del estuario del río Piedras (Huelva) durante el Holoceno. In: Galve JP, Azañón JM, Pérez-Peña JV et al (eds) Una visión global del Cuaternario. El hombre como condicionante de procesos geológicos. Granada, XIV Reunión Nacional de Cuaternario, 30 June–2 July 2015. AEQUA, Granada, pp 28–30
Lario J, Alonso-Azcárate J, Spencer C et al (2016) Evolution of the pollution in the Piedras River Natural Site (Gulf of Cadiz, southern Spain) during the Holocene. Environ Earth Sci 75:481–496. https://doi.org/10.1007/s12665-016-5344-8
Lillios KT, Blanco-González A, Drake BL et al (2016) Mid-late Holocene climate, demography, and cultural dynamics in Iberia: a multi-proxy approach. Quatern Sci Rev 135:138–153. https://doi.org/10.1016/j.quascirev.2016.01.011
López de Ayala P (1779) Crónicas de los reyes de Castilla don Pedro, don Enrique II, don Juan I, don Enrique III: Tomo I, que corresponde a la crónica del rey don Pedro. In: Llaguno Amirola E (ed) Con las enmiendas de […] Gerónimo Zurita. Antonio de Sancha, Madrid
López-Sáez JA, López-García P, Tixier C (2002) Crisis? What crisis?: l'anthropisation du milieu et la biodiversité dans la Baie de Cádiz (Espagne). Les Apports de la Palynologie. Orsis 17:91–99
López-Sáez JL, Pérez-Díaz S, Rodríguez-Ramírez A et al (2018) Mid-late Holocene environmental and cultural dynamics at the south-west tip of Europe (Doñana National Park, SW Iberia, Spain). J Archaeol Sci Rep 22:58–78. https://doi.org/10.1016/j.jasrep.2018.09.014
Luque L, Lario J, Zazo C et al (2001) Tsunami deposits as palaeoseismic indicators: examples from the Spanish coast. Acta Geologica Hispanica 36:197–211
Lyell C (1850) Principles of Geology or, the modern changes of the Earth and its inhabitants considered as illustrative of Geology. John Murray, London
Magnusson M (1973) Introducing archaeology. Book Club Associates, London
Mayet F, Tavares da Silva C (2002) L'Atelier d'amphores d'Abul (Portugal). Exploration archéologique du Sado. De Boccard, Paris
Medialdea T, Somoza L, Pinheiro LM et al (2009) Tectonics and mud volcano development in the Gulf of Cadiz. Mar Geol 261:48–63. https://doi.org/10.1016/j.margeo.2008.10.007
Menanteau L (1981) Les marismas du Guadalquivir. Exemple de transformation d'un paysage alluvial au cours du Quaternaire récent. Dissertation, Université de Paris-Sorbonne
Mitchell J (1760) Conjectures concerning the cause, and observations upon the phaenomena of earthquakes. Royal Society, London
Morales JA, Borrego J, San Miguel EG et al (2008) Sedimentary record of recent tsunamis in the Huelva Estuary (southwestern Spain). Quatern Sci Rev 27:734–746. https://doi.org/10.1016/j.quascirev.2007.12.002
Moreira de Mendonça JJ (1758) Historia Universal dos terremotos que tem havido no mundo, de que ha noticia, desde a sua creaçâo até o seculo presente. Antonio Vicente da Silva, Lisboa
Morgan LH (1877) Ancient Society. Holt, New York
Morton RA, Gelfenbaum G, Jaffe BE (2007) Physical criteria for distinguishing sandy tsunami and storm deposits using modern examples. Sed Geol 200:184–207
Osuna Ruiz M, Bedia García J, Domínguez Rico AM (2000) El santuario protohistórico hallado en la calle Méndez Núñez (Huelva). In: Cabrera Bonet P, Santos Retolaza M (eds) Ceràmics jònies d'època arcaica: centres de producció i comercialització al Mediterrani Occidental. Actes de la Taula Rodona, Empúries, 26–28 May 1999. Museu d'Arqueologia de Catalunya, Empúries, pp 177–188
Perrey A (1847) Sur les tremblements de terre de la Péninsule Ibérique. Annales de la SociétéRoyale d'Agriculture et Industrie de Lyon 10:461–513
Pozo M, Ruiz F, Carretero MI et al (2010) Mineralogical assemblages, geochemistry and fossil associations of Pleistocene-Holocene complex siliciclastic deposits from the Southwestern Doñana National Park (SW Spain): a palaeoenvironmental approach. Sed Geol 225:1–18. https://doi.org/10.1016/j.sedgeo.2010.01.002
Reimer PJ, Bard E, Bayliss A et al (2013) IntCal13 and Marine13 Radiocarbon Age Calibration Curves, 0–50,000 Years cal BP. Radiocarbon 55(4):1869–1887
Remesal J (2011) La Bética en el concierto del imperio romano. Real Academia de la Historia, Madrid
Renfrew C (2007) Prehistory: the making of the human mind. The Modern Library, New York
Rey GA (2011) Un terremoto y un tsunami en Huelva en el siglo VII a.C. Huelva Información 21 November 2011. https://www.huelvainformacion.es/opinion/articulos/terremoto-tsunami-Huelva-siglo-VII_0_535446794.html. Accessed 11 May 2020
Rodríguez-Ramírez A (1998) Geomorfología del Parque Nacional de Doñana y su entorno. Organismo Autónomo Parques Nacionales del Ministerio de Medio Ambiente, Madrid
Rodríguez-Ramírez A, Yáñez CM (2008) Formation of chenier plain of the Doñana marshland (SW Spain): observations and geomorphic model. Mar Geol 254:187–196
Rodríguez-Ramírez A, Rodríguez-Vidal J, Cáceres LM et al (1996) Evolución costera de la desembocadura del Guadalquivir en los últimos 6.000 años (SW de España). Geogaceta 20(5):1086–1088
Rodríguez-Ramírez A, Flores-Hurtado E, Contreras C et al (2014) The role of neo-tectonics in the sedimentary infilling and geomorphological evolution of the Guadalquivir estuary (Gulf of Cadiz, SW Spain) during the Holocene. Geomorphology 219:126–140. https://doi.org/10.1016/j.geomorph.2014.05.004

Rodríguez-Ramírez A, Pérez-Asensio JN, Santos A et al (2015) Atlantic extreme wave events during the last four millennia BP in the Guadalquivir estuary, SW Spain. Quatern Res 83:24–40. https://doi.org/10.1016/j.yqres.2014.08.005%3E

Rodríguez-Ramírez A, Villarías-Robles JJR, Pérez-Asensio JN et al (2016) Geomorphological record of extreme wave events during Roman times in the Guadalquivir estuary (Gulf of Cadiz, SW Spain): an archaeological and paleogeographical approach. Geomorphology 261:103–118. https://doi.org/10.1016/j.geomorph.2016.02.030

Rufete P (2002) El final de Tartessos y el Período Turdetano en Huelva. Huelva Arqueológica 17:7–204

Ruiz F, Rodríguez-Ramírez A, Cáceres LM et al (2004) Late Holocene evolution of the southwestern Doñana National Park (Guadalquivir Estuary, SW Spain): a multivariate approach. Palaeogeogr Palaeoclimatol Palaeoecol 204:47–64. https://doi.org/10.1016/S0031-0182(03)00721-1

Ruiz F, Rodríguez-Ramírez A, Cáceres L et al (2005) Evidences of high-energy events in the geological record: Mid-Holocene evolution of the southwestern Doñana National Park (SW Spain). Palaeogeogr Palaeoclimatol Palaeoecol 229:212–229. https://doi.org/10.1016/j.palaeo.2005.06.023

Salvany JM (2004) Tilting neotectonics of the Guadiamar drainage basin, SW Spain. Earth Surf Proc Land 29:145–160. https://doi.org/10.1002/esp.1005

Salvany JM, Custodio E (1995) Características lito-estratigráficas de los depósitos pliocuaternarios del bajo Guadalquivir en el área de Doñana: implicaciones hidrogeológicas. Revista de la Sociedad Geológica de España 8:21–31

Sánchez-León ML (1978) Economía de la Hispania Meridional durante la dinastía de los Antoninos. Universidad de Salamanca, Salamanca

Sánchez Navarro-Neumann MM (1921) Lista de los terremotos más notables sentidos en la Península Ibérica desde los tiempos más remotos, hasta 1917, inclusive, con ensayo de agrupación en regiones y periodos sísmicos. Estación Sismológica de Cartuja, Granada

Schneider H, Höfer D, Trog C et al (2010) Holocene estuary development in the Algarve Region (Southern Portugal): a reconstruction of sedimentological and ecological evolution. Quatern Int 221:141–158

Schulten A (1945) Tartessos, 2nd edn. Espasa-Calpe, Madrid

Sillières P (2006) Investigaciones arqueológicas en *Baelo*: balance, interpretación y perspectivas. In: Actas de las I Jornadas Internacionales de Baelo Claudia: balance y perspectivas (1966–2004), Cádiz, 25–27 October 2004. Consejería de Cultura de la Junta de Andalucía, Sevilla, pp 37–60

Soares AMM (2015) Radiocarbon dating of marine shells from the Gulf of Cadiz: the marine radiocarbon reservoir effect, its variability during the Holocene and palaeoenvironmental inferences. Cuaternario y Geomorfología 29(1–2):19–28

Spencer H (1876) The principles of sociology. Williams & Norgate, London

Stuiver M, Reimer PJ (1993) Radiocarbon calibration program. Rev. 4.2. Radiocarbon 35:215–230

Switzer AD, Jones BG, Bristow CS (2004) Geological evidence for large-scale washover events from coastal New South Wales, Australia: implications for management. In: Delivering Sustainable Coasts: connecting Science and Policy, Proceedings of Littoral 2004, Aberdeen, 20–22 September 2004. Cambridge Publications, Brookline, MA, vol 1, pp 390–395

Tejera-Gaspar A (1985) Excavaciones arqueológicas en el Huerto Pimentel (Lebrija, Sevilla), Noticiario Arqueológico Hispánico 26. Ministerio de Cultura, Madrid

The Jewish Publication Society of America (1978) The Prophets: a new translation of The Holy Scriptures according to the Masoretic text. The Jewish Publication Society of America, Philadelphia

Tsirkin JB (1987) The crisis of antique society in Spain in the third century (trans. Chistonogova L). Gerión 5:253–270

Tylor EB (1871) Primitive culture. John Murray, London

Udías A (2015) Historical earthquakes (before 1755) of the Iberian Peninsula in early catalogs. Seismol Res Lett 56(3):999–1005

Ventura A, Monterroso A (2003) Estudio sucinto de la campaña de excavación 1998–2000 en el Teatro Romano de Córdoba: la terraza media oriental. Anuario Arqueológico de Andalucía 2000 3(1):427–446

Viguier C (1977) Les grands traits de la tectonique du basin néogène du Bas Guadalquivir. Boletín Geológico Minero 88:39–44

Villani M (1729) Matthaei Villani eiusque filii Philippi Historia ab anno MCCCXLVIII ad annum MCCCLXIV. In: Moratori L A (ed) Rerum Italicarum Scriptores, vol 14. Società Palatina, Milano

Vizcaíno A, Gràcia E, Pallàs R et al (2006) Sedimentology, physical properties and ages of mass-transport deposits associated to the Marquês de Pombal Fault, Southwest Portuguese Margin. Norw J Geol 86:177–186

Voltaire F-MA (1877) Poème sur le désastre de Lisbonne, ou Examen de cet axiome: tout est bien. In: Ouvres complètes de Voltaire. Garnier Frères, Paris, vol 9, pp 470–478

Voltaire F-MA (1999) Cándido o el optimismo. Picazo MD, Gutiérrez F (eds) Orbis, Barcelona

Wallace AR (1855) On the law which has regulated the introduction of new species. Ann Mag Nat Hist 16:184–196 (2nd series)

Whelan F, Kelletat D (2005) Boulder deposits on the southern Spanish Atlantic coast: possible evidence for the 1755 AD Lisbon tsunami? Sci Tsunami Haz 23 (3):25–38

Willey GR, Sabloff JA (1980) A history of American archaeology, 2nd edn. WH Freeman & Co, San Francisco

Zazo C, Goy JL, Somoza L et al (1994) Holocene sequence of sea-level fluctuations in relation to climatic trends in the Atlantic-Mediterranean linkage coast. J Coast Res 10:933–945

Zazo C, Dabrio CJ, González J et al (1999) The records of the later glacial and interglacial periods in the Guadalquivir marshlands (Mari López drilling, SW Spain). Geogaceta 26:119–122

Zazo C, Mercier N, Silva PG et al (2005) Landscape evolution and geodynamic controls in the Gulf of Cadiz (Huelva coast, SW Spain) during the Late Quaternary. Geomorphology 68:269–290. https://doi.org/10.1016/j.geomorph.2004.11.022

Zeilinga de Boer J, Sanders DT (2005) Earthquakes in human history: the far-reaching effects of seismic disruptions. Princeton University Press, Princeton and Oxford

7 The Record of Extreme Wave Events in the Bay of Cadiz During Historical Times

Francisco Javier Gracia, Carlos Alonso, and José A. Aparicio

Abstract

The Bay of Cadiz is a complex coastal area, formed by confining sandy barriers, tidal flats, vegetated saltmarshes, fluvial mouths, and other coastal plains. Such physiographic characteristics have made them a very attractive place for human settlements since ancient times. At the same time this is a very vulnerable area, often affected by extreme wave events, both sea storms and tsunamis. Although such events produced damage in anthropic infrastructures and left different morpho-sedimentary records, subsequent human activity erased or distorted a substantial part of the remains. As a consequence, at present it is very difficult to identify correctly forms and deposits associated with events of this type, especially the oldest ones, for having suffered a higher number of later modifications. Only some places, like the Valdelagrana system of historical littoral ridges, have well-preserved indicators of historical extreme wave events. The systematic review and summary of historical records analyzed in the last decades by different research groups has allowed for establishing a chronology of historical energetic events, regardless their climatic or seismic origin (calibrated ages in years BP): 7.0–6.8, 5.7–5.6, 5.3–4.9, 2.7–2.3, 2.3–1.9 ka, 873–750, 269, and 245 (AD 1755). Some of them were very probably related to storms. Future research should focus on specific events recorded along the Gulf of Cadiz coast, in order to contrast dates, energy, and effects, which would help to gain a better understanding of their nature and to establish reliable return periods.

Keywords

Extreme wave event · Sea storm · Tsunami · Bay of Cadiz · Geoarchaeology · Evolution model

7.1 Introduction

During the last millennia the Bay of Cadiz and its surroundings have been preferential zones for the settlement of different human groups in Southern Iberia. Such communities knew navigation

F. J. Gracia (✉)
Departamento de Ciencias de la Tierra, Universidad de Cádiz, Cádiz, Spain
e-mail: javier.gracia@uca.es

C. Alonso
Instituto Andaluz del Patrimonio Histórico, Junta de Andalucía, Cádiz, Spain
e-mail: carlos.alonso.v@juntadeandalucia.es

J. A. Aparicio
Instituto Español Para la Reducción de los Desastres. Servicio de Emergencias, Cádiz, Spain
e-mail: aparicioflorido@gmail.com

M. Álvarez-Martí-Aguilar and F. Machuca Prieto (eds.), *Historical Earthquakes, Tsunamis and Archaeology in the Iberian Peninsula*, Natural Science in Archaeology,
https://doi.org/10.1007/978-981-19-1979-4_7

techniques (Vijande et al. 2015) and how to exploit not only marine resources but also terrestrial ones, especially those produced in the fertile valley of the river Guadalete. Such fluvial depressions offered easy access to the nearby lower Guadalquivir valley. Both physiographic units, the Bay of Cadiz-river Guadalquivir valley, were very closely related during different historical periods thanks to maritime trade.

The Bay of Cadiz, located in the southwest sector of the Iberian Peninsula, enjoys a privileged position due to its proximity to the main commercial routes connecting Europe and Africa, the Atlantic, and the Mediterranean. Phoenicians, Greeks, Carthaginians, Romans, or Arabs were all attracted by the site and, moved by their desire to control such trading activity, settled there founding colonies that would then evolve into the main urban nuclei of the bay. Centuries later, the discovery of America and the subsequent opening of sea routes to the Pacific also affected the economic relevance of the Bay of Cadiz: together with Seville, Cadiz became a bridgehead from which commerce coming from the New World was structured, organized, and distributed to other European harbors between the fifteenth and nineteenth centuries AD.

For centuries, the Bay of Cadiz was densely occupied by humans and modified as a consequence of the many infrastructures that were built to facilitate its defense, to engage in agriculture and animal husbandry and to distribute land produce and to trade with other distant harbors (Ruiz Gil et al. 1999; Alonso et al. 2001, 2003b, 2004; Alonso and Gracia 2004; Arteaga et al. 2008; Bernal 2008; López Amador and Pérez 2013). Such intensive historical activity has contributed to transform, blur and/or erase many possible markers of past extreme wave events (hereinafter EWEs) along this coast. This is especially the case of urban and saltmarsh zones, almost completely anthropized for the construction of saltworks (in Spanish, *salinas*) (Alonso et al. 2003a; Gracia et al. 2017), or their desiccation for agricultural purposes on the floodplain of the river Guadalete.

At present, it can be claimed that, after the last 20 years of research, there is a fairly good knowledge of the Holocene sedimentary records left by EWEs (tsunamis or ocean storms) along the coast of the Gulf and Bay of Cadiz. This is result of the work of several research groups focusing their efforts on describing and dating EWE deposits from different ages (Luque et al. 2002; Rodríguez-Ramírez et al. 2003; Reicherter et al. 2010; Rodríguez-Vidal et al. 2010; Morales et al. 2011; Lario et al. 2011). Some have put the accent on the geomorphological effects of such events (Alonso et al. 2004, 2015; Benavente et al. 2006; Gracia et al. 2006; Del Río et al. 2012; Ruiz et al. 2013), while others have concentrated on their structure from a purely sedimentological perspective (Luque et al. 2001; Gutiérrez-Mas et al. 2009a, b; Cuven et al. 2013, among others), although it is not easy to distinguish clearly their ascription to seismic events, like tsunamis, or climatic phenomena, like storms, cyclones, etc. (Lario et al. 2010; Medina et al. 2011; Gutiérrez-Mas and Mas 2013). The studies performed to date on the development, direct effects, and sedimentary records produced by present or very recent storm events in the most vulnerable zones of the Southern Atlantic seaboard of Spain (Benavente et al. 2006; Del Río et al. 2012; Anfuso et al. 2015) may be helpful in this respect.

An important unknown aspect is the impact that those historical events had on the area's coastal communities. An exception to the rule is the last big tsunami that hit the coast of the Gulf of Cadiz, associated with the Lisbon earthquake, in 1755; this event is well-documented due to the abundant information existing in historical archives (Martínez Solares 2001) and the numerous geomorphological and sedimentological records distributed along the Southern Portuguese, Spanish, and Northern Moroccan coastal fronts (Blanc 2008; Luque 2008; Campos 1992; Aparicio 2017, among others). Similar studies, focusing on a single event at different spatial scales and from a geoarcheological perspective, will be required to determine with a certain degree of accuracy aspects like impact level, chronology, significance, and geographical amplitude, genetic process, focus, effects on infrastructures and socioeconomic activity, etc.

7.2 The Bay of Cadiz. Potentiality of EWE Marker Preservation

The Bay of Cadiz is located less than 20 km to the south of the mouth of the river Guadalquivir, within the Guadalquivir Tertiary Depression. The bay is inset on low undulating hills modeled on Triassic and Neogene sedimentary materials as a consequence of the Plio-Pleistocene activation of strike-slip faults with a certain vertical component (Gracia et al. 2008). It is 30 km long in an N-S direction and 15 km wide. The bay is formed by an extensive littoral sedimentary plain behind confining sandy barriers comprising beaches and dunes, which shelter a complex space with tidal flats and saltmarshes, typical of a mesotidal coast (mean spring tidal range of 2.96 in the city of Cadiz; Benavente et al. 2007). Plio-Quaternary tectonics gave rise to several elevated morphostructural blocks, some of them of diapiric origin, forming islands (like Cadiz or San Fernando, Fig. 7.1) during periods of eustatic highstands; the summit of such islands is between 15 and 30 m above the present sea level. The tectonically subsided blocks recorded continuous coastal-marine flooding and sedimentary

Fig. 7.1 Location of the Bay of Cadiz (Google Earth) and the main place names cited in the text

filling throughout the late Quaternary, reaching a thickness of up to 30 m at some points (Dabrio et al. 2000). During sea level lowstands they acted as wide coastal plains traversed by the rivers Guadalquivir and Guadalete, plus other minor river courses (Mediavilla et al. 2004; Gracia et al. 2010).

Regarding wave energy, more than 70 per cent of annual waves are less than 1 m high, so Cadiz can be classified as a low-energy coast. The most energetic waves affect the coast in the winter, associated with Atlantic low pressure systems, and can reach a height of up to 4 m (Benavente et al. 2000). Waves usually arrive from the west, and their partial refraction in this NNW-SSE oriented coast produces a prevalent littoral drift flowing southwards.

The bay is structured around three main coastal embayments, separated by two central relieves of diapiric origin and NE-SW oriented: Ceuta Hill (in Puerto Real) and the island of San Fernando (Gracia et al. 2008). From this geomorphological point of view, the Bay of Cadiz can be divided in four well-defined zones (Fig. 7.1):

1. The outer confining barrier island
2. The northern bay
3. The central inner bay
4. The southern bay.

Each zone has a particular structure and orientation and, therefore, has a different level of exposition or shelter against the arrival of possible EWEs, regardless of their nature or origin. This factor, added to the amount of historical artificial transformations experienced by each coastal zone, directly controls the dispersion and type of high-energy deposits identified in the bay to date.

7.2.1 The Outer Confining Barrier Island

It is formed by a beach-dune system 17 km long running in a NNW–SSE direction, divided into two sectors. The first northern one is 11 km long and forms a tombolo connecting two rocky reliefs on Plio-Quaternary materials, currently occupied by the cities of Cadiz to the north and San Fernando in the center. This tombolo is the natural access to the city of Cadiz, and several remains of historical ancient roads can be identified along this shore, now partly covered by the beach and dunes. After a small rocky headland, the second southern sector of sandy barrier extends about 6 km to the south of the city of San Fernando, forming the Sancti Petri spit. This second stretch of the barrier island has been registering a continuous retreat and active overwashing in its northern half since the mid-nineteenth century (Fernández-Montblanc et al. 2018), partly conditioned by the bathymetry that promoted the differential dissipation of wave energy (Benavente et al. 2013).

The sandy barrier rests on previous Quaternary deposits. All along the confining barrier several cemented conglomeratic and sandstone units outcrop forming a more or less continuous and slightly undulating rocky platform about 500 m wide, which follows the coastline in the intertidal and subtidal zones, in some cases reaching 3 m above m.s.l. (Gracia et al. 2008). It is formed by a series of marine terraces of the Lower to Upper Pleistocene age (González-Acebrón et al. 2016). About one mile from this coast to the west a similar rocky shoal has developed parallel to the coastline, forming a submerged platform structurally controlled between 6 and 1 m below low-tide level. To the south some of these Quaternary terraces emerge to form the small island of Sancti Petri (Fig. 7.1). Other very shallow rocky shoals, all of them in all likelihood formed by Pleistocene cemented beachrock deposits, are also present in the northern external bay (Gutiérrez-Mas et al. 2004).

In this sector as a whole, different historical infrastructures constructed along the barrier (roads, defense walls, military fortresses, tuna fisheries, small docks, railways, etc.) certainly erased any imprints left by previous EWEs, identified in other places of the bay. Only the most recent tsunami event (in 1755) produced conspicuous effects recognizable at present, including several large and currently inactive overwash fans, the breakage of boulders from the Late Quaternary substratum and their transport and deposition inland, or the partial destruction of historical structures like roads and walls.

7.2.2 The Northern Bay

Between Puerto de Santa María and Rota, the so called "External Bay" (Fig. 7.1) is characterized by a mostly cliffed coast, excavated on Neogene sands and marls, and plenty of active mass movements where no record of past EWEs has been identified or cited. The southern reaches of the northern bay comprise a semi-confined tidal estuary, formed by an outer sand barrier N–S oriented (the Valdelagrana spit-barrier, 7 km long) and a wide extension of saltmarshes in the sheltered zone. The saltmarshes were comprehensively transformed for salt harvesting during historical times and artificially drained and desiccated in the 1950s for agricultural purposes, although the project failed due to the soil's high salinity.

The marshes feature two main drainage channels: the river Guadalete, one of the most important in Southern Spain, and the "river" San Pedro, a former course of the river Guadalete which now acts as a tidal channel, after its artificial disconnection from the main fluvial channel in the eighteenth century. The present mouth of the river Guadalete, located in the city of Puerto de Santa María, is an artificial channel initially excavated 2000 years ago for navigation purposes (Gracia et al. 2008).

The Valdelagrana spit-barrier exhibits a typical log-spiral plan morphology, linked to the mouth of the river Guadalete and the prevalent southwards littoral drift. This is the less transformed area in the northern bay and currently forms part of the Bay of Cadiz Natural Park. Its location, close to the river Guadalete and exposed to the Atlantic waves, favored the development of a complex system of late Holocene beach ridges, more than 20 according to Rodríguez Polo et al. (2009) and grouped in three main episodes by Dabrio et al. (2000), with ridges maintaining parallelism during the progradation of each episode. This sedimentary system has been the object of several studies by different authors over the past decades, including detailed geomorphological mapping and radiocarbon dating (Dabrio et al. 2000; Alonso et al. 2015, among others). Unfortunately, the reduced thickness of the sedimentary record in each ridge made them very vulnerable to EWEs. As a consequence, some of the deposits might have been mixed and/or altered, and dating values have often been contradictory. Nevertheless, the morphological study of the ridges and their dating by different authors has allowed for identifying a number of EWEs occurring during the last 3000 years. Other high-energy deposits have been identified as embedded sand layers within the clay sedimentary infilling of the estuarine saltmarshes of the river Guadalete (Alonso et al. 2015).

7.2.3 The Central Inner Bay

This area is formed by an open-water embayment between the cities of Puerto Real (Ceuta Hill) and San Fernando, directly connected to the sea to the north and protected from wave action by the Cadiz-San Fernando tombolo. This area historically served as a refuge for boats and an ideal place for developing docks, shipyards, military harbors, etc. A rim of active saltmarshes has developed along the inner zones of the bay, occupied since classical times by saltworks (Alonso et al. 2001, 2003a, 2015), which experienced their heyday in the nineteenth century. The construction of saltworks and salt harvesting activities transformed the saltmarsh surface, for which reason it is difficult to identify records of past EWEs, apart from the damage caused to historical infrastructures: an ancient road, an ancient powder magazine and a tidal mill, which fell into disuse after the 1755 tsunami (Alonso et al. 2003a; Aparicio 2017).

7.2.4 The Southern Bay

The city of San Fernando is located on an isolated relief of diapiric origin. Diapiric processes at this point started in the Late Pleistocene, affecting Triassic marls and gypsums. The diapiric rise has resulted in a hill 40 m high over the surrounding tidal flats and saltmarshes and is still active at present (Gracia et al. 2008). The southern bay extends to the south and southeast of the island of San Fernando, sheltered from the sea by the external confining barrier island. This area forms a wide NE–SW depression of fluvial origin (Mediavilla et al. 2004; Gracia et al. 2010), characterized by vegetated saltmarshes. The marshes were transformed into saltworks since pre-Roman times until the mid-nineteenth century (Alonso et al. 2003a). Most of them have since been abandoned and drained by the Sancti Petri tidal channel, and the area is watered by several minor river courses.

7.3 Methodology

The present synthesis has been elaborated in two stages:

In the first stage, an exhaustive bibliographic analysis was performed on works developed by other research teams in different places in the Bay of Cadiz. Special attention was paid to those that identified EWEs and included some type of dating. Due to the high number of works published in the last decades, a selection of papers and contributions was made in order to consider the most representative ones.

In the second stage, a comparative review of the aforementioned works helped to elaborate an interactive mapping of EWE markers in the Bay of Cadiz, which served as a basis for establishing time intervals for each event according to existing dating values. Finally, the results obtained were comprehensively reviewed in order to establish a proper interpretation and a definitive inventory of historical events in the bay.

One of the main problems encountered during the compilation was the reliability of datings made with ^{14}C techniques and their interpretation in relation to the reservoir effect existing in the Atlantic face of the Iberian Peninsula (Soares 2015). Some values were published after correction by reservoir effect, while others were not, and there were even some that did not provide enough information for evaluating the criteria used for their publication. This disparity was an important issue when trying to interpret the data and to correlate them on a chronological scale. Due to this problem, it was decided not to modify the dating values supplied by previous authors, insofar as the reason why the authors decided not to make such a correction or to follow different criteria is still a mystery.

Apart from this, radiocarbon dating poses another problem relating to the nature of the samples taken. An EWE (storm or tsunami) generates an important removal of both sublittoral and emerged coastal zones and waves transport debris of a different nature: bioclasts, ictiofauna, rock fragments, the remains of damaged anthropic coastal structures, elements eroded from different preexisting geomorphological or sedimentary units, etc. Those energetic waves can travel an important distance inland depending on the coastal morphology and topography, destroying previous forms until accumulating debris at given points, which then help to interpret and/or date such events. Those accumulations are often mixed, disordered, and heterogeneous deposits, as a result of a very energetic transport. In such conditions, we cannot use any bioclast or organic remains for dating. Only those bivalves that appear in their original life position can serve that purpose, since it is assumed that they were alive at the moment that the wave arrived. But even in those cases the results can be doubtful. Probably it would be more effective to date such sedimentary remains by dating the underlying and overlying levels, if possible.

7.4 Chronology of EWEs in the Bay of Cadiz

7.4.1 Prehistoric Deposits

7000 BP. The oldest documented records in the Bay of Cadiz are located in the northern bay, in the saltmarshes developed on the fringe of the shelter of the oldest Valdelagrana littoral ridge. At present they appear as relict washover deposits (Fig. 7.2), dated to cal. 7.0–6.8 ka BP (Lario 1996; Lario et al. 2011). These authors interpret the accumulation as a tsunami deposit generated at a moment during which the first Holocene prograding units began to develop, after the mid-Holocene (Flandrian) eustatic maximum (Zazo 2006; Zazo et al. 2008). On a regional scale, the first post-Flandrian littoral ridge, formed in cal. 6.9–4.5 ka BP (Zazo et al. 1996), has yet to be detected in the Bay of Cadiz. A tsunami deposit possibly coeval with this one has been described on the continental margin, facing the southern Portuguese coast, by Gràcia et al. (2010).

5700–5300 BP. A later EWE, during the Neolithic period, was also documented in the Valdelagrana complex (Fig. 7.2), dating back to cal. 5.7–5.6 ka BP (Lario 1996; Ruiz et al. 2007). The deposit could be coeval with other high-energy deposits identified on the nearby coast of Huelva, at Punta Umbría and in the Doñana spit system. Although the latter have been dated to cal. 5.3 ka BP (Ruiz et al. 2005; Cáceres et al. 2006), this is a somewhat moot point, since these authors consider the possibility of an origin

Fig. 7.2 Relict washover deposits (black arrows) behind the oldest Holocene littoral ridge at Valdelagrana (Google Earth). Red dashed line indicates the route of the ancient Roman road. Location in Fig. 7.1

relating to heavy storms. In fact, Rodríguez-Ramírez and Yáñez (2008), after a detailed study on the Doñana cheniers, concluded that they were associated with storm episodes and the inner estuary dynamics, not with an EWE. For Lario et al. (2010) all of them are associated with a unique tsunami event, despite chronological discrepancies. These last authors explain the ^{14}C dating deviations as a consequence of sampling different biological taxons and/or not applying the reservoir effect adjustments.

About 2 km to the southeast of Puerto Real, Gracia et al. (2000) found a littoral deposit located 2.5–3 m above the present sea level in the inner Bay of Cadiz, at a place completely sheltered from the waves during both the Holocene period and at present. The deposit was formed by less than 2 m of coarse beach sands with abundant mollusk bioclasts. Radiocarbon dating of the broken shells gave an age of cal. 4.9–5.3 ka BP, although no correction was made regarding the reservoir effect. The characteristics of the deposit suggest an energetic event (more probably a tsunami than a storm, due to its location) which could be correlated with the aforementioned episode.

4000 BP. Outside of the Bay of Cadiz, an event dated to cal. 4.0 ka BP has been identified at various points on the coast of the Gulf of Cadiz: a conspicuous deposit at Barbate beach interpreted as a tsunamite by Koster and Reicherter (2014), other similar accumulations in the Doñana spit system and marshes, dated to cal. 4.5–4.1 ka BP (Lario et al. 1995; Lario 1996; Ruiz et al. 2005; Cáceres et al. 2006), cal. 4.0, 3.55 and 3.15 ka BP, especially the first one which produced spit breaching, washover fans and deposition of a widespread detrital layer (Rodríguez-Ramírez et al. 2015), cal. 3.9–3.7 ka BP (Ruiz et al. 2005; Cáceres et al. 2006) and cal. 4.0–3.1 ka BP (Pérez et al. 2016). In Morocco, near Larache, other energetic deposits were indirectly dated to 5.0–3.0 BP (Mhammdi and Medina 2015; Mhammdi et al. 2015).

7.4.2 Deposits of the Antique Period

2700–2500 BP. Between 4.4 and 2.6 ka BP a quiescence period favored the development of a beach ridge system at the Valdelagrana barrier, equivalent to the H2 unit identified by Zazo et al. (1996). The ridges acted as a confining barrier that favored the initial generation of saltmarshes in the sheltered zones (Dabrio et al. 2000). The oldest radiocarbon dating obtained for this unit gave an age of 3.8 ka BP (Arteaga et al. 2008), coherent with the discovery of archeological remains associated with the occupation of the ridges by Bronze Age communities (Gómez Ponce et al. 1997). Other dating values gave younger ages (Zazo et al. 1996; Dabrio et al. 2000).

In the central sector of the Valdelagrana barrier, it is possible to identify a large ancient breach affecting the H2 ridge unit; the ridges at this point have developed several hooks bending inland (Gracia et al. 2005). Such a morphology could be explained by the impact of one or more EWEs (Lario et al. 1995; Dabrio et al. 2000) that were responsible for the capture and sudden outwash of the river Guadalete to the sea through the center of the barrier (its mouth was previously located to the south of the H2 ridge unit: Gracia et al. 2005; Alonso et al. 2015). It is difficult to specify the precise moment at which this episode occurred, although it must have taken place after the complete development of the H2 episode and before the establishment of the subsequent H3 ridge system (dated in Valdelagrana to cal. 2.3–1.1 ka BP by Dabrio et al. 2000, and in the Doñana barrier by Zazo et al. 1994, 1996; Rodríguez-Ramírez et al. 1996; Rodríguez-Vidal et al. 2014). Other coeval high-energy deposits were identified at other points along the Gulf of Cadiz by Lario (1996) and Lario et al. (2001, 2002), Cáceres et al. (2006), Ruiz et al. (2004) and Schneider et al. (2010), which point to the broad geographical scope of such an event, dated to between 2.7 and 2.3 ka BP. From an archaeological point of view, in 1998 during an excavation in Huelva, at Nos.

7–8, Méndez Núñez Street (Osuna et al. 2001), the remains of a Phoenician settlement were unearthed, with evidence of important damage and sudden abandonment at the beginning of the sixth century BC due to a seismic/tsunamigenic event, since the remains were covered by marine mollusk bioclasts typical of deep waters. During the first half of sixth century BC, that space remained partly flooded until renewed human occupation at about the second half of the century. All these data seem to indicate a seismic event. Be that as it may, a palaeoclimatic study performed by Martín Puertas et al. (2012) in the North Atlantic revealed that between 2.76 and 2.56 ka BP the zone was affected by intense atmospheric activity that very likely produced powerful storms, strong winds, and heavy rainfall in Southern and Central Europe. In any case, regardless the origin of such an event, the temporal coincidence or records and their wide geographical dispersion are evident, thus confirming an important EWE during the sixth century BC.

The historiographic tradition tends to explain the crisis of the Southern Iberian Tartessian culture in the sixth century BC as a slow, progressive process resulting from changes in the productive and commercial models of the metal industry (Wagner 1983; Alvar 1993). More recent studies suggest violent and traumatic processes (Escacena 1993; Ferrer Albelda 2007), interpreted by some historians as being associated with a possible natural catastrophe, and more specifically with the effects of an earthquake or a tsunami (Celestino 2014; Celestino and López-Ruiz 2016; a synthesis of such position can be found in Álvarez-Martí-Aguilar 2019).

2300–2200 BP. Apart from the tsunami following the Lisbon earthquake in 1755, one of the seismic events in the Gulf of Cadiz appearing most in the literature purportedly occurred at the end of third century BC (a review of the question has been performed by Álvarez-Martí-Aguilar 2017). This event was recorded in the classic seismic catalog compiled by Galbis (1932) as a series of earthquakes and tsunamis between 245 and 209 BC, causing widespread damage on the coast. However, Álvarez-Martí-Aguilar (2017) has demonstrated that the Spanish chronicler Florián de Ocampo (1543; 1553), cited by Galbis as his source, is highly unreliable. Rodríguez-Ramírez et al. (2016) already questioned the geological evidences of such energetic event in the Guadalquivir estuary.

Dated deposits associated with EWEs recorded along the coast of the Gulf of Cadiz between 218 and 209 BC are not uncommon, albeit showing a certain chronological divergence (Rodríguez-Vidal 1987; Lario et al. 1995, 2001, 2002; Lario 1996; Dabrio et al. 1999; Luque et al. 2001, 2002; Ruiz et al. 2004, 2008; Cáceres et al. 2006; Gràcia et al. 2010; Silva et al. 2015, among others). Rodríguez-Vidal et al. (2011) associate all those records to the event recorded in Galbis' catalog under the entry 218–209 BC events, which coincides with the end of the Second Punic War. The important damage and economic effects recorded in different archaeological settlements, like the one at Doña Blanca, near Puerto de Santa María (see Fig. 7.1 for location), were attributed to this conflict (Gómez et al. 2015). There is evidence that the Phoenician and Punic harbor at Doña Blanca was a very busy place between the eighth and third centuries BC, when it was suddenly abandoned for unknown reasons. Different authors have put forward hypotheses in the regard, one of which being the impact of a tsunami (Gómez et al. 2015). A new urban settlement surrounded by defensive walls recently discovered close to Doña Blanca, near the river Guadalete, will most surely provide very valuable information on the reason behind the harbor's abandonment and the possible role of an EWE in its destruction.[1]

[1] During 2017 a research team lead by L. Lagóstena and J. A. Ruiz (University of Cadiz, UCA) worked in the zone by applying georadar techniques, the initial results of which were published in the press: an urban settlement and harbor near the present-day Doña Blanca site. In the spring of 2019, a second team formed by F.J. Gracia, L. Barbero and J.A. López-Ramírez (UCA), the archaeologists C. Alonso and A. Higueras (Andalusian Institute for Historical Heritage), and the PhD student C. Caporizzo (University Parthenope, Naples, Italy) performed an aerial survey with an UAV using different sensors (optical, thermal and multi-spectral) in order to identify buried harbor infrastructures and to determine palaeosea levels. The results, still unpublished, revealed an extensive ancient urban area surrounded by walls, buried at a low depth (less than 1 m) close to the river Guadalete.

In the Bay of Cadiz sedimentary evidence of such an event is restricted to the northern side of the H2 ridge episode at the Valdelagrana barrier, perfectly recognizable in situ as washover lobes (Fig. 7.2), at about 3.5 m a.m.s.l. and with a thickness varying between 0.3 and 1 m. The deposit is formed by quartz-rich sands and plenty of complete and fragmented shells of *Glycimeris*, apart from other mollusks inherent to open- and deep-sea environments (Borja et al. 1999; Luque et al. 1999). Although it was initially thought to be related to the 1755 event (like other washover deposits identified in the central sector of the sand barrier, Fig. 7.3), subsequent historical, archeological, and radiometric studies (Luque et al. 2001; Luque 2008) have associated this EWE with a possible tsunami occurring between 218 and 216 BC, with waves higher than 2 m. However, these authors recognized that the AMS dating of a shell fragment taken from the deposit gave an age of cal. 1.91 ka BP, namely, the first century AD; this data points to a considerably later date and relates the event with a completely different historical horizon, as will be seen in the following paragraph.

2100–1800 BP. The Imperial Roman age is another period for which different references to EWEs can be found in the literature. An overall analysis of these references reveals different locations, from the coast of Huelva (Morales et al. 2008) to the Strait of Gibraltar (Arteaga and González 2004), and dates ranging from the first century BC to the third century AD.

On the southern Portuguese continental margin, near the submarine Marqués-de-Pombal Fault, four turbidite deposits were distinguished by Vizcaíno et al. (2006), one of them dating from between 47 BC and AD 61. In the Bay of Cadiz, a submerged sample featuring high-energy facies was dated to cal. 2.0–2.3 ka BP (Gutiérrez-Mas 2011). In the saltmarshes of Huelva, recent field research carried out on the island of Saltés (the complex mouth of the rivers Tinto and Odiel) characterized a washover deposit generated by an EWE, dating it to between cal. 2.1 and 1.9 ka BP, on top of which were the remains of several Roman salting factories (for example, that of La Cascajera), active during the fourth and fifth centuries BC (González-Regalado et al. 2019; Bermejo Meléndez et al. 2019). In Doñana, a system of Holocene littoral ridges and saltmarshes locally interrupted by successive minor EWEs, possibly linked to storm episodes or to extreme tidal events, was abruptly affected by an important energetic event dated to 1.8–1.7 ka BP (Ruiz et al. 2004; Cáceres et al. 2006; Morales et al. 2008; Rodríguez-Ramírez et al. 2016). This date coincides with the sudden, traumatic interruption in the activities of the salting factory at Cerro del Trigo nearby (the central Doñana ridge system), as well as the disappearance of many other coastal salting factories along the Gulf of Cadiz (Lagóstena 2001; Vidal and Campos 2008).

In the Bay of Cadiz, the reinterpretation of an AMS dating of a shell fragment extracted from the base of an old EWE deposit in Valdelagrana, places this event in 1.9 ka BP (Luque 2008). This record, together with others detected in the submerged zone of the bay (Gutiérrez-Mas 2011), reinforces the hypothesis of a tsunami occurring between the first and third centuries AD. That period was characterized by the proliferation of settlements (both urban and rural) and maritime trade and transport infrastructures. Such an energetic event might have been responsible for the heavy economic losses recorded along the coast of the Gulf of Cadiz during the Roman Imperial era (Alonso et al. 2003b), causing huge damage to (and even abandonment of) fishing grounds and urban enclaves, such as the Roman city of Baelo Claudia in the Strait of Gibraltar (Alonso et al. 2003a, b, c, 2004, 2007, 2009; Bernal et al. 2007).

7.4.3 Deposits and Forms from Roman to Early Modern Times (Third to Seventeenth Centuries AD)

Less known are the EWEs that may have occurred during medieval times, despite the information contained in Arab and Christian

Fig. 7.3 Location of the central and southern zones of the Valdelagrana barrier and the Holocene littoral ridges (Google Earth). White arrows indicate historical washover fans associated with the 1755 tsunami. Location in Fig. 7.1

chronicles (Bretón and Espinar 1996). Different works carried out in the Bay of Cadiz during the past 10 years have identified several EWE deposits, both at visible and submerged points in the external bay and in the Valdelagrana ridge system near Puerto Real (Gutiérrez-Mas 2011; Morales et al. 2011; Gutiérrez-Mas and García López 2015). The samples yielded dates of between the fourth (cal. 1.67 ka BP), sixth-eighth (cal. 1.44, 1.39 and 1.35 ka BP), ninth-twelfth (cal. 1.1, 0.95 and 0.87 ka BP), and eighteenth centuries AD (cal. 0.31 ka BP).

An important high-energy deposit, mainly composed by bioclasts, located about 8 m above the present sea level can be observed along the La Algaida Holocene littoral ridge (Fig. 7.3).

This ridge is equivalent to the H3 episode described by Zazo et al. (1996), and its morphological alteration helps to understand its evolution. Before the twelfth century (AD 1127 according to the earliest dating made in the deposits by Gutiérrez-Mas 2011), the river San Pedro (by that time it was the river Guadalete's main channel) ran to the east of the H3 ridge (Fig. 7.3), allowing for the formation of EWE deposits on La Algaida ridge. The opposite is very unlikely. If the river Guadalete had flowed to the west of the ridge, like the river San Pedro, no EWE deposit could have reached the H2 ridge unit, since the river channel is more than 200 m wide and very probably would have prevented the waves from reaching La Algaida ridge. The later (and current) circulation of the river Guadalete/San Pedro to the west of the H3 ridge means that at some moment after the twelfth century AD the H3 ridge was breached and the main channel flowed out through the central zones of the Valdelagrana barrier, leading to the generation of a new littoral ridge (H4). A borehole excavated on the H4 ridge in the southern zone of the Valdelagrana barrier included a high-energy deposit some meters below the present ridge surface, dated to cal. 0.75 ka BP (Alonso et al. 2015); this just might correspond to a storm or tsunami.

Indications of EWEs in a similar broad chronological range have been identified in other coastal locations along the Gulf of Cadiz: on the coast of the Portuguese Algarve dated to cal. 1.3–1.1 ka BP (Feist et al. 2019), in Huelva (Punta Umbría) dated to around cal. 1.56–1.51 ka BP (Ruiz et al. 2004), and in the Doñana spit barrier dated to cal. 1.6, 1.05, and 0.47 ka BP (Morales et al. 2008). This is a fairly wide chronological interval, only explainable by a high frequency of events, in all likelihood of a climatic origin. In his book *Historia de la dominación de los árabes en España* (*History of the Arab domination in Spain*), drawing from medieval chronicles (Bretón and Espinar 1996) the historian Antonio Conde (1820) refers to a possible tsunami in the Gulf of Cadiz at about the ninth century AD (AD 881?), the same date as several high-energy deposits found on the seabed of the external bay of Cadiz (Gutiérrez-Mas 2011; Morales et al. 2011).

During the fourteenth century AD several natural catastrophes, like earthquakes and heavy storms, affected different coastal settlements along the Gulf of Cadiz. For instance, Seville was severely damaged by an earthquake in 1356 (Gentil 1999). Nevertheless, there is no evidence of a tsunami associated with any of these events. There is more information on coastal storms at the time in historical archives. That is the case of the hurricane that occurred in 1464, according to the chronicles of Enrique IV of Castile (Espinar 1996), or other later events, identified thanks to documents housed in the *Archivo General de Indias*, like those recorded in 1580 (AGI/INDIFERENTE, 1956, L.3, F.98R-98V), 1595 (AGI/PATRONATO, 260, N.1, R.28), and 1685 (AGI/INDIFERENTE, 442, L.32, F.443-443V).

7.4.4 Late Modern to Recent Deposits and Forms (Eighteenth Century-Present-Day)

The intense industrial and commercial activity in the Bay of Cadiz as from the eighth century BC produced a series of historical markers on the current external confining barrier and the Valdelagrana spit barrier, very useful for identifying damage relating to historical EWEs: the Roman road (Aparicio 2017) called the Via *Augusta* and the Gades aqueduct (first century BC), a road built in the mid-eighteenth century, coastal watch towers (e.g. Torregorda, see Fig. 7.1 for location), bridges above tidal channels, defensive structures, fortresses and saltworks. These markers, when contrasted with documentary, archeological and geological data, help to identify, analyze and sometimes date such energetic events. Obviously, there is more accurate and reliable information on the latest and most energetic event occurring during the eighteenth century.

Between February and March 1731, a succession of EWEs relating to Atlantic storms affected the coasts of the Gulf of Cadiz. People reported "strange" tidal behavior, combined with storms and strong rip currents that caused deep erosion along the sandy shores between Cadiz and the island of Sancti Petri, in the external confining barrier. To the west, the strong low tides uncovered ancient Roman remains like coins, columns, basements, capitals, figurines and ruined buildings, among others. The minutes of Cadiz City Council of April 1731 described the breaching of three beaches near Torregorda, in a place known as the "Two-Seas" sentry box (currently El Chato beach; Fig. 7.4). It was given this name in reference to the rapid coastal erosion of that sector of the external barrier and the frequent opening of channels between 150 and 310 m wide, connecting the Atlantic to the central inner bay (see Fig. 7.1 for location). The return-to-normal, non-energetic conditions closed these breaches and the pedestrian connection between Cadiz and San Fernando could be recovered. The area affected by the breaches (c and d in Fig. 7.4) was traversed by a livestock trail, although dune development and mobility obliged people to go down to the beach and walk along the wide intertidal zone (Abreu 1866). Beyond the "Two-Seas" sentry box, the trail reached the La Gallega beach, where saltmarshes and saltworks extended eastwards; no other man-made structures were visible in this place, apart from the aforementioned guardhouse. The trail continued behind the Tower of Hercules, which had been built from the ruins of an old watch-tower (the present-day Torregorda military camp). It then passed close to a small fortress and bridge known as La Alcantarilla, before crossing the Arillo tidal channel and finally turning inland toward the city of San Fernando.

The abovementioned breaches unearthed a section of an ancient road, very probably the Roman road known as the *Via Augusta*, partly destroyed by wave action, whose existence had been completely unknown until then (Pemán 1948; Corzo 1992; Aparicio 2017). Built by the end of first century BC, it was 1.4 m above the backshore surface and 7 m wide, formed by two retaining walls made from Pliocene conglomerate masonry joined with lime mortar and filled with gravels, stones and sand, and covered with a flagstone pavement (Fig. 7.5). The whole structure rested on a sub-base 0.4 m thick, tamped down on the natural surface with different layers of gravels, clays and sands, as shown in Fig. 7.6. It was a fairly consistent structure in order to prevent overturning or collapse of walls due to underlying soft soils, or rapid deterioration from wave action.

Along the seashore, several blocks of the Roman Gades (Cadiz) aqueduct were also unearthed by the 1731 event. This stone water pipe was originally 82 km long and ran parallel to the road, until it reached the city's water storage cisterns (*castellum aquae*). In this final section (Santa María del Mar beach), the sea waves caused a landslide of the vertical scarp, outcropping a masonry water spring as part of the inner pipeline of this aqueduct. The widespread damage and the breached beaches indicate a fairly strong EWE, difficult to relate to a sea storm. A historical account (without details on dates or sources) mentions the sudden withdrawal of the sea for about one league (5.5 km) in the vicinity of the island of Sancti Petri (see Fig. 7.1 for location), uncovering the seafloor and making it possible to identify the site of the ancient Temple of Hercules (Matute 1887). This description led Galbis (1932) to include the event in his seismic catalog in relation to the Agadir earthquake, also recorded in the same year, although the significant sea withdrawal is not mentioned in the extant primary sources. A firsthand historical account is the testimony of Lope de los Ríos (Salas 2003), who talked about the "violence of the uncheckable surge" ("*violencia del desenfrenado golpe de mar*") that led to the discovery of archaeological remains in the vicinity of the island of Sancti Petri, the Roman *Via Augusta* (Aparicio 2017) and the main gates of Roman Gades.

Although Moreira (1993) claims that there is no coeval data confirming the occurrence of such an earthquake, Hoff (1840), citing the French traveler Verneur, remarked that in 1731 "an earthquake devastated the city of Santa Cruz de Aguer" (present-day Agadir in Morocco). Similarly, the English merchant Benjamin Bewick, who was living in Cadiz at the time of the 1755

Fig. 7.4 Location map (Google Earth) of the main severe impact points associated with the EWEs/tsunamis in 1731 (White arrows) and 1755 (Red arrows): **a** Santa Bárbara beach; **b** La Laguna neighborhood; **c** Cortadura and El Chato beaches; **d** La Gallega beach; **e** Torregorda; **f** La Albufereta embayment; **g** La Alcantarilla fortress and Urrutia beach; **h** La Alcantarilla bridge; **i** El Estanquillo saltworks; **j** the island and castle of Sancti Petri. Cartographic base: Google Earth

earthquake and tsunami, wrote a letter to a friend in London in which he told him that "about 25 years ago there was a small shock of an earthquake, but not attended with these horrid risings of the sea" (Bewick 1755). This date coincides with the 1731 seismic event and, since Bewick still remembered it 25 years later, it must have been quite strong. Martínez Solares and Mezcua (2002) located its epicenter in the Gulf of Cadiz, while some months before intense volcanic activity had been recorded on the island of Lanzarote in the Canary Isles, with lava flows and cinder emissions entirely covering several villages (Moreira 1758).

In sum, all this coastal damage may be related to a single sea storm, consistent with the

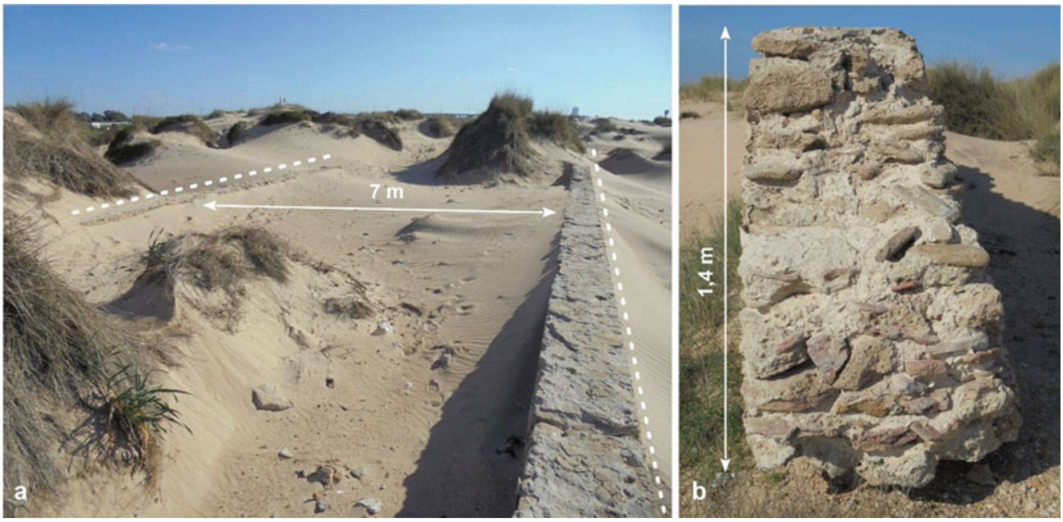

Fig. 7.5 Remains of the Roman road (*Via Augusta*) on La Gallega beach: **a** retaining walls, with the road embankment filled with aeolian sands and covered by vegetated dunes; **b** profile of a retaining wall with masonry joined with lime mortar

expected effects of a tsunami, which in some respects was very similar to that produced by the well-known 1755 tsunami. But no storm observed or described in modern times has been capable of causing such devastation. The most recent meteorological event, Storm Emma (February–March 2018), generated wave heights of up to 7.3 m and intense littoral currents coinciding with spring tides (coefficient of 1.6), producing intense erosion of beach berms, unearthing some archaeological remains of the Gades aqueduct and partially demolishing a small section of the coastal defense walls in the city of Cadiz, albeit without causing damage as severe as that produced by the 1731 event.

The great Lisbon earthquake, with an epicenter located to the southwest of Cape St. Vincent, occurred on November 1, 1755. In the Bay of Cadiz, the place hardest hit by the tsunami, gauged in the loss of human life and coastal damage, was again the external confining barrier between Cadiz and Sancti Petri, with the same points of impact as in the 1731 EWE (Fig. 7.4). Near the "Two-Seas" sentry box, a new breach was opened, causing an important inflow of sediments inside the central inner bay, making the navigation and anchoring of vessels difficult and isolating the city of Cadiz (minutes of the city council, May 29, 1756). A deposit of coarse imbricated discoid gravels, about 0.4 m thick, can currently be identified below the dunes at many points along the outer confining barrier, from Cadiz to the southern extreme of the Sancti Petri spit.

After the 1731 event, a new road had to be built along the barrier, but with a reinforced design: the thickness of the retaining walls was increased to 1.1 m, the width of the roadway to 11.2 m and height of the pavement to 2.4 m (Aparicio 2017), thus doubling its structural weight and resistance. However, it was completely destroyed by the tsunami's waves. The walls closest to the seashore overturned inwards, from west to east (Fig. 7.7a), uncovering some isolated remains of the original Roman road on the beach (Fig. 7.7b), plus fragments of the aqueduct used as masonry (Fig. 7.7c).

As the engineer Barnola observed (Martínez Solares 2001), new "thin" walls in a vertical position appeared near the Tower of Hercules (Torregorda). Judging by the building techniques, these remains belong to the original Roman wall and were uncovered by the removal of dunes (Fig. 7.7d, Aparicio 2017). The sub-base erosion and the gradually retreating

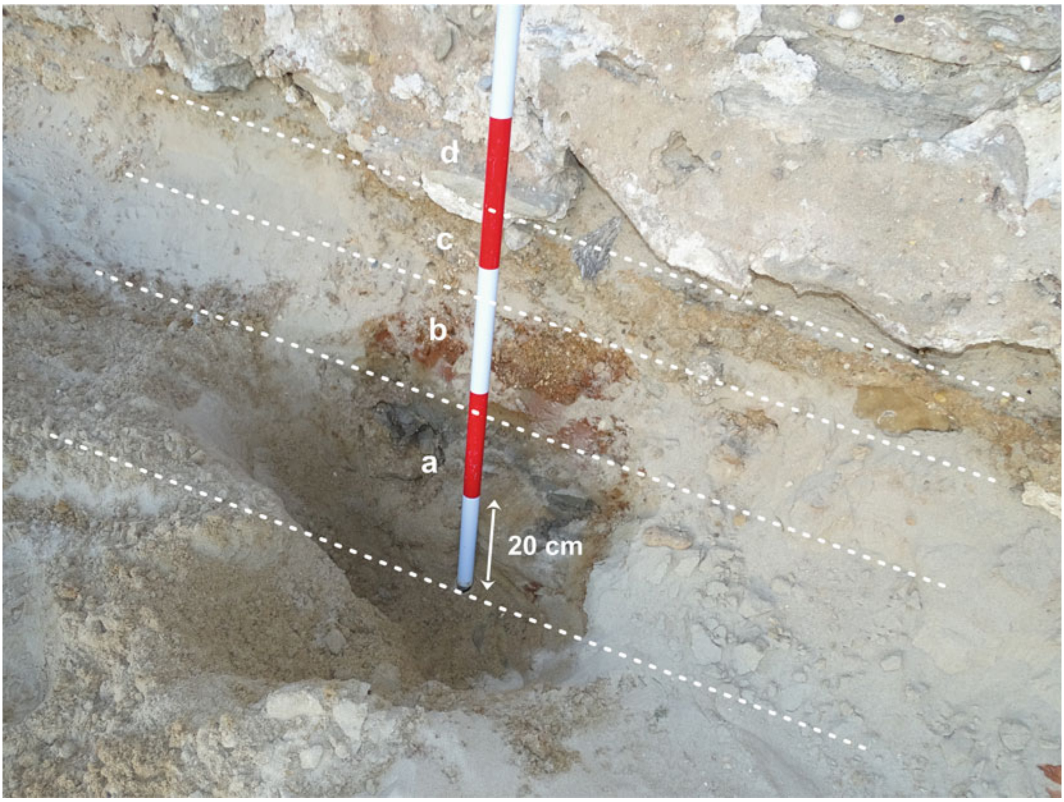

Fig. 7.6 Stratigraphic section of the sub-base of the Roman road (Torregorda): **a** pebble layer mixed with dried silts; **b** red clay layer; **c** basal layer with gravels mixed with yellow sands; **d** base of the Roman wall

shoreline in this area (Gracia et al. 2006), which is still occurring, left these walls very vulnerable to subsequent EWEs (Fig. 7.7e). It should be noted that, depending on the process, it is possible to distinguish two types of wall overturning: tsunami waves cause a massive, lined up and in-one-hit overturning, while minor EWEs (storms) cause limited rupture and random overturning in successive phases (Fig. 7.8).

Another stretch of several kilometers of the Roman road, previously covered by the dunes, came to light between the Tower of Hercules and La Albufereta, unearthed by the tsunami flood. On top of the road plane and inland there is a visible high-energy deposit 0.4 m thick, composed of a mixture of saltmarsh clays and clasts, very probably relating to the 1755 event. Only the retaining walls remained in their original position; but in La Albufereta the walls suffered a complete and lined-up collapse, with many fractured blocks being overturned in the direction of the back flow currents, plus some others on the opposite side in the inward flow direction. From this can be deduced a two-phase overturning: swash and backwash (Fig. 7.7f). Part of the direct impact of the tsunami waves was absorbed by the La Albufereta shore platform (see Fig. 7.4 for location). This can be seen in the large boulders lying on the rocky platform, one of them weighing up to about 40–50 tons, very similar to other boulder fields existing on the southwest coast of Iberia and interpreted as being typical of tsunamis (Fig. 7.9; Whelan and Kelletat 2005; Gracia et al. 2006).

Several huge washover fans formed in the Valdelagrana spit barrier (Fig. 7.3; Luque et al. 1999; Luque 2008) and also in the external confining barrier where they destroyed previous saltworks (Alonso et al. 2015). A wide washover lobe formed behind La Alcantarilla fortress and

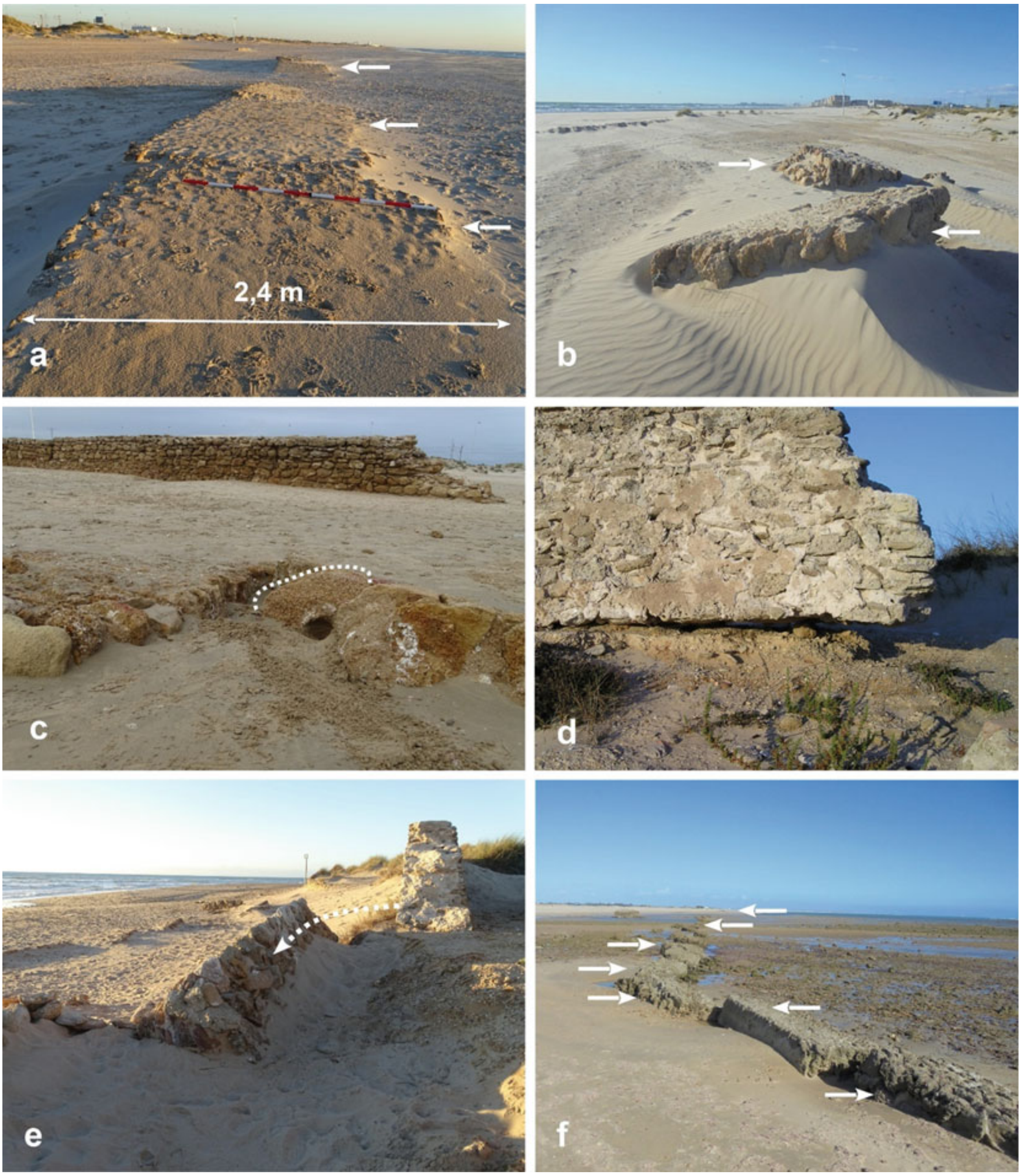

Fig. 7.7 EWE effects on ancient roads in the external confining barrier between Cadiz and Camposoto: **a** retaining walls of the road rebuilt in 1731 on Cortadura beach, overturned in the direction of arrival of the 1755 tsunami waves; **b** remains of the first-century-BC Roman road on Cortadura beach, overturned by the 1755 tsunami or other later events; **c** piece of the Roman aqueduct unearthed by the 1731 EWE, and reused as masonry in the construction of the new road; **d** Roman road wall in its original position (Torregorda beach) on the eroded sub-base with risk of collapse (photo taken in 2017); **e** the same wall finally overturned by loss of foundation support (photo taken in 2018); **f** walls of the ancient road in La Albufereta embayment, overturned in both directions by the swash and backwash of the 1755 tsunami waves

Fig. 7.8 Walls of the ancient Roman road on Torregorda-La Albufereta beach, randomly overturned by EWEs and erosional undermining. Dashed lines indicate the original position and orientation of the retaining walls of the road

Fig. 7.9 Boulder fields deposited on rocky shore platforms on the coast of Cadiz: above, La Albufereta embayment; below, Cape Trafalgar

bridge, where the road was completely destroyed (Fig. 7.10). The mayor of San Fernando reported the complete destruction of La Alcantarilla fortress and a nearby saltworks, while his counterpart in Chiclana de la Frontera (see Fig. 7.1 for location) claimed to have witnessed the arrival of three big waves higher than the castle of Sancti Petri, which demolished houses and saltworks located close to the Arillo tidal channel. Within the Bay of Cadiz, this was indeed the most severely flooded place, where up to 400 people drowned (Carbonell 1806).

7.5 Summary and Conclusions

In light of the foregoing, it can be concluded that a fair number of EWEs have been recorded in the Bay of Cadiz throughout history, many of them coinciding with similar events detected in other places along the Gulf of Cadiz (see Fig. 7.11 for the location of the main markers and deposits).

Without entering into the debate on their possible origin (climatic or tectonic), the list of events cited and described in this work and their reliability can be summarized as follows:

Fig. 7.10 Zone that suffered most from the 1755 tsunami: **a** Arillo channel; **b** flooded area forming a wide lagoon (dashed line); **c** old abandoned saltworks; **d** washover lobes (white line) formed by incoming waves; **e** ancient route of the Roman road (yellow line); the yellow dashed line indicates the destroyed section without archeological remains, coinciding with geological markers; **f** red line; route between Cadiz and San Fernando used in the eighteenth century. White arrows indicate the zone of barrier breaching. Base image: USAF aerial photograph taken in 1945–1946 (Serie A H1068_036_049, IGN)

– **cal. 7.0–6.8 ka BP**, present in the form of washover fans affecting the Valdelagrana spit barrier and interpreted as a tsunami deposit by Lario et al. (2011).
– **cal. 5.7–5.6 ka BP**, again recorded as washover fans affecting the Valdelagrana spit barrier. Regionally, its origin is controversial, although Lario et al. (2010) interpret the deposits as the result of a tsunami.
– **cal. 5.3–4.9 ka BP**, represented by a high-energy deposit in the most sheltered place of the central inner bay. They can be considered to have been caused by a tsunami, since it is highly improbable that a storm could have affected it and, if so, only after substantial energy dissipation. This event fits into the chronological range of an event identified in Morocco (Mhammdi and Medina 2015; Mhammdi et al. 2015).
– **cal. 2.7–2.5 ka BP**, inferred from the geometry of dated Holocene beach ridges at the Valdelagrana spit barrier (Gracia et al. 2005), and coeval with EWE deposits and archeological indicators identified along the Gulf of Cadiz. It might be associated with the crisis of the proto-historical Tartessian culture. The origin or nature of the event is uncertain.
– **cal. 2.3–1.9 ka BP**, EWE records from 218 to 216 BC have been widely documented throughout the Gulf of Cadiz, although their dating may be highly conditioned by the historical information contained in seismic

Fig. 7.11 Synthesis of historical EWE markers described in the Bay of Cadiz

catalogs. Their alleged destructive effects have sometimes been associated with warfare (end of the Second Punic War). Subtidal samples taken from the external bay of Cadiz by Gutiérrez-Mas (2011) have been associated with the period 2.3–1.9 ka BP, and may also be present in the Valdelagrana spit barrier (Luque 2008), as well as at different points in the Gulf of Cadiz. Its destructive effects along the coast might have led to a major economic crisis.

– **Ninth century to AD 1127–1250**, recorded as submerged levels, as a bioclast deposit on La Algaida littoral ridge (Gutiérrez-Mas 2011) and also as an EWE deposit in a borehole excavated near that zone (Alonso et al. 2015). They have been interpreted as being associated with strong storms and tsunamis, alike. Other records of EWEs dating back to medieval times, with a wide chronological interval, have been recorded along the Gulf of Cadiz.

– **1731 AD**. This event, described in a number of historical documents, caused greater damage to the most exposed infrastructures in the Bay of Cadiz than any storm ever recorded. If a tsunami, it might have been related to the Agadir earthquake.
– **1755 AD**. This is the most energetic and recent EWE, specifically a tsunami, produced by the Lisbon earthquake on November 1, 1755. Many indicators of the event can be identified along the coast of the bay, in the form of boulder fields, gravel deposits within the clayey marshes, washover fans, littoral ridge breaches, and also in many examples of damaged infrastructure all along the shore between Cadiz and San Fernando.

In conclusion, about eight EWEs have been identified in the Bay of Cadiz for the late Holocene, whose origin and nature is often difficult to determine. Surely some of them were related to a series of storms that hit the Gulf of Cadiz, causing damage. However, the dearth of remains and historical accounts describing them makes it hard to determine whether the rest were of climatic or tectonic origin. There is a need for further research focusing on the study of specific events and their effects along the coast of the Gulf of Cadiz, in order to contrast dates, energy level and a variety of characteristics, which may help to determine their nature with greater precision. This is essential for defining scientifically-supported return periods for tsunamis or strong storm events in this region.

References

Abreu P de (1866) Historia del saqueo de Cádiz por los Ingleses en 1596. Revista Médica, Cádiz

Alonso C, Gracia FJ (2004) La paleotopografía costera y el asentamiento de puertos, fondeaderos y zonas de producción del litoral gaditano durante la antigüedad. In: De Maria L, Turchetti R (eds) Evolución paleoambiental de los puertos y fondeaderos antiguos en el Mediterráneo Occidental. Proyecto europeo ANSER, European Progr. Interreg III B Medocc. Rubbettino, Roma, pp 167–195

Alonso C, Gracia FJ, Benavente J (2009) Evolución histórica del sector meridional de la Bahía Interna de Cádiz. RAMPAS 11:13–37

Alonso C, Menanteau L, Navarro M et al (2001) Antropización histórica de un espacio natural. Las salinas de la Bahía de Cádiz. Boletín del Instituto Andaluz del Patrimonio Histórico 35:172–185

Alonso C, Gracia FJ, Ménanteau L (2003a) Las salinas de la Bahía de Cadiz durante la antigüedad: visión geoarqueológica de un problema histórico. Spal 12:317–332

Alonso C, Ojeda R, Ménanteau L et al (2003b) Paleogeographie de l'anse de Bolonia (Tarifa, Espagne) à l'époque romaine. In: Fouache E (ed) The Mediterranean world environment and history. Environmental dynamics and history in Mediterranean areas, Paris, Université de Paris-Sorbonne, 24–26 avril 2002. Swamp areas and seashores dynamics/Dynamiques des zones humides et mobilite des lignes de rivage. Elsevier, Paris, pp 407–417

Alonso C, Ojeda R, Ménanteau L et al (2003c) Análisis geoarqueológico del sector meridional de Baelo Claudia (Tarifa, Cádiz). Boletín del Instituto Andaluz del Patrimonio Histórico 43:58–74

Alonso C, Gracia FJ, Anfuso G et al (2004) Registro morfosedimentario de eventos históricos de alta energía en el litoral atlántico del Estrecho de Gibraltar (Trafalgar–Tarifa). In: Benito G, Díez Herrero A (eds) Contribuciones recientes sobre Geomorfología. CSIC, Madrid, pp 263–271

Alonso C, Menanteau L, Gracia FJ et al (2007) Geoarqueología y paleomorfología litoral de la ensenada de Bolonia: primeros resultados y nuevas propuestas. In: Arévalo A, Bernal D (eds) Las *cetariae* de *Baelo Claudia*. Avance de las investigaciones arqueológicas en el barrio meridional (2000–2004). Universidad de Cádiz—Consejería de Cultura de la Junta de Andalucía, Cádiz-Sevilla, pp 521–538

Alonso C, Gracia FJ, Rodríguez Polo S et al (2015) El registro de eventos energéticos marinos en la bahía de Cádiz durante épocas históricas. Cuaternario y Geomorfología 29(1–2):95–117

Alvar J (1993) El ocaso de Tarteso. In: Alvar J, Blázquez JM (eds) Los enigmas de Tarteso. Cátedra, Madrid, pp 187–200

Álvarez-Martí-Aguilar M (2017) La tradición historiográfica sobre catástrofes naturales en la Península Ibérica durante la Antigüedad y el supuesto tsunami del Golfo de Cádiz de 218–209 a.C. Dialogues d'histoire ancienne 43(2):117–145

Álvarez-Martí-Aguilar M (2019) El retorno del cataclismo: de la Atlántida a Tarteso. In: Sánchez Moreno E (coord) Veinticinco estampas de la España antigua cincuenta años después (1967–2017). En torno a la obra de Antonio García y Bellido y su actualización científica. Universidad de Sevilla, Sevilla, pp 115–129

Anfuso G, Rangel-Buitrago N, Cortéz-Useche C et al (2015) Characterization of storm events along the Gulf of Cadiz (eastern central Atlantic Ocean). Int J Climatol 36:3690–3707

Aparicio JA (2017) 1755. El maremoto que viene. Q-book, Cádiz

Arteaga C, González JA (2004) Presencia de materiales marinos y dunares sobre un alfar romano en la Bahía de Algeciras (Cádiz, España). In: Benito G, Díez Herrero A (eds) Contribuciones recientes sobre Geomorfología, VIII Reunión Nacional de Geomorfología, Toledo. SEG-CSIC, Madrid, pp 393–400

Arteaga O, Schulz H, Roos AM (2008) Geoarqueología dialéctica en la Bahía de Cádiz. RAMPAS 10:21–116

Benavente J, Gracia FJ, López-Aguayo F (2000) Empirical model of morphodynamic beachface behaviour for low-energy mesotidal environments. Mar Geol 167:375–390

Benavente J, Del Río L, Gracia FJ et al (2006) Coastal flooding hazard related to storms and coastal evolution in Valdelagrana spit (Cadiz Bay Natural Park, SW Spain). Cont Shelf Res 26:1061–1076

Benavente J, Del Río L, Anfuso G et al (2007) Efecto de la marea en la clasificación morfodinámica de playas. In: Gomez-Pujol L, Fornós JJ (eds) Investigaciones recientes (2005–2007) en Geomorfología Litoral. Universitat de les Illes Balears-IMEDEA-SEG, Palma de Mallorca, pp 17–21

Benavente J, Del Río L, Plomaritis TA et al (2013) Impact of coastal storms in a Sandy Barrier (Sancti Petri, Spain). J Coast Res SI 65:66–671

Bermejo Meléndez J, Gómez Gutiérrez P, Montero ML et al (2019) A new roman fish-salting workshop in the Saltés Island (Tinto-Odiel Estuary, SW Spain): La Cascajera and its archaeological and geological context. Cuaternario y Geomorfologia 33:13–26

Bernal D (2008) Gades y su bahía en la Antigüedad. Reflexiones Geoarqueológicas y Asignaturas Pendientes. RAMPAS 10:267–308

Bernal D, Arévalo A, Lorenzo L et al (2007) Abandono en algunas insulae del barrio industrial a finales del siglo II D. C. In: Arévalo A, Bernal D (eds) Las *cetariae* de *Baelo Claudia*. Avance de las investigaciones arqueológicas en el barrio meridional (2000–2004). Universidad de Cádiz - Consejería de Cultura de la Junta de Andalucía, Cádiz-Sevilla, pp 383–454

Bewick B (1755) An account of the Earthquake at Cadiz, Novem. 1, 1755, in a letter from Mr. Benjamin Bewick, merchant there to Mr. Joseph Paice, merchant in London. Philos Trans XLIX(I):424–427

Blanc PL (2008) The tsunami in Cadiz on 1 November 1755: a critical analysis of reports by Antonio de Ulloa and by Louis Godin. CR Geosci 340:251–261

Borja F, Zazo C, Dabrio CJ et al (1999) Holocene aeolian phases and human settlements along the Atlantic coast of Southern Spain. Holocene 9(3):333–339

Bretón M, Espinar M (1996) Fenómenos sísmicos que afectaron a las tierras andaluzas en los siglos IX al XII según las crónicas musulmanas Homenaje al prof. Fernando de Miguel Martínez. Universidad de Granada, Granada, pp 47–76

Cáceres LM, Rodríguez Vidal J et al (2006) El registro geológico Holoceno como instrumento para establecer periodos de recurrencia de tsunamis. El caso de la costa de Huelva. In: V Asamblea Hispano Portuguesa de Geodesia y Geofísica, Sevilla, pp 1–4

Campos ML (1992) El riesgo de tsunamis en España. Análisis y valoración geográfica. IGN, Madrid

Carbonell A (1806) Razón de las circunstancias del terremoto acaecido en Cádiz a primero de noviembre de 1755 hallándose el día en la mayor serenidad. By D.A.C.B. as eye witness. Memorial Literario o Biblioteca Periódica de Ciencias y Artes, pp 200–207

Celestino S (2014) Tarteso. Viaje a los confines del Mundo Antiguo. Trébede, Madrid

Celestino S, López-Ruiz C (2016) Tartessos and the Phoenicians in Iberia. Oxford University Press, Oxford

Conde JA (1820) Historia de la dominación de los árabes en España, sacada de varios manuscritos y memorias arábigas. Imprenta que fue de García, Madrid

Corzo R (1992) Las vías romanas en Andalucía. Consejería de Obras Públicas y Transportes, Seville

Cuven S, Paris R, Falvard S, Miot-Noirault E et al (2013) High-resolution analysis of a tsunami deposit: case-study from the 1755 Lisbon tsunami in southwestern Spain. Mar Geol 337:98–111

Dabrio CJ, Zazo C, Goy JL (1999) El estuario del Guadalete. In: Durán JJ, Nuche R (eds) Patrimonio Geológico de Andalucía. Enresa, Madrid, pp 78–83

Dabrio CJ, Zazo C, Goy JL et al (2000) Depositional history of estuary infill during the last postglacial transgression (Gulf of Cadiz, Southern Spain). Mar Geol 162:381–404

Del Río L, Plomaritis TA, Benavente J et al (2012) Establishing storm thresholds for the Spanish Gulf of Cadiz coast. Geomorphology 143–144:13–23

Escacena JL (1993) De la muerte de Tartesos. Evidencias en el Registro Poblacional. Spal 2:183–218

Espinar M (1996) Terremotos (?) o fenómenos naturales en tiempos de Enrique IV de Castilla. Ideas de la época. In: Homenaje en honor al profesor Fernando de Miguel Martínez. Universidad de Granada, Granada, pp 51–172

Fernández-Montblanc T, Del Río L, Izquierdo A et al (2018) Shipwrecks and man-made coastal structures as indicators of historical shoreline position. An interdisciplinary study in the Sancti Petri sand spit (Bay of Cadiz, SW Spain). Mar Geol 395:152–167

Ferrer Albelda E (2007) Fenicios y cartagineses en el Tartessos postcolonial. In: Actas del V Congreso de Historia de Carmona. El nacimiento de la ciudad: la Carmona protohistórica. Ayuntamiento, Carmona, pp 95–223

Feist L, Frank S, Bellanova P et al (2019) The sedimentological and environmental footprint of extreme wave events in Boca do Rio, Algarve coast, Portugal. Sed Geol 389:147–160

Galbis J (1932) Catálogo sísmico de la zona comprendida entre los meridianos 5° E y 20° W de Greenwich y los

paralelos 45° y 25° N. Tomo I. Instituto Geográfico, Catastral y de Estadística, Madrid
Gentil P (1999) El riesgo sísmico de Sevilla. Servicio de Publicaciones Univ. Sevilla, Sevilla
Gómez F, Arruda AM, Rodríguez-Vidal J et al (2015) Eventos marinos de alta energía y cambios traumáticos en los asentamientos costeros del suroeste de la Península Ibérica. Cuaternario y Geomorfología 29(1–2):57–74
Gómez Ponce C, Borja F, Lagóstena L et al (1997) Primeras fases de la evolución de la flecha litoral de Valdelagrana (El Puerto de Santa María, Cádiz). Datos arqueológicos. In: Rodríguez Vidal J (ed) IV Reunión del Cuaternario Ibérico. AEQUA, Huelva, pp 165–167
González-Acebrón L, Mas R, Arribas J et al (2016) Very coarse-grained beaches as a response to generalized sea level drops in a complex active tectonic setting: Pleistocene marine terraces at the Cadiz coast, SW Spain. Mar Geol 382:92–110
Gràcia E, Vizcaino A, Escutia C et al (2010) Holocene earthquake record offshore Portugal (SW Iberia): testing turbidite palaeoseismology in a slow-convergence margin. Quatern Sci Rev 29(9–10):1156–1172
Gracia FJ, Alonso C, Abarca JM (2017) Evolución histórica y geomorfología de las explotaciones salineras en marismas mareales. Ejemplos de la bahía de Cadiz. Cuaternario y Geomorfología 31(1–2):45–72
Gracia FJ, Alonso C, Gallardo M et al (2000) Evolución eustática postflandriense en las marismas del sur de la Bahía de Cádiz. Geogaceta 27:71–74
Gracia FJ, Alonso C, Anfuso G et al (2005) Chapter IV: Historical evolution and erosion problems in the Cadiz Coast. In: Gracia FJ (ed) Geomorphology of the South-Atlantic Spanish Coast, 6th international conference on geomorphology, field trip guide A-4, Zaragoza, pp 40–58
Gracia FJ, Alonso C, Benavente J et al (2006) The different coastal records of the 1755 tsunami waves along the south Atlantic Spanish Coast. Z Geomorphol 146:195–220
Gracia FJ, Rodríguez-Vidal J, Belluomini G et al (2008) Diapiric uplift of an MIS 3 marine deposit in SW Spain. Implications in Late Pleistocene sea level reconstruction and palaeogeography of the Strait of Gibraltar. Quatern Sci Rev 27(23–24):2219–2231
Gracia FJ, Alonso C, Giles F et al (2010) Evidencias del paso del río Guadalquivir por el interior de la Bahía de Cádiz durante el Pleistoceno Medio. In: Cuaternario y Arqueología. Homenaje a Francisco Giles Pacheco. Diputación Provincial de Cádiz, Cádiz, pp 9–17
Gutiérrez-Mas JM (2011) Glycymeris shell accumulations as indicators of recent sea-level changes and high-energy events in Cadiz Bay (SW Spain). Estuar Coast Shelf Sci 92:546–554
Gutiérrez-Mas JM, Mas R (2013) Record of very high energy events in Plio-Pleistocene marine deposits of the Gulf of Cadiz (SW Spain): facies and processes. Facies 59:679–701
Gutiérrez-Mas JM, García-López S (2015) Recent evolution of the river mouth intertidal zone at the Río San Pedro tidal channel (Cadiz Bay, SW Spain): controlling factors of geomorphologic and depositional changes. Geol Acta 13:123–136
Gutiérrez-Mas JM, Achab M, Gracia FJ (2004) Structural and physiographic controls on the Holocene marine sedimentation in the Bay of Cadiz (SW Spain). Geodin Acta 17(2):47–55
Gutiérrez-Mas JM, Juan C, Morales JA (2009a) Evidence of high-energy events in shelly layers interbedded in coastal Holocene sands in Cadiz Bay (south-west Spain). Earth Surf Proc Land 34:810–823
Gutiérrez-Mas JM, López-Arroyo J, Morales JA (2009b) Recent marine lithofacies in Cadiz Bay (SW Spain) Sequences, processes and control factors. Sed Geol 218:31–47
Hoff KEA (1840) Geschichte der durch Überlieferung nachgewiesenen natürlichen Veränderungen der Erdoberfläche IV. Bei Justus Perthes, Gotha
Koster B, Reicherter K (2014) Sedimentological and geophysical properties of a ca. 4000 year old tsunami deposit in southern Spain. Sed Geol 314:1–16
Lagóstena L (2001) La producción de salsas y conservas de pescado en la Hispania romana. Collecció Instrumenta 11. Editorial Universidad de Barcelona, Barcelona
Lario J (1996) Último y presente Interglacial en el área de conexión Atlántico-Mediterráneo: Variaciones del nivel del mar, paleoclima y paleoambientes. Dissertation, Universidad Complutense, Madrid
Lario J, Zazo C, Dabrio CJ et al (1995) Record of recent Holocene sediment input on spit bars and deltas of South Spain. In: Ocre B (ed) Holocene cycles: climate, sea levels, and sedimentation. J Coast Res SI 17:241–245
Lario J, Zazo C, Plater AJ et al (2001) Particle size and magnetic properties of Holocene estuarine deposits from the Doñana National Park (SW Iberia): evidence of gradual and abrupt coastal sedimentation. Z Geomorphol 45(1):33–54
Lario J, Zazo C, Goy JL et al (2002) Changes in sedimentation trends in SW Iberia Holocene estuaries (Spain). Quatern Int 93–94:171–176
Lario J, Luque L, Zazo C et al (2010) Tsunami vs. storm surge deposits: a review of the sedimentological and geomorphological records of extreme wave events (EWE) during the Holocene in the Gulf of Cadiz, Spain. Zeitschrift für Geomorphologie 54(Suppl. 3):301–316
Lario J, Zazo C, Goy JL et al (2011) Holocene palaeotsunami catalogue of SW Iberia. Quatern Int 242:196–200
López Amador JJ, Pérez E (2013) El puerto gaditano de Balbo. Ed. El Boletín, Cádiz
Luque L (2008) El impacto de eventos catastróficos costeros en el litoral del Golfo de Cádiz. RAMPAS 10:131–153
Luque L, Zazo C, Goy JL et al (1999) Los depósitos del tsunami de Lisboa de 1755. Su registro en la Bahía de

Cádiz: flecha de Valdelagrana (Spain). In: Pallí L, Roqué C (eds) Avances en el estudio del Cuaternario español, Universidad de Girona, Girona, pp 63–66

Luque L, Lario J, Zazo C et al (2001) Tsunami deposits as paleoseismic indicators: examples from the Spanish coast. Acta Geológica Hispánica 36(3–4):197–211

Luque L, Lario J, Civis J et al (2002) Sedimentary record of a tsunami during Roman times, Bay of Cadiz, Spain. J Quat Sci 17:623–631

Martín Puertas C, Matthes K, Brauer A et al (2012) Regional atmospheric circulation shifts induced by a grand solar minimum. Nat Geosci 5:397–401

Martínez Solares JM (2001) Los efectos en España del terremoto de Lisboa (1 de noviembre de 1755). Instituto Geográfico Nacional, Madrid

Martínez Solares JM, Mezcua J (2002) Catálogo sísmico de la Península Ibérica (880 a. C.—1900). Instituto Geográfico Nacional, Madrid

Matute J (1887) Anales eclesiásticos y seculares de la muy noble y leal ciudad de Sevilla, vol I. Impr. E. Rasco, Seville

Mediavilla R, Antón-López L, Dabrio CJ et al (2004) Distribución y caracterización de los depósitos fluviales pleistocenos del subsuelo de la Bahía de Cádiz. Geotemas 6(5):203–206

Medina F, Mhammdi N, Chiguer A et al (2011) The Rabat and Larache boulder fields; new examples of high-energy deposits related to storms and tsunami waves in north-western Morocco. Nat Hazards 59:725–747

Mhammdi N, Medina F (2015) Recent tsunami deposits along the Moroccan Atlantic coast. In: Galve JP, Azañón JM, Pérez Peña JV et al (eds) Una visión global del Cuaternario. El hombre como condicionante de procesos geológicos. XIV Reunión Nacional de Cuaternario, Granada, pp 227–229

Mhammdi N, Medina F, Trentesaux A et al (2015) Sedimentary evidence of palaeo-tsunami deposits along the Loukkos estuary (Moroccan Atlantic coast). Sci Tsunami Hazards 34(2):83–100

González-Regalado ML, Gómez P, Ruiz F et al (2019) Facies analysis, foraminiferal record and chronostratigraphy of Holocene sequences from Saltés Island (Tinto-Odiel estuary, SW Spain): the origin of high-energy deposits. Estuar Coast Shelf Sci 218:95–105

Morales JA, Borrego J, San Miguel EG et al (2008) Sedimentary record of recent tsunamis in the Huelva Estuary (southwestern Spain). Quatern Sci Rev 27:734–746

Morales JA, Gutiérrez-Mas JM, Borrego J et al (2011) Sedimentary characteristics of the Holocene tsunamigenic deposits in the coastal systems of the Cadiz Gulf (Spain). In: Mörner NA (ed) The Tsunami threat—research and technology. InTech, Rijeka, pp 237–258

Moreira JJ (1758) Historia universal dos terremotos. Antonio Vicente da Silva, Lisboa

Moreira VS (1993) Historical tsunamis in mainland Portugal and Azores: case histories. Tsunamis in the world. In: Tinti S (ed) 15th international tsunami symposium. Springer, Dordrecht

Ocampo F de (1543) Los quatro libros primeros de la Cronica general de España que recopila el maestro Florian do Campo criado y cronista del Emperador Rey nuestro señor por mandado de su magestad Çesarea. Juan Picardo, Zamora

Ocampo F de (1553) Los cinco libros primeros de la Cronica general de España, que recopila el maestro Florian do Campo, Cronista del Rey nuestro señor, por mandado de su Magestad, en Zamora, Guillermo de Millis, Medina del Campo

Osuna M, Bedia J, Domínguez AM (2001) El santuario protohistórico hallado en la calle Méndez Núñez (Huelva). In: Cabrera P, Santos M (eds) Ceràmiques jònies d`època arcaica: centres de producció i comercialització al Mediterrani occidenta. Actes Taula Rodona, Empúries. Museu d'Arqueologia de Catalunya, Barcelona, pp 177–188

Pemán C (1948) Nuevas precisiones sobre vías romanas en la provincia de Cadiz. Arch Esp Arqueol 72:255–268

Pérez SC, Cerrillo E, León Á et al (2016) Razones geológicas, arqueológicas y antropológicas para la conservación de Doñana: el Proyecto Hinojos (2005–2013). In: Ferrer M (coord) Doñana: 50 años de investigaciones científicas. Anejos de Arbor 11. CSIC, Madrid, pp 81–100

Reicherter K, Vonberg D, Koster B et al (2010) The sedimentary inventory of tsunamis along the southern Gulf of Cadiz (southwestern Spain). Z Geomorphol 54 (3):147–173

Rodríguez Polo S, Gracia FJ, Benavente J et al (2009) Geometry and recent evolution of the Holocene beach ridges of the Valdelagrana littoral spit (Cadiz Bay, SW Spain). J Coast Res SI 56:20–23

Rodríguez-Ramírez A, Pérez-Asensio JN, Santos A et al (2015) Atlantic extreme wave events during the last four millennia in the Guadalquivir estuary, SW Spain. Quatern Res 83:24–40

Rodríguez-Ramírez A, Rodríguez-Vidal J, Cáceres LM et al (1996) Recent coastal evolution of the Doñana national park (SW Spain). Quatern Sci Rev 15:803–809

Rodríguez-Ramírez A, Ruiz F, Cáceres LM et al (2003) Analysis of the recent storm record in the southwestern Spanish coast: implications for littoral management. Sci Total Environ 303(3):189–201

Rodríguez-Ramírez A, Villarías-Robles J, Pérez-Asensio J et al (2016) Geomorphological record of extreme wave events during Roman times in the Guadalquivir estuary (Gulf of Cadiz, SW Spain): an archaeological and paleogeographical approach. Geomorphology 261:103–118

Rodríguez-Ramírez A, Yáñez CM (2008) Formation of chenier plain of the Doñana marshland (SW Spain): observations and geomorphic model. Mar Geol 254:187–196

Rodríguez-Vidal J (1987) Modelo de evolución geomorfológica de la flecha litoral de Punta Umbría, Huelva, España. Cuaternario y Geomorfología 1:247–256

Rodríguez-Vidal J, Ruiz F, Cáceres LM et al (2010) Holocene tsunami record in the Gulf of Cadiz. In:

Lamolda MA et al (eds) Geoevents, geological heritage and the role of the IGCP. European Regional Meeting of the IGCP, Caravaca de la Cruz, pp 178–179

Rodríguez-Vidal J, Ruiz F, Cáceres LM et al (2011) Geomarkers of the 218–209 BC Atlantic tsunami in the Roman Lacus Ligustinus (SW Spain): a palaeogeographical approach. Quatern Int 242:201–212

Rodríguez-Vidal J, Bardají T, Zazo C et al (2014) Coastal dunes and marshes in Doñana National Park. In: Gutiérrez F, Gutiérrez M (eds) Landscapes and landforms of Spain. Springer, Dordrecht, pp 229–238

Ruiz E, Borrego J, López-González N et al (2007) The geological record of a mid-Holocene marine storm in southwestern Spain. Geobios 40:689–699

Ruiz F, Rodriguez-Ramirez A, Cáceres LM et al (2004) Late Holocene evolution of the southwestern Doñana Nacional Park (Guadalquivir estuary, SW Spain): a multivariate approach. Palaeogeogr Palaeoclimatol Palaeoecol 204:47–64

Ruiz F, Rodríguez-Ramírez A, Cáceres LM et al (2005) Evidence of high energy events in the geological records: mid-Holocene evolution of the southwestern Doñana National Park (SW Spain). Palaeogeogr Palaeoclimatol Palaeoecol 229:212–229

Ruiz F, Abad M, Rodríguez-Vidal J et al (2008) The geological record of the oldest historical tsunamis in Southwestern Spain. Rivista Italiana di Paleontologia e Stratigrafia 114(1):145–154

Ruiz F, Rodríguez-Vidal J, Abad M et al (2013) Sedimentological and geomorphological imprints of Holocene tsunamis in southwestern Spain: an approach to establish the recurrence period. Geomorphology 203:97–104

Ruiz Gil JA, Giles F, López Amador JJ et al (1999) Geoarqueología en la desembocadura del río Guadalete. Aportaciones cronoestratigráficas en la ciudad de El Puerto de Santa María. Revista de Historia de El Puerto 23:11–29

Salas J (2003) Los interlocutores y temas tratados en la correspondencia. Universidad de Málaga, Málaga, El museo cordobés de Pedro Leonardo de Villacevallos

Schneider H, Höfer D, Trog C et al (2010) Holocene estuary development in the Algarve Region (Southern Portugal)—a reconstruction of sedimentological and evolution. Quatern Int 221:141–158

Silva PG, Bardají T, Roquero E et al (2015) Seismic palaeogeography of coastal zones in the Iberian Peninsula: understanding ancient and historic earthquakes in Spain. Cuaternario y Geomorfología 29(1–2):31–56

Soares AM (2015) Datación radiocarbónica de conchas marinas en el golfo de Cádiz: El efecto reservorio marino, su variabilidad durante el Holoceno e inferencias paleoambientales. Cuaternario y Geomorfología 29(1–2):19–29

Vidal N, Campos JM (2008) Relaciones costa-interior en el territorio onubense en época romana. Mainake 30:271–287

Vijande E, Domínguez-Bella S, Duarte J et al (2015) Social inequalities in the Neolithic of southern Europe: the grave goods of the Campo de Hockey necropolis (San Fernando, Cadiz, Spain). CR Palevol 14:147–161

Vizcaíno A, Gràcia E, Pallás R et al (2006) Sedimentology, physical properties and ages of mass-transport deposits associated to the Marqués de Pombal Fault, Southwest Portuguese Margin. Norvegian J Geol 86:177–186

Wagner CG (1983) Aproximación al proceso histórico de Tartessos. Arch Esp Arqueol 56:3–36

Whelan F, Kelletat D (2005) Boulder deposits on the Southern Spanish Atlantic coast: possible evidence for the 1755 AD Lisbon Tsunami? Sci Tsunami Hazards 23:25–38

Zazo C (2006) Cambio climático y nivel del mar: la Península Ibérica en el contexto global. Cuaternario y Geomorfología 20(3–4):115–130

Zazo C, Goy JL, Somoza L et al (1994) Holocene sequence of sea-level fluctuations in relation to climatic trends in the Atlantic-Mediterranean linkage coast. J Coast Res 10(4):933–945

Zazo C, Goy JL, Lario J et al (1996) Littoral zone and rapid climatic changes during the last 20.000 years. The Iberian study case. Z Geomorphol 102:119–134

Zazo C, Dabrio CJ, Goy JL et al (2008) The coastal archives of the last 15 ka in the Atlantic-Mediterranean Spanish linkage area: sea level and climate changes. Quatern Int 181:72–87

Part III

Historical Tsunamis, Paleotsunamis and Paleoearthquakes in the Iberian Peninsula: Case Studies

8 Archaeological and Geophysical Evidence of a High-Energy Marine Event at the Phoenician Site of Cerro del Villar (Malaga, Spain)

Manuel Álvarez-Martí-Aguilar, José Suárez-Padilla, Mª Eugenia Aubet, Francisco Machuca Prieto, Juan Manuel Martín-Casado, Lisa Feist, Cristina Val-Peón, and Klaus Reicherter

Abstract

The Mediterranean coast of Spain, much of which is built-up and densely populated, is today a tourist hot spot. Additionally, there are vital infrastructures, including airports, harbours and industrial facilities along its coastal motorways. In comparison with the western and southern Atlantic coastlines, the region is relatively protected from storms, while earthquake-related inundations, namely, tsunamis, are also rare. The very imprecise historical and sedimentary record of a tsunami in 1522 near Almeria bear this out. However, new evidence is provided here for the oldest extreme wave event (EWE) affecting human settlements on the Iberian Peninsula. The Phoenician site of Cerro del Villar, located near the Andalusian city of Malaga, in the estuary of the river Guadalhorce, suffered two episodes of destructive flooding at the beginning and at the end of the seventh century BC. In this paper, the initial interpretation of the former as a fluvial flood is recovered, while the latter is reinterpreted as an extreme wave event of a possible tsunami.

Keywords

Cerro del Villar · Phoenician · Spain · Extreme wave event (EWE) · Tsunami · Geoarchaeology

8.1 Introduction

Between the second quarter and the mid-eighth century BC, a Phoenician colony was established at Cerro del Villar on a former islet located in the

M. Álvarez-Martí-Aguilar (✉) · J. Suárez-Padilla · F. Machuca Prieto · J. M. Martín-Casado
Department of Historical Sciences, University of Malaga, Campus de Teatinos s/n. 29071, Malaga, Spain
e-mail: m_alvarez@uma.es

J. Suárez-Padilla
e-mail: josesuarez@uma.es

F. Machuca Prieto
e-mail: machucaprieto@uma.es

J. M. Martín-Casado
e-mail: JuanMMCasado@uma.es

M. E. Aubet
Departament d'Humanitats - Institut Universitari d'Història Jaume Vicens Vives, Laboratorio de Arqueología – LARQ, Universidat Pompeu Fabra, Barcelona, Spain
e-mail: eugenia.aubet@upf.edu

L. Feist · C. Val-Peón · K. Reicherter
Neotectonics and Natural Hazards, Dept. of Geosciences and Geography, RWTH Aachen University, Aachen, Germany
e-mail: l.feist@nug.rwth-aachen.de

C. Val-Peón
e-mail: c.val-peon@nug.rwth-aachen.de

K. Reicherter
e-mail: k.reicherter@nug.rwth-aachen.de

M. Álvarez-Martí-Aguilar and F. Machuca Prieto (eds.), *Historical Earthquakes, Tsunamis and Archaeology in the Iberian Peninsula*, Natural Science in Archaeology,
https://doi.org/10.1007/978-981-19-1979-4_8

Fig. 8.1 Location of the Bay of Malaga (Google Earth) and the main place names cited in the text

wide mouth of the river Guadalhorce (Malaga). The islet has since disappeared, now forming part of the alluvial plain of the lower Guadalhorce, located about 1000 m from the present-day Mediterranean coastline (Fig. 8.1).

The settlement, whose original Phoenician name is unknown, occupied a strategic position in the centre of the bay of Malaga, sheltered from the prevailing winds and currents, thus making it an ideal port. Furthermore, the islet dominated the approaches to the Guadalhorce valley and the Ronda highlands, both rich in agricultural and livestock resources, thus making it one of the main terrestrial communication routes to the Guadalquivir valley, namely, Tartessos.

At some point towards the end of the eighth century BC or during the first quarter of the following one, the settlement suffered an episode of violent destruction provoked by a flood event which was initially interpreted as having a fluvial origin and, subsequently, as having a marine origin (Aubet 1989; Aubet 1999b). Thenceforth, a major reorganisation of the population of the Bay of Malaga can be observed. From the mid-seventh century BC, *Malaka*, located on the left bank of the river Guadalmedina, became the main Phoenician settlement in this coastal territory, with Cerro del Villar apparently playing a secondary role as a production centre where pottery was manufactured, among other things. At the end of the seventh century BC, the settlement yet again suffered a violent flood, which in this chapter is tentatively interpreted as the result of an extreme wave event (hereinafter EWE).

This chapter provides evidences for the catastrophic events documented at Cerro del Villar, based on the results of different geoarchaeological and geophysical surveys performed at the site in recent decades.

8.2 Palaeogeographical Description

Located on the northern shore of the Alboran Sea, the bay of Malaga is shaped like a large amphitheatre, in the centre of which there is a wide alluvial plain bounded by two rivers, the Guadalhorce and the Guadalmedina and surrounded by the Malaga highlands to the east, the

Cártama highlands to the north and the Llana and Mijas mountain ranges to the west. Since pre-Roman times, the course of the river Guadalhorce was an important land route that connected the Mediterranean coast with the hinterland of the Ronda highlands, the Antequera region and, further to the west, the fertile lowlands of the Guadalquivir. This territory possessed agricultural and forestry resources and even some argentiferous lead and copper carbonate mines located in the nearby foothills (Aubet 1999a; García Alfonso 1999).

At the beginning of the first millennium BC, the mouth of the river Guadalhorce (Fig. 8.2) was a navigable estuary bordered by a series of open coastal spits, with sand-silt river bars in their interior, which were surrounded by riverbeds, marshes, and deltaic lagoons (Carmona 1999; Burjachs and Ros 1999; Aubet and Delgado 2003). It is in this coastal area of the province of Malaga, and in Huelva (González de Canales et al. 2004), where the first Phoenician presence in the Iberian Peninsula, dating to the mid-ninth century BC, has been documented. It was a sanctuary built on one of the islets located in the Guadalhorce estuary, known as La Rebanadilla, a site currently occupied by Malaga Airport (Arancibia et al. 2011; Arancibia and Fernández 2012; Sánchez et al. 2018; Suárez-Padilla et al. 2021). This place shows evidence of having been a meeting place for the settlers and the local population, who had also established themselves there and, around the same time, in a place known as San Pablo, located on the right bank of the nearby estuary of the river Guadalmedina (Suárez-Padilla et al. 2020, pp. 69–70). As a consequence of a significant territorial reorganisation, a new Phoenician settlement known as Cerro del Villar was created on another islet, located 1 km south of La Rebanadilla, during the second quarter of the eighth century BC (Fig. 8.2).

Palaeotopographical studies, reinforced by the results of recent geophysical surveys, indicate that the settlement was established on a gentle promontory located on an islet with a noticeably ellipsoidal shape. Its physiognomy is still recognisable today from a height of 3.5 m upwards, with a maximum preserved elevation of 6 m above the present-day sea level (Fig. 8.2).

8.3 The Destruction Layers of the Settlement (First Quarter of the Seventh Century BC and Last Quarter of the Seventh Century BC)

Following its discovery in 1965, several stratigraphic surveys were performed on Cerro del Villar in 1966–67 (Arribas and Arteaga 1975) and, later on, the site was systematically excavated from 1987 to 1999 (Aubet et al. 1999; Aubet 2018). The most recent excavations have revealed the characteristic features of the settlement in its most archaic phases during the eighth and seventh centuries BC, the most outstanding of which being its dimensions (with an inhabited area of about 80.000 m^2), the density and size of its buildings and domestic structures, and the regularity of its urban planning, documented in Sectors 2, 6, and 8 (Fig. 8.3).

It is worth mentioning two features characterising the socio-economic history of the settlement since its founding in the eighth century BC:

(1) Its role as a regional market and port of transit for agricultural products, cultivated in the immediate hinterland and destined for the export market. The colony dominated a hinterland that produced a significant volume of cereals (64%), legumes (20%), grapes and olives (16%) on land—probably worked by the indigenous population—in the lower and middle course of the river Guadalhorce at an estimated distance of up to 18 km. It acted as a regional trading centre between the indigenous hinterland of the valley and, in all likelihood, other Phoenician colonies in the Western Mediterranean, such as Carthage. Its most important infrastructures included a commercial street that ran through the city centre at the end of the eighth century BC (Aubet 1997). It had houses and shops on both sides, where fish, almonds, wine, oil

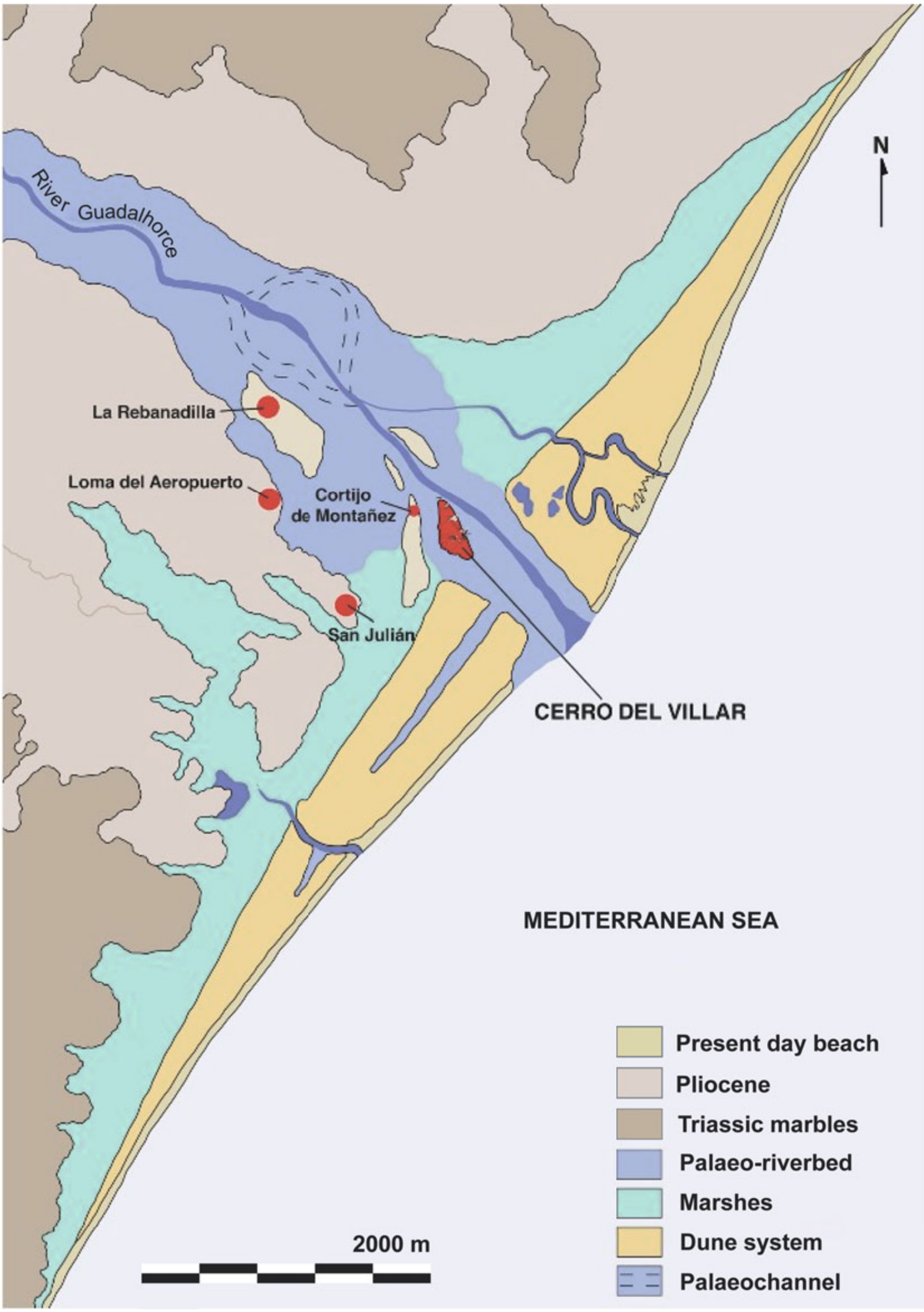

Fig. 8.2 Palaeogeographical reconstruction of the mouth of the river Guadalhorce (ca. 700 BC) and the location of the main archaeological sites mentioned in the text

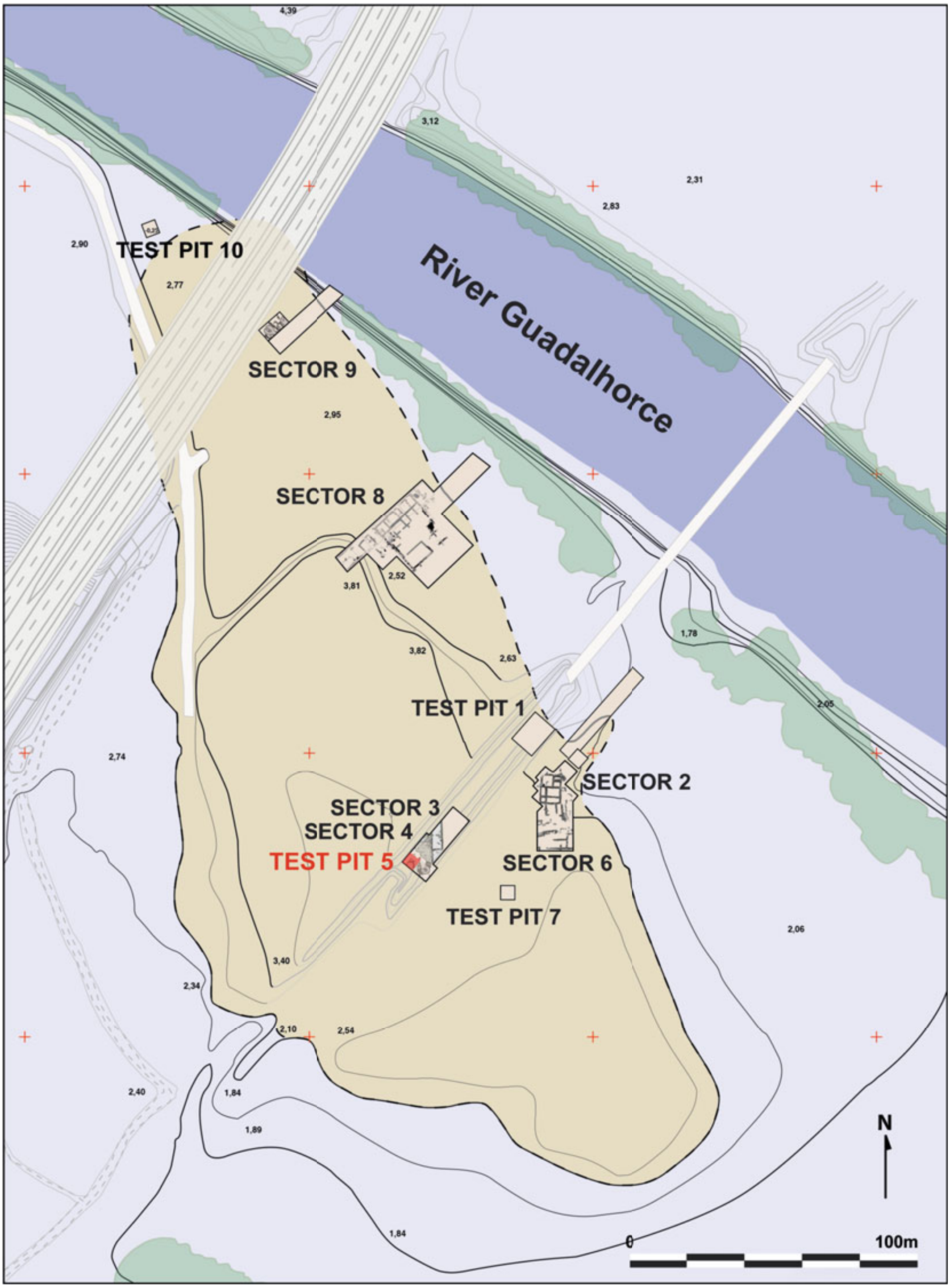

Fig. 8.3 Map showing the excavation sectors at the Phoenician site of Cerro del Villar

and cereals were displayed for sale, and metals were weighed in small blacksmiths and metal workshops.

(2) In terms of production volume, the second characteristic that defines the main functions of the Phoenician colony of Cerro del Villar is ceramic production. From the beginning, the good quality of the alluvial silt and clay outcrops around the river Guadalhorce favoured the development of an industrial activity revolving around pottery workshops located on the periphery of the colony, documented in Sector 9 (Fig. 8.3).

At the beginning of the seventh century BC, the settlement suffered a major destructive episode which in this chapter is interpreted as a fluvial flood, as initially proposed by Aubet (1989, p. 381). In the wake of the event, the site recuperated its activity focusing on intensive ceramic production revolving around the manufacture of containers and transport amphorae. This may have favoured significant changes in the environment, judging by the decline of the forest cover in the valley from the mid-seventh century BC onwards, probably due to the intensive use of wood as building material and fuel for pottery kilns and blacksmiths. Thus, the economic activity of the settlement may have partially contributed to the degradation of the immediate environment and the gradual silting of the estuary. By the end of the seventh century BC, the islet was on the verge of disappearing, surrounded by marshes and riverbeds in the midst of an inhospitable and highly vulnerable landscape. At that time, the islet suffered a new flood, which is tentatively interpreted here as an EWE.

8.3.1 Test Pit 5: The Archaeological Levels

In 1989, a test pit known as test pit 5 ("Corte 5") (Fig. 8.3) was opened in the highest part of the former islet, the only area preserving a section of the original promontory elevation at a maximum height of 6.49 m above sea level. The survey was carried out in one of the most densely populated areas of the colony (Aubet 1999b, p. 73 ff.). After several extensive excavations, the aim of this survey was to verify the vertical sequence of the site near the centre of the islet-promontory of Cerro del Villar and to establish a complete pollen and sedimentological column in order to analyse the characteristics and evolution of the environment during the Phoenician period.

The test pit, with a surface area of 3 × 3 m, reached a depth of almost 5 m, where the oldest archaeological levels appeared on top of sterile soil formed by alluvial silt and clay. Ten superimposed occupation levels were identified (S-I to S-X; Fig. 8.4), and a substantial record of archaeological materials and samples were extracted for soil, anthracological, and pollen analyses. The first Phoenician occupation level of the site, dated to the second quarter of the eighth century BC, was reached for the first time in test pit 5.

Stratum X is the oldest occupation level of Cerro del Villar in the test pit 5 area. It has an average thickness of 0.17 m and is composed of reddish-brown clays. The stratum, with few ceramic finds, sits on yellowish clay soil, which is directly superimposed on the sterile subsoil of the ancient fluvial islet.

Stratum IX is a thin (0.07–0.15 m) fluvial sedimentation level, composed of soft grey-brown clays, coarse sands and gravels, which yielded little pottery. The sediments accumulated on top of a yellowish ochre-coloured clay pavement.

Stratum VIII, with an average thickness of 0.16 m, is composed of light grey, very soft and sandy clayey soils, accumulated on top of a blackish burnt clay pavement. There are a large number of traces of combustion and charred wood associated with two circular ovens built directly on the pavement and formed by a ring-shaped wall of reddish-coloured adobe.

With a thickness of around 0.30 m, stratum VII consists of a stratum of clays, whose dark black-brown colour is due to the large quantity of coals and remains of combustion that it contains. It is a stratum associated with combustion structures or ovens, which continue the tradition

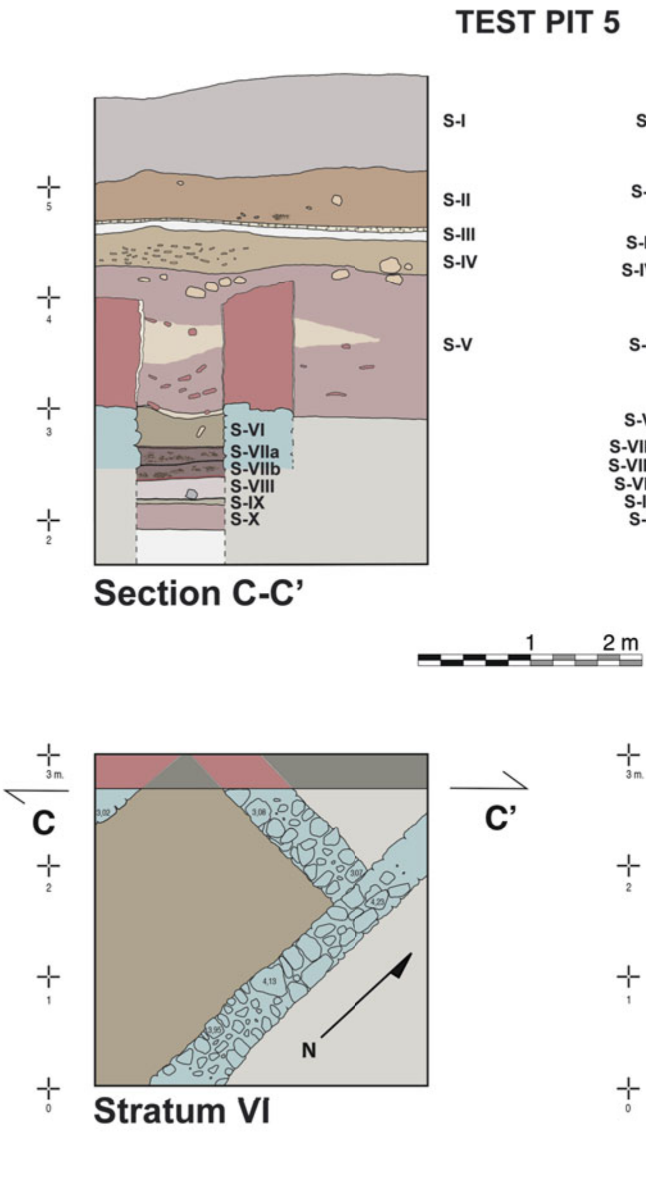

Fig. 8.4 Stratigraphic section of the site (test pit 5) showing strata V (S-V) and IV (S-IV)

of use documented in stratum VIII. In this case, its use is related to two moments clearly differentiated by a pavement, which is why the stratum was subdivided into two superimposed sublevels: stratum VIIa (0.15–0.25 m) and stratum VIIb (0.15 m).

Stratum VI is composed of dark brown clays with a maximum thickness of 0.35 m. The sedimentation of the stratum accumulated on top of a very fine, caked, dark red clay pavement, while there is a thin layer of sand between the beaten clay soil and the pebble base.

In the test pit 5 excavation, stratum V represents a change in the sedimentation (S-V; Fig. 8.4). It consists of a remarkably thick stratum composed of dark brown clayey soils, mixed with some limestones, small ore pockets and white or yellowish marls of alluvial origin. The thickest stratum in the test pit (1.15–1.30 m), it evinces rapid sedimentation, caused by a devastating, large-scale inundation that affected the remains of a rectangular-shaped house (Aubet 1999b, pp. 81–83).

The destruction observed in stratum V is confirmed by the arrangement of the abundant and practically intact pieces of pottery at the base, which appeared under plentiful rubble and fallen stones on a very hard pavement of reddish-coloured rammed clay at a height of 3 m above sea level (Fig. 8.5b). A very thin layer of sand that dips slightly to the south was documented on that pavement (Aubet 1999b, p. 82).

The base level of stratum V and the infills deposited over it left several architectural structures intact, such as the remains of two stone walls or plinths delimiting a rectangular room about 2.20 m wide. These served as the foundation for two 1 m-high rammed earth walls of dark brown clay, whose profile is preserved intact in the northern and western sections of the test pit (Figs. 8.4 and 8.5).

The mud-brick walls retain a yellowish clay plaster, in some sections of which it is still possible to glimpse the shape of the ancient adobes (Fig. 8.5b). They are probably remains of a dwelling or storehouse, judging by the large number of amphorae—both of Phoenician and Greek provenance—cooking pots (containing burnt fish remains) and tripods, which were preserved by the collapses.

The remains of an exceedingly unique piece were found in the upper part of stratum V (Fig. 8.5a): an amphora of Greek manufacture (Fig. 8.6a, b) which is a variant or imitation of Attic SOS amphorae, with a pyriform body covered with a very diluted brownish-blackish

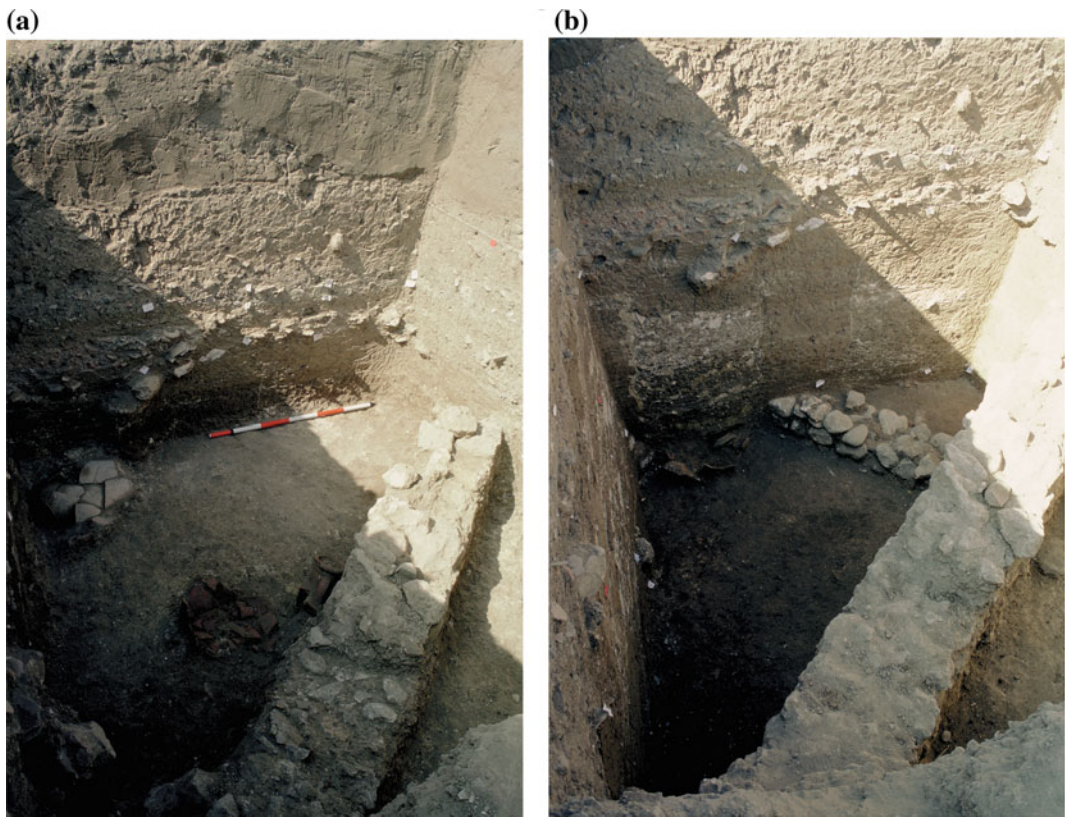

Fig. 8.5 Detail of stratum V from test pit 5. **a** Upper part of the stratum with the remains of the SOS-type Attic amphora (ca. 700 BC). **b** Base level of the stratum with a red clay pavement and remains of ceramic vessels

varnish on the neck and reddish-brown on the rest of the body (Vegas 1999). The composition of the clay, with abundant mica and limestone particles, points to an Euboean or Eastern Greek origin. The impression of an Egyptian seal—the Horus falcon—on one of the handles, under which a T-shaped graffito is preserved, is a strikingly unique feature. The amphora has been dated to between 700 BC and the first years of the seventh century BC, which provides a chronology consistent with that of the Phoenician ceramics from stratum V and, consequently, suggests a *terminus post quem* as a reference date for the destruction layer (i.e. stratum V).

Stratum IV, with an average thickness of 0.40 m, is composed of very loose, light brown sands and clays (S-IV; Fig. 8.4). It is a thick and irregular layer, with a large amount of microfaunal and ceramic remains that slopes steeply downwards to the south and that is formed on a light yellowish rammed clay pavement. This shows a rapid and powerful deposition, which was interpreted as a new energetic episode of flooding (Aubet 1999b, p. 81).

In this level some significant changes in the morphology, manufacture and uses of the Western Phoenician ceramics from Cerro del Villar can already be observed, with an increase in painted and grey pottery. The greater number of amphorae and items associated with ceramic production, such as prisms and slag, reflect a progressive specialisation of the colony's industrial activities in the central part of the islet, where dwellings and domestic structures had hitherto prevailed, mainly involving manufactured and agricultural products, which necessarily required the islet's reorganisation. The pottery from stratum IV places this transitional horizon in the last quarter of the seventh century BC (Aubet 1999c, pp. 45–46). Changes in the material culture point to the existence of a brief hiatus or abandonment of this part of the islet

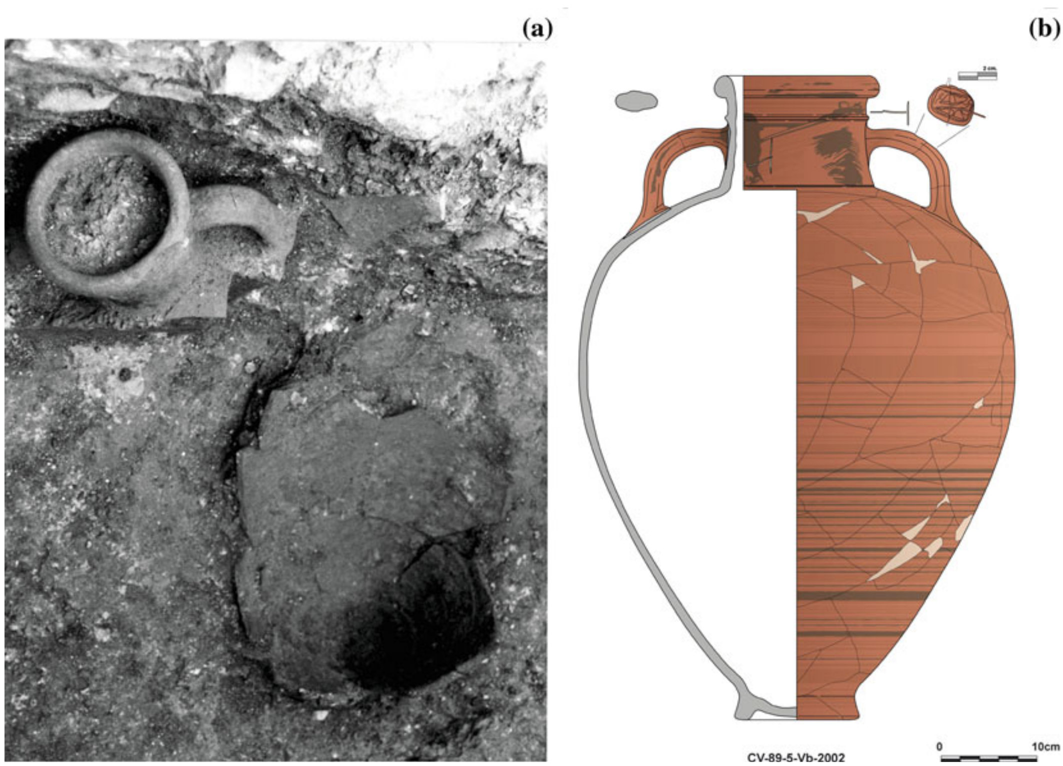

Fig. 8.6 **a** Remains of the Greek SOS-type amphora found in the stratum V in test pit 5. **b** Reconstruction of the amphora

between the second and third quarter of the seventh century BC, that is, subsequent to the destruction layer of stratum V.

In any case, the transformation of the centre of the islet into an industrial area culminated in about 600–570 BC (strata III-II), with the emergence of pottery workshops specialising in the manufacture of amphorae and large containers (Sector 3/4; Fig. 8.3), whose activity is dated by Eastern Greek and Etruscan imports (Aubet 2007). The transformation of Cerro del Villar into an industrial area dependent on the neighbouring Phoenician settlement of *Malaka* coincides with the abandonment of the islet's dwellings, warehouses and commercial street. The sediment analysis of this period reflects a clear evolution towards a landscape of stagnant waters and the disappearance of the islet as a consequence of the alluvial filling and seaward progression of the estuarine/deltaic area.

8.3.2 Test Pit 5: The Geological Strata

After defining the sequence of the archaeological levels in test pit 5 in 1989, in the 1991 campaign the test pit was reopened for a complete edaphological study by E. Villate and M. Millán, which also included the analysis of plant remains, fossil pollen and anthracological and microfaunal remains (Millán et al. 1999).

Villate and Millán identified 17 geological strata, compared to the 10 previously defined archaeological levels, each of which was formed by different geological layers of sedimentation, which is particularly evident in stratum V, the flood layer. The correspondence between the archaeological strata (in Roman numerals) and geological strata (in Arabic numerals) was recorded by Aubet (1999b) in a sketch (Fig. 8.7).

The sedimentological analysis performed by Villate and Millán included the sedimentary distribution of the fine and coarse fraction for each stratum, among other aspects. Archaeological stratum V consisted of four geological strata: 10, 11, 12 and 13 (Fig. 8.7).

With a thickness of between 10 and 50 cm, stratum 10 was described as one of sands with

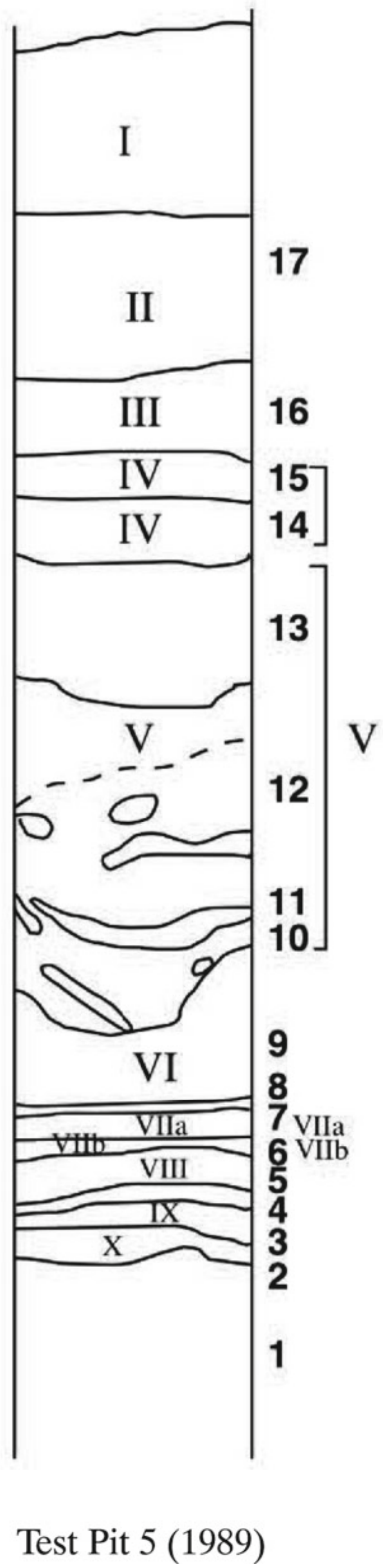

◀ **Fig. 8.7** Diagram showing the correspondence between the archaeological (in Roman numerals) and geological (in Arabic numerals) strata of test pit 5 ("Corte 5") (Modified from Aubet (1999b) Fig. 31)

red clay bands and displaced archaeological materials. It was interpreted by Millán et al. (1999, p. 11) as a "clear sweep" and attributed to a fast inundation event. The analysis of the fine fraction distribution highlighted the high percentage of coarse sands, which accounted for 70% of the sediment in the stratum. The stratum was interpreted as the result of a tsunami ("maremoto") or a very powerful tidal surge ("agitada marea de grandes proporciones") (Millán et al. 1999, p. 11). However, evidence of foraminifera and other marine biogenic components was not proven.

Stratum 11, with a thickness of about 8 cm, had a light yellow clayey-sandy texture. In the opinion of Millán et al. (1999, p. 12), it was linked to stratum 10 and showed a predominance of "marine features". The analysis of the fine fraction distribution led the authors to consider that the stratum was a consequence of a quiet sedimentation of the swept sediment in stratum 10. The stratum was dominated by coarse sands, with modest percentages of fine sands and clays, and few silts. As for the coarse fraction, the percentage of gravels (4.72%) indicated the transition to a normalisation represented by the next stratum (Millán et al. 1999, p. 22). Here also, no evidence for marine origin was proven.

With a thickness of around 70 cm, stratum 12 was composed of light grey sandy clay with loams and limestone. An analysis of the fine fraction distribution revealed a predominance of fine sands, with the authors identifying a gradation characteristic of suspension sorting, whereas silts and clays were more abundant. According to the authors, stratum 12 marked a new evolutionary stage defined by the predominance of fine sands over coarse sands (Millán et al. 1999, p. 12). As regards the coarse fraction, stratum 12 contained the gravel percentages of the middle band (9.95%). The grey colour of the stratum was attributed to the abundant clay of either a fluvial or marine origin, at a time of combined marine-fluvial action, although with a predominance of fluvial traction (Millán et al. 1999, p. 33). This interpretation, together with the vague marine origin and lack of evidence, leads us to interpret the entire stratum V as terrigenous flood deposits, and due to the large amount of sediment, this event was most probably catastrophic.

Stratum 13, with a thickness of about 40 cm, was composed of light yellowish-brown sandy clay. An analysis of the fine fraction revealed an intensification of the characteristics of the previous stratum, with a predominance of fine sands as opposed to a dearth of coarse sands. Silts and clays were also scarce. With respect to the coarse fraction, the stratum showed an intense decrease in the percentage of gravels, which almost disappeared. This was considered to indicate new rapid sweeping actions (Millán et al. 1999, p. 22).

Geological strata 14 and 15 corresponded to archaeological stratum IV. Stratum 14 had a sandy-clayey texture and a light brown colour, with archaeological remains and pebbles. The predominance of fine sands of the immediately preceding strata was maintained, while the coarse sands were once again significant. The histogram showed a double staggering in the sands, as in stratum 12. Silty-clays were scarce, as in the previous stratum. The percentage of gravels increased and approached the middle band (7.66%). Overall, the stratum was considered to reflect a return to equilibrium conditions (Millán et al. 1999, p. 22).

Stratum 15, about 10 cm thick, had a yellowish-brown sandy-clayey texture, with ceramic remains and remains of ovens. Very coarse sands were abundant, and it was interpreted as fluvial deposition on top of the alternating fluvial and marine conditions. Sands were abundant, both coarse and fine, and showed an inverse gradient, increasing the coarser and decreasing the finest. In the coarse fraction, there was a high abundance of gravels (39.45%). This led to interpret the stratum as the result of a rapid sedimentation, a flood with "catastrophic overtones" (Millán et al. 1999, p. 22).

At the time when Millán et al. (1999) performed their study, little was known of the sedimentological characteristics of high-energy marine deposits produced by tsunamis or storm surges in archaeological research contexts. Following the exponential increase in studies of high-energy marine deposits in the last few decades, two aspects should be highlighted. The multi-layered structure (geological strata 10–13) of archaeological stratum V is remarkable. These strata show features typical for alluvial flood deposits as the coarse-grained gravelly layers are rare.

The geological strata 14 and 15 of stratum IV comprise at the base coarsening upward and topwards fining-up layers with erosive base containing many ceramic rests of pottery, marine shells, bones, slag, fluvial gravels and charcoal. Again, the strata are multi-layered and partly channelled with basal scours. These layers document a remarkable change in the sedimentological system and may tentatively be associated with a marine high-energy event.

8.4 The Geological Field Campaign of 2019

In this section, the first results of a short field campaign (University of Malaga and RWTH Aachen University), carried out at the western end of the Guadalhorce palaeoestuary in October 2019, outside the boundaries of the archaeological site of Cerro del Villar, are presented. Two sediment cores (MAL-CV-1, ca. 3.70 m in length, and MAL-CV-2, ca. 4.69 m in length) were drilled southwest of the Phoenician site. A total of eight non-invasive ground-penetrating radar (hereinafter GPR) profiles were carried out in the surroundings of the cores, plus additional ones close to the beach so as to gain a better understanding of the changes in the depositional environment along the coast.

8.4.1 Methods

During fieldwork in October 2019, two sediment cores were drilled outside the boundaries of the Cerro del Villar Phoenician site, to the southwest, in the Guadalhorce palaeoestuary (Malaga, southern Spain) (Table 8.1). Both cores were drilled ca. 20 m apart with a petrol-driven Cobra drilling device (Atlas Copco, Rock Hill, SC, USA). For both cores, window sampling steel tubes with inner diameters of 60 mm (MAL-CV-1 0–2 m; MAL-CV-2 0–3 m) and 50 mm (MAL-CV-1 2–3.7 m; MAL-CV-2 3–4.69 m) were used for visual core descriptions and on-site sampling. All the samples were collected in plastic bags and stored in a refrigerator at ca. 4 °C. Visual core descriptions were conducted on both cores to identify the sediment units and their depositional environments. Characteristics such as grain size, sedimentary structures, the colour of the sediment (according to the 2009 revised washable edition of the Munsell Rock Color Chart), plant remains, shells and ceramic fragments were described, while a preliminary stratigraphic classification was also performed.

In preparation for grain size measurements, eight samples from each core were dried at 40 °C for a minimum of 24 h, before being homogenised using a mortar and sieved to <2 mm. The samples were pre-treated with hydrogen peroxide (H_2O_2, 15%) to remove organic matter and with sodium pyrophosphate ($Na_4P_2O_7$, 46 g/l) to avoid coagulation (Gee and Or 2002). Both cores were measured according to Schulte

Table 8.1 Drilling locations with core label, GPS coordinates, drilled depth and recovery

Core	GPS coordinates		Drilled depth (m)	Recovery (m)
	N	W		
MAL-CV-1	36° 40′ 12.651″	4° 27′ 54.882″	4.00	3.70
MAL-CV-2	36° 40′ 12.128’″	4° 27′ 54.436″	5.00	4.69

and Lehmkuhl (2018) with a laser diffraction particle size analyser (Beckman Coulter, Brea, CA, USA): core MAL-CV-1 at the Institute of Geography (University of Cologne), and core MAL-CV-2 at the Physical Geography and Geoecology Institute (RWTH Aachen University). Statistical calculations were performed based on Folk and Ward (1957) and employing GRADISTAT software version 8.0 (for unconsolidated sediments analysed by sieving or laser granulometry Kenneth Pye Associates Ltd., Crowthorne, UK; Blott and Pye 2001).

Two wood/charcoal samples from core MAL-CV-2 were radiocarbon dated at the Keck Carbon Cycle AMS Facility of the Earth System Science Department (University of California, Irvine). At the facility, the samples were treated with acid–base-acid (1 N HCl and 1 N NaOH, 75 °C) prior to combustion. Samples were calibrated with CALIB software version 8.2 (Stuiver and Reimer 1993; Stuiver et al. 2020) and the IntCal20 calibration dataset (Reimer et al. 2020).

In the immediate surroundings of the drilling sites, a total of eight non-invasive GPR profiles were carried out using the SIR 3000 instrument equipped with a 270 MHz antenna (GSSI Geophysical Survey Systems Inc., Nashua, NH, USA). Two of these profiles are presented here. Each profile was measured based on distance-mode, performed with a calibrated survey wheel, with a permittivity (ε) of 6. This relatively low ε was chosen based on dry soil conditions during the time of measurement. The collected data were processed at RWTH Aachen University using ReflexW software version 7.0 (Sandmeier geophysical research, Karlsruhe, Germany), including general and common processes and filters, such as move-start-time, background removal, remove-header-gain, energy-decay, average-xy-filter and band-pass Butterworth filter. A topographic correction was not necessary as the area is flat, and the GPR profiles were always taken in both directions, that is, doubled to avoid geophysical artefact reflections in the profiles caused by the concrete bridge and pillars in the area (Fig. 8.9 a). For further details regarding GPR processing and interpretation, see Frenken et al. (this volume) and Reicherter et al. (this volume).

8.4.2 Preliminary Results

8.4.2.1 Results from Cores MAL-CV-1 and MAL-CV-2

Core MAL-CV-1 recovered ca. 3.70 m of sediment, while core MAL-CV-2 recovered ca. 4.69 m of sediment (Table 8.1). Both cores present a similar stratigraphy comprised of three different sediment units: a basal sand unit A, followed by a large silt/clay unit B, plus another silt/clay unit C at the top. In core MAL-CV-1, units B and C are interrupted by two possible event units E2 and E1, respectively. Unit E2 is also present in core MAL-CV-2, but the upper unit E1 is replaced by an anthropogenic unit D, which may have concealed remains of a possible event unit E1 in this core. Detailed descriptions of both cores are given below and presented in Fig. 8.8.

Core MAL-CV-1

At the base, core MAL-CV-1 exhibits a dark grey medium sand unit from ca. 3.70 m b.s. (below surface) until 3.08 m b.s., which was washed out downcore by groundwater (unit A). Shell fragments are visible in this unit. The granulometric results indicate mean grain size values of 1–2 Φ.

The sand unit is topped by a thin dark organic-rich layer, followed by silt until ca. 1.89 m b.s. (unit B). Occasionally, calcium concretions, root fragments and other organic material are visible. The colour gradually changes upwards from medium dark grey to dark yellowish orange mixed with medium bluish grey and pale blue. Granulometric results reveal a mean grain size of 7.4 Φ for the silt unit.

Two dark grey medium sand layers are intercalated with the lower silt unit at 3.03–2.89 and 2.82–2.73 m b.s. (unit E2). The lower one displays an erosive basal contact with the

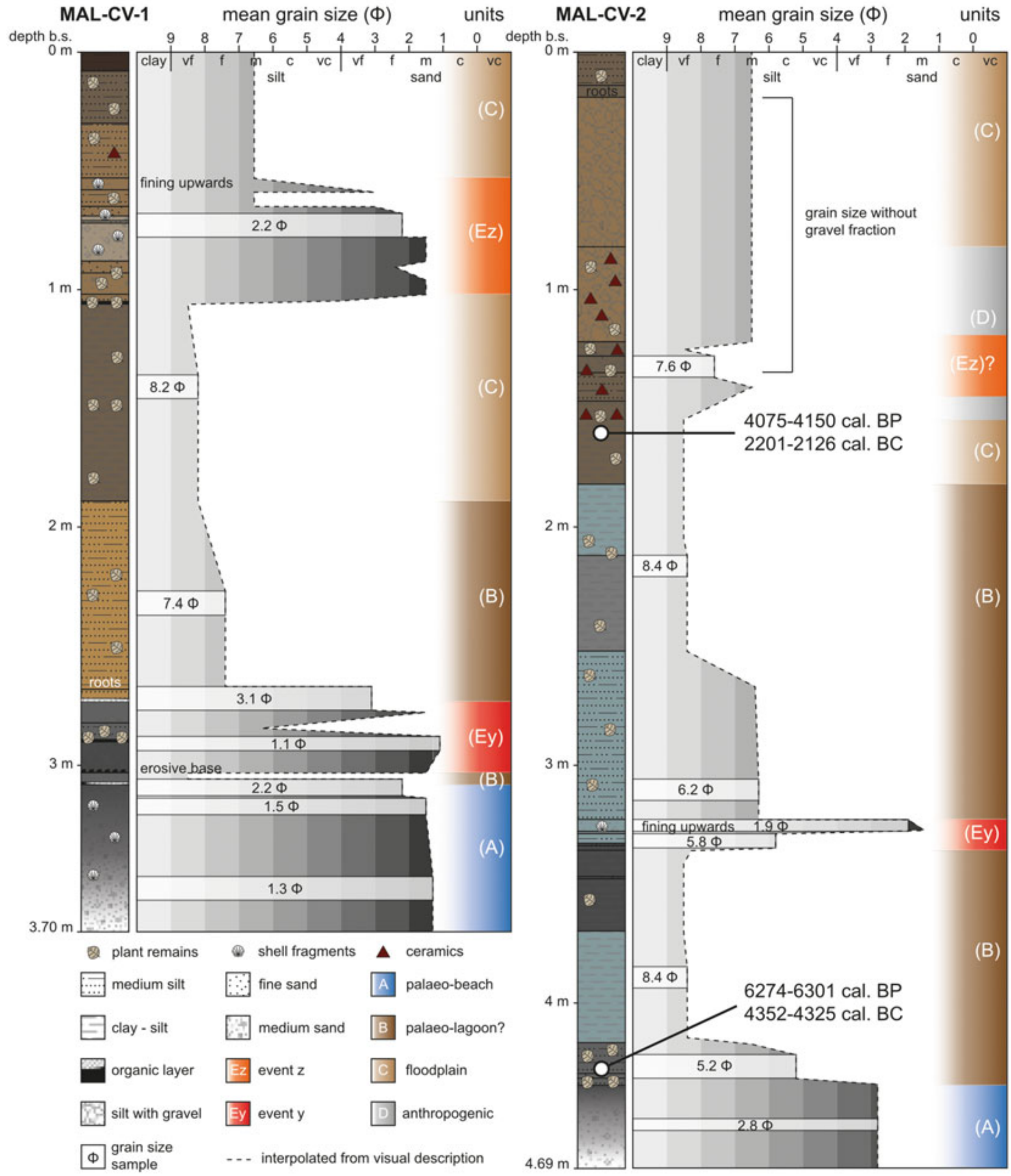

Fig. 8.8 Stratigraphic profiles and mean grain size (Φ) of cores MAL-CV-1 and MAL-CV-2, including two calibrated radiocarbon dates based on charcoal samples from core MAL-CV-2. b.s. below surface

underlying silt and is topped by a thin dark organic-rich layer. The upper one, which concludes at the end of a core section which conceals its basal contact, exhibits an irregular upper contact which is followed by many large root fragments. The granulometric results indicate a mean grain size of 1.1 Φ for the lower layer and 3.1 Φ for the upper contact of the upper layer.

The colour of the lower silt unit gradually changes to dark yellowish brown mixed with light olive grey (silty) clay and moderate dark yellowish, brown silt until the top (unit C). Some root fragments and organic material are visible. A piece of glass (1 cm) and a brick fragment (0.5 cm) are found at 0.55 and 0.54 m b.s., respectively. Towards the top, the sediment is very dry and less compact. Grain size slightly coarsens towards the top, and the mean grain size of a sample from the lower part of this unit is 8.2 Φ.

Several fine, medium and coarse sand layers are intercalated with the upper clay/silt unit at 1.02–0.65 and 0.58–0.53 m b.s. (unit E1). The layer at 1.02–0.72 m b.s. consists of moderate yellowish, brown medium sand mixed with a silt/clay matrix gradually changing upwards to pure medium sand, followed by fine sand that includes small roots and medium sand with shell fragments that coarsen towards the top. The lower contact to a thin silt layer is gradual, but a sharp contact to a black organic soil layer including many roots followed downcore. The upper contact is sharp, and a 1-cm-thin clay layer follows. The thin clay layer is topped with pale yellowish brown coarse sand and gravel, followed by fine sand with shell fragments at 0.71–0.65 m b.s. The mean grain size for these layers is 2.2 Φ. The upper contact to a silt layer mixed with roots is sharp. This is topped with another pale yellowish brown medium sand layer at 0.58–0.53 m b.s., which includes a few larger bioclasts (2 mm) and shell fragments and fines upwards. Both the contacts to the over- and underlying sediments are sharp.

Core MAL-CV-2

Similar to core MAL-CV-1, core MAL-CV-2 exhibits a dark grey medium sand unit at its base at ca. 4.69–4.34 m b.s. (unit A). Again, the lower part was washed out by groundwater. The granulometric results reveal a mean grain size of 2.8 Φ.

This unit is followed by a transition unit until ca. 4.16 m b.s., which consists of medium dark grey organic-rich silt intercalated with thin fine sand layers and lenses. Carbonate concretions are visible. The mean grain size of the transition unit is 5.2 Φ. The following medium (light) grey and pale blue clay and silt unit persists until 1.82 m b.s. (unit B). Organic material, bright brown carbonate concretions, iron and manganese staining are present throughout the unit. The mean grain size is 8.4 Φ in the lower part of this unit, becoming slightly larger in the middle part (6.2 Φ) before returning to 8.4 Φ in the upper part.

This clay and silt unit is interrupted by dark grey fine sand at 3.33–3.32 m b.s. and medium sand at 3.28–3.22 m b.s. (unit E2). The lower fine sand is intercalated with organic-rich silt and has a mean grain size of 5.8 Φ. The upper medium sand includes shell fragments and fined upwards with a mean grain size of 1.9 Φ.

The lower clay and silt unit is topped with light olive grey and dark yellowish brown clay until ca. 1.47 m b.s., and very dry and loose moderate yellowish brown gravel fragments in a silt matrix until the top, turning darker towards the top (unit C). There is an abundance of organic material and root fragments in this unit.

Different sized ceramic and brick fragments are present in this silt and gravel unit between 1.56–0.82 m b.s., forming an anthropogenically influenced unit (unit D). The silt matrix around the ceramic fragments and gravel has a mean grain size of 7.6 Φ.

Radiocarbon Ages of the Samples from Core MAL-CV-2

Two samples from core MAL-CV-2 were radiocarbon dated (Table 8.2). The wood/charcoal sample from 4.28–4.26 m b.s. is dated to 6284 cal. BP (6274–6301 cal. BP), for the transition between the lowermost sand unit A and the overlying clay and silt unit B. While the charcoal sample from 1.64–1.62 m b.s. is dated to 4092 cal. BP (4075–4150 cal. BP), for the clay unit C just below the anthropogenic unit D.

8.4.2.2 Results for the GPR Profiles

A total of eight GPR profiles were recorded to characterise the drill holes described above, two of which at an interpretable penetration depth of ca. 3.2 m—below which the groundwater table blurred the reflected signal—are described below. The groundwater table corresponds to the sea level of the nearby coast and, therefore, approximately the height of the drill sites above

Table 8.2 Radiocarbon ages of two wood/charcoal samples taken from core MAL-CV-2. The samples were dated at the Keck Carbon Cycle AMS Facility of the Earth System Science Department (University of California, Irvine) and calibrated using CALIB 8.2 software (Stuiver and Reimer 1993; Stuiver et al. 2020) and the IntCal20 (Reimer et al. 2020) dataset

Core	Lab code	Depth in core	Material	^{14}C age	Cal. ^{14}C age, 2σ and median cal. ^{14}C age	Cal. ^{14}C age, 2σ and median cal. ^{14}C age
MAL-CV-2	231,710	1.62–1.64 m	Charcoal	3735 ± 15 BP	4075–4150 cal. BP 4092 cal. BP	2201–2126 cal. BC 2143 cal. BC
MAL-CV-2	231,711	4.26–4.28 m	Wood/charcoal	5470 ± 15 BP	6274–6301 cal. BP 6284 cal. BP	4352–4325 cal. BC 4335 cal. BC

the present-day sea level. The quality of the radargrams is excellent, with almost no noise being recorded (Fig. 8.9b–e). For facilitating interpretations, the stratigraphic units were colour-coded (Fig. 8.8). Profile AAA085 ran ca. 9 m from NW towards SE. It is possible to trace the stratigraphic units of drill core MAL-CV-2 along the entire profile (Fig. 8.9c). There appears to be "noise" in the upper ca. 0.7 m, thus suggesting larger blocks or cobbles, possibly formed by anthropogenic modification and disturbances. Erosional features like unconformities, corresponding to the base of the alleged event layer E2, are detectable in part. Relatively horizontal layering is interpreted to mirror the lagoonal low-energy facies detected in the core. Below this and close to event layer E1, channelled and partly cross-bedded strata were identified, reflecting a high energy depositional environment.

With a length of ca. 28 m, the lithofacies of profile AAA081 (Fig. 8.9d, e) are almost comparable with those described in the shorter section. The simplified stratigraphy matches the core observation extremely well and provides evidence for two high-energy events (hereinafter HEEs) (E1 and E2) in the direct vicinity of the archaeological site of Cerro del Villar. The aforementioned unconformities associated with the erosional event are clearly evidenced by the channel structures and varying thickness of the individual layers. GPR proved to be a useful tool for extending the patchy drill core information to the wider area, strongly supplemented, of course, with ground truth drilling.

8.4.3 Preliminary Data Interpretation

The cores cover a stratigraphy of three different sediment units: a basal sand unit representing a palaeo-beach, followed by a large silt and clay unit developed in a lagoon environment, topped with another silt and clay unit representing floodplain conditions. At MAL-CV-1, two possible HEE units (E2 and E1) interrupt the low-energy silt and clay units. At MAL-CV-2, event unit E2 is also preserved, the other event unit E1 being concealed by an anthropogenic unit rich in ceramic, brick and glass fragments. The GPR profiles display the same stratigraphy and allow for a lateral continuation of the different units and event deposits. With the help of these GPR profiles, event unit E1 can be traced in between the anthropogenic unit of MAL-CV-2. In chronological terms, two radiocarbon dates establish the transition between the basal palaeo-beach and the lagoon at 4352–4325 cal. BC (6274–6301 cal. BP) and that the anthropogenic layer is younger than 2201–2126 cal. BC (4075–4150 cal. BP). The establishment of coastal freshwater lagoons with plentiful *Hydrobia* gastropods and ostracods resembles the last stage of

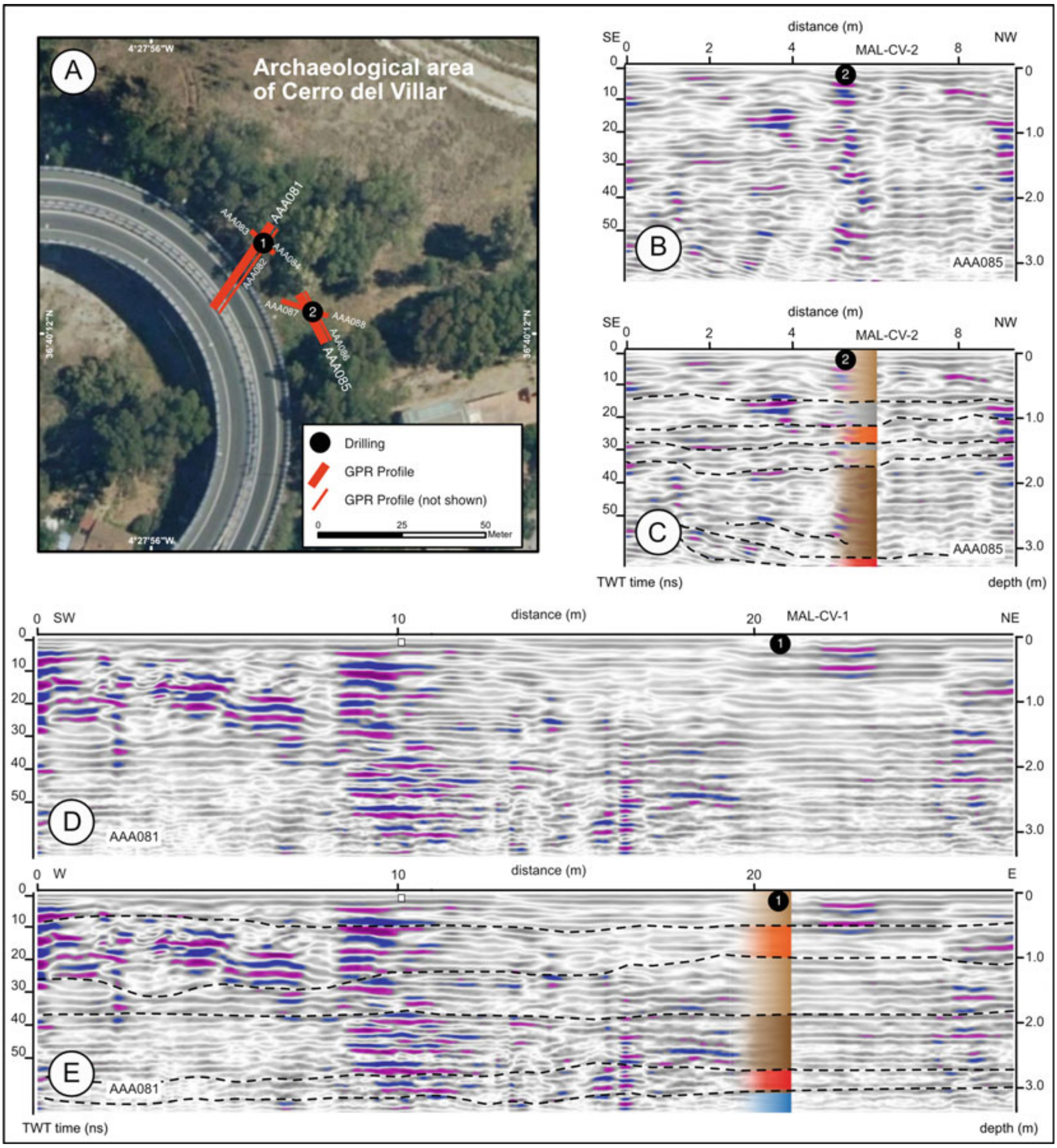

Fig. 8.9 **a** Location of GPR profiles taken outside the archaeological site of Cerro del Villar. **b** Radar line AAA085 crossing drill hole MAL-CV-2. **c** Interpretation of radar line AAA085, including the simplified stratigraphy of MAL-CV-2; stippled lines refer to units described in Fig. 8.8. **d** Radar line AAA081 crossing drill hole MAL-CV-1. **e** Interpretation of radar line AAA081, including the simplified stratigraphy of MAL-CV-1; stippled lines refer to units described in Fig. 8.8

the post-glacial sea level rise in the Mediterranean. In the future, these promising initial results will be extended by additional radiocarbon dates and a palynological study to gain a better understanding of the climate and palaeoenvironmental evolution.

8.5 Tsunamis on the Coast of Malaga

Evidence of the catastrophic high-energy marine event documented at the Cerro del Villar site around 625-600 BC raises the possibility that it was generated by a tsunami. Before assessing the possible tsunamigenic origin of the event, it is convenient to review the tsunamis that, according to the historiographical tradition and scientific literature, have been recorded on the coasts of the province of Malaga throughout the ages, before the period of instrumental records.

In seismic catalogues such as that of Soloviev et al. (2000, pp. 5, 29), it is stated that the 365 AD tsunami in the Eastern Mediterranean affected the coast of Malaga. This news is based on the interpolation that Miguel Lafuente made, in his *Historia de Granada* (Lafuente 1843), based on the description of the 365 AD tsunami by the Roman historian Ammianus Marcellinus (26.10.15–19). Udías (1983) showed that the text of Ammianus did not refer to Spain, thus ruling out the possibility that the 365 AD tsunami affected the Iberian Peninsula (Álvarez-Martí-Aguilar 2020, this volume). Nevertheless, this "false" event found its way into the seismic catalogues of the Iberian Peninsula and North Africa (Galbis 1932; 1940; Munuera 1963; Stahl 1971).

The archaeologist Pérez de Barradas claimed that the Palaeo-Christian basilica of Vega del Mar (San Pedro de Alcántara, Malaga), excavated between 1929 and 1930, suffered great damage between the fifth and sixth centuries AD. In light of the discovery of a layer of beach sand in the basilica and in some of the burials at the site, he linked its destruction to a tsunami ("maremoto"), dating it to 526 AD (Pérez de Barradas 1934, p. 42), without explaining how he had arrived at this conclusion. Since no tsunami is known to have occurred in the Mediterranean at that date (Guidoboni 1994), it seems that Pérez de Barradas was suggesting that the Antioch earthquake in 526 AD, for which there is no evidence that it caused a tsunami, affected the Western Mediterranean. Accordingly, there are still lingering doubts about the nature of this sand level at the Vega del Mar site, its possible EWE origin and its dating.

A high-energy marine deposit has recently been documented in the town of Estepona (Malaga), dated by archaeological materials to the last third of the ninth century AD (Tomassetti et al. 2019-2020). The researchers studying the findings have linked this deposit to the tsunami that, according to reference seismic catalogues (Galbis 1932; 1940), occurred on 26 May 881 AD, after a major earthquake that was felt in Andalusia and the Maghreb, and whose epicentre has often been located in the Gulf of Cadiz (IGN 2020).

It has also been argued that the earthquake that affected the city of Malaga on 9 October 1680 AD may have been accompanied by a tsunami. However, the review of the historical documentation on the earthquake (Goded 2006) suggests that its epicentre was inland, thus ruling out the possibility that it triggered a tsunami. In conclusion, there is no unequivocal historical evidence of the occurrence of tsunamis on the coast of Malaga (cf. Macías et al. 2012).

8.6 Tsunamigenic Sources in the Western Alboran Sea

In comparison with the Atlantic seaboard of the Gulf of Cadiz, the coasts of the provinces of Malaga, parts of Granada and Almeria are not liable to be affected by very high-magnitude earthquakes, like the 1755 AD Lisbon event, among others. Be that as it may, significant submarine slides can occur and have occurred in the past. The plate boundary in the western Alboran Sea is diffuse (Vázquez et al. this volume). Moreover, far-field tsunamis triggered by the Moroccan and Algerian margin and thrust and strike-slip faults should be borne in mind, although strong seismic events are relatively rare (Buforn et al. 2019). The eastern stretch of the Almeria margin has been comprehensively studied and its related faults have been well imaged seismically (Gràcia et al. 2006; Estrada et al. 2018). The area's major faults are of the sinistral (left-lateral) strike-slip faults of considerable length and palaeo-magnitudes, like the 1522 AD Almeria earthquake (Reicherter and Hübscher 2007; Reicherter and Becker-Heidmann 2009). Although this earthquake destroyed the medieval city, its epicentre has yet to be accurately established. Meanwhile, it is assumed that it was located off-shore in the Gulf of Almeria, along the Carboneras Fault system. Despite the fact that, in principle, strike-slip faults do not generate tsunamis, recent scientific model-based approaches have revealed that, besides triggering submarine slides, they may indeed do so (Elbanna et al. 2021). As to the 1522 AD Almeria earthquake, that the collapse of the head scarp of the Almeria canyon triggered a tsunami should not be precluded (Reicherter and Becker-Heidmann 2009). Along the west coast, until Estepona, palaeotsunami deposits are rare or non-existent, which may be explained by missing archives, like, for example, coastal lakes, lagoons, cliffs or highly dynamic coastal systems including dunes, beaches, deltas of larger rivers (e.g., Guadalfeo, Guadalhorce) and human activity in a very popular tourist destination. The seismicity in the Malaga area is fairly deep (Vázquez et al., this volume) and not necessarily tsunamigenic. Some submarine slides have occurred in a wider area, but not immediately in the vicinity of the Cerro del Villar site. Additionally, off-shore faults are rare and, in contrast to data provided by González et al. (2010), recent mapping has not revealed any major seismogenic or tsunamigenic faults near the site (Vázquez et al., this volume). The postglacial sea level rise and the islet-studded estuary of the river Guadalhorce, associated with sediment dynamics (e.g., Hoffmann 1988), are not conductive to the preservation of EWE deposits. So, the Cerro del Villar event(s) are somewhat exceptional in that they are at the moment probably the oldest historically or archaeologically related tsunami deposits.

8.7 Discussion

The nature of the "marine" inundation deposit documented in stratum V of test pit 5, at the Cerro del Villar site, led Aubet (1999b) and Millán et al. (1999) to posit that it was possibly caused by a strong tide or probably a tsunami with catastrophic consequences (Aubet 1999b, p. 81; Millán et al. 1999, p. 11), at a time when research on the characteristics of tsunami deposits was still in its infancy (Atwater 1987; Dawson et al. 1988). Here, we change the interpretation to an alluvial inundation leaving a thick stratified package of clayey deposits. However, archaeological stratum IV (geological strata 14 and 15) resembles multi-layered marine deposits which are relatively chaotic, sometimes with channelled bases and fining-up sequences. The multi-layered deposits are interpreted as deposits of a marine high energy event, possibly a tsunami.

Research on the characteristics of tsunami and palaeotsunami deposits has progressed by leaps and bounds in the past decades, especially thanks to the field work carried out after the 2004 Indian Ocean and the 2011 Japanese tsunamis (Dawson and Shi 2000; Scheffers and Kelletat 2003; Dominey-Howes et al. 2006; Fujiwara 2008; Chagué-Goff 2008; Chagué-Goff et al. 2011; Costa and Dawson 2015, among others). These studies have made it possible to specify the elements that characterise tsunami and palaeotsunami deposits. However, they have also shown that it is extremely difficult to differentiate them from those generated by large storms, as they share many of their sedimentological characteristics. For this reason, concepts such as EWEs (Lario et al. 2010) or HEEs have been defined, encompassing both types of geological evidence.

In this regard, for the French Mediterranean coast seven Holocene periods of increased storm activity have been recorded in 6300–6100, 5650–

5400, 4400–4050, 3650–3200, 2800–2600, 1950–1400 and 400–50 cal yr BP (during the Little Ice Age) (Sabatier et al. 2012). Significantly, the stormy period between 2800–2600 cal yr BP broadly coincides with the date of the riverine floods that affected the Phoenician site of Cerro del Villar, but also EWE.

Based on the information from the sedimentological study performed on the test pit 5 profile by Villate and Millán (Millán et al. 1999), it is possible to identify some of the elements that are nowadays considered characteristic of flood, storm surge and tsunami deposits, such as their multi-layered structure and, particularly, the fining upward sequence of the layers that constitute the sedimentary event in layers 14 and 15 (Costa and Dawson 2015).

Villate and Millán identified stratum 10 from test pit 5 as a catastrophic marine inundation, and stratum 11 as the result of the sedimentation caused by this marine inundation (Millán et al. 1999). However, the whole sequence formed by strata 10–13 might be considered as the product of a single sedimentary event composed of a multi-layered structure characteristic of flood deposits indicating widespread inundation in the estuary. In turn, the edaphological study of these strata clearly documents a depositional sequence of the fine fraction, with a predominance of coarse sands in strata 10 and 11, and fine sands in strata 12 and 13.

Another development in the literature on tsunami deposits in recent years has been the attention paid to the erosional and sedimentary action of the tsunami backwash phase (Dawson 1994, 1999). The peculiar sedimentological configuration of stratum 14 and 15 from test pit 5, in which marine components indicate sea water and EWE, could be explained as the result of the channelled current of the tsunami backwash acting on the settlement located on the islet, in the mouth of the Guadalhorce palaeoestuary.

Characteristics similar to those of test pit 5 were also observed in the sediment cores and GPR profiles obtained close to Cerro del Villar in October 2019. The stratigraphy shows a possible intercalated HEE deposit (E1) in sediments whose chronology broadly corresponds to that of the Phoenician settlement. This event deposit also has a multi-layered structure and fining upward sequences, similar to the findings from test pit 5. It can thus be correlated to strata 14 and 15, identified by Millán et al. (1999), even though further and more detailed analyses, as well as more precise dating, are still pending. Furthermore, numerous broken shell fragments and marine microfauna confirm the marine origin of deposit E1. Whereas the lagoonal deposits of the cores are constituting the equivalent to the layer 10–13 of fine-grained deposits of alluvial origin.

8.8 Conclusions

The bay of Malaga, located on the northern shore of the Alboran Sea, was one of the first places in which Phoenicians settled in the south of the Iberian Peninsula. Settlements of different types, dating from between the ninth and fourth centuries BC, were established on a series of islets in the palaeoestuary of the river Guadalhorce, an environment exposed to both marine and fluvial flooding.

The largest site is the Phoenician settlement of Cerro del Villar, which covers an area of more than 80.000 m^2 and has a well-defined layout documented from the second quarter of the eighth century BC. The sedimentological analyses carried out in the stratigraphic sequence of the settlement, specifically in test pit 5, allowed for assessing the occurrence of two destructive flood events. The first one occurred at the beginning of the seventh century BC, probably due to an alluvial flood, as initially proposed by Aubet (1989, p. 381), which resulted in the violent destruction of the settlement, while the second one occurred at the end of the seventh century BC, probably due to an EWE of tsunamigenic origin. Both episodes must have had a considerable impact on the daily life of the settlement, in particular, and on the structure of the Phoenician population in the bay of Malaga, in general (Suárez-Padilla et al. 2020).

Recent studies of the subsoil of the settlement and its immediate perimeter reinforce this hypothesis. The preliminary results from two geoarchaeological cores drilled in the immediate perimeter of the ancient islet have revealed the existence of an EWE which can only be dated to a period later than the end of the third millennium BC.

It warrants noting that, albeit rare, EWEs can occur in the Alboran Sea due to different circumstances, including large storms from the east to tsunamis triggered by submarine landslides. The analysis of historiographical sources and recent archaeological work allows us to assess the existence of some of these phenomena in the region.

Future geoarchaeological studies at the Phoenician site of Cerro del Villar, in the framework of a long-term research project, should provide a better understanding of the characteristics and nature of the EWE that affected the settlement, which, according to the available evidence, may have been a tsunami. In turn, this research should address the way in which the catastrophic event affected all facets of life of the inhabitants of the settlement on the ancient islet at the mouth of the river Guadalhorce.

Acknowledgements We would like to thank the Institute of Geography at University of Cologne and the Physical Geography and Geoecology Institute at RWTH Aachen University for their help with grain size measurements. Furthermore, we are indebted to C. Cämmerer and M. Chaumet for their assistance during the fieldwork, and to L. Broer for the sample preparation and lab work. This research has been conducted as part of the project *Earthquakes and Tsunamis in the Iberian Peninsula: Social Responses in the longue durée* (PGC2018-093752-B-I00), funded by the Spanish Ministry of Science, Innovation and Universities (MCIU), the Spanish State Research Agency (AEI) and the European Regional Development Fund (ERDF).

References

Álvarez-Martí-Aguilar M (2020) The historicity of the earthquakes occurring in the Iberian Peninsula before A.D. 881 recorded in Spanish and Portuguese seismic catalogs. Seismol Res Lett 91(6):3585–3594. https://doi.org/10.1785/0220200168

Arancibia A, Galindo L, Juzgado M et al (2011) Aportaciones de las últimas intervenciones a la arqueología fenicia de la Bahía de Málaga. In: Álvarez-Martí-Aguilar M (ed) Fenicios en Tartesos: nuevas perspectivas. Archaeopress, Oxford, pp 129–149

Arancibia A, Fernández LE (2012) El periodo fenicio arcaico en la Bahía de Málaga. In: García Alfonso E (ed) Diez años de investigación fenicia en la provincia de Málaga (2001–2010), Junta de Andalucía, Sevilla, pp 49–66

Arribas A, Arteaga O (1975) El yacimiento de la desembocadura del río Guadalhorce (Málaga). Universidad de Granada

Atwater BF (1987) Evidence for great Holocene earthquakes along the outer coast of Washington State. Science 236:942–944

Aubet ME (1989) Cerro del Villar 1989. Informe de la segunda campaña de excavaciones arqueológicas en el asentamiento fenicio de la desembocadura del Guadalhorce (Málaga). Anuario Arqueológico de Andalucía 1989, II. Actividades Sistemáticas. Informes y Memorias. Consejería de Cultura y Medio Ambiente de la Junta de Andalucía, Dirección General de Bienes Culturales, Sevilla, pp 377–381

Aubet ME (1997) A Phoenician market place in Spain. In: Pongratz-Leisten B, Kühne H, Xella P (eds) Beiträge zu altorientalischen und mittelmeerrischen Kulturen. Neukirchen Verlag, Neukirchen-Vluyn, Festschrift W. Röllig, pp 11–22

Aubet ME (1999a) Recursos potenciales y vías de comunicación. In: Aubet ME, Carmona P, Curiá E et al (eds) Cerro del Villar-I. El asentamiento fenicio en la desembocadura del río Guadalhorce y su interacción con el hinterland. Junta de Andalucía, Sevilla, pp 41–46

Aubet ME (1999b) La estratigrafía del Corte 5. In: Aubet ME, Carmona P, Curiá E et al (eds) Cerro del Villar-I. El asentamiento fenicio en la desembocadura del río Guadalhorce y su interacción con el hinterland. Junta de Andalucía, Sevilla, pp 76–86

Aubet ME (1999c) La secuencia arqueo-ecológica del Cerro del Villar. In González A (ed) La cerámica fenicia en Occidente: centros de producción y áreas de comercio. Actas del I Seminario Internacional sobre Temas Fenicios. Guardamar del Segura, 21–24 de noviembre de 1997. Diputación Provincial de Alicante - Instituto Alicantino de Cultura Juan Gil-Albert, Alicante, pp 41–69

Aubet ME (2007) East Greek and Etruscan pottery in a Phoenician context. In: Ben-Tor A, Dever WG, Mazar A et al (eds) Essays in the archaeology and history of the eastern Mediterranean in honor of S. The Israel Exploration Society, Jerusalem, Gitin, pp 447–460

Aubet ME (2018) La colonia fenicia del Cerro del Villar. In: Botto M (ed) De Huelva a Malaka. Consiglio Nazionale dell Ricerche (Collezione di Studi Fenici 48), Roma, pp 325–349

Aubet ME, Carmona P, Curià E et al (eds) (1999) Cerro del Villar-I. El asentamiento fenicio en la desembocadura del río Guadalhorce y su interacción con el hinterland. Junta de Andalucía, Sevilla

Aubet ME, Delgado A (2003) La colonia fenicia del Cerro del Villar y su territorio. In: Gómez Bellard C (ed) Ecohistoria del paisaje agrario. Universidad de Valencia, Valencia, pp 57–74

Blott SJ, Pye K (2001) GRADISTAT: a grain size distribution and statistics package for the analysis of unconsolidated sediments. Earth Surf Proc Land 26 (11):1237–1248

Buforn E, Coco P, Bezzeghoud M et al (2019) The destructive 1790 Oran (NW Algeria) earthquake in a region of low seismicity. Tectonophysics 759:1–14

Burjachs F, Ros M (1999) Paleovegetación del Cerro del Villar. In: Aubet ME, Carmona P, Curiá E et al (eds) Cerro del Villar-I. El asentamiento fenicio en la desembocadura del río Guadalhorce y su interacción con el hinterland. Junta de Andalucía, Sevilla, pp 65–72

Carmona P (1999) Evolución paleogeográfica y geomorfológica del entorno del Cerro del Villar. In: Aubet ME, Carmona P, Curiá E et al (eds) Cerro del Villar-I. El asentamiento fenicio en la desembocadura del río Guadalhorce y su interacción con el hinterland. Junta de Andalucía, Sevilla, pp 33–41

Chagué-Goff O (2008) Bedforms and sedimentary structures characterizing tsunami deposits. In: Shiki T et al (eds) Tsunamiites: features and implications. Elsevier Science, Amsterdam, pp 51–62

Chagué-Goff C, Schneider JL, Goff JR et al (2011) Expanding the proxy toolkit to help identify past events—lessons from the 2004 Indian Ocean Tsunami and the 2009 South Pacific Tsunami. Earth Sci Rev 107:107–122

Costa PJM, Dawson S (2015) Tsunami Sedimentology. In: Meyers RA (ed) Encyclopedia of complexity and systems science. Springer Science - Business Media, New York, pp 1–17

Dawson AG (1994) Geomorphological effects of tsunami run-up and backwash. Geomorphology 10:83–94

Dawson AG (1999) Linking tsunami deposits, submarine slides and offshore earthquakes. Quat Int 60:119–126

Dawson AG, Long D, Smith DE (1988) The Storegga slides: evidence from eastern Scotland for a possible tsunami. Mar Geol 82:271–276

Dawson AG, Shi S (2000) Tsunami deposits. Pure Appl Geophys 157:875–897

Dominey-Howes DT, Humphreys GS, Hesse PP (2006) Tsunami and palaeotsunami depositional signatures and their potential value in understanding the late-Holocenetsunami record. The Holocene 16:1095–1107

Elbanna A, Abdelmeguid M, Ma X et al (2021) Anatomy of strike-slip fault tsunami genesis. PNAS 118. https://doi.org/10.1073/pnas.2025632118

Estrada F, Galindo-Zaldívar J, Vázquez JT et al (2018) Tectonic indentation in the central Alboran Sea (westernmost Mediterranean). Terra Nova 30(1):24–33. https://doi.org/10.1111/ter.12304

Folk RL, Ward WC (1957) Brazos River bar [Texas]; a study in the significance of grain size parameters. J Sediment Res 27(1):3–26

Fujiwara O (2008) Bedforms and sedimentary structures characterizing tsunami deposits. In: TsujiY, Yamazaki T, Minoura K (eds) Tsunamiites. Elsevier, Amsterdam, pp 51–62

Galbis J (1932) Catálogo Sísmico de la Zona comprendida entre los meridianos 5° E. y 20° W.de Greenwich y los paralelos 45° y 25° N. Tomo I. Instituto Geográfico, Catastral y deEstadística, Madrid

Galbis J (1940) Catálogo Sísmico de la Zona comprendida entre los meridianos 5° E. y 20° W. de Greenwich y los paralelos 45° y 25° N. Tomo II. Instituto Geográfico y Catastral, Madrid

García Alfonso E (1999) La cuenca baja del Guadalhorce. In: Aubet ME, Carmona P, Curiá E et al (eds) Cerro del Villar-I. El asentamiento fenicio en la desembocadura del río Guadalhorce y su interacción con el hinterland. Junta de Andalucía, Sevilla, pp 48–56

Gee GW, Or D (2002) Particle-size analysis. In: Dane JH, Topp GC (eds) Methods of soil analysis. Part 4—physical methods. In: Soil science society of America book series 5, Madison, Wisconsin, pp 255–293

Goded T (2006) Reevaluación de daños de los terremotos de Málaga de 1494 y 1680. Dissertation. Universidad Complutense de Madrid

González M, Medina R, Olabarrieta M et al (2010) Tsunami hazard assessment in the Southern coast of Spain. Turkish J Earth Sci 19:351–366

González de Canales F, Serrano L, Llompart J (2004) El emporio fenicio precolonial de Huelva (ca. 900–770 a. C.) Biblioteca Nueva, Madrid

Gràcia E, Pallàs R, Soto JI et al (2006) Active faulting offshore SE Spain (Alboran Sea): implications for earthquake hazard assessment in the Southern Iberian Margin. Earth Planet Sci Lett 241(3–4):734–749

Guidoboni E (ed) (1994) Catalogue of ancient earthquakes in the Mediterranean area up to the 10th century; with the collaboration of A. Comastri and G. Traina. Istituto Nazionale di Geofisica, Rome

Hoffmann G (1988) Holozänstratigraphie und Küstenlinienverlagerung an der andalusischen Mittelmeerküste. Berichte, Fb Geowissenschaften. Univ. Bremen, Nr 2:1–173

IGN (2020) Earthquake catalog. https://www.ign.es/web/ign/portal/sis-catalogo-terremotos Accessed 30 Apr 2020

Lario J, Luque L, Law C et al (2010) Tsunami vs. Storm surge deposits: a review of the sedimentological and geomorphological records of extreme wave events (EWE) during the Holocene in the gulf of Cádiz, Spain. Zeitschrift für Geomorphologie 54(3):301–316

Lafuente M (1843) Historia de Granada, comprendiendo las de sus cuatro provincias Almería, Jaén, Granada y Málaga. Desde remotos tiempos a nuestros días… Imprenta y Librería de Sanz, Granada

Loke MH (2004) RES2DINV ver. 3.54. Ed. M.H. Loke, Penang
Macías Sánchez J, Fernández Salas LM, González Vida JM et al (2012) Deslizamientos submarinos y tsunamis en el Mar de Alborán. Un ejemplo de modelización numérica. IEO, Madrid
Millán M, Villate E, Bernuz M (1999) Análisis del sedimento y del entorno. In: Aubet ME, Carmona P, Curiá E et al (eds) Cerro del Villar-I. El asentamiento fenicio en la desembocadura del río Guadalhorce y su interacción con el hinterland. Junta de Andalucía, Sevilla. Anexo II, 82 pp
Munuera JM (1963) Datos básicos para un estudio de sismicidad en el área de la península Ibérica (Seismic Data). Memorias Del Instituto Geográfico y Estadístico 33:1–47
Pérez de Barradas J (1934) Excavaciones en la necrópolis visigoda de Vega del Mar (San Pedro Alcántara, Málaga). Memorias de la Junta Superior de Excavaciones y Antigüedades, 128. Madrid, Tipografía de Archivos
Reicherter K, Becker-Heidmann P (2009) Tsunami deposits in the western Mediterranean: Remains of the 1522 Almería earthquake? Geological Society Special Publication, 316, London, pp 217–235
Reicherter K, Hübscher C (2007) Evidence for a seafloor rupture of the Carboneras Fault Zone (southern Spain): Relation to the 1522 Almería earthquake? J Seismolog 11(1):15–26
Reimer PJ, Austin WEN, Bard E et al (2020) The IntCal20 northern hemisphere radiocarbon age calibration curve (0–55 cal kBP). Radiocarbon 62(4):725–757
Sabatier P, Dezileau L, Colin C et al (2012) 7000 years of paleostorm activity in the NW Mediterranean Sea in response to Holocene climate events. Quart Res 77:1–11
Sánchez VM, Galindo JL, Juzgado M et al (2018) La Rebanadilla, santuario litoral fenicio en el sur de la Península Ibérica. In: Botto M (ed) De Huelva a Malaka. Los fenicios en Andalucía a la luz de los descubrimientos más recientes. Consiglio Nazionale dell Ricerche (Collezione di Studi Fenici 48), Roma, pp 305–324
Scheffers A, Kelletat D (2003) Sedimentologic and geomorphologic tsunami imprints worldwide—a review. Earth Sci Rev 63(1–2):83–92
Schulte P, Lehmkuhl F (2018) The difference of two laser diffraction patterns as an indicator for post-depositional grain size reduction in loess-paleosol sequences. Palaeogeogr Palaeoclimatol Palaeoecol 509:126–136
Soloviev SL, Solovieva ON, Go CN et al (2000) Tsunamis in the Mediterranean Sea 2000 B.C.–2000 A.D. Springer Science-Business Media, Dordrecht Springer
Stahl P (1971) La séismicité de Tanger et de sa région. In: Mémoire explicatif de la Carte géotechnique de Tanger au 1/25 000. Contribution à la connaissance du Tangérois. Notes et Memoires du Service Geologique du Maroc, 222 bis. Ed. Serv. Géol. Maroc, Rabat, pp 101–109
Suárez-Padilla J, Jiménez-Jáimez V, Caro JL (2021) The Phoenician diaspora in the westernmost Mediterranean: recent discoveries. Antiquity 95(384):1495–1510. https://doi.org/10.15184/aqy.2021.105
Stuiver M, Reimer PJ (1993) Extended 14C data base and revised CALIB 3.0 14C age calibration program. Radiocarbon 35:215–230
Stuiver M, Reimer PJ, Reimer RW (2020) CALIB 8.2 [WWW program] at http://calib.org. Accessed 2020-12-8
Suárez-Padilla J, Ramon Torres J, Mora Serrano B et al (2020) La cronología fundacional de la Malaka fenicia: investigaciones en el solar del Rectorado de la Universidad de Málaga. Spal 29(1):41–77. https://doi.org/10.12795/spal.2020.i29.02
Tomassetti JM, Navarro I, Suárez-Padilla J (2019-2020) Tsunami en la Estepona omeya: primera evidencia arqueológica del maremoto del año 881 d. C. Mainake 38:249–264
Udías A (1983) El terremoto del 21 de Julio 365, erróneamente atribuido a la costa de Málaga. Sismicidad Histórica de la Región de la península Ibérica. Asociación Española de Ingeniería Sísmica, Madrid, pp 53–55
Vegas M (1999) El ánfora griega del estrato V. In: Aubet ME, Carmona P, Curiá E et al (eds) Cerro del Villar-I. El asentamiento fenicio en la desembocadura del río Guadalhorce y su interacción con el hinterland. Junta de Andalucía, Sevilla, 136

9

High-Energy Events and Human Settlements in the Bay of Lagos (Portugal) in the Iron Age and Roman Times

Ana Margarida Arruda

Abstract

Archaeological and geological surveys carried out in several sites in the Bay of Lagos (Portugal) have brought to light new evidence of high-energy events (earthquakes and tsunamis) during Antiquity. Twenty-eight sediment cores performed along Lagos's waterfront yielded diverse intertidal strata, some of which are composed of sandy silt that may correspond to such events. Indeed, high-energy events of this kind might have aborted the first Phoenician occupation of Lagos and Pamares between the seventh and sixth centuries BC. In turn, it is possible that the Bay of Lagos was affected by other events, such as the extreme wave event that allegedly struck the seaboard of the Gulf of Cadiz at the end of the third century BC. In Monte Molião, some structural alterations are evident in walls dating from the first century BC, plus sand layers have been detected in the transition from the Iron Age to Roman times. An analysis of faunal remains, specifically shells, has revealed changes in the estuary's dynamics, which may be related to the effects of an extreme wave event.

A. M. Arruda (✉)
UNIARQ - Centro de Arqueologia da Universidade de Lisboa, Faculdade de Letras da Universidade de Lisboa, Alameda da Universidade, 1600-214 Lisboa, Portugal
e-mail: ana2@campus.ul.pt

Keywords

Earthquakes · Tsunamis · Algarve coast · Lagos · Monte Molião

9.1 Introduction

The Bay of Lagos and the eponymous city, located on the right bank of the river Bensafrim (Fig. 9.1), in the Algarve, are located in an important seismogenic and tsunamigenic region, as is highlighted in several chapters of this book. The urban core of the city of Lagos can be considered as a "Natural Hazard Area", as evidenced by geotectonic studies and the city's history of seismic events and tsunamis (Trindade 2014, p. 4). The city is also highly vulnerable due to its topographic and, above all, morphological profile (Trindade 2014). The river Bensafrim and its relatively wide estuary are a favourable entry point for extreme waves (see Fig. 9.2). Furthermore, Lagos shares obvious similarities with other urban centres impacted by such disastrous high-energy events.

Historical data on the impact of the 1755 earthquake (also known as the Lisbon earthquake) and the subsequent powerful tsunami are fairly abundant for the southwest coast of Portugal, where the event was particularly devastating. The height of the waves possibly reached 13 m and would have pushed 4 km inland at

M. Álvarez-Martí-Aguilar and F. Machuca Prieto (eds.), *Historical Earthquakes, Tsunamis and Archaeology in the Iberian Peninsula*, Natural Science in Archaeology,
https://doi.org/10.1007/978-981-19-1979-4_9

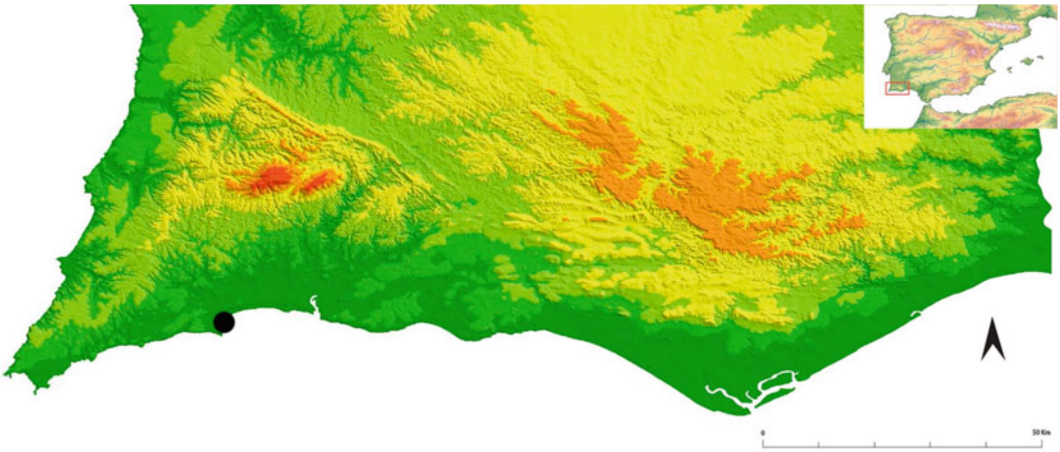

Fig. 9.1 Location of Lagos, Portugal (Reprinted from Pereira et al. (2019, Fig. 1) Copyright 2019)

Fig. 9.2 Lagos, the ocean and the Bensafrim estuary (Google Earth)

Lagos. The description offered in the historical sources compiled by Pereira de Sousa (1919) is striking to say the least:

> *Pelas 9 1/2 horas da manhã do predicto 1° de Novembro, estando o dia claro e sereno como de estio, vento N. O., ouviu-se um grande trovão surdo; logo passado 3 ou 4 minutos principiou a tremer a terra com espantosa violência; o mar recolheu-se em parte mais de 20 braças, deixando as praias em seco; e arremetendo imediatamente para a terra com tamanho ímpeto, entrou por ela dentro mais de uma légua, sobrepujando as mais altas rochas; tornando a retrair-se e rompendo por mais três vezes dentro de poucos minutos, arrasando no fluxo e refluxo enormes massas de penhascos e edifícios; e deixando por isso arrazadas quase todas as povoações marítimas.*
> At 9.30 am on 1 November, on a clear and calm summer day with a northwest wind, a deafening rumble was heard; after about 3 or 4 minutes the earth began to tremble with a shocking violence; the sea retreated more than 20 fathoms (ca. 40 m), leaving the beaches dry; and then returned with such impetus that it pushed more than a mile inland, passing over the highest rocks; retreating and returning three more times in a few minutes, destroying with its ebb and flow huge sections of the cliffs and buildings; and devastating nearly all of the costal populations.

An eyewitness account reads as follows: "[…] an awful earthquake with alteration in the sea, which in a few minutes devastated the city […]" (Rocha 1991, in Costa et al. 2005; see Baptista and Miranda 2004, p. 29). The earthquake had a disastrous impact on Lagos, which lost more than 10% of its population. It was immediately replaced as the capital of the Algarve by Faro and remained virtually uninhabited for approximately 50 years (Costa 2005, among others).

Information on this event has been supplemented by several geological studies performed along the coast of the Algarve, revealing the presence of massive blocks bearing marks of biocorrosion by live marine beings, found hundreds of metres inland from the river mouth—namely, the estuary of Barranco de Benaçoitão and Furnas (Costa et al. 2008, Fig. 1). The specific morphology of the sand barrier of Formosa also evinces its breaching (Andrade 1990, 1992). Additionally, a few elements show traces of seawater in the Salgados lagoon (Moreira et al. 2014, 2017; Costa et al. 2012, 2014; Fig. 1), among other places. The 1755 tsunami has also been well-recorded in Boca do Rio by geological studies (Dawson et al. 1995; Font et al. 2010, 2012, 2013; Feist et al. 2019; Hermann et al., this volume), as well as by an archaeological survey in Cerro da Vila, located in the mouth of the Quarteira estuary (Teichner 2017; Teichner et al. 2014).

Simulations for different wave-height scenarios (2.4 and 6 m) in the Bay of Lagos, using digital land models, were originally made for establishing prevention plans in order to assess vulnerability and establish evacuation routes (Trindade 2014). However, they can also be used to analyse events of the same nature occurring in Antiquity, namely the Iron Age and Roman times (see Figs. 9.3 and 9.4).

It should also be recalled that the 1755 earthquake was not a one-off phenomenon. The morpho-sedimentary and sedimentological record of extreme wave events (hereinafter EWEs) in the southwest of the Iberian Peninsula and, specifically in the Algarve, indicates that they must have also occurred in pre-historical and proto-historical time frames (Costa et al., this volume).

One such EWE, possibly equaling the 1755 event in terms of magnitude, has left a clear geoarchaeological record in Donaña (480–140 cal. BC; 390–40 cal. BC) and the Bay of Cadiz (340–70 cal. BC) (Rodríguez-Vidal et al. (2011). These authors have associated this record with the earthquakes and sea floods that, according to Galbis' (1932) seismic catalogue, occurred in Cadiz between 218 and 209 BC, information that ultimately derives from the *Crónica General de España* written by Florián de Ocampo (1553; see Álvarez-Martí-Aguilar, this volume). Similar episodes have been identified in the same area, at the mouth of the river Guadalquivir, inside Doñana National Park, in 5309 BP, 4200–4100 BP, 3900–3700 BP, 2400–2250 BP, and 2020–1990 BP (Cáceres et al. 2006; see also Rodríguez-Ramirez et al., this volume).

Only one source might possibly provide information on the 219–208 BC event, viz. Silius Italicus's epic poem *Punica*, which describes an

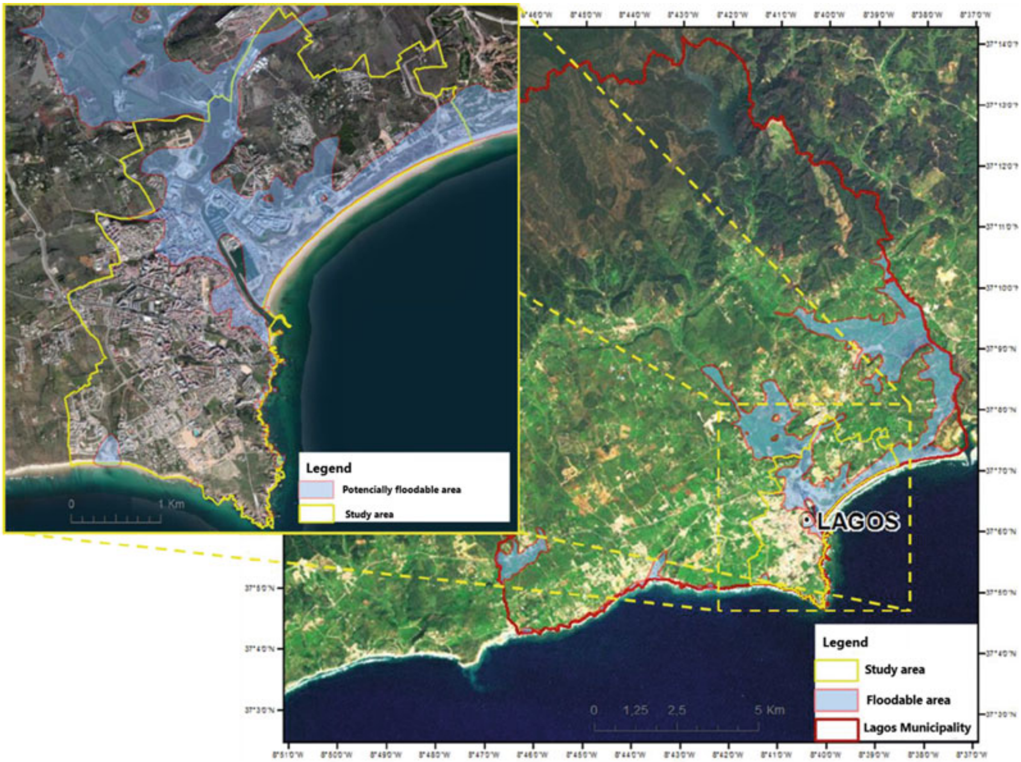

Fig. 9.3 Potentially floodable area in Lagos (Modified from Trindade (2014, Fig. 20) Copyright 2014)

episode that Hannibal would have witnessed near the shrine of Melqart (in Gadir, present-day Cadiz):

> When Hannibal's eyes were sated with the picture of all that valour, he saw next a marvellous sight the sea suddenly flung upon the land with the mass of the rising deep, and no encircling shores, and the fields inundated by the invading waters. For, where Nereus rolls forth from his blue caverns and churns up the waters of Neptune from the bottom, the sea rushes forward in flood, and Ocean, opening his hidden springs, rushes on with furious waves. Then the water, as if stirred to the depths by the fierce trident, strives to cover the land with the swollen sea. But soon the water turns and glides back with ebbing tide; and then the ships, robbed of the sea, are stranded, and the sailors, lying on their benches, await the waters' return. It is the Moon that stirs this realm of wandering Cymothoe and troubles the deep; the Moon, driving her chariot through the sky, draws the sea this way and that, and Tethys follows with ebb and flow (Sil. *Pun*., 3.45–60; transl. Duff 1927).

We know that Hannibal was in Cadiz precisely at the end of 219 BC, so it is tempting to relate this passage (Gómez et al. 2015) to the evidence of EWEs documented in the geological record of the Gulf of Cadiz, which yielded duly calibrated 14C dating, according to the ocean's reservoir effect, between the fifth and first centuries BC (Rodriguez-Vidal et al. 2011; Cáceres et al. 2006; see above).

However, as has been discussed in recent years (Álvarez-Martí-Aguilar 2017a, b, this volume), the relationship between the data collected in the geological survey and those deriving from the classical and historical sources is not that clear at first sight. Silius Italicus' account, which has usually been interpreted as an extremely high tide, perhaps refers to the tsunami that might have occurred in 219–218 BC. At any rate, this testimony does not seem to have been Florián de

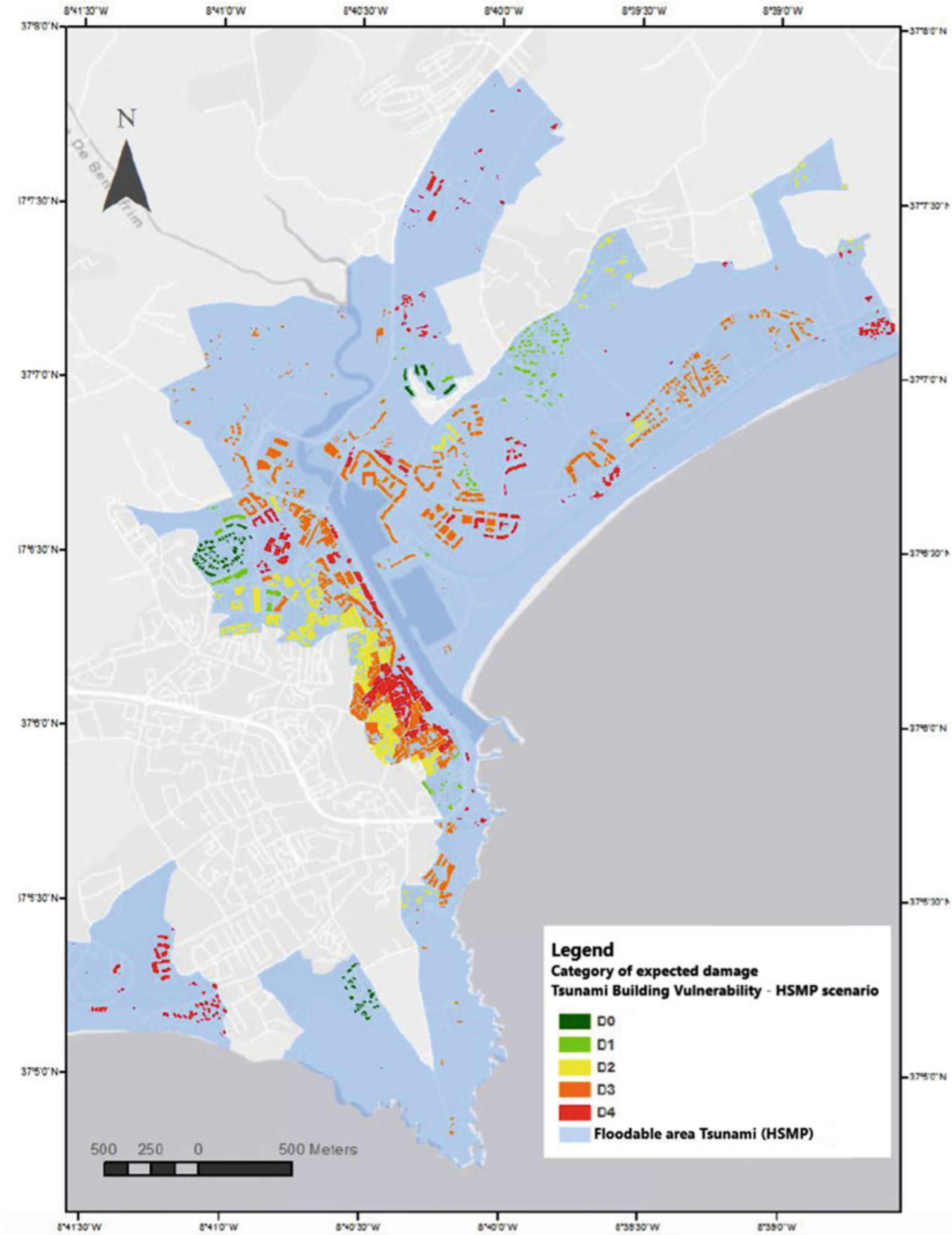

Fig. 9.4 Simulations for a 6 m wave-height in the Bay of Lagos, using digital land models (Modified from Trindade (2014, Fig. 28) Copyright 2014)

Ocampo's source of inspiration, whose *Crónica General de España* (Ocampo 1553) includes the first reference to an earthquake and a sea flood in the ancient Phoenician city of Gadir (modern-day Cadiz) in 216 BC, the year to which the Spanish chronicler erroneously dates the departure of Hannibal's expedition for Italy (218 BC being the correct date). No such episode is mentioned in the classical literature, which is odd because for the period of the Second Punic War, which exactly coincides with the proposed dates, the sources about the Iberian Peninsula are abundant.

9.2 The Bay of Lagos: Data

As regards the specific case of the Bay of Lagos, the results obtained from several geological sediment cores on both banks of the river Bensafrim, as well as on the city's waterfront, are unfortunately less clear. Be that as it may, the first probes, with their respective 14C radiometric dating, made it possible to determine that, up until approximately 2800 BP, the river had had an open estuary in which ocean dynamics prevailed (Gomes 2010). This matched other data previously obtained in the same area (Pereira et al. 1994), as well as data resulting from research in other estuaries of the Algarve. The sand barrier forming in the river mouth in the second half of the ninth century BC was overrun by the sea on several occasions, as evidenced by the sand interspersed with finer sediments.

Field work on the city's waterfront (28 sediment cores) has also yielded relevant data, namely, levels corresponding to an Iron Age I occupation (seventh-sixth century BC), with objects relating to the presence of Western Phoenicians in westernmost Iberia. These levels were followed by many intertidal strata, some composed of sandy silts (Arteaga and Barragán 2010), which may correspond to high-energy events. Even though information on the ancient occupation is unfortunately very scarce, the site seems to have remained unoccupied throughout the second half of the first millennium. Human occupation at the site was only resumed in the first century AD, this time well-documented by traces of fish-based products.

Geographically and topographically speaking, the presence of human communities at Lagos in the first centuries of the first millennium BC is identical to other cases along the Portuguese coast—of which Castro Marim and Tavira, also on the Algarve—are excellent examples (Arruda 2002, 2005). Surprisingly, however, the settlement was abandoned in the first half of the first millennium BC—something that has not been recorded at the other places mentioned above.

Apparently, this also occurred at another site in the Bay of Lagos, specifically Palmares (Fig. 9.5). We know even less about this site, as findings are very recent. An occupation dating from the Late Bronze Age has been identified, consisting of circular domestic structures, over which materials clearly associated with the Western Phoenician world have been found—specifically, R1-type amphorae and ceramics with a red engobe coating. Although the date of abandonment is unclear, it doubtless occurred in the first half of the first millennium BC (personal information—Manuel Pica, Arkaios, and Lúcia Miguel, Era Arqueologia). The site was re-occupied only in the Islamic period.

In my opinion, Lagos and Palmares might have been abandoned due to EWEs, phenomena similar to those described in this book, especially because people did not actually leave the region, but rather looked for safer places to settle, while maintaining easy access to the sea and control over the territory and the river Bensafrim, the waterway leading into the hinterland. One such place was precisely Monte Molião, founded in the fourth century BC, as evidenced by archaeological materials, namely Greek ceramics (Arruda et al. 2011). Other artefacts, like Kuass-type ceramics (Sousa and Arruda 2014), amphorae and both painted and common pottery (Arruda et al. 2011), show that this occupation lasted throughout the third century BC, with no major incidents (see Figs. 9.5 and 9.6).

However, the site remained exposed to the high-energy events that impacted the bay area, and there are available data to assess such a

Fig. 9.5 Lagos, Monte Molião and Palmares in the Bay of Lagos (Google Earth)

Fig. 9.6 The river Bensafrim and Monte Molião (*Photo* Rui Parreira)

reality. On the one hand, it should be stressed that the transition from the Iron Age to the Roman republican era is characterised by thick layers of fine sand, possibly relating to the micaceous silt from the *Formação de Ameijeira*, studied by a team from the University of Lisbon (Pereira et al. 2007) a few years ago. In any case, I believe that the sand deposit at Monte Molião was created by a tsunami-like phenomenon, probably the one that might have occurred in 219–218 BC, despite its debatable chronology, as noted above. It is interesting to observe that the Portuguese Cistercian monk Bernardo de Brito also mentions an earthquake that purportedly struck the Portuguese seaboard in 217 BC, which he tries to relate to the one occurring during the Battle of Lake Trasimene in Italy (Brito 1597), a connection devoid of credibility (Álvarez-Martí-Aguilar 2017b, this volume).

However intense the EWE might have been, human occupation of the site was not affected. In fact, the occupation of Monte Molião during the Roman republican era was highly significant and started early on, at about the beginning of the second century BC—if not in the last years of the previous century (Arruda and Sousa 2013; Sousa and Arruda 2014).

The place was struck again, in this case by a seismic event. This event is recorded on the walls of the first phase of the republican buildings (end of the second century-first decades of the first century BC), and led to the construction of new buildings in the first century BC, overlapping the older ones (Figs. 9.7 and 9.8).

The event documented in Monte Molião might be related to the earthquake occurring in Cordova between 79–72 BC, which is mentioned in Sallust's *Histories* (2.28; see Álvarez-Martí-Aguilar, this volume), although it is difficult to confirm this on the strength of the data currently available. On the other hand, another of the cataclysms recorded in Bernardo de Brito's work is dated to 63 BC. According to the Portuguese chronicler, in that year there was an earthquake and sea floods on the Portuguese and Galician coasts:

> *At around that time, or a few years before, there was a notable earth tremor on the coasts of Portugal and Galicia, which destroyed many places and killed so many people that the rest (as if beside themselves) fled from the villages to the hills, parents leaving behind their children and husbands abandoning their wives, all believing that*

Fig. 9.7 Monte Molião—Roman republican walls fractured by an earthquake (*Photo* Monte Molião Project)

Fig. 9.8 Monte Molião—Roman republican wall displaced by an earthquake (*Photo* Monte Molião Project)

> *they had been very fortunate to save their own lives, without having preserved those of others. And the sea, surpassing its ordinary limits in some places, covered much of the land where it had never shown signs of reaching, while leaving it exposed in other parts. Aladio refers to many other freak occurrences during those years, which I will not go into because they seem to me to be very special for such an ancient time, given that otherwise everything that this author writes adds up and appears to me to be very true* (Brito 1597, 316r–316v).

However, Brito's description is based on spurious sources and, therefore, lacks all credibility (see Andrade et al. 2016; Álvarez-Martí-Aguilar 2017b, this volume). Anyway, the possibility that an earthquake and a tsunami struck the Bay of Lagos in the first century BC may be corroborated by other types of evidence. The previously published study of malacological fauna at the site of Monte Molião has showed that cockle (*Cerastoderma edule*) recollection during the Roman republican era decreased sharply—a decline accompanied by the increased recollection of other species, such as mussels and clams (Detry and Arruda 2013). Since biometrical data do not bear out the hypothesis of over-exploitation, which can only be considered when values drop below 300 mm—which is not the case at Monte Molião—everything points to a change in paleo-environmental drivers (see Fig. 9.9). In fact, predation can cause serious unbalances and even the partial or total extinction of certain species, mainly slow-moving ones (e.g. molluscs), which are always the most affected because they are more sensitive to anthropic activity (Detry and Arruda 2012).

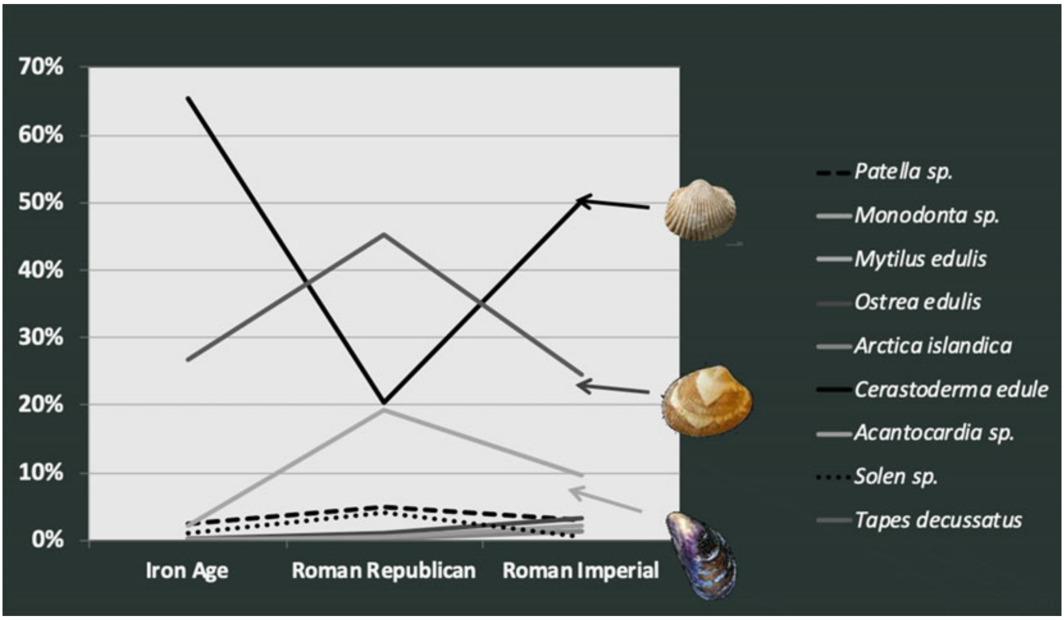

Fig. 9.9 The evolution of mollusc consumption in Monte Molião throughout its occupation (*Source* Detry and Arruda (2013))

Thus, if during the Iron Age the silting of the mouth of the river Bensafrim had provided an estuary sheltered and protected by sandy, marsh-type barriers, the occurrence of a high-energy event (such as a tsunami) must have had an impact on the change in the estuary ecosystem by opening the marshes to the influence of the sea, after breaching the protective barrier (Detry and Arruda 2012).

9.3 Final Remarks

The silting of the river Bensafrim's left mouth, following the possible tsunami that led to the abandonment of Lagos and Palmares in the mid-first millennium BC, had created a sheltered estuary, protected by sand barriers, by the fourth century BC, the accepted chronology for the commencement of human occupation at Monte Molião. After that, a high-energy event (or several) destroyed the dune system and changed the shape of the estuary, exposing it to the ocean, as the faunal remains in the republican levels at Monte Molião have revealed. Consumption of *C. edule* was resumed during the Roman Principate, specifically in the first century BC, which shows that the dune system that had once shaped the estuary recovered swiftly. In the field work carried out at the same site, we had the opportunity to verify other high-energy events. At the beginning of the second century AD, a large building collapsed, probably due to a strong earthquake. However, there is no evidence of any tsunami.

The abandonment of the site in the first quarter of the third century AD, and the reoccupation of Lagos, on the opposite bank of the river Bensafrim, were not due to any phenomenon of this nature, but to the progressive silting of the river, which prevented the arrival of vessels, and, therefore, imported products. In any case, the Bay of Lagos and the eponymous city did not remain untouched by the catastrophes resulting from these types of events, as borne out by the historical sources and archaeological data.

Acknowledgements This contribution to the book *Historical Earthquakes, Tsunamis and Archaeology in the Iberian Peninsula* is a result of the project "Monte Molião na Antiguidade".

References

Álvarez-Martí-Aguilar M (2017a) La tradición historiográfica sobre catástrofes naturales en la Península Ibérica durante la Antigüedad y el supuesto tsunami del Golfo de Cádiz de 218–209 a.C. Dialogues d'histoire ancienne 43(2):117–145

Álvarez-Martí-Aguilar M (2017b) Terremotos y tsunamis en Portugal en época antigua: el legado deBernardo de Brito y su Monarchia Lusytana (1597–1609). Euphrosyne 45:183–204

Andrade C (1990) Estudo da susceptibilidade ao galgamento da Ria Formosa. Geolis 4(1–2):69–76

Andrade C (1992) Tsunami generated forms in the Algarve barrier islands (South Portugal). Sci Tsunami Hazard 10:21–33

Andrade C, Freitas MC, Oliveira MA et al (2016) On the sedimentological and historical evidences of seismic triggered tsunamis on the Algarve Coast of Portugal. In: Duarte JC, Schellart WP (eds) Plate boundaries and natural hazards. American Geophysical Union, Washington, pp 219–232

Arruda AM (2002) Los fenicios en Portugal: Fenicios y mundo indígena en el centro y sur de Portugal (siglos VIII-VI a.C.). Universidad Pompeu Fabra, Barcelona

Arruda AM (2005) O 1º milénio a. n. e. no Centro e no Sul de Portugal: leituras possíveis no início de um novo século. O Arqueólogo Português, Série IV 23:9–156

Arruda AM, Sousa E (2013) Ânforas republicanas de Monte Molião (Lagos, Algarve, Portugal). SPAL 21:93–133

Arruda AM, Sousa E, Pereira C et al (2011) Monte Molião: um sítio púnico-gaditano no Algarve (Portugal). Conímbriga 50:5–32

Arteaga O, Barragán D (2010) Investigaciones geoarqueológicas en la Rua da Barroca (Lagos). Xelb 10:82–102

Baptista MA, Miranda JM (2004) Revision of the Portuguese catalog of tsunamis. Nat Hazards Earth Syst Sci 9:25–42

Brito B (1597) Monarchia Lusytana. Composta por Frey Bernardo de Brito, Chronista geral & Religioso da ordem de s. Bernardo, professo no Real mosteiro de Alcobaça. Parte Primeira. Mosteiro de Alcobaça

Cáceres LM, Rodríguez-Vidal J, Ruiz F et al (2006) El registro geológico Holoceno como instrumento para establecer periodos de recurrencia de tsunamis. El caso de la costa de Huelva. In: V Asamblea Hispano Portuguesa de Geodesia y Geofísica, Sevilla, pp 1–4

Costa A, Andrade C, Seabra C et al (2005) 1755: Terramoto no Algarve. Centro Ciência Viva do Algarve, Faro

Costa P, Andrade C, Oliveira MA et al (2008) High energy boulder deposition in Barranco and Furnas lowlands, western Algarve (south Portugal). In: Second international field symposium—IGCP Project 495, Ostuni (Italy) and Ionian Islands. GI2S Coast Research Publication 6, pp 19–22

Costa P, Andrade C, Freitas MC et al (2012) A tsunami record in the sedimentary archive of the central Algarve coast, Portugal: characterizing sediment, reconstructing sources and inundation paths. The Holocene 22(8):899–914

Costa P, Andrade C, Freitas MC et al (2014) Reconhecimento de um depósito de tsunami na Lagoa dos Salgados (Algarve, Portugal). In: VIII Congresso Nacional de Geologia (Braga, 12–16 de Julho de 2010). Universidade do Minho, Braga, vol 1, pp 5–15

Dawson AG, Hindson R, Andrade C et al (1995) Tsunami sedimentation associated with the Lisbon earthquake of 1 November AD 1755: Boca do Rio, Algarve, Portugal. The Holocene 5(2):209–215

Detry C, Arruda AM (2012) Acerca da influência ambiental e humana nos moluscos de Monte Molião (Lagos, Portugal). In: Campar Almeida A, Bettencourt A, Moura D et al (eds) Environmental changes and human. Interaction along the Wester Atlantic edge. Associação Portuguesa para o Estudo do Quaternário, Coimbra, pp 171–184

Detry C, Arruda AM (2013) A fauna da Idade do Ferro e época romana de Monte Molião: continuidades e rupturas na dieta alimentar. Rev Port Arqueol 16:213–226

Duff JD (1927) Silius Italicus. Punica, Vol. I: Books 1–8. William Heinemann Ltd., London; Harvard University Press, Cambridge, MA

Feist L, Frank S, Bellanova P et al (2019) The sedimentological and environmental footprint of extreme wave events in Boca do Rio, Algarve coast, Portugal. Sed Geol 389:147–160. https://doi.org/10.1016/j.sedgeo.2019.06.004

Font E, Nascimento C, Omira R et al (2010) Identification of tsunami-induced deposits using numerical modeling and rock magnetism techniques: a study case of the 1755 Lisbon tsunami in Algarve, Portugal. Phys Earth Planet Inter 184(1–2):106–117

Font E, Veiga-Pires C, Ruiz F et al (2012) Testing rock magnetic and AMS methods in tsunami and storm induced deposits. 13th Castle Meeting, Zloven. Poster session

Font E, Veiga-Pires C, Pozo M et al (2013) Benchmarks and sediment source(s) of the 1755 Lisbon tsunami deposit at Boca do Rio Estuary. Mar Geol 343:1–14

Galbis J (1932) Catálogo Sísmico de la Zona comprendida entre los meridianos 5° E. y 20° W. de Greenwich y los paralelos 45° y 25° N. Tomo I. Instituto Geográfico, Catastral y de Estadística, Madrid

Gomes, JPA (2010) Estuário da Ribeira de Bensafrim: leitura geo-arqueossismológica. Dissertation. Universidade de Lisboa, Lisboa

Gómez F, Arruda AM, Rodríguez-Vidal J et al (2015) Eventos marinos de alta energia y cambios traumáticos en los asentamientos costeros del Suroeste de la Península Ibérica. Cuaternario y Geomorfología 29(1–2):57–74

Moreira S, Costa P, Andrade C et al (2014) Geochemical signature in a tsunami deposit detected in Lagoa dos

Salgados (Portugal). 9th ISC 2014, 18–22 August, Geneva, p 511
Moreira S, Costa P, Andrade C et al (2017) High resolution geochemical and grain-size analysis of the AD 1755 tsunami deposit: insights into the inland extent and inundation phases. Mar Geol 390:94–105
Ocampo F de (1553) Los cinco libros primeros de la Cronica general de España, que recopila el maestro Florian do Campo, Cronista del Rey nuestro señor, por mandado de su Magestad, en Zamora, Guillermo de Millis, Medina del Campo
Pereira AR, Dias JA, Laranjeira MM (1994) Evolução holocénica da linha de costa da baía de Lagos. In: Pereira AR et al (eds) Contribuições para a Geomorfologia e Dinâmicas Litorais em Portugal. Linha de Acção de Geografia Física, Relatório nº. 35, Centro de Estudos Geográficos, Lisboa, pp 75–89
Pereira AR, Ramos C, Neves M (2007) Dinâmica dos sistemas litorais: uma componente esquecida no ordenamento do território. O exemplo de Porto de Mós (Lagos). In: Geomorfologia: Ciência e Sociedade. Associação Portuguesa de Geomorfólogos, Lisboa, pp 237–247
Pereira C, Arruda AM, Sousa E (2019) Os artefactos metálicos da Idade do Ferro de Monte Molião (Lagos, Portugal). Lucentum 38:77–88. https://doi.org/10.14198/LVCENTVM2019.38.03
Pereira de Sousa FL (1919) O terremoto do 1.º de Novembro de 1755 em Portugal e um estudo demográfico. Vol 1: Distritos de Faro, Beja e Évora. Serviços Geológicos, Lisboa
Rodríguez-Vidal J, Ruiz F, Cáceres LM et al (2011) Geomarkers of the 218–209 BC Atlantic tsunami in the Roman Lacus Ligustinus (SW Spain): a palaeogeographical approach. Quatern Int 242(1):201–212
Sousa E, Arruda AM (2014) A cerâmica comum romano-republicana de Monte Molião (Lagos). Onoba 2:55–91
Teichner F (2017) Cerro da Vila: A rural commercial harbour beyond the Pillars of Hercules. In: Campos J, Bermejo J (eds) Los puertos atlánticos, béticos y Lusitanos y su relación comercial con el Mediterráneo. Universidad de Huelva, Huelva, pp 403–435
Teichner F, Mäusbacher R, Daut G et al (2014) Investigações geo-arqueológicas sobre a configuração do litoral algarvio durante o Holoceno. Rev Port Arqueol 17:141–158
Trindade A (2014) Risco de Tsunami da cidade de Lagos. Avaliação da vulnerabilidade e modelação de rotas de evacuação numa abordagem SIG. Dissertation. Universidade de Lisboa, Faculdade de Ciências, Lisboa

Check for updates

10 At the Mercy of the Sea—Vulnerability of Roman Coastal Settlements in the Algarve (Portugal). Boca do Rio as an Emblematic Example of a Key Maritime Industry

Florian Hermann, Lisa Feist, Felix Teichner, João Pedro Bernardes, Klaus Reicherter, and Helmut Brückner

Abstract

The Roman fish-salting industry in the Western Mediterranean was concentrated in a high-risk geological area as regards extreme wave events. It underwent a significant and sudden decline and reorganisation between the second and third centuries AD. The few explanations that have been hitherto offered for this abrupt transformation range from political and economic disruptions to vague speculations on natural causes. Accordingly, this chapter focuses on determining the possibility of an extreme wave event as the cause behind the restructuring of this industry. For this purpose, the results of 3 years of archaeological and geoscientific field research in Boca do Rio (Vila do Bispo, Algarve) are presented and evaluated. Although far-reaching changes in the building stock of this Roman industrial settlement have been dated to between the second and third centuries AD, and a short series of high energy events has been identified, there is no evidence of the direct influence of a single event (a flood, storm surge, tsunami, etc.) as a trigger for the changes in the settlement and the local Roman economy. Rather, medium-term environmental changes seem to have been the driving force behind them. Additionally, a previously unknown late medieval event layer is described in detail.

F. Hermann (✉) · F. Teichner
Department of History and Cultural Studies, Institute of Prehistoric Archaeology, University of Marburg, Marburg, Germany
e-mail: florian.hermann0@gmail.com

F. Teichner
e-mail: teichner@staff.uni-marburg.de

L. Feist · K. Reicherter
Department of Geosciences and Geography, Neotectonics and Natural Hazards, RWTH Aachen University, Aachen, Germany
e-mail: l.feist@nug.rwth-aachen.de

K. Reicherter
e-mail: k.reicherter@nug.rwth-aachen.de

J. P. Bernardes
Centro de Estudos em Arqueologia Artes e Ciências do Património CEACCP, University of Algarve, Faro, Portugal
e-mail: jbernar@ualg.pt

H. Brückner
Department of Geosciences, Coastal Morphology, Geoarcheology, and Geochronology, Institute of Geography, University of Cologne, Cologne, Germany
e-mail: h.brueckner@uni-koeln.de

M. Álvarez-Martí-Aguilar and F. Machuca Prieto (eds.), *Historical Earthquakes, Tsunamis and Archaeology in the Iberian Peninsula*, Natural Science in Archaeology,
https://doi.org/10.1007/978-981-19-1979-4_10

Keywords

Roman marine industry · Garum · Fish-salting · Third-century crisis · Tsunami · High-energy event · Coastal settlement · Environmental change

10.1 The Roman Fish-Salting Industry, Its Development and Connection to Tsunami Research

In the Hispanic and North African provinces of the Roman Empire, to the classical ‘Mediterranean triad’ of grain, wine and olive oil should be added preserved marine resources, above all salted fish (*salsamenta*) and fish sauces (*liquamen, garum*, etc.), as the fourth pillar on which the economy rested (Fabião 1992; Bekker-Nielsen 2002; Teichner 2014a).

Especially in the western provinces, the characteristic large vats—*cetariae*—lined with hydraulic concrete or plaster (*opus signinum* or *caementitium*) are well documented (Fig. 10.1). The lower scale production in the eastern part of the Empire employed ceramic vessels (*dolia, pithoi*) and is, therefore, less well known (Curtis 1991). The concentration of production sites on both sides of the Strait of Gibraltar and the Strait of Sicily and on the Atlantic seaboard of *Lusitania*, *Mauretania Tingitana* and *Gallia Lugdunensis*, however, is only partly true due to the difficulties in detecting sites. Rather, it is assumed to be connected with the movement of shoals of migratory fish species, such as tuna and mackerel, which regularly passed through those areas (Opp., *Hal*. III.620–648; Bekker-Nielsen 2005; Wilson 2007). The processing of catches required a complex network of facilities and manpower, including production facilities, amphora potteries, fresh water, saltworks or salt evaporation ponds, fisheries and traders (Fig. 10.2).

Since this phenomenon was systematically explored for the first time by Ponsich and Tarradell in 1965, almost 300 sites relating to fish salting have been detected in the Western Mediterranean (Fig. 10.1; <ramppa.uca.es> 01.05.2022). This impressive number should not, however, conceal the fact that large areas of the Mediterranean and Atlantic regions are still blank on distribution maps, while in view of the local topography, known fish migration routes (Fig. 10.2) and the written sources this is hardly to be expected. Furthermore, a majority of the known sites were only superficially identified or researched in rescue excavations during the first half of the twentieth century or before, namely, usually without recording stratigraphic connections. In the past, the regionally very varied state of the knowledge led to a biased representation and interpretation of the economic dominance of the *Baetica* over the *Mauretania Tingitana* (Ponsich and Tarradell 1965; Teichner and Pujol 2008; Trakadas 2015), which is now also being discussed for southern *Lusitania* during the first and second centuries AD (Fabião 2004).

The state of research allows for arriving at some basic conclusions on the distribution and organisation of fish-salting facilities, of which the most important regarding the research questions posed here are a follows:

- Settlements specialising in the ‘development and processing of maritime goods’ (Teichner 2008), established in areas unsuitable for agriculture, to wit, in river estuaries or bays or generally near the coast (Fabião 1992). Contrary to earlier assumptions (e.g. Trakadas 2005), both urban and extra-urban areas were involved in this maritime economy. While most of the facilities, including the largest, were still located outside cities, some of the best researched are located within or in the environs of ancient cities (Wilson 2006; Bernal Casasola 2009; Expósito Álvarez et al. 2018).
- It can be assumed that the majority of the facilities were devoted to the sale and export of their products and required a supra-regional or even Empire-wide market (Curtis 1991; Étienne et al. 1994; Martin-Kilcher 1994; Ehmig 2001).
- The majority of the identified settlements are concentrated along seismically active and, therefore, high-risk coastal areas (Lario et al. 2011; Duarte et al. 2013).

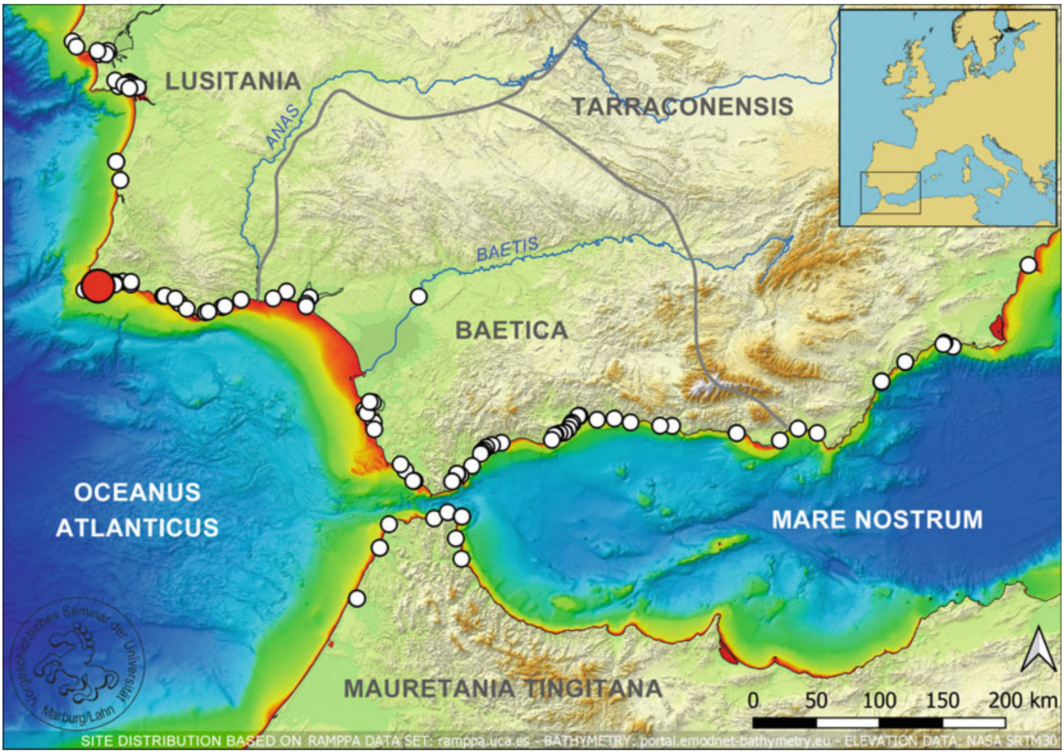

Fig. 10.1 Distribution of Roman fish-salting facilities around the Strait of Gibraltar in the southern Hispanic and North African provinces of the Roman Empire, with the red circle marking Boca do Rio's position

Possibly based on a Punic-Carthaginian tradition, the earliest evidence of fish preservation in southern Hispania in Roman times was dated to the late Republic (Bernal Casasola 2009; Bernal Casasola et al. 2018; Bernal Casasola and Vargas Girón 2019). From the first century BC onwards, the first facilities equipped with *opus signinum* lined vats—which would be subsequently commonplace during the Roman imperial period—began to appear (Bernal Casasola 2009; Trakadas 2015). After the turn of eras, numerous small and large facilities were built in the *Lusitania* province, including the supra-regional production centre of Tróia next to Setúbal (Fabião 2009; Vaz Pinto et al. 2014). The ongoing construction of new facilities and the associated growth of the aggregated vat capacities continued well into the second century AD, at the end of which a sudden upheaval can be observed (Lagóstena Barrios 2001). This is illustrated by a significant reduction in the overall vat capacity in *Hispania* due to the complete or partial abandonment of individual facilities (Wilson 2006).

Traditionally, this development is associated with the 'crisis of the third century', which is well documented for the Hispanic region, or the *bellum mauricum* and its economic and political repercussions (Reece 1981; Fabião 2008; Bombico 2015; *bellum mauricum*: Fabião 2004; Trakadas 2005).

Apart from the aforementioned anthropogenic influences, more recently natural factors have been suggested as an explanation for the changes occurring between the second and third centuries AD. On the one hand, all Roman coastal settlement were heavily dependent on the development and stability of their immediate natural environment, which has been clearly demonstrated in the settlement of Cerro da Vila in Vilamoura (Hilbich et al. 2005; Teichner 2014b, 2016, 2017; Teichner et al. 2014). On the other, Mayet and Silva (2010) suggested the possibility

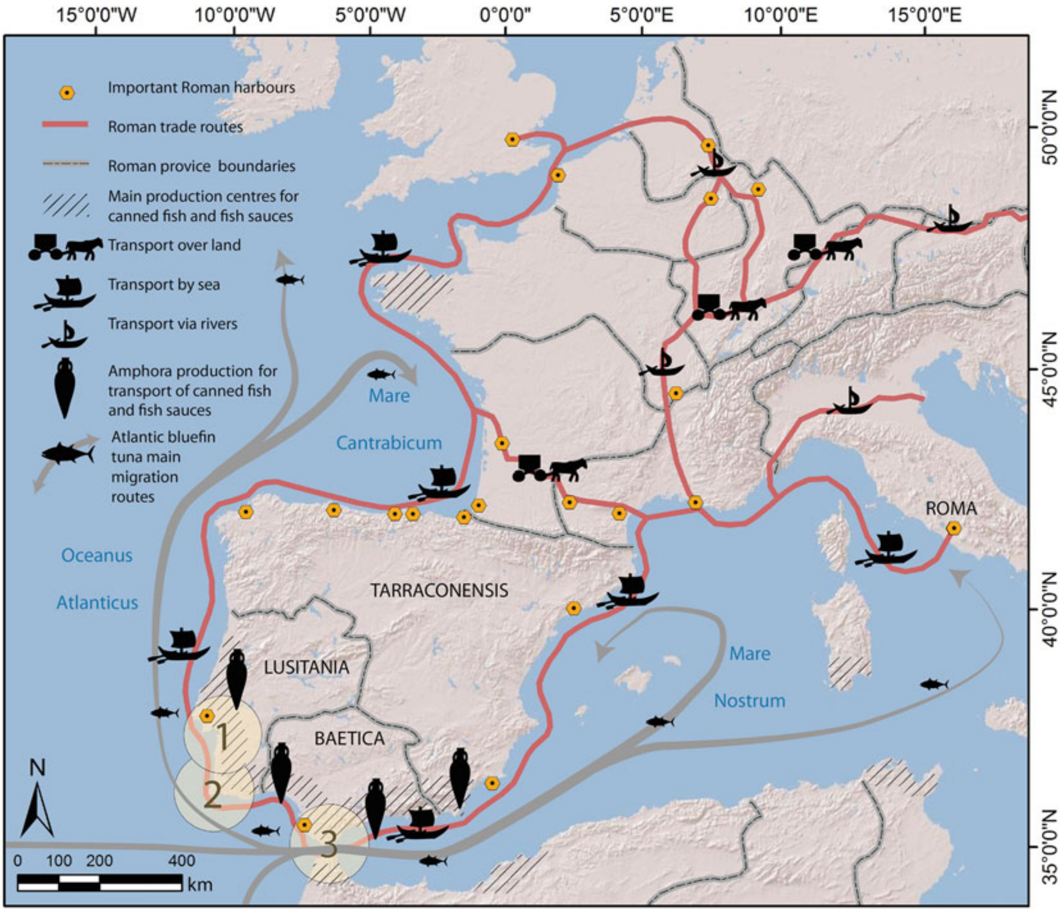

Fig. 10.2 Simplified Roman trade routes and the location of the three key regions covered by the research project: (1) the Costa Alentejana, Tróia; (2) the western Algarve, Boca do Rio (presented in this study); and (3) the Strait of Gibraltar, *Baelo Claudia* (Bolonia). Own elaboration; Atlantic bluefin tuna migration routes, after Fromentin and Powers (2005)

of a major flood or tsunami as a trigger. They based their hypothesis on destruction horizons and vat fillings in a handful of Portuguese (Tróia, Setubal, Sines and Ilha do Pessegueiro), southern Spanish (*Baelo Claudia*) and northern Moroccan (Cotta) sites which may be dated to this period. Although their hypothesis was subsequently taken up in the literature (e.g. Vaz Pinto et al. 2014), this alleged event has yet to be geologically or archaeologically evaluated. Be that as it may, it serves as a working hypothesis for the study described in this chapter.

The vats built after this change, viz. from the third century AD onwards, are usually smaller than their predecessors. Additionally, the subdivision of existing vats is often observed in the case of the continued use of facilities (Wilson 2006). However, the biggest change in *Lusitania* was the introduction of new, locally produced fish sauce amphorae (Diogo 1987; Fabião 2004) and the construction of new facilities in the previously underrepresented Algarve region. This is interpreted as a decoupling of the Lusitanian economy, in particular that of the Algarve, from that of the hitherto dominant province of *Baetica*, only made possible by this ‘crisis’ (Fabião 1992; Teichner 2008; Bernardes and Viegas 2017).

By the end of the fifth century AD, most of the sites had ceased production, although some continued to operate on a much smaller scale during the following centuries (Wilson 2006; Maghreb: Trakadas 2015; Hispania: Lagóstena Barrios 2001; Portugal: Teichner 2008; Fabião 2009).

10.2 Testing the Tsunami Hypothesis—'Vulnerability' of the Algarve Coast to Extreme Wave Events

In the light of new data, natural causes have yet again been put forward as an explanation for the observed breaks in coastal settlement patterns in Antiquity in general, especially in the second and third centuries AD. Particular emphasis has been placed on the possible role of single events like earthquakes or extreme wave events (hereinafter EWEs) (Étienne et al. 1994; Grützner et al. 2012; Röth et al. 2015; Gómez et al. 2015; Silva et al. 2016; Teichner 2017; Arruda, this volume; Frenken et al., this volume). This hypothesis—among other natural causes—was tested in a 3-year research project funded by the German Research Foundation (DFG). Specifically, three key regions of the fish-salting industry were identified, and in each one of them a reference site was selected and investigated: (1) the Costa Alentejana with the site of Tróia on a peninsula just outside the port of *Caetobriga* (Setúbal); (2) the western Algarve with the settlement of Boca do Rio west of Roman *Lacobriga* (Lagos); and (3) the city of *Baelo Claudia* (Bolonia) in the Strait of Gibraltar (Fig. 10.2). In this chapter, the results from Region 2 and its reference site of Boca do Rio are presented and discussed.

The Algarve coast—with Boca do Rio as the reference site—has a high potential for earthquakes and associated tsunamis due to its tectonic setting within the Gulf of Cádiz, close to the Eurasia-Africa plate boundary (Lario et al. 2011; Duarte et al. 2013). Several tsunamis hit the Algarve coast in historical times (60 BC, AD 382, 1722, 1755, 1761, 1941, 1969 and 1975—Portuguese tsunami catalogue: Baptista and Miranda 2009). It should be noted, however, that not all of the listed events affecting the Algarve region have been accepted as tsunamis in view of the sedimentary analyses performed to date. In particular, the reliability of the events dated to 60 BC and AD 382 is debatable, as their descriptions in the written sources are in all likelihood associated with events occurring at different times and places, such as the 63–65 BC Syrian and AD 365 Cretan tsunamis (Andrade et al. 2016), or their historicity is very questionable (Baptista and Miranda 2009; Álvarez-Martí-Aguilar 2020, this volume). Further east along the coast of the Spanish Gulf of Cádiz, one or more additional events occurring during the Republican period (ca. 250 ± 50 cal. BC; Lario et al. 2011; Costa et al., this volume) have been reported at several locations based on geological evidence (e.g. Bay of Cádiz: Luque et al. 2002; Guadalquivir estuary: Rodríguez-Ramírez et al. 2016). Similarly, Bermejo Meléndez et al. (this volume) and Gutiérrez-Rodriguez et al. (this volume) focus on events occurring in the areas of Huelva and Seville in Imperial times and late Antiquity, respectively. Of all events listed in the catalogues, only the devastating tsunami following the AD 1755 Lisbon earthquake has been comprehensively analysed. Along the Algarve coast, the sedimentary footprint of the AD 1755 tsunami is well preserved (e.g. Andrade et al. 2004; Kortekaas and Dawson 2007; Dinis et al. 2010; Schneider et al. 2010; Costa et al. 2011, 2012a; Trog et al. 2015; Quintela et al. 2016), especially at the site of Boca do Rio, where the AD 1755 deposit is sandwiched between finer grained floodplain strata, which has led to numerous studies focusing on various characteristics of the event deposit (e.g. Dawson et al. 1995; Hindson et al. 1996; Hindson and Andrade 1999; Oliveira et al. 2009; Cunha et al. 2010; Costa et al. 2012b; Font et al. 2013; Feist et al. 2019).

Apart from the relatively high tsunami potential, storms frequently trigger EWEs along the Algarve coast (Ferreira et al. 2008); however, only a few sedimentary imprints have been documented for the coastal lowlands of Martinhal, close to Boca do Rio (Kortekaas and

Dawson 2007), and for the Ria Formosa barrier island system of Faro further to the east (Andrade et al. 2004).

Besides this excellent setting for tsunami research, there was a Roman fish-salting settlement in the valley of Boca do Rio (Bernardes and Medeiros 2016; Bernardes et al. in press; Hermann et al. 2022, in press). The combination of these two factors led to the selection of this settlement site and its immediate surroundings for the study at hand, whose aim—as will be explained below—is to answer the following research questions:

1. Since few details are known about the industrial area of the settlement of Boca do Rio: what was its size and what role did it play in the fish-salting industry network?
2. Were there any changes and/or hiatuses in this settlement between the second and third centuries AD, as has been recorded in other coastal settlements? If so, how can they be characterised?
3. Are there traces of EWEs in the sediments of the immediate surroundings and/or in the archaeological remains? If so, can the traces of identified upheavals (no. 2) and EWEs be correlated, that is, can the former be attributed to the latter?

10.3 Topographical–Geological Environment and Archaeological Overview of the Site of Boca do Rio

Boca do Rio is located on the south-western Algarve coast, Portugal (08°48.5'W and 37° 04'N; Hindson and Andrade 1999), approximately 18 km east of Cape St Vincent (Sagres) and 15 km west of the town of Lagos (Fig. 10.1). It is a formerly V-shaped, flat-floored, sediment-filled river valley, dissecting a coast with prominent Jurassic and Cretaceous cliffs to the west and east, and bordered by the Atlantic to the south (Hindson et al. 1999). This floodplain valley, consisting of mostly fine-grained Holocene sediments (silt, clay), extends up to 1 km inland, where it is divided into three sub-valleys by the rivers Budens, Vale de Boi and Vale de Barão (Hindson and Andrade 1999). The highly variable and seasonally blocked gravelly and sandy river mouth influences the surrounding floodplain and beach, depending on the river's water level (Costa et al. 2012b; Feist et al. 2019). A dune complex, bordered by steep terrain with an eroding cliff and a beach break with coarse gravel and boulders from the cliff, is situated to the west of the floodplain (Feist et al. 2019). This dune complex covers the Roman ruins.

At the beginning of the Roman occupation of the site in the second half of the first century AD, it is assumed that the bay was still largely open to the sea, but protected by a barrier. Identified palaeochannels of the aforementioned rivers on the western edge of the present alluvial plain, however, indicate that the estuary was practically unnavigable (Feist et al. 2019). The retreating coastline on the other hand, offered ideal conditions for the production of salt in salt gardens due to an extensive salt marsh on its edges and high evaporation during the summer months (Bernardes 2007; Fabião 2009; general prerequisites: Lagóstena and Palacios 2010; for comparison: Teichner et al. 2014).

As the siltation of the estuary progressed, it gradually lost its littoral character, while fluvial and alluvial conditions as precursors of the present geomorphology began to prevail, until the current direction of the watercourse along the eastern edge of the valley was established (Hindson et al. 1996; Allen 2003; Vigliotti et al. 2019; Feist et al. 2019). This process was greatly accelerated by the impact of the AD 1755 tsunami, which not only introduced a large amount of additional sediment but also severely restricted river discharge (Font et al. 2013).

The settlement site comprises three principal areas (Hermann et al. 2022). Firstly, a very densely built-up area to the south, divided into the *pars urbana*, or residential area with a *thermae* building and adjoining industrial complexes featuring fish-salting workshops (Fig. 10.3, between markers 'harbour' and 'cliff'); and, separated from this area, a group of buildings further north-west, including 'industrial'

Fig. 10.3 Overview of the results of the geomagnetic measurements at the site of Boca do Rio. The marked spots are mentioned in the text

structures, such as two kilns belonging to a pottery workshop (Fig. 10.3, marker 'kiln II').

The existing interpretation of Boca do Rio's building stock is based on an 1878 plan of the area on the present-day cliff (da Veiga 1910; Figs. 10.3 and 10.5 for details). Although most of the structures recorded at that time have since deteriorated due to coastal erosion (Hermann et al. 2022; Fig. 10.5), this old record has recently been reviewed and reinterpreted by Bernardes and Medeiros (2016). For these authors, they are residential and utility buildings constructed in the third century AD. The settlement's fish-salting workshops, on the other hand, have yet to be documented in detail (Alves 1997). Nevertheless, it is believed that they must have included facilities for the processing of marine resources (Bernardes 2007). So far, the dating of the site is largely based on Bernardes' stratigraphic work around the ruins of the eighteenth-century buildings of the Portuguese Royal Fishing Company (Fig. 10.4 for location), specifically, in the areas in which the residential and utility buildings of the Roman settlement were located (Bernardes et al. in press). On this basis, the earliest phase of settlement can be dated to the Flavian period (AD 69–96; Bernardes and Medeiros 2016). The area close to the beach was comprehensively reorganised as of the third century AD, which involved demolishing previous structures. Their earlier existence is only indirectly borne out by dominant levelling layers (see below section profiles for details). Thus, the majority of the building structures documented by da Veiga (1910) can be dated to this later period (Bernardes 2007; Teichner and Mañas 2018). Over its approximately 150 years of use, the building complex underwent numerous minor additions and alterations, such as repairs to the mosaics and the application of several layers of painted plaster on the walls. The last traces of the settlement's activity were reported in the form of African red slip (ARS) and Chiara C and D ware, datable to the end of the fourth or to the beginning of the fifth century AD. A vast coin hoard discovered in 1938, mostly consisting of emissions from the last third of the fourth century AD (the latest struck during the reign of Honorius), also points to this time horizon (Santos 1971; most complete coverage by Conejo Delgado 2019). Thereafter, the area was abandoned and probably only resettled in the fifteenth or sixteenth century. After the 1755 Lisbon tsunami, new short-lived buildings belonging to the aforementioned Portuguese Royal Fishing Company were constructed, the ruins of which are still visible (Bernardes and Medeiros 2016; Bernardes 2007; also Figs. 10.3 and 10.4).

10.4 Extent of the Fieldwork and applied Methodology

The campaigns conducted during the three years of fieldwork were based on a comprehensive survey of the site in the spring of 2017. This included geological drillings in the alluvial plain (Fig. 10.4; Feist et al. 2019), a geophysical measurement campaign (Fig. 10.3; Bernardes et al. in press; Hermann et al. 2022) and a detailed archaeological recording of the marine cliff's stratigraphy in 11 profiles (Fig. 10.5).

The results of the geophysical prospection (geomagnetic, resistivity and georadar) allowed for the analysis of the site as a whole, as well as the detailed identification of the individual building structures. Based on these insights, those structures whose outer shape and features ensured a heterogeneous sampling, especially as regards their chronology, and thus a representative cross-section of the history of the site's industrial area,

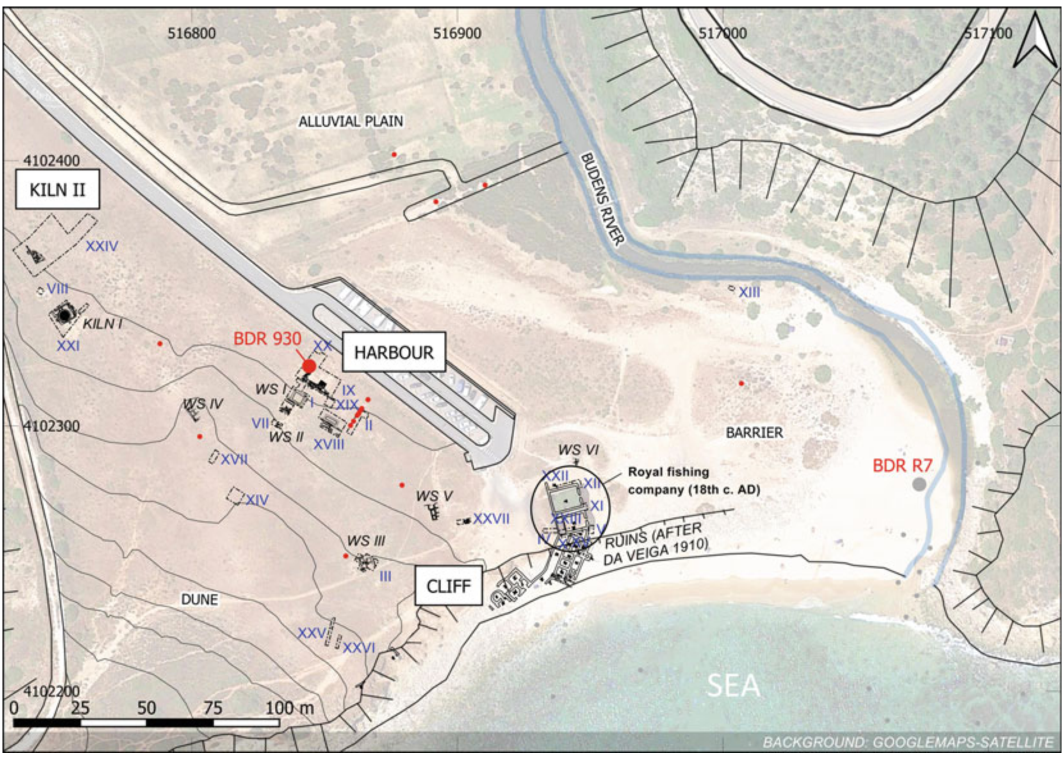

Fig. 10.4 Location of the archaeological trenches (blue, numbering after Table 10.1), sediment cores (red) and reference sites (grey), highlighting the three areas covered in this study (cliff, harbour and kiln II)

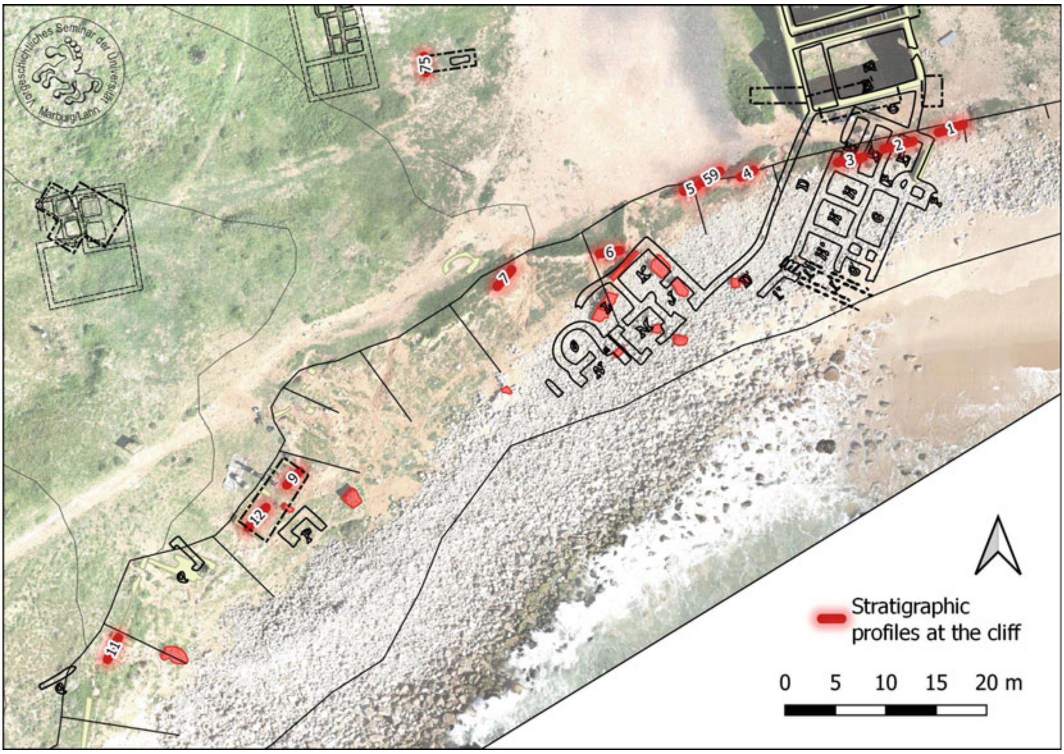

Fig. 10.5 Orthographic view of the beach area indicating the structures documented in 1878 (da Veiga 1910) and the cliff profiles mentioned in the text. Further inland, the partially excavated workshops III (west) and V (north) are shown (cf. Fig. 10.4). For the recent highly dynamic development of the cliff and its possible impact on the coastal settlement, see Hermann et al. (2022). Background image: own orthographic photograph, spring 2017

were selected systematically in 18 archaeological diagnostic trenches excavated during the subsequent campaigns (Fig. 10.4; Table 10.1). Following the excavation of first trenches during the 2017 summer campaign, three fish-salting workshops (WS I–III, Fig. 10.4) could be identified, thus supplementing the three unearthed previously in Alves' excavation (WS IV–VI, Fig. 10.4; Alves 1997). Of the first group, trenches I and II, and subsequently also IX, XVIII, XIX and XX, consecutively recorded relevant parts of workshop I and the associated harbour

Table 10.1 List and characteristics of selected trenches excavated in the industrial area, plus their connection to trench profiles and samples as mentioned in the text. For their location, see Fig. 10.4

	Campaign	Excavated structure	Investigated area (m^2)
I	Summer 2017	Workshop I, production area and harbour facilities	57.0
II	Summer 2017	Workshop I, storage rooms	12.5
IX	Summer 2018	Harbour facilities in front of workshop I	8.0
XIX	Summer 2018	Workshop I, production area	9.5
XX	Spring 2019	Harbour basin in front of workshop I **Profile 58, sediment core 930, bulk samples**	61.0
XIV	Summer 2019	Kiln II **Profile 58**	70.0

facilities (Bernardes et al. in press). In 2018, workshop II was investigated in trenches VII and XVIII, while workshop III was documented in trench III during the 2017 summer campaign (Fig. 10.4). After the promising results yielded by test trenches VI and VIII in the spring of 2018, a part of the pottery workshop to the north of the settlement was investigated in trenches XXI and XXIV in the following year. At two different locations, a Roman waste dump extending along the south-western edge of the settlement's boundary was documented in trenches XIV, XVII, XXV and XXVI.

In this study, a number of archaeological and geological features (walls, levelling layers, event layers, etc.), whose unique IDs is given in brackets (…), are addressed. This follows the excavation documentation based on stratigraphic units (UE, 'unidade estratigráfica').

10.5 Results and Interpretation

10.5.1 The Settlement

According to the geophysical measurements, the Roman settlement extended in a NW–SE direction approximately 180 m along the palaeo-estuary (Hermann et al. 2022; Fig. 10.3). Most of the remaining structures are fish-salting workshops, as demonstrated by recent excavations (Bernardes et al. in press). Their estimated accumulated vat volume distinguishes Boca do Rio as a supra-regional centre of this non-agricultural economy. Parts of these workshops, three of which have been diagnostically excavated in 2017–2019, are presented in this chapter. The northern part of the settlement is occupied by a small pottery workshop with two pottery kilns, of which kiln II will be briefly described here.

10.5.2 The Cliff

The profiles mapped along the current sandy cliff in the spring of 2017 (profiles 1–7, 9, 11–12), the spring of 2019 (profile 59) and the summer of 2019 (profile 75 in trench 27) were primarily intended to provide a stratigraphic overview (Fig. 10.5). Since numerous archaeological features (walls, debris layers, etc.) were already visible in the eroded coastal profile, a broad chronological cross section of the settlement's development on the site could be anticipated.

The connection between the stratified wall segments identified in the profiles of the active cliff, and the structures known from earlier investigations is of great importance for the interpretation of the settlement's development. Yet, the ground plans of the walls are only known with sufficient certainty in individual cases, such as profiles 9 and 12 (building P in da Veiga 1910) and profiles 2 and 3 ('*thermae*' building B/E in da Veiga 1910). Profile 11 was located directly between the two uppermost parts of the building (121) on the dune, which are only partially known ('cistern', building Q in da Veiga 1910). Of the 11 profile sections documented, profiles 2 and 3 forming the lower part, and 9 and 12, the higher part of the cliff, offer the aforementioned valuable connection with the building structures, which is why they are discussed here in detail. As the general stratigraphy observed in those profiles is similar to that of the other profiles, they are taken as representative of the cliff's general evolution.

Profiles 2 and 3 (Fig. 10.6) are located between the walls (138) to the west and (1) to the east, which belong to corridor D and rooms B/E, after da Veiga (1910) in Fig. 10.5. The archaeological features found are therefore primarily the filling of the interior of this building. The two separating walls of room E, as noted by da Veiga (1910), which divide the two profiles (71, 110), were also documented.

The oldest recorded structure in relative chronology is the remnant of a wall (97) with a preserved top at 3.70 m a.s.l. (above mean sea level), built directly on top of the boulder beach surface (Fig. 10.6). With a green compact loam band at 3.60 m a.s.l. further west (87), a loamy rammed earth floor probably associated with this wall is fragmentarily preserved.

The following levelling works (83, 85, 86; 92, 108) form a horizontal stratum covering the wall

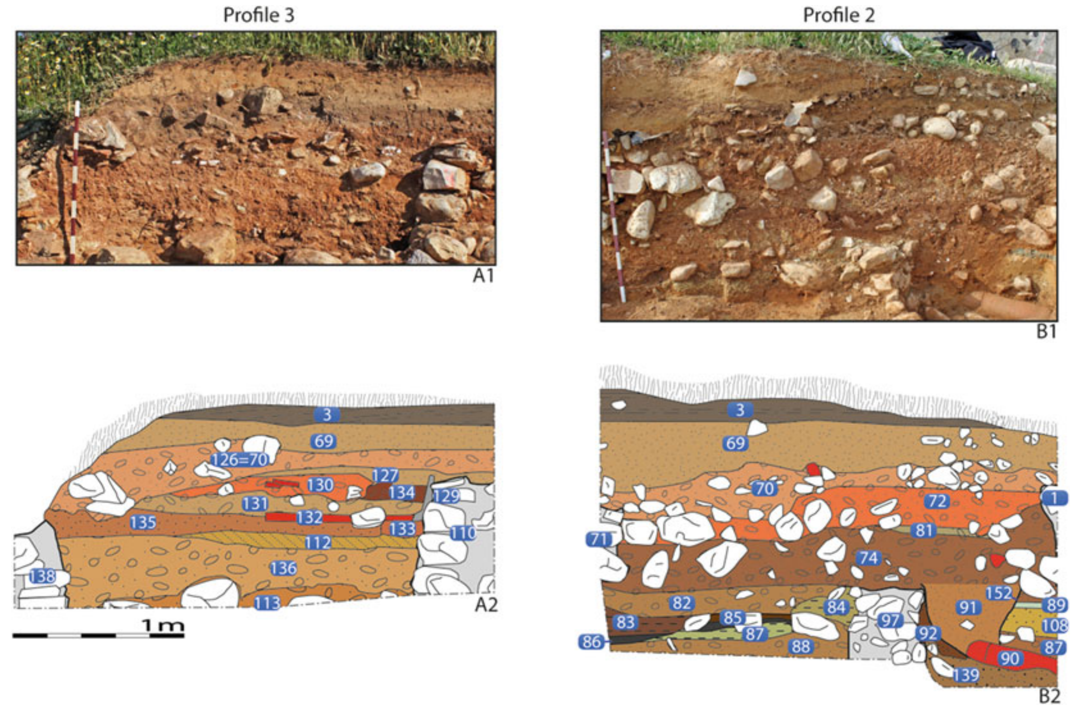

Fig. 10.6 Photograph and schematic presentation of neighbouring cliff profiles 3 (A) and 2 (B). The profiles are limited by the walls of the surrounding Roman structures; only the main features mentioned in the text are numbered. Profiles face south

(97) at 3.75 m a.s.l. In places, it can be seen that their common upper edge is terminated by a compact greenish loam layer (89 = 84). This shaped an occupation level and is only documented between the walls (1) and (110), whereas it seems to be non-existent to the west, namely, towards the wall (138). However, this wall (138) has the same depth of foundation as the walls (110) and (1), that is, directly down to the beach surface. It is possible that the floor in the area between the walls (110) and (138), which would have consisted only of rammed clay, was destroyed to such an extent in later times so as to be currently unidentifiable (see below). This, however, cannot be clarified without further archaeological interventions. On the other hand, it is certain that the floor (89 = 84) identified between the walls (110) and (1) is linked to the earliest use of those later walls.

This floor (84/89) had subsequently been affected by the digging of a pit (152) for the construction of a water pipe (90). The filling of the pit with silty sand and rubble (91), together with a further levelling layer (82), formed a new walking horizon, which was raised by 0.18 m to an absolute height of 3.93 m a.s.l. In this phase, the area between the walls (110) and (1) was also further divided by the construction of a small wall (71) above the old walking level (84). For the first time, a walking level in the form of a red rammed earth floor (132) can also now be detected to the west of the wall (110), namely, between the walls (110) and (138). At 4.40 m a.s.l., this is slightly higher than the walking level between the walls (110) and (1) and has a foundation of massive levelling of the area between the walls (138) and (110), formed by the layers (113), (136), (112), (133) and (135). The connection between the floor level (132) and these walls is marked by the corresponding plaster (129) on both faces of the wall (110). Subsequent layers indicate centuries of decay of the structures, while the uppermost layers (69) and (70 = 126) are the result of earlier archaeological interventions, like Alves' excavation in 1982 (Alves 1997).

Unfortunately, there is no stratified, datable archaeological material available in profiles 2 and 3. However, the surface formed by the red rammed earth floor (132), (89 = 84) as well as the plastering (129) on the wall (110), is the southern continuation of the features excavated in 2010 by Bernardes and Medeiros (2016), who identified a fragment of South Gaulish Samian Ware Drag. 29 found beneath the layer (87). According to their results, the second stage of construction identified in the profiles, that is, the walls (1), (110) and (138), as well as the plaster (129) and the surface (132), may therefore date, at the earliest, to the first half of the third century AD. The preceding construction, namely the wall (97), is thus of a relatively earlier date (late first / early second century AD), while the segmentation of the eastern space E'/E' by means of the wall (71) is somewhat later.

Profiles 9 and 12 (Fig. 10.7) are located in the eastern (9) and western (12) parts of two rooms visible in the cliff. In da Veiga (1910), they are documented as part of building P (Figs. 10.5 and 15.7). In profile 9, a trench was excavated to a depth of 2.50 m below the preserved floor level of the rooms at 7.65 m a.s.l, and in profile 12, to a depth of 1.60 m. In this way, it was also possible to document the deeper sand layers of the dune, namely (119, 114, 120, 117, 33), in profile 9.

The oldest identified layers are well stratified dune sands (profile 9: 119, 120, 33; profile 12: 115, 116) with up to 0.20 m thick reddish brown, slightly loamy horizontal discolourations with clear traces of bioturbation—signs of incipient soil formation on the dune surfaces (114, 117). On top of one of these surfaces (114), at 6.30 m a.s.l., the coarsely fragmented remains of a Dressel 7–11 fish sauce amphora and some quarry stones were found. In contrast, the other sand layers did not yield any archaeological finds.

The upper part of the sand (33 = 116) shows a grey humus section with clear traces of bioturbation (31 = 118). It seems to have been exposed for a long time and to have been overgrown by vegetation. Finally, clayey layers (profile 9: 28, 24, 25; profile 12: 42, 41), with inclusions of building material, in particular lime mortar (27, 34), and a layer of ash and charcoal (26), were deposited on top of it in close temporal succession—most likely the building layers associated with the surrounding structure.

In both profiles, but especially in profile 9, the change from the use of a natural, unpaved surface within the dune, i.e., the layers (114) and (117), to the construction of the building can be clearly observed. The ceramic material from the sand (115) (profile 12), samian ware of Gaulish as well as Hispanic provenance (115–006, 007, 008; 115–002), as well as the Dressel 7–11 fish sauce amphora, plainly indicate a time horizon for the use of these surfaces between the first and second centuries AD. This is supported by the ^{14}C dating of a piece of charcoal from the layer (114), which hints at a second century AD origin (BDR-17–145; Table 10.2). In the upper layers (33) and (28) in profile 9, and the layers (116), (42) and (41) in profile 12, the early ceramic material (28: 028–001; 33: 033–004, 005; 116: 116–006; 41: 041–001, 004, 42: 042–005, 009) still predominates. The presence of African kitchenware in (33), however, indicates a later date, namely, well into the second century AD or the beginning of the following one (33: 033–001, African kitchenware Hayes 181 B). The filling (42) under the later floor may then already date from the fourth century AD, as indicated by African kitchenware Hayes 196/185D shards (042–002, 003). It gives a *terminus post quem* for the overlying layers, namely, the ones linked to the building's construction horizon above the sand surfaces (31) in profile 9 and (118) in profile 12.

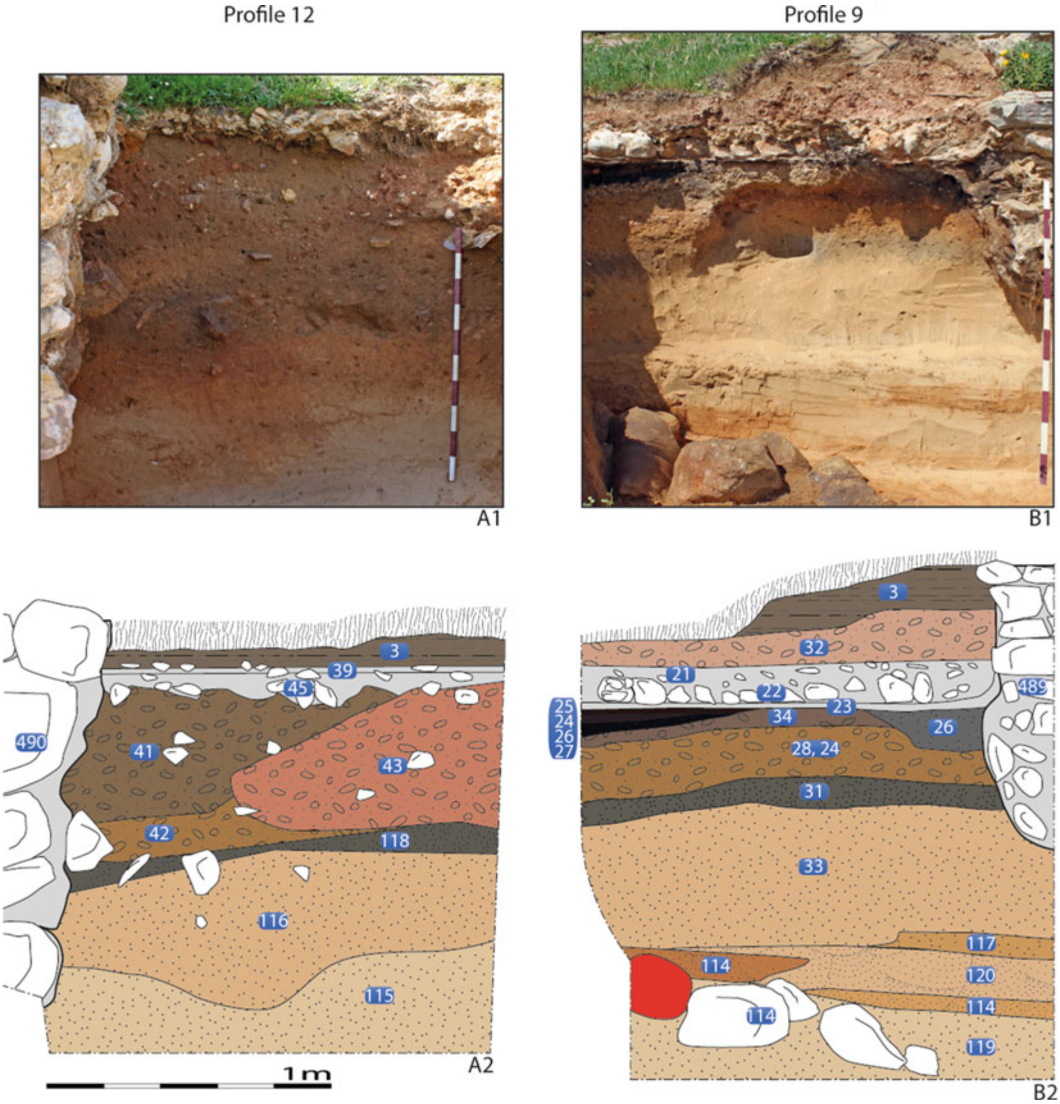

Fig. 10.7 Photograph and schematic presentation of profiles 12 (A) and 9 (B) at the cliff, limited by the Roman wall structures. Main features mentioned in the text are numbered. Profiles face south-east

10.5.3 The Harbour

The identified harbour facilities include parts of a large workshop, listed here as workshop I. A rectangular, NW-SE oriented building, 45.0 m long and 9.5 m wide, is clearly visible in the geophysical measurement data (Fig. 10.3). The regular internal division—production vats—was also evident geophysically and, thanks to the excavation results, a detailed interpretation was possible (Hermann et al. 2022, in press; Bernardes et al. in press). In front of the central segment of the complex, it was discovered that a stone quay, with direct access to the interior of the workshop, had been built.

10.5.3.1 The Quay: Harbour Front, Ramp and Platform

The building was accessible via an elevated rectangular platform measuring 1.20 m × 1.50 m

Table 10.2 Results of ^{14}C (upper part) and OSL (lower part) dating of selected samples mentioned in the text

Sample code (1)	Lab code	Material	Others	14C years (2)	Calendar years (calibrated 2σ)	
BDR-17–145	Poz-104454	Charcoal		1850 ± 30 BP	121-248 cal AD	0.944
Context	Beach profile, PR 9, UE 114					
BDR-18–853	Poz-115463	Charcoal	0.6 mg C	1785 ± 30 BP	210-265 cal AD / 272-351 cal AD	0.342 / 0.608
Context	Trench I (extension spring 2019), Unit I/harbour basin, UE 249					

Radiocarbon dating by ^{14}C-laboratory Poznan. Calibration with Calib 8.2 [calib.org]

Sample code	Lab code	Burial depth (m)	H_2O (%)	U (ppm)	Th (ppm)	K_2O (%)	Cosmic (Gy)	Dose rate (Gy/ka)	Age (ka) before sampling in 2019	Calendar years (calibrated 1σ)	Model (3)
BDR-T1-2019 35–38 cm	UNL4484	0.365	3.4	0.58	1.11	0.35	0.20	0.682 ± 0.030	0.447 ± 0.030	1572 ± 30	MAM-3
BDR-T1-2019 36–45 cm	UNL4485	0.405	3.2	0.65	0.97	0.32	0.20	0.668 ± 0.029	0.610 ± 0.036	1409 ± 36	MAM-3
BDR-T1-2019 48–51 cm	UNL4486	0.490	3.2	0.45	1.24	0.46	0.19	0.749 ± 0.033	1.05 ± 0.05	969 ± 50	CAM

OSL-dating lab: Luminescence Geochronology Laboratory of the University of Nebraska

1 = BDR + Year of sampling + internal reference number / depth

2 = rounded to closest 5-year step (T. Goslar, Poznan laboratory, 15.07.2019)

3 = Model used to calculate age, CAM = Central Age Model, MAM-3 = 3 term Minimum Age Model, after Galbraith et al. (1999)

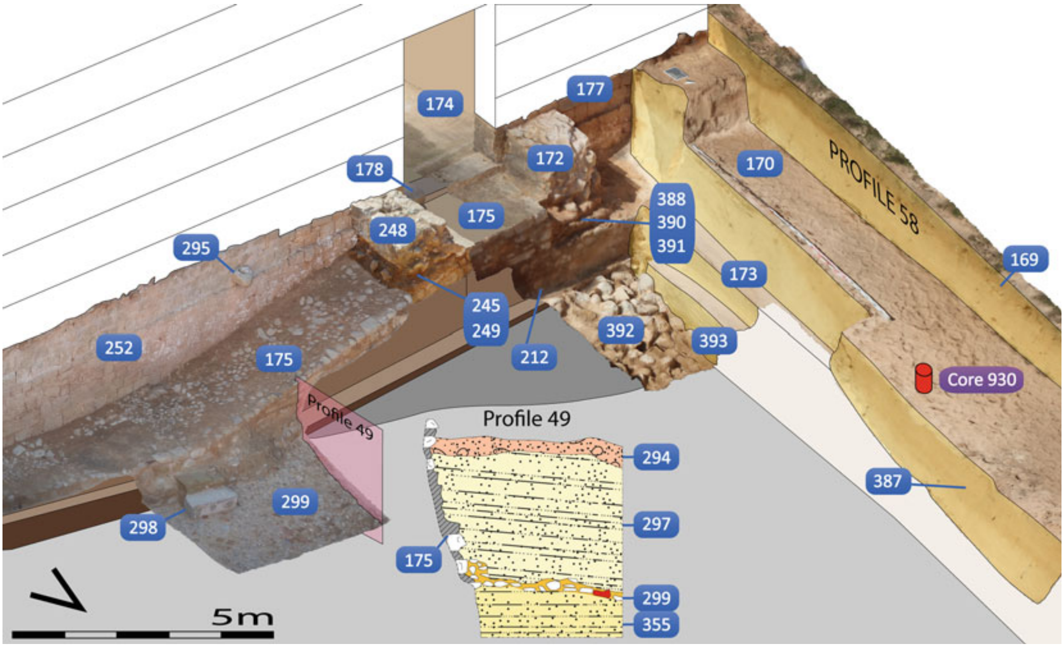

Fig. 10.8 Isometric view of the harbour facilities and the entrance to workshop I, with the position of profile 58 (Fig. 10.13), core 930's sample location and a schematic reconstruction of unexcavated features. The given view equals the proven minimal extent of the event layer (387). The inset shows profile 49 with the preceding palaeo-beach (355) and the early sedimentation layers (297) and (294)

1.30 m at its north-east façade, with a walking surface at 3.12 m a.s.l. (Fig. 10.8). Towards the north-west, this platform drops vertically down to a mat foundation (212) beneath it. To the south-east, however, a 0.15 m step connects the platform with a ramp (175), which has a gradient of around 9.1° and a minimum height of 2.1 m a.s.l. A two-stage staircase (298) built of *lateres* and a monolithic limestone ashlar is attached. Approximately 1.0 m above the level of the ramp (175), a vertically perforated mooring stone (295) protrudes 0.26 m from the façade of the wall (252) towards the former estuary. It shows clear signs of local abrasion along the edges of the inner side of its 0.10 m wide bore hole.

Typical biological markers such as barnacles (*Chthamalus* spp.) for the upper littoral zone, or limpets (Patellidae) for the middle littoral zone (cf. Laborel and Laborel-Deguen 1994, 2005), were not identified on the structures of the ramp or its foundation.

An approximately 5 cm thick layer of poorly sorted pebbles diameters of 2–6 cm (299) was found just below the bottom step of the staircase. It was mixed with medium-sized shattered and partially much worn ceramic material, broken shell fragments and traces of lime plaster. With its upper edge sloping slightly towards the north-east, this ancient surface can be interpreted as an intentional, anthropogenically reinforced beach section between 1.37 and 1.26 m a.s.l.

Beside the quay, an approximately 2.4 m-wide rampart of boulders (392) was placed in front of the walls (177 = 252) and their foundations (212) to support and protect the structures from waves and tides.

The quality of the construction, namely, the use of representative ashlar masonry in the quay wall, recalls the structure of kiln II (see below), as well as the earliest construction phase documented in the *thermae* area (Bernardes et al. in press). These structures may have formed part of the same building programme, which would have been carried out in the second century AD.

However, the decisive factor for the initial dating is the *terminus ante quem* given by the material of the subsequent modification of the quay (see below).

10.5.3.2 Changes in the Building Stock of the Quay and the Sedimentation of the Harbour Basin

In a second construction phase, roughly constructed quarry stone walls were erected on both sides of the rectangular platform (175), orthogonally adjacent to the outer wall (177 = 252). These—(248) to the south-east and (172) to the south-west—are between 0.90 and 0.95 m wide and extend over the width of the ramp (175) and the foundations (212) below. Due to their coarse type of construction, the two walls are quite distinctive in comparison to the original structure. Remarkably, both walls were erected at a distance of 0.25 m from the original platform (175), thus leaving 1.40 m long rectangular gaps, with a width of 0.25 m and a depth ranging from 0.15 to 0.20 m, between them.

They were both built on top of a more or less complex sequence of sediments and levelling layers. South-east of the ramp, on the original surface of the harbour basin, corresponding to the gravel layer (299), medium-sized sand (297) was deposited in 1–10 cm fine horizontal stratification layers (Fig. 10.8). Between these slightly NE-declining levels, isolated ceramic material and the bone fragments of small fish were found. This sediment reached the upper edge of the stairs (298) and the foundations (212). The sand layer (297) was overlaid by a light yellow, loose fine sand (294), with a thickness of about 0.60 m, which extends over the upper part of the ramp (175).

To the south-east, these naturally deposited layers (297, 393, 294) were followed by the clayey levelling layers (245) and (249), with the wall (248) resting directly on their surface. An accumulation of small to medium-sized field and quarry stones in the top levelling layer (249) served to reinforce the foundations.

To the north-west of the ramp (175), three levelling layers (391), (390) and (388), together only 0.5 m thick, were stacked on top of the foundations (212). With an irregular layer of small and medium-sized stones, the uppermost layer (388) formed the solid ground on which the wall was built (172) (Fig. 10.9).

The dating of this modification is mainly based on ceramic material from the aforementioned levelling layers. Regarding the construction of the walls built on top of them, they give a *terminus post quem*. Two fragments originate directly from the wall (248) itself (248-001: African kitchenware Hayes 23 B, 248-005; and Hispanic samian ware (TSH) base 27 or 24/25). Since the material is quite homogeneous, these works might have been carried out more or less simultaneously. In contrast, material from the sediments dating from before the modification work already contains African red slip ware (ARS-D) (236-033), which did not appear in the levelling layers below. This absence indicates that the modification took place, at the latest, in the first decades of the third century AD. A fragment of charcoal (BDR-18-853, Table 10.2) from the levelling layer (249) was ^{14}C-dated to 210-351 cal AD. In connection with the aforementioned chronological range of the ceramic finds, the overall picture of the levelling layers and the wall (248) points to the late second or the first half of the third century AD as a probable date for the modification work.

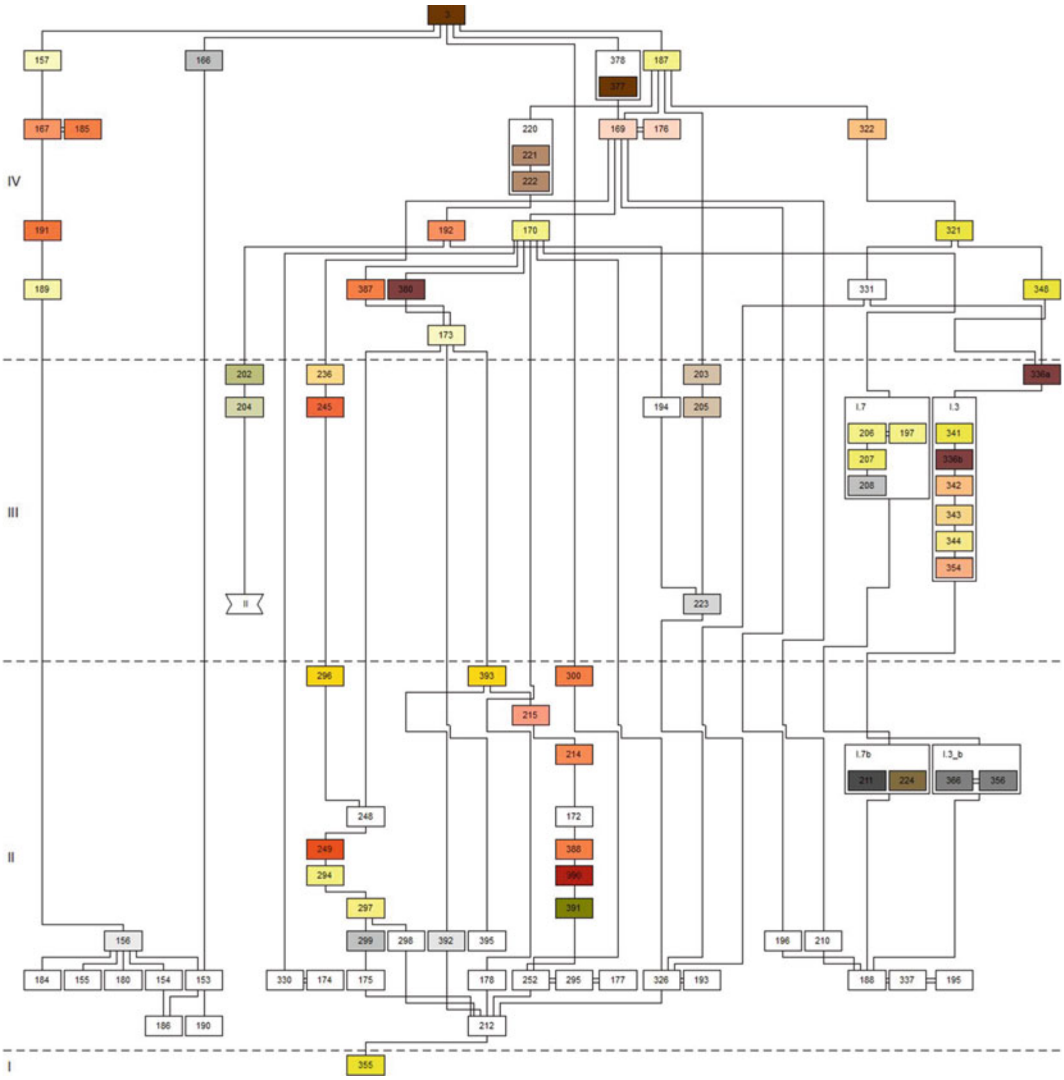

Fig. 10.9 Schematic representation of the stratigraphic units identified in sections I, IX, XVII, XVIII and XXI (see Fig. 10.4). The colours represent an approximation to the original colour of the layers. The white boxes represent construction elements (walls, floors/reinforced surfaces, etc.)

10.5.4 Kiln II

Of kiln II, located to the north of kiln I, only parts of the combustion chamber and the fire tunnel remain. As indicated in the results of the geomagnetic measurements (Fig. 10.3), the north-eastern half of these structures is lacking. It was not a stand-alone kiln, but integrated into a building made of clay pit walls with a stone base (442, 453). Parts of the rising wall structure were found to the west and south-west of the kiln in a collapsed position.

The stratigraphy around kiln II is mainly composed of undisturbed sands (457), as shown in profile 69 (Fig. 10.10). Sedimentary indicators hint at a subaerial beach environment at least for the lower part of (457). Below, a palaeo-riverbed (486) can be seen, indicating a former course very different from the river's present position in the east of the valley (Fig. 10.4). Roman tile

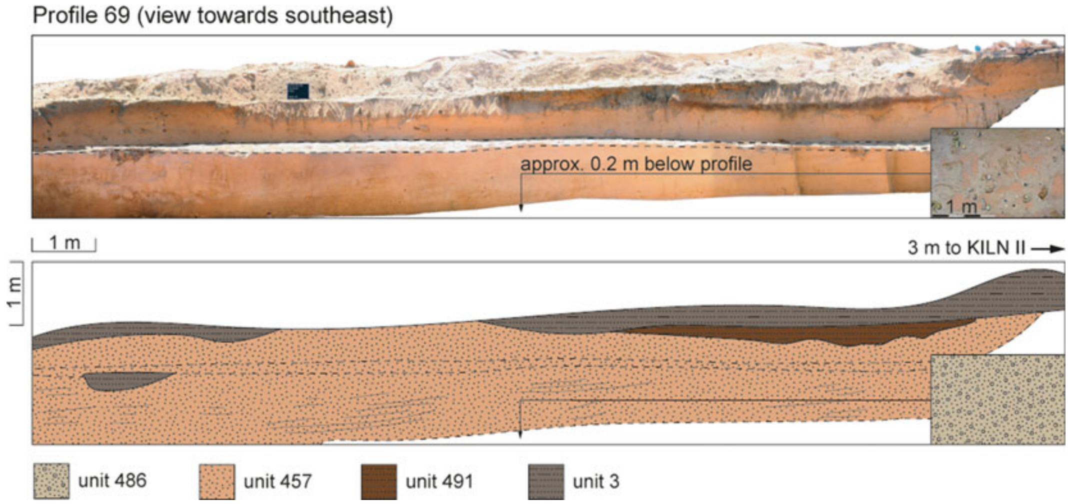

Fig. 10.10 Photo and simplified stratigraphy of profile 69. Unit 486 describes a palaeo-riverbed ca. 0.2 m below the documented profile (inlet). Unit 457 is composed of undisturbed sands, unit 491 is composed of silt and possibly part of a late Roman dirt track, and unit 3 is the uppermost top soil. The dashed lines highlight the stepped profile

fragments scattered on top of this surface already indicate an anthropogenic, that is, Roman, presence during that time. Due to the established general development of the settlement (see above), this surface should not be dated to earlier than the first century AD, the beginning of the settlement activity in Boca do Rio. The sand (457) is covered by the current top soil (3) and a silty layer, possibly a (late Roman) dirt road (491).

10.5.4.1 The Structure and Features of Kiln II

Kiln II was constructed as an updraft kiln, with the firing and combustion chambers aligned vertically. A round central column in the combustion chamber supported the perforated floor of the firing chamber (Figs. 10.11 and 10.12).

From the 1.68 m high preserved combustion chamber (435) a slightly elliptical semicircle with a width of 2.20 m is still visible. On the basis of the existing curvature, this can be reconstructed pointing to internal dimensions of 2.45 m × 2.20 m.

In the middle, there was a collapsed column of mud bricks, 0.60 m in diameter. The exterior wall (442) of the kiln building provided a representative façade and enclosed a rectangular area of at least 7.50 m × 4.0 m. Due to the massive destruction of the feature (see below), it is no longer possible to clarify its eastern extension with certainty. Only its length can be apparently established with certainty by the corner of the foundations to the north. Thus, there was an enclosed area of at least 3 m × 3 m in the apron of the fire tunnel. The contemporaneous occupation layer at 3.30 m a.s.l. consisted of a compact layer of red silty loam mixed with small fragments of limestone and sandstone (464). Due to its bad state of preservation, it was only found on a 0.40 m × 1.50 m strip west of the fire tunnel.

Inside the kiln, a single-layer floor paving of fired bricks (465) was laid out at 2.54 m a.s.l. Along its entire lower edge, and clearly less so below the fire tunnel, the sand underneath was partly vitrified. The fire tunnel to the north-west had a total length of about 1.60 m and was spanned by a round brick arch. The latter is only partially preserved, but based on the imprints of the bricks of the paving on the underlying vitrified sand, its reconstruction indicates that it would have had a width of approximately 0.70–0.80 m.

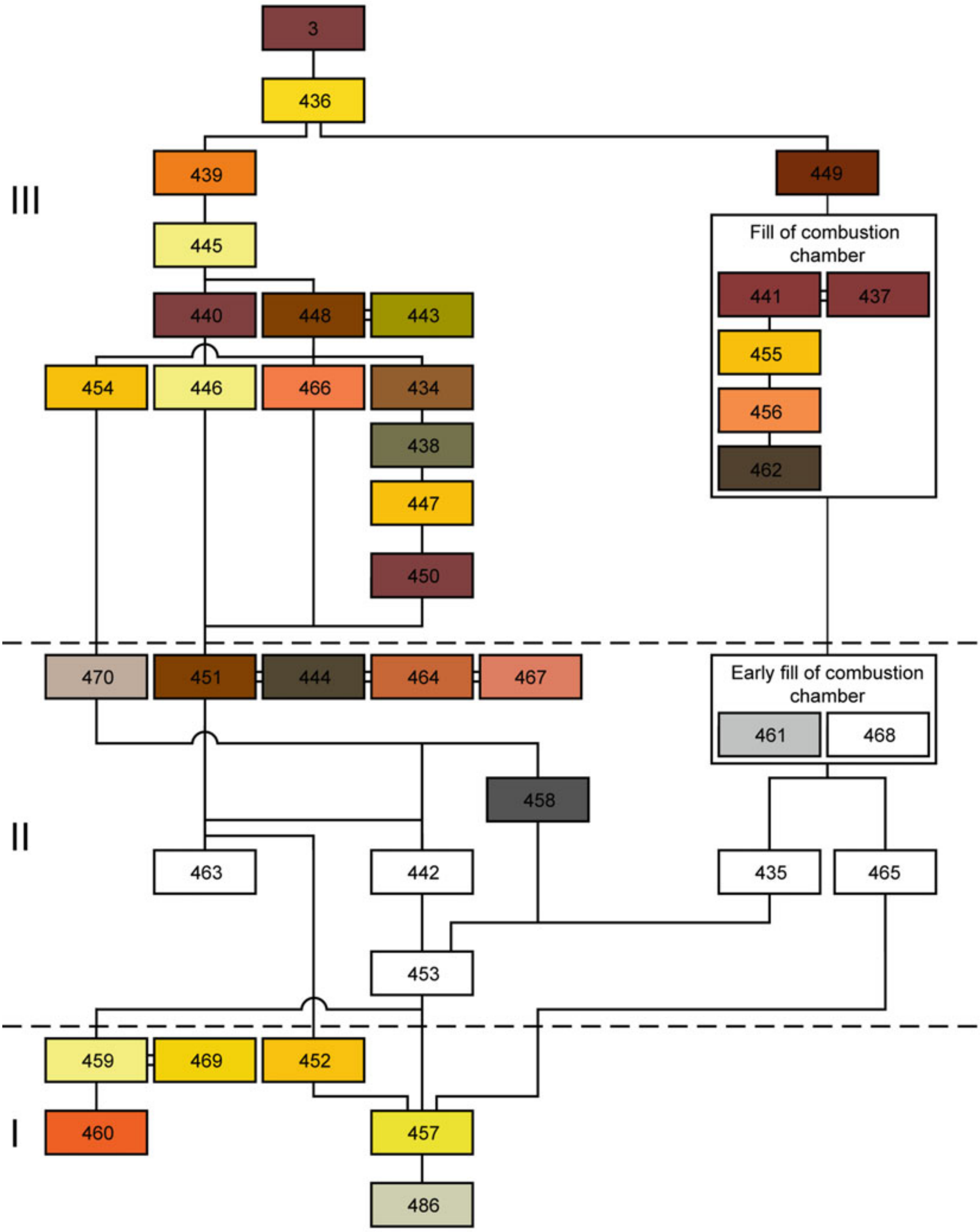

Fig. 10.11 Schematic representation of the stratigraphic units identified in trench XXIV (see Fig. 10.4) in the summer of 2019. The colours represent an approximation to the original colour of the features. Note the distribution of undisturbed (aeolian or littoral) sands in light yellow and anthropogenically influenced areas (loamy; reddish, brown). The white boxes represent architectural elements (walls, paving, etc.). Also, the three phases of the kiln (I = until construction, II = use and III = abandonment) are already visible

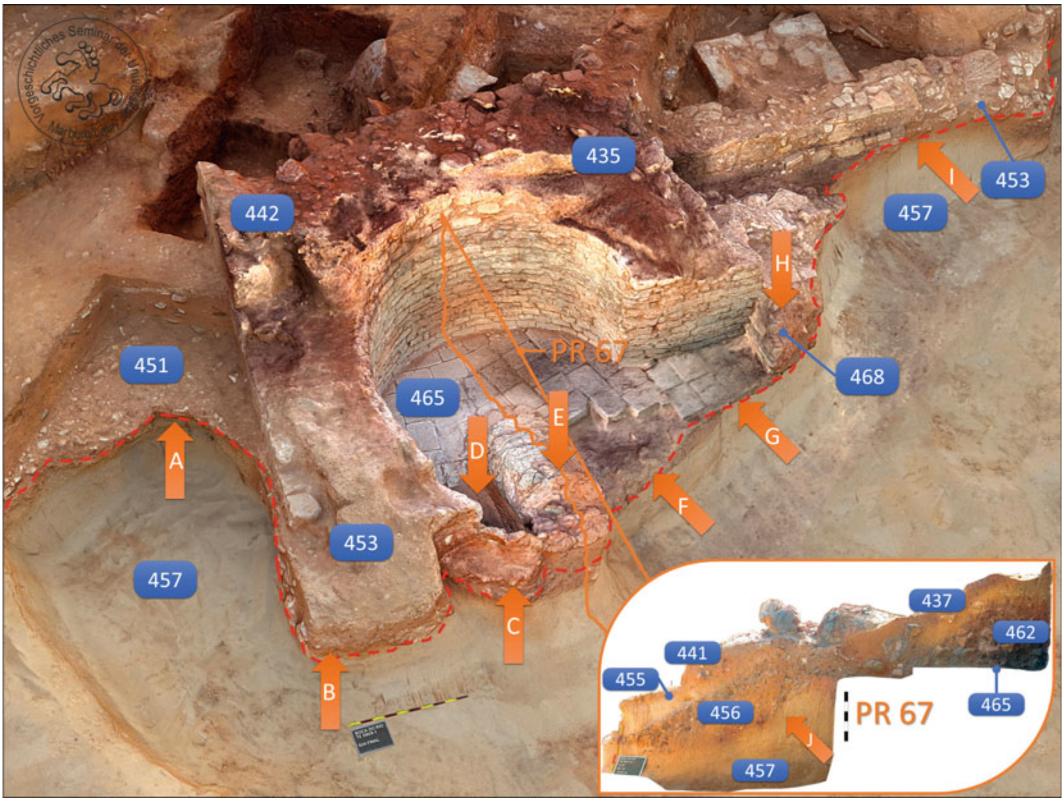

Fig. 10.12 Kiln II, highlighting the damage to the structure (orange arrows) and the limit of its conservation (red dashed line). Selected UE numbers mentioned in the text are noted in blue. Perspective from the east. Inset: NE–SW profile 67

Outside the kiln, a continuous paved surface was found to the west, south-west and south (458, 470 = 444 = 451 = 467) at about 3.30 m a.s.l. Due to its correlation to the upper edge of the foundations (453), it can be considered to have been in use at the same time as the structure.

From the area of trench XXIV, 11 datable ceramic pieces have so far been recovered and identified. The six pieces of African, three South Gaulish and two Hispanic kitchenware originate from three contexts: Post or late use waste layers (441) and (443), plus a surface used before the reinforced paving (458) around the kiln. In spite of the problems associated with their exiguousness, these pieces roughly indicate a possible period of activity of the kiln area between the second half of the first and the mid-third centuries AD.

Two of the early South Gaulish *sigillatae* (458-001: TSG Drag. 18, and 458-002: undefined base TSG) were recovered from the walking level (458), which correlates with the first usage of the kiln (see above). They provide a *terminus post quem* in the second half of the first century AD for the kiln's construction and usage. Taking into account the later deposits (434, 441), the kiln was most likely built at the end of the first or at the beginning of the second century AD.

The next datable deposit comprises the waste layers to the south-west of the kiln (434, 441). They contained organic and plentiful ceramic finds, of which the fine ceramics were chronologically quite homogeneous, with just three exceptions. Only two types of African kitchenware were found: one Hayes type 196 and five type 197. The other three pieces are Hispanic

Drag. 15 and 33, and a South Gaulish form (434-023: TSH Drag. 15, 434-024: TSH Drag. 33, 434-025: TSG, undefined base). Due to the great homogeneity of the pieces of African kitchenware, which provide a *terminus post quem* for their deposition in the last third of the second century AD, it may be assumed that the older pieces are scrap.

As later material is absent, the deposition of this settlement waste, namely, the continuous use of the exterior area of the kiln, probably took place during the circulation time of the aforementioned ceramic forms, that is, between the end of the second and the middle of the third century AD. The findings' homogeneous composition points to an abandonment of the area shortly afterwards. In fact, it might have been linked to the destruction of the kiln, whose characteristics are described in detail below.

10.5.4.2 The Destruction and Abandonment of the Kiln

The kiln and its extensions are heavily damaged along a NW–SE axis running across the structure (Fig. 10.12, red dashed line). While the parts of the structure to the west of this axis have been preserved, those to the east no longer exist.

First, the solid surface level (451) surrounding the kiln displays, especially in the southern part, a concave incision. Originally, it would have surrounded the structure (Fig. 10.12 A). At the easternmost point, the foundations are preserved only in a low-lying stone layer (B), above which only (later) collapsed material of the kiln wall (442) was found (E). A similar degradation can be observed to the north (I, H). At point C, the outer façade of the kiln wall (435) is reduced to the more stable vitrified inner half of the wall which was originally roughly 0.5 m thick; besides, the entire eastern flank of the kiln has disappeared without a trace. The debris layer (456) documented in profile 67 includes the collapsed material of the kiln's superstructure, like the firing chamber's floor, but not that of the enclosure (J, Fig. 10.12; inlet with profile 67). Inside the combustion chamber and fire tunnel, only the western part of that paving is preserved (C, D, G). Below the central column, the eastern part of the floor is also missing, which subsequently led to its collapse. Surprisingly, the underlying partially vitrified sand (= surface of 457) is still in place. The debris layers (456) and (441) deposited to the east of the kiln reach below the walking level of (465) inside. This underlines the fact that the sand (457) supporting the paving (465) had a distinct eastward slope at the time when these layers were deposited (Fig. 10.12 PR67). Originally, however, this substratum must have reached up to the lower edge of the paving (465). During or (shortly) before the destruction of the kiln, substantial parts of the sand appear to have been removed.

From these observations, the following conclusions can be drawn regarding the destruction of the kiln: it was an erosive process or an event that changed the appearance of both the building structure and the underlying sand (457). It was fast or repetitive enough to prevent sediment from being introduced to compensate for the void in the underlying sand (457), before the building material of the kiln collapsed into the created hollow. It was unsystematic, namely, it was not that certain parts of the building structure were damaged while others were spared; it took place on a broad front, affecting the entire structure and its surroundings. Ultimately, the destruction was massive enough to weaken the statics of the structure to such an extent that it disintegrated completely and a large portion of debris was carried away.

10.5.5 An Event Layer in the Harbour Basin and its Geophysical Description, UE 387

Still considered as being part of the sands (170) in the 2017 summer campaign, a very characteristic sediment layer (387) sandwiched between the deposits (173) and (170) was identified in the course of the following year's campaign (Fig. 10.13). This layer has been shown to

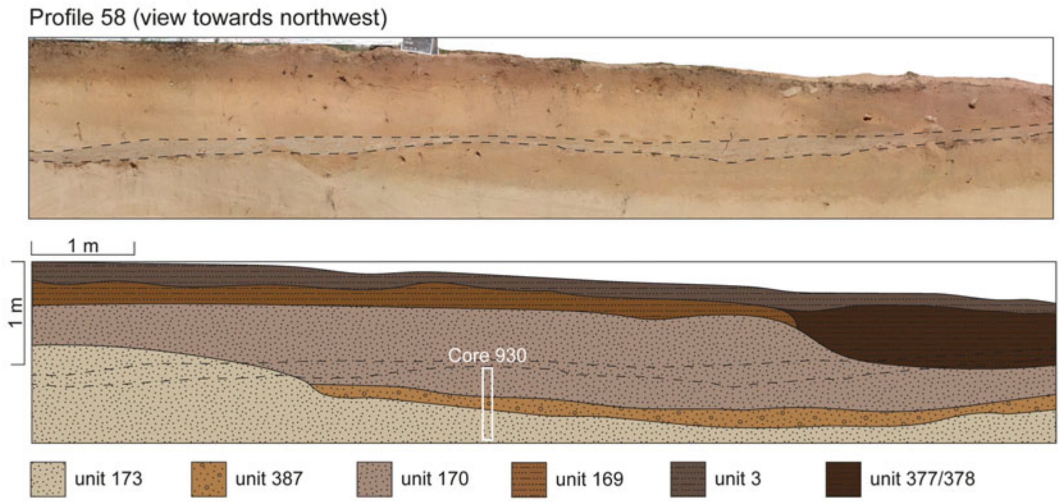

Fig. 10.13 Photograph and simplified stratigraphy of profile 58, including the location of sediment core BDR 930 (Figs. 10.4 and 10.8). The harbour facilities are located to the left. The dashed lines highlight the stepped profile

have a minimum extension over the entire harbour basin of 11 m × 9 m (=area excavated so far) (Figs. 10.8 and 10.13).

The most recent deposit in the area of the harbour basin is an approximately 0.2 m thick layer of debris (169). This layer extends up to the middle of workshop I, before slowly beginning to thin out uphill. Inclusions in this poorly sorted sediment are very often small to medium-sized stones from quarries and fields, shell fragments and mortar and plaster remains. This younger event layer (169) presumably matches that of the AD 1755 Lisbon tsunami, which has been widely preserved in the Boca do Rio floodplain and other locations along the Algarve coast.

For further analysis, a 71 cm long sediment core BDR 930 was drilled, which covered the sequence of early sedimentation of the basin (173-387-170; Fig. 10.13) (Table 10.3).

Composition of core 930

In general, the stratigraphy of the 71 cm long core BDR 930 is composed of three different sediment units. The lowermost unit (173), at a core depth of 37–71 cm (Fig. 10.14), consists of poorly sorted medium sand (1.6 Φ; Table 10.4). The upper part, until a core depth of approximately 45 cm, is slightly richer in shell fragments than the lower part of this unit. The colour is greyish orange (10 YR 7/4, Munsell Rock Color Chart 2009), while the magnetic susceptibility results give an average of $-1.4 * 10^{-5}$ SI, with $-5.0 * 10^{-5}$ SI as the lowest absolute value at the end of the core. Fe, Ca and Ca/Fe have the lowest values of the whole core (Fe: 1307 ppm, Ca: 50,685 ppm, Ca/Fe: 39). This unit is followed by 5 cm (387, 32–37 cm core depth, Fig. 10.14) of moderately sorted bioclastic medium sand (1.2 Φ; Table 10.4) which is slightly coarser than the other two units. Its colour is light brown (5 YR 5/6). The basal contact to the lowermost sediment unit (173) is clearly erosive. Magnetic susceptibility values for (387) rise to an average of $7.7 * 10^{-5}$ SI, with $12.0 * 10^{-5}$ SI being the highest absolute value at a core depth of 34.0 cm. Fe and Ca increase to 2744 ppm and 79,188 ppm, respectively, while Ca/Fe decreases to 29. The uppermost unit (170, 0–32 cm core depth, Fig. 10.14) consists of well-sorted medium sand (1.6 Φ; Table 10.4) with scattered shell fragments. At a core depth of 7.0 cm, a dark lens is visible, probably representing the remains of plant components. The colour of the uppermost sediment unit is dark yellowish orange (10 YR 6/6). The magnetic susceptibility of this unit

Table 10.3 Sampling and treatment process of the geological samples of the harbour basin

Methodologal approach		Resolution	Device
Volume-specific magnetic susceptibility		2 cm	Bartington MS2 Magnetic Susceptibility System with MS2K Sensor
Elementary composition, X-ray fluorescence (XRF)		2 cm	Hand-held Niton analytical device; exposure time of 45 s
Geochemical analysis of elements Ca, Fe and Ca/Fe ratio	Differentiation between terrestrial and marine environments (Cuven et al. 2013)	Supra	
Textural analysis by wet sieving of bulk samples from the core and its surroundings		10 cm intervals, except possible event layer (387). Idem in 4 cm intervals (29–33 cm upper contact, 33–37 cm possible event layer, 37–41 cm lower contact)	Retsch AS 200 sieve shaker; standard set of sieves in the range of −2 to 4 Φ in whole phi intervals
Micropalaeontological analysis		10 cm intervals, except possible event layer (387). Idem in 4 cm intervals (29–33 cm upper contact, 33–37 cm possible event layer, 37–41 cm lower contact); homogenised fraction of ca. 5–6 g per sample, sieved to >0.063 mm	Zeiss Stemi 2000 C microscope
Foraminifera content, qualitative and quantitative analysis	Minimum 100 benthic foraminifera for low diversity onshore assemblages (Fatela and Taborda 2002) not reached; hence, the distribution to the dominant (>10%), subsidiary (5–10%) and minor (<5%) classes should be considered with caution		

varies, with an average of 3.1 * 10^{-5} SI. Average Fe, Ca and Ca/Fe values for the unit (170) are 2002 ppm, 69,758 ppm and 35, respectively.

All bulk samples are mainly composed of quartz grains (>80% of all grains), with less than 5% of bioclasts. A peculiarity of the sample from a core depth of 33–37 cm (387) are charcoal fragments of different sizes up to 3 mm. The overall micropalaeontological content of all the bulk samples is predominately shell fragments (mainly bivalvia). Enchinoidea and bryozoa fragments exist in smaller amounts, as well as rare (whole or fragmented) foraminifera, ostracoda, gastropoda and whole bivalvia. The foraminifera assemblages of all the bulk samples identified at a species or, at least, genus level can be found in Table 10.5. In all the samples, *Cibicides lobatulus* (Walker and Jacob 1798) and *Elphidium crispum* (Linnaeus 1758) are dominant or at least subsidiary species. Furthermore, *Elphidium* spp. and *Quinqueloculina seminula* (Linnaeus 1758) are dominant species in the two samples from (173; 48–52 cm, 58–62 cm). However, these two samples present the lowest total number of individuals, as well as the lowest diversity in terms of the number of species

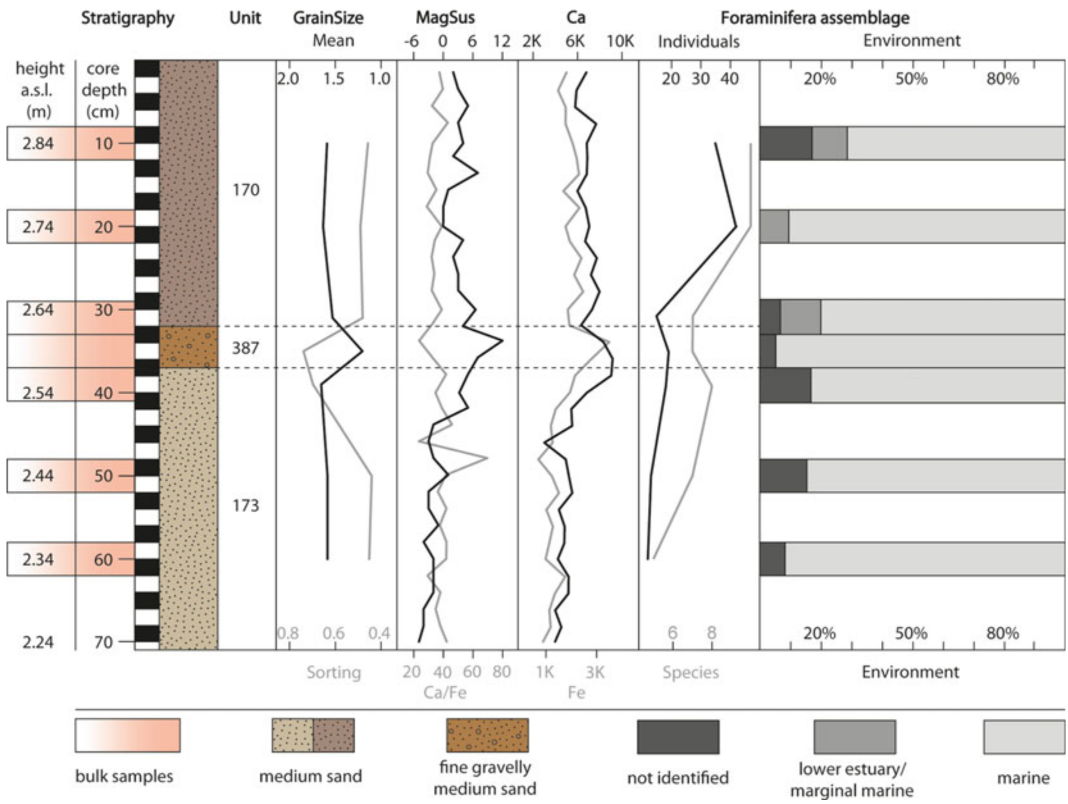

Fig. 10.14 Stratigraphy, sediment units, mean grain size (Φ), sorting (Φ), magnetic susceptibility (*10^{-5} SI) and Ca/Fe, Ca (ppm) and Fe (ppm) results, total number of individual foraminifera, total number of foraminifera species and the suitable environment of the foraminifera assemblage for sediment core BDR 930. The bulk sample depths for grain size and micropalaeontological analyses are highlighted in red

(Fig. 10.14). *Elphidium discoidale* predominates in sample 37–41 cm, the lower contact of (387) (d'Orbigny 1839). In the foraminifera assemblage of unit 387 (sample 33–37 cm), *Ammonia beccarii* (Linnaeus 1758) and *Ammonia* spp. are dominant species. The total numbers of individuals and species are still low, but slightly higher than for unit 173 (Fig. 10.14). *Elphidium williamsoni* (Haynes 1973) and *Haynesina* spp. appear exclusively in the samples from the upper contact of (387; 29–33 cm) and (170; 8–12 cm, 18–22 cm), but only as subsidiary or minor species. Furthermore, *A. beccarii* and *A.* spp. are dominant species in the uppermost sample (8–12 cm). Samples from (170) do not only present the highest numbers of individuals but also exhibit the highest species diversity (Fig. 10.14). For a better identification of palaeoenvironments, the identified foraminifera assemblages of the bulk samples were sorted into marine (*Ammonia* spp., *A. beccarii*, *Cibicides lobatulus*, *Elphidium* spp., *E. crispum*, *E. discoidale*, *Quinqueloculina* spp., *Q. seminula*) and lower estuarine (*E. williamsoni*, *Haynesina* spp.) species (Fig. 10.14). The division was made following Quintela et al. (2016), according to standard environments largely documented in micropalaeontological studies.

Sediment unit (387) consists of a medium sand deposit with an erosive basal contact and abundant shell fragments (Fig. 10.14). The granulometric results, especially a coarser mean grain size and poorer sorting (Table 10.4), differentiate it from the over- and underlying littoral sediments (units 170 and 173; Fig. 10.14). Calcium (Ca) and iron (Fe) values are also high

Table 10.4 Grain size statistics calculated after Folk and Ward (1957) for seven bulk samples from sediment core 930 and reference samples from bulk sample 855 (palaeobeach, trench 9) and the present-day beach berm R7. Sample 33–37 cm from core BDR 930 marks the possible event layer

Sample core depth (cm)	Mean (Φ)		Sorting (Φ)		Skewness (Φ)		Kurtosis (Φ)	
8–12	1.583	Medium sand	0.455	Well sorted	0.171	Fine skewed	1.12	Leptokurtic
18–22	1.631	Medium sand	0.49	Well sorted	0.215	Fine skewed	1.109	Mesokurtic
29–33	1.527	Medium sand	0.478	Well sorted	0.07	Symmetrical	1.217	Leptokurtic
33–37	1.194	Medium sand	0.74	Moderately sorted	−0.1	Symmetrical	0.86	Mesokurtic
37–41	1.643	Medium sand	0.699	Moderately well sorted	0.065	Symmetrical	1.291	Leptokurtic
48–52	1.576	Medium sand	0.44	Well sorted	0.17	Fine skewed	1.116	Leptokurtic
58–62	1.583	Medium sand	0.451	Well sorted	0.171	Fine skewed	1.12	Leptokurtic
Bulk sample (855)	1.693	Medium sand	0.527	Moderately well sorted	0.248	Fine skewed	1.089	mesokurtic
R7 Beach berm	1.578	Medium sand	0.442	Well sorted	0.169	Fine skewed	1.114	Leptokurtic

(Fig. 10.14). The coarser grain size indicates a higher energy flow regime compared to the surrounding sediment units. Elevated Ca values result from the abundance of shell fragments and other marine bioclasts in the layer (Chagué-Goff et al. 2017 and references therein). In addition to shell fragments and other marine biota, calcium also derives from detrital calcite/dolomite found in the Boca do Rio area, as well as from boulders accumulated on the upper beach (Font et al. 2013). Therefore, parts of the calcium signature can be attributed to the erosion and redistribution of these sediments. Elevated Fe concentrations can be related to siliciclastic components, especially clay minerals and iron oxides that generally correspond to the terrigenous sediment fraction of Boca do Rio's floodplain (Font et al. 2013). Thus, the sediment of unit (387) presents a mixture of marine and terrestrial signatures. The foraminifera assemblage indicates littoral conditions with all identified species deriving from shallow marine environments (Fig. 10.14). Lower estuary or even brackish species are absent in unit (387). Only *Ammonia beccarii* has typically been assigned to hyposaline lagoons and estuaries, but its natural environment is highly variable as this species also occurs frequently among sandy sediments in inner shelf environments (e.g. Murray 1971, 1991). The results of this study show that the lateral distribution of unit (387) is restricted to the area near the Roman harbour (Fig. 10.8). This may be explained by the harbour walls serving as sediment traps, leading to the accumulation of unit (387) behind them.

The sedimentary indicators discussed above lead to the conclusion that unit (387) was deposited by an as yet undocumented high-energy event. Based on micropalaeontological and compositional results, a marine origin of the sediment can be assumed, although the geochemical composition is not fully conclusive. However, the marine origin excludes river flooding as a possible generating mechanism for the event layer; deposition by an EWE, severe storm or tsunami, seems more likely. Nowadays, storms are frequent along the Algarve coast (Ferreira et al. 2008) and geological evidence of

Table 10.5 Foraminifera assemblages of seven bulk samples from sediment core BDR 930. Sample 33–37 cm marks the possible event layer. The following classes have been used to describe the foraminifera assemblage of each sample: + = dominant (>10%), o = subsidiary (5–10%), − = unidentifiable (<5%). Some foraminifera individuals were unidentifiable at a species or genus level due to broken and/or abraded tests

Sample core depth (cm)	*Ammonia* spp.	*A. beccarri*	*Cibicides* spp.	*Elphidium* spp.	*E. crispum*	*E. discoidale*	*E. williamsoni*	*Haynesina* spp.	*Quinqueloculina* spp.	*Q. seminula*	Unidentifiable
8–12	+	+	+	o	+	o	–	o	–	o	+
18–22	o	–	+	o	+	+	–	o		+	–
29–33			+		+	o	o	o	o	+	o
33–37	+	+	+		o	+			+		+
37–41		o	+	o	o	+			o	+	+
48–52		o	+	+	o	o				+	+
58–62			o	+	+					+	o

the storm-induced flooding of the coastal lowlands has been identified at Martinhal (Kortekaas and Dawson 2007) and the Rio Formosa barrier island chain (Andrade et al. 2004). The OSL age of AD 1409 ± 36 (AD 1373–1445, 1σ) matches one of the North Atlantic Holocene storm periods (HSP V: AD 1300–1650; Sorrel et al. 2012), marked by rapid global climate change, influencing the strength and location of westerly winds. Although Andrade et al. (2004) were not able to correlate their results from the Rio Formosa barrier island chain with Holocene storm periods, they identified multiple events of storm-induced overwash of different magnitudes and spatial expressions. Therefore, a storm event is likely to have caused the deposition of unit (387). A tsunami event as the generating mechanism for this unit is provisionally excluded, as there are not enough sedimentary indicators, no similar event layers have been detected in other locations of the Boca do Rio valley and there are no historical records in the Portuguese tsunami catalogue in this respect (Baptista and Miranda 2009).

10.6 Discussion

10.6.1 Size and Importance of the Fish-Salting Facilities of Boca do Rio

Due to the excellent natural conditions for processing marine resources in situ—sufficient salt and good fishing grounds—the site was interpreted early on as a hub in the tight network of the Roman maritime economy. Its connection to the sea has been stressed for a long time (Santos 1971; Alves 1997; more recently: Medeiros 2015; Bernardes and Medeiros 2016; Teichner 2016), while the most recent research has made it possible to characterise it more precisely. It can now be considered proven that the developed area roughly extended over the entire dune slope (Hermann et al. 2022) and that most of these buildings should be regarded as fish-salting facilities (Bernardes et al. in press). Because of its extensive industrial quarter and the total volume of production vats estimated at roughly 700 m^3, the complex was certainly one of the larger ones in the Hispanic provinces of the Roman world (cf. Wilson 2006; Medeiros 2015). Undoubtedly, it must have played a major role in the regional economy.

10.6.2 Identification of Major Upheavals in the Settlement's Development

In the studied sections of the cliff, stratigraphically older and younger anthropogenic alterations, such as building structures and levelling layers, are apparent. In profiles 12 and 9, thick sand deposits form a distinctive separating layer between those older (profile 9: 114, 117) and younger (profile 9: 22, 21, 32) features. Prominent levelling layers indicate the aforementioned changes inside the rooms in profiles 2 and 3. These stratigraphically separated horizons can also be distinguished from each other in absolute chronology. As shown above, the unpaved surface (114) in profile 9, and the wall (97) in profile 2 date from before the third century AD. This contrasts with the stratigraphically younger (building) features, namely the walls (1, 110, 138) in profiles 2 and 3, and the structures in profiles 9 and 12, all of which can be dated to the third or fourth century AD. Since a generally similar, although more fragmentary image also appears in the other cliff profiles (Fig. 10.5), we can assume that this was the general course of the settlement's development in the present-day cliff area.

A comparable process can be observed in kiln II, on the settlement's northern outskirts, which was built in the second half of the first century AD. The latest evidence of its use dates to the end of the second century AD—a finding that in all likelihood should be linked to its destruction. As indicated by the lack of younger ceramic material, the area seems to have been abandoned shortly afterwards. No direct parallel can be drawn between the kiln's destruction and its abandonment, as the material only provides a *terminus post quem* for its destruction.

Also, at the very heart of the settlement, in the large fish-salting facilities, a distinct change can be observed. At the beginning of the third century AD, new facilities were erected there, while the interior of early second century AD workshop I underwent a general overhaul, with its quay—i.e. the harbour facilities—being comprehensively modified.

Changes in the settlement's structures as of the third century AD have been recently reported by Bernardes and Medeiros (2016), although their dataset is only viable for the reduced area around the ruins of the halls of the Portuguese Royal Fishing Company, viz., the alleged *pars urbana*. In light of these accounts, it can now be assumed that, instead of local events or modifications, these changes point to an upheaval affecting the entire settlement and resulting in its comprehensive restructuring, including the location of the local pottery production area. A fundamental change between the high and late imperial periods can be evinced here. The conversion and extension of the settlement from the third century AD onwards seems to have been preceded by a period of relative calm, during which existing building structures or areas were abandoned and siltation became dominant, following which these buildings were demolished.

A remarkable change—especially with regard to the discussed research questions—is the replacement of the previous stone quay by a wooden structure. This measure elevated the entrance level by about 1.0 m (Fig. 10.15). While a certain amount maintenance work on the fish-salting facilities, especially the production vats, was necessary at more or less regular intervals (Driard 2014), there is a more complex reason behind the adjustment of the quay's surface level.

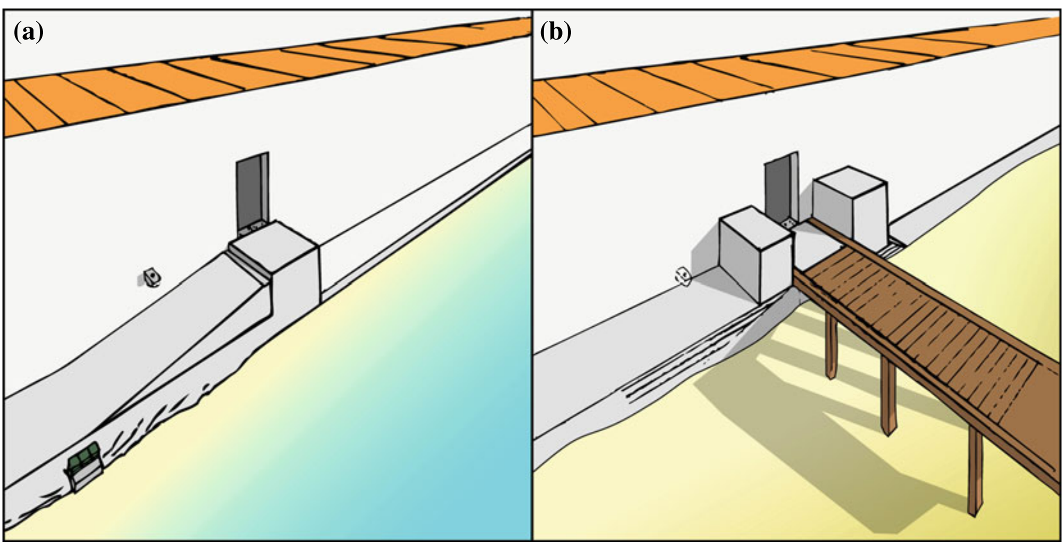

Fig. 10.15 Schematic reconstruction of the entry to workshop I before (**a**) and after (**b**) the third century AD overhaul. In the second phase, it is more than likely that a wooden quay allowed access to what was then a more distant navigable watercourse. Of the original structure, only the platform was still in use, while the former ramp was entirely covered by sediment and levelling layers

10.6.3 Identification and Correlation of EWEs and the Identified Disruption in the Settlement's Development

As yet, no tsunami deposits, apart from those generated by the AD 1755 Lisbon tsunami, have been identified in the field site of Boca do Rio. However, the aim of many previous studies (e.g. Dawson et al. 1995; Hindson et al. 1996; Hindson and Andrade 1999; Cunha et al. 2010; Costa et al. 2012b; Font et al. 2013) was to find and characterise precisely the AD 1755 deposits (and not their possible predecessors). This might explain why no further deposits of previous events have been found to date. Feist et al. (2019) were the first to detect another interesting layer, but this was restricted to one coring site and the evidence was insufficient to confirm a storm or tsunami origin. However, they definitely identified another EWE stratum.

In this study, another interesting layer associated with an EWE, tentatively interpreted as a severe storm event, was detected. The ages and foraminifera assemblages of the layers identified by Feist et al. (2019) and of those presented here do not match, whereby these layers have been interpreted as deriving from different events. This has led to the assumption that additional geological footprints of EWEs, in general, and tsunami events, in particular, may exist at Boca do Rio, but no study has so far been able to detect all of them. It is noteworthy that the tsunami catalogues (Baptista et al. 1998; Baptista and Miranda 2009; Lario et al. 2011) list other as yet geologically undocumented events on the Algarve coast and in the Spanish Gulf of Cádiz.

In this chapter, two profiles covering the entire stratigraphy of the evolution of the estuarine area since Roman times have been presented and discussed (see above, harbour and kiln II). However, only in the harbour basin, perfectly illustrated by profile 58 (Figs. 10.8 and 10.13), have two plausible events been identified. No clearly erosive layer boundaries, signalling the existence of other (earlier) erosive processes, have been found. It can be assumed that the sediments older than the layer (387) are entirely present and that an undisturbed geo-archive of the development of the immediate harbour basin during the Roman era indeed exists.

While the stratigraphically younger event layer (169) presumably corresponds to the 1755 Lisbon tsunami, geologically detected in the Boca do Rio area at many locations, the older event layer, probably the result of a severe storm (see above), was previously unknown. According to the OSL age of AD 1409 ± 36 (AD 1373–1445; 1σ), it dates to late medieval times. Based on these age estimates, both of the identified events should be considered to be irrelevant to the research question of possible EWEs in Roman times. In addition, since a coherent stratigraphic sequence of the harbour basin without any event indicator has been detected (profile 58, Figs. 10.8 and 10.13), the existence of such an event—including its theoretically associated implications for the development of the settlement and the fish-salting industry—should be rejected.

The position of the harbour and the palaeoriverbed in profile 69 indicates that the river followed a different course during the Roman occupation than today. Thus, the estuarine and littoral conditions observed by Allen (2003) and Feist et al. (2019) are supported by our findings. During the Roman age, a wide river mouth was located west of the present-day floodplain, close to the harbour and kiln II. It can be expected to have been considerably larger than it is today, with enough space for the harbour basin and related structures. Major parts of profile 58 close to the Roman harbour structures are composed of quartz-rich littoral sands typical of coastal environments (e.g. nearshore, beach and dune). This is supported by the detailed analysis of core 930 presented above, although only for a limited timeframe (as the core only comprises three units of the stratigraphy). The core's lowermost unit (173) describes the environmental conditions at least until approximately AD 969 ± 50 (OSL age: AD 919–1019, 1σ; Table 10.2). Grain size statistics reveal medium sand size (1.6 Φ) and good sorting (0.45 Φ), very similar to those of the foredunes at Martinhal (mean: 1.6 Φ, sorting: 0.3 Φ; Kortekaas and Dawson 2007) and the present-day subaerial beach berm (Table 10.3). This points to aeolian transport as the main mode for sediments in (173). The foraminifera assemblage further highlights a littoral environment for (173), exclusively containing shallow marine species (Fig. 10.14, Table 10.5). The dominant species *C. lobatulus*, *E. crispum* and *Q. seminula* all derive from the inner shelf (e.g. Murray 1971, 1991, 2006; Mendes et al. 2013), while the latter can also be found at mid-shelf depths or in the outer parts of tidal inlets (e.g. Murray 1971; Hayward et al. 1999). However, the foraminifera assemblage of this unit is severely limited, whereby further analyses are necessary to definitely classify the palaeoenvironment based on foraminifera species alone. Still, the identified environment based on foraminifera concurs with other characteristics of the unit indicating wind-blown littoral sediments. Unit (173) was abruptly covered by the possible high-energy event (387) discussed above.

The still littoral environmental conditions, featuring exclusively shallow marine species, with the ongoing aeolian sediment transport point to the gradual siltation of the harbour basin. Measures to remove these sediments, such as dredging, have not been identified.

The site of Cerro da Vila near Vilamoura (Quarteira), 60 km further east, provides a close parallel to Boca do Rio's harbour situation, and in particular to the modification of its facilities. There, at the edge of the palaeo-estuary, two differently levelled waterfront facilities have been identified. At first, a supposedly earlier wooden pier existed, which was subsequently replaced by a stone waterfront fortification, the former dating from pre-Flavian times and the latter from Flavian times onwards; in a second phase, the quay was modified in the third century AD (Teichner 2017, 2018). The confirmed gradual and strong siltation of the Vilamoura estuary, which seems to have made this necessary (Teichner et al. 2014), is striking. It should be stressed that the same researchers, although focusing on the development of the estuary, did not find any evidence of EWEs in their core-drillings either (Teichner et al. 2014).

Similarly, it can be concluded that the ongoing siltation (297, 173), following the construction of Boca do Rio's harbour facilities, produced a shift in the river course towards the north-east in the short and medium terms. Access to what was already a more distant navigable watercourse was then further ensured by modifying the quay, namely, its elevation and replacement by a wooden footbridge.

The same development, that is, the change in the river course, can be further specified based on the results for kiln II. No event layer could be detected there either—neither on the features themselves nor in the surrounding area. However, clear traces of an erosive process are documented, as this destruction was not caused by a deliberate, anthropogenically initiated event, such as the reuse of building materials. Presumably the erosive force of the watercourse was visible here, which did not move in a straight line along its entire length to the east at the time, but did so in a meandering manner. In the area of kiln II, a cut bank of this meandering river must have existed at least for a short period. As a result of this temporary, small-scale westward shift, this section of the settlement was literally milled off, namely, continuously eroded. Occasional extreme rainfall events, affecting the Algarve region in the past and at present, may have strengthened this effect (Pereira et al. 1994; Bernardes 2006). This fluvial erosion is roughly comparable to the marine erosive process in the cliff area (Carrasco et al. 2007; Bernal Casasola 2015; Hermann et al. 2022), where tides and winter storms have a highly destructive effect on the conservation status of coastal monuments.

10.7 Conclusion

There is no doubt that Boca do Rio was a major regional player in the fish-salting industry in the Roman Empire, most likely from as early as the second century AD. This is evidenced by the 'halieutic cycle', namely, that all the steps of the fish-salting process—fishing, salting, potting, etc.—were carried out in Boca do Rio.

The pottery kilns and the construction of the harbour facilities, described in detail in this chapter, were important for the functioning of the settlement. They underwent a major upheaval in the third century AD, which can also be traced in the rest of the settlement (see Sect. 10.5.2). In particular, the kilns were abandoned and even suffered, in part, from erosion. As part of the harbour, the level of the quay of one of the largest fish-salting facilities in the settlement was raised and replaced by a wooden footbridge, in order to guarantee is continued functioning.

Two high-energy events have been detected in the sediments of the harbour basin. One is the well-known AD 1755 Lisbon tsunami and the other presumably a storm event during the fourteenth century AD. While the complete stratigraphy covers the entire Roman period, no traces of an older event have been found. On the contrary, a changed sedimentation and erosion behaviour of the river bordering the settlement has indeed been detected; the modification of the harbour and the destruction of the pottery area can at least be attributed to a change in its course.

It should therefore be concluded that no definite evidence of a tsunami event during the time of the Roman occupation has been detected. The findings in Boca do Rio thus do not confirm the assumption that single events—like earthquakes or EWEs—may have led to the sudden, radical change in production.

Acknowledgements This research was conducted as part of the project 'Vulnerability of complex Roman production networks on the Atlantic coast of southern Hispania', funded by the German Research Foundation (DFG; grant nos. TE 580/8-1, RE 1361/28-1, BR 877/36-1), which is gratefully acknowledged. Special thanks are due to Pedro José Miranda da Costa (University of Coimbra) for the funding of the dating of the OSL samples used in this paper, our local partner Ricardo Soares (Câmara Municipal Vila do Bispo) for logistical support, and to Margret Mathes-Schmidt, Piero Bellanova (both from RWTH Aachen University) and Hannes Laermanns (University of Cologne) for their support during the geological fieldwork, the subsequent analyses and the discussion of the results.

References

Allen HD (2003) A transient coastal wetland: from estuarine to supratidal conditions in less than 200 years – Boca do Rio, Algarve, Portugal. Land Degrad Dev 14:265–283

Álvarez-Martí-Aguilar M (2020) The historicity of the earthquakes occurring in the Iberian Peninsula before A.D. 881 recorded in Spanish and Portuguese seismic catalogs. Seismol Res Lett 91(6):3585–3594

Alves FJS (1997) Em torno dos projectos da Boca do Rio e do Oceán. In: Silva CT, Soares J (eds) I Encontro de Arqueologia a costa Sudoeste. Homenagem a Georges Zbyszewski. Setúbal Arqueológica 11–12:225–239

Andrade C, Freitas MC, Moreno J, Craveiro SC (2004) Stratigraphical evidence of Late Holocene barrier breaching and extreme storms in lagoonal sediments of Ria Formosa, Algarve, Portugal. Marine Geol 210 (1–4):339–362

Andrade C, Freitas MC, Oliveira MA et al (2016) On the sedimentological and historical evidences of seismic-triggered tsunamis on the Algarve Coast of Portugal. In: Duarte JC, Schellart WP (eds) Plate Boundaries and Natural Hazards, Geophysical Monograph 219, Hoboken, pp 219–238

Baptista MA, Miranda JM (2009) Revision of the Portuguese catalog of tsunamis. Nat Hazard 9(1):25–42

Baptista MA, Miranda PMA, Miranda JM, Victor LM (1998) Constrains on the source of the 1755 Lisbon tsunami inferred from numerical modelling of historical data. J Geodyn 25(1–2):159–174

Bekker-Nielsen T (2002) Fish in the ancient economy. In: Ascani K, Gabrielsen V, Kvist K (eds) Ancient history matters. Studies presented to Jens Erik Skydsgaard on his seventieth birthday. Analecta Romana Instituti Danici Supplementum vol 30. L'Erma di Bretschneider, Rome, pp 29–38

Bekker-Nielsen T (2005) The technology and productivity of ancient sea fishing. In: Bekker-Nielsen T (ed) Ancient fishing and fish processing in the Black Sea region. Proceedings of an interdisciplinary workshop on marine resources and trade in fish products in the Black Sea region in antiquity, University of Southern Denmark, Esbjerg, April 4–5, 2003. Black Sea Studies vol 2. Aarhus University Press, Aarhus, pp 83–96

Bernal Casasola D (2009) Roma y la producción de garvm y salsamenta en la costa meridional de Hispania. Estado actual de la investigación. In: Bernal Casasola D (ed) Arqueología de la pesca en el Estrecho de Gibraltar. De la prehistoria al fin del mundo antiguo. Universidad de Cádiz, Cádiz, pp 133–182

Bernal Casasola D (2015) Viveros y yacimientos haliéuticos. Importancia y fragilidad del patrimonio pesquero-conservero hispanorromano. In: Olcina Domènech M, Pérez Jiménez R (eds) La Illeta dels Banyets y los viveros romanos de la costa mediterránea Española.

Cuestió de conservación. Diputación de Alicante, Alicante, pp 16–41
Bernal Casasola D, Vargas Girón JM (2019) El Testaccio haliéutico de Gades. In: Bernal Casasola D, Vargas Girón JM, Lara Medina M (eds) 7 metros de la historia de Cádiz. Arqueología en el Olivillo y en el Colegio Mayor Universitario. Universidad Cádiz, Cadiz, pp 237–328
Bernal Casasola D, Expósito Álvarez JÁ, Díaz Rodríguez JJ (2018) The Baelo Claudia paradigm: the exploitation of marine resources in Roman Cetariae. J Marit Archaeol 13(3):329–351
Bernardes JP (2006) Existem pontes romanas no Algarve? In: Pereira A (ed) Actas das I Jornadas. As vias do Algarve – da época romana à actualidade. São Brás de Alportel, pp 14–19
Bernardes JP (2007) Boca do Rio. 130 anos depois. In: Actas do 4º Encontro de Arqueologia do Algarve: Percursos de Estácio da Veiga. Silves, 24 e 25 de Novembro 2006. Xelb 7:341–354
Bernardes JP, Medeiros IE (2016) Boca do Rio (Budens, Vila do Bispo). Novos dados de uma villa piscícola romana. Rev Port Arqueol 19:265–286
Bernardes JP, Viegas C (2017) A produção oleira Romana no Algarve. In: Fabião C, Raposo JMC, Guerra AMR (eds) Olaria Romana/Roman pottery works. Seminário Internacional e Ateliê de Arqueologia Experimental/International and Experimental Archaeological Workshop, Seixal, pp 239–256
Bernardes JP, Teichner F, Hermann F, Soares R (in press) Novos dados do sítio pesqueiro romano da Boca do Rio. In: Actas do X Encuentro de Arqueología del Suroeste Peninsular, Zafra
Bombico S (2015) Salted fish industry in Roman Lusitania: trade memories between Oceanus and Mare Nostrum. In: Barata FT, Rocha JM (eds) Heritages and memories from the sea. 1st international conference of the UNESCO chair in intangible heritage and traditional know-how: linking heritage, 14–16 January 2015, Évora, Portugal, conference proceedings. Évora, pp 19–39
Carrasco AR, Ferreira Ó, Matias A et al (2007) Historic Monuments Threatened by Coastal Hazards at Boca do Rio, Algarve, Portugal. Coast Manag 35(2–3):163–179
Chagué-Goff C, Szczuciński W, Shinozaki T (2017) Application of geochemistry in tsunami research: a review. Earth Sci Rev 165:203–244
Conejo Delgado N (2019) Economía monetaria de las áreas rurales de la Lusitania romana. Dissertation, Universidades de Lisboa, Lisboa (https://repositorio.ul.pt/handle/10451/39321) [01.07.2020]
Costa PJM, Andrade C, Freitas MC et al (2011) Boulder deposition during major tsunami events. Earth Surf Proc Land 36:2054–2068
Costa PJM, Andrade C, Freitas MC et al (2012a) A tsunami record in the sedimentary archive of the central Algarve coast, Portugal: characterizing sediment, reconstructing sources and inundation paths. The Holocene 22(8):899–914
Costa PJM, Andrade C, Dawson AG et al (2012b) Microtextural characteristics of quartz grains transported and deposited by tsunamis and storms. Sed Geol 275–276:55–69
Cunha PP, Buylaert JP, Murray AS et al (2010) Optical dating of clastic deposits generated by an extreme marine coastal flood: the 1755 tsunami deposit in the Algarve (Portugal). Quat Geochronol 5:329–335
Curtis RI (1991) Garum and Salsamenta. Production and commerce in materia medica. Studies in Ancient Medicine Series 3, Brill, Leiden
Cuven S, Paris R, Falvard S et al (2013) High-resolution analysis of a tsunami deposit: case-study from the 1755 Lisbon tsunami in southwestern Spain. Mar Geol 337:98–111
da Veiga SPME (1910) Antiguidades do Algarve. Capitulo V. Tempos historicos. O Archeologo Português 15:209–232
Dawson AG, Hindson R, Andrade C et al (1995) Tsunami sedimentation associated with the Lisbon earthquake of 1 November AD 1755: Boca do Rio, Algarve, Portugal. The Holocene 5(2):209–215
Diogo AMD (1987) Quadro tipológico das ânforas de fabrico lusitano. O Arqueólogo Português 5:179–191
Dinis J, Andrade C, Oliveira MA et al (2010) Geomorphological constraining of tsunami (?) run-up in the Alcantarilha coastal lowland (Central Algarve, Portugal). In: Conferência Coastal Hope – Iberian Coastal Holocene Paleonvironmental Evolution, Lisbon, pp 40–41
Driard C (2014) Les sauces de poisson dans l'ouest de la province romaine de lyonnaise. Reflexions sur l'élaboration et la nature des produits. In: Botte E, Leich V (eds) Fish & Ships. Production and commerce of salsamenta during Antiquity; production et commerce des salsamenta durant l'Antiquité. actes de l'atelier doctoral, Rome, 18–22 juin 2012. Bibliothèque d'archéologie méditerranéenne et africaine 17:47–60
Duarte JC, Rosas FM, Terrinha P et al (2013) Are subduction zones invading the Atlantic? Evidence from the southwest Iberia margin. Geology 41(8):839–842
Ehmig U (2001) Hispanische Fischsaucen in Amphoren aus dem mittleren Rhônetal. Münstersche Beiträge zur antiken Handelsgeschichte 20(2):62–71
Étienne R, Makaroun Y, Mayet F (1994) Un grand complexe industriel à Tróia (Portugal). De Boccard, Paris
Expósito Álvarez JÁ, Bernal Casasola D, Díaz Rodríguez JJ (2018) The urban halieutic workshops of Baelo Claudia (Baetica, Hispania). In: La città che produce. Archeologia della produzione negli spazi urbani. Atti delle Giornate Gregoriane, X edizione (10–11 dicembre 2016). Bibliotheca Archaeologica, Edipuglia, Bari, pp 289–295. https://doi.org/10.4475/851
Fabião C (1992) Garum na Lusitania rural? Alguns comentários sobre o povoamento romano do Algarve. Studia Historica. Historia Antigua 10–11:227–252
Fabião C (2004) Centros oleiros da Lusitania: balanço dos conhecimentos e perspectivas de investigação. In:

Bernal Casasola D, Lagóstena Barrios L (eds) Figlinae Baeticae. Talleres alfareros y producciones cerámicas en la Bética romana (ss. II a.C. – VII d.C.), Universidad de Cádiz, Noviembre 2003. BAR International series vol 1266. BAR Publishing, Oxford, pp 379–410

Fabião C (2008) Las anforas de Lusitania. In: Bernal Casasola D, Ribera Lacomba A (eds) Cerámicas hispanoromanas. Un estado de la cuestión. Actas del XXVI Congreso Internacional de la Asociación Rei Cretariae Romanae Fautores, Cádiz, pp 501–521

Fabião C (2009) Cetárias, ânforas e sal: a exploração de recursos marinhos na Lusitania. In: Luís Cardoso J (ed) Estudos Arqueológicos de Oeiras. Volume comemorativo do XX aniversário do Centro de Estudos Arqueológicos do Concelho de Oeiras, Oeiras, pp 555–594

Fatela F, Taborda R (2002) Confidence limits of species proportions in microfossil assemblages. Mar Micropaleontol 45:169–174

Feist L, Frank S, Bellanova P et al (2019) The sedimentological and environmental footprint of extreme wave events in Boca do Rio, Algarve coast, Portugal. Sed Geol 389:147–160

Ferreira Ó, Dias JA, Taborda R (2008) Implications of sea-level rise for continental Portugal. J Coastal Res 24(2):317–324

Folk RL, Ward WC (1957) Brazos river bar: a study in the significance of grain size parameters. J Sediment Petrol 27:3–26

Font E, Veiga-Pires C, Pozo M et al (2013) Benchmarks and sediment source(s) of the 1755 Lisbon tsunami deposit at Boca do Rio Estuary. Mar Geol 343:1–14

Fromentin JM, Powers JE (2005) Atlantic bluefin tuna: population dynamics, ecology, fisheries and management. Fish Fish 6:281–306

Galbraith RF, Roberts RG, Laslett GM, Yoshida H, Olley JM (1999) Optical dating of single and multiple grains of quartz from Jinmium Rock Shelter, Northern Australia: Part I, experimental design and statistical models. Archaeometry 41:339–364

Gómez F, Arruda AM, Rodríguez-Vidal J et al (2015) Eventos marinos de alta energía y cambios traumáticos en los asentamientos costeros del Suroeste de la Península Ibérica. Cuaternario y Geomorfología 29(1–2):57–74

Grützner C, Reicherter K, Hübscher C, Silva PG (2012) Active faulting and neotectonics in the Baelo Claudia area, Campo de Gibraltar (Southern Spain). Tectonophysics 554–557:127–142

Hayward BW, Grenfell HR, Reid CM, Hayward KA (1999) Recent New Zealand shallow-water benthic foraminifera: taxonomy, ecologic distribution, biogeography, and use in paleoenvironmental assessment. Institute of Geological & Nuclear Sciences, Lower Hutt, vol 21

Hermann F, Teichner F, Brückner H et al (2022) Geoarchäologische Forschungen zur römischen Fischsaucenproduktion in Lusitanien: Boca do Rio und Tróia. In: Engel M, Stock F, Brückner H (eds), Coastal Geoarchaeology in the Mediterranean – on the Interdependence of Landscape Dynamics, Harbour Installations and Economic Prosperity in the Littoral Realm, Panel 2.3, Archaeology and Economy in the Ancient World 5, pp 5–25

Hermann F, Bernardes JP, Teichner F (in press) "Hum caes … de boa cantaría" en el extremo oeste del mundo romano. Las instalaciones portuarias de las aglomeraciones secundarias de Boca do Rio y Cerro da Vila (Algarve) - The harbour installations of the coastal settlements of Boca do Rio and Cerro da Vila (Algarve, Portugal) In: Congreso internacional Entre Mares: Emplazamiento, infraestructuras y organización de los puertos romanos. Irún, 24–26 de noviembre, 2020

Hilbich C, Mügler I, Daut G et al (2005) Geophysikalische, sedimentologische und mikrofaunistische Methoden zur Rekonstruktion der Paläogeographie einer römischen Hafensiedlung: Die Landschaftsgenese der Lagune von Vilamoura (Portugal) während der letzten 6000 Jahre. In: Beck N (ed) Neue Ergebnisse der Meeres- und Küstenforschung. Schriften des Arbeitskreises Landes- und Volkskunde 4, Koblenz, pp 51–71

Hindson RA, Andrade C (1999) Sedimentation and hydrodynamic processes associated with the tsunami generated by the 1755 Lisbon earthquake. Quat Int 56:27–38

Hindson RA, Andrade C, Dawson AG (1996) Sedimentary processes associated with the tsunami generated by the 1755 Lisbon earthquake on the Algarve Coast, Portugal. Phys Chem Earth 21(1–2):57–63

Hindson RA, Andrade C, Paris R (1999) A microfaunal and sedimentary record of environmental change within the late Holocene sediments of Boca do Rio (Algarve, Portugal). Geol Mijnbouw 77:311–321

Kortekaas S, Dawson AG (2007) Distinguishing tsunami and storm deposits: an example from Martinhal, SW Portugal. Sed Geol 200:208–221

Laborel J, Laborel-Deguen F (1994) Biological Indicators of Relative Sea-Level Variations and of Co-Seismic Displacements in the Mediterranean Region. J Coast Res 10(2):395–415

Laborel J, Laborel-Deguen F (2005) Sea-level indicators, biologic. In: Schwartz, M (ed) Encyclopedia of Coastal Science, Dordrecht, pp 833–834

Lagóstena L (2001) La producción de salsas y conservas de pescado en la Hispania Romana (II a.C. – VI d.C.). Collecció Instrumenta, vol 11, Universitat de Barcelona, Barcelona

Lagóstena LG, Palacios JL (2010) Salinae maritimae en Baetica. Condiciones ambientales y consideración jurídica. In: Hermon E (ed), Riparia dans l'Empire romain. Pour la définition du concept: actes des journeés d'etude de Quebec, 29–31 octobre 2009. BAR International series, vol 2066. BAR Publishing, Oxford, pp 67–84

Lario J, Zazo C, Goy JL et al (2011) Holocene palaeotsunami catalogue of SW Iberia. Quat Int 242 (1):196–200

Luque L, Lario J, Silva PG et al (2002) Sedimentary record of a tsunami during Roman times, Bay of Cadiz, Spain. J Quat Sci 17(5–6):623–631

Martin-Kilcher S (1994) Die römischen Amphoren aus Augst und Kaiseraugst. Ein Beitrag zur römischen Handels- und Kulturgeschichte. Die Amphoren für Wein, Fischsauce, Südfrüchte (Gruppen 2–24). Forschungen in Augst, vol 7(2). Museum Augusta Raurica, Basel

Mayet F, Silva CT (2010) Production d'amphores et production de salaisons de poisson: rythmes chronologiques sur l'estuaire du Sado. Conimbriga 49:119–132

Medeiros IE (2015) Conservas de peixe na Lusitânia. O quadro produtivo da Boca do Rio e das restantes cetariae do Algarve. An Arqueol Cordobesa 25–26:115–144

Mendes I, Dias JA, Schönfeld J et al (2013) Living, dead and fossil benthic foraminifera on a river dominated shelf (northern Gulf of Cadiz) and their use for paleoenvironmental reconstruction. Cont Shelf Res 68:91–111

Murray JW (1971) An Atlas of British recent Foraminiferids. Pearson, London

Murray JW (1991) Ecology and palaeoecology of benthic foraminifera. Taylor & Francis, London

Murray JW (2006) Ecology and applications of benthic foraminifera. Cambridge University Press, Cambridge

Oliveira MA, Andrade C, Freitas MC, Costa PJM (2009) Modeling volume transfer between beach-foredune and the backshore by the 1755 Lisbon Tsunami at Boca do Rio Lowland, Algarve (Portugal). J Coast Res, Special Issue 56:1547–1551

Pereira AR, Dias JA, Laranjeira MM (1994) Evolução holocénica da linha de costa da baía de Lagos. In: Pereira AR et al (eds) Contribuições para a Geomorfologia e Dinâmicas Litorais em Portugal. Linha de Acção de Geografia Física, Relatório nº. 35, Centro de Estudos Geográficos, Lisboa, pp 75–89

Ponsich M, Tarradell M (1965) Garum et industries antiques de Salaison dans la méditerranée occidentale. Bibliothéque de l'Ecole des Hautes Etudes Hispaniques, vol 36. Presses Universitaires de France, Paris

Quintela M, Costa PJM, Fatela F et al (2016) The AD 1755 tsunami deposits onshore and offshore of Algarve (south Portugal): sediment transport interpretations based on the study of Foraminifera assemblages. Quat Int 408:123–138

Reece R (1981) Roman third century: crisis or change? In: King A, Henig M (eds) The Roman West in the third century. BAR international series vol 108. BAR Publishing, Oxford, pp 27–38

Rodríguez-Ramírez A, Villarías-Robles JJR, Pérez-Asensio JN et al (2016) Geomorphological record of extreme wave events during Roman times in the Guadalquivir estuary (Gulf of Cadiz, SW Spain): an archaeological and paleogeographical approach. Geomorphology 261:103–118

Röth J, Mathes-Schmidt M, García Jiménez I et al (2015) The Baelo Claudia tsunami hypothesis: results from a multi-method sediment analysis of late-Roman deposits (Gibraltar Strait, Southern Spain). In: Blumetti AM et al (eds) 6th international INQUA meeting on Paleoseismology, Active Tectonics and Archaeoseismology, 19–24 April 2015, Pescina, Fucino Basin, Italy. Miscallenea INGV 27:418–422

Santos ML (1971) Arqueologia Romana do Algarve, vol I. AAPL, Lisboa

Schneider H, Höfer D, Trog C et al (2010) Holocene estuary development in the Algarve Region (Southern Portugal). A reconstruction of sedimentological and ecological evolution. Quat Int 221:142–158

Silva PG, Giner-Robles JL, Reicherter K et al (2016) Los terremotos antiguos del conjunto arqueológico romano de Baelo Claudia (Cádiz, Sur de España): Quince años de investigación arqueosismológica. Estud Geol 72(1): e050

Sorrel P, Debret M, Billeaud I et al (2012) Persistent non-solar forcing of Holocene storm dynamics in coastal sedimentary archives. Nat Geosci 5:892–896

Teichner F (2008) Entre tierra y mar. Zwischen Land und Meer – Architektur und Wirtschaftsweise ländlicher Siedlungsplätze im Süden der römischen Provinz Lusitanien (Portugal). Studia Lusitana 3, Merida

Teichner F (2014a) Von Exportschlagern und *Cash Crops* – Zum Wirtschaftsleben Hispaniens. In: Panzram S (ed) Städte in Spanien. Moderne Urbanität seit 2000 Jahren. Nünnerich-Asmus, Mainz, pp 81–92

Teichner F (2014b) Mensch, Umwelt, Wirtschaft: Zum Landschaftsbezug wirtschaftlichen Handelns im antiken Hispanien. In: Kemmers F, Maurer T, Rabe B (eds) Lege artis. Festschrift für Hans-Markus von Kaenel. Frankfurter Archäologische Schriften, vol 25. Rudolf Habelt, Frankfurt, pp 61–76

Teichner F (2016) A multi-disciplinary approach to the maritime economy and palaeo-environment of Southern Roman Lusitania. In: Vaz Pinto I, de Almeida RR, Martin A (eds) Lusitanian amphorae. Production and distribution. Published on the occasion of the 30th Congress of the Rei Cretariae Romanae Fautores, Lisbon, 2016. Roman and Late Antique Mediterranean Pottery, vol 10. Archaeopress, Oxford, pp 241–255

Teichner F (2017) Cerro da Vila: a rural commercial harbour beyond the Pillars of Hercules. In: Campos Carrasco JM, Bermejo Meléndez J (eds) Los puertos romanos Atlánticos Béticos y Lusitanos y su relación comercial con el Mediterráneo. L'Erma di Bretschneider, Roma, pp 399–434

Teichner F, Mañas Romero I (2018) The mosaics from Abicada and Boca do Rio (Portugal). A new perspective thirty years later. J Mosaic Res 11:257–271

Teichner F, Pujol LP (2008) Roman amphora trade across the Straits of Gibraltar. An ancient 'anti-economic practice'? Oxford J Archaeol 27(3):303–314

Teichner F, Mäusbacher R, Daut G et al (2014) Investigações geo-arqueológicas sobre a configuração do litoral algarvio durante o Holoceno. Rev Port Arqueol 17:141–158

Teichner F (2018) O establecimento portuário do Cerro da Vila (Vilamoura): de aglomerado romano a aldeia islâmica. In: Catálogo de exposição "Loulé – Território, Memória e Identidade". Museu Nacional de Arqueologia, Belem, Lisboa, pp 278–291

Trakadas A (2005) The archaeological evidence for fish processing in the Western Mediterranean. In: Bekker-Nielsen T (ed) Ancient Fishing and Fish Processing in the Black Sea Region. Proceedings of an interdisciplinary workshop on marine resources and trade in fish products in the Black Sea region in Antiquity, University of Southern Denmark, Esbjerg, April 4–5, 2003. Black Sea Studies 2:47–82

Trakadas A (2015) Fish-salting in the Northwest Maghreb in antiquity. A gazetteer of sites and resources. Archaeopress, Oxford

Trog C, Hempel R, Frenzel P, Mäusbacher R (2015) Holocene palaeoenvironmental changes in three lagoons on the Algarve coast of Portugal. Palaeobiodiversity and Palaeoenvironments 95(2):203–221

Vaz Pinto I, Magalhães AP, Brum P (2014) An overview of the fish-salting production centre at Tróia (Portugal). In: Botte E, Leich V (eds) Fish & Ships. Production and commerce of salsamenta during Antiquity; production et commerce des salsamenta durant l'Antiquité. actes de l'atelier doctoral, Rome, 18–22 juin 2012. Bibliothèque d'archéologie méditerranéenne et africaine 17:145–157

Vigliotti L, Andrade C, Freitas MC et al (2019) Paleomagnetic, rock magnetic and geochemical study of the 1755 tsunami deposit at Boca do Rio (Algarve, Portugal). Palaeogeogr Palaeoclimatol Palaeoecol 514:550–566

Wilson A (2006) Fishy business: Roman exploitation of marine resources. J Roman Archaeol 19(2):525–537

Wilson A (2007) Quantification of fish-salting infrastructure capacity in the Roman world. http://oxrep.classics.ox.ac.uk/working%20papers/quantification_fishsalting_infrastructure_capacity_roman_world/. Accessed 01 May 2022

11 The Impact of High-Energy Events on the Economy and Coastal Changes Along the Coast of Huelva in Ancient Times

Javier Bermejo Meléndez, Francisco Ruiz Muñoz, Juan M. Campos Carrasco, Joaquín Rodríguez-Vidal, and Luis M. Cáceres Puro

Abstract

Over the past two decades, historical extreme wave events have occupied an important place on the research agenda. The succession of these types of events and their impact on coastal populations is currently an interesting line of research, in which archaeological and geological studies should be performed together. There are increasingly more studies in this regard, which are of special interest in understanding coastal settlements and their transformations and economic development throughout different historical periods. Accordingly, this paper reviews the tsunami evidence (archaeology, economy, sedimentology, palaeontology and dating) on the southern seaboard of Spain, specifically on the coast of Huelva, during the third and fourth centuries AD.

Keywords

Coast of Huelva · Cetariae · Tsunami · Earthquake · Late antiquity

Introduction

Archaeological research in the province of Huelva (Southern Spain) has revealed a steady occupation of the entire coast during the Roman period, from high Imperial times to late Antiquity. This confirms that this coastal territory participated in the same commercial maritime and fishing activities as the rest of the southwestern reaches of the peninsula, and even with a particular ascendency between the fourth and fifth centuries AD, a period during which this industry experienced its heyday (Campos et al. 1990, 1999b; Campos and Gómez 2001), until sixth century AD. The fifth century AD would be the most prosperous for this industry, unlike what occurred in the *Fretum Gaditanum*, which was plunged into a period of recession. Bernal (2007) relates this period to the levels of abandonment and destruction of various factories in

J. Bermejo Meléndez (✉) · F. Ruiz Muñoz · J. M. Campos Carrasco · J. Rodríguez-Vidal · L. M. Cáceres Puro
Centro de Investigación en Patrimonio Histórico, Cultural y Natural (CIPHCN), Facultad de Humanidades, Universidad de Huelva, Campus del Carmen. Avda. Tres de Marzo, s/n. 21071, Huelva, Spain
e-mail: javier.bermejo@dhis1.uhu.es

F. Ruiz Muñoz
e-mail: ruizmu@dgyp.uhu.es

J. M. Campos Carrasco
e-mail: campos@uhu.es

J. Rodríguez-Vidal
e-mail: jrvidal@dgeo.uhu.es

L. M. Cáceres Puro
e-mail: mcaceres@uhu.es

M. Álvarez-Martí-Aguilar and F. Machuca Prieto (eds.), *Historical Earthquakes, Tsunamis and Archaeology in the Iberian Peninsula*, Natural Science in Archaeology,
https://doi.org/10.1007/978-981-19-1979-4_11

the Strait of Gibraltar (Villa de Puente Grande—Algeciras—*Septem*) caused by the Vandals while en route to Africa at the beginning of the fifth century AD. In this connection, highly interesting sites, such as El Eucaliptal (Punta Umbría), El Terrón (Lepe), Mazagón Poblado III (Moguer), Fontanilla (Moguer), Las Cojillas (Aljaraque), Urberosa (Cartaya), etc., have been brought to light or rediscovered. The current situation plan includes a large network of sites on the coast of Huelva, some of which have been excavated to a greater or lesser extent, while surface research has only been performed on others (see Fig. 11.1).

The diachronic study of these archaeological sites has revealed periods of occupation and activity versus others of recession, when records are very poor or almost non-existent. In addition, all the sites show that these last periods of inactivity were followed by stages of recovery, as regards industrial and artisanal areas, housing, etc. There are therefore several especially interesting moments in relation to the evolution of the coast's occupation and the successive occurrence of several types of natural events during these centuries. In this area, the sedimentary records reveal the existence of a series of exceptional catastrophic events, such as tsunamis or storms (Andrade 1992; Dabrio et al. 1999; Luque et al. 2002; Whelan and Kelletat 2003; Rodríguez-Ramírez et al. 2003; Alonso et al. 2004; Ruiz et al. 2005, 2008, 2012; Gracia et al. 2006; Morales et al. 2008; Gutiérrez-Mas et al. 2009; Baptista and Miranda 2009; Lario et al. 2010; Rodríguez-Vidal et al. 2011a, b; Rodríguez-Ramírez et al. 2015; 2016; Abad et al. 2019; Pozo et al. 2020; Guerra et al. 2020). This series of periodic events affected the coastal settlements and their inhabitants, inflicting important human and economic losses (Campos 2011; Alonso et al. 2015). Prior to this geomorphological research, in some coastal archaeological sites,

Fig. 11.1 Google Earth image of the coast of Huelva, indicating Roman archaeological sites—(first-sixth centuries AD) (*Source* Campos et al. (2015) Fig. 1)

such as El Eucaliptal, a hiatus in the archaeological record was detected in the middle of the third century AD (Campos et al. 1996). This was also observed at Cerro del Trigo, in both the oldest records of Schulten and Bonsor and the most recent ones (Bonsor 1928; Campos et al. 2002a, b). This contrasts with the archaeological records of settlements a little further inland, to wit, the territory's *villae rusticae* (Almagra, Cantarranas, Bojeos, etc.), where there is no evidence of this drop in activity, all of which led us to perform a preliminary analysis on the existence of an extraordinary event that might have been behind that recession. With this evidence, we then decided to fine-tune the analysis by incorporating geomorphological studies, while waiting for opportunities for new interventions that would allow us to confirm or discard our initial hypothesis.

However, it should be stressed that the vast majority of excavations at archaeological sites predate geological studies of tsunamites or archaeo-seismicity, for which reason the interconnection between disciplines has been all but non-existent until recently. Nevertheless, there are certain archaeological sites on the coast of Huelva where geoarchaeological data are very revealing for detecting possible catastrophic events in the absence of analytics.

Thus, from this long stretch of coast, several areas have been selected for this study, according to the degree of knowledge that we currently have of the different archaeological sites that diachronically reveal interruptions in their occupation and production activities, especially in the third century AD. Our initial hypothesis involves relating these hiatuses to a possible high-energy event that produced an extraordinary coastal inundation.

Study Area

11.2.1 The South-Western Coast of Spain

The Atlantic seaboard of the Iberian Peninsula extends from the Portuguese border to the Strait of Gibraltar, almost 300 km of which borders the Gulf of Cadiz. The coast of Huelva, occupying its northern sector, is made up of extensive dune

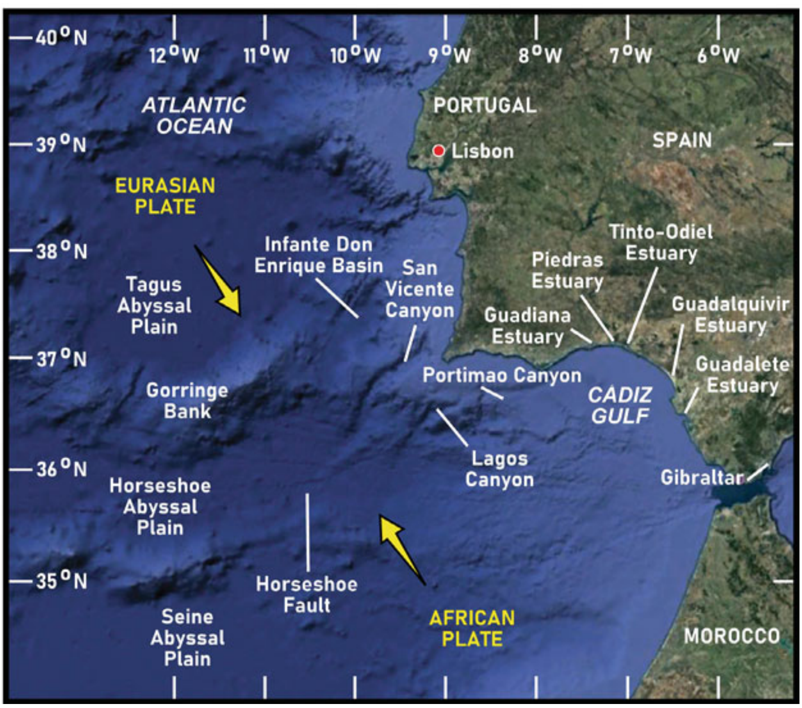

Fig. 11.2 Location of the study area (Google Earth image), including the tsunamigenic sites and the main structural elements of the Eurasian-African plate boundary

complexes interrupted by four estuaries (see Fig. 11.2: Rivers Guadiana, Piedras, Tinto-Odiel and Guadalquivir). These estuaries have a high degree of colmatation, with inland areas consisting mainly of extensive marshes partially protected by sandy spits.

This area is located near the Africa-Eurasia plate boundary, the westernmost part of the Alpine-Himalayan collisional belt. This boundary is characterised by a WNW-ESE oblique dextral convergence between Africa and Eurasia of 4–5 mm/yr (Stich et al. 2006; Nocquet 2012). Its physiography is very irregular, with extensive abyssal plains (see Fig. 11.2: Tagus abyssal plain, Horseshoe abyssal plain, Seine abyssal plain), elongated canyons (San Vicente canyon, Portimao canyon, Lagos canyon), numerous active faults (e.g. Horseshoe fault) and several seamounts (e.g. Gorringe Bank) (Gràcia et al. 2010).

The strain is accommodated by moderate- to large-magnitude earthquakes at shallow to intermediate depths of up to 60 km, most of them clustering along lineations usually with a NNE-SSW or WNW-ESE orientation (Neres et al. 2016). Very high magnitude historical earthquakes and associated tsunamis occurred in Morocco, Portugal and Spain, such as the 1531 Tagus earthquake ($M_w \sim 10$) or the 1755 great Lisbon earthquake (M_w: 8.5–9) (Baptista and Miranda 2009). The sedimentary record of these high-energy events has been extensively studied over the past 30 years (see previous references).

Between the third and fifth centuries AD, the coastal settlements of the south-western seabord of Spain were engaged in sea trade and fishing, the latter experiencing an unprecedented boom between the fourth and fifth centuries AD (Campos et al. 1990, 1999b; Campos and Gómez 2001). This coastal territory had a high human occupation, with an extensive network of Roman fish-salting factories (*cetariae*). The diachronic study of these factories and other archaeological sites have revealed periods of occupation and activity versus others of recession, especially in the third century AD (Bonsor 1928; Campos et al. 1996, 2002a, b).

This chapter reviews the archaeological and geological evidence of a high-energy event occurring in the study area during this century, based on the initial hypothesis that these hiatuses resulted from an extraordinary coastal inundation.

11.2.2 Geomorphologic Context

About 1,600 years ago, the physiographic structure of the Huelva seaboard was very different from now (e.g. Ruiz et al. 2004; Cáceres et al. 2018; see Fig. 11.3). This sector had an irregular layout, with large inlets (e.g. flooded marine estuaries) and headlands (e.g. interfluvial areas). The action of different littoral agents (waves, littoral drift currents and tides) progressively smoothed the coastal outline by eroding the headlands, shaping cliffs and filling entrances. Several sandy barriers and spits developed at the river mouths, protecting inland areas where marshes gradually developed.

In the eastern sector, the river Guadalquivir was partially closed by two sandy spits

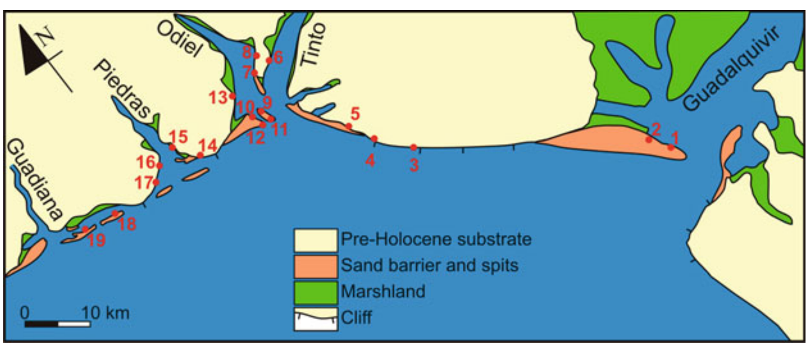

Fig. 11.3 The coast of Huelva in the fourth century AD: Roman fish-salting factories

(Rodríguez-Ramírez et al. 1996; Ruiz et al. 2004; see Fig. 11.3), with two factories located on the westernmost one (Fig. 11.3, 1: Cerro del Trigo, 2: Las Navas).

In the Tinto-Odiel estuary, some of these factories were established on a Neogene substrate or the adjacent salt marshes (Fig. 11.3, 6: El Rincón, 7: Huelva, 8: La Orden, 13: Las Cojillas). Archaeological evidence of these industrial fishing activities has also been found on coastal spits (Fig. 11.3, 10: Peguera, 12: El Eucaliptal) and barrier islands (Fig. 11.3, 9: Saltés, 11: Cascajera). Near this estuary, three factories were sited on the edges of the cliffs (Fig. 11.3, 3: Mazagón-Poblado III, 4: Torre del Loro, 5: Fontanilla).

In the western sector, numerous barrier islands ran parallel to the coast between the mouths of the rivers Guadiana and Piedras (Zazo et al. 1994). Some of them had already been stabilised and occupied by fish-salting factories (Fig. 11.3, 18: La Viña, 19: Punta del Moral). While other factories were located in the more protected inland areas (Fig. 11.3, 14: Urberosa, 15: Tenerías, 16: El Terrón, 17: Valsequillo). In all of them, there are direct or indirect indications of their relationship with fishing activities, like, for example, the fish salting vats discovered at the archaeological sites of Eucaliptal and La Viña and fishing gear and shells unearthed at that of La Cascajera.

11.2.3 Historical Tsunamis in Spain, Portugal and Morocco

Some of the aforementioned earthquakes caused tsunamis that have been recorded in the Spanish and Portuguese literature, of which a historical review is currently being performed (Galbis 1932; Campos 1991; Martínez-Solares2005; Baptista and Miranda 2009; Kaabouben et al. 2009). The oldest historical tsunamis (218–209 BC) are only cited in the Spanish historical catalogue. The archaeological research performed to date on the Portuguese-Spanish littoral seems to indicate that these tsunamis seriously affected the coastal settlements of both countries around the third century BC, with the subsequent abandonment of some of them or the partial destruction of their defensive structures, among other damage. The 60 BC tsunami, included in the Portuguese historical catalogue (Baptista and Miranda 2009), affected Portugal and the north-western coast of Spain (Moreira de Mendonça 1758). In contrast, there is no historical evidence of its impact on south-western Spain or Morocco.

The purported tsunami off Cape St Vincent (SW Portugal) in AD 382, allegedly described by Brito (1609), would have been caused by a 7.5 M_w earthquake (Martins and Mendes-Victor2001). Although there is neither historical evidence of this tsunami nor of that of AD 1531 in south-western Spain or Morocco, both events have been considered as regional or Atlantic-wide by Baptista and Miranda (2009). This also seems to be the case with the tsunami striking the Moroccan and Spanish coasts in AD 881 (Sánchez Navarro-Neumann1917; El Mrabet 2005; Alonso et al. 2015).

However, current historiography considers that the historicity of the alleged earthquakes and tsunamis in 218–209 and 60 BC and in AD 382, described by Galbis drawing from the sixteenth-century chroniclers Florián de Ocampo and Bernardo de Brito, is moot (Udías 2015; Álvarez-Martí-Aguilar 2017a, b, 2020, this volume). This review had led us to treat these earthquakes or catastrophic marine events with caution, at least in terms of historical evidence.

The eighteenth century was a time of remarkable seismic activity in this region, with six associated tsunamis in AD 1722, 1731, 1755 (two tsunamis), 1756 and 1761. The most important was the Lisbon tsunami on 1 November 1755, which caused thousands of deaths and widespread damage (El Mrabet 1991; Baptista et al. 1998; Martínez-Solares and López 2004). In addition, the North Atlantic tsunami on 31 March 1761 affected the Portuguese and Spanish coasts and even Barbados (Baptista and Miranda 2009).

There is no evidence of tsunamis during the nineteenth century, in contrast with the 10 tsunamis that occurred during the following one. Most of them were very small tsunamis only detected by tide gauges, with the 1969 tsunami being the only important one at a regional level, although its run-up did not exceed 1 m on most of this coast (Martínez-Solares2005).

11.2.4 Geological Evidence of High-Energy Events in South-Western Spain

Research on the Holocene geological record of high-energy events (i.e. storms and tsunamis) in south-western Spain, particularly in the estuaries of its main rivers (see Fig. 11.2: The estuaries of the rivers Piedras, Tinto-Odiel, Guadalquivir and Guadalete) and on some its beaches and rocky coasts (see Fig. 11.2: Gibraltar), has increased substantially over the past three decades—a review of this record can be consulted in Lario et al. (2010) and Ruiz et al. (2012, 2013). These imprints include beach erosion, the filling of intertidal channels, the deposition of bioclastic layers, washover fans, reworked aeolian sheets and the breaching of spits and tombolos.

The resulting sedimentary bodies have been dated on numerous occasions, but the results are mainly restricted to the last 6 kyr. This restriction may be largely due to the fact that these estuaries were flooded at the peak of the Flandrian transgression (ca. 6500–6000 ^{14}C yr BP; Zazo et al. 1994). Consequently, most of the Holocene tsunamigenic deposits prior to this date have disappeared or are to be found in submerged sedimentary sequences in the Gulf of Cadiz.

Coastal Settlements in Huelva in Roman Times

11.3.1 Archaeological and Historical Issues

The study of the coastal settlements in Huelva began in an incipient way in the 1920s, with the excavations carried out by G. Bonsor in Cerro del Trigo (Almonte), inside Doñana National Park. This archaeological research revealed a Roman fish-salting factory, as well as the habitat and necropolis associated with it since the second century AD (Bonsor 1928). Subsequently, it would not be until the mid-1970s that new factories were excavated, this time in the metropolitan area of Huelva (Del Amo 1976).

This research would be followed by Ponsich's (1988), which uncovered new Roman settlements on the coast, such as Las Naves (Almonte), Torre del Loro (Moguer), El Rincón (Huelva), etc. In the 1990s, a survey programme (Campos et al. 1990; Campos and Gómez 2001) revealed a high occupation of the entire coast during the Roman period, from the high Empire to late Antiquity, with an extensive network of enclaves (see Fig. 11.1). A comparative analysis of this coastal settlement model has revealed a common characteristic: the interruption of fishing activity and of the use of habitats and cemeteries in the middle of the third century AD, possibly relating to a traumatic episode, namely, a tsunami or high-energy marine event, which would explain this hiatus (Campos 2011; Campos et al. 2015).

Therefore, a multidisciplinary perspective, encompassing geology, archaeology and history, is required to identify possible catastrophic events that might have conditioned the coastal settlement model over time. Different sites have been selected for this study from this extensive coastline, according to the knowledge that we currently have of the different settlements that developed in the transition from the high Empire to late Antiquity.

In this vein, in the easternmost area, there is the archaeological site of Cerro del Trigo, in Doñana (Almonte), close to the mouth of the river Guadalquivir and adjacent to the Lucio del Membrillo marsh area (Bonsor 1928; Schulten 1945; Campos et al. 2002a, 2013) (Fig. 11.3, 1). This site has been dated between the second and sixth centuries AD. Throughout this long period, there are no environments, structures, etc., that can be clearly dated to the mid-third century AD. Indeed, its reoccupation, as in the case of the necropolis sector, has only been documented as of the second half of the century.

A little further to the west, there are several archaeological sites around the mouth of the rivers Tinto and Odiel, among which El

Eucaliptal (Punta Umbría) stands out as one of the most researched to date (Fig. 11.3, 12), yielding plenty of data that allow for its diachronic reconstruction (Campos et al. 1997, 1999a; Campos and Vidal 2004; López et al. 2003, 2005). The El Eucaliptal site, whose factory units, necropolis and habitats reflect a similar hiatus in the first half of the third century AD, is one of the best-known where production areas with salting basins would have been reused from the middle of the century. Dated to this same period, there are a number of housing and burial units on which a level of sterile sand has been recorded, and on top of which the new settlement would have been established already in the fourth century AD. From the middle of the third century AD onwards, the industrial and residential activity in this settlement was generally interrupted.

The factory of Onoba was located very close to the El Eucaliptal site in the port neighbourhood of the ancient colony, in the modern-day city centre of Huelva (Fig. 11.3, 7), where an important complex of salting basins was excavated on Palos, Tres de Agosto and Cardenal Cisneros Streets in the 1970s (Del Amo 1976), to which should be added those discovered more recently on Cardenal Cisneros Street (Lozano and González 2004). All these salting basins appear to have fallen into disuse at the beginning or in the middle of the third century AD, in a context of the widespread crisis detected all along the coast of Huelva. In the case of the salting basins discovered on Cardenal Cisneros Street, there is no evidence that they were put to new use after having been abandoned during the first decades of the third century AD, while a resumption of activities has indeed been documented in the rest, which remained in use until the mid-fifth century AD, a moment when they were abandoned once and for all (Vidal 2007). This decline and disappearance of archaeological indicators in Onoba have also been confirmed not only in industrial quarters but also in necropolises and residential areas, which possibly points to a hiatus relating to a major natural catastrophe.

Later on, in the fourth and fifth centuries AD, another important fishing settlement would be established: La Orden (Fig. 11.3, 8), with its necropolis and pottery production, probably in the context of a new occupation model following another natural event at the end of the fourth century AD (Del Amo 1976).

At the archaeological site of El Terrón, at the mouth of the river Piedras (Fig. 11.3, 16), which seems to have been in use from the second century AD to the sixth century AD, it has been possible to identify industrial-artisanal areas and necropolises (Campos et al. 2001a, b). A similar interruption seems to have occurred here, where records after the time of Gordian III (238–244 AD) are non-existent and where there are no evident signs of activity until the middle of the fourth century AD.

Of all the industrial installations and settlements found along the coast of Huelva, the archaeological sites listed above are the best known, given that various excavation campaigns have yielded a huge amount of data. The remaining sites are only known thanks to several surface prospections, news of isolated findings, etc., which makes it impossible to identify precisely their phases of occupation and diachrony. Therefore, the aim of this study is to analyse certain geoarchaeological indicators documented at these sites, with the intention of establishing a connection between the interruption in their activities and natural high-energy events.

11.3.2 Disruption in the Third Century AD

11.3.2.1 Archaeological Evidence

The analysis of the geoarchaeological records obtained in the different fish-salting factories, both in the excavated ones and to a lesser extent in the surface surveys, has led us to establish a general time frame that extends production in Roman times from the second half of the first century BC until the middle of the sixth century AD.

In this protracted period, we have been able to identify two moments that seem to point to traumatic episodes relating to high-energy marine events. The first has been dated to the central decades of the third century AD, while the second, well-known in the Gulf of Cadiz, occurred at the end of the fourth century AD and has also been detected fairly clearly on the coast of Huelva.

The following geoarchaeological data are available for the aforementioned sites. In the case of Cerro del Trigo (Doñana, Almonte), the remains of its necropolis reveal a clear interruption or drop in activity during the first half of the third century AD; a level of burials from the second century AD would have been followed by another as from the middle or the second half of the third century AD (Fernández 2020, p. 135). These data were provided by Bonsor, who as a result of his excavations also noted the existence of a group of structures damaged, by his reckoning, by seismic activity (Bonsor 1928, pp. 8 and 12). The most recent research also indicates that the production and residential areas were in use as a burial place during the fourth and fifth centuries AD, that is, certain areas of the settlement were put to different uses.

The El Eucaliptal site (Punta Umbría, Huelva) seems to have undergone a similar process. In this enclave in the Odiel estuary, a significant contraction of the settlement can be seen, represented by a major remodelling of the production sector in high Imperial period during which different burials would be performed. At this moment in the first half of the third century AD, some of the salting basins were filled and reused (see Fig. 11.4) (Campos et al. 2015, pp. 81–82).

Similarly, in the fishing and industrial quarter of Onoba, there is archaeological evidence of a stagnation or discontinuance of production in the factories by the middle of the third century AD (Campos 2011). This can be seen in the reuse of salting basins, such as the cases documented on Fernando el Católico and Tres de Agosto Streets (see Fig. 11.5) (Del Amo 1976; Lozano and González 2004; Campos et al. 2015).

Another of the coastal sites in which this recession can be conjectured is El Terrón (Lepe). In the third century AD, the factory and the settlement seem to have continued in use at least until the first half of the century, as evidenced by coinage struck during the reign Gordian III (AD 238–241). However, thenceforth—from the middle to the end of the century—there are no materials or elements that allow us to speak of continuity. This trend seems to have changed in the fourth century AD, a period in which the settlement resumed its activity, with new industrial quarters, channels and salting basins. Nevertheless, a whole set of structures dating to the end of this same century has been recovered. This level is represented by a regular deposit throughout the sector of the industrial quarter, with the collapse and filling of infrastructures, channels, slop ponds and so on, which seems to correspond to a high-energy event (see Fig. 11.6)

Fig. 11.4 Salting basin at El Eucaliptal site reused in the middle of the third century AD (*Source* Campos et al. (2015) Fig. 4)

Fig. 11.5 Archaeological remains at Onoba

(Campos and Gómez 2001; Campos et al. 1999b).

There is a general lack of population and productive indicators at coastal archaeological sites in different areas of the Atlantic seabord of Iberia for the third century AD. In this regard, on the Atlantic coast of Lusitania, there are signs of abandonment of Roman halieutic installations at this time, relating to a rise in the sea level. A good example of this is the Abul factory, in the Sado estuary, where palaeogeographic studies have shown that this occurred in the middle of the third century AD, making it necessary to move the industrial quarter (Mayet and Tavares da Silva 2002).

Another recorded case is the fish-salting factory of Tróia, also in this same estuary, which experienced a revival in the middle of the third century AD, coinciding with the start of the manufacturing of Almagro 50- and 51C-type vessels (Etienne et al. 1994).

Something similar occurred in the city of Ossonoba, after the mid-third century AD, when it began to prosper anew, before consolidating its importance during the final decades of the century and at the beginning of the following one (Bernardes 2012). In the case of the Cadiz area, research in the city of Baelo Claudia has brought to light evidence of a seismic event in the mid-third century AD, which would explain the collapse and destruction of buildings (Grützner 2011; Silva et al. 2009, 2016). After the final decades of the third century AD, when there is evidence that the factories began very slowly to resume their activities, the beginning of the following century would be accompanied by widespread activity and occupation in many of the old coastal settlements.

In other words, the archaeological context of the fish-salting factories on the Atlantic coast, in both Huelva and Portugal, points to a strange hiatus and general crisis in the fishing industry in the middle of the third century AD, after which it would have fully recovered by the beginning of the following century, as illustrated by the resumption of activities in some of the settlements and factories described above.

11.3.2.2 Geological Evidence

The geological evidence of this tsunami has been contrasted at three sites on the Gulf Cadiz and in the adjacent Mediterranean areas (see Fig. 11.2). This includes cheniers and bioclastic layers in estuaries (rivers Guadalquivir and Guadalete) and on rocky coasts (Gibraltar). Ages have been calibrated for 2σ intervals, with the application of the reservoir effect correction (-108 ± 31 ^{14}C yr) calculated by Martins and Soares (2013) for this area.

Guadalquivir Estuary

Several sandy layers and cheniers have been attributed to the effects of a tsunami during this period (see Fig. 11.7, A-B), with similar calibrated ages (cal. AD 150–490). They have the following features: (1) an erosive base that sometimes contains clasts from the underlying clay sediments; (2) basal bioclastic layers, with increasing amounts of silts and sands; (3) the presence of numerous disarticulated or fragmented valves of molluscs (mainly *Cerastoderma edule*, *Glycymeris* spp., *Ruditapes decussatus*) in this basal layer; (4) an upper layer with a decreasing mean grain size and more dispersed bioclastic fragments; (5) the partial replacement of foraminiferal assemblages typical of internal lagoon environments (e.g. *Haynesina germanica*) present in the underlying clays by others characteristic of more external lagoon environments or infralittoral marine areas (e.g. *Ammonia* spp., *Elphidium* spp., miliolids); and (6) the presence of ostracods from the adjacent marine palaeoenvironments (e.g. *Pontocythere*, *Urocythereis*, *Semicytherura*) (Ruiz et al. 2004, 2005; Guerra 2014).

Guadalete Estuary

The river Guadalete (157 km long), which flows into the Bay of Cadiz, can be divided into an internal area and an external area (see Fig. 11.8, A-B). Gutiérrez-Mas et al. (2009) note the presence of a tsunami deposit in the latter, composed of fine silty sands with shell fragments and boulders. The age of this layer is almost identical to that of the aforementioned cheniers of Doñana (1960 ± 110 yr BP; cal. AD 50–580).

Fig. 11.6 Channel at the El Terrón site, filled with sea deposits at the end of the fourth century AD (*Source* Campos et al. (2015) Fig. 3)

The Rock of Gibraltar

The Rock of Gibraltar is located on the Mediterranean coast adjacent to these Atlantic areas. Near its south-western end, it includes the bay of Rosia (see Fig. 11.9), with a high cliff of Jurassic dolostones. These rocks have a strong karstification, with the presence of numerous deep open crevices on their surface. Some of them have been filled with bioclastic sediments with ages very similar to those indicated above (Rodríguez-Vidal et al. 2015).

Final Reflection

The occupation of the Huelva coast, since the second century AD up until the moment of its disappearance at the middle of the sixth century AD, had its ups and downs.

Beyond the general historical causes, the so-called"crisis of the third century AD", there is a variety of archaeological and geological evidence that allows for establishing a succession of several high-energy events, namely, cycles of strong storms or tsunamis, which affected the area's coastal settlements. The revision of the historical record of tsunamis has led to the proposal of

Fig. 11.7 Geological evidence (I): Doñana Guadalquivir estuary

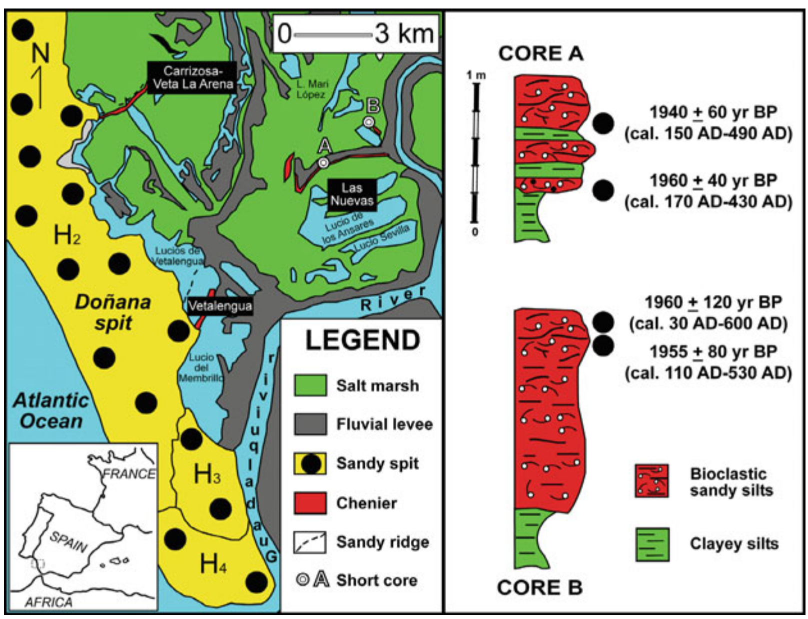

Fig. 11.8 Geological evidence (II): Guadalete estuary

different periods of recurrence for these events—1200–1500 years (Lario et al. 2011); 700–1000 years (Ruiz et al. 2013). On the other hand, the analysis of active faults in the Gulf of Cadiz has allowed Matias et al. (2013) to posit an earthquake recurrence period of around 700 years for M_w 8.0 events and of 3500 years for M_w 8.7 events, two possible causes of the tsunamis, together with more localised landslides or tectonic displacements (see examples in Baptista and Miranda 2009).

The research carried out in the last decades shows how in the third century AD there was an important and widespread stagnation or discontinuance of activity at many of the archaeological sites of seabord of the province of Huelva, as can be seen from the available geoarchaeological evidence at those such as Cerro del Trigo, El Eucaliptal, Huelva and El Terrón. At all of them, there are clear signs of disruption in their habitats, factories, necropolises, etc., in the central decades of the third century AD.

To this should be added the geological evidence of extreme wave events (EWEs) in the marshes of the Guadalquivir, where an episode of these characteristics has been documented in the third century AD, which has led us to relate it to the adjacent settlement of Cerro del Trigo. Furthermore, on a broader scale, identical data have been collected on the Portuguese Atlantic coast in the Sado estuary, in the Algarve, and in the Gulf of Cadiz at points such as the Guadalete estuary, the Roman city of Baelo Claudia and the Rock of Gibraltar.

Finally, there was a second similar episode at the end of the fourth century AD. There are interesting indicators that now clearly confirm a tsunami that destroyed and modified the coastline, devastating numerous settlements and fish-salting factories that would then begin to recover at the beginning of the fifth century AD. On the one hand, at the archaeological site of El Terrón (Lepe), there is evidence of a level of marine flooding that would have destroyed the settlement's industrial quarter, channels and settling ponds. This episode seems to be somewhat similar to another occurring in El Eucaliptal (Punta Umbría). At this archaeological site, a sandy sediment was documented during the mid-Empire period, just above which there is a level of occupation with abundant material from the second half of the fourth and early fifth centuries AD.

It also coincided with the occupation of new areas, such as La Cascajera immediately afterwards and the establishment of halieutic installations in the suburban areas to the north of the city of Onoba (La Orden), more protected from the open sea. On the other hand, the most recent geoarchaeological studies have confirmed the existence of a tsunami in the Atlantic area of Huelva, in particular, and in the area of the Gulf of Cadiz, in general, at the end of fourth century AD (Campos et al. 2015, pp. 86–87). This archaeological evidence dated to the end of the

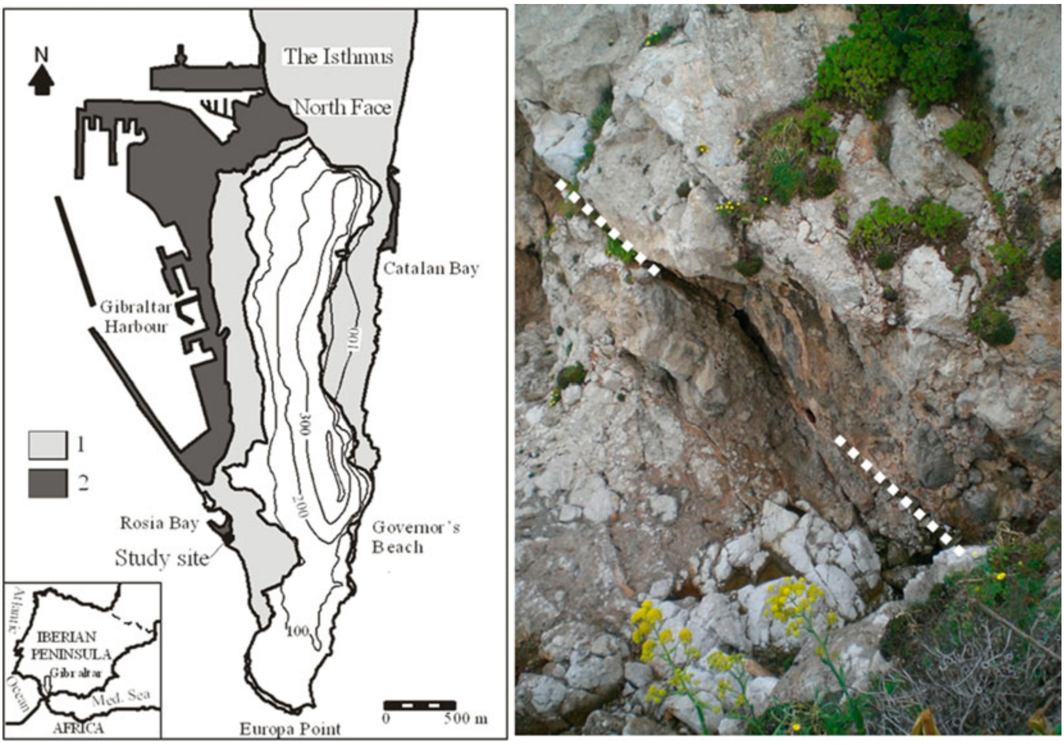

Fig. 11.9 Left: Geographical location of the Gibraltar Rock and the study area (Bay of Rosia). Legend: 1. Late Pleistocene formations, 2. Reclaimed land

fourth century AD and especially as of the following one, points to the recovery of the coastal sites in its wake. This recovery took longer after the event occurring in the third century AD than after that in the following one, probably due to the decline of the municipal order of the urban world and the economic and political crises at the time.

In other words, after the first episode, the reactivation of the halieutic industry cannot be confirmed until the end of the third or at the beginning of the fourth century AD, which curiously coincides with the administrative action and measures adopted by the Tetrarchs aimed at its reorganisation, with the re-exploitation of some farms in the mining district of Urium (Pérez 2006). After the second episode, the coastline as a whole apparently recovered more swiftly in the early fifth century AD, which would coincide with the heyday of this industry on the coast of Huelva, with numerous factories in areas as significant as the estuary of the rivers Tinto and Odiel.

The recovery of the fishing industry over a period of about 20–25 years was perhaps due to the intervention of the bishop of Niebla and to the urban ecclesiastical hierarchy of cities like Onoba, who might have had a stake in its reconstruction (Campos et al. 2015). Therefore, we believe that this recovery is related to the emergence of a strong political or ecclesiastical economic power. Although further research should be performed on this issue, we believe that the revival of this important and thriving industry would have been impossible without the intervention of the political and economic powers that be at the time.

Acknowledgements This study has been performed in the framework of the following projects: (1) DGYCIT project CTM2006-06722/MAR; (2) DGYCIT project CGL2006-01412; (3) "From the Atlantic to the Tyrrhenian. The Hispanic ports and their commercial relations with Ostia Antica. DEATLANTIR II—HAR2017-89154-P—(Plan Nacional de I+D+i); and (4) "Análisis geoarqueológico y paleoambiental en puertos y distritos marítimos atlántico-mediterráneos: el arco atlántico del suroeste hispano (Onoba, Huelva) y la desembocadura del Tíber (Portus, Roma)" (UHU-1260298; Project I+D+i FEDER 2014-2020). Also funded by the Andalusian regional government (groups HUM-132, RNM-238 and RNM-293), it is a contribution of the Research Centre in Historical, Cultural and Natural Heritage (CIPHCN) of the University of Huelva.

References

Abad M, Muñoz AF, González-Regalado ML et al (2019) Evolución paleoambiental de una turbera finiholocena en el sector suroccidental del Parque Nacional de Doñana (S. O. de España). Estudios Geológicos 75: e087

Alonso C, Gracia FJ, Del Río L et al (2004) Registro morfosedimentario de eventos históricos de alta energía en el litoral atlántico del Estrecho de Gibraltar (Trafalgar-Tarifa). In: Benito G, Díez Herrero A (eds) Contribuciones recientes sobre Geomorfología. SEG-CSIC, Madrid, pp 263–271

Alonso C, Gracia FJ, Rodríguez-Polo S et al (2015) The record of energetic marine events in the bay of Cádiz during historical times. Cuaternario y Geomorfología 29:95–117

Andrade C (1992) Tsunami generated forms in the Algarve barrier islands. Sci Tsunami Hazard 10:21–33

Álvarez-Martí-Aguilar M (2017a) Terremotos y tsunamis en Portugal en época antigua: el legado de Bernardo de Brito y su Monarchia Lusytana (1597–1609). Euphrosyne 45:183–204

Álvarez-Martí-Aguilar M (2017b) La tradición historiográfica sobre catástrofes naturales en la Península Ibérica durante la Antigüedad y el supuesto tsunami del Golfo de Cádiz de 218–209 a.C. Dialogues d'histoire ancienne 43(2):117–145

Álvarez-Martí-Aguilar M (2020) The historicity of the earthquakes occurring in the Iberian Peninsula before A.D. 881 recorded in Spanish and Portuguese seismic catalogs. Seismol Res Lett 91(6):3585–3594. https://doi.org/10.1785/0220200168

Baptista MA, Miranda JM (2009) Revision of the Portuguese catalog of tsunamis. Nat Hazard 9:25–42

Baptista MA, Heitor S, Miranda JM et al (1998) The 1755 Lisbon tsunami: evaluation of the tsunami parameters. J Geodyn 25:143–157

Bernal D (2007) Contextos cerámicos en el área del estrecho de Gibraltar (ss. V-VII d.C.). Hacia el replanteo de la dinámica urbana, económica y comercial tardorromana. In: LRCW2. Late Roman Coarse Wares, Cooking Wares and Amphorae in the Western Mediterranean. Archaeology and Archaeometry. Archaeopress, Oxford, pp 109–117

Bernardes JP (2012) A cidade de Ossónoba e o seu territorio. Anais do Município de Faro 37:11–26

Bonsor G (1928) Tartesos. Excavaciones practicadas en 1923 en el cerro del Trigo. Término de Almonte (Huelva). Junta Superior de Excavaciones y Antigüedades 97. Tipografía de Archivos, Madrid

Brito B de (1609) Segunda parte da Monarchia Lusytana em que se continuão as historias de Portugal desde o nacimento de nosso Salvador Iesu Christo até ser dado em dote ao Conde dom Henrique. Pedro Crasbeeck, Lisboa

Cáceres LM, Gómez P, González-Regalado ML et al (2018) Modelling the mid-late Holocene evolution of the Huelva Estuary and its human colonization, South-Western Spain. Mar Geol 406:12–26

Campos JM (2011) Onoba Aestuaria. Una ciudad portuaria en los confines de la Bética. Ed. Ayuntamiento de Huelva, Huelva

Campos JM, Gómez F (2001) La Tierra llana de Huelva: Arqueología y Evolución del paisaje. Arqueología Monografías 13. Ed. Consejería de Cultura Junta de Andalucía, Sevilla

Campos JM, Vidal N (2004) Las salazones del litoral onubense: la cetaria de 'El Eucaliptal.' Huelva en su Historia 11:51–82

Campos JM, Castiñeira J, García JM et al (1990) Arqueología y evolución del paisaje: un proyecto geoarqueológico en la Tierra Llana de Huelva. Cuadernos del Suroeste 2:43–70

Campos JM, Vidal N, Pérez JA et al (1996) Excavaciones arqueológicas en la factoría y necrópolis de El Eucaliptal (Punta Umbría, Huelva). Campañas 1993 y 1994. Inédito. Memoria de investigación. Delegación territorial de Educación, Cultura y Deporte. Junta de Andalucía, Huelva

Campos JM, Alzaga M, Benabat Y et al (1997) Factoría de salazones de El Eucaliptal (Punta Umbría, Huelva). Anuario Arqueológico de Andalucía/1993, vol III:313–323

Campos JM, Pérez JA, Vidal NO (1999a) El Eucaliptal, una necrópolis romana de pescadores (Punta Umbria, Huelva). Huelva en su Historia 7:195–231

Campos JM, Pérez JA, Vidal NO (1999b) Las cetariae del litoral onubense en época romana. Universidad de Huelva, Huelva

Campos JM, Pérez JA, Vidal NO et al (2001a) Intervención de emergencia en el yacimiento romano de El Terrón-La Bella (Huelva). Julio de 1996. Anuario Arqueológico de Andalucía/1996, vol III:235–246

Campos JM, López MA, Benabat Y et al (2001b) Intervención Arqueológica de emergencia en el asentamiento romano de El Terrón (Lepe, Huelva). Anuario Arqueológico de Andalucía/1997, vol III:359–364

Campos JM, Gómez A, Vidal NO et al (2002a) La factoría romana de El Cerro del Trigo (Doñana, Almonte, Huelva). Anuario Arqueológico de Andalucía/1999, vol III-1:330–349

Campos JM, Pérez JA, Vidal NO et al (2002b) Las industrias de salazones del litoral onubense: Los casos del Eucaliptal (Punta Umbría) y Cerro del Trigo (Almonte). Huelva en su Historia 9:76–96

Campos JM, Vidal M, Gómez A (2013) La cetaria de “el cerro del trigo” (Doñana, Almonte, Huelva) en el contexto de la producción romana de salazones del sur peninsular. Universidad de Huelva, Huelva

Campos JM, Bermejo J, Rodríguez-Vidal J (2015) La ocupación del litoral onubense en época romana y su relación con eventos marinos de alta energía. Cuaternario y Geomorfología 29(1–2):75–93

Campos ML (1991) Tsunami hazard on the Spanish coasts of the Iberian Peninsula. Sci Tsunami Haz 9:83–90

Dabrio CJ, Goy JL, Zazo C (1999) The record of the tsunami produced by the 1755 Lisbon earthquake in Valdelagrana spit (Gulf of Cadiz, southern Spain). Geogaceta 23:31–34

Del Amo M (1976) Restos materiales de la población romana de Onuba. Huelva Arqueológica 2. Diputación Provincial, Huelva

El Mrabet T (1991) La sismicité historique du Maroc. Thése de 3éme cycle, Université Mohammed V, Rabat

El Mrabet T (2005) Les grands séismes dans la région maghrébine. Dissertation, Université Mohammed V, Rabat

Etienne R, Makaroun F, Mayet F (1994) Un grand complexe industriel a Tróia (Portugal). Ed. De Boccard, Paris

Fernández L (2020) Espacios y usos funerarios en la ciudad portuaria de Onoba y su área de influencia entre los siglos II a.C. – VII d.C. Universidad de Huelva, Huelva

Galbis J (1932) Catálogo sísmico de la zona comprendida entre los meridianos 5º E y 20º W de Grenwich y los paralelos 45º y 25 º N, vol 1. Instituto Geográfico, Catastral y de Estadística, Madrid

Gracia FJ, Alonso C, Benavente J et al (2006) The different coastal records of the 1755 tsunami waves along the South Atlantic Spanish coast. Zeitschrift für Geomorphologie Suppl 146:195–220

Gràcia E, Vizcaino A, Escutia C et al (2010) Holocene earthquake record offshore Portugal (SW Iberia): testing turbidite paleosismology in a slow-convergence margin. Quatern Sci Rev 29:1156–1172

Grützner C (2011) The Baelo Claudia earthquake problem. Dissertation, RWTH Aachen University

Guerra LC (2014) GIS and Palaeontology integrated application for the recognition of tsunamigenic events in Doñana National Park. Master Thesis, Universidad do Algarve

Guerra L, Veiga-Pires C, González-Regalado ML et al (2020) Late Holocene benthic foraminifera of the roman Lacus Ligustinus (SW Spain): a paleoenvironmental approach. Ameghiniana 57:419–432

Gutiérrez-Mas JM, Juan C, Morales JA (2009) Evidence of high-energy events in shelly layers interbedded in coastal Holocene sands in Cádiz Bay (south-west Spain). Earth Surf Proc Land 34:810–823

Kaabouben F, Baptista MA, Iben Brahim A et al (2009) On the moroccan tsunami catalogue. Nat Hazard 9:1227–1236

Lario J, Luque L, Zazo C et al (2010) Tsunami vs. storm surge deposits: a review of the sedimentological and geomorphological records of extreme wave events (EWE) during the Holocene in the Gulf of Cadiz, Spain. Zeitschrift für Geomorphologie 54 (Supp. 3):301–316

Lario J, Zazo C, Goy JL et al (2011) Holocene palaeotsunami catalogue of SW Spain. Quatern Int 242:196–200

López MA, Castilla E, Haro J de (2003) Intervención arqueológica de urgencia en el Eucaliptal (Punta Umbría, Huelva). Informe Preliminar. Inédito. Delegación territorial de Educación, Cultura y Deporte. Junta de Andalucía, Huelva

López MA, Castilla E, Haro J de (2005) Intervención arqueológica de urgencia en el yacimiento romano de El Eucaliptal (Punta Umbría, Huelva). Anuario Arqueológico de Andalucía/2002, vol III-1:562–572

Lozano C, González D (2004) Excavación arqueológica de urgencia en la C/ Cardenal Cisneros nº 11 de Huelva. Anuario Arqueológico de Andalucía/2001, vol III-1:527–530

Luque L, Lario J, Civis J et al (2002) Sedimentary record of a tsunami during Roman times, Bay of Cadiz (Spain). J Quat Sci 17:623–631

Martínez-Solares JM (2005) Tsunamis en el contexto de la Península Ibérica y del Mediterráneo. Enseñanza de las Ciencias de la Tierra 13:52–59

Martínez-Solares JM, López AL (2004) The great historical 1755 earthquake. Effects and damage in Spain. J Seismolog 8:275–294

Martins JMM, Soares AMM (2013) Marine radiocarbon reservoir effect in Southern Atlantic Iberian coast. Radiocarbon 55:1123–1134

Martins I, Mendes-Victor LA (2001) Contribution to the Study of Seismicity in the West Margin of Iberia. IGIDL Pub 25. Universidade de Lisboa, Lisboa

Matias LM, Cunha T, Annunziato A et al (2013) Tsunamigenic earthquakes in the Gulf of Cadiz: fault model and recurrence. Nat Hazard 13:1–13

Mayet F, Tavares da Silva C (2002) L'atelier d'amphores d'Abul (Portugal). Ed. Ausonius, París

Morales JA, Borrego J, San Miguel EG et al (2008) Sedimentary record of recent tsunamis in the Huelva estuary (Southwestern Spain). Quat Sci Rev 27:734–746

Moreira de Mendonça JJ (1758) Historia universal dos terremotos, que tem havido no mundo, de que ha noticia, desde a sua creaçaõ até o seculo presente. … Antonio Vicente da Silva, Lisboa

Neres M, Carafa MMC, Fernandez RMS et al (2016) Lithospheric deformation in the Africa-Iberia plate boundary: improved neotectonic modeling testing a basal-driven Alboran plate. J Geophys Res Solid Earth

121(9):6566–6596. https://doi.org/10.1002/2016JB013012
Nocquet JM (2012) Present-day kinematics of the Mediterranean: a comprehensive overview of GPS results. Tectonophysics 579:220–242
Pérez JA (2006) La huella de Roma. Diputación Provincial, Huelva
Ponsich M (1988) Aceite de oliva y salazones de pescado. Factores geo-económicos de Betica y Tingitana. Universidad Complutense, Madrid
Pozo M, Ruiz F, González-Regalado ML et al (2020) The origin and evolution of Late Holocene tsunamiites in the Doñana National Park (SW Spain): trace elements as geochemical proxies. Minerals 10:956
Rodríguez-Ramírez A, Rodríguez-Vidal J, Cáceres LM et al (1996) Recent coastal evolution of the Doñana National Park (SW Spain). Quat Sci Rev 15:803–809
Rodríguez-Ramírez A, Ruiz A, Cáceres LM et al (2003) Analisis of the recent storm record in the southwestern Spanish coast: implications for littoral management. Sci Total Environ 303:189–201
Rodríguez-Ramírez A, Pérez-Asensio JN, Santos A et al (2015) Atlantic extreme wave events during the last four millennia in the Guadalquivir estuary, SW Spain. Quat Res 83:24–40
Rodríguez-Ramírez A, Villarías-Robles JR, Pérez-Asensio JN et al (2016) Geomorphological record of extreme wave events during Roman times in the Guadalquivir estuary (Gulf of Cadiz, SW Spain): an archaeological and paleogeographical approach. Geomorphology 261:103–118
Rodríguez-Vidal J, Ruiz F, Cáceres LM et al (2011a) Geomarkers of the 218–209 BC Atlantic tsunami in the Roman Lacus Ligustinus (SW Spain): a palaeogeographical approach. Quat Int 242:201–212
Rodríguez-Vidal J, Cáceres LM, Abad M et al (2011b) The recorded evidence of the AD 1755 Atlantic tsunami on the Gibraltar coast. J Iber Geol 37(2):177–193
Rodríguez-Vidal J, Cáceres M, González-Regalado ML et al (2015) Las grietas de acantilado como un nuevo tipo de registro de tsunamitas: ejemplo en la costa de Gibraltar. In: Galve JP, Azañón JM, Pérez Peña JV et al (eds) Una visión global del Cuaternario. El hombre como condicionante de procesos geológicos. XIV Reunión Nacional de Cuaternario, Granada, June-July 2015, pp 31–32
Ruiz F, Rodríguez-Ramírez A, Cáceres LM et al (2004) Late Holocene evolution of the southwestern Doñana National Park (Guadalquivir Estuary, SW Spain): a multivariate approach. Palaeogeogr Palaeoclimatol Palaeoecol 204:47–64
Ruiz F, Rodríguez-Ramírez A, Cáceres LM et al (2005) Evidence of high-energy events in the geological record: mid-holocene evolution of the southwestern Doñana National Park (SW Spain). Palaeogeogr Palaeoclimatol Palaeoecol 229:212–229
Ruiz F, Abad M, Rodríguez-Vidal J et al (2008) The geological record of the oldest historical tsunamis in southwestern Spain. Riv Ital Paleontol Stratigr 114:147–156
Ruiz F, González-Regalado L, Abad M et al (2012) El registro geológico de tsunamis holocenos en el estuario del río Tinto (SO de España). Geotemas 13:641–644
Ruiz F, Rodríguez-Vidal J, Abad M et al (2013) Sedimentological and geomorphological imprints of Holocene tsunamis in southwestern Spain: an approach to establish the recurrence period. Geomorphology 203:97–104
Sánchez Navarro-Neumann MM (1917) Ensayo sobre la sismicidad del suelo español. Boletín de la Real Sociedad de Historia Natural 46:83–109
Silva PG, Reicherter K, Grützner Ch et al (2009) Surface and subsurface palaeoseismic records at the ancient Roman city of Baelo Claudia and the Bolonia Bay area, Cádiz (south Spain). Geological Society of London, Special Publications 316:93–121
Silva PG, Giner-Robles JL, Reicherter K et al (2016) Los terremotos antiguos del conjunto arqueológico romano de Baelo Claudia (Cádiz, Sur de España): Quince años de investigación arqueosismológica. Estud Geol 72(1): e050. https://doi.org/10.3989/egeol.42284.392
Stich D, Serpelloni E, Mancilla FL et al (2006) Kinematics of the Iberia-Maghreb plate contact from seismic moment tensors and GPS observations. Tectonophysics 426:295–317
Schulten A (1945) Tartessos. Espasa Calpe, Madrid
Udías A (2015) Critical revision of earthquakes in the Iberian Peninsula before year 1000. Seismol Res Lett 86(3):2–23. Electronic supplement. https://www.seismosoc.org/Publications/SRL/SRL_86/srl_86-3_udias-esupp. Accessed 12 May 2020
Vidal NO (2007) Análisis Arqueológico de la Romanización del territorio onubense. Universidad de Huelva, Huelva
Whelan F, Kelletat D (2003) Analysis of tsunami deposits at Cabo de Trafalgar, Spain, using GIS and GPS technology. Essener Geographische Arbeiten 35:11–25
Zazo C, Goy JL, Somoza L et al (1994) Holocene sequence of relative sea level highstand lowstand in relation to the climatic trends in the Atlantic-Mediterranean linkage coast: forecast for future coastal changes and hazards. J Coast Res 10(4):933–945

12 A Third Century AD Extreme Wave Event Identified in a Collapse Facies of a Public Building in the Roman City of *Hispalis* (Seville, Spain)

Mario Gutiérrez-Rodríguez,
José N. Pérez-Asensio,
Francisco José Martín Peinado,
Enrique García Vargas, Miguel Ángel Tabales,
Antonio Rodríguez Ramírez, Eduardo Mayoral Alfaro,
and Paul Goldberg

Abstract

The southwestern coast of the Iberian Peninsula has been considered a low-probability tsunamigenic area. However, both onshore and offshore studies have characterized the occurrence of several extreme wave events (tsunamis and storm surges) in the Gulf of Cadiz during the Holocene. Among all the events reported in literature, in recent years the third century AD EWE events are being progressively gaining importance. Sedimentary records of these events are now more evident than previously stated and can be traced in a large regional scale. Some authors have proposed that such events would explain certain abandonment facies in coastal archaeological settlements in the area. In this context, we present a high-energy deposit identified in the suburbs of the Roman city of *Hispalis* (Seville), in a third century AD

M. Gutiérrez-Rodríguez (✉)
Instituto Universitario de Investigación en Arqueología Ibérica, Universidad de Jaén, Edificio C-6, Campus Las Lagunillas, 23071 Jaén, Spain
e-mail: mgrodrig@ujaen.es

J. N. Pérez-Asensio
CEREGE UM34, Aix Marseille Université, CNRS, IRD, INRAE, Coll France, 13545 Aix-en-Provence, France
e-mail: perez@cerege.fr

F. J. Martín Peinado
Departamento de Edafología y Química Agrícola, Universidad de Granada, Avenida de la Fuente Nueva 2, 18001 Granada, Spain
e-mail: fjmartin@ugr.es

E. García Vargas
Departamento de Prehistoria y Arqueología, Universidad de Sevilla, Doña María de Padilla s/n, 41004 Seville, Spain
e-mail: egarcia@us.es

M. Á. Tabales
Departamento de Construcciones Arquitectónicas II, Universidad de Sevilla, Avenida Reina Mercedes nº 4 B, 41012 Seville, Spain
e-mail: tabales@us.es

A. Rodríguez Ramírez · E. Mayoral Alfaro
Departamento de Ciencias de la Tierra, Universidad de Huelva, Avenida 3 de Marzo s/n, 21007 Huelva, Spain
e-mail: arodri@uhu.es

E. Mayoral Alfaro
e-mail: mayoral@uhu.es

P. Goldberg
Institut für Naturwissenschaftliche Archäologie, Eberhard Karls University of Tübingen, Rümelinstraße 23, 72070 Tübingen, Germany
e-mail: paulberg@bu.edu

M. Álvarez-Martí-Aguilar and F. Machuca Prieto (eds.), *Historical Earthquakes, Tsunamis and Archaeology in the Iberian Peninsula*, Natural Science in Archaeology,
https://doi.org/10.1007/978-981-19-1979-4_12

context of traumatic collapse of a Roman public building. This paper aims to present the sedimentary structures, bedforms, and features of this deposit in its archaeological context, exploring its possible origin in a combined action of an extreme wave event and fluvial flooding. Also, a critical review of the literature about the third century AD event(s) is done.

Keywords

Extreme wave event · Micromorphology · Hispalis · Roman building · Traumatic collapse

12.1 Extreme Wave Events in Southwestern Iberia During Roman Times: Debating the Third Century AD Event(s)

The mouth of the river Guadalquivir is a very complex network of tidal channels in a marshy environment which was greatly altered by agricultural colonization in the twentieth century. However, it still preserves the landscape characteristics of a large basin that has been clogged over the centuries by the sedimentation of the Guadalquivir, retained by the Doñana sandy coastal bar. This led to the transformation of the sea gulf into a lagoon, and although the filling process is by and large well known, it is difficult to establish the status of this marshy landscape for each specific historical period (Borja et al. 2018; Rodríguez-Ramírez et al. 2019).

The first literary description of the cities established on the margins of this coastal landscape is provided by Strabo of Amasia, who wrote his *Geography* in the change of era (*Geographica*, 3.2.5). He did not know the region first hand, but drew on authors such as Posidonius who, a hundred years earlier, had traveled to Cadiz to study the phenomenon of the tides, confirming that the estuaries or channels that characterized this marshy area served as navigation and communication routes for the population.

From the end of the Roman Republic and throughout the development of the Roman Empire, the consolidation of the supralittoral marshes and the floodplain was a noteworthy consequence of the development of the dune system in the Guadalquivir's mouth, and the spit bars of Doñana and La Algaida. In around AD 400, the sea penetrated only a small sector of the ancient gulf (Borja et al. 2018), creating a lagoon usually called *Lacus Ligustinus* after the coetaneous description of Avienus in his *Ora Maritima* (279–280). Although in the first century AD Pomponius Mela mentions a lake at the mouth of the Guadalquivir (Mel. 3.5), the *Ligustinus* place name is only found in Avienus. It surely responds to the transposition of a Greek toponym from the Aegean and the Phocaean colonies of the Gulf of Leon (where the current *Liguria* giving its name to this *lacus* is located) to the West. This toponym would have been drawn from the ancient periplus that Avienus would have consulted and sometimes recreated with his poetic imagination (Ferrer Albelda 2012).

Around this *lacus*, its marshes and the rivers that flowed into it, the settlement is distributed on vertical axes in three major sectors (García Vargas 2008): (1) A western sector around Campo de Tejada (*Ituci, Ostur*) and the river Guadiamar or *Maenuba*, on whose banks, from north to south, *Lastigi*, *Laelia*, and *Olontigi* were located; (2) a central axis represented by the river Guadalquivir between *Caura* (Coria del Río), *Osset* (San Juan de Aznalfarache), and *Ilipa Magna* (Alcalá del Río); and (3) the southeastern limit of the lake between *Orippo* (Torres de los Herberos, Dos Hermanas) and *Hasta Regia*, currently located in the Guadalquivir estuary near Jerez de la Frontera.

The mining and metallurgical economy of the Guadiamar axis, at the eastern end of the SW pyrite belt, to which the Rio Tinto mines also belong, was very important at least until the end of the second century BC (Amores et al. 2014). Here, surveys at *Laelia* (Cerro de la Cabeza, Olivares) have revealed an important development of cupellation and metallurgy of silver in a wide sector of the mine. The axis of the Guadalquivir, with *Hispalis*, its main port suitable for large trading vessels, was still navigable for medium-sized ships up river to *Ilipa Magna* (Alcalá del Río). This sector was devoted to agriculture and, above all, trade, connecting the bountiful countryside of the lower and middle Guadalquivir basin, and the mining areas of Sierra Morena with the Atlantic and Mediterranean seaboards. The cities from the Guadalquivir estuary to the Jerez countryside were located in agricultural areas increasingly given over to wine and oil production.

It is in this historical and archeological context that several extreme wave events (hereinafter EWEs) have been identified in the region during Roman times. The origin of these tsunamis is related to the seismic activity of the Gulf of Cadiz, specifically to the Azores-Gibraltar transformation faults. The tectonics of this area include a strike-slip fault movement in the west (Azores) and a north–south compression fault in the east (Gibraltar) (Udías et al. 1976; Buforn et al. 1988; Lario et al. 2011).

The information on these events comes from very diverse sources, while most of the evidence derives from a large number of geological and sedimentological studies. During the last three decades, a very fruitful line of research led by geologists has been developed, focusing on the identification and characterization of these deposits on the southwest coast of the Iberian Peninsula (Costa et al. this volume). Specifically, several teams have carried out surveys, identifying high-energy events in different basins and estuarine systems such as the Guadalquivir (Lario et al. 1995, 2001, 2002; Rodríguez-Ramírez et al. 1996, 2015, 2016, this volume; Luque et al. 2001; Ruiz et al. 2004, 2005, 2008; Rodríguez-Vidal et al. 2008, 2011), Tinto-Odiel (Ruiz et al. 2007; Morales et al. 2008; Campos et al. 2015; Bermejo Meléndez et al. this volume; Rodríguez-Vidal et al. 2015; González-Regalado et al. 2019a, b) and Guadalete basins (Lario et al. 1995; Dabrio et al. 1999; Luque et al. 2001, 2002; Gutiérrez-Mas et al. 2009; Gutiérrez-Mas 2011; Gracia et al. this volume), the coastal landscape of the southeast coast of the Gulf of Cadiz (Luque et al. 2002; Alonso et al. 2003a, b, 2004; Whelan and Kelletat 2003; Gracia et al. 2006; Arteaga et al. 2015; Vázquez et al. this volume), the abyssal plain of the Gulf of Cadiz (Vizcaíno et al. 2006; Gràcia et al. 2010), and finally the Algarve and Portugal (Andrade 1992; Dawson et al. 1996; Scheffers and Kelletat 2005; Andrade et al. 2016; Feist et al. 2019). Consequently, this has led to the compilation of a catalog of tsunamis occurring on the southwestern seaboard of Iberia during the Holocene (Lario et al. 2010, 2011). This catalog identifies seven EWEs over the last 7000 years. However, not all these events would correspond to tsunamis. In view of the data that it contains, it is possible to estimate a return period of 1200–1500 years for tsunamis in the southwest of the Iberian Peninsula (Morales et al. 2008; Lario et al. 2011).

As to the written sources, the tsunami and earthquake catalog compiled by José Galbis (1932) stands out. An exhaustive compilation of historical references to earthquakes and marine floods from protohistory and Classical Antiquity up until the beginning of the twentieth century, it identifies 20 references to seismic events from 1030 BC to AD 585. Some of these earthquakes and tsunamis would have struck the southwestern seaboard of Iberia, as is the case of the events dated to 218–209 and 60 BC. For decades, geological studies have attempted to correlate the chronology of the tsunami deposits identified with the events described by Galbis (Table 17.1). However, a recent systematic and critical historiographic analysis of the sources used by Galbis, carried out by Manuel Álvarez-Martí-Aguilar (2017a, b, 2020, and this volume; Rodríguez-Ramírez et al. 2016), has demonstrated the unreliability of the vast majority of them for identifying the events described in the catalog. This leads to another major challenge in the state of the art of EWE deposit research in this study area: their absolute dating and regional correlation.

Finally, archeology is another source for approaching tsunami events in the region. Albeit entering this debate at a relatively late date, archeologists have begun to collaborate with geologists. Their research has been more specific than systematic, except for examples like the study of the effects of seismic events in *Baelo Claudia* (a synthesis in Silva et al. 2010). Although on many occasions the traumatic destruction of architectural structures has been linked to seismic events without major empirical support, there is indeed an increasing body of evidence of the impact of earthquakes and tsunamis in southwestern Iberia, a topic that has recently found its way onto the archeological research agenda in this area (Bernal et al. 2015, this volume).

After decades of research, several of the events identified in the Holocene would have occurred during Roman times, according to the current state of the art (Fig. 12.1):

(a) 218–209 BC. Plenty of evidence of high-energy events has been found along the coast of the Gulf of Cadiz, which, according to radiocarbon dating, would be located within a broad chronological range between 2700 and 2200 cal. yr BP. This evidence includes the erosion and breaching of littoral spit bars, sandy inputs with marine bioclasts into estuaries and marshes, the reworking of cheniers, and turbiditic deposits in the Atlantic abyssal plain (Rodríguez-Vidal et al. 2011; Ruiz et al. 2008, 2013a, b; Vizcaíno et al. 2006; Gràcia et al. 2010; Scheffers and Kelletat 2005). Although these indicators may correspond to both storms and tsunamis, the presence of wash-over fans toward the interior of the marshes, exhibiting fining-upward sequences, plus marine fauna, rounded clasts, and a silty-clay layer at the top of the high-energy deposit, probably indicate a tsunami origin. This event would have remodeled the landscape significantly in some areas of the Atlantic coast, and would have contributed to the reorganization of the drainage network in some basins, such as the Guadalquivir and Guadalete estuaries (Lario et al. 2010). By comparing these data with the description contained in Galbis' seismic catalog (1932), this event has been dated to 210–209 BC. As Lario et al. (2011, p. 168) have observed, "Age discrepancies for this apparently single event are probably due to flaws in the radiocarbon dating method […] it is also possible that a given particular event was assigned to different ages in separate localities." Uncertainties about this event from the geological and historiographic perspectives were evinced by Rodríguez-Ramírez et al. (2016).

(b) 60 BC-first century AD. Alonso et al. have identified this event in the Bay of Bolonia (Cadiz) in a deposit of bioclastic sands (Alonso et al. 2003a, b, 2004). Arteaga et al. have also identified possible tsunami deposits dating back to the first century AD in the Bay of Algeciras (Arteaga et al. 2015). The reliability of this event and its possible evidences in Galicia and north Portugal are discussed in Costa et al. (this volume). For Lario et al. (2011), however, this evidence should be understood as preliminary data, somehow associated with the 60 BC tsunami event reported in Galbis' seismic catalog (1932).

(c) Third century AD: This event was included in the EWE catalog after the identification of geomorphological and sedimentological evidences in the Guadalquivir, Guadalete and Tinto-Odiel estuaries (Morales et al. 2008; Gutiérrez-Mas 2011; Rodríguez-Ramírez et al. 2016). In the Doñana marshland a bioclastic sandy silt layer was initially identified (Ruiz et al. 2004). According to their authors, this deposit would have been generated during a violent storm and it would be dated in 2050–2000 cal. yr BP. Subsequent research, after a recalibration of the radiocarbon dating of those same deposits, and together with other geological evidence, placed the event in the second–third century AD (Rodríguez-Ramírez et al. 2016). According to Lario et al. (2010, p. 311): "considering that the sedimentological data are inconclusive, and

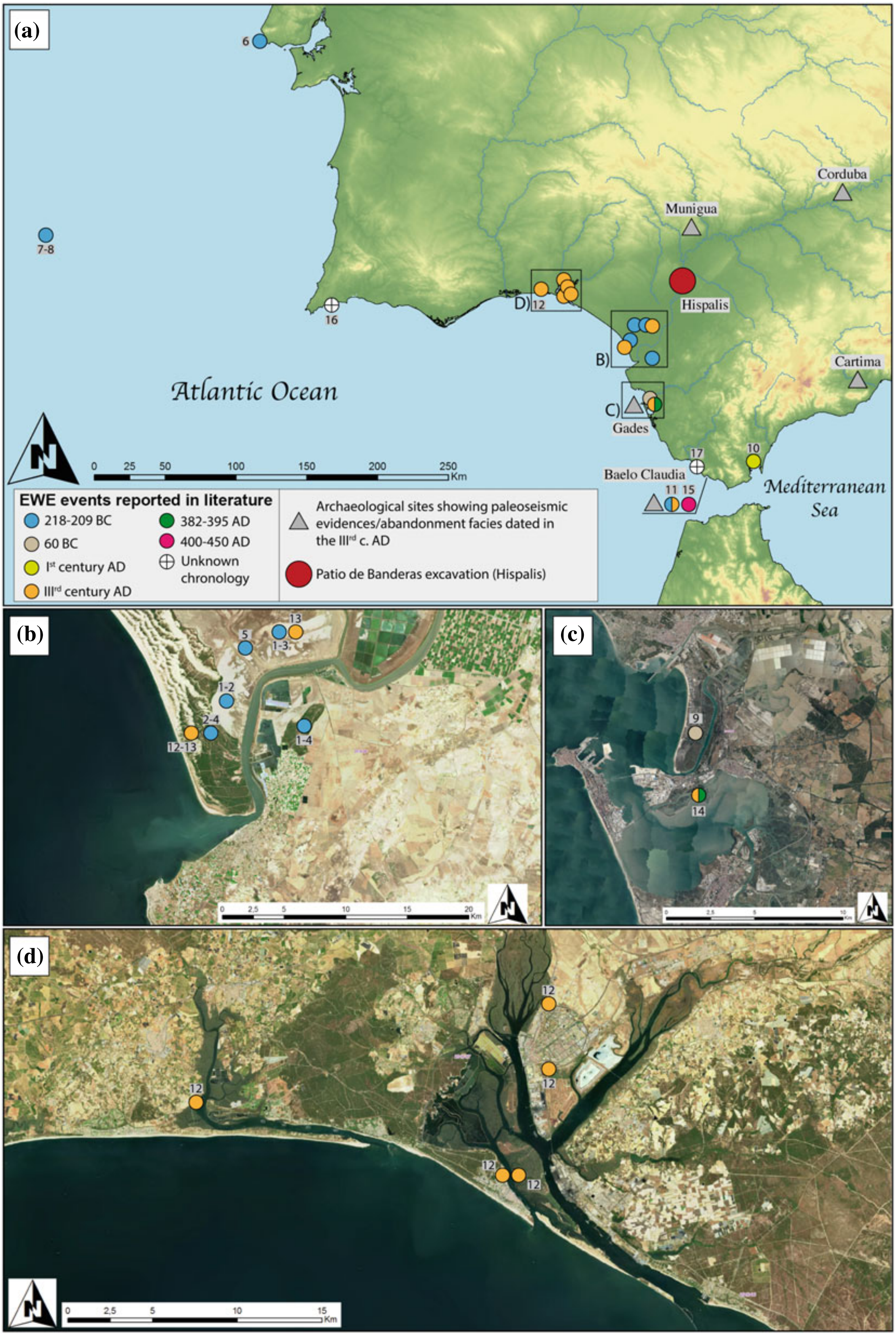
(a)
Corduba
Munigua
Hispalis
Cartima
Gades
Baelo Claudia
Atlantic Ocean
Mediterranean Sea
EWE events reported in literature
218-209 BC
60 BC
I[st] century AD
III[rd] century AD
382-395 AD
400-450 AD
Unknown chronology
Archaeological sites showing paleoseismic evidences/abandonment facies dated in the III[rd] c. AD
Patio de Banderas excavation (Hispalis)
(b)
(c)
(d)

◀ **Fig. 12.1** **a** Tsunami and EWE deposits of Roman chronology identified in the SW coast of Spain and location of the high-energy deposit identified in the Patio de Banderas excavation in the Roman city of Hispalis (modern Seville). **b** Detail of the Guadalquivir estuary. **c** Detail of the Guadalete estuary. **d** Detail of the Tinto-Odiel estuary. Numbers refer to the following references: 1. Rodríguez-Vidal et al. 2011; 2. Ruiz et al. 2004; 3. Ruiz et al. 2008; 4. Rodríguez-Ramírez et al. 1996; 5. Lario et al. 2001; 6. Scheffers and Kelletat 2005; 7. Gràcia et al. 2010; 8. Vizcaíno et al. 2006; 9. Luque et al. 2001, 2002; 10. Arteaga et al. 2015; 11. Alonso et al. 2003a, b, 2004; 12. Campos et al. 2015; 13. González-Regalado et al. 2019a and b; 14. Gutiérrez-Mas 2011; 15. Röth et al. 2015; 16. Feist et al. 2019; 17. Reicherter et al. 2010

the local occurrence of these deposits, this layer may represent an EWE with limited impact only." However, subsequent research has brought to light more data about this event, identifying clear sedimentary evidence in the Doñana (Rodríguez-Ramírez et al. 2016), Tinto-Odiel (Campos et al. 2015; González-Regalado et al. 2019a, b), and Guadalete estuaries (Gutiérrez-Mas 2011). Some of these evidences were identified as storm deposits (González-Regalado et al. 2019a, b), while others were described as tsunami deposits (Gutiérrez-Mas 2011; Rodríguez-Ramírez et al. 2016). In this situation, it is challenging to assess if these evidences correspond to the same or different events, and also, in the case of the tsunami hypothesis, it turns difficult to evaluate its extent.

(d) 382–395 AD: This event is mentioned in Galbis' seismic catalog (1932), but only some researchers have associated sedimentary evidence with it, based on a recalibration of the radiocarbon dates of previous studies, such as that performed by Ruiz et al. (2013a) on the deposit identified by Gutiérrez-Mas (2011). Nowadays, this event has no reliability and has been discarded (Andrade et al. 2016).

(e) 400–450 AD: This event is only identified by Röth et al. (2015) as a tsunami event that, presumably and according to the authors, contributed to the eventual ruin of the Roman city of *Baelo Claudia*. However, the studied deposits have been interpreted as uniquely anthropogenic by the archeologists in charge of the excavations where the samples come from (Bernal et al. 2016).

(f) Unknown chronology, albeit in Roman times. A possible tsunami deposit containing Roman pottery has been reported by Reicherter et al. (2010) on the coast between Barbate and Zahara de los Atunes (Cadiz, Spain).

A detailed analysis of the data currently available makes it certainly possible to claim, on the one hand, that EWEs struck the southwestern seaboard of Iberia during Roman times. But, on the other, in our opinion it poses a long list of unanswered questions or even contradictions (Fig. 12.1). One of the main problems is the chronology of these events. Apart from the abovementioned lack of historicity of the commonly used Galbis' seismic catalog (Galbis 1932), other difficulties include the reservoir effect, which has been extensively considered in the area (Ruiz et al. 2008; Lario et al. 2010; Monge Soares 2015), and the lack of consistency of these radiocarbon dates with archeological finds. In this sense, ceramic assemblages are very eloquent, insofar as they allow for establishing a more precise chronology for the deposits when combined with radiocarbon dates. The many different events identified in Roman times are somewhat difficult to interpret taking into account the return period already established for the southwest of the Iberian Peninsula. Another problem is the regional correlation of the data, which is sometimes a difficult task. On certain occasions the same sedimentary evidence has been interpreted in diverse ways by different authors (for example, the La Algaida deposits in Rodríguez-Vidal et al. 2011 and Rodríguez-Ramírez et al. 2016), or reinterpreted (for example, reinterpretations of several studies across the Guadalquivir estuary in Ruiz et al. 2008). In this connection, there are events that have been recognized in the same geographical area by different authors, but never in the same stratigraphic sequence (in the case of the Las Nuevas chenier, for instance, one team—Ruiz et al. 2004, 2008; Rodríguez-Vidal et al. 2011—reported the 218–209 BC event, while another—Rodríguez-Ramírez et al. 2016 – the third century AD event in the same location, but without correlating the C14 data with Galbis' seismic catalog). Besides, while the broad diversity of independent studies performed in this respect in the area has certainly served to enrich the debate over the past decades, another consequence has been the lack of common data recording and research protocol strategies, which has made it difficult to compare the nature and composition of the tsunami deposits in the southwest of the Iberian Peninsula as a whole. These conditioning factors have also hindered the identification of a specific catalog of events along the southwestern seaboard of Iberia and their impact on the landscape, at least in Roman times, especially when considering the EWE return periods established for the area (1200–1500 years for Lario et al. 2011; 700–1000 years for Ruiz et al. 2013b; Costa et al., this volume).

Finally, all these questions become even more difficult to answer when considering the different paleogeographic reconstructions of the *Lacus Ligustinus* in Roman times (Fig. 12.2), thus impeding the establishment of the progradation and effects of these phenomena. The evolution of the *Lacus Ligustinus* has been very rapid in the last thousands of years (Rodríguez-Ramírez et al. 1996, 2014, 2015, 2016). Its sedimentary filling begins clearly and quickly about 3200 yrs BP, being especially intense in the last two millennia with rapid progradation of coastal spits. Around the first century AD the Algaida spit was still an island, surrounded by two arms of the river, but from the first–second century AD it will be joined by a tombolo to the mainland. In the estuary, the progressive sedimentary infilling occurs following the model of digited deltas for areas of significant tidal range and low waves interrupted by the succession of winter storms that formed the shelly cheniers. The tsunami of the second–third century AD resulted in significant paleogeographic changes, especially in coastal spits. In the second–fourth century AD an important chenier was formed (Las Nuevas-Isla Mayor) and developed toward the interior of the estuary, although according to Rodríguez Ramírez et al. (2016) it would not be related to the tsunami event.

Of all the events reported in the literature, in recent years the third century AD event has progressively gained importance. The studies performed by Rodríguez-Ramírez et al. (2016) and Gutiérrez-Mas (2011) demonstrate that the

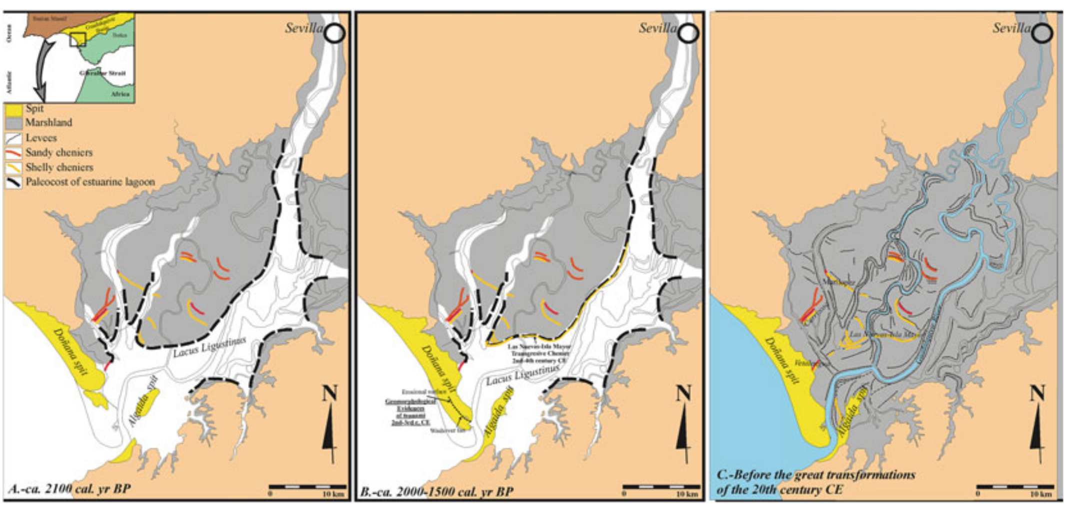

Fig. 12.2 Paleogeography of Guadalquivir Estuary during Roman times and present time (Modified from Rodríguez-Ramírez et al. 2016)

sedimentary imprints of this event are more evident than previously stated (Lario et al. 2010) and can be traced on a large regional scale, especially if the evidence presented by Feist et al. (2019) is finally proven to be dated to Roman times. Some authors have suggested that such an event would explain certain abandonment facies in coastal archeological sites in the area, as well as a temporal decline in the fish processing and amphorae industries in southwest *Hispania*, which would not recover until the fourth century AD (Campos et al. 2015; Rodríguez-Vidal et al. 2015; Hermann et al., this volume; Bermejo et al., this volume). In this context, this chapter focuses on a high-energy deposit identified in the suburbs of the Roman city of *Hispalis*, in the excavation of Patio de Banderas, in a third century AD context of traumatic collapse of a Roman public building. The aims of this chapter are to present this deposit in its archaeological context, as well as to explore its sedimentary origin. In sum, this chapter is a contribution on the third century AD event(s).

12.2 Roman *Hispalis* (Modern Seville): A Port Opened to the Atlantic and the Mediterranean

The location of *Hispalis* at the bottom of the old marine lagoon made it a place of special importance because, as Strabo pointed out, large trading vessels plying the Atlantic could reach the city to unload goods at its port and to load metals and foodstuffs from the lower and middle Guadalquivir countryside for their exportation (Strabo, *Geographica*, III, 2, 3). Of all these goods, Baetican olive oil was especially important, since more than 180.000 Dressel 20 amphorae (equivalent to more than 18.000 tons of freight traffic) were annually processed in the port of *Hispalis* and shipped in large cargo vessels to Rome and other cities in the Roman Empire (García Vargas et al. 2017; Cabrera 2019).

Although the port of *Hispalis* comprised a series of facilities (warehouses, craft areas, wharves, etc.), linearly arranged from the southern end of the city to way beyond its northern limits, the truth is that the port nucleus was always to be found on the southern esplanade (García Vargas et al. 2017) (Fig. 12.3), a triangular area whose longest side was over 1 km long. This was due to its location between two rivers, the smallest (the river Tagarete) flowing into the largest (the river Guadalquivir). It is in the fluvial port, located at 6 m.a.s.l. (Borja 2014), where trade facilities and port services are documented, such as large warehouses built in Republican (Patio de Banderas), Early Imperial (Patio de Banderas, Avenida de Roma, Florida), and Flavian times (Patio de Banderas and Avenida de Roma), with a grid plan of which some road sections intersecting at right angles (Avenida de Roma, calle San Fernando) are still preserved (García Vargas et al. 2017; Cabrera 2019).

Upstream, along the course of the Guadalquivir in Roman times, buildings relating to commercial traffic have also been recorded, such as the calle Francos construction (*schola*?). Additionally, piers and docks have been identified, such as those on the Avenida de la Constitución-Sierpes, and even anchorages, like the present-day Plaza Nueva, where the remains of boats have been documented: specifically the late Roman iron anchor of a large ship and a riverboat dated to the eleventh century AD (González Acuña 2011; García Vargas et al. 2017; Cabrera 2019).

Finally, the location of an artisanal-commercial space in the Plaza de La Encarnación area, at the northern end of the Roman city, can be explained by the presence of secondary piers to which the ashlar constructions of Plaza de la Campana may correspond (Jiménez Sancho et al. 2014). The suburban landscape outside *Hispalis* was completed with necropolises and suburban villas that reflected the commercial influence of the fluvial port, even in areas far from the city walls. This is the case of the warehouses located in the hospice on calle

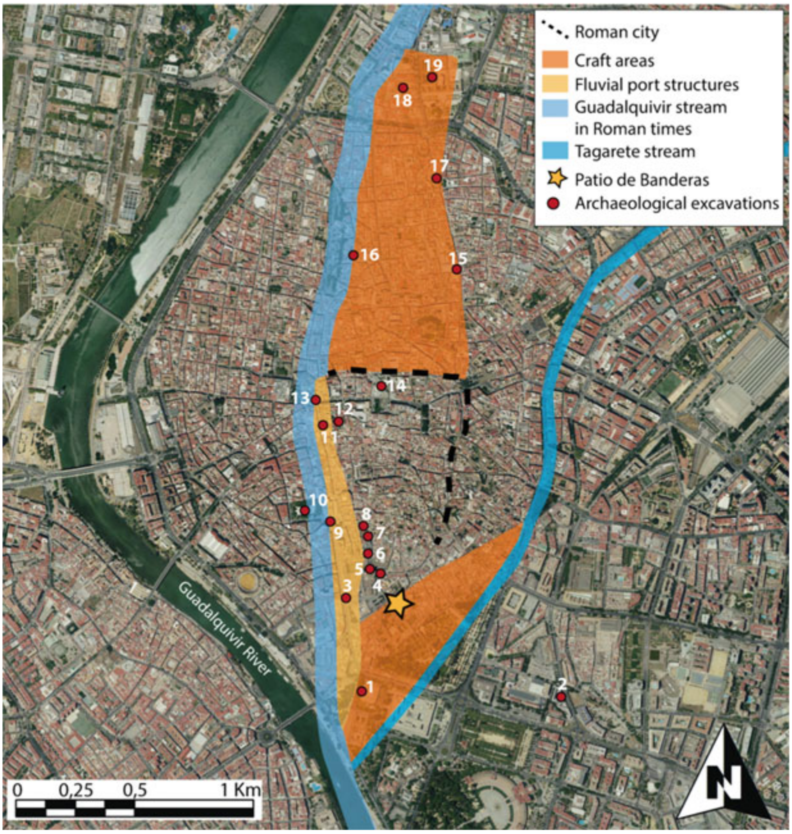

Fig. 12.3 Location of the Patio de Banderas excavation in the suburban environment of Roman *Hispalis*. The red points show archeological excavations were Roman buildings associated with the fluvial port have been documented.1. Avenida de Roma, 2. Plan Especial de San Bernardo, 3. Pabellón de oficinas de la catedral, 4. Plaza de la Virgen de los Reyes, 5. Palacio Arzobispal, 6. Calle Alemanes 25, 7. Calle Placentines nº 7, 8. Calle Francos 41, 9. Avenida de la Constitución, 10. Plaza Nueva, 11. Antiguo Cine Imperial, 12. Calle Cuna 10, 13. Martín Villa-La Campana, 14. Plaza de la Encarnación, 15. Calle San Luis nº 29, 16. Calle Joaquín Costa nº 32, 17. Calle San Luis nº 95, 18. Calle Esperanza 6–10, 19. Antiguo Hospital de las Cinco Llagas

San Luis and, closer to the river, the Julio-Claudian and Flavian amphorae production center of the Hospital de las Cinco Llagas, the current seat of the Andalusian parliament (Tabales Rodríguez 2003).

It is in one of these locations associated with the fluvial port of *Hispalis*, namely, the excavation conducted at Patio de Banderas (Fig. 12.3), where a high-energy deposit was found in a third century AD context of the traumatic collapse of a Roman public building.

12.3 The Third Century AD Collapse Facies Documented in the Patio De Banderas Excavation

The 2009–2014 excavations in the Patio de Banderas (Reales Alcázares, Seville) were carried out in the framework of a research project whose aim was to obtain a complete stratigraphic sequence at this point in Seville. The excavations

Fig. 12.4 **a** Plan of the Roman public building documented in Patio de Banderas excavation. The yellow arrow indicates the location of the sampled profile. The red line indicates the location of the section shown in **b**, where the red and blue colors indicate the Republican and Imperial constructions, respectively. Note that collapses are documented in the southern part of the building, the sector of the excavation closest to the river Guadalquivir

revealed an impressive urban stratigraphy dated between the ninth century BC and the thirteenth century AD, showing some temporary hiatuses (Tabales Rodríguez 2012, 2015). From all these findings, a very well-preserved Roman public building found at 6 m.a.s.l. stands out. This building, constructed in *opus africanum* during the Late Republic (60–30 BC), is organized around a central courtyard, which had a colum-nated gallery at its southern end (Figs. 12.4 and 12.5). These columns, made of semicircular bricks, were plaster coated. The presence of four stone pillars in the courtyard (constructed in *opus quadratum*) allows for identifying an upper floor (Tabales Rodríguez 2015). As already noted, this building was located in the southern suburban area of the Roman city. The material evidence and the construction itself makes it possible to identify this space as a commercial and administrative construction associated with the fluvial port of *Hispalis* and its huge volume of fluvial and maritime exports (Tabales Rodríguez 2012, 2015). This construction was repaired several times during its active life, most of the repair work being carried out in Flavian times (AD 70–90), when new canalizations were added and new walls in *opus testaceum* were built (Tabales Rodríguez 2015).

However, the most important phase of the building in terms of material evidence, volume, and variety is dated to AD 200–225 (Tabales Rodríguez 2015). At that moment, the widespread collapse of the architectural remains has been documented. Most of the southern walls appear to have been displaced from their original position and to have subsequently collapsed on top of the pavements, always in the same direction, toward the northwest. All these architectural remains were discovered in a 80 cm-thick microlaminated deposit, alternating sandy and silty beds, and with abundant fresh-fragmented shells across it as a whole. It is important to note

Fig. 12.5 Architecture of the studied building. **a** Columnated gallery in the southern part of the building, indicating the sampled stratigraphic profile (yellow arrow). **b** Detail of the *opus africanum* fabric

that several brick column fragments were reworked and incorporated in the deposit (Figs. 12.6 and 12.7). Of all the reworked architectural elements in this context, some stand out: several calcarenite ashlars showing in situ plaster and paintings, a fluted calcarenite column, fragmented marbles from different quarries across the Mediterranean, an inscription, and a complete marbled votive relief depicting feet, which is typical of Isis worship (Fig. 12.8). These materials do not belong to the building excavated in the Patio de Banderas, since it was constructed with different materials (mainly limestone and bricks) and techniques. All these elements have been interpreted as boulders integrated into a collapse facies that resulted from a highly energetic event which even transported exogenous construction materials to this public building (Tabales Rodríguez 2015). This context has been dated to 197–225 AD, thanks to the profuse ceramic assemblage studied and three C14 dates on different materials: bone, charcoal, and shell (Tabales Rodríguez 2015; Table 12.1). In part, this event and the subsequent collapse would explain the good state of preservation of the entire construction, since the area does not

Fig. 12.6 Finely stratified deposits alternating sands and silty clay sediments deposited during the sedimentary event (from the orange arrows to the bottom of the sequence). These deposits incorporate reworked architectural elements, such as brick column fragments integrated into the sandy clay deposit (blue arrows indicate both the reworked architectural elements and their original position)

show any evidence of human occupation until the fifth century AD, when a new building was constructed (Tabales Rodríguez 2015).

While this excavation has been extensively published (Tabales Rodríguez 2012, 2015; García Vargas 2015), the collapse facies required a complete geoarchaeological study in order to understand the site formation processes involved in the genesis of this particular archeological context. One of the objectives of the Patio de Banderas research project was to characterize the paleotopography of this area during different historical periods. Such a study was preliminarily performed by M. A. Barral-Muñoz and F. Borja, who made a visual characterization of the different sedimentary deposits and a tentative paleotopographic reconstruction by linking these descriptions to previous studies in the surroundings of this area of the city (Barral-Muñoz and Borja 2015). For these authors, it was clear that this deposit corresponded to an EWE, but its origin was difficult to assess. On the one hand, the presence of marine shells and bedded sandy and silty deposits could indicate a tsunami as a possible origin of these materials. However, some arguments led them to discard the tsunami hypothesis: (a) the deposit is located at 6.70 m.a.s.l., and the distance from *Hispalis* to the shores of the *Lacus Ligustinus* (30–40 km) would have required a highly energetic event to inundate not only the *Lacus Ligustinus*, but also the lower area of the Guadalquivir floodplain. As already observed, while the paleogeographic evolution of the *Lacus Ligustinus* has been studied, there are still several doubts about its dimensions in Roman times. As Barral-Muñoz and Borja stated, “Currently, there is a lack of data to accurately delimit the extent and spatial arrangement of these tidal flats around the second century AD, as well the width of the channel, or channels, of the river Guadalquivir in that same period” (free translation of Barral-Muñoz and Borja 2015, p. 47); (b) Galbis’ seismic catalog and the geological tsunami literature on the southwestern coast of the Iberian Peninsula has traditionally suggested events in 218–209 BC, 60 BC, and the third century AD. While there were tsunami deposits chronologically contemporaneous with the Patio de Banderas sequence in the Guadalquivir estuary, previous literature suggested that this event would have had a limited impact on the landscape (Lario et al. 2011), very far removed from the highly energetic event required to reach the city of *Hispalis*. All considered, and while accepting the marine provenance of the shell assemblage of the third century collapse

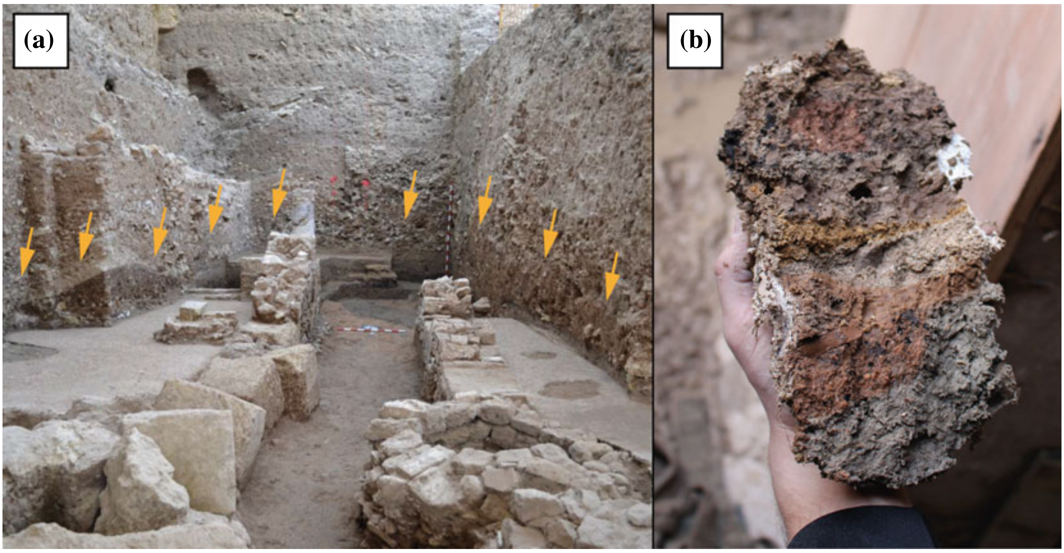

Fig. 12.7 **a** Extension of the high-energy deposit, sealing the Roman public building (from the orange arrows down). **b** Sample 1, showing the microlaminated nature of the deposit

context in the Patio de Banderas excavation, Barral-Muñoz and Borja (2015) suggested a high-energy fluvial event as the origin of these deposits. However, Alonso et al. tentatively proposed that this deposit was generated during a marine EWE (Alonso et al. 2015).

In our opinion, a visual characterization of the facies identified in the Patio de Banderas excavation was not enough to assess the sedimentary origin of this deposit. Accordingly, we conducted a multiproxy and interdisciplinary study, combining methods and techniques from the macro to the microscale, where most of the evidence seems to be reflected given the microlaminated nature of the deposit. First, the chronological assessment of the deposit was made based on C14 dating and the ceramic assemblage. Regarding the deposit, soil micromorphology has been the backbone of the entire study in order to perform a precise microfacies analysis. Besides, we have characterized the mineralogy and geochemistry of the different microfacies units identified, plus bivalve and micropaleontological characterization.

12.4 Materials and Methods

Undisturbed and oriented sediment micromorphology samples were collected from the chronostratigraphic profiles produced during the 2014 excavation season. The blocks, stabilized by plaster of Paris bandages, were then oven-dried at 50 °C for 24 h. Impregnation was carried out under vacuum with polyester resin (Palatal P4-01), styrene monomer, and MEK catalyst. A total of 14 thin sections of the entire stratigraphic sequence were studied, of which five correspond to the high-energy event. They were analyzed under plane-polarized (PPL), cross-polarized (XPL), and oblique incident (OIL) lights, as well fluorescence ultraviolet microscopy (UV). Descriptive standard criteria were followed (Stoops 2003). Additionally, 8 samples for micropaleontological analyses were systematically collected from every stratigraphic unit, in tandem with a sampling of the micromorphology blocks.

Fig. 12.8 Building blocks and ornamental materials (boulders) trailed by the event: **a** and **b** show a flutted column and calcarenite blocks with attached mural painting panels. These materials do not belong to the building discovered in Patio de Banderas excavation. **c** Detail (cenital view) of shell concentrations present in most of the deposit, but especially at the top of the sequence. **d** Selection of some of the mural painting and marble fragments identified in the destruction layer. An inscription, a marbled votive relief depicting feet typical of Isis worship, and several architectural elements are highlighted

The microfacies concept is used here, following Flügel, to refer to the arrangement of sedimentary constituents by distinct and recurrent groups of similar composition and organization within a particular thin section (Flügel 2004). Thus, through microfacies analysis similar characteristics of lithological composition, geometric association, and post-depositional changes can be grouped, allowing for recognizing patterns in different thin sections. This is based on the principle that distinct events, depositional environments, and post-depositional processes produce a particular set of microfacies units that, in turn, can be associated with a

Table 12.1 Absolute C14 radiocarbon dates of the studied deposit

Laboratory code	Type of material	Context	Radiocarbon age (BP)	Calibrated date (95% confidence) Cal AD
CNA2422.1.1	Shell	S.U. 2284	1810 ± 30 BP	128–258 AD
CNA2423.1.1	Wood	S.U. 2284	2095 ± 35 BP	167–387 AD
CNA2424.1.1	Bone	S.U. 2284	1880 ± 30 BP	67–221 AD

specific microfacies type (Courty 2001; Flügel 2004; Goldberg et al. 2009).

After microfacies analysis was made, microdrilling was used for sub-sample extraction from resin-impregnated micromorphology blocks using a Dremel® multi-tool. Sampling was made in correlation with microfacies analysis. A total of 23 samples were taken in addition to a resin reference sample. These bulk samples were used for geochemical (ICP-MS/OES) and mineralogical (XRD) analyses.

Total concentration of chemical elements was analyzed in the CIC laboratory of the University of Granada, after fine grinding and acid digestion ($HNO3$ + HF + HCl). Major elements (Al, Ca, Fe, K, Mg, Na, P, and S) were analyzed by ICP-OES in a PERKIN-ELMER OPTIMA 8300 instrument; trace elements were analyzed by ICP-MS in a PE SCIEX ELAN-5000 A spectrometer. A calibration standard was used with the studied analyze at five different concentrations.

The mineralogy was studied by X-ray diffraction (XRD) in a Philips PW-1710 instrument with CuKα radiation, Ni-filter, and graphite monochromator, using the method of disoriented crystalline powder (Davis and Pawlowski 1987). Semiquantitative interpretation of the main minerals was estimated according to the software XPowder Ver. 2016.01.15 (http://www.xpowder.com/).

The macrofossils contained in the deposit were analyzed, identifying types and diversity of species (faunal composition and shell taphonomy). Several samples were collected from the bulk sediment of each sample and were washed through a 1 mm sieve. Bivalves and gastropods were identified to the species level and then counted in order to determine the semi-quantitative distribution. The presence and relative abundance of other groups were also noted.

Micropaleontological analyses were performed on 8 samples of 50 g along the studied section. Samples were wet-sieved over a 63 µm mesh and oven-dried at 40 °C. Then, they were split with a microsplitter to obtain sub-samples containing at least 300 benthic foraminifera. These sub-samples were dry-sieved over a 125 µm mesh and benthic foraminifera were counted and identified at species level. A quantitative taphonomic analysis of 200 benthic foraminiferal shells was carried out in order to characterize microfossil shell preservation (Pérez-Asensio et al. 2017). Six taphonomic traits were quantified using different preservation categories, grade 0 meaning that the specific taphonomic signature was absent: (1) fragmentation (0–4), (2) abrasion (0–3), (3) dissolution (0–3), (4) borings (0–3), (5) recrystallization (0 = absence; 1 = coatings on the foraminiferal tests), and (6) fillings (0 = absence, 1 = calcite). Furthermore, a qualitative biostratigraphic dating based on the presence and absence of planktic foraminiferal biomarkers was performed.

Three samples of the high-energy deposit were taken for C14 dating. These three samples corresponded with charcoal, shell, and wood, respectively. All dates were measured using accelerator mass spectrometry and dated by CNA laboratories (Santos Arévalo et al. 2009). All results were calibrated using the calib radiocarbon calibration program (v. 7.0) (Reimer et al. 2013). Also, the chronology of the studied deposit and the destruction context of the Roman public building was established after a detailed and systematic study of the ceramic assemblages recovered in the excavation.

12.5 Results

12.5.1 Archaeological Materials and C-14 Dating: Assessing the Chronology of the Studied Deposit

Most of the stratigraphic contexts whose ceramic materials characterize and date the studied deposit were excavated at the southern end of the public building. The most expressive units, from both a stratigraphic and a chronological perspective, were those laying directly on top of the signinum pavements of southern limit of the excavation (Fig. 12.4). They provide an immediately *ante quem* date for the collapse of the ceilings and walls of the entire edification. Specifically, they correspond to the campaigns of archaeological excavations carried out between 2013 and 2014 in areas XVII (stratigraphic units 2129, 2127, 2130, 2135) and XVIII (stratigraphic units 2226, 2240, 2276, 2284, 2289, 2290–91) (Tabales Rodríguez 2015). The pottery found includes material from local workshops but also large quantities of imported wares whose very precisely established dates in their respective original production areas allows us to adjust the chronological frame of this archaeological context complementing and refining their radiocarbon dating.

The main ceramic-dating groups provided by these contexts are African table wares and amphorae. The last class includes forms Dressel 20, late Dressel 28, Beltrán IIB, Keay XVI, Dressel 14, Lusitana 3, Gauloise 4, Dressel 2–4, Almond-Rim Type amphorae, M254, African IIA, Tripolitana III, Agora G199, Ephesos J46/47, Sinopian "carrot amphorae," and Kapitän II (Fig. 12.9).

The generic chronology of these contexts in the Severan period is suggested by the presence of ARS A table wares (Fig. 12.10) (forms H.3 A and B, H.6, H.8A, H.9A and B, H. 14, H 16) and the presence of an early ARS C Atlante XXXI.18 "water bottle." Types Hayes 16 in ARS A and Atlante XXXI.18 in ARS C have been traditionally dated to the early third century AD, but there is nothing to suggest that a date in the last decade of the second century AD is necessarily wrong.

The stamp IIAVRHERACLAE/PATETFILFBAR [(Duorum) AVR(elii) HERACLAE/PAT(er) ET FIL(ius) F(iglina) BAR(ba)], from SU 2289 comes from *figlina Barba* (Fig. 12.10). This pottery workshop belongs to a group of Imperial possessions located right by the river, which also included the *Grumense* and *Ceparia* pottery workshops. All these workshops share stamps that demonstrate the fact that they were the property of the early Severan emperors: Septimius Severus and Antonino Caracalla first; Septimius Severus, Caracalla, and Geta from 209 AD; the latter two after Severus' death (211 AD), and Caracalla alone after Geta's death (212 AD). Stamps of the *Aurelii Heraclae*, father and son, followed by the name of the *figlina* are also known in these three workshops. The *Aurelii Heraclae* (Moros Díaz 2014) should be identified with the Imperial freedmen who were in charge of managing the workshops as *procuratores* in the years of Septimius Severus principate, that is between 197 and 207 AD, because the sons of Severus began to use the *augustus* title even before their official designation as such *augusti* in 209 AD. May be also that the stamps of the *Aurelii* and the first stamps of the three *Augusti* were roughly contemporary.

We have, in conclusion, a chronology of 197–225 AD or slightly later for these deposits and the associated ceramics. This chronology fits quite well with the presence in these ceramic assemblages of Lusitana 3 amphorae (Fig. 12.9: 7) and Käpitan II from the northern Aegeus (Fig. 12.9: 15). In addition to that, several amphora types or subtypes the production of

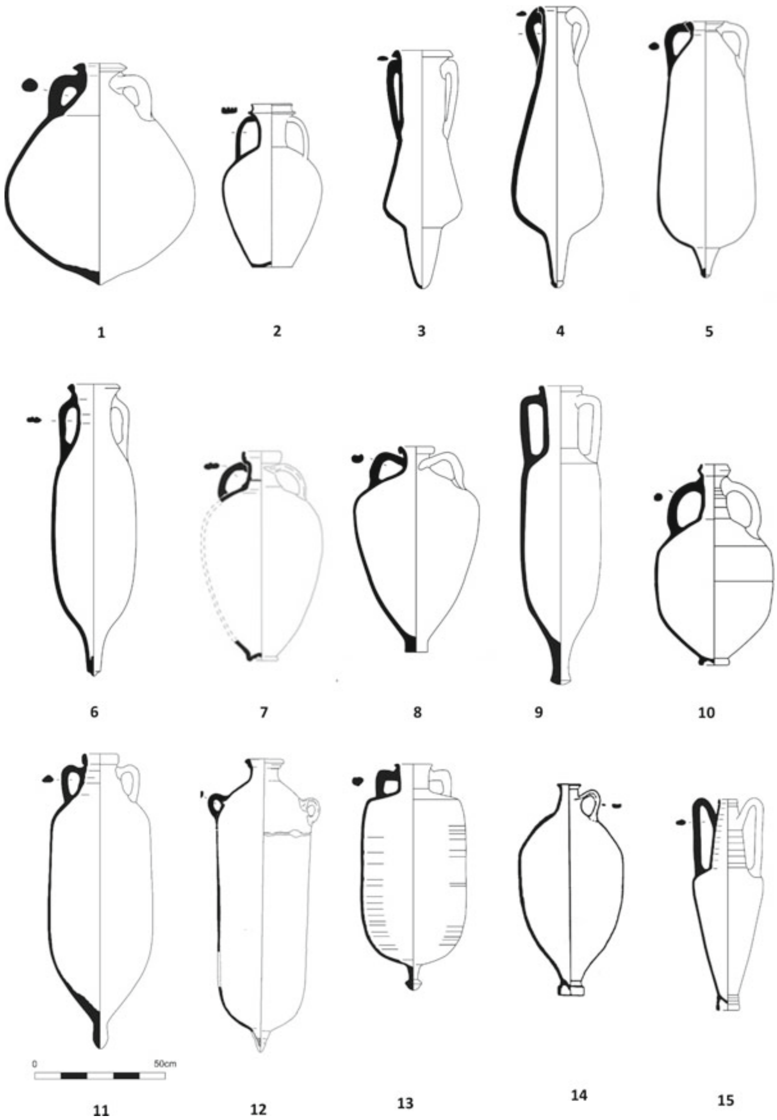

Fig. 12.9 Amphoric types documented in the destruction context of the Patio de Banderas excavation. 1: Dressel 20; 2: Late Dressel 28; 3: Beltrán IIA; 4: Beltrán IIB; 5: Keay XVI; 6: Dressel 14; 7: Lusitana 3; 8: Gauloise 4; 9: Dressel 2–4 and Campanian almond-rim amphora; 10: MRA 1b variant; 11: Africana II A-B; 12: Tripolitana II; 13: Agora G-199; 14: Ephesian J. 46–47; 15: Kapitän II

which terminates precisely in the initial decades of the third century AD are well represented in the ceramic record of Patio de Banderas. Among them, we should stress the presence of variant MRA 1b (Ostia III 564; Fig. 81, nº 216 in 15) of the Sicilian (Catania) amphorae type Agora M254 (Fig. 12.9: 10), which has recently been incorporated into the earlier group of Sicilian Flat-Bottomed Amphorae (Franco and Capelli 2014). Other types also present in Patio de Banderas, which were also in the final stage of their production, are the Gauloise 4 (Fig. 12.9: 8), from the region around the Rhône, and the Dressel 14 (Fig. 12.9: 6), predominantly from the Tagus/Sado Valleys, which is the later variant of Beltrán IIA and B types. The Tripolitana III amphora (Fig. 12.9: 12) started to be produced in the second half of the second century CE (Bonifay 2004), and their presence was already common in Mediterranean consumption contexts by the early third century AD. Type G199 (Pinched-handle Amphora) is mostly dated to between the late second century and the late Severan period, like the J46/47-type amphora

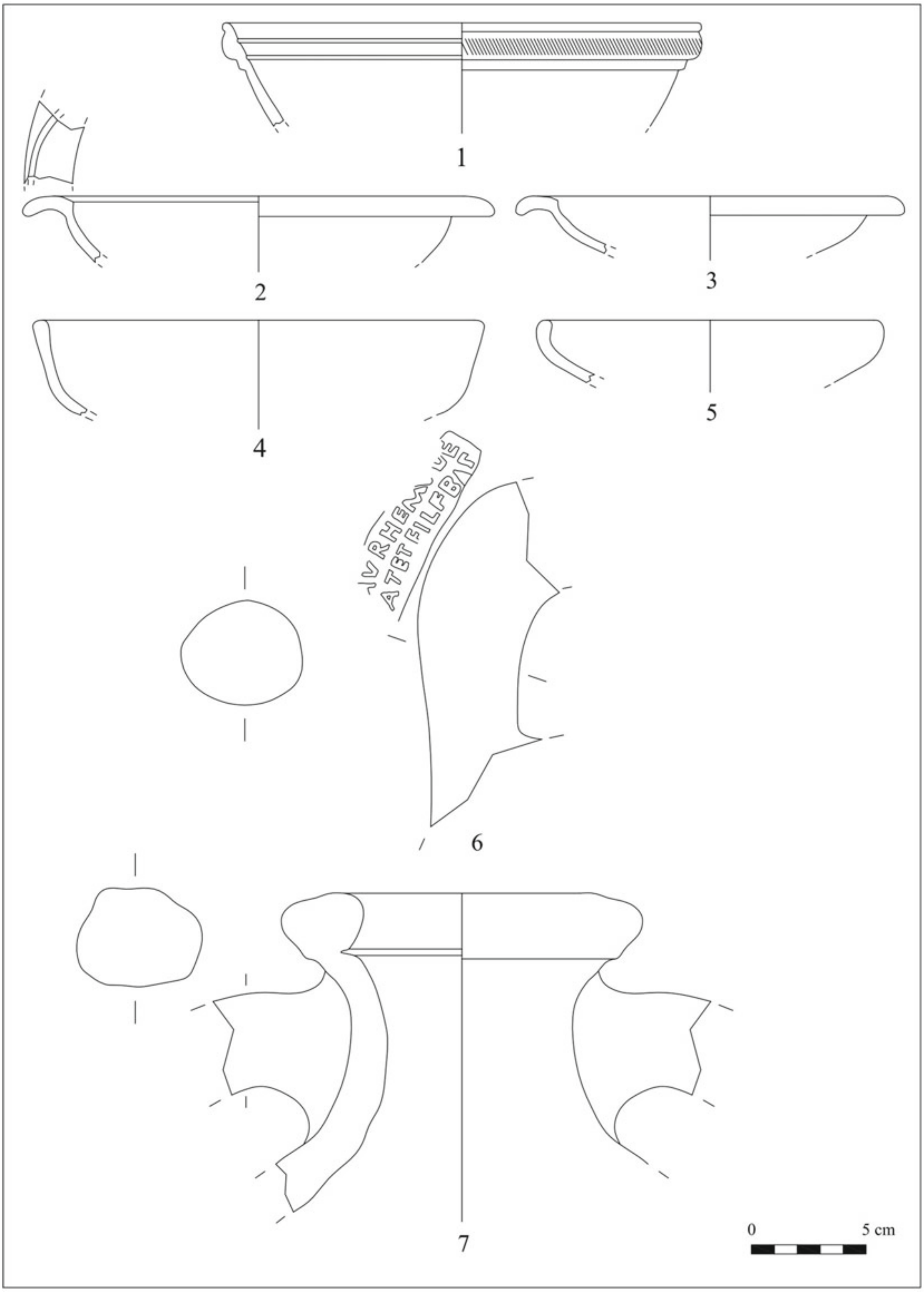

Fig. 12.10 1–5: African Red Slip ware (ARS); 6: Stamp on Dressel 20 handle *M.AVRHERACLAE/PATETFILFBAB*; 7: Dressel 20

from Ephesus (Fig. 12.9: 14), which was in circulation in the late second and the early third century AD (Bezeczky 2013).

Besides, three samples have been taken at the destruction level of the Roman building for radiocarbon dating (Table 12.1). All of them contain statistically significant dates by exceeding 95% confidence. It has been sought to analyze different materials (wood, shell, and bone) to obtain precise chronological information. The result of the three radiocarbon dates opens a wide chronological range that oscillates between the years 67 and 387 AD although they show a coincidence in the period between the years 167 and 221 AD.

This chronological framework is very consistent with the abovementioned chronological evidence that ceramics provide (197–225 AD or slightly later). We therefore consider that the high-energy event occurred within that interval of time.

From an economic point of view, the ceramic materials documented in the studied deposit constitute a first-hand account of the trade of food bottled in amphorae in *Hispalis* during the first decades of the third century AD. African table pottery and oil, wine and salted-fish amphorae, from the Iberian Peninsula, southern Gallia, Italy, Sicily, and the Aegean document a commercial activity spread throughout the Atlantic-Mediterranean area allow us to understand the fundamental role of the port of Seville in the commercial exchanges during this historical moment. To this, must be added the well-known role of the port of Seville in the administrative framework responsible for supplying olive oil to the population of Rome and to the legionaries of the German *limes*.

The volume of private and state commercial traffic, the testimonies of literary sources (Strabo, *Geographica* 3.2.2) and the size and extension of the port structures documented in the city by Archaeology ensure the arrival to the port of *Hispalis* of merchant ships of good tonnage for the time and sufficient draught (García Vargas et al. 2017; Cabrera Tejedor 2019).

12.5.2 Soil Micromorphology

The high-energy deposit identified in the Patio de Banderas excavation was sampled for micromorphology, covering the 80 cm-thick sequence with five samples located in the contacts of the different sedimentary layers that compose the microlaminated deposit. A macroscopic characterization of the deposit was sufficient to detect a succession of bioclastic-rich silty and sandy layers, sometimes showing sharp contacts. These deposits show discontinuous parallel to planar bedding. The first sample, in contact with the *opus signinum* pavement, shows three different microfacies units (Fig. 12.11). The first one in contact with the pavement is an iron-poor silt with horizontally disposed shells and benthic foraminifera (Fig. 12.11a, b), indicating a sedimentary input of marine/estuarine origin. This microfacies unit shows chemical post-depositional features such as vivianite coatings and intercalations, as well iron staining, which are indicative of water saturation and iron and phosphate mobilization. Furthermore, evidence of organic material input and decay is recorded in pseudomorphic voids, fresh organic tissues, and authigenic phosphate nodules. Microfacies unit 2 is a faster and more traumatic deposition. It is mainly composed of anthropogenic materials, especially earth-based materials such as mud-bricks (Fig. 12.11a, c), which exhibit typical pseudomorphic voids after organic binder decay (chaff and straw). In fact, the silty clay groundmass of this microfacies resulted from the erosion and transport of these earth-based materials. Also, mortar fragments, potteries, and big fragments of charcoal are commonplace. This microfacies seems to be a transported debris of construction and anthropogenic materials, while also containing rip-up clasts of structural crusts and Bt horizons with clay illuviation features. These rip-up clasts are especially significant in microfacies unit 3 (Fig. 12.11a, d, e), which is composed of a well-sorted silt constituting a muscovite-rich “mud lamina” (Fig. 12.11e). This microfacies resulted from sedimentation of

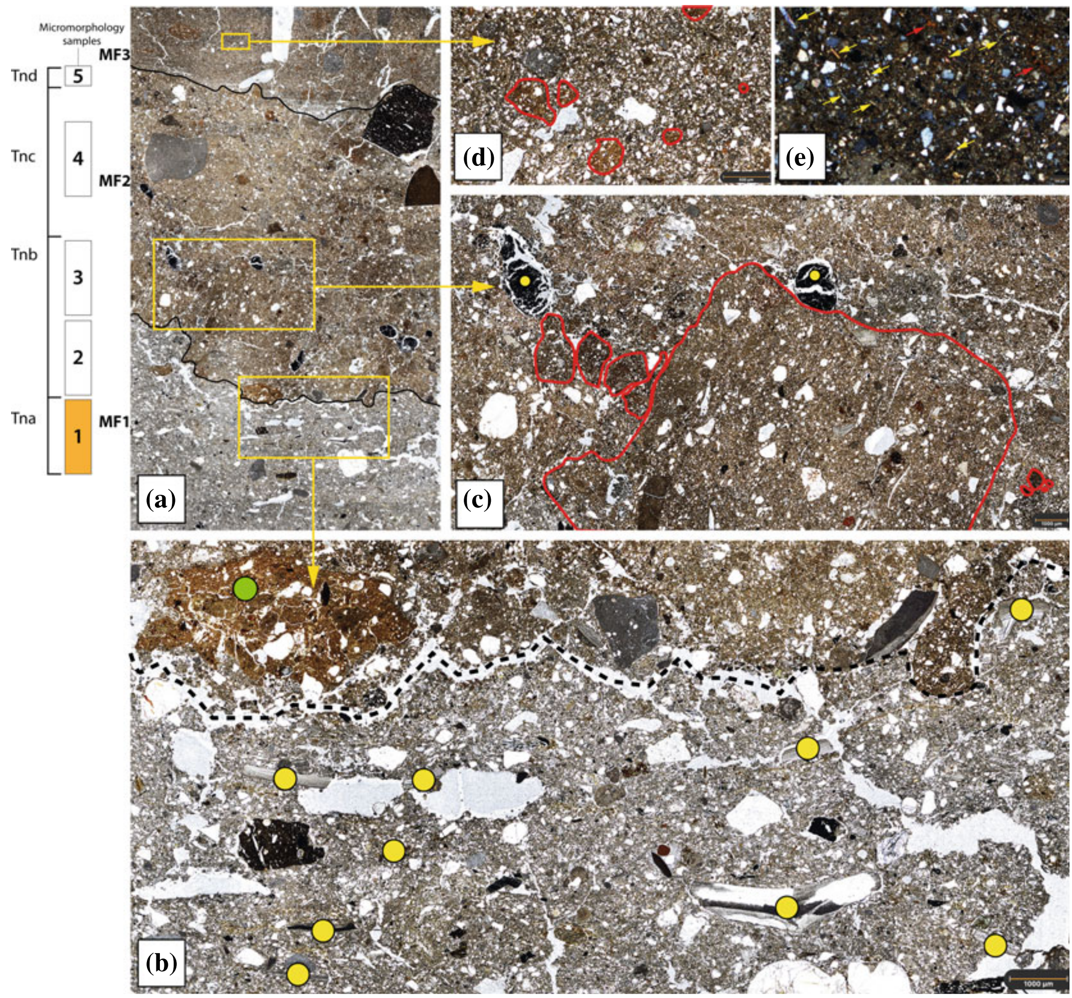

Fig. 12.11 Soil micromorphology. Sample 1. **a** Scan of the complete thin section showing the identified microfacies units and specific features. **b** Contact between microfacies Units 1 and 2 (black dotted line). Yellow points indicate the presence of shells horizontally disposed in microfacies Unit 1, an iron-poor silt. The green points correspond to a rip-up clast. **c** Detail of microfacies Unit 2, namely, anthropogenic debris composed above all of earth-based materials, such as mudbricks, (red lines) and other anthropogenic materials, such as charcoal (yellow points). **d** and **e** Detail of microfacies unit 3, a well-sorted silt constituting a muscovite-rich "mud lamina." In this microfacies, rip-up clasts (red lines), incipient clay illuviation features (red arrows), and muscovite (yellow arrows) are very common

suspension fallout of coarse and fine silt, clay, and organic remains, in a lower energetic deposition environment compared to the previous microfacies. In this microfacies unit there are common incipient clay illuviation features, suggesting clay flocculation and mobilization through pores.

Sample 2 (Fig. 12.12), however, contains coarser sandy deposits. In this regard, microfacies Unit 1 (Fig. 12.12a), composed of well-sorted siliceous sands, and microfacies Unit 2, a glauconite-rich calcarenite sandy material, represent the coarser sedimentary material of the whole sequence. This granulometric change compared to the previous sample, along with the absence of fine material, suggests a highly energetic sedimentation environment for these two microfacies. The grain orientation also indicates

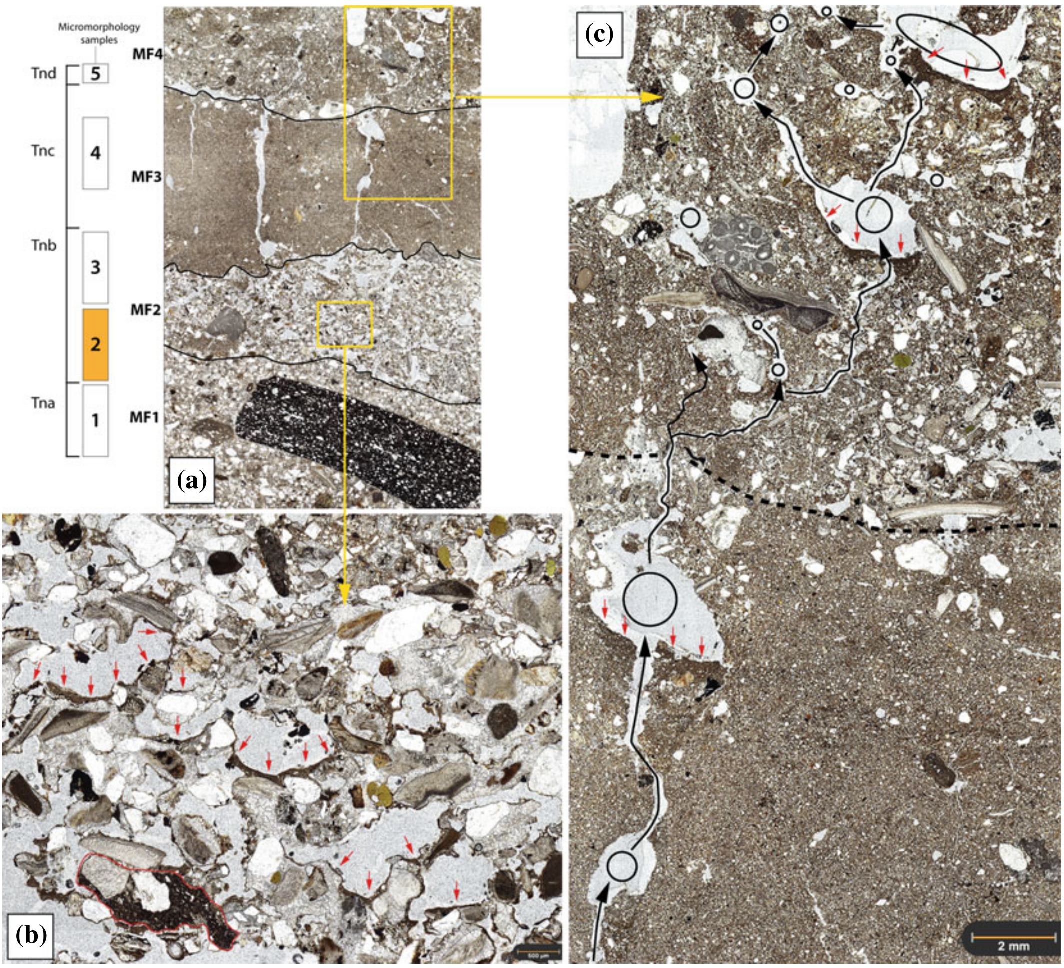

Fig. 12.12 Soil micromorphology. Sample 2. **a** Scan of the complete thin section showing the identified microfacies units and specific features. **b** Sandy microfacies exhibit laminated silt coatings gravitationally sedimented within pores (red arrows). **c** Detail of a "mud lamina" microfacies. In this thin section there is a significant porosity system of vesicular pores vertically interconnected with planar voids (black arrows), formed by the evacuation of trapped air in the lower sandy microfacies, which also generated laminated silt coatings gravitationally sedimented within pores (red arrows)

changes in the flow direction regime, the first microfacies pointing seaward and the second landward (Fig. 12.12). These sandy microfacies are sealed by a "mud lamina" and a bioclastic-rich silty microfacies (Fig. 12.12a). In this sample silty layered coatings gravitationally sedimented, connected by vesicles and planar voids, are very common (Fig. 12.12b, c). These pedofeatures, connecting microfacies of different granulometry and mineralogical and lithological composition, indicate trapped air escaping upwards. These features, along with the granulometry of the sandy microfacies units, would indicate a high-energy deposition.

Sample 3 (Fig. 12.13) shows two microfacies units. These are, as before, a poorly sorted iron-poor marine/estuarine silt with shells (Figs. 12.13a–c), and a poorly sorted silty clay rich in mudbricks and anthropogenic material (Fig. 12.13a, d). In this case, the vertical arrangement of the shells suggests a more energetic depositional environment and, in addition,

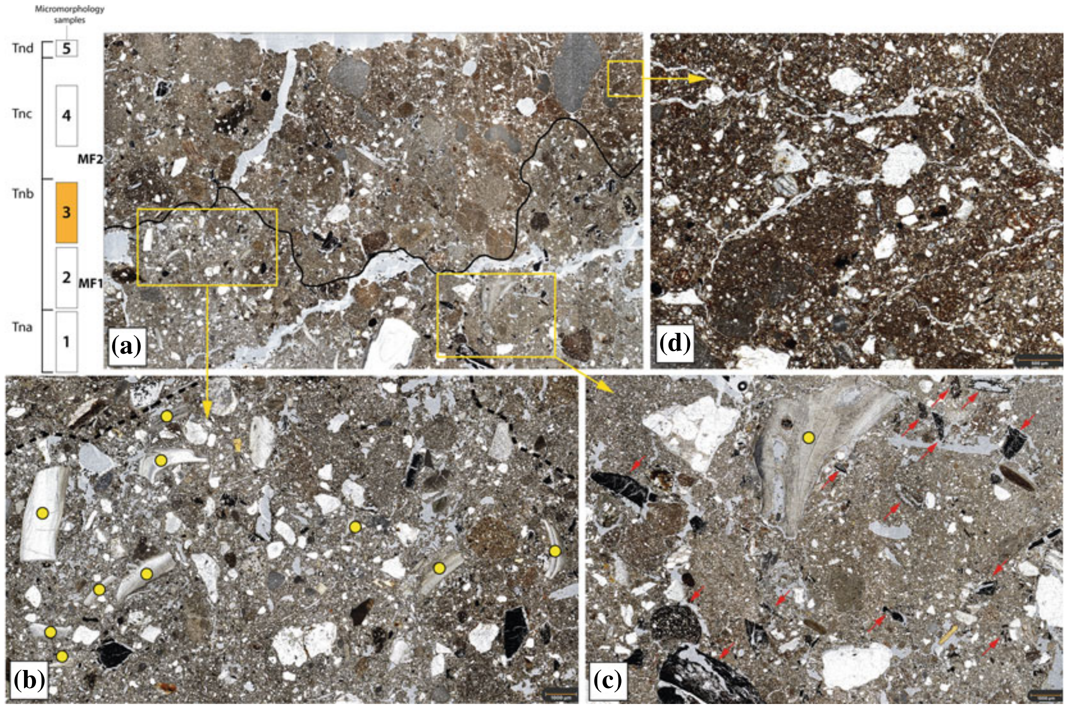

Fig. 12.13 Soil micromorphology. Sample 3. **a** Scan of the complete thin section showing the identified microfacies units and specific features. **b** and **c** show a detail of microfacies Unit 1, an iron-poor marine/estuarine silt with abundant vertically and chaotically deposited shells (yellow points) and fresh organic tissues (red arrows). **d** Detail of microfacies Unit 2, an anthropogenic debris composed above all of earth-based materials such as mudbricks

abundant remains of fresh organic matter and tissues are identified. Both microfacies indicate a highly energetic sedimentation environment, and an input of bioclastic and organic material in the case of microfacies Unit 1, and of anthropogenic materials in that of microfacies Unit 2.

Sample 4 (Fig. 12.14) contains finer material, namely, sandy silt, which would indicate a lower energy sedimentation environment. This poorly sorted sandy loam eventually shows an intercalated siliceous sand microfacies resulting from an energetic pulse (Fig. 12.14b). Rip-up clasts are also common in this microfacies, but in this sample there is a greater lithological diversity of these transported aggregates: calcareous crusts aggregates also being present (Fig. 12.14c).

Finally, sample 5 (Fig. 12.15) ends with a well-sorted mud cap microfacies, formed by suspension fallout. This massive material shows common pseudomorphic voids after organic matter decay. Again, rip-up clasts of structural crusts (Fig. 12.15b) and rip-up clasts from Bt horizons (Fig. 12.15c) are common. Also, incipient illuviation coatings and trapped air evacuation features are present (Fig. 12.14c).

12.5.3 Geochemistry and Mineralogy

In general, Late Roman and Medieval deposits (Fig. 12.16, samples 14–23) show lower concentrations and variability of major and trace elements than the samples associated with the high-energy event, which are characterized by a higher variability (Fig. 12.16, samples 1–13). Among elemental concentrations in the high-energy deposit samples, the strongest anomalies (both positives and negatives) are localized in the most energetic phase (energetic pulse 2). Ba, Pb, Cu, and Zn concentrations, and Ti/Zr ratio, are

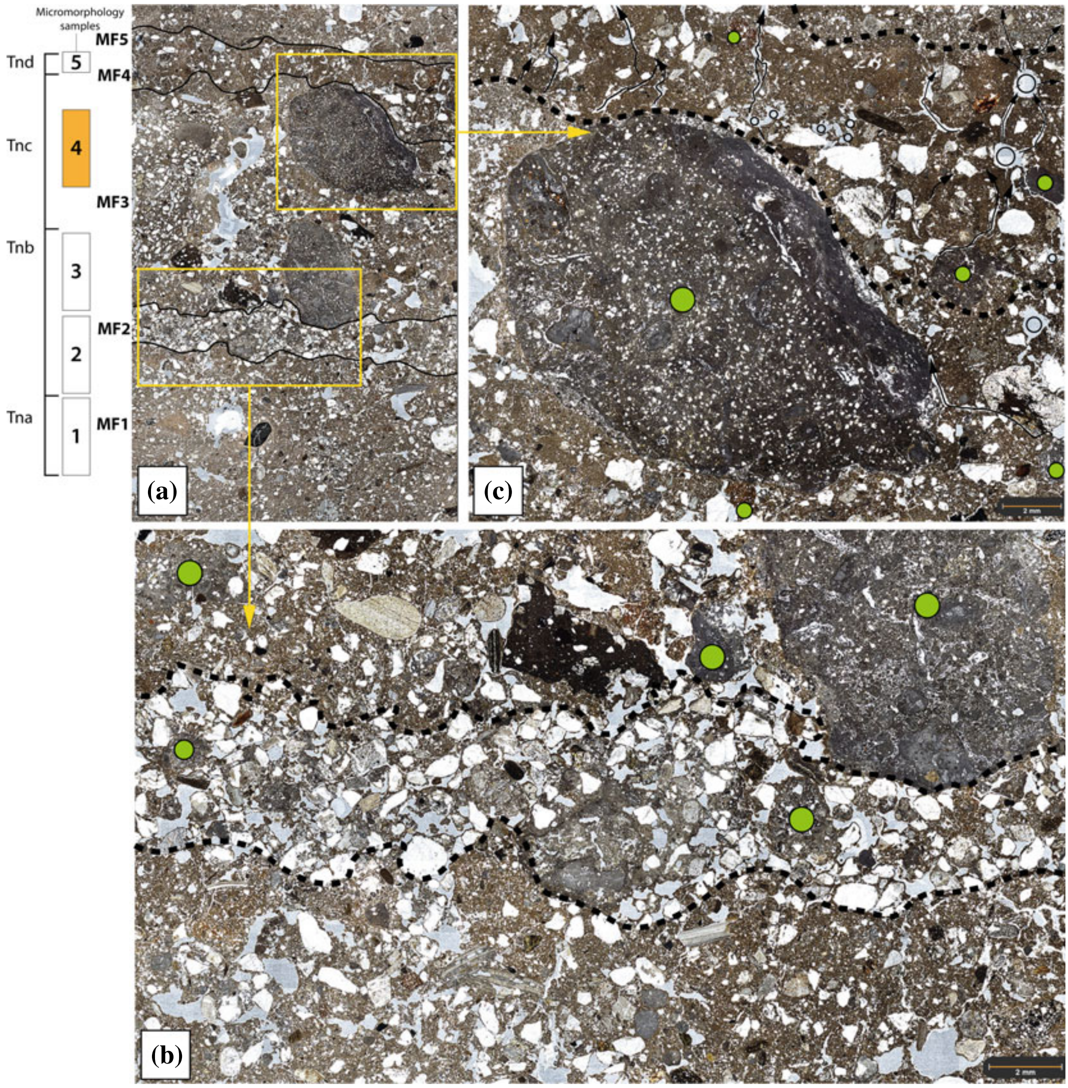

Fig. 12.14 Soil micromorphology. Sample 4. **a** Scan of the complete thin section showing the identified microfacies units and specific features. **b** Detail of the sharp contact (dotted line) of microfacies Unit 2 (well-sorted quartz sand) with microfacies Units 1 and 3 (sandy loam). **c** Detail of microfacies Units 3 and 4 (mud lamina). Green points indicate calcareous rip-up clasts. Black arrows and circles indicate vesicular pores vertically interconnected with planar voids

indicative of high-energy inputs, coinciding with the entrance of sandy and coarser materials as shown in microfacies analysis. Na, Ba, and S concentrations, as well Ba/Ti ratio, show an increase in paleosalinity, which is especially remarkable in the first energetic flow. Ca and calcite concentrations are related to the significant entrance of bioclastic material, coinciding with shell-rich microfacies. Si and quartz concentrations are an important proxy for the identification of siliceous sands input and detrital material. Also, Si enrichment defines the whole high-energy deposit, as shown in Si/Ti and Si/Al ratios. K and mica concentrations, as well K/Si ratio, are indicative of clay and silt sedimentation in stagnation periods between energetic pulses, corresponding with the mud laminae and mud cap.

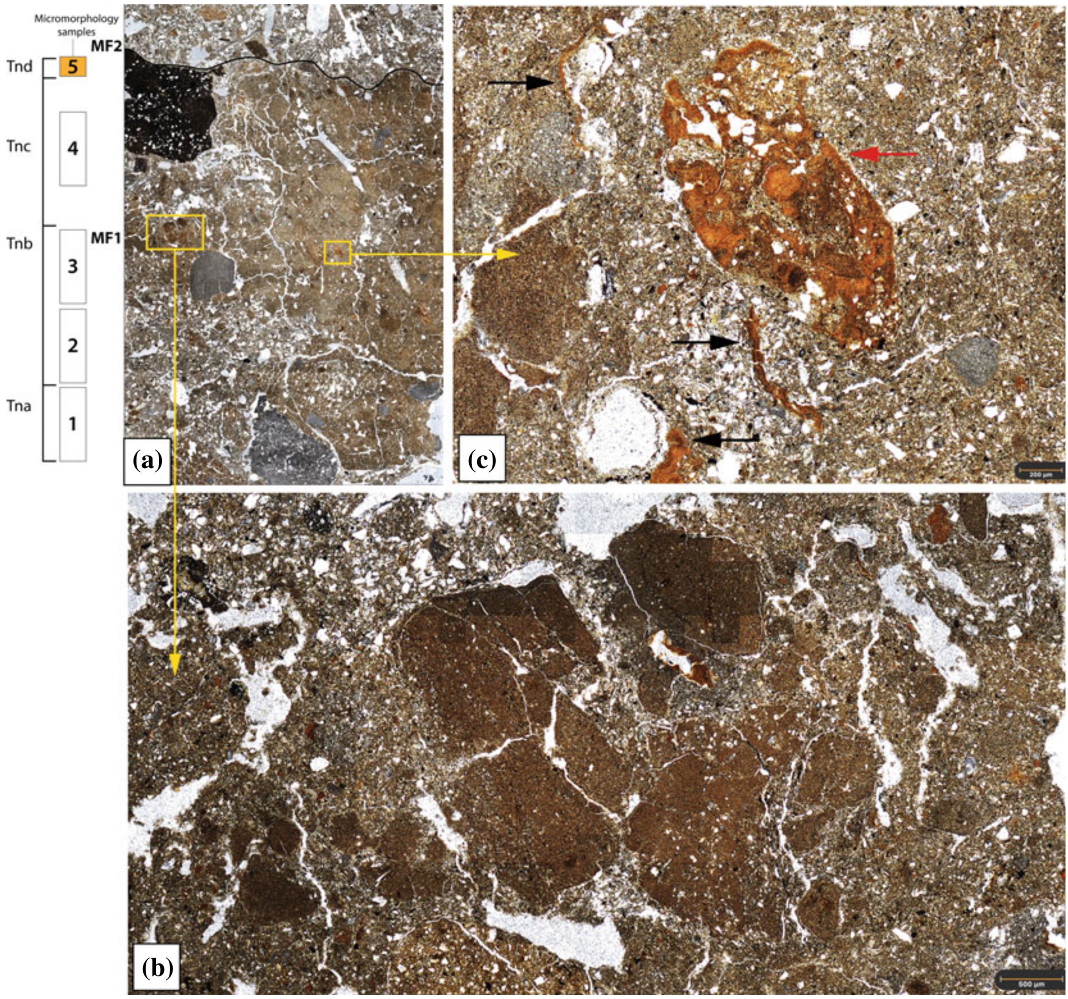

Fig. 12.15 Soil micromorphology. Sample 5. **a** Scan of the complete thin section showing the identified microfacies units and specific features. **b** Detail of the mud cap, showing rip-up clasts of transported structural crusts. **c** Incipient clay illuviation coatings (black arrows) and rip-up clasts from Bt horizons (red arrow)

12.5.4 Malacology and Micropaleontology

Malacofaunal and micropaleontological assemblages were characterized. Concerning the trophic structure of malacofauna, epifaunal benthic organisms of filtering suspensivorous habit dominate, with 73.8% being *Ostrea stentina* the most dominant. Infaunal bivalves potentially vagile are the minority, with 11%, also dominating those of suspensivorous filtering habit, among them *Cerastoderma glaucum* with 9%. Gastropods are dominated by carnivorous, vagile, epifaunal organisms (14.3%), most notably *Nassarius reticulatus* (12.5%). The analysis of the malacofauna (Fig. 12.6) as a whole indicates the intertidal (foreshore) or shallow infralittoral (shoreface, <5 m) character of paleobiocenosis, mostly corresponding to coarse and/or muddy sandy bottoms.

From a taphonomic point of view, all bivalves are disarticulated, with evidence of abrasion and no signs of bioerosion. Only the single specimen of *Ostrea edulis* identified, which is the largest in the studied assemblage (12 cm), has evidence of *Entobia*, an ichnotaxon related to the boring

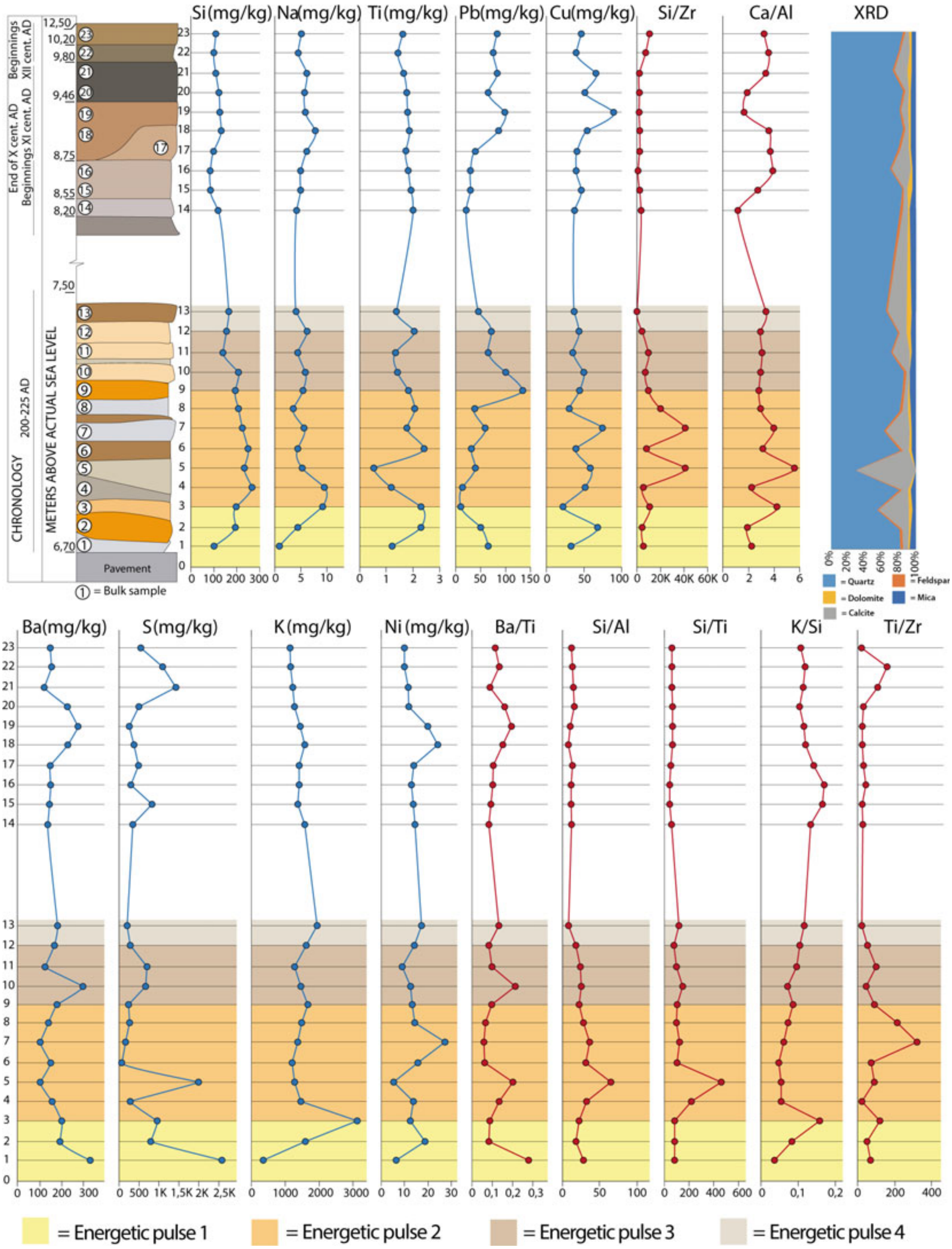

Fig. 12.16 ICP-MS/OES and XRD results in relation to microfacies analysis with chronological and vertical contextualization (present-day m.a.s.l.)

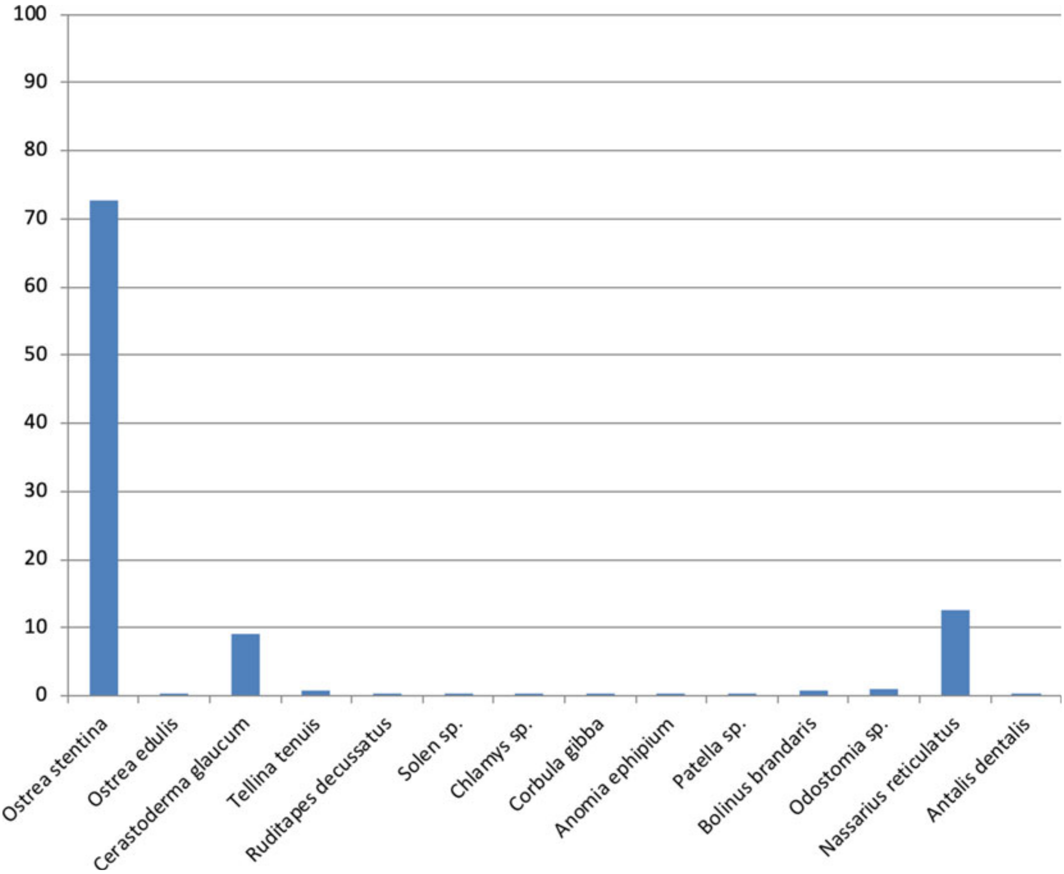

Fig. 12.17 Malacofauna species identified in the destruction context of Patio de Banderas

activity of clionaid sponges, as well as signs of rupture in its ventral edge.

The fauna has a relatively high percentage of shell fragments (59%), less than 5 mm in size. The almost absolute absence of evidence of bioerosion implies a short time of permanence of the shells in the bottom. These characteristics are congruent with a resedimented state of conservation that evidences a seafloor winnowing and an almost immediate transport of the exhumed specimens. Once the deposit was produced, it had to be reworked in situ by the action of currents or waves, since 41% of the assemblage are fragments less than 5 mm, which coexist with the rest of larger shells not fragmented (41%). These malacofaunal assemblages present certain similarity to the deposits of shelly cheniers of the Guadalquivir marshland (Fig. 12.17).

Regarding benthic foraminiferal shell preservation, the high-energy deposits (samples MP1 and MP2) are characterized by the highest abrasion (highest abrasion grade 1 and lowest abrasion grade 0), low dissolution and low recrystallization (Fig. 12.18). These taphonomic features indicate an energetic and rapid deposition consistent with high-energy deposits. In contrast, the rest of the archaeological sediments (samples MP3 to MP8) show lower abrasion (lower abrasion grade 1 and higher abrasion grade 0), higher dissolution and higher recrystallization. Lower abrasion in these samples might point to non-energetic and slow deposition. In addition, higher dissolution and recrystallization of microfossils suggest diagenetic processes due to circulation of pore fluids.

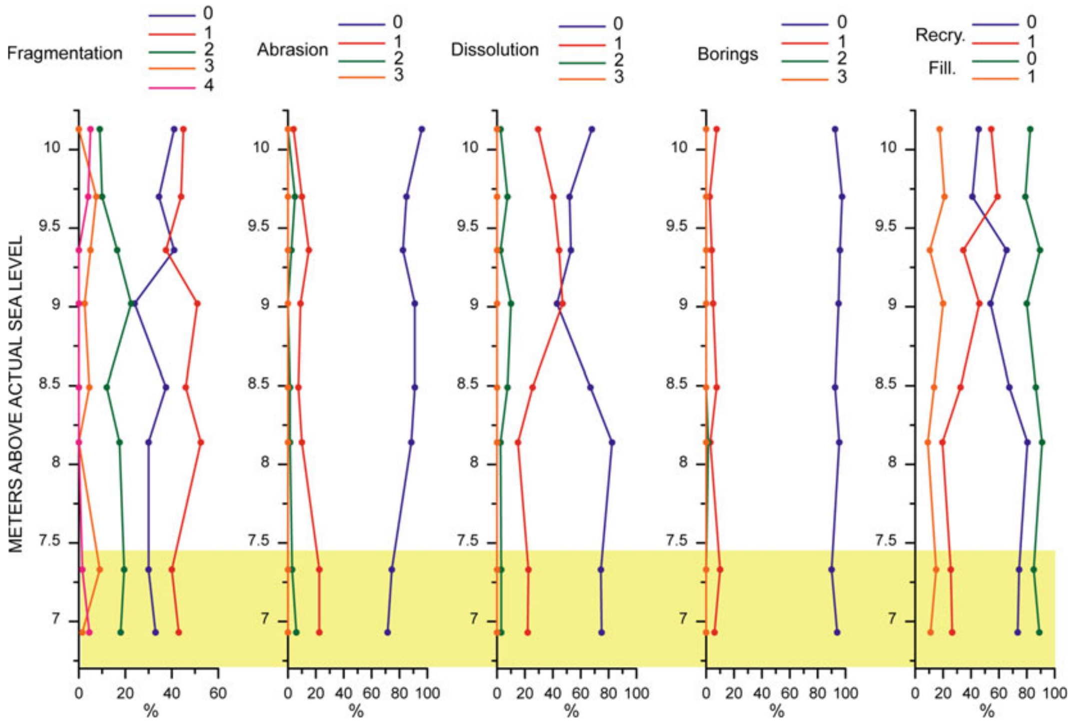

Fig. 12.18 Distribution of the different taphonomic traits from benthic foraminifera: fragmentation, abrasion, dissolution, borings, recrystallization, and fillings (calcite). 0 represents the absence of the specific taphonomic signature. Yellow horizontal shading is the high-energy deposit

In the high-energy deposits, presence of early Pliocene (4.3–3.84 Ma) (Wade et al. 2011) planktic foraminifera (*Globorotalia margaritae, Globorotalia crassaformis*) and upper slope and shelf benthic foraminifera (*Cibicidoides mundulus, Cibicidoides* sp., *Cibicides refulgens, Cibicides* sp., *Ammonia beccarii, Ammonia* sp., *Cassidulina laevigata*) indicate reworking of early Pliocene marine sediments from the Neogene Formations outcropping near Sevilla (Pérez-Asensio et al. 2012, 2018). Therefore, the energetic event would have eroded a limited area and transported the early Pliocene foraminifera into the studied site. The rest of the archaeological deposits (Late Roman alluvial and Medieval occupation deposits) also contain similar upper slope and shelf benthic foraminifera, however, planktic foraminiferal biomarkers (*Globorotalia miotumida, Globorotalia scitula, Globorotalia margaritae, Globorotalia crassaformis*) range from late Miocene to early Pliocene (Sierro et al. 1993; Wade et al. 2011; Pérez-Asensio et al. 2012, 2018). This wider temporal range of reworked foraminifera might be related to different sediment sources covering a wider area.

12.6 The Sedimentary Origin of the Third Century AD Collapse Facies of Patio De Banderas

The abovementioned deposits were transported and sedimented in the same event, since there are no features indicating soil exposure and formation. Besides, some sedimentary components like rip-up clasts, and features such as gravitational silt coatings formed due to trapped air scaping upwards, are present in all the microfacies described, suggesting a common origin of these microfacies in the same sedimentary event (Fig. 12.12). These deposits, the sedimentary structures identified, and their composition fit with several EWE deposits identification criteria described in the literature (Goff et al. 2012; Costa and Dawson 2015). In the deposit identified in Patio de Banderas, grain sizes vary from boulders (transported constructive, decorative, and epigraphic materials) to sandy, silt, and finally mud laminae microfacies. This is indicative of a high-energy sedimentary event with energetic pulses that caused structural damage to the Roman city of *Hispalis*. Each wave or energetic pulse formed distinct sedimentary microfacies, resulting in specific bedforms, like the case of storm deposits and microlaminated tsunami deposits (Fujiwara 2008; Lario et al. 2010; Goff et al. 2012; Costa and Dawson 2015). In this sense, the 14 microfacies units identified with micromorphology would be related to the physical properties of the flows of an EWE event, such as speed, density, viscosity, and dominant grain size of the different energetic pulses of the event. These changes in the energetic deposition are discernible due to the presence of mud laminae, which are good indicators of stagnation periods between pulses (Fujiwara and Kamataki 2007, 2008; Fujiwara 2008; Nanayama 2008), and to granulometric changes identified, ranging from silty to sandy microfacies. Discordant and sharp contacts between microfacies also depend on changes in the energetic sedimentation environment along the event that entailed erosion. The cyclical repetition of microfacies units along the sequence is very common in the studied deposit. This is the case of poorly sorted iron-poor marine/estuarine silt layers with shells, which are followed by poorly sorted silty clay levels rich in mudbricks and anthropogenic materials in micromorphological samples 1 and 3 (Figs. 12.10 and 12.12). Another indicator of EWE deposits present in Patio de Banderas is the abundant and constant presence of rip-up clasts, aggregates of reworked soil material which, under thin section, exhibit their own porosity, b-fabric, and mineralogical composition. These rounded aggregates have been classified into three different types according to their provenance: reworked Bt horizon aggregates, calcareous, and sedimentary crusts aggregates. Also, individual shells and shell-rich units are typical of EWE deposits (Lario et al. 2010; Morton et al. 2007). In Patio de Banderas, shell-rich layers were identified both macroscopically during the excavation process and microscopically through micromorphology. Their distribution and bedding degree provided significant data about energetic changes during sedimentation, being horizontally arranged during the early stages of the event (micromorphological sample 1) and chaotically distributed in the most energetic moment of the event (micromorphological sample 3). Also, shell, wood, and less dense debris are often found "rafted" at or near top of sequence in tsunami and EWE deposits (Goff et al. 2012). In this respect, while shells and organic remains are abundant all across the studied deposit, as seen in thin section, during excavation it was identified a significant shell debris in the upper part of the deposit (Fig. 12.8c). Lastly, a muddy layer with plant debris formed by suspension fallout on the top of the deposit, such as the one identified in micromorphological sample 5 (Fig. 12.15), is often generated during the backwash process and the returning to low-energy conditions after storms and tsunamis (Lario et al. 2010). In some of these mud laminae and the final mud cap there are incipient clay illuviation features. These features were formed due to clay flocculation and mobilization through pores. Thus, regarding clay illuviation features, we distinguish those inherited from Bt horizons aggregates of soils eroded by the event from those generated in situ (Fig. 12.15c). In this sequence, anthropogenic materials such as construction materials, pottery, and charcoal are localized in specific microfacies that we associate with the transport of the debris generated by the structural damage in the city due to the impact of the EWE inundation. Finally, another distinctive EWE feature identified in Patio de Banderas is the identification of several microfacies and laminae that, going from sand to loam and finally mud, constitute a fining upwards sequence.

The abovementioned sedimentary components and features offer, when considered together, significant information about the sedimentary processes and post-depositional evolution of the studied deposit. The sequence starts with micromorphological sample 1 (Fig. 12.11), which shows a succession of three microfacies that corresponds to the first energetic pulse and to relatively small waves in the early stages of an EWE event. Thus, microfacies 1 result from estuarine muds with abundant shell remobilization and sedimentation. Microfacies 2 was deposited relatively fast and traumatically, associated with the transport and sedimentation of the anthropogenic debris generated by the high-energy event. Finally, microfacies unit 3 corresponds with water saturation, energy flow decrease, and a stagnant period between flows. Micromorphological sample 2 (Fig. 12.12) showing a succession of 4 microfacies, and the two microfacies identified in micromorphological sample 3, would correspond with relatively large waves. Microfacies 1 and 2 comprise coarse sandy components deposited in a highly energetic pulse, while microfacies 3 corresponds with a stagnant and water saturation period between pulses. Microfacies 4 of micromorphological sample 2, together with micromorphological sample 3 (Fig. 12.13) show, again, an increase in energy and the input of estuarine muds with shells and anthropogenic debris. Micromorphological sample 4 (Fig. 12.14) shows a set of 5 microfacies that correspond with the waning stage of the inundation. Thus, the waves deposited more fine material as the energy was decreasing. This resulted in a succession of sandy loam microfacies (microfacies 1, 3, and 5) which eventually incorporate a quartz sand microfacies (microfacies 2) and a mud lamina (microfacies 4, reflecting energetic changes). Finally, micromorphological sample 5 (Fig. 12.15) shows a mud cap layer that corresponds with a water saturation period and the backwash process.

The sedimentary units identified in microfacies analysis, as well as the different energetic pulses, have also been identified in the geochemical and mineralogical analyses developed. We find that element concentrations are related to the geochemical input associated with the event. This is the case of Ba, an important component of marine biota that plays an important role in the marine biogeochemical cycle (Gonneea and Paytan 2006). In sediments, it represents the organic and mineral fraction associated to biological activity (organic matter, carbonates, opal, and barite). Greater amounts of concentrations are detected in estuarine geomorphological environments than in the open sea (Wedepohl 1971). By normalizing Ba with elements such as Al or Ti (Murray et al. 2000), associated with terrigenous materials, marine biological activity stands out. In this case study, this normalization can be understood as a good marker of EWE deposits (Cuven et al. 2013). In the Patio de Banderas sequence, the Ba/Ti normalization shows clear increases in moments of input and higher energetic sedimentation pulses. Specifically, it is the case of sample 1, dominated by the input of shell-rich estuarine material (Fig. 12.16). It is also identified in sample 5, composed of sands derived from the erosion and weathering of glauconitic-rich calcarenites, or sample 10, which corresponds to the first input of sandy loams of the third energetic pulse. Besides, S is often related to post-depositional diagenetic processes in marine/brackish environments, as well as in peat bogs. S has been reported as an indicator of input of marine material, paleosalinity, and frequency of flooding in tsunami events (Cuven et al. 2013; Chagué-Goff 2010; Chagué-Goff et al. 2017). Again, as with the Ba, S shows the significant enrichments associated to high-energy deposition. Specifically, it is the case of samples 1, 5, and 10 (Fig. 12.16). Of these enrichments, the most prominent is that of sample 1 at the base of the sequence, the same situation identified in the deposits of the Lisbon tsunami of 1755 AD, in the sequence identified in Los Lances (Cuven et al. 2013).

Furthermore, Ca can be indicative of the entrance of bioclastic materials (Fig. 12.16). Although this element shows significant anomalies, we have normalized this element with Al (Fig. 12.16). This normalization expresses the importance of the silicate proportion residing in the lithogenic fraction. Therefore, an increase in the Ca/Al ratio can show increases in biogenic carbonate in storm and tsunami deposits (Cuven et al. 2013). In samples 1, 3, 5, and 7 (Fig. 12.16), normalization shows significative enrichments, which corresponds to the identification of shell-rich microfacies in soil micromorphology. Also, a decrease of this ratio is observed in the mud laminae, siliceous sands, and sandy silts microfacies (Fig. 12.16).

Another paleosalinity indicator is Na (Fig. 12.16). Cuven and collaborators highlighted how, in general terms, there is an enrichment of this element in tsunami and storm deposits with respect to non-tsunami and anthropogenic deposits. This situation occurs in the Patio de Banderas sequence. Besides, it should be noted that both S and Na, although they are good salinity indicators, they are highly mobile and generally subject to leaching by meteoric waters (Chagué-Goff et al. 2017, 2012). Therefore, the use of these elements as paleosalinity indicators is risky due to their solubility. In this sense, studies about Indonesia tsunami deposits event (2004) identified enrichments of Na and other soluble salts that, after a rainy season, were significantly reduced in terms of concentration (Szczuciński et al. 2007).

The considerable contribution of Si in tsunami deposits has also been highlighted in literature (Morton et al. 2007; Cuven et al. 2013; Chagué-Goff et al. 2017; Goff et al. 2012). It is associated with the input silica-rich sands. The concentration of Si, in the high-energy deposit of the Patio de Banderas, is very prominent with respect to the rest of the sequence, showing only a decrease in samples 11 and 12 (Fig. 12.16). These samples are associated with the deceleration process and the backwash, and therefore with the cessation of the entry of exogenous material. This decrease has been reported in other case studies, such as the Lisbon tsunami sequence in Los Lances (Cuven et al. 2013). In addition, the normalization of other elements with Si is very useful, since it is an indicator of detrital material. For example, the Si/Al and Si/Ti ratios represent quartz-rich sandy horizons and increase with respect to terrigenous deposits (Cuven et al. 2013; Chagué-Goff et al. 2017), which in the Patio de Banderas is especially intense in samples 5, 7 and 10–12 (Fig. 12.16). These samples represent, respectively, glauconitic sand, estuarine sandy silts, and finally, sandy silts with a high content of quartz. After the event, these normalizations stabilize, being these values the typical geochemical background of the study area.

As proposed by Kuwatani et al. (2014), the Si is a good element to discriminate EWE deposits. To do this, matrix dispersion graphs have been made comparing the concentrations of the elements analyzed with respect to Si (Fig. 12.19). In all the matrices, two statistically significant populations are distinguished: the EWE deposits on the one hand and the alluvial Late Roman sediments and Medieval anthropogenic sediments on the other hand. In the case of the Late Roman and Medieval sediments, the concentrations show a greater clustering that indicates a more stable geochemical environment, compared to the high-energy deposits that are characterized by a greater dispersion caused by the continuous and violent succession of sedimentary inputs, showing more variable geochemical compositions. Therefore, Si is a good indicator of EWE deposits in the context of the Patio de Banderas. In general, the Late Roman and Medieval deposits have lower values than the sediments associated with the high-energy event.

The variation of concentrations of some elements is related to the mud laminae that were deposited among the different energetic pulses of the wave train. These layers are characterized by a decrease in values of Si, Ba, and Ca while, on the contrary, there is a significant enrichment in K, reflecting an increase in proportions of silt and clay fractions (Fig. 12.16). The maximum value of K occurs in sample 3 (Fig. 12.16). Soil micromorphology analysis highlights the high content of muscovite in this microfacies, which is a potassium-rich mica (Fig. 12.16). Also, the K/Si ratio is indicative of fine material sedimentation (silt and clays) (Fig. 12.16). As in the case of the Lisbon tsunami of 1755 in the sequence identified in the Lances (Cuven et al. 2013), in the Patio de Banderas there is an increase of this ratio in backwash and deceleration process.

Regarding heavy metals, Pb, Cu, and Ni show significant anomalies in concentrations

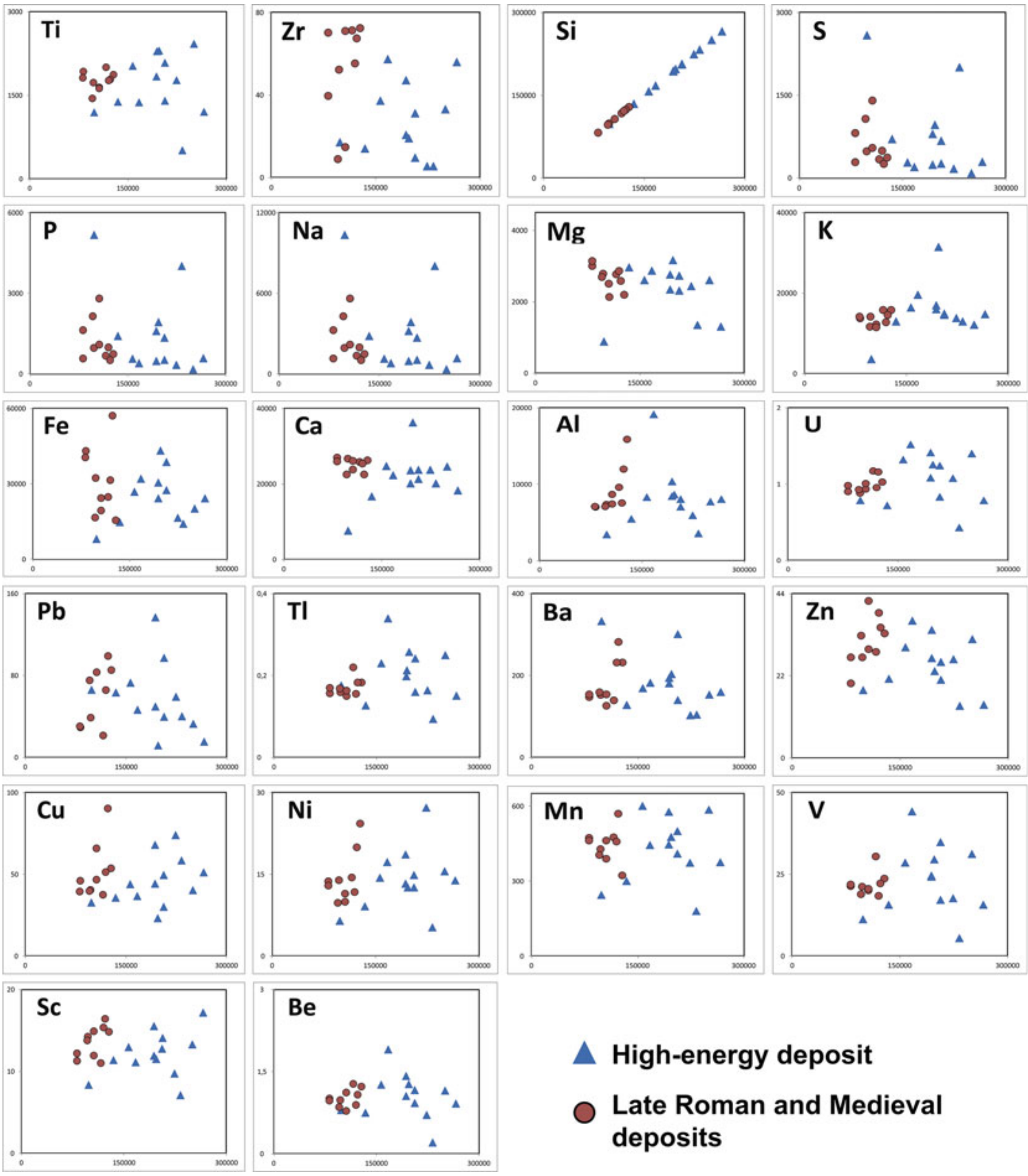

Fig. 12.19 Scatter diagrams of the ICP-MS, ICP-OES results. The horizontal axis is Si, and the vertical axes are the elements named at the top of each diagram. Blue triangles indicate the high-energy deposit, and the red circles indicate the Late Roman and Medieval deposits. All diagrams are expressed in ppm

depending on changes in energy and sedimentation environments. At the same time, these anomalies clearly reflect the different energetic moments (initial sedimentation, maximum energetic pulses and deceleration), according to the sedimentary units identified. Specifically, Pb shows a negative significant anomaly in moments of energetic deposition, as shown in samples 3, and 4–8 (Fig. 12.16). After an increase in sample 9, there is a progressive decrease in Pb concentrations in samples 10–13 (Fig. 12.16). Cu and Ni, however, show a different behavior, with positive anomalies in moments of energetic deposition, as is specially clear in samples 2, 4, and 7 (Fig. 12.16). Besides, Cu and Ni show, as in the case of Pb, a progressive decrease in their concentrations in samples 8–13 (Fig. 12.16).

XRD analysis shows significant mineralogical anomalies related to the EWE event. Quartz content shows anomalies related to the different energetic pulses (Fig. 12.16). Thus, an increase of quartz in samples 1 and 2 is observed, when there is an input of estuarine silts and anthropogenic materials-rich silty clay, but especially in sample 4, with the input of quartz sand. This mineral shows decreases in certain samples, such as 3 and 13, with the entrance of the mud laminae, or in sample 5, which shows a sand input produced by the erosion and weathering of glauconitic-rich calcarenites. In these samples, while there is a decrease in the amount of quartz, there is also an increase in other minerals, such as calcite and mica, which are associated with moments of higher input of bioclastic calcitic material and clayey silt respectively. Finally, XRD analysis shows smaller amounts of feldspar and dolomite, which do not show significant differences in concentration along the sequence (Fig. 12.16). Therefore, quartz, calcite, and mica are the minerals that present significant differences associated to the high-energy event and, in particular, to the energetic pulses identified. In this sense, the main anomalies are located in samples 3–12, when the event was more violent.

Finally, a principal component analysis was carried out, using the varimax method, and analyzing some very significant geochemical ratios, such as Si/Ca, Si/Al, and K/Si (Fig. 12.20). The use of these normalizations is given by the results of the matrix analysis, which revealed that Si was a good indicator of detrital material in this context, differentiating two populations: the EWE deposits and the Late Roman alluvial sediments and Medieval occupation deposits. In addition, Ca allows to discriminate the input of bioclastic material, as well as Al and K are good markers of terrigenous and silty clay material input respectively. Therefore, with these values, an analysis of principal components of rotated solution and regression method was carried out. The result of this analysis discriminates two components in which the first group, the ratios Si/Ca and K/Si, with inverse relationship between them, explains 57.9% of the variance. The second component is associated with the Si/Al ratio with a positive coefficient, which explains 38.4% of the variance. The percentage of variance explained between the two components is 96.3%, which denotes a good explanation of the variability in the distribution of the samples.

The results of the PCA analysis have been plotted under two different grouping criteria: EWE deposits versus Late Roman and Medieval sediments, and, in addition, sedimentary units identified in microfacies analysis. Discrimination between EWE sediments and Late Roman and Medieval deposits is clearly shown in Fig. 12.19. In this regard, Late Roman and Medieval samples are strongly conditioned by the K/Si ratio, showing higher values in this geochemical ratio than the EWE deposits. As for the sedimentary units, in the non-EWE deposits two subpopulations are discriminated: on the one hand, the Late Roman alluvial deposits with a higher K/Si ratio, and, on the other, Medieval anthropogenic deposits also dominated by a high ratio K/Si, but with lower values than alluvial deposits. On the contrary, EWE deposits show greater variability. However, component two (positive coefficient of Si/Al) allows to discriminate four subpopulations related to the different energetic pulses of the high-energy event, and, ultimately, granulometric differences within the deposit. Those pulses of lower energy and finer granulometry, such as the mud cap, and the initial moment of the event, are characterized by lower values in the Si/Al ratio. In contrast, samples 3–12 show an increase in this ratio, coinciding with the presence of thicker granulometric fractions and more energetic depositional environments (Fig. 12.16).

The malacological analysis shows the transport and input of intertidal or shallow infralittoral species, mostly corresponding to coarse and/or muddy sandy bottoms. The studied assemblage shows signs of abrasion but no bioerosion. Micropaleontological analyses reveal rapid and energetic deposition (high abrasion, low

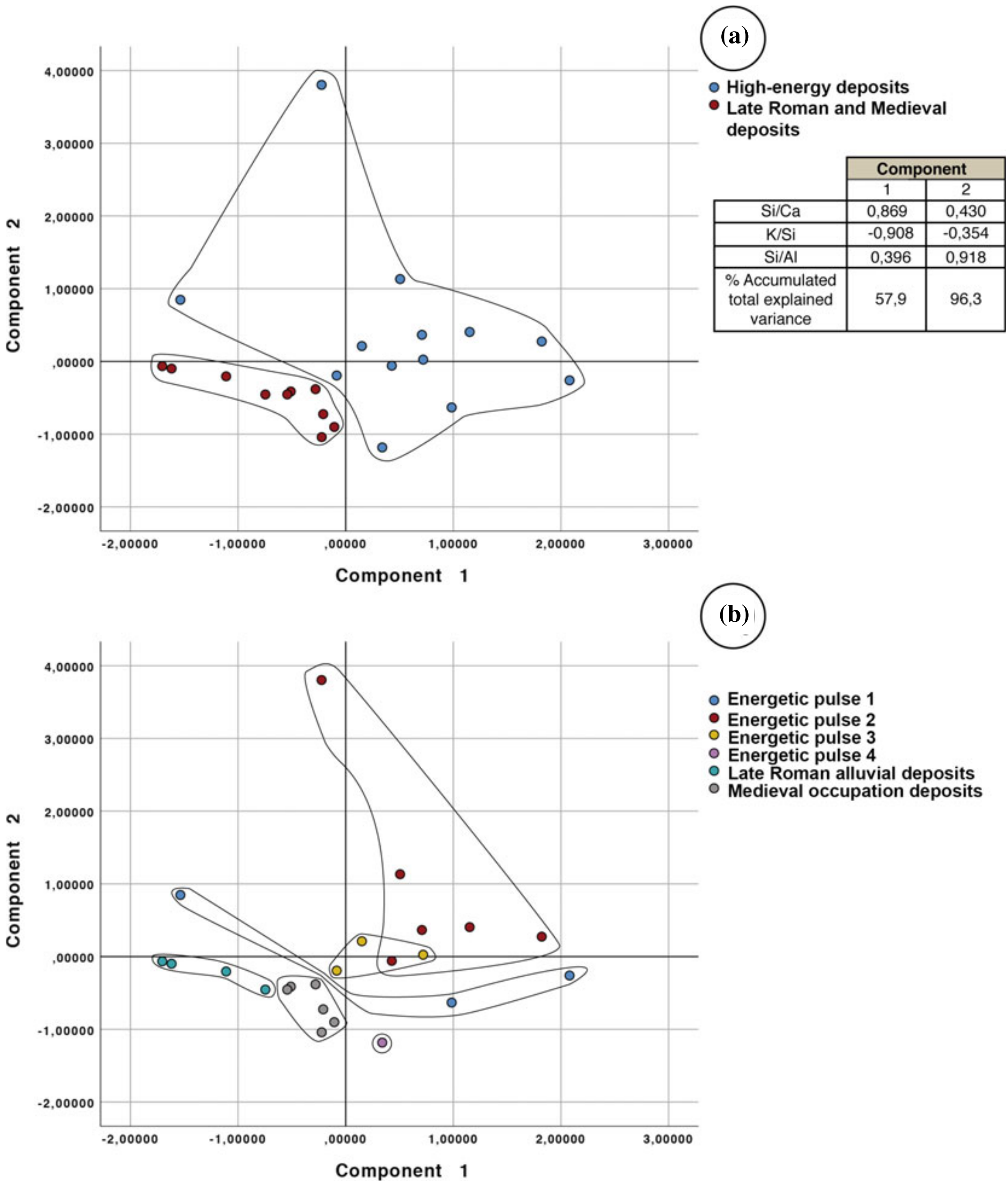

	Component 1	Component 2
Si/Ca	0,869	0,430
K/Si	-0,908	-0,354
Si/Al	0,396	0,918
% Accumulated total explained variance	57,9	96,3

Fig. 12.20 Principal component analysis of the studied deposits. Plot **a** labels refer to the EWE and Late Roman and Medieval samples, while Plot **b** labels refer to the geomorphological setting and sedimentation phases identified in the EWE event. The different clusters in this plot show granulometric differences in the deposit. Thus, the EWE deposit shows a thicker granulometry, especially when it is documented a sandy input in the most energetic pulse

dissolution, and low recrystallization) in the EWE deposit and slow and non-energetic deposition (low abrasion, high dissolution, and high recrystallization) in Late Roman and Medieval deposits.

In our opinion, the Patio de Banderas deposit was generated during an extreme wave event, even though it is difficult to assess its sedimentary origin. Our interpretation is limited by the nature and extent of the excavation. In this sense, it must be remembered that the deposit identified in Patio de Banderas was found inside a Roman building, a sedimentary trap for the transported sediments and anthropogenic debris, creating a thick deposit. In the future, new excavations in the suburbs of *Hispalis* will allow to conduct new geoarchaeological analyses in order to confirm the vertical and horizontal extension of the deposit, as well as to profound in its sedimentary origin. With the data we actually have, and considering the distance from this point to the coast in Roman times and also similar synchronic regional evidence, we affirm that the most probable origin for the deposit identified is the combined action of an energetic storm, that might have produced waves and currents in the *Lacus Ligustinus* energetic enough to transport estuarine and marine fauna, together with intense rainfall and flooding from the Guadalquivir River. However, this deposit seems to be synchronous with a tsunami event identified in the coast of southwestern Spain.

12.7 Contextualization of the Patio de Banderas High-Energy Deposit in the Third Century AD EWE Event(s) in Southwestern Iberia

In recent years, the third century AD event has progressively gained importance as more evidence has been being reported. Even though this event was considered to have had a limited impact until recent years (Lario et al. 2010), new evidence has been reported in the Doñana spit bar and marshland. The main evidence of this tsunami in the estuary is a fine layer of sediment about 10–15 cm thick with marine fauna, studied in a core taken in the Guadalquivir marsh about 10 km from the coast, and other geomorphological evidence in the littoral spit bars (Rodríguez-Ramírez et al. 2016).

One of the main geomorphological characteristics of the Guadalquivir estuary is a chenier plain, although it is not evidence of tsunamis (Rodríguez-Ramírez and Yáñez 2008), In this sense, Las Nuevas chenier, one of the main estuarine shelly ridges of the chenier plain, was operating from the second to the fourth century AD, at least, and fed from all the detrital particles available in the basin (supplied by storms, tides, and tsunamis). It is a transgressive chenier that migrated toward land experiencing recycling and reworking of its own deposits and extending into the estuary for more than 20 km (Rodríguez-Ramírez 2009; Rodríguez-Ramírez and Yáñez 2008; Rodríguez-Ramírez et al. 2016). According to the paleogeographic reconstruction of their study, the tsunami, storms, and tides input would have promoted sedimentary accumulation in Las Nuevas chenier, which crested between the second and the fourth centuries AD and especially in the third century AD. This development can be explained as the result of the reworking and subsequent build-up of the basal residual lag in the estuary (Rodríguez-Ramírez et al. 2016). The new chronology of Las Nuevas chenier proposed in Rodríguez-Ramírez et al. (2016) (and not 218–209 BC as proposed by Rodríguez-Vidal et al. 2011; Ruiz et al. 2013b) takes into account the considerable reworking of these contexts and the residual nature of the faunal assemblage, something crucial for the radiocarbon dating. For Rodríguez-Ramírez et al. (2016), despite such geomorphological and sedimentary effects, however, the event failed to break through, by means of inlets, the Doñana spit as well as the tombolo that linked the mainland to La Algaida spit bar, thereby limiting the sedimentary marine input into the inner estuary. Other regional contemporaneous evidence for this event is located in the Guadalete estuary, where Gutiérrez-Mas (2011) observed shelly sandy layers in both subtidal zones and emerged areas. These biogenic deposits consist of bivalve shells (mainly

Glycymeris sp.), sometimes imbricated, showing abrasion, impact marks, and dissolution. These lithofacies show sedimentary structures compatible with high-energy flows, such as erosive bases, reactivation surfaces, imbricated shells, cross-stratification (Gutiérrez-Mas 2011). Also, the washover fans identifies in the Tinto-Odiel estuary are contemporaneous to this event (González-Regalado et al. 2019a, b). However, their authors have interpreted these deposits in different ways with time. While a tsunami was hypothesized as a possible origin for these washover fans (Ruiz et al. 2013a), nowadays these deposits are now interpreted as storm deposits (González-Regalado et al. 2019a, b). When considered together, all these deposits depict a supra-regional correspondence that encompasses a significant part of the Gulf of Cadiz (Fig. 12.1). Additionally, they show some similarities, such as the high bioclastic content exhibiting bioerosion and an abundant presence of *Glycimeris sp.* (Gutiérrez-Mas 2011; Rodríguez-Ramírez et al. 2016; González-Regalado et al. 2019b). In sum, the geomorphological and sedimentary evidence for the estuarine environments in the southwest of the Iberian Peninsula calls for a model of evolution punctuated by successive small EWEs, possibly storm surges, and disrupted by a considerably larger event, likely a tsunami, in the second–third century AD.

Regarding the contemporaneous archaeological record, there is seismological evidence and abandonment facies dated to the third century AD in southwestern Iberian archaeological settlements which some archaeologists have tried to correlate with a large-scale event (Ramallo Asensio and Quevedo Sánchez 2015; Rodríguez-Vidal et al. 2015; while Ruiz-Bueno 2017 is more cautious about the extent of such an event), specifically its impact on the region's cities. This is the case of *Baelo Claudia* (Bolonia, Cadiz), where two different earthquakes have been reported in 40–60 and 260–290 AD. This last event caused structural damage to several buildings and constructions across the city, such as the *basilica* (Sillières 2013), the *macellum*, the *capitolium*, the Isis temple (Fincker et al. 2008), the *forum* square, the theater, the city walls and one of the city's aqueducts (Silva et al. 2010). There are several appreciable seismological effects on the city's architecture, such as impacts on pavements due to the fall of architectural elements, the collapse of columns and entire buildings in a preferential direction, tilted and folded walls, displaced arch voussoirs, etc. (Silva et al. 2005, 2010). In this sense, new findings in the eastern necropolis are very promising, since a collapsed funerary monument has been discovered in recent years. However, its chronology (preliminarily ascribed to the end of the fourth century AD) and seismological origin of the collapse deposit is still under study (Prados Martínez 2019; Reicherter et al., this volume). Regarding possible synchronous tsunami deposits in *Baelo Claudia*, a recent geoarchaeological study shows no sign of any high-energy deposit in the lower area of the *forum* (Gutiérrez-Rodríguez et al. 2020).

Similarly, collapse and destruction facies caused by an earthquake are common in *Munigua* (Villanueva del Río y Minas, Seville). In this city, several public buildings that had totally collapsed were discovered in the excavations carried out by the German Archaeological Institute (Schattner 2003). This is the case of the so-called "Pórtico de dos pisos," a construction devoted to the exhibition of a Flavian statuary cycle of the Imperial family, and the small temple of Mercury nearby. Their entire façades had collapsed onto the street. Most of the city's contemporaneous constructions exhibit the effects of this earthquake (Giner-Robles et al. 2016): the houses, the *thermae* (Gutiérrez-Rodríguez et al. 2019), the forum, and the impressive sanctuary crowning the granitic hill. This earthquake has been dated to the end of the third century AD, in light of archeological finds (Schattner 2003), but this chronology is still broad and ambiguous. An inventory of the earthquake effects revealed two different orientations of maximum deformation or preferential ground movement: NNW-SSE and ENE-WSW. The authors related the first orientation to an origin on the northern border of the Guadalquivir basin (Giner-Robles et al. 2016).

Seismological effects have also been documented in third century AD archeological contexts in *Corduba* (Cordova), the capital of the *Baetica* province. During decades, destruction facies have been documented at several points in the city. Ruiz-Bueno (2017) compiled all the evidence to perform a critical review on them from an archeological perspective, while Morín et al. (2014) conducted a preliminary archeo seismological study. According to Ruiz-Bueno (2017), evidence in several domestic contexts, namely, the thermal complex of calle Concepción, the *Forum Provinciae*, and the *Forum Coloniae*, are ambiguous. However, the evidence from the theater and the *Aqua Augusta Vetus* is much clearer (Morín et al. 2014; Ruiz-Bueno 2017). In the theater, excavations revealed several collapses, impacts on pavements, and parallel fissures 8 m long and 25 cm wide in the foundations and the geological substrate on which the theater was constructed (Monterroso Checa 2002). The aqueduct's *specus* was disabled and deformed at several points along its course during the third century AD, more specifically AD 250–260 (Ventura and Pizarro 2010). This evidence has been interpreted by Morín et al. (2014) as an earthquake with a magnitude of IX on the ESI-07 scale.

Another city with collapse/destruction facies dating to the third century AD is *Cartima* (Cártama, Malaga), where a building identified as the forum's *basilica* shows signs of traumatic destruction at the end of the second or the beginning of the third century AD. The entire roof had collapsed on the marble floor, after which it remained abandoned until the fourth century AD. While this context has been interpreted as the consequence of the invasion of the *Baetica* province by North African tribesmen (*Mauri*) (Melero García 2007; Berlanga Palomo and Melero García 2015), the chronological coincidence with the other regional evidence discussed in this paper is thought-provoking. In any case, neither the sediments nor the possible earthquake effects have been studied until now.

Finally, in *Gades* (Cadiz) generalized abandonment facies discovered in several locations of the city have been dated to the third century AD (Bernal and Lara Medina 2012). This has traditionally been associated with the text of Avienus (*Ora Maritima*, 270–272), who depicted an image of a devastated city in ruins. Typical urban conditions limiting archeological excavations must be taken into account, as well the regional urban dynamics of this area of the Roman Empire from the third century AD onwards: cities became smaller after losing some of their functions and were concentrated in a number of economic and craft enclaves, especially in port cities such as *Gades* (Bernal and Lara Medina 2012). However, contemporaneous tsunami evidence of this abandonment facies has been reported in the Guadalete estuary (Luque et al. 2001, 2002; Gutiérrez-Mas 2011). Further geoarchaeological research on urban deposits in *Gades* is needed in order to assess the possible evidence of this tsunami and to identify the site formation processes involved in such abandonment facies.

Similar abandonment facies have been detected in *cetariae* (fish processing coastal archeological sites) and *figlinae* (amphorae production centers) in Portugal and Spain. In southwestern Portugal amphorae ceased to be made in the third century AD (Mayet and Tavares 2002; Fabião 2008), as well on the coast of Huelva (Campos et al. 2015). This decline in the Atlantic coastal economy and trade would be temporarily restricted to the third century AD, and for some authors this economic crisis would have been partially caused by the third century AD tsunami, whose effects would have reached archeological sites like La Orden, *Onuba*, El Eucaliptal, and La Cascajera, some of them 12–14 linear km inland from the Tinto-Odiel estuary (Fig. 12.1) (Campos et al. 2015; Bermejo Meléndez et al., this volume). This hypothesis has given rise to a geoarchaeological research line whose aim is to correlate both the archeological and geological records in these coastal sites in order to identify the possible relationship between EWEs and the third century AD decline in the coastal economy of southwestern Iberia (González-Regalado et al. 2019a, b). The detailed publication of the archeological sedimentary sequence, the archeological materials, and the analysis of these deposits will be crucial to understand the extent of the third century AD event(s).

Both the geological and archeological records seem to coincide in the occurrence of a high-energy event in the third century AD, in all likelihood a tsunami. But could it have penetrated inland with sufficient energy to cause structural damage to the settlements on the shores of the *Lacus Ligustinus*? If so, could it have reached the city of *Hispalis*? Abril et al. (2013) performed a modeling study of the 1755 Lisbon tsunami, with the coastal geomorphology in Tartessian and Roman times, in order to evaluate its possible propagation. It took into account not only the geomorphology of the *Lacus Ligustinus* after the sea level rise 6900 years BP, but also the evolution of certain forms of the coastal landscape and the progressive filling of the basin. As a result, the coastline and bathymetry were reconstructed (Abril et al. 2013, p. 4499).

The necessary data for this reconstruction come from studies by Menanteau (1980, 1984), Schubart (1990), Schulz et al. (1995), but, fundamentally, from the "Guadalquivir Marshes Project" led by O. Arteaga. This led to the reconstruction of the paleogeography of the basin in different historical periods (Arteaga and Roos 1995; Arteaga et al. 1995; Roos et al. 1995). The knowledge of the ancient geography of the basin was supplemented by the review of the coastal evolution of Doñana carried out by Rodríguez Ramírez et al. (1996), and by the analysis of sediments from cores by Ruiz et al. (2005), in which four phases of evolution were established in the Guadalquivir estuary during the Late Holocene.

The results of their model reveal an insignificant impact on the inland coast of *Lacus Ligustinus* in Roman times. If a tsunami occurred in this chronology, it might have caused severe damage along the Atlantic seaboard of southwestern Iberia, from Cadiz to Huelva, but never in the interior of the basin. According to the model, the development of the Doñana and La Algaida coastal arrows would have minimized the impact of the tsunami (Abril et al. 2013). This is in contradiction with the tsunami deposits present in the geological record of the Guadalquivir estuary.

However, Abril et al. themselves emphasize that very little is known about the bathymetry of the *Lacus Ligustinus* (Abril et al. 2013). Certainly, the fact that the reconstruction of the bathymetry and its evolution is based on the geographical reconstruction performed in the framework of the "Guadalquivir Marshes Project" (Arteaga et al. 1995) casts doubt on the validity of this model, due to the paucity of primary research data published until now (stratigraphic sequences, cores, sedimentological analyses, etc.). Despite being plentiful and valuable, these data are not enough to establish a bathymetry with the level of detail required for accurate modeling, such as that proposed by Abril et al. In fact, these authors prudently assure that the proposed bathymetry, the subsequent basis of the entire interpretation of the study, would only be tentative (Abril et al. 2013). Nevertheless, the modeling and the methodology used by Abril et al. (2013) are very promising lines that should be explored in light of new data.

The geographical dispersion of the geological and archeological evidence dated to the third century AD is broad enough to cover a significant part of the Gulf of Cadiz and the Guadalquivir valley. If they are truly contemporaneous and belong to a same seismic event, it would entail a high-magnitude earthquake. The highest magnitude event recorded in the area is the 1755 AD earthquake. Concerning this event, there is a vast amount of information on its geological imprint and material effects. Regarding its effects on the city of Seville, the intensity was VIII (EMS-1998) and there are numerous historical records about specific buildings that were completely destroyed or damaged. This information has been mapped, showing that the effects on the lower area near the river, in the surroundings of the Cathedral, the Real Álcázar, and Patio de Banderas, were considerable (Martínez Solares 2001; Rodríguez-Pascua et al. 2016). Also, other geological phenomena such as liquefaction have been identified (Martínez Solares 2001).

The current state of the art about the third century AD event is promising, but inconclusive.

The geomorphological and sedimentary evidence calls for a model of evolution punctuated by successive small EWEs, possibly storm surges, and disrupted by a considerably larger event, likely a tsunami, in the second–third century AD. We still do not know the extent of these events. The corpus of geological and archaeological data is progressively growing, but a closer correlation about them is needed in order to confirm the consequences of such events. In this context, the evidence of Patio de Banderas in Seville seems to be key to exploring new directions or to discarding the hypothesis of a high-magnitude event with material consequences along the southwest coast of Iberia and up the Guadalquivir Valley to Cordova.

12.8 Conclusions: Further Research is Needed

Both the geological and archeological records of the southwest of the Iberian Peninsula seem to coincide in the identification of high-energy and collapse deposits, respectively, at the end of the second or at the beginning of the third century AD. The spatial distribution and chronological concordance of these deposits along the southwestern seaboard of the Iberian Peninsula suggests a succession of storm surges and the disruption of a larger tsunami event. However, several questions remain opened, making it difficult to distinguish among these events or to evaluate their magnitude and extent. One of those unanswered questions is the absolute dating and regional correlation of the EWE and collapse deposits. Now that it has been proven that the Galbis catalog and its sources are not useful for the chronological ascription of the events that occurred in Roman times (Rodríguez-Ramírez et al. 2016; Álvarez-Martí-Aguilar 2017a, b, 2020, this volume), the current tsunami catalog should be reconsidered, as has been done in Costa and colleagues (this volume). Also, and regarding the event discussed in this paper, the chronological span of most of the C14 datings of the events identified in Roman times is relatively wide, and in some cases the most recent dates according to the calibrations are close to the third century AD. C14 calibration and the reservoir effect are both recurrent problems in this area, an aspect that has been addressed in several studies and reviews of the available dates. However, a comprehensive study of all these absolute dates for the Roman period in order to explore the regional correlation of these deposits and to assess the third century AD event is still lacking.

In such a hypothetical study, it would be useful to expand the absolute dating series, both horizontally and vertically in each one of the deposits of interest, in order to explore possible chronological coincidences between them from a Bayesian statistical perspective. In this line of research, the role of archeology will be important, due to the greater chronological resolution provided by the archeological materials in tandem with the absolute dates, and also due to the presence of settlements on the southwestern seaboard of the Iberian Peninsula with phases of occupation contemporaneous with these events identified in the geological record, such as Cerro del Trigo. In this respect, archeologists have a great contribution to make to the possible third century AD event. As shown in Boca do Rio (Portugal), new excavations in archeological sites along the southwest coast, implementing a specific sampling protocol, will provide very conclusive data not only for gaining further insights into the effects of this event on local settlements, but also for corroborating the existence of such event(s). In our opinion, another possible line to be explored by archeologists is the study of the sociopolitical reactions to these catastrophic natural events (Ñaco and Nappo 2013). Specifically, we are referring to the study of the honorific epigraphic record in the Roman cities of this area, looking for possible urban refurbishments, new architectural programs, or tax benefits granted by the Imperial administration in the wake of the seismic event, which, as previously shown, have been archeologically identified in some cities of the *Baetica* province. In this connection, two inscriptions from *Astigi* (Écija), dated to AD 245–253, demonstrate that the *Baetica* province was temporarily exempted from paying taxes (*prouincia immunis*) due to unknown causes (Sáez Fernández et al. 2005; Ruiz-Bueno 2017). This measure, among others, was commonplace in the event of various kinds of crises, such as the effects of natural disasters. Could the origin of this exceptional measure be the third century AD seismic event? Maybe an exhaustive study of the *Baetican* epigraphic record could help to flesh out the material effects of this possible event.

In sum, further geological, archaeological, and specially geoarchaeological research is needed in order to confirm the occurrence of the third century AD events, their magnitude and extent. This necessary collaboration between geologists and archaeologists will enrich the debate, making it possible then to systematize the currently available data and to elaborate a more complex and complete sampling and analytical strategy for the study of storm and tsunami deposits, specially the microlaminated ones. In this scenario, the geoarchaeological research conducted at Patio de Banderas excavation in Seville potentially plays a significant role from various perspectives. On one hand, the interpretation of the third century AD collapse layer as a combined action of energetics waves together with intense rainfall and flooding from the river Guadalquivir proposed in this chapter shows that storm surges in the third century AD were energetic enough to reach the Roman city of *Hispalis* and transport estuarine materials. This possibility highlights that a better knowledge of the geomorphological and paleogeographical evolution of the *Lacus Ligustinus* is still needed in order to know where the coastline was at the third century AD. The presence of this high-energy deposit containing estuarine and marine fauna in Patio de Banderas, along with the fact that large merchant ships annually reached *Hispalis* suggests, in our opinion, that the coastline was closer to the city and the marsh channels were wider and deeper than currently thought. On the other, the methodology and results summarized here show how significant information about this high-energy sedimentation event was contained only at the microscale. The Patio de Banderas case study has implications for the future characterization protocols of EWE deposits, since most of the microfacies identified and a wide range of sedimentary features are only recognizable at the microscale, and specifically through micromorphology.

Acknowledgements Authors wish to acknowledge the financial support provided by institutions involved in this research. The archaeological investigations carried out in the Patio de Banderas from 2009 to 2014 are included within the framework of the General Research Project "Archaeological Analysis of the Alcázar de Seville II", directed by M.A.T.R., approved by the Dirección General de Bienes Culturales of the Junta de Andalucía and financed by the Patronato del Real Alcázar de Seville. "Campus de Excelencia Internacional en Patrimonio" of University of Jaén supported the project "Gea versus Chronos, Geoarchaeological Research in Roman Contexts of Andalusia," origin of this paper. University of Granada provided a postdoctoral grant to M.G.-R. in the School of Archaeology and Ancient History of University of Leicester (Programa 8. Perfeccionamiento de Doctores, Plan Propio del Vicerrectorado de Investigación). M.G.-R. thanks the support and funding received from the Juan de la Cierva-Formación Subprogramme (FJC2019-041335-I) funded by the Ministry of Science and Innovation of Spain (MCIN/AEI/ 10.13039/501100011033) and by the European Union (NextGenerationEU/PRTR). J.N.P.-A, A.R.R. and E.M.A. thank the Research Groups RNM-190 and RNM-276 (Junta de Andalucía) and Climate Research Group (CEREGE). Authors wish to acknowledge Antonio Pamies Bertrán and Charles Bashore for revising the text, the authors mentioned in the figure captions who kindly permitted the reproduction of their figures, as well as the reviewers and editors for their constructive comments.

References

Abril JM, Periáñez R, Escacena JL (2013) Modeling tides and tsunami propagation in the former Gulf of Tartessos, as a tool for Archaeological Science. J Archaeol Sci 40:4499–4508. https://doi.org/10.1016/j.jas.2013.06.030

Alonso C, Gracia-Prieto FJ, Ménanteau L et al (2003a) Paléogéographie de l'anse de Bolonia (Tarifa, Espagne) à l'époque romaine. In: Fouache E (ed) The Mediterranean World Environment and History. Environmental dynamics and history in Mediterranean areas, Paris, Université de Paris-Sorbonne, 24–26 avril 2002. Swamp areas and seashores dynamics/Dynamiques des zones humides et mobilite des lignes de rivage. Elsevier, Paris, pp 407–417

Alonso C, Ojeda Calvo R, Ménanteau L et al (2003b) Análisis geoarqueológico del sector meridional de Baelo Claudia (Tarifa, Cádiz). PH 43:58–75

Alonso C, Gracia FJ, Del Río L et al (2004) Registro morfosedimentario de eventos históricos de alta energía en el litoral atlántico del Estrecho de Gibraltar (Trafalgar–Tarifa). In: Benito G, Díez Herrero A (eds) Contribuciones recientes sobre Geomorfología. SEG-CSIC, Madrid, pp 263–271

Alonso C, Gracia Prieto FJ, Rodríguez Polo S et al (2015) El registro de eventos energéticos marinos en la bahía de Cádiz durante épocas históricas. Cuaternario y Geomorfología 29:95–117. https://doi.org/10.17735/cyg.v29i1-2.29935

Álvarez-Martí-Aguilar M (2017a) Terremotos y tsunamis en Portugal en época antigua: el legado de Bernardo de Brito y su "Monarchia Lusytana" (1597–1609). Euphrosyne 45:183–204

Álvarez-Martí-Aguilar M (2017b) La tradición historiográfica sobre catástrofes naturales en la Península Ibérica durante la Antigüedad y el supuesto tsunami del Golfo de Cádiz de 218–209 a.C. Dialogues D'histoire Ancienne 43:117–145

Álvarez-Martí-Aguilar M (2020) The historicity of the earthquakes occurring in the Iberian Peninsula before A.D. 881 Recorded in Spanish and Portuguese seismic catalogs. Seismol Res Lett 91(6):3585–3594. https://doi.org/10.1785/0220200168

Amores F, García Vargas E, Garrido González P et al (2014) Los paisajes históricos del valle del Guadiamar (Sevilla): La minería y la metalurgia en el extremo oriental del cinturón ibérico de piritas. Cuadernos de Prehistoria y Arqueología de la Universidad de Granada 24:203–237. https://doi.org/10.30827/cpag.v24i0.4093

Andrade C (1992) Tsunami generated forms in the Algarve barrier islands. Sci Tsunami Hazards 10:21–33

Andrade C, Freitas MC, Oliveira MA et al (2016) On the sedimentological and historical evidences of seismic-triggered tsunamis on the Algarve Coast of Portugal. In: Duarte JC, Schellart WP (eds) Plate boundaries and natural hazards. Wiley, Hoboken, pp 219–238

Arteaga C, Blánquez J, Roldán L (2015) Consideraciones paleogeográficas en la bahía de Algeciras. Acerca de un posible tsunami en la Carteia romana (San Roque, Cádiz). Cuaternario y Geomorfología 29:137–156

Arteaga O, Roos AM (1995) Geoarchäologische Forschungen im Umkreis der Marismas am Río Guadalquivir (Niederandalusien). Madrider Mitteilungen 36:199–218

Arteaga O, Schulz HD, Roos AM (1995) El problema del "Lacus Ligustinus": investigaciones geoarqueológicas en torno a las marismas del bajo Guadalquivir. In: Tartessos 25 años después, 1968–1993. Actas del Congreso conmemorativo del V Symposium internacional de Prehistoria peninsular. Ayuntamiento de Jerez de la Frontera, Jerez de la Frontera, pp 99–135

Barral-Muñoz MA, Borja F (2015) 3.2. Análisis geoarqueológico. In: Tabales-Rodríguez MA (ed) Excavaciones arqueológicas en el Patio de Banderas, Alcázar de Sevilla: memoria de investigación 2009–2014. Patronato del Real Alcázar, Sevilla, pp 40–51

Berlanga Palomo MJ, Melero García F (2015) Nuevos datos para el estudio del espacio forense de la ciudad de Cartima (Cártama, Málaga). Romula 14:127–160

Bernal D, Lara Medina M (2012) Desenterrando a Gades: hitos de la arqueología preventiva, mirando al futuro. In: Beltrán Fortes J, Rodríguez Gutiérrez O (eds) Hispaniae vrbes. Investigaciones arqueológicas en ciudades históricas. Secretariado de Publicaciones, Universidad de Sevilla, Sevilla, pp 423–473

Bernal D, Expósito JA, Díaz JJ et al (2015) Evidencias arqueológicas de desplomes paramentales traumáticos en las Termas Marítimas de Baelo Claudia. Reflexiones Arqueosismológicas. Cuaternario y Geomorfología 29:119–136

Bernal D, Expósito JA, Díaz JJ et al (eds) (2016) Las Termas marítimas y el Doríforo de Baelo Claudia. The maritime Baths and the Doryphoros of Baelo Claudia. Editorial Universidad de Cádiz; Consejería de Cultura de la Junta de Andalucía, Cádiz

Bezeczky T (2013) The Amphorae of Roman Ephesus. Österreichischen Archäologischen Institut in Wien, Wien

Bonifay M (2004) Etudes sur la céramique romaine tardive d'Afrique. Archaeopress, Oxford

Borja F (2014) Sevilla (1500 a.C.-1500 d.C.): Estudio de geoarqueología urbana. In: Beltrán Fortes J, Rodríguez Gutiérrez O (eds) Sevilla arqueológica. La ciudad en época protohistórica, antigua y andalusí. Editorial Universidad de Sevilla. Ayuntamiento de Sevilla, Instituto de la Cultura y las Artes de Sevilla (ICAS), Sevilla, pp 276–305

Borja F, Borja C, Jiménez Sancho A, García Vargas E (2018) Evolución de la llanura aluvial del bajo Guadalquivir durante el Holoceno medio-superior. Geoarqueología y reconstrucción paleogeográfica de la vega de Itálica (Sevilla, España). Bol Geol Min 129:371–420

Buforn E, Udías A, Colombás MA (1988) Seismicity, source mechanisms and tectonics of the Azores-Gibraltar plate boundary. Tectonophysics 152:89–118. https://doi.org/10.1016/0040-1951(88)90031-5

Cabrera C (2019) From Hispalis to Ishbiliyya. The ancient port of Seville, from the Roman. Empire to the end of the Islamic period (45 BC–AD 1248). Archaeopress, Oxford

Campos JM, Bermejo J, Rodríguez-Vidal J (2015) La ocupación del litoral onubense en época romana y su relación con eventos marinos de alta energía. Cuaternario y Geomorfología 29:75–93. https://doi.org/10.17735/cyg.v29i1-2.31570

Chagué-Goff C (2010) Chemical signatures of palaeotsunamis: a forgotten proxy? Mar Geol 271:67–71. https://doi.org/10.1016/j.margeo.2010.01.010

Chagué-Goff C, Andrew A, Szczuciński W et al (2012) Geochemical signatures up to the maximum inundation of the 2011 Tohoku-oki tsunami—implications for the 869AD Jogan and other palaeotsunamis. Sed Geol 282:65–77. https://doi.org/10.1016/j.sedgeo.2012.05.021

Chagué-Goff C, Szczuciński W, Shinozaki T (2017) Applications of geochemistry in tsunami research: a review. Earth Sci Rev 165:203–244. https://doi.org/10.1016/j.earscirev.2016.12.003

Costa PJM, Dawson S (2015) Tsunami Sedimentology. In: Meyers RA (ed) Encyclopedia of complexity and systems science. Springer Science-Business Media, New York, pp 1–17

Courty M-A (2001) Microfacies analysis assisting archaeological stratigraphy. In: Goldberg P, Holliday VT, Ferring CR (eds) Earth sciences and archaeology. Springer, Boston, MA, pp 205–239

Cuven S, Paris R, Falvard S et al (2013) High-resolution analysis of a tsunami deposit: case-study from the 1755 Lisbon tsunami in southwestern Spain. Mar Geol 337:98–111. https://doi.org/10.1016/j.margeo.2013.02.002

Dabrio CJ, Zazo C, Lario J et al (1999) Sequence stratigraphy of Holocene incised valley fills and coastal evolution in the Gulf of Cádiz (southern Spain). Geologie En Minjbow 77:23–281

Davis BL, Pawlowski GA (1987) Quantitative determination of mineral content of geological samples by X-ray diffraction; discussion and reply. Am Miner 72:438–443

Dawson S, Smith DE, Ruffman A et al (1996) The diatom biostratigraphy of tsunami sediments: examples from recent and middle holocene events. Phys Chem Earth 21:87–92. https://doi.org/10.1016/S0079-1946(97)00015-3

Fabião C (2008) Las ánforas de Lusitania. In: Bernal D, Ribera i Lacomba A (eds) Cerámicas hispanorromanas. Un estado de la cuestión. Servicio de Publicaciones de la Universidad de Cádiz, Cádiz, pp 725–745

Feist L, Frank S, Bellanova P et al (2019) The sedimentological and environmental footprint of extreme wave events in Boca do Rio, Algarve coast, Portugal. Sed Geol 389:147–160. https://doi.org/10.1016/j.sedgeo.2019.06.004

Ferrer Albelda E (2012) Confusiones contemporáneas sobre geografía antigua. A propósito del Sinuus Tartesii y del Lacus Ligustinus. Spal 21:57–67

Fincker M, Sillières P, Dardaine S, Lancha J (2008) Belo VIII. Le sanctuaire d'Isis, Madrid

Flügel E (2004) Microfacies of carbonate rocks: analysis, interpretation and application. Springer, Berlin, Heidelberg

Franco C, Capelli C (2014) New archaeological and archaeometric data on Sicilian wine amphorae in the Roman period (1st to 6th century AD). Typology, origin and distribution in selected western Mediterranean contexts. In: Rei Cretariae Romanae Fautorum Acta 43. Bonn, pp 547–555

Fujiwara O (2008) Bedforms and sedimentary structures characterizing tsunami deposits. In: Tsuji Y, Yamazaki T, Minoura K (eds) Tsunamiites. Elsevier, Amsterdam, pp 51–62

Fujiwara O, Kamataki T (2008) Tsunami depositional processes reflecting the waveform in a small bay: interpretation from the grain-size distribution and sedimentary structures. In: Tsuji Y, Yamazaki T, Minoura K (eds) Tsunamiites. Elsevier, Amsterdam, pp 133–152

Fujiwara O, Kamataki T (2007) Identification of tsunami deposits considering the tsunami waveform: an example of subaqueous tsunami deposits in Holocene shallow bay on southern Boso Peninsula, Central Japan. Sed Geol 200:295–313. https://doi.org/10.1016/j.sedgeo.2007.01.009

Galbis J (1932) Catálogo sísmico de la zona comprendida entre los meridianos 5° E y 20° W de Greenwich y los paralelos 45° y 25° N. Dirección General del Instituto Geográfico, Catastral y de Estadística, Madrid

García Vargas E (2008) La romanización del Bajo Guadalquivir: Ciudad, territorio y economía (siglos II-I a.C.). Mainake 30:247–270

García Vargas E (2015) Ánforas vinarias de los contextos severianos del Patio de Banderas de Sevilla. In: Aguilera Aragón I, Beltrán Lloris F, Dueñas Jiménez MJ et al (eds) De las ánforas al museo. Estudios dedicados a Miguel Beltrán Lloris. Institución Fernando el Católico. Excma. Diputación de Zaragoza, Zaragoza, pp 395–412

García Vargas E, Ordóñez Agulla S, Cabrera C (2017) El puerto romano de Hispalis. Panorama arqueológico actual. In: Campos JM, Bermejo J (eds) Los Puertos Atlánticos Béticos y Lusitanos y su relación comercial con el Mediterráneo. Universidad de Huelva, Huelva, pp 245–285

Giner-Robles JL, Bardají T, Rodríguez-Pascua MA et al (2016) Análisis arqueosismológico del conjunto arqueológico romano de Mulva-Munigua (Sevilla, España). Resultados Preliminares. Geo-Temas 16:605–608

Goff J, Chagué-Goff C, Nichol S et al (2012) Progress in palaeotsunami research. Sed Geol 243–244:70–88. https://doi.org/10.1016/j.sedgeo.2011.11.002

Goldberg P, Miller CE, Schiegl S et al (2009) Bedding, hearths, and site maintenance in the Middle Stone Age of Sibudu Cave, KwaZulu-Natal, South Africa. Archaeol Anthropol Sci 1:95–122. https://doi.org/10.1007/s12520-009-0008-1

González Acuña D (2011) Forma Urbis Hispalensis: el urbanismo de la ciudad romana de Hispalis a través de los testimonios arqueológicos. Universidad de Sevilla, Fundación Focus-Abengoa, Sevilla

González-Regalado ML, Gómez P, Ruiz F et al (2019a) Facies analysis, foraminiferal record and chronostratigraphy of Holocene sequences from Saltés Island (Tinto-Odiel estuary, SW Spain): The origin of high-energy deposits. Estuar Coast Shelf Sci 218:95–105. https://doi.org/10.1016/j.ecss.2018.12.005

González-Regalado ML, Gómez P, Ruiz F et al (2019b) Holocene palaeoenvironmental evolution of Saltés Island (Tinto and Odiel estuary, SW Spain) during the Roman period (1st century BC–5th century AD). J Iber Geol 45:129–145. https://doi.org/10.1007/s41513-018-0089-8

Gonneea ME, Paytan A (2006) Phase associations of barium in marine sediments. Mar Chem 100:124–135. https://doi.org/10.1016/j.marchem.2005.12.003

Gràcia E, Vizcaíno A, Escutia C et al (2010) Holocene earthquake record offshore Portugal (SW Iberia): testing turbidite palaeoseismology in a slow-convergence margin. Quatern Sci Rev 29:1156–1172

Gracia FJ, Alonso C, Benavente J et al (2006) The different coastal records of the 1755 tsunami waves along the South Atlantic Spanish coast. Z Geomorphol 146:195–220

Gutiérrez-Mas JM (2011) Glycymeris shell accumulations as indicators of recent sea-level changes and high-energy events in Cadiz Bay (SW Spain). Estuar Coast Shelf Sci 92:546–554. https://doi.org/10.1016/j.ecss.2011.02.010

Gutiérrez-Mas JM, Juan C, Morales JA (2009) Evidence of high-energy events in shelly layers interbedded in coastal Holocene sands in Cadiz Bay (south-west Spain). Earth Surf Proc Land 34:810–823

Gutiérrez-Rodríguez M, Goldberg P, Martín Peinado FJ et al (2019) Melting, bathing and melting again. Urban transformation processes of the Roman city of Munigua: the public thermae. Archaeol Anthropol Sci 11:51–67. https://doi.org/10.1007/s12520-017-0527-0

Gutiérrez-Rodríguez M, Brassous L, Rodríguez Gutiérrez O et al (2020) Site formation processes and urban transformations during Late Antiquity from a high-resolution geoarchaeological perspective: Baelo Claudia, Spain. Geoarchaeology 35:258–286. https://doi.org/10.1002/gea.21769

Jiménez Sancho A, Borja F, Oliva Muñoz P (2014) La orilla de Sevilla desde época altoimperial al período califal. In: Beltrán Fortes J, Rodríguez Gutiérrez O (eds) Sevilla arqueológica. La ciudad en época protohistórica, antigua y andalusí. Editorial Universidad de Sevilla. Ayuntamiento de Sevilla, Instituto de la Cultura y las Artes de Sevilla (ICAS), Sevilla, pp 304–305

Kuwatani T, Nagata K, Okada M et al (2014) Machine-learning techniques for geochemical discrimination of 2011 Tohoku tsunami deposits. Sci Rep 4:7077. https://doi.org/10.1038/srep07077

Lario J, Zazo C, Dabrio CJ et al (1995) Record of recent Holocene sediment input on spit bars and deltas of south Spain. J Coastal Res 17:241–245

Lario J, Zazo C, Dabrio CJ et al (2001) Particle size and magnetic properties of Holocene estuarine deposits from the Donana National Park (SW Iberia): evidence of gradual and abrupt coastal sedimentation. Zeitschrift Fur Geomorphologie 45:33–54

Lario J, Spencer C, Plater AJ et al (2002) Particle size characterisation of Holocene back-barrier sequences from North Atlantic coasts (SW Spain and SE England). Geomorphology 42:25–42. https://doi.org/10.1016/S0169-555X(01)00071-X

Lario J, Luque L, Zazo C et al (2010) Tsunami vs. storm surge deposits: a review of the sedimentological and geomorphological records of extreme wave events (EWE) during the Holocene in the Gulf of Cadiz, Spain. Z Geomorphol 54:301–316

Lario J, Zazo C, Goy JL et al (2011) Holocene palaeotsunami catalogue of SW Iberia. Quatern Int 242:196–200. https://doi.org/10.1016/j.quaint.2011.01.036

Luque L, Lario J, Zazo C et al (2001) Tsunami deposits as paleoseismic indicators: examples from the Spanish coast. Acta Geologica Hispanica 36:197–211

Luque L, Lario J, Civis J et al (2002) Sedimentary record of a tsunami during Roman times, Bay of Cadiz, Spain. J Quat Sci 17:623–631. https://doi.org/10.1002/jqs.711

Martínez Solares JM (2001) Los efectos en España del terremoto de Lisboa (1 de noviembre de 1755). Dirección General del Instituto Geográfico Nacional, Madrid

Mayet F, Tavares C (2002) L'Atelier d'amphores d'Abul (Portugal). Exploration archéologique du Sado. De Boccard, Paris

Melero García F (2007) El estudio de la Cartima romana (Cártama, Málaga) a través de los nuevos hallazgos. In: Corrales Aguilar M (ed) Tiempos de púrpura: Málaga antigua y antigüedades hispanas. Servicio de Publicaciones de la Universidad de Málaga, Málaga, pp 339–355

Menanteau L (1980) Les Marismas du Guadalquivir: Exemple de transformation d'un paysage alluvial au cours du Quaternaire récent. Université de Paris-Sorbone, Paris

Menanteau L (1984) Evolución histórica y consecuencias morfológicas de la intervención humana en las zonas húmedas: el caso de Las Marismas del Guadalquivir. In: Las zonas húmedas en Andalucía. Ministerio de Obras Públicas y Urbanismo, Sevilla, pp 43–76

Monge Soares AM (2015) Datación radiocarbónica de conchas marinas en el golfo de Cádiz: El efecto reservorio marino, su variabilidad durante el Holoceno e inferencias paleoambientales. Cuaternario y Geomorfología 29:19–29. https://doi.org/10.17735/cyg.v29i1-2.29541

Monterroso Checa A (2002) La secuencia estratigráfica. Evolución histórica del teatro de Colonia Patricia. In: Ventura Villanueva A, Márquez C, Monterroso A, Carmona MA (eds) El Teatro Romano de Córdoba. Universidad de Córdoba, Córdoba, pp 133–146

Morales JA, Borrego J, San Miguel EG et al (2008) Sedimentary record of recent tsunamis in the Huelva Estuary (southwestern Spain). Quatern Sci Rev 27:734–746

Morín J, Silva PG, Rodríguez MA et al (2014) Evidencias arqueosismológicas en la Colonia Patricia romana de Córdoba (Valle del Guadalquivir, España). In: Álvarez JA, Martín F (eds) Una aproximación multidisciplinar al estudio de las fallas activas, los terremotos y el riesgo sísmico. Segunda reunión Ibérica sobre fallas activas y paleosismología Lorca (Murcia, España), del 22 al 24 de octubre de 2014. Instituto Geológico y Minero de España, Madrid, pp 159–162

Moros Díaz J (2014) La intervención severiana en la producción del aceite bético. In: Blázquez Martínez

JM, Remesal Rodríguez J (eds) Estudios sobre el Monte Testaccio (Roma) VI. Publicacions i Edicions de la Universitat de Barcelona, Barcelona, pp 773–859

Morton RA, Gelfenbaum G, Jaffe BE (2007) Physical criteria for distinguishing sandy tsunami and storm deposits using modern examples. Sed Geol 200:184–207. https://doi.org/10.1016/j.sedgeo.2007.01.003

Murray RW, Knowlton C, Leinen M et al (2000) Export production and terrigenous matter in the Central Equatorial Pacific Ocean during interglacial oxygen isotope Stage 11. Global Planet Change 24:59–78. https://doi.org/10.1016/S0921-8181(99)00066-1

Nanayama F (2008) Sedimentary characteristics and depositional processes of onshore tsunami deposits: an example of sedimentation associated with the 12 July 1993 Hokkaido–Nansei-Oki earthquake tsunami. In: Tsuji Y, Yamazaki T, Minoura K (eds) Tsunamiites. Elsevier, Amsterdam, pp 63–80

Ñaco T, Nappo D (2013) When the waters recede: the economic impact of tsunamis in the Graeco-Roman world. Revue belge de philologie et d'histoire - Belgisch tijdschrift voor filologie en geschiedenis Fasc 1: Antiquitè 91:45–68

Pérez-Asensio JN, Aguirre J, Schmiedl G et al (2012) Messinian paleoenvironmental evolution in the lower Guadalquivir Basin (SW Spain) based on benthic foraminifera. Palaeogeogr Palaeoclimatol Palaeoecol 326–328:135–151

Pérez-Asensio JN, Aguirre J, Rodríguez-Tovar FJ (2017) The effect of bioturbation by polychaetes (Opheliidae) on benthic foraminiferal assemblages and test preservation. Palaeontology 60:807–827

Pérez-Asensio JN, Larrasoaña JC, Samankassou E (2018) Magnetobiochronology of Lower Pliocene marine sediments from the lower Guadalquivir Basin: Insights into the tectonic evolution of the Strait of Gibraltar area. GSA Bull 130:1791–1808

Prados Martínez F (2019) Bailo-Baelo. Deux emplacements pour une ville du détroit de Gibraltar. Une perspective à travers sa nécropole. In: Hamrouni MR, El Bahi A (eds) Actes du VIIème Colloque International du Département d'Archéologie. Villes et archéologie urbaine au Maghreb et en Méditerranée. Faculté des Lettres et des Sciences Humaines de l'Université de Kairouan. Université de Kairouan, Tunis

Quevedo A, Ramallo Asensio SF (2015) La dinámica evolutiva de "Carthago Nova" entre los siglos II y III. In: Brassous L, Quevedo A (eds) Urbanisme civique en temps de crise: Les espaces publics d'Hispanie et de l'Occident romain entre le IIe et le IVe siècle. Casa de Velázquez, Madrid, pp 161–178

Reicherter K, Vonberg D, Koster B et al (2010) The sedimentary inventory of tsunamis along the southern Gulf of Cadiz (southwestern Spain). Zeitschrift Für Geomorphologie Suppl Issues 54:147–173. https://doi.org/10.1127/0372-8854/2010/0054S3-0023

Reimer PJ et al (2013) IntCal13 and Marine13 radiocarbon age calibration curves 0–50.000 years cal BP. Radiocarbon 51:1869–1887

Rodríguez-Pascua MA, Morales Manzanos FJ, Perucha MA et al (2016) Los efectos orientados del terremoto de Lisboa (1755) en el patrimonio de Sevilla (Valle del Guadalquivir, España). Geo-Temas 16:399–402

Rodríguez-Ramírez A (2009) Discussion of the paper "The Geological record of the oldest historical tsunamis in southwestern Spain" by Francisco Ruiz, Manuel Abad, Joaquín Rodríguez-Vidal, Luis Miguel Cáceres, María Luz González-Regalado, María Isabel Carretero, Manuel Pozo, and Francisco Gómez Toscano [published by Rivista Italiana di Paleontologia e Stratigrafia. (2008), 114(1): 147–156]. Rivista Italiana di Paleontologia e Stratigrafia 115(1):133–134

Rodríguez-Ramírez A, Rodríguez-Vidal J, Cáceres L et al (1996) Recent coastal evolution of the Doñana National Park (SW Spain). Quatern Sci Rev 15:803–809. https://doi.org/10.1016/S0277-3791(96)00068-6

Rodríguez-Ramírez A, Flores-Hurtado E, Contreras C et al (2014) The role of neo-tectonics in the sedimentary infilling and geomorphological evolution of the Guadalquivir estuary (Gulf of Cadiz, SW Spain) during the Holocene. Geomorphology 219:126–140. https://doi.org/10.1016/j.geomorph.2014.05.004

Rodríguez-Ramírez A, Pérez-Asensio JN, Santos A et al (2015) Atlantic extreme wave events during the last four millennia in the Guadalquivir estuary, SW Spain. Quatern Res 83:24–40. https://doi.org/10.1016/j.yqres.2014.08.005

Rodríguez-Ramírez A, Villarías-Robles JJR, Pérez-Asensio JN et al (2016) Geomorphological record of extreme wave events during Roman times in the Guadalquivir estuary (Gulf of Cadiz, SW Spain): an archaeological and paleogeographical approach. Geomorphology 261:103–118. https://doi.org/10.1016/j.geomorph.2016.02.030

Rodríguez-Ramírez A, Villarías-Robles JJR, Pérez-Asensio JN, Celestino-Pérez S (2019) The Guadalquivir Estuary: Spits and Marshes. In: Morales JA (ed) The Spanish coastal systems. Springer, Cham, pp 517–541. https://doi.org/10.1007/978-3-319-93169-2_22

Rodríguez-Ramírez A, Yáñez CM (2008) Formation of chenier plain of the Doñana marsh- land (SW Spain): observations and geomorphic model. Mar Geology 254:187–196

Rodríguez-Vidal J, Campos JM, Cáceres Puro LM (2015) Eventos marinos y asentamientos costeros en el suroeste de Iberia. Cuaternario y Geomorfología 29:5–28

Rodríguez-Vidal J, Ruiz F, Cáceres LM et al (2008) Morphosedimentary features of historical tsunamis in the Guadalquivir estuary (SW of Spain). In: 2nd international tsunami field symposium. IGCP Project 495. GI2S Coast Res. Publ. 6, pp 139–141

Rodríguez-Vidal J, Ruiz F, Cáceres LM et al (2011) Geomarkers of the 218–209 BC Atlantic tsunami in the Roman Lacus Ligustinus (SW Spain): a palaeogeographical approach. Quatern Int 242:201–212. https://doi.org/10.1016/j.quaint.2011.01.032

Roos AM, Schulz HD, Arteaga O et al (1995) El problema del “Lacus Ligustinus”: investigaciones geoarqueológicas en torno a las marismas del bajo Guadalquivir. In: Tartessos: 25 años después, 1968–1993. Ayuntamiento de Jérez de la Frontera, Jerez de la Frontera, pp 99–135

Röth J, Mathes-Schmidt M, García Jiménez I et al (2015) The Baelo Claudia tsunami hypothesis- results from a multi- method sediment analysis of late- roman deposits (Gibraltar Strait, Southern Spain). In: 6th international inqua meeting on paleosismology, active tectonics, and archaeosismology, 14–19 April 2015, Pescina, Fucino Basin, Italy

Ruiz F, Rodríguez-Ramírez A, Cáceres LM et al (2004) Late Holocene evolution of the southwestern Doñana National Park (Guadalquivir Estuary, SW Spain): a multivariate approach. Palaeogeogr Palaeoclim Palaeoecol 204:47–64. https://doi.org/10.1016/S0031-0182(03)00721-1

Ruiz F, Rodríguez-Ramírez A, Cáceres LM et al (2005) Evidence of high-energy events in the geological record: mid-holocene evolution of the southwestern Doñana National Park (SW Spain). Palaeogeogr Palaeoclimatol Palaeoecol 229:212–229. https://doi.org/10.1016/j.palaeo.2005.06.023

Ruiz F, Borrego J, López-González N et al (2007) The geological record of a mid-Holocene marine storm in southwestern Spain. Geobios 40:689–699. https://doi.org/10.1016/j.geobios.2006.12.003

Ruiz F, Abad M, Rodríguez Vidal J et al (2008) The geological record of the oldest historical tsunamis in southwestern Spain. Riv Ital Paleontol Stratigr 114:145–154

Ruiz F, Abad M, Rodríguez-Vidal J et al (2013a) Morpho-sedimentary evidence of Holocene tsunamis in the southwestern spanish estuaries: a summary. In: VIII Reunión de Cuaternario Ibérico. La Rinconada - Sevilla, pp 145–149

Ruiz F, Rodríguez-Vidal J, Abad M et al (2013b) Sedimentological and geomorphological imprints of Holocene tsunamis in southwestern Spain: an approach to establish the recurrence period. Geomorphology 203:97–104. https://doi.org/10.1016/j.geomorph.2013.09.008

Ruiz-Bueno MD (2017) Actividad sísmica en el mediodía ibérico durante el siglo III d.C. La incidencia arqueológica en Corduba (Córdoba). Pyrenae 48:29–51

Sáez Fernández P, Ordóñez S, Saquete JC et al (2005) Hispania Baetica, provincia immvnis. Z Papyrol Epigr 154:299–311

Santos Arévalo FJ, Gómez Martínez I, García León M (2009) Radiocarbon measurement program at the Centro Nacional de Aceleradores (CNA), Spain. Radiocarbon 51:883–889

Schattner T (2003) Munigua: Cuarenta años de investigaciones. Junta de Andalucía, Instituto Arqueológico Alemán, Sevilla

Scheffers A, Kelletat D (2005) Tsunami relics in the coastal landscape west of Lisbon, Portugal. Sci Tsunami Haz 23:3–16

Schubart H, Arteaga O, Hoffman G et al (1990) Investigación geológica-arqueológica sobre la antigua línea de costa en Andalucía. Campaña 1988. Anuario Arqueológico de Andalucía 1988, II:185–189

Schulz HD, Felis T, Hagedorn C et al (1995) La línea costera holocena en el curso bajo del río Guadalquivir entre Sevilla y su desembocadura en el Atlántico. Informe preliminar sobre los trabajos de campo realizados en Octubre y Noviembre de 1992. Anuario Arqueológico De Andalucía 1992:323–327

Sierro FJ, Flores JA, Civis J et al (1993) Late Miocene globorotaliid event-stratigraphy and biogeography in the NE-Atlantic and Mediterranean. Mar Micropaleontol 21:143–168

Sillières P (ed) (2013) Belo IX. La Basilique. Casa de Velázquez, Madrid

Silva PG, Borja F, Zazo C et al (2005) Archaeoseismic record at the ancient Roman City of Baelo Claudia (Cádiz, south Spain). Tectonophysics 408:129–146

Silva PG, Reicherter K, Giner-Robles JL et al (2010) Arqueosismología del Conjunto Arqueológico Romano de Baelo Claudia (Cádiz, Sur de España): estado de la cuestión. In: II Jornadas Internacionales de Baelo Claudia: Nuevas Investigaciones. Consejería de Cultura de la Junta de Andalucía, Sevilla, pp 63–92

Stoops G (2003) Guidelines for analysis and description of soil and regolith thin sections. Soil Science Society of America Inc., Madison, Wisconsin

Szczuciński W, Niedzielski P, Kozak L et al (2007) Effects of rainy season on mobilization of contaminants from tsunami deposits left in a coastal zone of Thailand by the 26 December 2004 tsunami. Environ Geol 53:253–264

Tabales Rodríguez MA (2003) El complejo alfarero localizado en el Parlamento de Andalucía. In: Vázquez Labourdette A (ed) Arqueología y rehabilitación en el Parlamento de Andalucía. Investigaciones arqueológicas en el antiguo Hospital de las Cinco Llagas de Sevilla. Parlamento de Sevilla, Sevilla, pp 139–162

Tabales Rodríguez MA (2012) El subsuelo del Patio de Banderas entre los siglos IX a.C. y XII d.C. Apuntes Del Real Alcazar De Sevilla 13:8–53

Tabales Rodríguez MA (ed) (2015) Excavaciones arqueológicas en el Patio de Banderas, Alcázar de Sevilla: memoria de investigación 2009–2014. Patronato del Real Alcázar, Sevilla

Udías A, López Arroyo A, Mezcua J (1976) Seismotectonic of the Azores-Alboran region. Tectonophysics 31:259–289. https://doi.org/10.1016/0040-1951(76)90121-9

Ventura A, Pizarro G (2010) El Aqua Augusta (acueducto de Valdepuentes) y el abastecimiento de agua a Colonia Patricia Corduba: investigaciones recientes (2000–2010). Las técnicas y las construcciones en la ingeniería romana. V congreso de las obras públicas romanas. Fundación de la Ingeniería Técnica de Obras, Madrid, pp 177–203

Vizcaíno A, Gràcia E, Escutia C et al (2006) Characterizing holocene paleoseismic record in the SW Portuguese margin. Geophys Res Abstr 8:08469

Wade BS, Pearson PN, Berggren WA et al (2011) Review and revision of Cenozoic tropical planktonic foraminiferal biostratigraphy and calibration to the geomagnetic polarity and astronomical time scale. Earth Sci Rev 104:111–142

Wedepohl KH (1971) Environmental influences on the chemical composition of shales and clays. Phys Chem Earth 8:307–333. https://doi.org/10.1016/0079-1946(71)90020-6

Whelan F, Kelletat D (2003) Analysis of tsunami deposits at cabo de Trafalgar, Spain, using GIS and GPS technology. Essener Geographish Arbeiten 35:11–25

The *Baelo Claudia* Tsunami Archive (SW Spain)—Archaeological Deposits of High-Energy Events

13

Klaus Reicherter, Fernando Prados, Helena Jiménez-Vialás, Ivan García-Jiménez, Lisa Feist, Cristina Val-Peón, Nicole Höbig, Margret Mathes-Schmidt, José Antonio López-Sáez, Joschka Röth, Simoni Alexiou, Pablo G. Silva Barroso, Christoph Cämmerer, Laetitia Borau, Simon Matthias May, Werner Kraus, Helmut Brückner, and Christoph Grützner

Abstract

Over the past decades, substantial progress has been made in tsunami research. Be that as it may, little is still known about tsunami deposits and their related depositional mechanisms in coastal areas in historical and archaeological contexts. In particular, the Phoenician, Greek and Roman trade and military networks along the Mediterranean and Atlantic coasts, with their cities, harbours

K. Reicherter (✉) · L. Feist · C. Val-Peón · N. Höbig · M. Mathes-Schmidt · J. Röth · C. Cämmerer · W. Kraus
Neotectonics and Natural Hazards, Department of Geosciences and Geography, RWTH Aachen University, Aachen, Germany
e-mail: k.reicherter@nug.rwth-aachen.de

L. Feist
e-mail: l.feist@nug.rwth-aachen.de

C. Val-Peón
e-mail: c.val-peon@nug.rwth-aachen.de

N. Höbig
e-mail: n.hoebig@fz-juelich.de

M. Mathes-Schmidt
e-mail: m.mathes@nug.rwth-aachen.de

J. Röth
e-mail: joschka.roeth@emr.rwth-aachen.de

C. Cämmerer
e-mail: c.caemmerer@nug.rwth-aachen.de

W. Kraus
e-mail: w.kraus@nug.rwth-aachen.de

F. Prados
Instituto de Arqueología Y Patrimonio Histórico (INAPH), Universidad de Alicante, Alicante, Spain
e-mail: fernando.prados@gcloud.ua.es

H. Jiménez-Vialás
CEPOAT-Universidad de Murcia, Murcia, Spain
e-mail: vialas@um.es

I. García-Jiménez
Conjunto Arquelógico de Baelo Claudia (CABC), Agencia Andaluz de Instituciones Culturales, Ensenada de Bolonia, Tarifa, Cádiz, Spain
e-mail: ivan.garcia@juntadeandalucia.es

J. Antonio López-Sáez
Research Group Environmental Archaeology, Institute of History, CSIC, Madrid, Spain
e-mail: joseantonio.lopez@cchs.csic.es

M. Álvarez-Martí-Aguilar and F. Machuca Prieto (eds.), *Historical Earthquakes, Tsunamis and Archaeology in the Iberian Peninsula*, Natural Science in Archaeology,
https://doi.org/10.1007/978-981-19-1979-4_13

and additional facilities, are susceptible to serving as archives for extreme wave events. The ruins of the Roman city of *Baelo Claudia*, located on the Bay of Bolonia Bay (southern Spain), offer a unique environment for studying historical tsunamis in the Gulf of Cadiz. *Baelo Claudia* suffered at least two earthquakes in Roman times, namely, in the first and fourth centuries CE. The latter, associated with a tsunami, led to the city's destruction and subsequent decline. Accordingly, three tsunami deposits in *Baelo Claudia*, dated to ca. 4000 cal BP (2000 BCE), ca. 400 CE and 1755 CE, the last corresponding to the Lisbon tsunami, are described here. The multi-disciplinary research conducted on the sedimentary, archaeological and palaeontological records has revealed event deposits, together with major landscape changes in the environs of the bay after tsunami landfall. Furthermore, the significant archaeoseismic damage detected in recently excavated buildings has been dated to the end of the fourth-century CE. The results presented here serve to supplement the earthquake and tsunami record of coastal Iberia.

S. Alexiou
Department of Natural Resources Management and Agricultural Engineering, Agricultural University of Athens, Athens, Greece
e-mail: sim.alexiou@aua.gr

P. G. Silva Barroso
Dpto. Geología, Escuela Politécnica Superior de Ávila, Universidad Salamanca, Ávila, Spain
e-mail: pgsilva@usal.es

L. Borau
Institut AUSONIUS UMR 5607, Université Bordeaux Montaigne, Pessac, France
e-mail: laetitia.borau@u-bordeaux-montaigne.fr

S. Matthias May · H. Brückner
Department of Geosciences, Institute of Geography, University of Cologne, Cologne, Germany
e-mail: mays@uni-koeln.de

H. Brückner
e-mail: h.brueckner@uni-koeln.de

C. Grützner
Institute of Geosciences, University of Jena, Jena, Germany
e-mail: christoph.gruetzner@uni-jena.de

Keywords

Tsunami deposits · Event dating · Archaeology · Landscape changes · Extreme wave events · Spain

13.1 Introduction

Sedimentary imprints of extreme wave events (hereinafter, EWEs) in coastal areas are commonly found and studied in so-called geoarchives that protect deposits from erosion (e.g. Dawson and Stewart 2007; Hoffmann et al. 2013, 2020; Hoffmann and Reicherter 2016; Reicherter et al. 2019a; Costa and Andrade 2020; Dawson et al. 2020). EWEs or high-energy events (hereinafter, HEEs) are umbrella terms for tsunamis and storm surges. In many cases, the deposits generated by EWEs and HEEs cannot be clearly distinguished. Geoarchives for palaeo-tsunami deposits are, as a rule, diverse in the Mediterranean and in the Gulf of Cadiz: floodplains (e.g. Lario et al. 2002a; Mathes-Schmidt et al. 2013; Cuven et al. 2013), lagoons, swamps, sabkhas and salt marshes (e.g. Reicherter and Becker-Heidmann 2009; Costa et al. 2012; Koster et al. 2015), coastal lowlands (e.g. Lario 1996; Gracia et al. 2006; Reicherter et al. 2010; Frenken et al. 2022, this volume), estuaries (e.g. Dawson et al. 1995; Luque et al. 2001, 2002, 2004; Lario et al. 2002b; Andrade et al. 2003; Morales et al. 2008; Feist et al. 2019), rocky cliff coasts (Whelan and Kelletat 2003, 2005; Gracia et al. 2006; Costa et al. 2011; Gibraltar: Rodríguez-Vidal et al. 2011) and even offshore shelves (e.g. Smedile et al. 2011, 2020; Goodman-Tchernov et al. 2016; Reicherter et al. 2019b). Nowadays, tsunamis can directly affect coastal settlements, as well as industrial complexes, infrastructures and plants with processes such as inundation, erosion and sediment transport and deposition, while sometimes completely destroying them. In Antiquity, coastal settlements and harbours were affected by EWEs, which blocked or destroyed travel and trade routes (e.g. Goodman-Tchernov and Austin Jr. 2015; Hermann et al. 2022, this volume). However, tsunami deposits in ancient ports or settlements have been found especially in the Eastern Mediterranean and the Aegean (e.g. Pirazzoli et al. 1992; Dominey-Howes et al. 1999; Stiros and Papageorgiou 2001; Stiros 2001, 2010; Vött et al. 2008; Bruins et al. 2008; Bony et al. 2012; Hadler et al. 2013, 2020; Röth et al. 2015; Werner et al. 2018, 2019a).

In the Western Mediterranean and on the Atlantic seaboard of the Iberian Peninsula, there was a succession of Bronze Age, Phoenician, Greek and Roman networks, settlements and colonies. These first began to be appear around 1000 BCE with the foundation of *Onuba* (Huelva), *Gadir* (Cadiz), *Malaca* (Malaga), *Iulia Traducta* (Algeciras), *Carteia* (San Roque, Bay of Algeciras) in Spain and *Tingis* (Tangiers) and *Lixus* (Larache) in Morocco (Fig. 13.1). The seaboard of the Roman province of *Baetica* (*Hispania ulterior Baetica*, which took its name from the Baetis, the modern-day Guadalquivir river) encompassed the Gulf of Cadiz in the Atlantic and the southern Mediterranean coast. The spotlight is placed here on a small but important part of the Costa de la Luz, on which the Bay of Bolonia and the ruins of *Baelo Claudia* are to be found approximately 23 km northeast of Tarifa, in the Strait of Gibraltar. The ruins of the ancient Roman town of *Baelo Claudia* are located in the modern-day village of Bolonia. The settlement was originally located on the nearby hilltop site of La Silla del Papa, before its population migrated to the Atlantic coast in the Augustan Age and transformed the pre-existing fish factory into a city, which was subsequently granted the status of *municipium* by Emperor Claudius. The intention here is to describe the tsunami deposits and associated earthquake damage in this area, thus updating the tsunami and earthquake history of *Baelo Claudia* (Ménanteau et al. 1983; Goy et al. 1994; Sillières 1997; Silva et al. 2005, 2009, 2014; Grützner et al. 2010; Bernal et al. 2015; Röth et al. 2015).

The geological and plate tectonic or seismotectonic setting west of the Strait of Gibraltar has been described in many papers and geological maps (Gonzáles Lastras et al. 1991; Gutscher et al. 2002, 2006; Silva et al. 2006, 2009; Grützner et al. 2010, 2012; Pedrera et al. 2011). For the closer environs, a simplified geological overview shows that the location of the study area is dominated by the Alpine nappes of different flysch units in the so-called "Campo de Gibraltar Flysch complex". The ages of the individual thrust nappes, which are all intensely

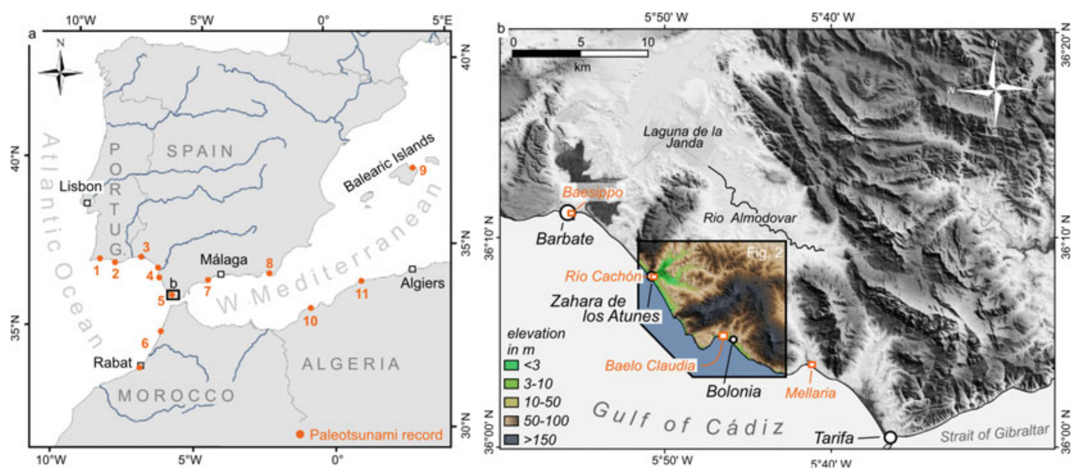

Fig. 13.1 **a** Overview and location of the study area in the Western Mediterranean/Eastern Atlantic and the areas where palaeo-tsunami deposits have been documented: 1. Boca do Rio/Portugal; 2. Algarve coast; 3. Huelva coast, Ayamonte; 4. Guadalquivir estuary and the Cadiz area; 5. *Baelo Claudia*; 6. Atlantic coast of Morocco; 7. Malaga coast; 8. Cabo de Gata; 9. Balearic Islands; 10. Oran; 11. Algerian coast. **b** Regional setting and location of the study area and the Roman settlements along the coast (orange)

folded and faulted, range from the Middle to the Late Cretaceous to the Aquitanian stage (Almarchal Formation of Cretaceous to Eocene, Bolonia Fm. and Aljibe Flysch Fm. of the Aquitanian to the early Burdigalian; Silva et al. 2005, 2006, 2009; Grützner et al. 2012). Later on, post-orogenic deposits, mainly shallow-marine carbonates from the Tortonian to the Pliocene unconformably overlaid the faulted flysch units, including the famous “Piedra or Roca Ostionera” limestone, the main building material available in the area, in addition to Almarchal sandstone and minor Aljibe sandstone in *Baelo Claudia*. Although the coastal and shallow-marine deposits of the Plio-Quaternary were influenced by sea-level changes, they generally form marine terraces (Zazo et al. 2008) and deltaic deposits, associated with aeolian dunes (e.g. Borja et al. 1999) and beaches (e.g. Goy et al. 1995).

The intense Alpine deformation caused by the collision of the Eurasian and African plates formed large stacks of nappes and thrust faults, along with uplift. The collapse of the nappe stacks and parts of the orogen led to new stress orientations and an E-W extension (Reicherter and Peters 2005; Silva et al. 2005; Fernández-Ibáñez et al. 2007; De Vicente et al. 2008; Grützner et al. 2012). The extension is represented by young graben structures that are also seismically active, and neoformed N-S striking normal faults (Zazo et al. 1999; Grützner et al. 2012; Silva et al. 2015, 2019). These faults continue offshore in the Bay of Bolonia and off the Cabo de Gracia; Grützner et al. (2012) provide a palaeostress history and an active fault map of the area.

13.2 Prehistoric and Historical Records of Tsunamis and Earthquakes in the Western Mediterranean and the Gulf of Cadiz

In recent years, many geological and archaeological studies have focussed on natural hazards, earthquakes and tsunamis in the Western Mediterranean and the Gulf of Cadiz, motivated by the huge damage produced by 1755 CE Lisbon earthquake and tsunami and, of course, in search of comparable past catastrophes (Fig. 13.1; summaries in Álvarez-Martí-Aguilar and Machuca, this volume; Costa et al., this volume). The 1755 CE tsunamis deposits in Boca do Rio and other sites on the Algarve coast in Portugal have been especially well documented (e.g. Dawson et al. 1995; Costa et al. 2012; Feist et al. 2019). The Huelva coast, the Guadalquivir estuary and the Cadiz area have also been comprehensively studied, because the landscape changes were very impressive, including wash over fans, breached spits and filled estuaries (e.g. Lario et al. 1995, 2002b; Lario 1996; Rodriguez-Ramírez et al. 1996, 2015, 2016; Morales et al. 2008; Ruiz et al. 2004, 2013; Alonso et al. 2015; Klein et al. 2016; López-Sáez et al. 2018; for further information, see Costa et al., this volume). Although several different features, such as sand sheets and boulder deposits, have been documented along the coast from Conil to Gibraltar, including the *Baelo Claudia* area, this research has often been hampered by imprecise dating. Nonetheless, deposits associated with the 1755 CE Lisbon event have also been identified here (e.g. Lario 1996; Alonso Villalobos et al. 2003; Whelan and Kelletat 2003, 2005; Luque et al. 2001, 2002; Gracia et al. 2006; Becker-Heidmann et al. 2007; Lario et al. 2009, 2011; Reicherter et al. 2010; Rodríguez-Vidal et al. 2011; Cuven et al. 2013; Koster and Reicherter 2014; Gutierrez-Mas et al. 2016). The Atlantic coast of Morocco has yielded different types of tsunami deposits which, depending on the coastal topography, usually take the shape of boulder ridges on rocky cliff coasts and sand sheets on floodplains (e.g. Kaabouben et al. 2009; Mhammdi et al. 2015; El Talibi et al. 2016), although the interpretation of the former is still a moot point (Brill et al. 2021).

The intention here is not to discuss the uncertainties in the tsunami history of the Gulf of Cadiz, but to focus on sedimentary evidence of tsunami inundations that left deposits. Evidence of tsunamis during Roman times, documented, by and large, in geological archives along the southern Atlantic coast of the Strait of Gibraltar, from the Doñana marshlands to Cadiz (a discussion in Álvarez-Martí-Aguilar, this volume; and a summary in Costa et al., this volume; Lario et al. 2002a; Luque et al. 2002; Ruiz et al. 2004), allegedly occurred between ca. 219 and 60 BCE (Campos 1991; Luque et al. 2001). EWEs before and after that period have rarely been described, the exception to the rule being the 1755 CE Lisbon event. Although several deposits have been documented, the tsunami history of the Bay of Bolonia and its environs is far from being precise. An ambiguous deposit discovered in the Arroyo del Alpariate, a small stream to the east of *Baelo Claudia*, points to probable tsunamis in cal. 2150–1825 BP (Fig. 13.2a; Alonso Villalobos et al. 2003) and in the fifteenth and sixteenth centuries (Becker-Heidmann et al. 2007). Gracia et al. (2006) described several deposits relating to the 1755 CE Lisbon event, based on stratigraphic evidence, but without providing any age dating. The dating problem also prompted Reicherter et al. (2010) to ascribe the tsunami deposits detected to the south of Barbate to the 1755 CE event. ^{14}C-14 dating on *Acanthocardium* and *Cerastoderma* mollusc shells, in all likelihood the remnants of a palaeo-beach during MIS 3, when the sea level was 60 m lower than today, revealed ages of $\geq$30.000 years (i.e. measurements close to detection limits). Koster and Reicherter (2014) subsequently dated the event layer with optically stimulated luminescence (hereinafter OSL) on quartz sand grains to ca. 4000 ± 200 BP. The deposits also display features typical of a tsunami backwash, such as channels, seaward imbricated clasts and the reworking of beach deposits. In the Cachón estuary in Zahara de los Atunes, drilling revealed an EWE layer, dated to 3125 BP or earlier by radiocarbon dating, tentatively interpreted as a tsunami deposit (Koster and Reicherter 2014). This event drastically transformed the coast from a marine (sublittoral) into a limnic (back-barrier coastal lake) environment. May et al. (2021) did not detect any indications of catastrophic marine inundations further inland from Zahara de los Atunes. Convincing evidence of tsunami deposits in *Baelo Claudia* was discovered during the excavations of the Roman baths (Fig. 13.2 TM; Fig. 13.3b) outside the city walls. Röth et al. (2015) described sedimentary evidence of a tsunami in the Roman baths and related charcoal dates between 255–263 CE and the 260–290 CE earthquake (Silva et al. 2009; Grützner et al. 2010), while also documenting an event associated with a tsunami in ca. 400 CE, which they correlated with the earthquake occurring between 350 and 395 CE (Silva et al. 2005), first described by Ménanteau et al. (1983). Bernal et al. (2015) dated the abandonment of the bath complex to the late third/early fourth-century CE (the Diocletian or Constantine period). In summary, the evidence of tsunamis in the Bay of Bolonia discovered by all other authors has been based on radiocarbon dating, with the sole exception of the archaeological dating proposed by Bernal et al. (2015). Radiocarbon dates of pieces of charcoal embedded in tsunami deposits (the "*terminus a quo*" which an attempt in being made to establish here) should be not regarded as "event dating", but as a "*terminus ante quem*", which means that this is the date of the charcoal formation (i.e. much older), rather than that when it was deposited by an EWE. In other words, all the EWE layers may be much younger than the age provided by the charcoal.

The first destructive earthquake in *Baelo Claudia*, dated to 40–60 CE, left no indications of tsunami deposits (e.g. Silva et al. 2005; Grützner 2011). Goy et al. (1994) provided the first description of earthquake evidence in *Baelo Claudia*, while suggesting that the pop-up structures in the forum were the result of liquefaction. Subsequently, the dates of 40–60 CE and 365–395 CE were proposed in light of the archaeological dating of the two destruction events recorded at *Baelo Claudia* (Silva et al. 2005). Based on the ^{14}C-14 dating of the soil layer underneath the fallen columns, like, for example, in the Temple of Isis, Silva et al. (2009) tentatively dated the second earthquake damage to the third century CE. As before, however, these are *terminus ante quem* dates, the archaeological dates around the late fourth-century CE

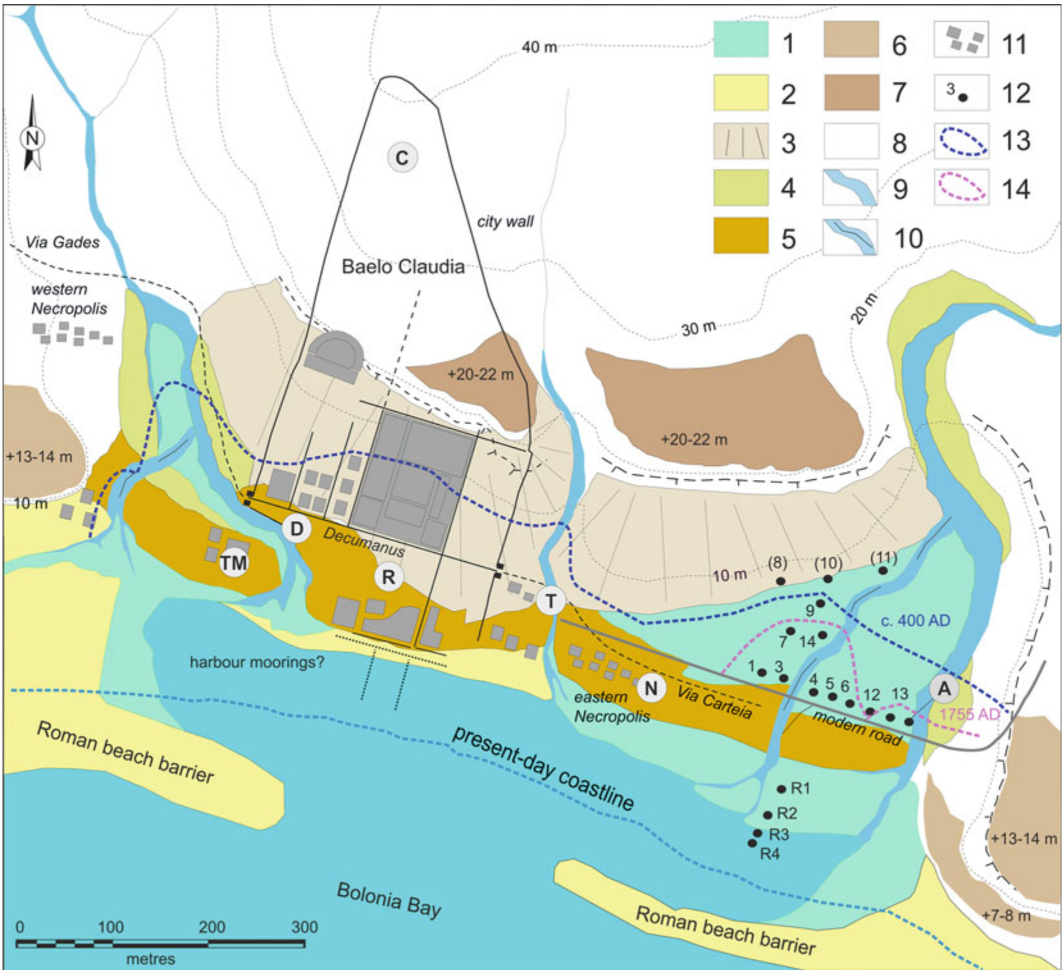

Fig. 13.2 Palaeogeography of *Baelo Claudia* (after Alonso Villalobos et al. 2003; and Silva et al. 2016): 1. River plains and floodplain; 2. Beach; 3. Colluvium; 4. Fluvial terrace deposits; 5. Beach barrier ca. 4 ka BP (Atlantic stage); 6. and 7. Pleistocene marine terraces; 8. Almarchal Fm. (Cretaceous-Eocene); 9. Active channels; 10. Palaeochannels; 11. Roman buildings; 12. Sample (R1-4, recent beach) and drilling sites (coordinates: Table 13.1 and Fig. 13.5; sites 2, 8–11 not shown); 13. Extent of the fourth-century-CE tsunami deposit; 14. Extent of the 1755 CE Lisbon tsunami deposit; A. Tsunami deposit documented by Alonso Villalobos et al. (2003); N. Eastern necropolis; R. Radar profile 205 in Fig. 13.5d, T. Mausoleum T-31 (Fig. 13.3a, d); TM. Maritime baths (Fig. 13.3b); C. Small cistern (Fig. 13.3e); and D. *Decumanus Maximus* (Fig. 13.3c)

provided by Ménanteau et al. (1983) and Bernal et al. (2015), based on coin and ceramic finds, being in all likelihood more reliable.

In the following pages, the EWE deposits discovered in the ruins of *Baelo Claudia* and its environs in the Bay of Bolonia are described by employing new dating approaches, shallow drillings, shallow geophysics (ground-penetrating radar, hereinafter, GPR), palaeoenvironmental analyses based on pollen data and archaeological earthquake-related data from the latest excavation campaign. In doing so, an attempt is made to update the history of earthquakes and tsunamis in this part of the Gulf of Cadiz, while concluding that the late fourth-century-CE or ca.-400-CE event sealed the fate of the late Roman city of *Baelo Claudia*, leading to its decline and ultimate abandonment.

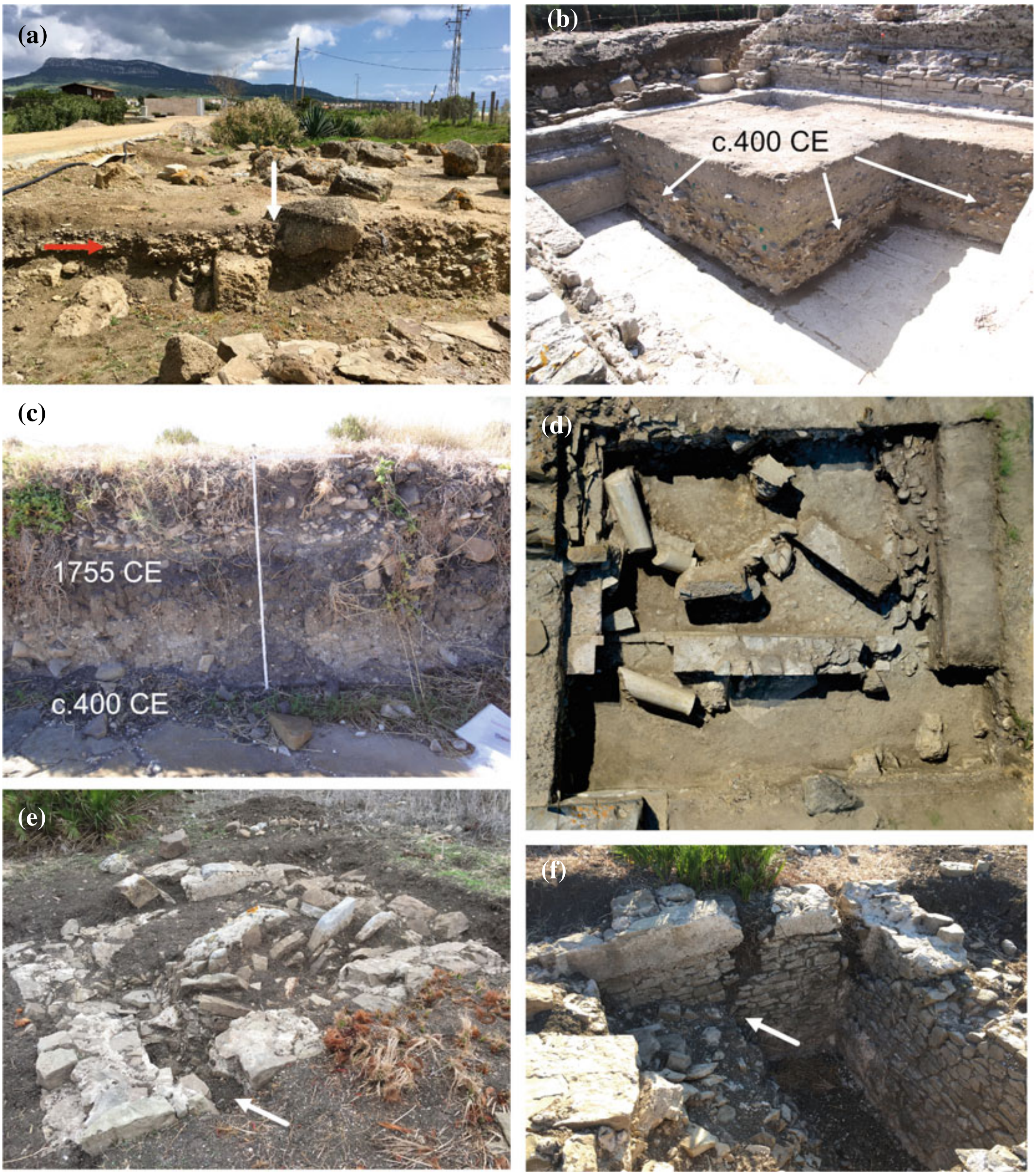

Fig. 13.3 **a** Eastern outcrop T (see Fig. 13.2 for location), the red arrow marks the tsunami backwash deposit of the ca. 400-CE event, while the white arrow marks the limit of backwash at a wall; **b** Maritime Roman baths (TM in Fig. 13.2) with palaeo-tsunami deposits ("black layer" at the base) within the basin; **c**. *Decumanus Maximus* outcrop with two palaeo-tsunami deposits (D in Fig. 13.2); **d** Orthophoto of Tomb T-32 with fallen columns, whose lower margin is displayed in A; **e** and **f** Small cistern before and after excavation, with the white arrow marking the dated crack (C in Fig. 13.2)

13.3 Methodology

To perform a multi-proxy study, based on archaeological and geological methods including different lab, dating and geochemical analyses, samples were taken from different sectors of the *Baelo Claudia* archaeological site. Classical archaeological excavations were carried out along the Via *Carteia*, passing the eastern necropolis to the east of the city walls. The focus was initially placed on Mausoleums T-31 and T-32 (Fig. 13.2 T), plus the remains of a small cistern, located uphill in the central part within the city walls (Fig. 13.2c), analysed using archaeoseismic methods (e.g. Rodríguez-Pascua et al. 2011). Following this, the finds documented in the maritime baths (Fig. 13.2 TM) were reinvestigated and re-interpreted (Bernal et al. 2015; Röth et al. 2015), while additional GPR data from Grützner (2011) were reanalysed. Although other fossils were taken into consideration, those of foraminifera were of special interest here, insofar as they can offer an indication of the prevailing marine conditions, while planktic forms are inherent to EWE deposits (e.g. Mendes et al. 2013; Camacho et al. 2015; Quintela et al. 2016, Werner et al. 2018, 2019a, b; Smedile et al. 2020). Palynomorphs were also considered for studying land-use changes (e.g. López-Sáez et al. 2018). Additionally, nine soil profiles around Mausoleums T-31 and T-32, nine drillings in the lagoonal area east of the city (Fig. 13.2; additional drillings in brackets are not shown) and four reference beach samples (R1-4 in Fig. 13.2) were selected for micropalaeontological examination using the residues of grain size analysis or washed samples.

13.3.1 Vibracoring, Micropalaeontology and Palynomorphs

A total of 14 vibracores, up to 7 m in length and with open window samplers, were taken for sedimentological analyses and microfossil investigations, eight of which in the so-called “lagoonal” area that formed behind the beach berm (after Silva et al. 2015; Fig. 13.2; Table 13.1). Additional samples were taken from three areas along the *Decumanus Maximus*, from the maritime *thermae* basin (TM, *extra-muros*) and from the present-day beach (references in Fig. 13.2, R1-4). A total of 86 samples of

Table 13.1 Coordinates of the samples and GPR profiles and the altitude of the event layers in the drill cores (Fig. 13.6). All altitudes are given in metres above the current mean sea level (m a.s.l.)

Name	Location (coordinates)	Altitude (surface)	Altitude of 1755 CE event layer (Ez)	Altitude of 400 CE event layer (Ey)	Altitude of 2000 BCE event layer (Ex)
BOL1	36.08777 N 5.770463 W	2.7	2.13 (base)	1.04 (top) ? base	–
BOL3	36.087713 N 5.770218 W	2.3	1.84 (base)	0.78 (top) ? (base)	–
BOL4	36.087657 N 5.770014 W	2.3	2.14 (base)	1.0 (top) ? (base)	–
BOL5	36.087607 N 5.769802 W	2.5	2.23 (base)	1.42 (top) 0.64 (base)	–
BOL6	36.087559 N 5.7695892 W	2.6	2.33 (base)	0.83 (top) −0.4 (base)	−0.9 (top) −1.2 (base)
BOL7	36.088063 N 5.770118 W	3.9	3.4 (base)	2.65 (top) ? (base)	–
BOL8	36.087607 N 5.769802 W	5.1	–	–	–

(continued)

Table 13.1 (continued)

Name	Location (coordinates)	Altitude (surface)	Altitude of 1755 CE event layer (Ez)	Altitude of 400 CE event layer (Ey)	Altitude of 2000 BCE event layer (Ex)
BOL9	36.088252 N 5.769869 W	4.4	–	2.6 (top) ? (base)	–
BOL10	36.088647 N 5.769777 W	5.4	4.51 (base)	–	–
BOL11	36.088517 N 5.769072 W	5.0	–		
BOL12	36.087512 N 5.769378 W	3.6	–	2.6 (top) 1.75 (base)	–
BOL13	36.087429 N 5.769154 W	3.2	2.20 (base)	2.19 (top) 0.66 (base)	0.5 (top) ? (base)
BOL14	36.087971 N 5.769798 W	3.4	2.63 (base)	2.03 (top) ? (base)	
Maritime baths	36.088999 N 5.7764059 W	5.0	–	ca. 3.5 (top)	–
Cistern	36.092449 N 5.774877 W	39	–	–	–
T-31	36.088780 N 5.773375 W	ca. 4.0	-	ca. 3.3 (top)	–
Eastern necropolis	36.087912 N 5.772042 W	ca. 2.0–3.0, mean 2.5	–	–	ca. 1.8–1.2 (top)
GPR line 205	36.089165 N 5.775080 W (start)	5.0	ca. 4.0 (base)	–	ca. 0.5 (top)

microfossils were selected, although the foraminiferal content was very low and insufficient for performing quantitative and statistical analyses, thus yielding only qualitative data.

Nine palynomorphs samples were collected from different sectors of the *Baelo Claudia* archaeological site: three from the *Decumanus Maximus* at different levels and six from different profiles in Mausoleums T-31 and T-32. Of the total of nine samples, four were sterile and thus discarded.

All samples were chemically treated with HCl to remove carbonates, with KOH to remove humic acids and with sodium polytungstate (SPT, $3Na_2WO_4{\cdot}9WO_3{\cdot}H_2O$) at 2.0–2.1 cm^3 for densiometric separation. Pollen concentration was estimated by adding one *Lycopodium clavatum* tablet to each sample (Stockmarr 1971). The final residue obtained after the treatment was mounted on slides with the use of glycerol. Palynomorphs were counted using an optical microscope at 400× and 1000× to a minimum pollen sum of 150 terrestrial pollen grains. Fossil pollen grains, spores and non-pollen palynomorphs were identified using published keys (Jarzen and Elsik 1986; López-Sáez et al. 1998; 2012; Moore et al. 1991; Pals et al. 1980; Reille 1992, 1995; Scott 1992; van Geel 1978, 1986, 1992; van Geel et al. 1980, 1989, 2003) and the modern pollen reference collection of the CSIC in Madrid, Spain. Diagrams were plotted using TiliaIT software, version 2.0.41 (Grimm 2012–2015), in order to identify the main taxa of pollen grains, spores and non-pollen palynomorphs, represented as relative frequencies and concentrations.

13.3.2 Radiocarbon Dating

The radiocarbon dating of the selected charcoal and soil samples was carried out at Beta Analytics (Miami, FL, USA; radiocarbon.com) and the CologneAMS (University of Cologne, Germany) facilities. Carbonate mollusc shells were not dated owing to the fact that the marine reservoir effect can lead to significant errors, especially in the Gulf of Cadiz. All data were calibrated with IntCal20-calibration (Reimer et al. 2020) and cross-checked with archaeological finds, such as ceramics and coins (Table 13.2; Fig. 13.8a).

13.3.3 OSL Dating

In the sediments containing no charcoal or organic material, instead of marine shells, quartz samples were dated using OSL (Table 13.3; Fig. 13.8d). This technique for dating coastal sediments has already been applied successfully along the southern coast of Spain, to the north of *Baelo Claudia*, near Barbate (Koster and Reicherter 2014). For OSL dating, steel tubes were hammered into the freshly cleaned vertical sections of the investigated profiles. The tubes were directly sealed from sunlight with opaque tape and black bags. Three quartz samples (Ne-II-OSL3, OSL1 and OSL4; from the bottom to the top of the profile) were OSL dated in the Cologne Luminescence Lab (CLL; Institute of Geography, University of Cologne, Germany). The single-aliquot-regenerative-dose (SAR) approach proposed by Murray and Wintle (2000) was applied for D_e determination. Preheat-plateau and dose-recovery tests substantiated the measurement protocol (a preheat temperature of 220 °C resulted in ratios of measured dose to given dose of 0.93–1.03). The central age model (CAM, Galbraith et al. 1999) was applied for final equivalent dose (D_e) determination. Environmental dose rates and OSL ages were calculated using DRAC (Durcan et al. 2015).

13.3.4 GPR

To detect and trace subsurface evidence of particular layers not only in the *Decumanus Maximus* area and the eastern necropolis of *Baelo Claudia* (Fig. 13.2), but also in other parts of the city (compilation in Grützner 2011), non-destructive GPR measurements were taken. The SIR 3000 coupled to 400 and 300 MHz antennas (Geophysical Survey Systems Inc.) was used. The frequency of the antennas and a permittivity (ε) of six allowed for high-resolution measurements to be taken in dry conditions, from the surface to depths of up to 3.7 m; deeper penetration was hampered by the groundwater table (i.e. mean sea level). GPS measurements were used to determine the start and finish points of the profiles, along with a calibrated survey wheel for measuring the length of the profiles. Data processing, including move start time, background removal, remove header gain, energy decay, average xy filter and bandpass Butterworth filter, was carried out using the ReflexW software (Sandmeier Scientific Software, version 7.0). A topographic correction is not necessary in flat environments. All datasets have since been published and are freely available at PANGEA (Grützner and Reicherter 2021). For the location of the profiles, see Figs. 13.2 and 13.5.

13.4 Results

13.4.1 Archaeological Excavations and Archaeoseismic Finds

13.4.1.1 Eastern Necropolis and Mausoleums of the "Carteia Gate"

In recent years, the necropolis and mausoleums of the "Carteia Gate" (eastern entrance to the city) have been excavated along the proximities of the *Decumanus Maximus* (Fig. 13.2 T;

Table 13.2 Dating of radiocarbon samples (Cologne AMS, Beta Analytics), calibration with IntCal20 (Reimer et al. 2020; Stuiver et al. 2020)

Location	Sample ID	Sample code	Core/depth in m	Material	Age	Cal age 2 σ
Eastern necropolis	Beta-441864	Ne-III-01	0.12	Organic sediment	1,960 ± 30 BP	1,990–1,822 BP 41 BCE–128 CE
Eastern necropolis	Beta-441863	Ne-II-08	0.18	Charcoal	2,120 ± 30 BP	2,291–1,998 BP 342–49 BCE
Eastern necropolis	Beta-441862	Ne-II-02	0.2	Charcoal	2,060 ± 30 BP	2,111–1,933 BP 162 BCE–17 CE
Maritime baths	COL2443.11	BOL1	0.06–0.17	Charcoal	Modern	Modern
Maritime baths	COL2444.11	THE1c(1)	0.93–1.2	Charcoal	1,830 ± 36 BP	1826–1624 BP 131–326 CE
Maritime baths	COL2445.11	THE1c(2)	1.55	Charcoal	1,809 ± 34 BP	1821–1612 BP 129–338 CE
Lagoon	Beta-471027	BOL4_17_40-45	0.4–0.45	Organic sediment	Modern	Modern
Lagoon	Beta-471028	BOL4_18_85-90	0.85–0.9	Organic sediment	710 ± 30 BP	694–644 BP 1256–1306 CE
Lagoon	Beta-471029	BOL4_19_120-124	1.2–1.24	Organic sediment	930 ± 30 BP	925–785 BP 1025–1165 CE
Lagoon	Beta-471030	BOL4_21_150-154	1.5–1.54	Organic sediment	2520 ± 30BP	2,643–2,491 BP 694–542 BCE
Lagoon	Beta-471032	BOL9_S9_365-375	2.97–3.07	Organic sediment	4660 ± 30 BP	5,468–5,314 BP 3519–3365 BCE
Cistern	Beta-459040	BAELO-4–37	basal crack fill, after rupture	Organic sediment	1590 ± 30 BP	1550–1405 BP

Figs. 13.4, 13.5; Prados Martínez et al., 2020). Hardly any traces of these two monuments (called T-31 and T-32) were visible on the surface (Fig. 13.3a, d; top view in Fig. 13.5a). The excavation attempted to shed light on their structure, their position in relation to the *Decumanus Maximus* and their chronology. Accordingly, an excavation was carried out in an open area where there was evidence of plundering in ancient times and which had been damaged by an

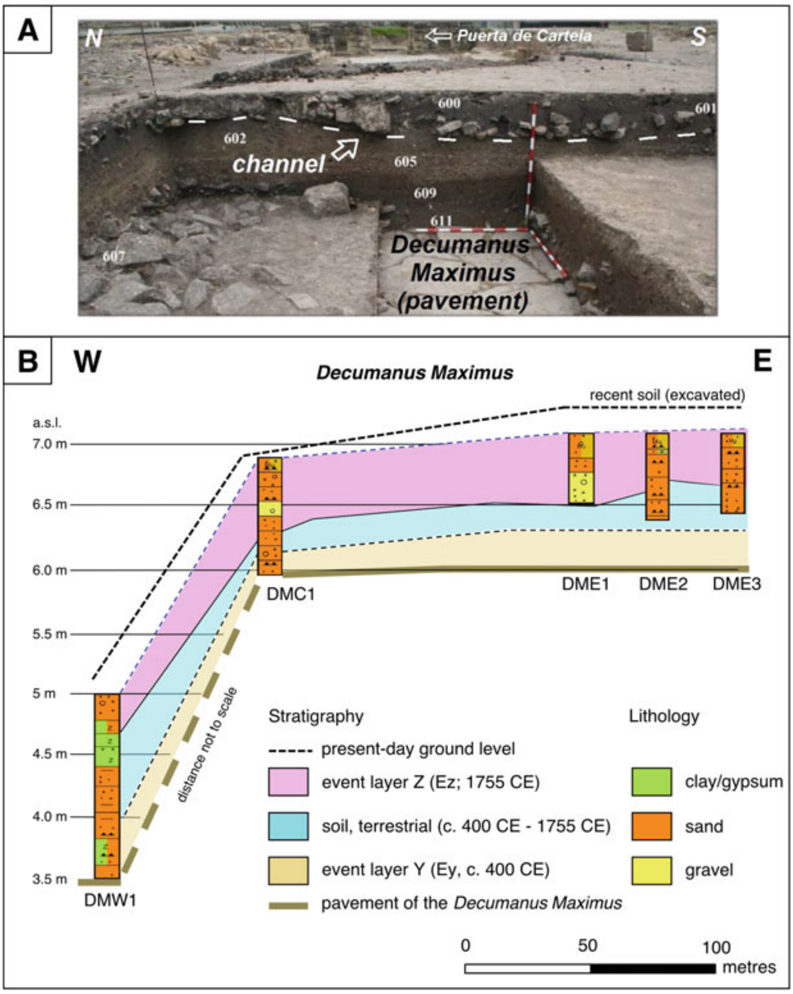

Fig. 13.4 **a** Eastward view of a fluvial channel feature on top of the eastern *Decumanus Maximus* (with the Carteia Gate in the background; from Conjunto Arqueológico de Baelo Claudia 2013). The pavement is ca. 6 m a.s.l., with a vertical profile thickness of 1.20 m (the white numbers correspond to the archaeological units, see text); **b** Profile correlation of the *Decumanus Maximus* intervention (colour code as in Figs. 13.5 and 13.6). DMW. western *Decumanus Maximus*; DMC. Central *Decumanus Maximus*; DME. Eastern *Decumanus Maximus*; distance to the slope towards the west not to scale

earthquake. This seismic event led to the collapse of the buildings towards the northeast (Fig. 13.5a), as evidenced by the crescent-shaped "halo" of fallen blocks, indicating an SW direction of propagation already discussed by Silva et al. (2009). Later on, they were covered with rubble and aeolian sands, sealing many of their fallen decorative elements. The excavation thus made it possible to recover these well-preserved elements, especially from T-32. The complete architectural orders, which were executed in marble, are remarkable, as well as the unique funerary epigraph made of gilded bronze letters crowning the building. This is an important find both for the quality of the architectural decoration and for the fact that it is one of the few preserved *litterae aureae* from the Western Roman Empire.

Despite the continuous plundering to which they had been subjected, the two monuments must have been very impressive, perhaps reflecting the city's heyday during the first and second centuries CE. Before Mausoleum T-31 was partially excavated, a basement made of bioclastic calcarenite ashlars (Roca Ostionera), covering an area of more than 15 × 15 m, which had been conscientiously plundered, was already visible. It was totally devoid of decorative elements, though some corner blocks with highly eroded remains of pilasters could be seen at the base. At the top, an anthropomorphic tomb had been carved out, which, due to its shape and

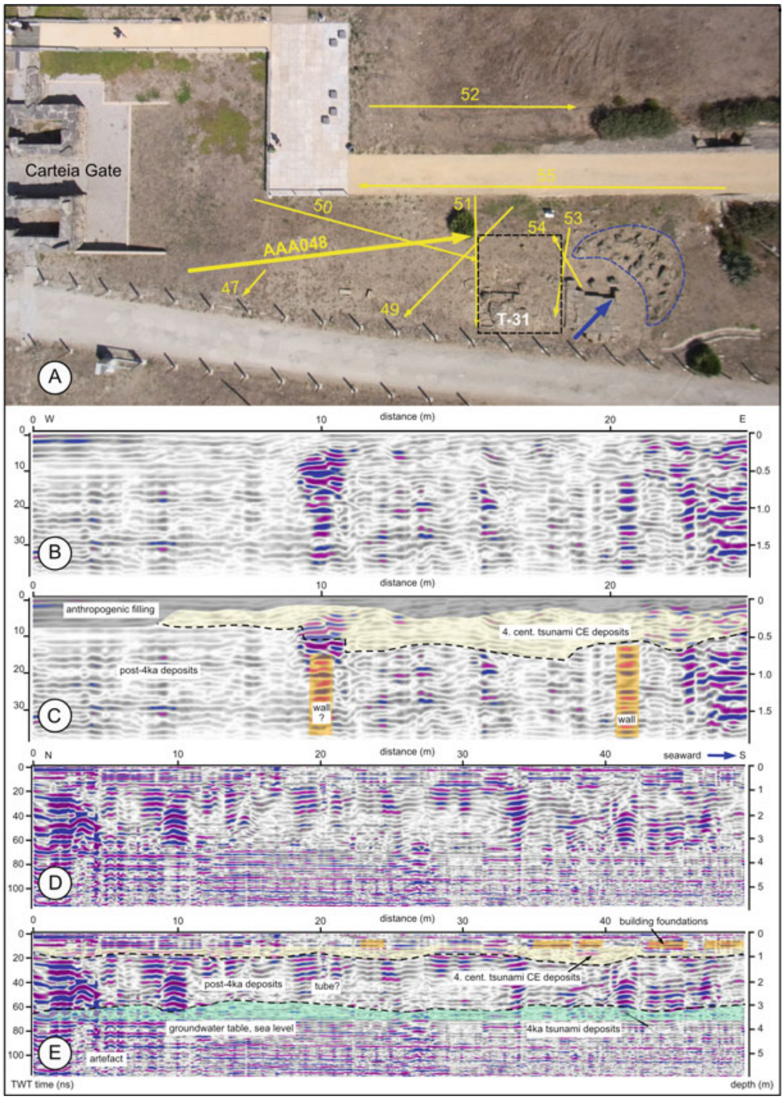

Fig. 13.5 GPR (georadar) profiles in the *Decumanus Maximus* and T-31 areas. A. Location of the profiles; the blue arrow indicates the shock direction (SW) and crescent-shaped block debris of the mausoleum; B. Profile AAA048 with a 400 MHz antenna; C. Profile AAA048 interpreted; D. Profile 205 with a 300 MHz antenna (Grützner and Reicherter 2021); and E. Profile 205 interpreted. Coordinates in Table 13.1, colour code as in Fig. 13.6

southern orientation, may be interpreted as an Islamic or late Roman burial (sixth–seventh centuries CE, sketched by Bonsor, in Paris et al. 1926). This provides relevant information: in late Antiquity or the Middle Ages, the mausoleum was already in the same state as it is to be found today.

The back part of the building could not be excavated as it lies beneath the enclosure of the site and the current road (Fig. 13.5a). The intervention on its façade, however, allowed for documenting numerous architectural elements, cornices, pilasters and remains of stucco. Since it had been thoroughly transformed and eroded and no associated movable material culture had been documented, it was decided to concentrate on the intermediate space separating both mausoleums. This was excavated in order to reach their foundations and construction levels and thus determine their date of construction. Besides, the intervention made it possible to carry out a stratigraphic correlation between the two, separated by a *diverticulum* a little over 2 m wide which, running in an N-S direction, connected the *Decumanus Maximus* with the port area. The stratigraphy corroborated that the two mausoleums were practically contemporaneous, forming part of the same process of urban development of this space outside the city walls.

Thanks to the excavation, it is now possible to confirm that Mausoleum T-32 rests on geological strata, as with the aforementioned alley or *diverticulum*. Above the geological level, and prior to its construction, some late republican materials, specifically, Italic Terra Sigillata fragments, were discovered. Above that, the documented archaeological finds dating to the initial half of the first century CE were associated with the use of this alley. The intervention also confirmed that the *opus quadratum* blocks forming the base of this mausoleum were stuccoed, including several parts with remains of paint preserved in situ. These materials date the construction of the monument to the mid first century CE, that is, in the first phase of use of the city's eastern necropolis (Prados Martínez et al. 2020; Prados Martínez and Jiménez-Vialás 2015).

Mausoleum T-31, which is in a poor state of preservation, shared the same fate as T-32. Some of the dislodged blocks had fallen into existing gaps in its base, as result of previous looting. The mausoleum was already in disuse and had been plundered before the destructive event (an earthquake and subsequent tsunami) occurred. The remains of the collapse of T-31 are covered by a clayey, very plastic, black layer, which seems to have come from geological deposits in the adjacent lagoon. Containing hardly any archaeological material, it is related to the "black level" documented in other parts of the city, especially the *Decumanus Maximus*, and attributed to a EWE (Bernal et al. 2015; Röth et al. 2015; Silva et al. 2016). This black layer, or level, covers all the units described above, therefore it was clearly subsequent to the collapse of the mausoleums and the abandonment of this sector of the necropolis. It was first described by Bernal-Casasola et al. (2007) in the southern part of the Carteia Gate, dated to the fourth–fifth century CE and related to a natural event. During the excavation, the discovery of upsection remains (two warning signals) dating from the First Spanish Republic (1873–1874 CE) would suggest a very young covering soil or anthropogenic modifications.

Mausoleum T-32 is currently in an even worse state of preservation than T-31, since many more of its blocks have been looted. Moreover, around what is left standing are different late tombs, some literally carved out of their foundations, while others are placed right next to them. In all cases, the tombs, some featuring sarcophagi, are associated with the previous structure of T-32, which must have already been all but derelict at that time. The prolific number of burials is striking and, in a way, offers a glimpse of how important the original building must have been.

A funerary monument crowned the structure of T-32, which was dismantled down to its foundations. The excavation was carried out at the foot of the mausoleum, inside a funeral enclosure or garden at the front, with a wall facing the sepulchral way section of the *Decumanus Maximus* to the north and another facing the *diverticulum* to the east. Mausoleum T-32 is outstanding because of its two high-quality Corinthian columns and capitals made of marble, as well as the sculpted and painted decorative elements forming part of its ornamentation. These perfectly preserved finds appeared immediately below the levels of collapse. The later tomb of a child, whose body had been placed in an amphora, was excavated from the rubble, sealing off the destruction levels. Both this burial and those mentioned above attest to the fact that the funerary and symbolic value of this area had not been lost over time.

The excavation of the interior of the funeral enclosure or garden provided very complete information about the entire sequence, since all the layers down to the geological and sterile basement were unearthed. In the opposite direction to the excavation, and in chronological order, a layer associated with the construction of the mausoleums was documented. As the materials that it contained (fragments of Italic Terra Sigillata, a Gallic Terra Sigillata and a thin-walled base) can be dated to the reigns of Tiberius/Claudius, the date of construction of the mausoleum can be established in the mid first century CE. The floor was made of highly compacted yellowish soil, about 10 cm thick. Materials relating to its last uses were found above this soil layer, but without discovering any funerary deposits. The abundance of organic material, such as charcoal, Sus, Bos and fish bones, seems to reflect the rituals that must have been performed in this space. Along with the fauna, several metal rivets, a Trajan bronze coin and some other completely illegible coins were unearthed. The ceramic fragments recovered correspond to open, almost complete forms of Gallic and Marmorata Terra Sigillata, which can be logically linked to the celebration of commensal rituals. The lower third part of a high Imperial amphora, specifically cut out to contain an offering, with the remains of a bird inside, was also exhumed. As these materials can be readily dated to the first or second century CE, they thus provide a clear chronology of the life of the monument. A barren layer with a thickness of between 20 and 40 cm and important sedimentary input was found above these archaeologically rich layers, which indicates the moment when this space, and surely the mausoleum as a whole, fell into disuse after its destruction. The destruction level can be dated to the fourth-century CE at the latest by several coins, two of which were discovered under the marble elements that were toppled by the event (*terminus ante quem*; two bronze coins of Constantius II which, as they were minted at the Constantinople officina, must have been struck between 348 and 351 CE; Fig. 13.8a). Once the building had collapsed and a kind of artificial tell had been formed, there is evidence that it continued to be used for funerary purposes, albeit with much more modest structures. Returning to the aforementioned child burial in the amphora, the head of the boy, who died in perinatal period, points to the west. The corpse, which was buried without any trousseau (grave goods), is only accompanied by a few remains of ichthyofauna. The container is a Dressel 23/Keay XIIIa oil amphora, a type manufactured in from the fourth-century CE and used to export oil from the Guadalquivir valley during the first half of the fifth century CE (Keay 1984; Remolà 2000; Berni and Moros 2012). This evidence provides a *terminus post quem* for the seismic event, thus establishing it after the mid fourth and before the mid fifth century CE.

Although the two mausoleums had been looted and greatly modified, it was possible to detect earthquake archaeological effects (hereinafter EAE, Rodríguez-Pascua et al. 2011) in the excavation: (1) The oriented collapse of fallen columns and other architectural elements, with no sediments between them, clearly indicates that they collapsed contemporaneously. The capitals of the columns and the architrave of the monument were discovered over 2 m from the base. The *opus quadratum* blocks form a crescent-shaped "halo" around the mausoleum (Fig. 13.5 a) and (2) the foundation blocks did not undergo large displacements, but have various cracks with an SW-NE orientation. The eastern wall of the funeral enclosure or garden also displays cracks and a lateral displacement of some of its courses (Fig. 13.8c).

13.4.1.2 The Decumanus Maximus

The *Decumanus Maximus*, the main road connecting the "Carteia Gate" to the east with the "Gades Gate" (Puerta de Cadiz) to the west (Fig. 13.2d), displays many peculiar EAE related deformation patterns described by Silva et al. (2009, 2014) and Rodríguez-Pascua et al. (2011). To this should be added that a "black level or layer" was found throughout the scarlet of the wall facing the seafront (García-Jiménez 2011), which has also been documented in other parts of the city, especially in the eastern necropolis, and which has been attributed to an EWE, specifically, a tsunami (Röth et al. 2015; Silva et al. 2016). The "black level" is a chaotic layer, with unsorted material and a distinct coarsening-upward sequence, which means large components remained "floating" on the top (Fig. 13.3c). It was possible to identify marine pebbles with bivalve borings (*Lithophaga* sp.), Roman ceramics and tiles, angular chunks of stucco, glass fragments and sandstone, bones and fish bones, and other marine species. Röth et al. (2015) described marine fauna including different foraminifera. Above the "black level", land gastropods in a brownish, humic, fine-grained soil layer, with a thickness of ca. 10–15 cm, indicate a terrestrial environment. This layer is again truncated by a second sandy black layer, containing all kinds of Roman debris, marine bivalves, fish bones and microfauna, plus a medieval pocket knife, pointing yet again to a marine inundation reaching a height of 5–6 m above the current sea level. Excavations of the *Decumanus Maximus* revealed a comparable stratigraphy (García-Jiménez 2011): during the 2009–2010 campaign carried out by the archaeologist Ivan García-Jiménez, an erosive channel feature, dated by archaeological evidence to between the fifth and sixth centuries CE, was recovered from inside the stratigraphic column of the *Decumanus Maximus*. This N-S section traverses the deposits covering an ancient street junction (Fig. 13.4a; the white numbers are units defined by archaeologists). On the one hand, Layers 607/609/611 form a rubble horizon, with coarse components and a fining-up sequence resting directly on top of the clean pavement of the *Decumanus Maximus*. On the other, Layers 602/605, which contain identical fine-grained, brownish soil material, have been incised and eroded by a "high-energy channel", suggesting an E-W flow direction, and as before (layers 600/601), have coarse-grained deposits at the base and a dark, clayey matrix. Finally, a beautiful, large, enigmatic marble basin was discovered floating on the dark layers, or debris, at the *Decumanus Maximus*, although its original location is still a mystery.

To sum up, in their study of seven vertical outcrops along the *Decumanus Maximus* Röth et al. (2015) found that the "black level" rested directly on the pavement, covered by a layer of humic soil, and, in turn, by a sandy black layer (Fig. 13.4b). They also speculated on two EWE deposits in the area, located at ca. 5–6 m above the current sea level and descending westward to the Gades Gate to about 3.5 m (Fig. 13.4b). However, they could not provide any chronological information on the layers/events.

In the eastern necropolis (Fig. 13.3a), between T-31 and T-32, a comparable "black level" was found in front of the entrance door of a house (marked by the white arrow). Flow indications (the red arrow in Fig. 13.3a) suggest a backwash-type of deposition. It can be assumed that the waters did not get past the door, as no "black layer" deposits were discovered inside (to the right and seaward).

In short, the lower "black layer" seems to be present throughout the lower area of *Baelo Claudia*, reaching a height of about 5–6 m and possibly even 8 m a.s.l. (Silva et al. 2016). In light of the archaeological context (plus that of the *Decumanus Maximus*) and coin finds, it is possible to date the layer to the mid fourth-century CE. It is striking that the first EWE layer was deposited on the clean pavements of the streets of *Baelo Claudia*, because, following the event, they appear to have fallen into disuse, without them ever having been cleaned/restored, as evidenced by soil formation. On top of the sequence, however, another second dark sandy layer, with a thickness of up to 50 cm, probably evinces an inundation as a result of the 1755 CE Lisbon tsunami. The channel (Fig. 13.4a) offers clear evidence of high-energy transport. In this second event layer, the foraminifera is generally more numerous and diverse. The chess board pattern of the streets, formed by the *Decumanus* and *cardines*, might have facilitated inundation, backwash and the associated deposition of sediments and debris.

Further evidence of the ca. 400-CE event has been documented in the maritime baths, namely, the *extra-muros thermae* (Fig. 13.2 TM). The maritime baths, which are a relatively recent discovery, have been studied in detail by Bernal et al. (2017). According to these authors, the heyday of the baths, with their mosaics and other decorative elements, was in the second and third centuries CE. The considerably large *natatio* (swimming pool/basin) is also impressive, and even more so the sedimentary filling of the basin, again on a clean floor (Fig. 13.3b), indicating that it was in use. The sedimentary infill is characterised by a coarse basal layer with blocks and cobbles, marine macro- and microfauna, and a clear fining-up sequence wedging out landward to the north. The basal layer, which dips almost

25°, is also covered with wedge-shaped, coarse-grained deposits, interbedded with finer layers. The entire "basin" fill has a maximum thickness of 1.40 m, which indicates that the pool was almost completely filled with sediments, the lower portion most probably during a single event. The thinning-up and fining-up layers of the event deposit suggest a sedimentation produced by several waves (Fig. 13.8c), while backwash is observed due to the trapping of sediments. Up-section Roman material and components are more plentiful (ceramics, bones, shells, charcoal, cinder resulting from iron smelting, etc.). The charcoal was dated to between 129–338 CE and, as it was redeposited, this was interpreted as its formation age—a *terminus ante quem* predating the event. A stratigraphical study performed on the archaeological remains discovered in the infill revealed different well-dated phases, from the late third to the early fourth century up until the sixth century CE, indicating anthropogenic modification within the area of the *extra-muros thermae* (Bernal-Casasola et al. 2016), thus pointing to a post-event settlement in *Baelo Claudia* unrelated to the fourth-century-CE event.

Water played an important role in *Baelo Claudia*, as evidenced by the fact that the city walls were traversed by at least three main aqueducts. The aqueduct of Realillo ran from the north into the city, supplying the large cistern at the end of the channel and above the three main temples. Along the course of the channel, several levelling and drop shafts, water towers, settling ponds and a small quadratic basin (Figs. 13.2c and 13.3e, f) were discovered during the excavation campaigns carried out from 2013 to 2016 (Borau 2017). The small basin/cistern measuring 3.3 × 3.3 m and with a depth of ca. 1.7 m, halfway between the large end cistern (Borau 2017) and the city walls, had open cracks that were well documented after the excavation (Fig. 13.3f). The wall failure also resulted in the basin falling into disuse, as documented by the ceramics found inside the cistern. There were no visible signs of repair. The youngest pottery discovered in the oldest infill at the base dates to the fifth or sixth century CE; a radiocarbon sample of the oldest covering soil (bulk soil sample) within the crack dates to 1550–1405 BP (*terminus post quem*). All these data show that the large cistern and the aqueduct of Realillo had not been excavated or disturbed/modified at least since the fifth-century CE.

13.4.2 GPR Profiles

GPR investigations within and around *Baelo Claudia* commenced in 2000, with Grützner (2011) subsequently performing them in the city as a whole and its surroundings, and with Prados Martínez (2015) following suit, especially in the eastern necropolis and recently in the area around Mausoleums T-31 and T-32, as described above. Two representative and characteristic examples of the GPR profiles, with different frequency and penetration depths, are provided below. AAA048 was performed in the unexcavated environs of the T-31 and T-32 area, in the vicinity of the Carteia Gate (Fig. 13.5A–C), whereas Profile 205 (coordinates in Table 13.1) was carried out in the unexcavated area to the south of the *Decumanus Maximus*, where a small church and fishermen's houses were demolished, along with the Guardia Civil barracks, which also served as the dig's headquarters in the early 2000s, before the construction of the museum (Grützner and Reicherter 2021). The foundations and pipes of these modern buildings were detected and located in the radargram (Fig. 13.5D, E). Profile AAA048 shows the remains of the walls of buildings which are interrupted by a distinct chaotic layer with an erosional base. This chaotic layer corresponds to the lower "black level" characterised as tsunami deposits dating from the late fourth-century CE. Modern ground levelling, anthropogenic changes (the "Carteia Gate" area was excavated) and filling were found on top of this layer. Profile 205 offers deeper insights into the sediments, and once again a chaotic layer, corresponding to the fourth-century-CE EWE, is clearly visible. Below that, parallel reflectors indicate a period of relatively "quiet" non-erosive deposition. At the base of the profile—more or less parallel to the groundwater table (sea level)

—there is another "noisy" pattern corresponding to coarse-grained deposits. The excavations in the eastern necropolis reached this level, which was possible to date (Fig. 13.8d). The coarse-grained level was also previously excavated by Prados Martínez (2015), having been detected by GPR and described by Gracia et al. (2006) beforehand. Furthermore, the drillings in the flat floodplain area (Fig. 13.2) reached this level at a depth of ca. 4 m. In the main, the GPR profile corroborates the archaeological and geological investigations in *Baelo Claudia*.

13.4.3 Drilling in the Floodplain: Sedimentological and Palaeontological Results

Several sediment cores were drilled in the unexcavated part of the environs of *Baelo Claudia*—outside the city walls—in an area that is very flat and to which others have referred as a "lagoon" (Alonso Villalobos et al. 2003; Silva et al. 2016). The entire flat area is barren of Roman and other archaeological remains. Besides some completely altered and well-rounded ceramic fragments, no archaeological artefacts were found in the cores. Several parallel holes were drilled in an E-W direction, after which an attempt was made to trace and map the wash over and high-energy deposits uphill (Fig. 13.2; Table 13.1 for coordinates). The higher drill points did not contain 1755 CE tsunami deposits, so the run-up here was around 5–6 m above sea level, corresponding to the elevations in the *Decumanus Maximus* and the mausoleums. By and large, the drill cores contained seven facies of different environmental conditions, but not all were recovered (Fig. 13.6). The height of the individual layers varied, probably due to the area's palaeotopography which is traversed by a dry palaeochannel (Fig. 13.2), although it was possible to perform a correlation study on the strata (Fig. 13.6).

The longest cores BOL12 and BOL6 reach back to mid Holocene times, most probably to the Atlantic period around 6–7 ka BP. The basal sediments are medium-grained sands with molluscs/shell debris inherent to beach deposits.

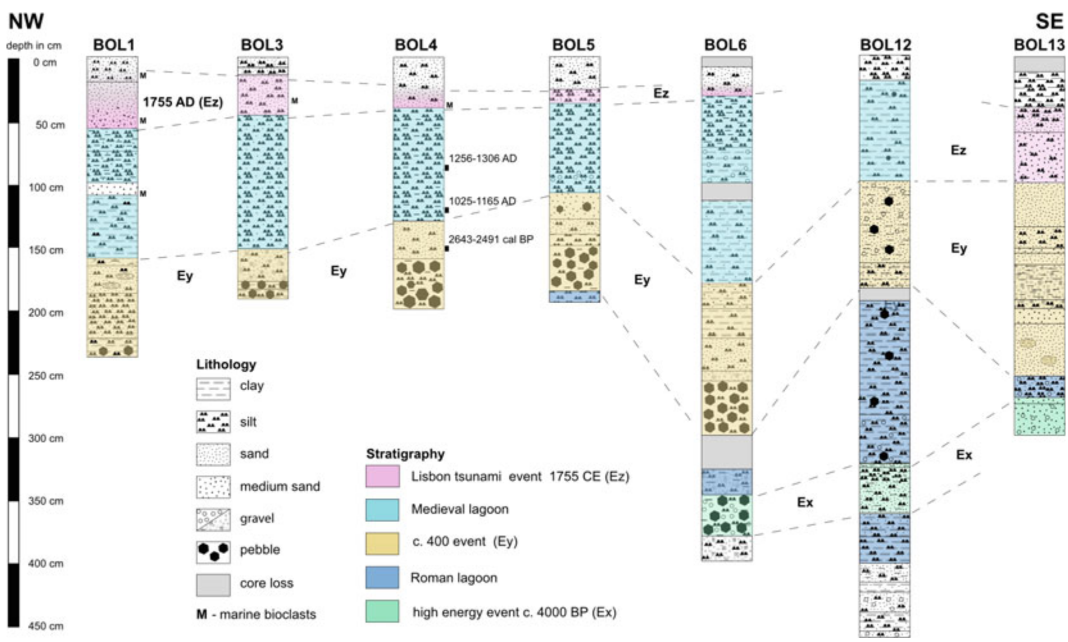

Fig. 13.6 Drill core profiles (locations in Fig. 13.2 and Table 13.1); Cores 7–11 are not shown; radiocarbon dates in Table 13.2. Description in the text

In view of the sea-level curves in the area and the Gulf of Cadiz (e.g. Zazo et al. 2008), this is interpreted as the beach formation at the end of the Holocene sea-level rise (Fig. 13.6). The basal sediments are followed by massive, unstructured coarse sands and pebbles, probably the result of an EWE and the formation of the beach berm with coarse marine pebbles (evidenced by the *Lithophaga* borings) and shell debris (high-energy environment, oysters, *Mactra* spp. and *Glycimeris* spp.). This unit is called "tsunami event Ex" (the oldest of three) as it transformed the open beach into a closed fresh water lagoon/alluvial plain. These are the deposits of the beach berm on which the eastern necropolis was built later on. Afterwards, the environment changed completely with the development of a back-barrier lagoon (Fig. 13.2), called the "Roman lagoon", since it still existed in late Roman times (Silva et al. 2016). Marine species are very rare, with the occasional presence of gyrogonites of charophytes as a freshwater indicator. Sediments are fine-grained bluish-black clays, interpreted as wash-off deposits from small creeks and the outcropping Cretaceous Almarchal units. The foraminiferal assemblages of the cores from the inner part of the lagoonal area are characterised by reworked, agglutinated foraminifera of the Cretaceous flysch facies (Almarchal Fm.), with a typical grey-dark grey or brownish colour—*Paratrochamminoides* spp., *Textularia* spp., *Glomospira* spp., *Trochamminoides* spp., *Haplophragmoides* spp. and *Ammodiscus* spp.—mostly in a good state of preservation. There are also elongated forms, including *Bathysiphon* spp., *Subreophax* spp., *Reophax* spp. and various *Astrorhizidae* and *Lituotubidae*, corresponding to the deep-water flysch fauna of the Cretaceous.

The fine-grained deposits are covered by an event deposit characterised by gravelly sands, some shells and Roman ceramics (Fig. 13.6). With a considerable thickness of several tens of centimetres, this layer, which was encountered in all the drillings, contains a low-diversity foraminifera fauna, including *Cibicides* sp., *Elphidium* sp., *Ammonia* sp. and *Miliolidae*, as well as *Quinqueloculina*. These foraminifers can be divided into two groups according to their state of preservation: on the one hand, those that are broken around the aperture and, barring a few exceptions, hardly lithified; and, on the other, those that are strongly abraded or partly polished and often no longer determinable. They are interpreted as having been reworked from the beach or dunes. Other marine faunal elements include gastropods and bivalve shells, fish remains, fragments of sea urchin spines and bryozoans. Due to its widespread presence and the fact that its characteristics are typical of an HEE (erosive base, mixed provenance, fining-up sequence, clearly open marine and beach sediments), the layer is called "tsunami event Ey". Its sedimentary characteristics allow for correlating it with the aforementioned archaeological layer ("black level") discovered in the T-31 and T-32 areas and, accordingly, it should also be dated to ca. 400 CE. Radiocarbon dating of the bulk sediment (Fig. 13.6; Table 13.2a), however, yielded much older ages of ca. 2500 cal BP.

Above the tsunami event Ey, there are yet again fine-grained, dark lagoonal deposits which are clearly non-marine. Radiocarbon dates suggest a medieval age (Fig. 13.6, Table 13.2a). *Characeae* and ostracods show that the silts were sedimented in a non-marine aquatic environment. The fine-grained deposits are intercalated with two coarse layers, probably relating to storm/flood events, between 930 ± 30 cal BP (1025–1165 CE) and 710 ± 30 cal BP (1256–1306 CE). Finally, these deposits with a thickness of up to 100 cm are covered by a non-continuous event layer attributed to the 1755 CE Lisbon tsunami and called "tsunami event Ez". The layer is characterised by chaotic, non-stratified black deposits containing sediments from all the units described above, plus Roman debris, as is to be expected for catastrophic layers. The layer displays a fining-up sequence and marine components. The modern soil layer, which has developed on top of layer Ez, has been greatly modified due to anthropogenic actions (agricultural land use, a military road, a fishing village and a chapel, the Guardia Civil barracks and more than 120 years of archaeological excavations). Finally, modern beach sand samples were analysed for comparison. They are characterised by a foraminifera assemblage containing *Elphidium* sp., *E. crispum*, *Ammonia* sp., *A. beccarii*, *Cibicides sp.* and *C. lobatulus*, plus the occasional presence of *Quinqueloculina* sp. (Fig. 13.2 R1–4). Every so often, reworked *Globigerinoides* with a typical orange colour is present, as with other typical microfossils such as sea urchin spines, bryozoan fragments and well-rounded bioclasts, as is to expect for beach sediments.

13.4.4 Pollen Data and Environmental Characterisation

Pollen samples were collected so as determine the environmental changes along the coastal strip, interpreted as having been caused by HEEs. The samples collected from the *Decumanus Maximus* and Mausoleum T-31 (Fig. 13.7; in the following called UE 31,005, according to the archaeological stratigraphy, Fig. 13.8) have been dated to the fourth and fifth centuries CE. They indicate the existence of a patchy landscape characterised by typical Mediterranean woodlands and shrub lands of evergreen oaks (evergreen *Quercus*), stone pines (*Pinus pinea*), wild olives (*Olea europaea*), mock privets (*Phillyrea*) and junipers (*Juniperus*), along with open areas of grassland (*Poaceae*). These characteristics seem to confirm that the current vegetation had already been established by then. The presence of anthropogenic-nitrophilous herbs, such as *Asteracea*, *Asteroideae* and *Cichorioideae*, together with coprophilous and saprophytic fungi (mainly *Sordariaceae*, *Sporomiella* and *Coniochaeta*) are indicative of nitrate-rich environments deriving from livestock pressure and/or animal husbandry. The presence of *Glomus* (HdV-207) and *Pseudoschizaea circula* imply the existence of erosive processes occurring at the site: the first is associated with dry or desiccated areas, root activity and/or crop rotation (Anderson et al. 1984; López-Sáez et al. 2000; van Geel et al. 1989); the

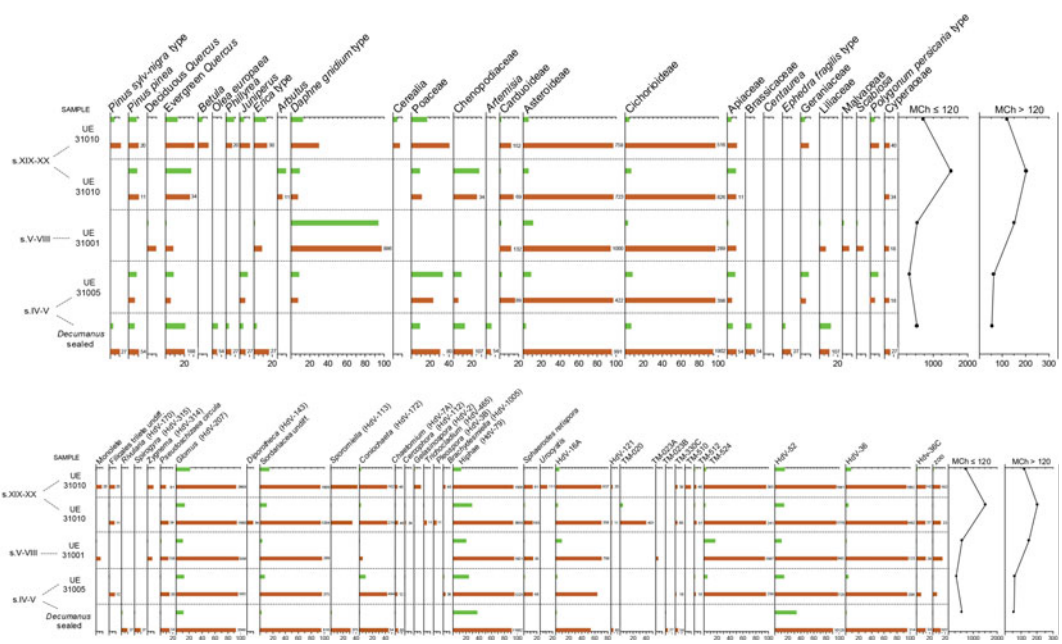

Fig. 13.7 Diagrams of pollen (upper part) and non-pollen (lower part) palynomorphs indicating the taxa identified in the different stratigraphic units (UE). The green histograms represent relative frequencies (%), while the orange histograms show concentrations (grains/gr of dry sediment). The black line graphs indicate microcharcoal concentrations (particles/gr of dry sediment)

latter is related to seasonal droughts and/or rapid sedimentation processes (Carrión and Navarro 2002; Pantaleón-Cano et al. 1996; Scott 1992). Sample HdV-207, which was collected from the "black level", namely, the event layer Ey, reflects the prevailing conditions during the Roman period.

The sample collected from Section UE 31,001 (Fig. 13.8 lower east profile), dated to between the fourth and eighth centuries CE, exhibits a peak of *Daphne gnidium* type, at similar concentrations, which could signify the local presence of this shrub taxon at the site, probably from an unintended indirect contribution. Some other taxa appear in lower values, such as evergreen and deciduous oaks (*Quercus*) and heath (*Erica* type). The landscape is mainly dominated by anthropogenic-nitrophilous herbs, although with a low presence of coprophilous and saprophytic fungi. *Glomus* and *Pseudoschizaea* are also present, the latter exhibiting the highest values among the samples, revealing the intensity of the erosive processes affecting the site. This sample, which was collected from the layers above Ey (location in Fig. 13.8a), evinces the post-event relief phase of the landscape and vegetation (Fig. 13.6).

The samples collected from Section UE 31,010, which can be dated to between the nineteenth and twentieth centuries and are thus modern, are characterised by Mediterranean vegetation comprising woodland and shrub land, such as evergreen oaks (*Quercus*), stone and Scots pines (*Pinus pinea* type and *Pinus sylvestris-nigra* type, respectively), wild olives (*Olea europaea*), mock privets (*Phillyrea*), junipers and heath (*Erica* type), among others. Grassland and anthropogenic-nitrophilous herbs represent the most abundant non-arboreal taxa, accompanied by high levels of coprophilous and saprophytic fungi (mostly *Sordariaceae* and *Coniochaeta*) and indicators of erosive processes (*Glomus* and *Pseudoschizaea*). Both samples exhibit the highest microcharcoal concentrations, suggesting intense local and regional fires, especially in the sample corresponding to the eastern sector. This sample represents the present-day pollen assemblage, as well as being subrecent and characteristic of the post-1755 CE Lisbon deposits.

13.5 Dating Results, Interpretation of Events and Discussion

In *Baelo Claudia* and the environs of the Bay of Bolonia, three possible event layers can be distinguished and dated by means of archaeological and geological/radiogenic dating methods. The oldest tsunami event Ex, only detectable in the deeper sections of BOL6 and BOL12, is evidenced by a distinct change in grain size. It was excavated in a trench within the eastern necropolis of *Baelo Claudia* and dated to an approximate mean age younger than 5000 cal BP. Radionuclide data for all the samples are shown in Table 13.3. No significant disequilibrium was observed in the ^{238}U decay chain. The three OSL samples show low to moderate scatter in the dose distributions with overdispersion values of between ~14 and ~23%, which can be assumed to reflect complete bleaching during sediment transport. The final OSL ages are 5.2 ± 0.3 ka (Ne-II-OSL-1), 4.9 ± 0.2 ka (Ne-II-OSL-3) and 2.5 ± 0.1 ka (Ne-II-OSL-4, post-event). Furthermore, the GPR profiles indicate coarse-grained layers in the area to the south of the *Decumanus Maximus*. The event layer Ex was also previously detected with GPR and in excavations carried out by Prados Martínez (2015). Gracia et al. (2006), who had already discovered it nearly a decade before, interpreted this event layer as a tsunami deposit, associating it with deposits left by the 1755 CE Lisbon event. We are inclined to attribute the coarse-grained deposits to an older event that completely modified the Bay of Bolonia and the coastal situation in the Middle Holocene (the Subboreal or Northgrippian/Meghalayan transition (Head 2019); in the archaeological context, it encompasses the Neolithic and Bronze Age). The event led to, or facilitated, the formation of a huge beach barrier (Fig. 13.2), due to a large amount of available sediment from the beach. The barrier

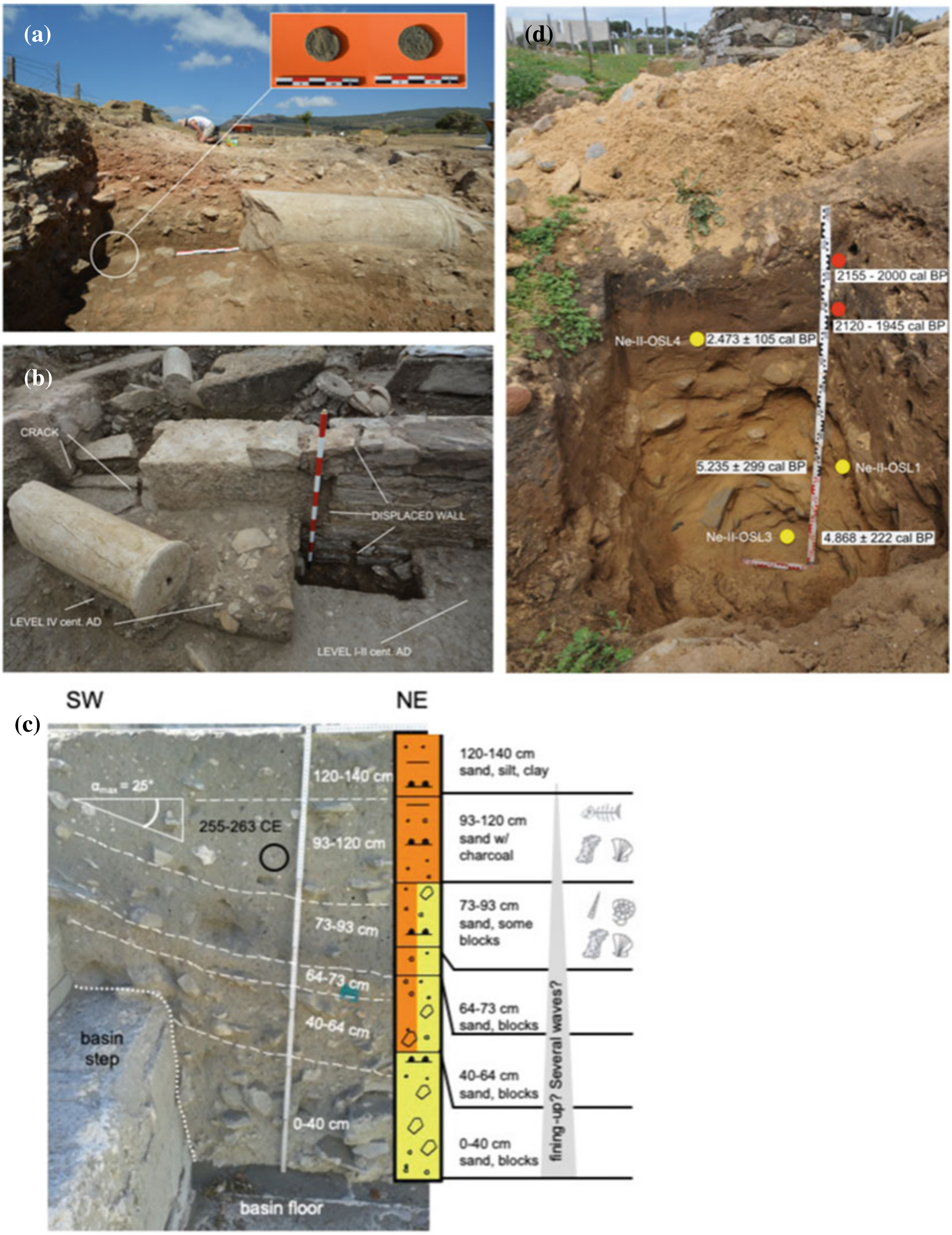

Fig. 13.8 Dating of events (see Table 13.2). **a** Coins in T-31 (location T in Fig. 13.2); **b** T-31 archaeological dating and archaeoseismic damage; **c** Maritime baths (TM in Fig. 13.2), charcoal age in *natatio* basin fill; note the fining-up sequence and marine fossils; and **d** Excavation in the eastern necropolis (N in Fig. 13.2), lower OSL ages (yellow dots) date the first EWE that caused beach berm development), and pieces of charcoal indicate first-century-CE Roman burials (^{14}C ages, red dots)

Table 13.3 OSL dating chart. Samples are from the eastern necropolis of *Baelo Claudia* (Spain)

Sample code	Lab code	Sample depth (m b.s.)	WC (%)	n_a	^{238}U (ppm)	^{232}Th (ppm)	^{40}K (%)	OD (%)	CAM De (Gy)	Total dose rate (Gy/ka)	OSL age (ka)
Ne-II-OSL-1	CL-4136	0.95	5.43	22	0.41 ± 0.04	1.44 ± 0.12	0.52 ± 0.01	22.53 ± 3.70	4.48 ± 0.22	0.856 ± 0.025	5.235 ± 0.299
Ne-II-OSL-3	CL-4138	1.4	3.15	27	0.43 ± 0.04	1.38 ± 0.12	0.36 ± 0.01	14.77 ± 2.38	3.46 ± 0.11	0.711 ± 0.023	4.868 ± 0.222
Ne-II-OSL-4	CL-4139	0.5	9.57	32	0.57 ± 0.04	2.97 ± 0.19	0.65 ± 0.01	16.99 ± 2.38	2.71 ± 0.09	1.096 ± 0.029	2.473 ± 0.105

The measurements were carried out in the Cologne Luminescence Lab (CLL). WC = water content; na = number of accepted aliquots; OD = overdispersion; and CAM = Central Age Model (Galbraith et al. 1999). DRAC was used for dose rate and age calculation (Durcan et al. 2015). OSL ages in years before 2015 CE temporarily closed the mouths of the streams (*arroyos*) and led to the formation of a back-barrier, freshwater-dominated floodplain and, possibly, a partly brackish lagoon. Many years later, the Romans used this elevated beach barrier area for the construction of fish factories, the eastern necropolis ("*Isola Sacra*" after Prados Martínez 2015) and, ultimately, the *extra-muros thermae* (Bernal et al. 2015, 2017). The city was constructed on the hillside behind the beach barrier, but not in the periodically flooded area of the lagoon. Neither the Romans nor the later inhabitants built on the lagoon/floodplain, as evidenced by the scarcity of archaeological finds. Down to this day, the area has been used as grassland which is occasionally flooded, with palynological data revealing marked changes in land-use patterns.

Gracia et al. (2006) did not date the pebbly deposits along the beach outcrops. We have preferred to re-interpret their finds as material of the tsunami event Ex, which was then reworked during the tsunami event Ez (i.e. the 1755 CE Lisbon tsunami). Hence, the interpretation made by Gracia et al. (2006) is reasonable and fits our own. The cannibalism of HEE deposits by younger ones is also observed in the event layer Ey, which was also affected by the last major event, the 1755 CE Lisbon tsunami (as observed in the *Decumanus Maximus* section, Fig. 13.4). This event is not substantiated by any earthquake-related damage or effects in the area. However, the layer corresponds to an event that affected long stretches of the coastline (e.g. Reicherter et al. 2010; Koster and Reicherter 2014). May et al. (2021) recently studied the environmental changes in the adjacent Bay of Zahara de los Atunes, in the Rio del Cachón catchment. They discovered a closure of the bay and the formation of a brackish, fresh water lagoon before 6000 BP, interpreting this as the mid Holocene sea-level "standstill". Additionally, Reicherter et al. (2010) and Koster and Reicherter (2014) described a ca. 4000-year-old HEE layer in the lagoon, which may correspond to the same layer in *Baelo Claudia* and the tsunami event Ex.

The next event layer is the massive layer, or "black level", attributed to the tsunami event Ey. This is found along all the sections of the *Decumanus Maximus* in GPR profiles and in the excavations of *Baelo Claudia* up until a height of ca. 8 m above sea level (which corresponds to the height of the forum to the north of the *Decumanus Maximus*). Furthermore, this is the destruction level of the earthquake that led to the abandonment of the city described by Silva et al. (2005, 2009, 2016). In the wake of the disaster, *Baelo Claudia* became more and more detached from the Roman Empire. The political power of the Empire disintegrated slowly, although the economy, local administration and urban life still flourished in some regions of the *Baetica* province, especially in the Strait of Gibraltar thanks to the fish and *garum* factories and trade. Possibly, the Vandals passed by *Baelo Claudia* on their way to Africa, causing the abandonment of some areas in the Strait of Gibraltar in the early fifth-century CE (Bernal-Casasola 2018). The Strait of Gibraltar area even formed part of the Byzantine Empire in the sixth century CE, resulting in a relative growth in trade and wealth. Recent excavations in *Baelo Claudia*, near the eastern *Decumanus Maximus* and the basilica, unearthed houses occupying ancient public buildings (Brassous et al. 2017; Gutiérrez Rodríguez et al. 2019), while in the necropolis a large number of tombs covering the ruins and rubble of the earthquake were discovered (Prados Martínez 2015). Monumental destruction in the necropolis and all the low-lying areas of the city has been documented. The water supply through the aqueduct and channels leading to the system of cisterns was disrupted during this event, while large cracks appeared in the walls of the basin causing it to leak. Archaeological damage and disruption are coeval with the Ey-related flooding of the lower part of the city. The archaeoseismic record also allows for dating the destruction of the water channels and small cistern to the same time span as the filling of the basin of the *extra-muros thermae*, viz. around the end of the fourth-century CE (Bernal et al. 2015; Röth et al. 2015). The *cetariae* (fish salting plants) located between the beach and the sampled archaeological areas were not entirely abandoned until the early fifth century CE (Díaz and Bernal-Casasola 2020). Furthermore, no "black layer" has been identified in this area, but only sandy strata (Expósito Álvarez and Bernal-Casasola 2020). The event also led to the catastrophic filling of the basin of the *extra-muros thermae* (Röth et al. 2015), which has been dated with charcoal samples.

The event layer Ey was encountered in all the drillings, with the exception of the northernmost BOL8, BOL 10 and BOL11. Sedimentary features are mainly changes in grain size and in the element concentration of Ti, Ca and Sr (Patock 2017). Thanks to the archaeological evidence and unearthed coins, it was possible to date the event layers very precisely to the end of the fourth-century CE. The dating of organic matter in the lagoon (BOL4) revealed older ages. To our mind, the material was reworked during the EWE. These high-energy deposits may correspond to the layer described by Alonso Villalobos et al. (2003), who, taking into account the reworked material, dated it to ca. 200 years before. Additionally, the possible evidence of an older event should not be ruled out, as older EWEs have been described in the Gulf of Cadiz (Lario et al. 2011; Álvarez-Martí-Aguilar 2019; Costa et al., this volume). In conclusion, we are of the mind that the tsunami event Ey completely destroyed the Roman city of *Baelo Claudia*, after which it never recovered, although it continued to be inhabited until the seventh-century CE. We endorse the dates proposed by Ménanteau et al. (1983) and Silva et al. (2005), while correcting those suggested by Silva et al. (2009) and Grützner et al. (2010) to the late fourth-century CE. The dates of 260–290 CE should be interpreted as a *terminus ante quem*, predating the earthquake and tsunami. We have also been the first to interpret the mixed chaotic "black level" as a tsunami layer, which reworked the Roman archaeological stratigraphy completely, but left a prominent and traceable event horizon in the city and the lagoonal area. In contrast to the 1755 CE Lisbon earthquake and tsunami, however, we have detected and documented severe earthquake damage in *Baelo Claudia* (Silva et al. 2005, 2009; Grützner et al. 2010, 2012), which points to a different and closer seismic source, possibly somewhere in the Gulf of Cadiz.

The youngest event layer Ez corresponds to the 1755 CE Lisbon earthquake and tsunami, as already assumed by Gracia et al. (2006), who found several indications of tsunami action in the Bay of Bolonia. The high-energy deposits are obvious in BOL1, BOL3 and BOL4. It is also possible to detect traces of this tsunami in BOL5, weaker signatures in BOL 6, BOL7, BOL13 and BOL14 and, ultimately, none whatsoever in BOL12 (Fig. 13.6). The event is also traceable in some of the GPR profiles, especially in the lower parts of the city. The high-energy deposits that Becker-Heidmann et al. (2007) found near the western end of the beach, close to Roman remains and a coastal defensive bunker built during the Franco dictatorship, contained charcoal dated to ca. 500 yrs BP. In light of a *terminus ante quem* interpretation, the dated charcoal can be considered as having been reworked by wave action, while the multiple fining-up layers could correspond to the 1755 CE Lisbon tsunami and its multiple waves, whose inundation distance was clearly shorter than that of 400-CE event. The associated earthquake did not cause any material damage in the area, which was relatively unpopulated at that time, which is yet another argument that can be deployed in favour of a different seismic source area for the fourth-century-CE event, which sealed the fate of *Baelo Claudia*.

13.6 Conclusions

The results of more than 20 years of transdisciplinary research in the Bay of Bolonia and the ruins of the Roman city of *Baelo Claudia*, combining different archaeological and geoscientific methods, including sedimentology, dating techniques and shallow geophysics and micropalaeontology, demonstrate the difficulties posed by archaeological sites for studying catastrophic and cascading events. Not every earthquake triggers a tsunami and not every tsunami is triggered by an earthquake in situ. The different dating techniques and sampling strategies employed by different teams can lead to important errors when estimating ages. We can conclude that the most reliable dates in historical contexts are of the archaeological kind, especially in the Roman age, when coins and ceramics, building techniques, habits and fashions changed as in modern times, thus allowing for dating that avoids the errors associated with radiocarbon dating. Successive event layers of earthquakes and inundation events always involve the reworking of dated material, the erosion of basal pre-event layers, omissions or time-lags in subsequent post-event layers and anthropogenic or faunal modifications (bioturbation, burrows). Interpretations should include *terminus ante quem* and *terminus post quem* considerations and discussions. Additionally, several other factors modifying the study area over time, like sudden landscape changes, land-use changes (e.g. by pollen analyses), sea-level changes, wind-direction changes, short-term climatic variations, barrier and shelter positions (sand banks) and, of course, morphogenetic earthquakes, large-scale tectonic uplift, seismic and tsunamigenic sources and source areas (i.e. faults) all need to be taken into consideration and evaluated. In order to summarise our investigations and interpretations of a huge dataset with respect to tsunami landfall and EWE destruction in the Bay of Bolonia, we postulate three major events in the last ca. 4000 years severely affecting the coastline with inundation distances of ca. 200–250 m:

(a) A prehistoric EWE (in all likelihood a tsunami, Costa et al., this volume; but a severe storm surge, albeit very rare in the area, should not be ruled out) left coarse-grained deposits along the beach that indirectly would have facilitated the formation of a beach barrier around 4000 BP and, at the latest, before c. 2500 BP. The elevated cobble beach ridges later served as a settlement area for the Romans in the lower coastal environs of the bay. Behind the ridge, a "lagoon" formed as a result of the blocking of the mouth of the Arroyo del Alpariate.

(b) A Roman earthquake and tsunami in the late fourth-century CE led to the city's decline (although not to its total abandonment as there are younger, but rather poor, constructions on top of the event layer, as described by Brassous et al. 2017). The central water system/cistern of the aqueduct of Realillo was destroyed. Several buildings collapsed on "clean" ground (which means in use) and multiple impact marks are visible on the Roman pavements, like, for example, in the *basilica*, *Decumanus Maximus* and *Macellum* (Silva et al. 2016, 2019). Prestigious monuments in the eastern necropolis collapsed. Further significant earthquake-related destruction was mapped by Silva et al. (2009). The waves flooded the *forum* area until heights of ca. 8 m above the modern mean sea level. The collapsed buildings close to the sea in the *Decumanus Maximus* area were covered by a "black level", which has been interpreted as a tsunami layer. There is a clear sequence in the event deposits: first earthquake destruction, then flooding. Although the currently accepted date is around the late fourth-century CE, it might be slightly older, as Bernal et al. (2015) suggested.

(c) The preservation and distribution of the 1755 CE Lisbon tsunami is now more accurately established than before. The Bay of Bolonia and *Baelo Claudia* were affected by waves during the event, although sheltered by Cape Camarinal, probably due to their refraction and reflexion. Although these waves did not reach the run-up level of the fourth-century CE event, they reworked and redeposited many of the older sediments.

Besides these three major events, we should not forget that a local earthquake struck *Baelo Claudia* in the first century CE (40–60 CE; Sillières 1997; Silva et al. 2009, 2019; Grützner 2011). No tsunami deposits relating to this event have as yet been detected. In terms of a multi-hazard area, the Bay of Bolonia offers a large portfolio. However, the valuable natural amphitheatre formed by the Miocene Sierras de la Plata and Bartolomé and *Baelo Claudia* offers much more.

Acknowledgements The authors are grateful to German Science Foundation (DFG grant, RE 1361/28-1) and the MINECO-FEDER Spanish Research Project CGL2015-67169-P (QTECSPAIN-USAL) for their support. They would also like to thank Prof. Javier Gracia (University of Cadiz) for his thorough review of the manuscript. Furthermore, they express their gratitude to the BA and MA students at RWTH Aachen and Cologne University involved in the field- and lab work. Lastly, they are indebted to Dr Georgina King, Dr Melanie Bartz (both from the University of Lausanne, Switzerland) for the OSL dating, and to Prof. Manuel Álvarez-Martí-Aguilar (University of Malaga), Prof. Darío Bernal-Casasola (University of Cadiz) for their valuable comments.

References

Alonso C, Gracia F, Del Río L, Anfuso G et al (2004) Registro morfosedimentario de eventos históricos de alta energía en el litoral atlántico del Estrecho de Gibraltar (Trafalgar-Tarifa). In: Benito G, Díez Herrero A (eds) Contribuciones recientes sobre Geomorfología. SEG-CSIC, Madrid, pp 263–272

Alonso C, Gracia F, Rodríguez-Polo S, Martín Puertas C (2015) El registro de eventos energéticos marinos en la bahía de Cádiz durante épocas históricas. Cuaternario y Geomorfología 29(1–2):95–117

Alonso-Villalobos F, Gracia-Prieto F, Ménanteau L, Ojeda R et al (2003) Paléogeographie de l'anse de Bolonia (Tarifa, Espagne) à l'époque romaine. In: Fouache E (ed) The Mediterranean world environment and history—IAG working group on geoarchaeology symposium proceedings. Elsevier, Mayenne, pp 407–417

Álvarez-Martí-Aguilar M (2019) El retorno del cataclismo: de la Atlántida a Tarteso. In: Sánchez Moreno E (ed) Veinticinco estampas de la España Antigua. Cincuenta años después (1967–2017). En torno a la obra de Antonio García y Bellido y su actualización científica. Universidad de Sevilla, Sevilla, pp 115–130

Anderson RS, Homola RL, Davis RB, Jacobson GL Jr (1984) Fossil remains of the mycorrhizal fungal Glomus fasciculatum complex in postglacial lake sediments from Maine. Can J Bot 62(11):2325–2328

Andrade C, Freitas MC, Miranda JM, Baptista MA et al (2003) Recognizing possible tsunami sediments in the ultradissipative environment of the Tagus estuary (Portugal). In: Davis RA (ed) Coastal sediments, vol 3—the 5th international symposium on coastal engineering and science of coastal sediment processes, Clearwater Beach, Florida, 18–23 May, 14 pp

Becker-Heidmann P, Reicherter K, Silva PG (2007) 14 C-dated charcoal and sediment drilling cores as first evidence of holocene tsunamis at the southern spanish coast. Radiocarbon 49(2):827–835

Bernal D, Expósito JA, Díaz JJ et al (2015) Evidencias arqueológicas de desplomes paramentales traumáticos en las Termas Marítimas de Baelo Claudia. Reflexiones arqueosismológicas. Cuaternario y Geomorfología 29(1–2):119–136

Bernal D, Díaz JJ, Expósito JA (2017) Les thermes maritimes de Baelo Claudia et le suburbium occidental. Mélanges De La Casa De Velázquez, Nouv Sér 47 (1):133–150

Bernal-Casasola D, Díaz JJ, Expósito JA et al (2016) Arquitectura y fases de ocupación de las Termas Marítimas de Baelo Claudia. Las Termas Marítimas y el Doríforo de Baelo Claudia. Universidad de Cádiz, Cádiz, pp 18–97

Bernal-Casasola D, Arévalo A, Expósito JA, Díaz JJ (2007) Reocupaciones del espacio y continuidad habitacional en el Bajo Imperio. In: Las cetariae de Baelo Claudia. Avance de las investigaciones arqueológicas en el barrio meridional (2000–2004). Junta de Andalucía, Sevilla, pp 455–487

Bernal-Casasola D (2018) Continuidad y cesura en las ciudades tardorromanas del Estrecho de Gibraltar. El Fretum Gaditanum, un ámbito hispano-africano singular. In: Panzram S, Callegarin L (eds) Entre civitas y madīna. El mundo de las ciudades en la Península Ibérica y en el norte de África (siglos IV–IX). Collection de la Casa de Velázquez (167), Madrid, pp 105–118

Berni Millet P, Moros Díaz J (2012) Los sellos in planta pedis de las ánforas olearias béticas Dressel 23 (primera mitad siglo V A.C.). Arch Esp Arqueol 85:193–219

Bony G, Marriner N, Morhange C et al (2012) A high-energy deposit in the Byzantine harbour of Yenikapı, Istanbul (Turkey). Quatern Int 266:117–130

Borau L (2017) L´eau dans la fabrique de la ville: état de la recherche à *Baelo Claudia*. Mélanges De La Casa De Velázquez, Nouv Sér 47(1):97–120

Borja F, Zazo C, Dabrio CJ et al (1999) Holocene aeolian phases and human settlements along the Atlantic coast of southern Spain. The Holocene 9(3):333–339

Brassous L, Deru X, Rodríguez Gutiérrez O et al (2017) Baelo Claudia dans l´Antiquité tardive. Mélanges De La Casa De Velázquez, Nouv Sér 47(1):167–200

Brill D, May SM, Mhammdi N et al (2021) OSL rock surface exposure dating as a novel approach for reconstructing transport histories of coastal boulders over decadal to centennial timescales. Esurf Discussions. https://doi.org/10.5194/esurf-2020-46

Bruins HJ, MacGillivray JA, Synolakis CE et al (2008) Geoarchaeological tsunami deposits at Palaikastro

(Crete) and the Late Minoan IA eruption of Santorini. J Archaeol Sci 35(1):191–212
Camacho S, Moura D, Connor S et al (2015) Ecological zonation of benthic foraminifera in the lower Guadiana Estuary (southeastern Portugal). Mar Micropaleontol 114:1–18
Campos ML (1991) Tsunami hazard on the Spanish coasts of the Iberian peninsula. Sci Tsunami Haz 9:83–90
Carrión JS, Navarro C (2002) Cryptogam spores and other non-pollen microfossils as sources of palaeoecological information: case-studies from Spain. Ann Bot Fenn 39(1):1–14
Conjunto Arqueológico de Baelo Claudia (2013) Informe preliminar intervención arqueológica puntual Decumanus Maximus Baelo Claudia, Bolonia. Junta de Andalucía
Costa PJM, Andrade C (2020) Tsunami deposits: present knowledge and future challenges. Sedimentology 67 (3):1189–1206
Costa PJM, Andrade C, Freitas MC et al (2011) Boulder deposition during major tsunami events. Earth Surf Proc Land 36(15):2054–2068
Costa PJM, Andrade C, Freitas MdC et al (2012) A tsunami record in the sedimentary archive of the central Algarve coast, Portugal: characterizing sediment, reconstructing sources and inundation paths. The Holocene 22(8):899–914
Cuven S, Paris R, Falvard S et al (2013) High-resolution analysis of a tsunami deposit: case-study from the 1755 Lisbon tsunami in southwestern Spain. Mar Geol 337:98–111
Dawson AG, Stewart I (2007) Tsunami deposits in the geological record. Sed Geol 200(3–4):166–183
Dawson AG, Hindson R, Andrade C et al (1995) Tsunami sedimentation associated with the Lisbon earthquake of 1 November AD 1755: Boca do Rio, Algarve, Portugal. The Holocene 5(2):209–215
Dawson S, Costa PJM, Dawson A, Engel M (2020) Onshore archives of tsunami deposits. In: Engel M, Pilarczyk J, May SM et al (eds) Geological records of tsunamis and other extreme waves. Elsevier, Amsterdam, pp 95–111
De Vicente G, Cloetingh S, Muñoz-Martín A et al (2008) Inversion of moment tensor focal mechanisms for active stresses around the microcontinent Iberia: tectonic implications. Tectonics 27(1):TC1009, 22. https://doi.org/10.1029/2006TC002093
Díaz JJ, Bernal-Casasola D (2020) Excavaciones en la Cetaria XI y el mantenimiento de las conservas baelonenses hasta época tardorromana. In: Bernal-Casasola D, Díaz JJ, Expósito JA, Palacios V (eds) Baelo Claudia and the secrets of Garum. Tunas, whales, oysters, sardines and other marine resources in the Roman halieutic chaîne opératoire. Cádiz, Universidad de Cádiz, pp 68–83
Dominey-Howes D, Dawson A, Smith D (1999) Late Holocene coastal tectonics at Falasarna, western Crete: a sedimentary study. Geol Soc Lond 146(1):343–352
Durcan JA, King GE, Duller GA (2015) DRAC: Dose Rate and Age Calculator for trapped charge dating. Quat Geochronol 28:54–61
Expósito Álvarez JA, Bernal-Casasola D (2020) Una fábrica de excepcional productividad y con una producción diversificada: la Cetaria XII. In: Bernal-Casasola D, Díaz JJ, Expósito JA, Palacios V (eds) Baelo Claudia and the secrets of Garum. Tunas, whales, oysters, sardines and other marine resources in the Roman halieutic chaîne opératoire. Cádiz, Universidad de Cádiz, pp 84–97
Feist L, Frank S, Bellanova P et al (2019) The sedimentological and environmental footprint of extreme wave events in Boca do Rio, Algarve coast, Portugal. Sed Geol 389:147–160
Fernandez-Ibañez F, Soto J, Zoback M, Morales J (2007) Present-day stress field in the Gibraltar Arc (western Mediterranean). J Geophys Res: Solid Earth 112: B08404, 25. https://doi.org/10.1029/2006JB004683
Frenken M, Cämmerer C, Bellanova P, Chaumet M, Daehling K, FeistL, Schulte P, Lehmkuhl F, Schwarzbauer J, Reicherter K (2022) Multi-proxy analysis of the AD 1755 Lisbontsunami deposits in Conil de la Frontera, Spain. In: Álvarez-Martí-Aguilar M, Machuca-Prieto F (eds) HistoricalEarthquakes and Tsunamis in the Iberian Peninsula: an interdisciplinary dialogue. Springer, Heidelberg, Germany,Chapter ##, pp xxx–xxx
Galbraith RF, Roberts RG, Laslett GM et al (1999) Optical dating of single and multiple grains of quartz from Jinmium rock shelter, northern Australia: Part I, experimental design and statistical models. Archaeometry 41(2):339–364
García-Jiménez I (2011) Memoria Preliminar Excavación Arqueológica Puntual Decumanus Maximus Baelo Claudia (Tarifa. Unpublished excavation notes, Archive CABC; Baelo Claudia, Cadiz, Cádiz)
van Geel B (1992) Fungal spores as extra indicators for human impact in the past. In: Abstracts 8th international palynological congress. Université Aix en Provence-Marseille III, Marseille
van Geel B (2006) Quaternary non-pollen palynomorphs. Rev Palaeobot Palynol 141(1–2)
González Lastras J, García de Domingo A, Hernaiz P et al (1991) Cartografía geológica y memoria de la hoja 13–47 (Tarifa). Mapa Geológico de España, Escala 1:50.000, Plan MAGNA, 2ª Serie. IGME, Madrid
Goodman Tchernov B, Katz T, Shaked Y et al (2016) Offshore evidence for an undocumented tsunami event in the 'low risk'Gulf of Aqaba-Eilat, Northern Red Sea. PloS one 11(1):e0145802, 14. https://doi.org/10.1371/journal.pone.0145802
Goodman-Tchernov BN, Austin JA Jr (2015) Deterioration of Israel's Caesarea Maritima's ancient harbor linked to repeated tsunami events identified in geophysical mapping of offshore stratigraphy. J Archaeol Sci Rep 3:444–454
Goy J, Zazo C, Mörner N et al (1994) Pop up-like deformation of a Roman floor and liquefaction

structures in SW Spain as possible paleoseismic indicators. Bulletin of the INQUA Neotectonics Comisión 17:42–44
Goy J, Zazo C, Silva P et al (1995) Evaluación geomorfológica del comportamiento neotectónico del Estrecho de Gibraltar (Zona Norte) durante el Cuaternario. In: Esteras M (ed) IV Coloquio Internacional sobre el Enlace Fijo del Estrecho de Gibraltar, vol 2. SECEG, Madrid, pp 51–69
Gracia F, Alonso C, Benavente J et al (2006) The different coastal records of the 1755 tsunami waves along the south Atlantic Spanish Coast. Z Geomorphol Suppl 146:195–220
Grimm EC (2012–2015) Tilia, Tilia-Graph and TGView, Springfield, Illinois State Museum. Available at: https://www.tiliait.com
Grützner C, Reicherter K (2021) Georadar survey in the Roman Ruins of Baelo Claudia. PANGAEA, Spain. https://doi.org/10.1594/PANGAEA.927835
Grützner C, Reicherter K, Silva PG (2010) Comparing semiquantitative logic trees for archaeoseismology and paleoseismology: the Baelo Claudia (southern Spain) case study. Ancient Earthquakes 471:129–144
Grützner C, Reicherter K, Hübscher C, Silva PG (2012) Active faulting and neotectonics in the Baelo Claudia area, Campo de Gibraltar (southern Spain). Tectonophysics 554:127–142
Grützner C (2011) The Baelo Claudia earthquake problem. Dissertation, RWTH Aachen University
Gutiérrez Mas JM, Gómez Fernández V, García López S et al (2016) Comparative analysis of the deposits left by the tsunami that followed to the Lisbon Earthquake (1755 AD), on the Castilnovo beach and the Old Tuna Factory of La Chança (Conil de la Frontera, SW Spain). Revista De La Sociedad Geológica De España 29(1):21–33
Gutiérrez Rodríguez MA, Brassous L, Rodríguez Gutiérrez O et al (2019) Site formation processes and urban transformations during Late Antiquity from a high-resolution geoarchaeological perspective: Baelo Claudia, Spain. Geoarchaeology 35(2):258–286
Gutscher M-A, Malod J, Rehault J-P et al (2002) Evidence for active subduction beneath Gibraltar. Geology 30(12):1071–1074
Gutscher M-A, Baptista MA, Miranda JM (2006) The Gibraltar Arc seismogenic zone (part 2): constraints on a shallow east dipping fault plane source for the 1755 Lisbon earthquake provided by tsunami modeling and seismic intensity. Tectonophysics 426(1–2):153–166
Hadler H, Vött A, Koster B et al (2013) Multiple late-Holocene tsunami landfall in the eastern Gulf of Corinth recorded in the palaeotsunami geo-archive at Lechaion, harbour of ancient Corinth (Peloponnese, Greece). Zeitschrift Für Geomorphologie, Supplementary Issues 57(4):139–180
Hadler H, Fischer P, Obrocki L et al (2020) River channel evolution and tsunami impacts recorded in local sedimentary archives–the ‘Fiume Morto’ at Ostia Antica (Tiber River, Italy). Sedimentology 67(3):1309–1343
Head MJ (2019) Formal subdivision of the quaternary system/period.: present status and future directions. Quat Int 500:32–51
Hermann F, Feist L Teichner F, Bernardes JP, Reicherter K, Brückner H (2022) At themercy of the sea. Vulnerability of Roman coastal settlements in the Algarve-Region (Portugal). Boca do Rio as anemblematic example of a marine key industry. In: Álvarez-Martí-Aguilar M, Machuca-Prieto F (eds) HistoricalEarthquakes and Tsunamis in the Iberian Peninsula: an interdisciplinary dialogue. Springer, Heidelberg, Germany,Chapter 10, pp xxx–xxx
Hoffmann G, Reicherter K, Wiatr T et al (2013) Block and boulder accumulations along the coastline between Fins and Sur (Sultanate of Oman): tsunamigenic remains. Nat Hazards 65:851–873
Hoffmann G, Grützner C, Schneider B et al (2020) Large Holocene tsunamis in the northern Arabian Sea. Mar Geol. https://doi.org/10.1016/j.margeo.2019.106068
Hoffmann G, Reicherter K (2016) Geohazards: coastal disasters. In: Harff J, Meschede M, Petersen S, Thiede J (eds) Encyclopedia of marine geosciences. Encyclopedia of Earth Sciences Series. Springer, Dordrecht, pp 276–283
Jarzen DM, Elsik WC (1986) Fungal palynomorphs recovered from recent river deposits, Luangwa Valley, Zambia. Palynology 10(1):35–60
Jiménez-Vialás H (2017) Carteia y Traducta. Ciudades y territorio en la orilla norte del Estrecho de Gibraltar (siglos VII a. C. al III d. C.). Edicions de la Universitat de Barcelona, Barcelona
Kaabouben F, Baptista MA, Brahim AI et al (2009) On the moroccan tsunami catalogue. Nat Hazard 9 (4):1227–1236
Keay SJ (1984) Late roman amphorae in the western mediterranean. A typology and economic study: the catalan evidence. Bar international series, vol. 1.136. Archaeopress, Oxford
Klein T, Bebermeier W, Krause J et al (2016) Sedimentological evidence of an assumed ancient anchorage in the hinterland of a Phoenician settlement (Guadiana estuary/SW-Spain). Quatern Int 407:110–125
Koster B, Reicherter K (2014) Sedimentological and geophysical properties of a ca. 4000 year old tsunami deposit in southern Spain. Sed Geol 314:1–16
Koster B, Vött A, Mathes-Schmidt M, Reicherter K (2015) Geoscientific investigations in search of tsunami deposits in the environs of the Agoulinitsa peatland, Kaiafas Lagoon and Kakovatos (Gulf of Kyparissia, western Peloponnese, Greece). Zeitschrift Für Geomorphologie Supplementary Issues 59 (4):125–156
Lario J, Zazo C, Dabrio CJ et al (1995) Record of recent Holocene sediment input on spit bars and deltas of south Spain. J Coastal Res Special Issue 17:241–245
Lario J, Spencer C, Plater A et al (2002a) Particle size characterisation of Holocene back-barrier sequences from North Atlantic coasts (SW Spain and SE England). Geomorphology 42(1–2):25–42

Lario J, Zazo C, Goy J et al (2002b) Changes in sedimentation trends in SW Iberia Holocene estuaries (Spain). Quatern Int 93:171–176

Lario J, Zazo C, Goy J et al (2011) Holocene palaeotsunami catalogue of SW Iberia. Quatern Int 242 (1):196–200

Lario J, Luque L, Zazo C et al (2009) Tsunami deposits at Torre de Castilnovo, Conil de la Frontera. In: Lario J, Silva PG, Reicherter K et al (eds) Palaeoseismicity and active tectonics during the quaternary in the gibraltar strait (Betic Cordillera, South Spain). 1st INQUA-IGCP 567 international workshop on earthquake archaeology and palaeoseismology. IGME, Madrid, pp 85–96

Lario J (1996) Último y presente interglaciar en el área de conexión Atlántico-Mediterráneo (sur de España): variaciones del nivel del mar, paleoclima y paleoambientes. Dissertation, Universidad Complutense de Madrid

López-Sáez JA, van Geel B, Farbos-Texier S, Diot MF (1998) Remarques paléoécologiques à propos de quelques palynomorphes non-polliniques provenant de sédiments quaternaires en France. Rev Paléobiol 17 (2):445–459

López-Sáez JA, Pérez-Díaz S, Rodríguez-Ramírez A et al (2018) Mid-late Holocene environmental and cultural dynamics at the south-west tip of Europe (Doñana National Park, SW Iberia, Spain). J Archaeol Sci Rep 22:58–78

López-Sáez JA, Van Geel B, Martín Sánchez M (2000) Aplicación de los microfósiles no polínicos en Palinología Arqueológica. In: Actas 3 Congresso de Arqueologia Peninsular. Contributos das Ciências e das Technologias para a Arqueologia da Península Ibérica, IX, Adecap, Porto, Portugal, pp 11–20

Luque L, Lario J, Zazo C et al (2001) Tsunami deposits as paleoseismic indicators: examples from the Spanish coast. Acta Geologica Hispanica 36(3):197–211

Luque L, Lario J, Civis J et al (2002) Sedimentary record of a tsunami during Roman times, Bay of Cadiz, Spain. J Quatern Sci 17(5–6):623–631

Luque L, Zazo C, Lario J et al (2004) El efecto del tsunami del año 1755 en el litoral de Conil de la Frontera (Cádiz). In: Baquedano Pérez E, Rubio Jara S (eds) Miscelánea En Homenaje a Emiliano Aguirre 1. Geología. Comunidad de Madrid, Museo Arqueológico Regional, Madrid, pp 72–82

Mathes-Schmidt M, Schwarzbauer J, Papanikolaou I et al (2013) Geochemical and micropaleontological investigations of tsunamigenic layers along the Thracian Coast (Northern Aegean Sea, Greece). Zeitschrift Für Geomorphologie Supplementary Issues 57(4):5–27

May SM, Norpoth M, Pint A et al (2021) Mid- to late Holocene environmental changes and human–environment interactions in the surroundings of La Silla del Papa, SW Spain. Geoarchaeology 36:573–600. https://doi.org/10.1002/gea.21846

Ménanteau L, Vanney JR, Zazo C (1983) Belo II: Belo et son environement (Détroit de Gibraltar), Etude physique d'un site antique. Pub. Casa de Velázquez, Serie Archéologie 4. Editions Broccard, Paris

Mendes I, Dias JA, Schönfeld J et al (2013) Living, dead and fossil benthic foraminifera on a river dominated shelf (northern Gulf of Cadiz) and their use for paleoenvironmental reconstruction. Cont Shelf Res 68:91–111

Mhammdi N, Medina F, Trentesaux A et al (2015) Sedimentary evidence of palaeo-tsunami deposits along the Loukkos estuary (Moroccan Atlantic coast). Sci Tsunami Haz 34(2):83–100

Miola A (2012) Tools for non-pollen palynomorphs (NPPs) analysis: a list of Quaternary NPP types and reference literature in English language (1972–2011). Rev Palaeobot Palynol 186:142–161

Moore PD, Webb JA, Collison ME (1991) Pollen analysis. Blackwell scientific publications, Oxford

Morales J, Borrego J, San Miguel E et al (2008) Sedimentary record of recent tsunamis in the Huelva Estuary (southwestern Spain). Quatern Sci Rev 27(7–8):734–746

Murray AS, Wintle AG (2000) Luminescence dating of quartz using an improved single-aliquot regenerative-dose protocol. Radiat Meas. https://doi.org/10.1016/S1350-4487(99)00253-X

Pals JP, Van Geel B, Delfos A (1980) Paleoecological studies in the Klokkeweel bog near Hoogkarspel (prov. of Noord-Holland). Rev Palaeobot Palynol 30:371–418

Pantaleón-Cano J, Pérez-Obiol R, Yll E, Roure J (1996) Significado de Pseudoschizaea en secuencias sedimentarias de la vertiente mediterránea de la Península Ibérica e Islas Baleares. In: Ruíz Zapata B (ed) Estudios palinológicos. Universidad de Alcalá, Alcalá de Henares, pp 101–105

Paris P, Bonsor G, Laumonier A et al (1926) Fouilles de Belo (Bologna, Province Of Cadix) (1917–1921), T. II: La Nécropole. Bibliothèque De L'école Des Hautes Etudes Hispaniques, Bordeaux

Patock P (2017) A multi-proxy approach fo the reconstruction of palaeo-environments: sediment-physical, micropalaeontological and geochemical analyses of Bolonia Bay drill cores, Southern Spain. Unpubl BSc thesis, RWTH Aachen University

Pedrera A, Ruiz-Constan A, Galindo-Zaldívar J (2011) Is there an active subduction beneath the Gibraltar orogenic arc? Constraints from Pliocene to present-day stress field. J Geodyn 52(2):83–96

Pirazzoli P, Ausseil-Badie J, Giresse P, Hadjidaki E, Arnold M (1992) Historical environmental changes at Phalasarna harbor, West Crete. Geoarchaeology 7 (4):371–392

Prados Martínez F, Jiménez Vialás H, Abad Casal L (2020) Primeros avances de la intervención arqueológica en los mausoleos de la puerta sureste de Baelo Claudia: el monumento de Iunia Rufina. Zephyrus 85:163–184

Prados Martínez F, Jiménez-Vialás H (eds) (2015) La muerte en Baelo Claudia. Necropolis y ritual en el confín occidental del Imperio. Universidad de Cádiz-Universitat d'Alacant, Cádiz-Alicante

Prados Martínez F (2015) La necrópolis oriental de Baelo Claudia. Paisaje y arquitectura funerarios. In: Prados Martínez F, Jiménez-Vialás H (eds) La muerte en Baelo Claudia. Necropolis y ritual en el confín occidental del Imperio. Universidad de Cádiz-Universitat d'Alacant, Cádiz-Alicante, pp 81–96

Quintela M, Costa PJM, Fatela F et al (2016) The AD 1755 tsunami deposits onshore and offshore of Algarve (south Portugal): sediment transport interpretations based on the study of Foraminifera assemblages. Quat Int 408:123–138

Reicherter K, Becker-Heidmann P (2009) Tsunami deposits in the western Mediterranean: remains of the 1522 Almería earthquake? Geol Soc Lond 316 (1):217–235

Reicherter KR, Peters G (2005) Neotectonic evolution of the central Betic Cordilleras (southern Spain). Tectonophysics 405(1–4):191–212

Reicherter K, Vonberg D, Koster B et al (2010) The sedimentary inventory of tsunamis along the southern Gulf of Cádiz (southwestern Spain). Zeitschrift Für Geomorphologie, Supplementary Issues 54(3):147–173

Reicherter K, Vött A, Mathes-Schmidt M, Papanikolaou I (2019a) Signatures of extreme events recorded in geological archives of the Mediterranean. Zeitschrift Für Geomorphologie Supplementary Issues 62(2):1–6

Reicherter K, Vött A, Feist L et al (2019b) Lisbon 1755, Cruise No. M152/1, 02.11. - 14.11.2018, Funchal (Portugal)—Hamburg (Germany). Electronic report, METEOR-Berichte M152, Gutachterpanel Forschungsschiffe, Bonn. https://doi.org/10.2312/cr_m152

Reille M (1992) Pollen et spores d'Europe et d'Afrique du nord: Laboratoire de botanique historique et palynologie. URA CNRS, Marseille

Reille M (1995) Pollen et spores d'Europe et d'Afrique du nord Supplement 1, Laboratoire de botanique historique et palynologie. URA CNRS, Marseille

Reimer PJ, Austin WE, Bard E et al (2020) The IntCal20 Northern Hemisphere radiocarbon age calibration curve (0–55 cal kBP). Radiocarbon 62(4):725–757

Remolà Vallverdú JA (2000) Las ánforas tardo-antiguas en Tarraco (Hispania tarraconensis): siglos IV-VII d. C. Universitat de Barcelona, Barcelona

Rodríguez-Pascua MA, Pérez-López R, Giner-Robles JL et al (2011) A comprehensive classification of Earthquake Archaeological Effects (EAE) in archaeoseismology: application to ancient remains of Roman and Mesoamerican cultures. Quatern Int 242(1):20–30

Rodríguez-Ramírez A, Rodríguez-Vidal J, Cáceres L et al (1996) Recent coastal evolution of the Doñana national park (SW Spain). Quatern Sci Rev 15(8–9):803–809

Rodríguez-Ramírez A, Pérez-Asensio JN, Santos A et al (2015) Atlantic extreme wave events during the last four millennia in the Guadalquivir estuary, SW Spain. Quatern Res 83(1):24–40

Rodríguez-Ramírez A, Villarías-Robles JJ, Pérez-Asensio JN et al (2016) Geomorphological record of extreme wave events during Roman times in the Guadalquivir estuary (Gulf of Cadiz, SW Spain): an archaeological and paleogeographical approach. Geomorphology 261:103–118

Rodriguez-Vidal J, Caceres L, Abad M et al (2011) The recorded evidence of AD 1755 Atlantic tsunami on the Gibraltar coast. J Iberian Geol 177–193

Röth J, Mathes-Schmidt M, García Jiménez I et al (2015) The Baelo Claudia tsunami hypothesis: results from a multi-method sediment analysis of late-Roman deposits (Gibraltar Strait, Southern Spain). In: Blumetti AM (ed) 6th international inqua meeting on paleoseismology, active tectonics and archaeoseismology. INQUA 2015, 19–24 April, Pescina, Italy, pp 418–422

Ruiz F, Rodríguez-Ramírez A, Cáceres LM et al (2004) Late Holocene evolution of the southwestern Doñana National Park (Guadalquivir Estuary, SW Spain): a multivariate approach. Palaeogeogr Palaeoclimatol Palaeoecol 204:47–64

Ruiz F, Rodríguez-Vidal J, Abad M et al (2013) Sedimentological and geomorphological imprints of Holocene tsunamis in southwestern Spain: an approach to establish the recurrence period. Geomorphology 203:97–104

Scott L (1992) Environmental implications and origin of microscopic Pseudoschizaea Thiergart and Frantz ex R. Potonié emend. in sediments. J Biogeogr 19 (4):349–354

Sillières P (1997) Baelo Claudia: una ciudad romana de la Bética. Junta de Andalucía-Casa de Velázquez, Madrid

Silva PG, Borja F, Zazo C et al (2005) Archaeoseismic record at the ancient Roman city of Baelo Claudia (Cádiz, south Spain). Tectonophysics 408(1–4):129–146

Silva PG, Goy JL, Zazo C et al (2006) Neotectonic fault mapping at the Gibraltar Strait Tunnel area, Bolonia Bay (South Spain). Eng Geol 84:31–47

Silva PG, Reicherter K, Grützner C et al (2009) Surface and subsurface palaeoseismic records at the ancient Roman city of Baelo Claudia and the Bolonia Bay area, Cádiz (south Spain). Geol Soc Lond 316(1):93–121

Silva PG, Bardají T, Roquero E et al (2015) Seismic palaeogeography of coastal zones in the Iberian Peninsula: understanding ancient and historic earthquakes in Spain. Cuaternario y Geomorfología 29(1–2):31–56

Silva PG, Giner-Robles J, Reicherter K et al (2016) Los terremotos antiguos del conjunto arqueológico romano de Baelo Claudia (Cádiz, Sur de España): Quince años de investigación arqueosismológica. Estudios Geologicos 72(1):1–24. https://doi.org/10.3989/egeol.42284.392

Silva PG, Rodríguez-Pascua MA, Giner-Robles JL et al (2014) Catálogo de los efectos geológicos de los terremotos en España. Serie Riesgos Geológicos y Geotecnia, 4. IGME, Madrid

Silva PG, Rodríguez-Pascua MA, Giner-Robles JL et al (2019) Catálogo de Efectos Geológicos de los terremotos en España. 2ª edición (revisada y ampliada). Serie Riesgos Geológicos y Geotecnia, 6. IGME, Madrid

Smedile A, De Martini P, Pantosti D et al (2011) Possible tsunami signatures from an integrated study in the Augusta Bay offshore (Eastern Sicily–Italy). Mar Geol 281(1–4):1–13

Smedile A, Molisso F, Chagué C et al (2020) New coring study in Augusta Bay expands understanding of offshore tsunami deposits (Eastern Sicily, Italy). Sedimentology 67(3):1553–1576

Stiros SC (2001) The AD 365 Crete earthquake and possible seismic clustering during the fourth to sixth centuries AD in the Eastern Mediterranean: a review of historical and archaeological data. J Struct Geol 23(2–3):545–562

Stiros SC, Papageorgiou S (2001) Seismicity of Western Crete and the destruction of the town of Kisamos at AD 365: archaeological evidence. J Seismolog 5(3):381–397

Stiros SC (2010) The 8.5+ magnitude, AD365 earthquake in Crete: Coastal uplift, topography changes, archaeological and historical signature. Quatern Int 216(1–2):54–63

Stockmarr J (1971) Tabletes with spores used in absolute pollen analysis. Pollen Spores 13:615–621

Stuiver M, Reimer PJ, Reimer RW (2020) CALIB 7.1. [WWW program] at http://calib.org. Accessed 2020–1–9

El Talibi H, El Moussaoui S, Zaghloul MN et al (2016) New sedimentary and geomorphic evidence of tsunami flooding related to older events along the Tangier-Asilah coastal plain, Morocco. Geoenviron Disasters 3:14, 21. https://doi.org/10.1186/s40677-016-0049-6

van Geel B (1978) A palaeoecological study of Holocene peat bog sections in Germany and The Netherlands, based on the analysis of pollen, spores and macro- and microscopic remains of fungi, algae, cormophytes and animals. Rev Palaeobot Palynol 25:1–120

van Geel B (1986) Application of fungal and algal remains and other microfossils in palynological analyses. In: Berglund BE (ed) Handbook of holocene palaeoecology and palaeohydrology. Wiley & Sons Ltd., Chichester, pp 497–505

van Geel B, Bohncke S, Dee H (1980) A palaeoecological study of an upper Late Glacial and Holocene sequence from “De Borchert”, The Netherlands. Rev Palaeobot Palynol 31:367–448

van Geel B, Coope GR, van der Hammen T (1989) Palaeoecology and stratigraphy of the Lateglacial type section at Usselo (The Netherlands). Rev Palaeobot Palynol 60(1–2):25–129

van Geel B, Buurman J, Brinkkemper O et al (2003) Environmental reconstruction of a Roman Period settlement site in Uitgeest (The Netherlands), with special reference to coprophilous fungi. J Archaeol Sci 30(7):873–883

Vött A, Brückner H, May M et al (2008) Strong tsunami impact on the Bay of Aghios Nikolaos and its environs (NW Greece) during Classical-Hellenistic times. Quatern Int 181(1):105–122

Werner V, Baika K, Fischer P et al (2018) The sedimentary and geomorphological imprint of the AD 365 tsunami on the coasts of southwestern Crete (Greece)–examples from Sougia and Palaiochora. Quatern Int 473:66–90

Werner V, Baika K, Tzigounaki A et al (2019a) Mid-Holocene tectonic geomorphology of northern Crete deduced from a coastal sedimentary archive near Rethymnon and a Late Bronze Age Santorini tsunamite candidate. Geomorphology 326:167–189

Werner V, Baika K, Tzigounaki A et al (2019b) Extreme wave events recorded in sedimentary archives of the Geropotamos River (north-central Crete, Greece). Zeitschrift Für Geomorphologie Supplementary Issues 62(2):63–100

Whelan F, Kelletat D (2003) Analysis of tsunami deposits at Cabo de Trafalgar, Spain, using GIS and GPS technology. Essener Geographische Arbeiten 35:11–25

Whelan F, Kelletat D (2005) Boulder deposits on the southern Spanish Atlantic coast: possible evidence for the 1755 AD Lisbon tsunami. Sci Tsunami Haz 23(3):25–38

Zazo C, Silva P, Goy J et al (1999) Coastal uplift in continental collision plate boundaries: data from the Last Interglacial marine terraces of the Gibraltar Strait area (south Spain). Tectonophysics 301(1–2):95–109

Zazo C, Dabrio CJ, Goy J et al (2008) The coastal archives of the last 15 ka in the Atlantic-Mediterranean Spanish linkage area: sea level and climate changes. Quatern Int 181(1):72–87

14 A Late Roman Earthquake on the Southern Shore of the Strait of Gibraltar: Archaeoseismological Evidence in *Septem*

Darío Bernal-Casasola, Fernando Villada Paredes, Klaus Reicherter, José A. Retamosa Gámez, José L. Portillo Sotelo, and Rosario García Giménez

Abstract

Recent archaeological work in the so-called "Baluarte de la Bandera" in *Septem* (modern Ceuta), on the African coast of the Strait of Gibraltar, has led to the discovery of a series of defensive features. These probably belonged to the city wall built in the late second or early third century AD. The upper section of a wall, which was originally over 3 m high, appears to have collapsed dramatically. Together with various large vertical cracks, this suggests that it was caused by an earthquake. Part of the wall fell on top of a stratigraphic sequence which has been securely dated, based on the associated ceramic material and radiocarbon dates, to the second half of the seventh-century AD, which is, therefore the *post quem* date for the earthquake.

This work presents the hitherto unpublished constructive phases discovered during the 2018 excavation season, as well as seismic damage caused by an earthquake which is conspicuous by its absence in existing catalogues. It is the first earthquake to be detected in North Africa during this period. Similarly, we also analyse broader issues relating to the *Fretum Gaditanum*, where several seismic events are attested for the Roman period, especially in the nearby city of *Baelo Claudia*, while re-examining the chronology of these late Roman seismic events (tsunamis and earthquakes) based on archaeological indicators.

Keywords

Late antiquity · Ceuta · North Africa · Earthquake · Archaeoseismology · Seventh-century AD

D. Bernal-Casasola (✉) · J. A. Retamosa Gámez · J. L. Portillo Sotelo
Departamento de Historia, Geografía y Filosofía, Facultad de Filosofía y Letras, Universidad de Cádiz. Área de Arqueología, Avda. Dr. Gómez Ulla 1, 11003 Cádiz, España
e-mail: dario.bernal@uca.es

J. A. Retamosa Gámez
e-mail: jose.retamosa@uca.es

J. L. Portillo Sotelo
e-mail: joseluis.portillo@uca.es

F. Villada Paredes
Consejería de Educación y Cultura. Sección de Patrimonio Cultural. c/Ingenieros s/n, Ciudad Autónoma de Ceuta, 51001 Ceuta, España
e-mail: fvillada@ceuta.es

K. Reicherter
Lehr- und Forschungsgebiet Neotektonik und Georisiken, RWTH Aachen University, Lochnerstr. 4-20, 52056 Aachen, Germany
e-mail: k.reicherter@nug.rwth-aachen.de

R. García Giménez
Departamento de Geología y Geoquímica, Facultad de Ciencias, Universidad Autónoma de Madrid, C/Francisco Tomás y Valiente, 7, 28049 Madrid, Spain
e-mail: rosario.garcia@uam.es

M. Álvarez-Martí-Aguilar and F. Machuca Prieto (eds.), *Historical Earthquakes, Tsunamis and Archaeology in the Iberian Peninsula*, Natural Science in Archaeology,
https://doi.org/10.1007/978-981-19-1979-4_14

14.1 Introduction: Ceuta, the Principal Late Roman City in the Strait of Gibraltar

The Strait of Gibraltar has played a crucial historical role as the hinge between the Atlantic and the Mediterranean, and as the conduit for the active maritime commerce adopted as a *modus vivendi* by all the human groups that have inhabited, at least since the arrival of the Phoenicians in the Archaic period. In late Antiquity, seen from a *longue durée* perspective—i.e. between the third century and the arrival of Islam in the early eighth century AD (Brown 2012)—the core of the so-called "Circle of the Strait", that is, the region between Ceuta, Tangier, Tarifa and Algeciras (Bernal-Casasola 2016), became even more important when these harbours assumed the commercial activity that *Gades* had virtually monopolised until the early second century AD.

The key cities on the European shore of the Strait of Gibraltar during the late Antiquity were *Carteia* and *Traducta*. The former was in decline as of the late fifth century, but it was still important until at least the late sixth century AD. Meanwhile, the *garum* factories of Algeciras continued in full swing until the early sixth century AD, before the Byzantine occupation (Bernal-Casasola and Jiménez-Camino 2018). On the African shore, *Mauretania Tingitana*, mention should go to *Tamuda*, the northernmost military camp on the south-western frontier, which remained active until the early fifth century AD (probably until the reign of Honorius), and the capital *Tingi* (modern Tangier), which is likely to have been the most important city in northern Morocco, although we cannot say for certain for its archaeology is very poorly known as a result of its recent urban development (Villaverde 2001, pp. 78–96).

Other important cities, referred to in the Classical sources as *fortissimae civitates*, are located inland, in an attempt to avoid the dangers of the coastline in a convulse age; this process of *incastellamento* is wonderfully illustrated by the city of *Sidonia*—modern Medina Sidonia (for synthesis see Bernal-Casasola 2018).

However, if one city stood out from the rest on the seaboard of the *Fretum Gaditanum* during late Antiquity that would have been *Septem Fratres* (modern Ceuta), the word *Septem* referring to the seven hills that could be seen from the sea (Gozalbes 1990). This city was both strategically located and easy to defend, two features that were to play a central role throughout its history (Fig. 14.1a, b). It was also among the few to have maintained a stable population from the Roman period to the eighth century AD, as well as the only western city to be privileged by Justinian during his project to reconquer the Roman Empire; the city, after being taken by the Byzantines in 533, would maintain close links with the east until the late seventh-century AD. This relationship is at the root of the tale of Count Don Julián (called Urban in other sources), who allegedly paved the way for the Islamic conquest of *Hispania* out of hatred for his arch-enemies, the Visigoths (for a historical perspective, see Gozalbes 1986; Vallejo 1993, 2012, for the archaeological evidence, see Bernal-Casasola 2013).

In Ceuta, the archaeology preceding the Islamic period is complex, as later urban developments have tended to erase the topography and urbanism of its predecessors (Roman, late Roman, medieval, early modern and modern). In addition, owing to its strategic location, after the Portuguese conquest of 1415, the city was surrounded by a comprehensive and very well-preserved system of fortifications (see Fig. 14.1c)—the Murallas Reales—which were modified and expanded several times (Villada 2012). These walls, which literally "surrounded" the whole isthmus between Monte Hacho and Campo Exterior, still house the remains of older fortification systems. Since 2003, archaeological works have been exploring the interior of the Murallas Reales: first, the excavation and display of the so-called "Puerta Califal" (Caliphal Gate), which has a very long archaeological sequence spanning from the Palaeolithic up to the present day; and second, since 2014, in the so-called "Baluarte de la Bandera" (or del Torreón), on which this chapter focuses (Villada and Bernal-Casasola 2019). The excavation was complex since, as noted, it took place inside the Portuguese and Early Modern defensive system (Fernández Ahumada and Villada 2017, pp. 64–66), under the space created by the fortified vaults (see Fig. 14.1c, d). The archaeological sequence spans from the Roman period up to the present day. To date, the results of these recent excavations remain unpublished, except for a brief note (Villada and Bernal-Casasola 2019, pp. 201–205). Accordingly, in order to analyse clearly the evidence for the earthquake, we must first describe the different construction phases in detail and establish their chronology. We will first summarise the archaeological works undertaken to date (Sect. 14.2), followed by a description of the features dated to the Severan (Sect. 14.3) and late Roman (Sect. 14.4) periods, before addressing the earthquake (Sect. 14.5) and the associated strata and chronological markers. Lastly, we will present archaeoseismological parallels in the area of the Straits during late Antiquity and also the project's future prospects (Sect. 14.6).

14.2 Archaeology in the Baluarte de la Bandera (Excavations, Phases and Features)

In October 2018, the autonomous city of Ceuta and the University of Cádiz began a joint project for the study of the pre-Islamic sequence inside the Baluarte de la Bandera, or del Torreón. The project's primary aim was to clarify the site's complex architectural sequence; a large number of substantial pre-Islamic features (between 3 and 4 m high) were known to exist, but their function and chronology was unclear; in addition, these structures presented a series of pathologies which, owing to their severity, could be taken as an indication of an earthquake.

Three previous excavation seasons had been conducted, in 2014, 2016 and 2017. The aim of excavation was to progressively explore the archaeological sequence in the Baluarte de la Bandera (165 m^2) by a succession of soundings that adapted to the modern structures and the many associated logistical problems, which are the main reason that forced us to rule out an open area approach (see Fig. 14.2). The ultimate objective is to excavate the inside fully and to exhibit the most relevant structures in a future *Centro de Interpretación de la Muralla Real*, the project which is already in progress.

The first of these excavation seasons consisted in three soundings: two in the bastion's main room (Soundings 1 and 2) and another to the south, far from the area of most interest to us, which did not result in any significant pre-Islamic findings. The other two soundings identified the top of three substantial walls (hereinafter, these walls will be referred to with their final number, as illustrated in Fig. 14.3): on the one hand, a thick section of Ceuta's Caliphate period wall, whose façade is lined with blocks of calcarenite laid out in a characteristic stretcher and double-header pattern. This was identified in Sounding 1, and in several smaller soundings to the north and south of the bastion. There can be little doubt that this belongs to the fortifications built by Abd al-Rahman III in the third quarter of the tenth-century AD (Hita and Villada 2009, pp. 249–252). Other sections of these walls have been found in the Baluarte de los Mallorquines, the Puerta de Santa María, Queipo de Llano Street, the Baluarte de la Coraza and especially in the Puerta Califal (Hita et al. 2008; Hita and Villada 2004). The building technique responds to the typical Cordovan model, also found in the nearby *alcázar* of Tarifa (Villada and Gurriarán 2013). In addition, the excavation uncovered the top of another set of walls (M-2, M-8 and M-3/M-4), which were preliminarily dated to late Antiquity (Villada and Ortuño 2014).

In the 2016 season (BMR'16), seven soundings were planned (A-G), Sounding G being the only one in the main space of Baluarte de la Bandera (see Fig. 14.3), while the rest were opened inside the vaults that were built abutting the Muralla Real in the eighteenth century (Vaults 1, 2 and 3). The site's main phases were established during this season, which also led to

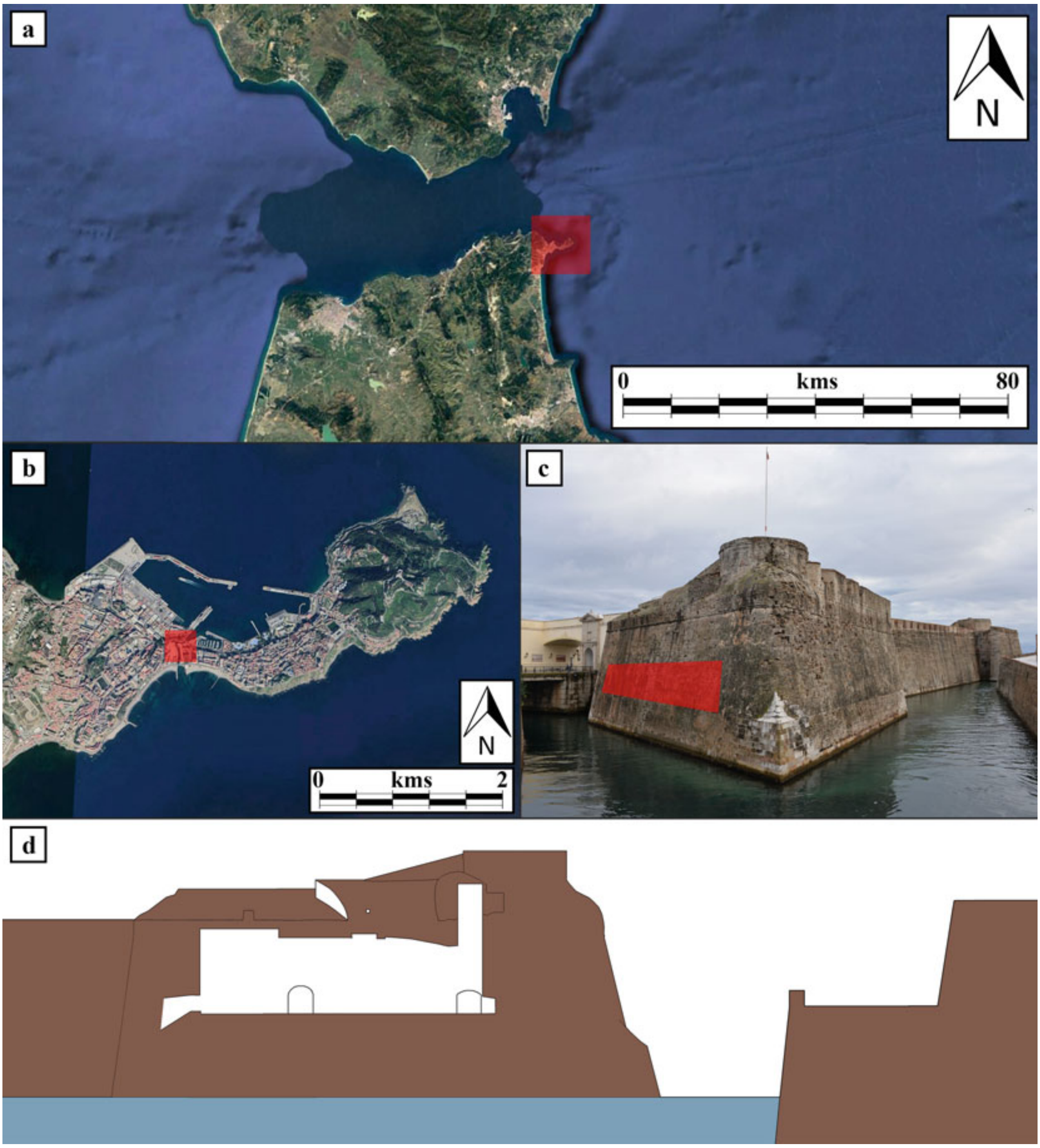

Fig. 14.1 Ceuta in the Strait of Gibraltar region (**a**), with urban topography and the location of the excavation in the seismic area (**b**); the Baluarte de la Bandera from the outside (**c**); N–S section of the Baluarte, based on historical plans, and a perspective of the interior of the excavated vault (**d**)

the uncovering of a series of structures tentatively identified as "pre-Islamic, possibly late-Roman and Byzantine in date"; these were beneath a much more recent phase (a forge) and the layers corresponding to the construction of the bastion by the Portuguese and Castilians (Villada and Godoy 2007, pp. 59–64). Especially interesting are a series of anomalous burials dated to the seventh century, during the Byzantine period. The bodies, which had their limbs amputated and were cremated in situ, were found in association with some remains of wool fabric and a belt made with the leaves of date palms. The humble nature of their clothing, along with the remaining evidence, suggests that they may have been executed (Bernal-Casasola et al.

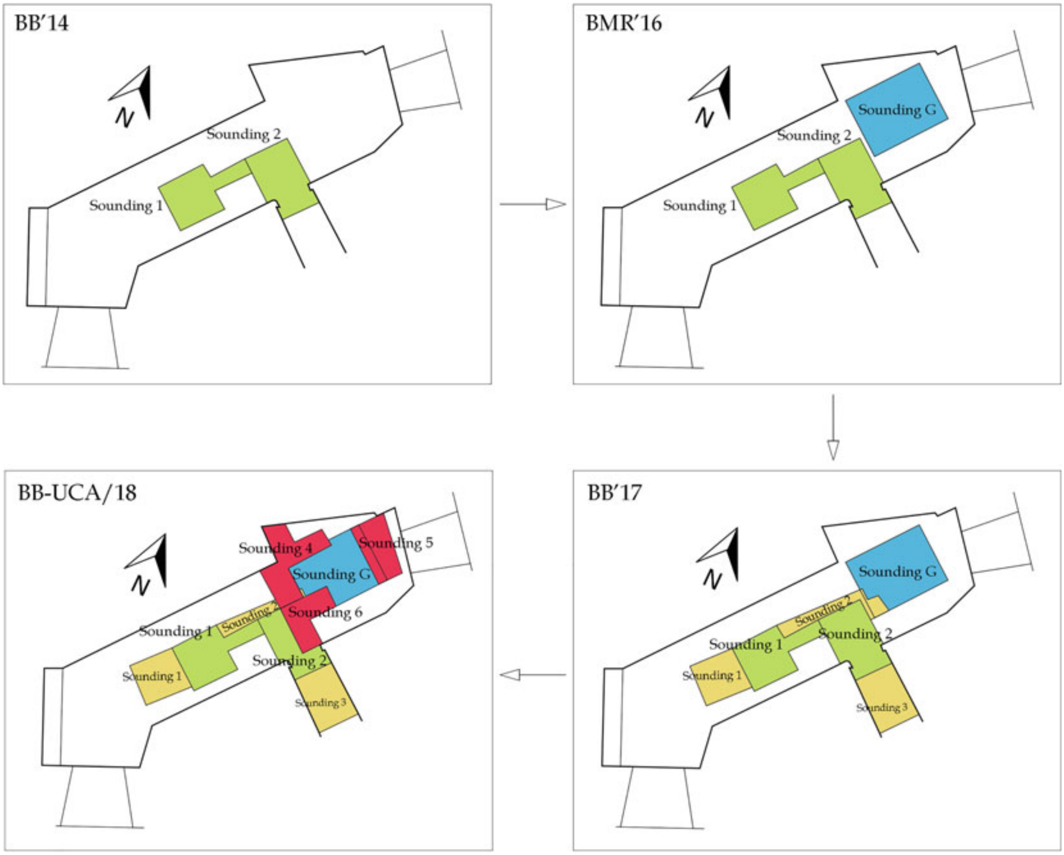

Fig. 14.2 Areas excavated in the Baluarte de la Bandera between 2014 and 2018

2020a); this excavation season also resulted in the identification of several ashlar blocks reused in the foundations of the late Roman wall—to which we will return shortly—as well as several coins—including an *As* from Cástulo dated to 165–80 BC (CNH 335–336, no. 38–41)—and pottery—possible Haltern 70 and Beltrán II A amphorae—which suggest that the construction of these walls cut through earlier deposits (Villada and Bernal-Casasola 2019, pp. 201–203), above all dating to the reigns of Juba II or Augustus, which is the earliest archaeological horizon (largely constituted by non-contextualised finds) of *Septem Fratres* as a Roman city (Bernal-Casasola 2013).

In the 2017 season (BB'17), the excavation area was extended, linking Soundings 1 and 2 from the 2014 season and G from the 2016 season (see Fig. 14.3). In order to do this, three more soundings (1, 2 and 3) were opened, resulting in an excavated area occupying virtually the whole of the interior of the Baluarte de la Bandera (Villada et al. 2017).

The soundings have reached the bottom of the archaeological sequence in most areas of the site. The main exceptions are the fills in the areas adjacent to the structures, which were left in place so as not to undermine them. However, in 2018 a new excavation was undertaken to facilitate the interpretation of the sequence. This aimed to chronologically and functionally characterise the standing features (BB-UCA/18). In order to meet this target, three small soundings were opened (4, 5 and 6). They were "high precision" soundings opened around Sounding G, with a view to performing a more detailed

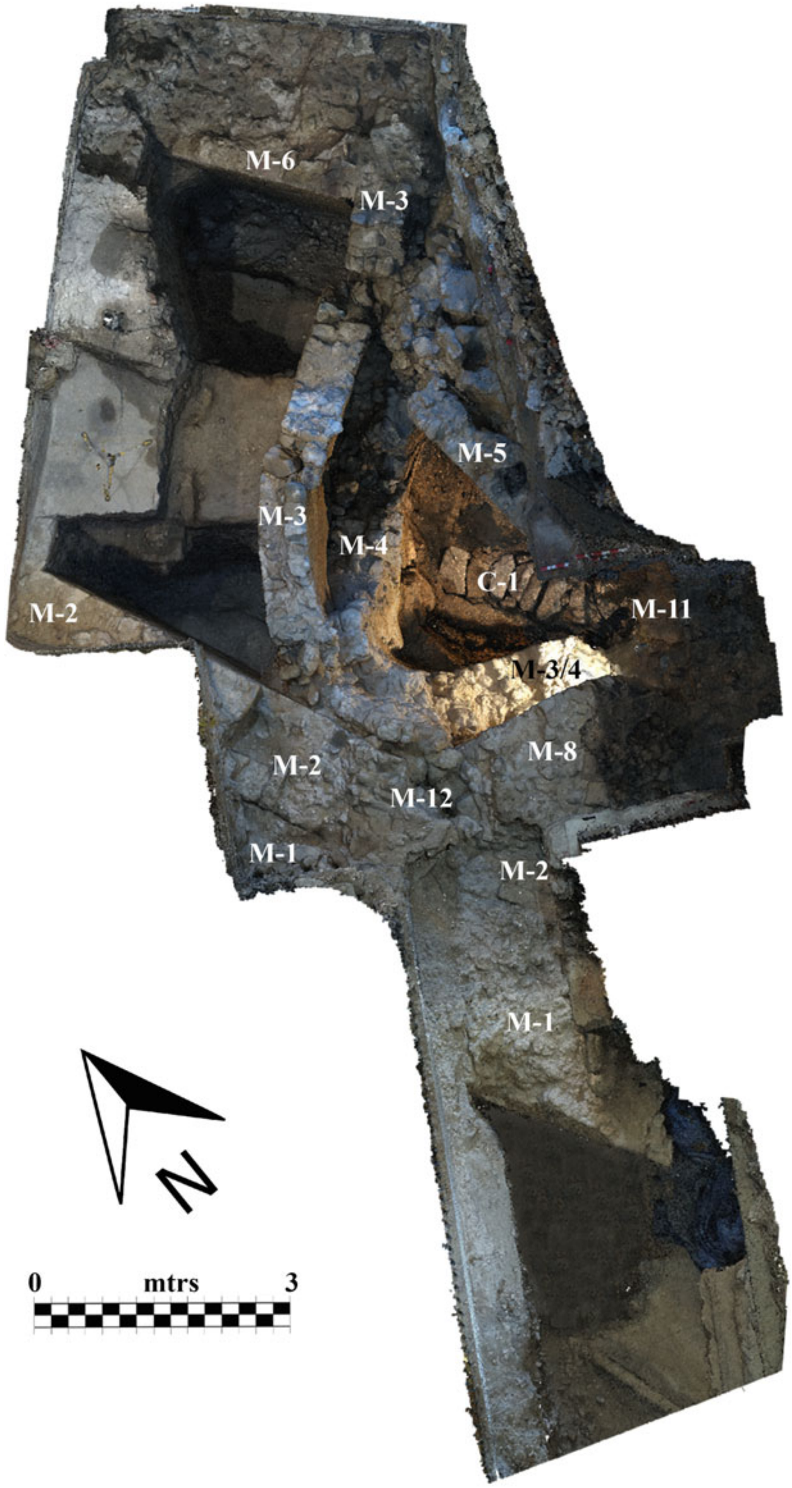

Fig. 14.3 Wall built during the Caliphate period (M-1) and late Roman structures found in the Baluarte de la Bandera (ortophotograph based on photogrammetric imaging—2018)

autopsy of the emerging features and to remove the fills with which they were levelled during Antiquity.

The results of the 2018 season, along with the data collected in previous seasons, allowed us to define a series of archaeo-historical horizons spanning the whole sequence of the site. As illustrated by the correlation matrix (see Fig. 14.4), seven phases were defined. These are briefly described below, before examining the late Roman phases (II, III and IV) in more detail.

14.2.1 Phase I. Late Republican–Early Imperial: Unknown Function

This phase could be identified only at the bottom of Sounding G, to the west of M-6, excavated in 2016. It consists of a possible pavement (C044) laid out with amphorae fragments and other late Republican or first-century-AD material (Haltern 70 and Beltrán IIA amphorae), and was where the *As* struck in Cástulo, which is probably a relict (Villada and Godoy 2017), was unearthed. In addition, the 2017 season led to the identification of a similar pavement above Channel C-1, which was preliminarily interpreted as the interior frequentation level of a possible tower (UE 2023) (Villada et al. 2017). The 2018 excavation of Sounding 4, however, did not reach this level, which will hopefully be explored in the near future. At any rate, the Byzantine levels have yielded some ceramic material from this period, found in a secondary position, especially two Vesuvian amphorae fragments (UE 4006) and several fragments of Pompeian red slip ware (UE 4007), which indirectly confirm the existence of remains dated to the Augustan period, if not earlier, at the site. Several such relicts have also been identified in more recent layers, including fragments of amphorae made in Cádiz in the early Imperial period (their typology could not be defined) (UE 6000/6001) and the wall of a Dressel 20 oil amphora made in the Guadalquivir valley in the fill of Channel C-1 (UE 6003).

These finds tally with what we know about the archaeological sequence of *Septem Fratres*. The earliest remains known to date, in the nearby Puerta Califal, are dated to Claudius' (AD 40–60) and Trajan's (AD 98–117) reigns, although out-of-context remains from earlier periods have also been attested (Bernal-Casasola 2013, p. 16, note 12); especially of note are the Italian *sigillatas* published by Posac and Daura, the re-examination of which has recently led to the sound identification of several known shapes and more than 10 stamps dated to between the Augustan period and the AD 30s (Bustamante 2010, pp. 74–83, appendices II and III). Indirectly, other finds have been interpreted as evidence for the proximity of public buildings: several architectural elements—including four ashlar blocks, three of which present carved half-columns—possibly from the façade of one of these late Mauritanian or early Imperial buildings, were reused in the foundations of the earliest late Roman urban wall (Bernal-Casasola et al. 2020b), as we shall see shortly.

14.2.2 Phase II. Early Late Roman (from the Late Antonine to the Early Severan Period): Construction and Use of Possible Defensive Structures

Most of the features identified are dated to this period (especially M-3/M-4, M-11 and Channel C-1). In view of the building techniques employed and their dimensions, these structures are reminiscent of the sort of fortifications found in military camps, being interpreted as *Septem Fratres*'s urban wall. The building techniques used (lime mortars and *opus vittatum* with pseudo-courses of brick) and the reuse of ceramic fragments date this wall to the late second or early third century AD onwards, as will be seen in more detail in Sect. 14.3. Some later structures appear abutting it, such as the interior supporting wall (M-5) or the external tower (M-6). These

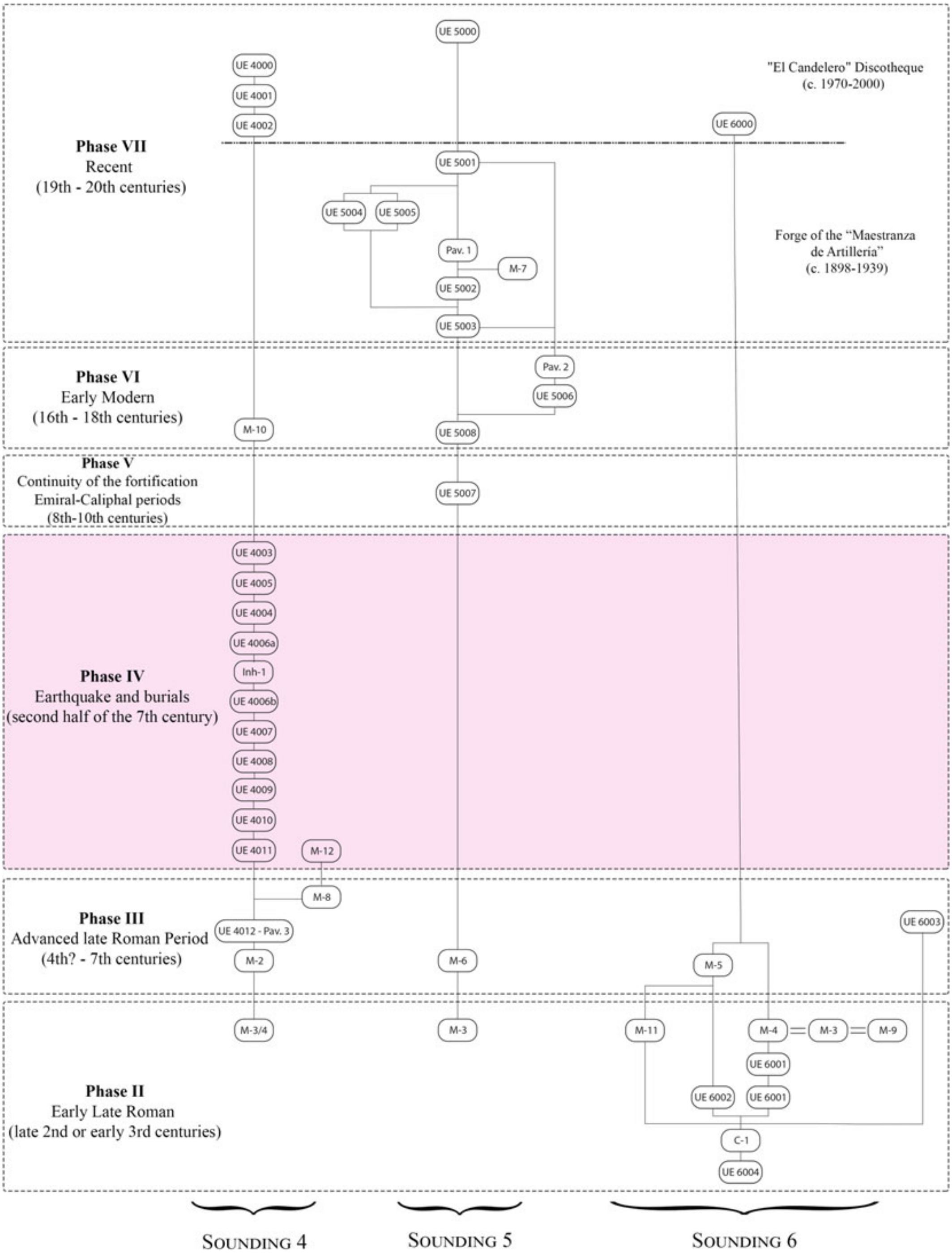

Fig. 14.4 Stratigraphic matrix for the 2018 season

features are, as noted, later in date, and will be examined in detail in the following section. Based on the stratigraphy, it is difficult to establish a clear-cutting point between both phases.

14.2.3 Phase III. Advanced Late Roman Period (from the Late Imperial Period or the Vandal Period, to the First Half of the Seventh Century): Addition of Defensive Elements and Construction of the (Byzantine?) Wall

It has proven to be impossible to assign a precise date to the features that belong to this construction phase, because the foundation trenches of its three main features remain unexcavated: the supporting wall (M-5), built in the interior angle of the urban wall, on top of a previous feature; a wall, interpreted as belonging to a square tower (M-6) built outside the urban wall; and, finally, a solid structure (M-2), the orientation of which (NE-SW) is clearly different from those of the two previous features, and must, therefore, belong to a different building programme (the building techniques suggest that M-2 is significantly later than M-6, although there is no way of confirming this with the evidence available). We can only posit an *ante quem* date for these features, based on the sedimentary sequence found between M-2 and M-3 (Sounding 4), which is dated to the second half of the seventh century (this sequence overlays M-2 and M-6, which are therefore earlier).

14.2.4 Phase IV. Second Half of the Seventh Century: Earthquake and Burials

The city wall exhibits several pathologies: on the one hand, the fracture, collapse and horizontal movement of M-3/M-4 (this event led us to take M-3—top part—and M-4—bottom part—separately); and, on the other, a number of large vertical cracks at the base of the walls, matching with the joints between the abovementioned reused blocks that lie at its base (Bernal-Casasola et al. 2020b). In M-3, the horizontal crack is compounded by three vertical cracks that made different sections collapse unevenly. The two westernmost sections, 2 and 3, did not collapse northwards, as they should have done, but shifted horizontally, rotated vertically (which is interpreted as indicative of seismic motion) and buckled slightly. The fills that accumulated in the northern sector of Sounding 4 arrested the fall of this wall section. Therefore, the chronology of this fill represents a *post quem* date for the earthquake, which has thus been dated to the second half of the seventh century (Bernal-Casasola et al. 2020c). In addition, M-3 seems to have collapsed against M-2 as a result of the earthquake, causing the fracture between M-2 and M-8. It seems that this crack was repaired with mortar immediately after the event (M-12) (see Fig. 14.3).

The strata overlying this sedimentary sequence, deposited in the immediate aftermath of the seismic event, still contain material dated to the second half of the seventh century. They are associated with a series of peculiar burials: the bodies had their limbs amputated and were cremated in situ (Villada and Godoy 2017). As already noted, their carbonised attires have survived (Bernal-Casasola et al. 2020a).

14.2.5 Phase V. Emirate-Caliphate Periods (Eighth to Tenth Centuries): Possible Continuity of the Fortification, and Construction of Abd Al-Rahman III's Fortification

The main event in this phase was the construction of a major wall lined with blocks of calcarenite, laid out in stretchers and double headers (M-1), which used M-2 as its foundations. This is a section of the tenth-century urban wall which, according to the written sources, was initiated by Abd al-Rahman al-Nasir (d. 961) and finished by his heir al-Hakam (915–976) (Hita et al. 2008; Villada and Bernal-Casasola 2019, p. 200). A levelling fill laid out over the late Roman structures (M-6 and M-3) was identified in the eastern sector of Sounding 5 and in the area between both structures (UE 5007/C041): the discovery of a lamp with a short nozzle and a wide base and common and glazed ware help to date this fill to the period of the Emirate or Caliphate. Owing to its extremely compact nature, part of this fill has yet to be removed. All the evidence suggests that the fill inside tower M-6 was deliberate, whose aim was to create a solid flat terrace, so we may date it to the opening years of this phase. The fact that the tenth-century wall (M-1) abuts the late Roman wall (M-2) indicates that the latter was still visible during this period, and it seems likely that these walls remained fully in use until the arrival of the Umayyads (Hita and Villada 2009, pp. 207–217).

14.2.6 Phase VI. Early Modern (XVI–XVIII)

This period witnessed the construction of the sixteenth-century Portuguese fortification. These defensive structures remained in use until the eighteenth century: for this period, the written record is abundant, and we also possess many plans, maps and written documents (Braga and Braga 2009; Carmona 2009; Martín Corrales 2009). In addition, these fortifications have received a good deal of archaeological attention and, as this period lies well outside the scope of this chapter, readers with further interest should consult the references provided (Villada 2012). During our 2018 excavation, we documented only one feature relating to these fortifications: a ball of mortar used to support the foot of the blind arch to the north of the bastion, identified during the excavation of Sounding 5 (UE 5006).

14.2.7 Phase VII. Recent (XIX–XX)

This phase can be divided into two periods. The first is related to the military use of these structures up until the Spanish Civil War, including the forge and other evidence for metalworking identified in 2016. In addition, numerous Mauser bullet shells, metal scoria and ashes, probably associated with an armoury, have been identified (Contreras 2010). The second period corresponds to the use of this area as a nightclub, after it was sold to Empresa Nacional de Turismo (ENTURSA), resulting in the installation of various pavements and wall claddings, benches, air conditioning systems, etc., which are also well outside the scope of this chapter.

14.3 The Earliest Late Roman Structures—Late Antonine to Early Severan Period (Phase II)—Affected by the Late Roman Earthquake

14.3.1 Dating Problems

The first question that should be addressed is the chronology of these structures, which are the largest at the site and which, as already observed, are related to other defensive structures in the city (M-3/M-4, C-1 and M-11 and later reforms: M-5 and M-6). Previous excavations confirmed the complex stratigraphy of the area and the absence of clear strata relating to the features. This was confirmed once more in 2018. As a result, other ways had to be devised to try to define the chronology of these structures.

One was the archaeometric analysis of the mortars used in the features that had already been revealed prior to the 2018 excavation. Five features were analysed in this way.[1] X-ray diffraction was used to characterise the mineralogical composition of the mortars and the lime/sand ratio. This technique is both easy to apply and reliable, because as lime carbonates fast it can easily be detected in the form of calcite; it is also an effective way of characterising sand (González Limón and De Buergo Ballester 2002; Sánchez et al. 2004). After grinding the mortars in an agate mortar, they were analysed by X-ray diffraction (XRD) using the random powder method for the bulk sample and the oriented slides method for the <2 μm fraction. The X-ray diffractometer is a SIEMENS D-5000 with a Cu anode, operated at 30 mA and 40 kV using divergence and reception slits of 2 and 0.6 mm, respectively. The XRD profiles were measured in 0.04 2θ goniometer steps for 3s.

As shown in Fig. 14.5f, the mortars were characterised as follows:

(a) Based on the mineralogical analysis. Sands were silicated. C-1 and M-3 contained very high proportions of quartz (77% and 68%, respectively; see Fig. 14.5a, c); and M-4 and M-6 (see Fig. 14.5b, e) had a similar proportion of quartz and feldspars.

(b) Based on the lime/sand ratios, which were similar in C-1 and M-3 and in M-4 and M-6. Two pairs could be clearly distinguished: Channel C-1 and Wall M-3, and Features M-4 and M-6. The mortar found in M-5 was different, containing low proportions of quartz (33%) and silicates and a high lime/sand ratio. In addition, the mineralogical analysis included multiple inclusions of ground volcanic rock, which was visible in the form of dark spots. These compositional differences suggest that these mortars were made in different periods, thus confirming the stratigraphic disposition of the features, which presented substantial *decalage* between them.

Another way to try to establish the chronology of these features was by analysing the pottery reused in some of them, especially in Walls M-3/M-4 and M-5 and to a lesser extent in M-2 and M-6, in order to obtain dates *post quem*. The structures were thoroughly examined, and eight large diagnostic fragments were selected (see Fig. 14.6). As noted, M-3/M-4 exhibited multiple fragments in both the interior and on the surfaces. Over 50 individual ones were recorded, a much greater concentration than normal. Over 50% of these fragments corresponded to walls of amphorae (with sides between 5 and 10 cm long), plus the occasional *tegulae* and bricks; fragments of coarse wares and large containers were much rarer. The eight samples selected are as follows (see Figs. 14.6 and 14.7).

Upper interface M-3/M-4

- CER-1. Rim of a Baetican amphora, subrectangular. Puerto Real I/II type. It was extracted alongside Mortar Sample 3.
- CER-2. Rim of a Baetican amphora. Puerto Real I/II type. It bears a retrograde "SOCI" stamp, *in collo*, behind the handle. Yellowish fabric. Coming from the bay of Cadiz, it formed a cluster with other similar fragments, all of which were strongly bound by mortar.
- CER-03. Near CER-2, the wall of two African amphorae was identified, owing to their characteristic white slip and red fabric with quartz-based tempers. Albeit cylindrical, their specific type is unclear.
- CER-04. Found in the northern cornice of the upper interface. Rim of a large open shape. Common ware.

Northern face of M-3/M-4

- CER-05. Found 20 cm below CER-04. Two fragments of the semi-circular rim of a short-necked Baetican oil amphora, folded outwards and shallowly concave in profile. Both fragments are heavily worn in contrast with the

[1] Mortar A1. Interior of the covering of the Roman channel (C-1), on the west side of one of the closing slabs; A2. Upper part of the interior facing of M-4; A3. Core of the upper interface of M-3; A4. Half height of the M-5 facing; A5. West facing of M-6, below the square hole. M-2 could not be sampled as it had not yet been clearly individualised when this archaeometric study was performed.

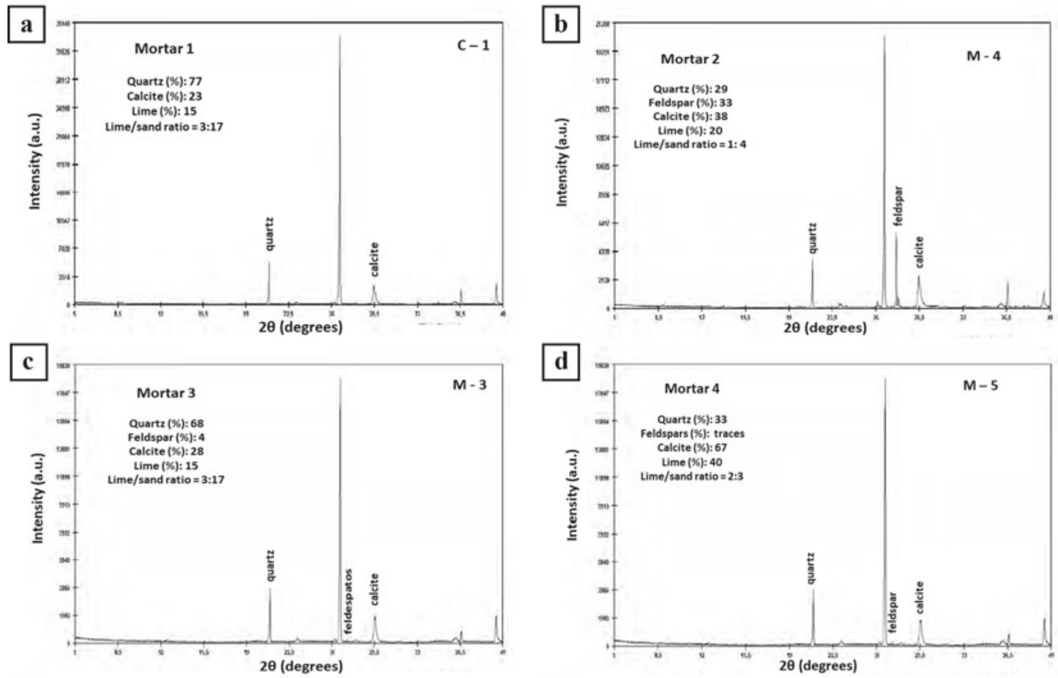

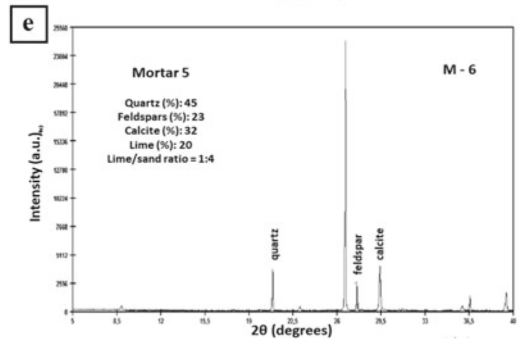

f

CHEMICAL COMPONENTS

Mortar	Quartz (%)	Feldspar (%)	Calcite (%)	Lime/sand ratio
1	77	n.d.	23	3/17
2	29	33	38	1/4
3	68	4	28	3/17
4	33	n.d.	67	2/3
5	45	23	32	1/4

Fig. 14.5 Diffractograms of the samples collected in Channel C-1 (**a**), and Walls M-4 (**b**), M-3 (**c**), M-5 (**d**) and M-6 (**e**), and a table with the mineralogical composition of the mortars (**f**)

others, the breaks of which are much sharper. Although the profile is reminiscent of the Dressel 23 type, a residual Dressel 20 type seems more likely.

Southern face of M-3/M-4

– CER-06. Extracted from the topmost section of the wall. The fill has yielded approximately 10 fragments of amphorae and also tableware. Wall of an open shape (plate or dish) in ARSW (African Red Slip Ware) A.[2] It has substantial mortar remains.
– CER-07. Same location CER-06, but slightly to the east. Indeterminate shape in ARSW A[1].

Northern face of M-5

– CER-08. Found above a limestone slab in the western central area of the wall, approximately 1.60 m from its base. As the fragment was deeply embedded in the wall, and was hard to see, it had to be extracted with a trowel. It belongs to an Almagro 51c amphora type, with the stem of the handle and a white slip. The intense red clay with white quartz-

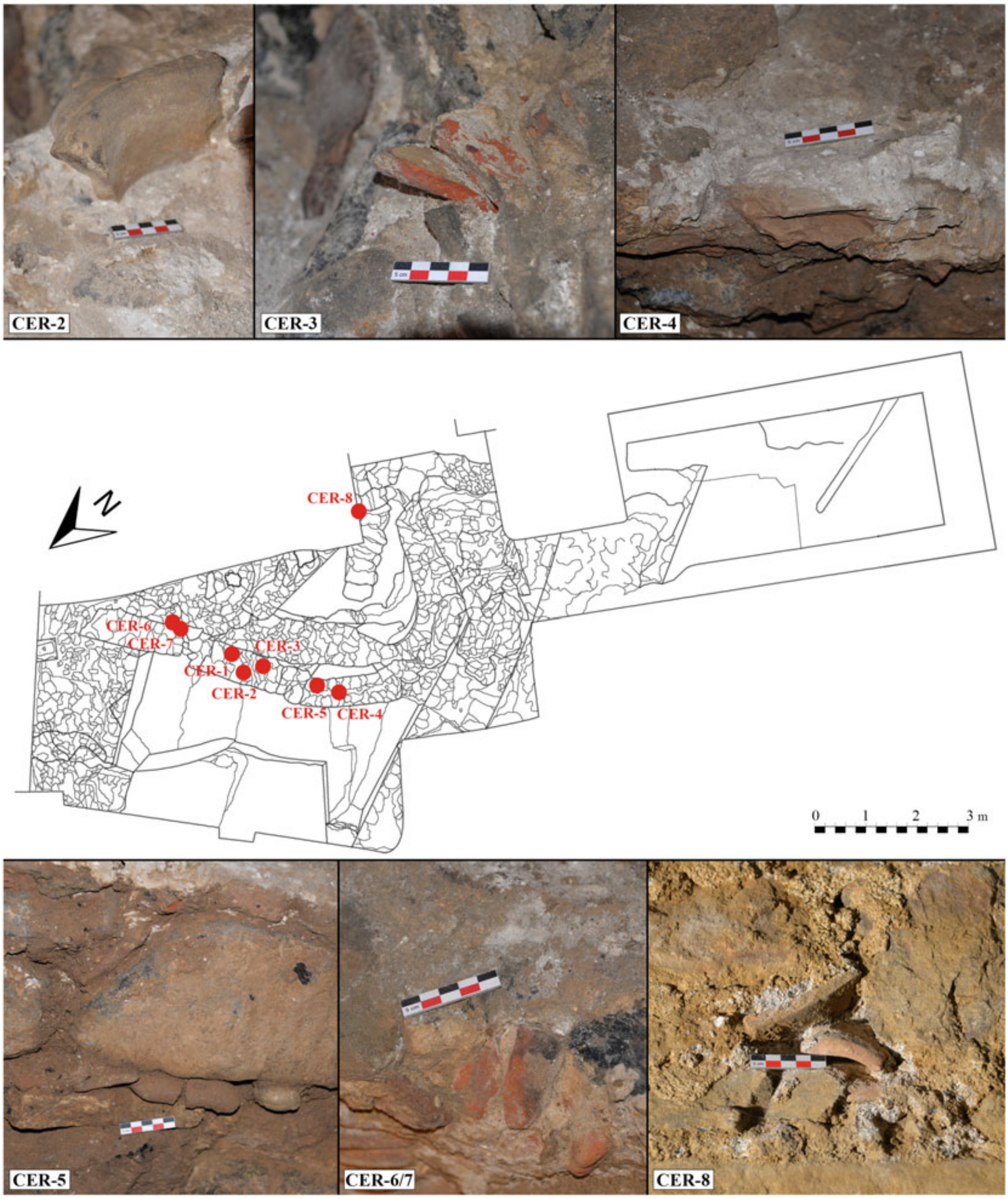

Fig. 14.6 Location of the pottery fragments extracted from the features

based tempers suggests an origin in *Lusitania*. The joint between the handle and the well-developed neck indicates that the handle was rather wide. These morphological features suggest that the fragment belongs to one of the earliest varieties of the type.

The fragments extracted from M-3/M-4 point to a date between AD 175 and 225. This date is derived from the two Puerto Real I/II type amphora fragments (see Figs. 14.6 and 14.7, 1 and 2). It can be argued that they belong to Variety II because these same contexts have also

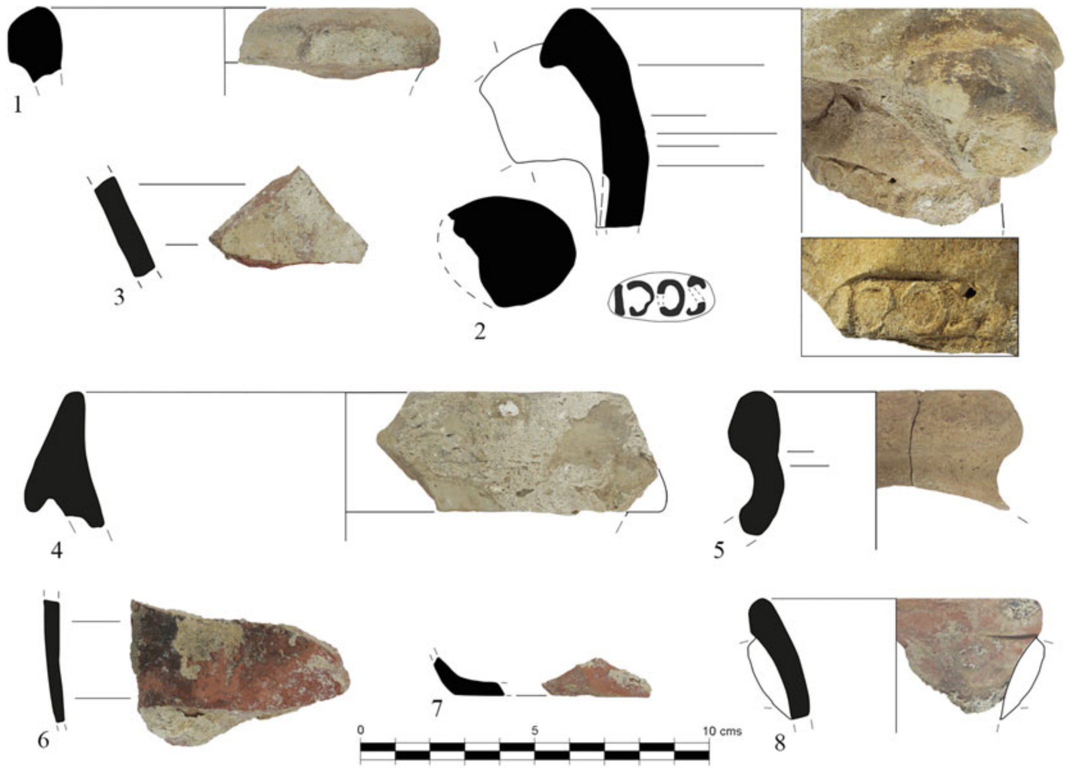

Fig. 14.7 Pottery found within the fabric of architectural features in the Baluarte de la Bandera: 1–2. Puerto Real I/II; 3. Wall of non-diagnostic African amphora; 4. Rim of open shape, common ware; 5. Heavily-worn Dr. 20 amphora fragment; 6–7. Non-diagnostic fragments of African *sigillata* (ARSW A); 8. Rim of Almagro 51c amphora

yielded several fragments of the umbilicated bases that are characteristic of the type. At any rate, both types are dated to the same period, straddling the late Antonine and the early Severan periods (García Vargas and Bernal-Casasola 2016), as recent studies have confirmed (Bernal-Casasola 2019, pp. 587–589). This is the most common type of amphora in fish processing plants in *Septem Fratres* during this period. They have been documented (some specimens even bear stamps) in Paseo de las Palmeras and Mirador I (Bernal-Casasola and Pérez 2001). The well-known retrograde SOCI stamp is also dated to the late second or early third century (Lagóstena 2001, pp. 423–427). The tableware also corroborates this chronology; these are limited to African *sigillatas* (African red slip ware) of both the A^2 (see Fig. 14.7, 6) and A^1 production (see Fig. 14.7, 7), dating from the late second or early third century, in any case earlier than the ARSW C, which appeared around AD 200 (VV. AA. 1981, p. 58) but which was not to be found in foreign markets until the second quarter of the third century (Járrega 2019, pp. 161–162). Therefore, the absence of ARSW C tableware indicates a *terminus ante quem* for the wall of around AD 220/230. On the other hand, the walls of African amphorae, one of which is illustrated in Fig. 14.7, 3, are also a good fit for this chronological interval. The earliest common Tunisian amphorae (Africana I and Africana II A types) appeared in the markets of the *Fretum Gaditanum* in the late second or early third-century AD (Bonifay 2004, pp. 107 and 111); both types have been documented in Ceuta (Bernal-Casasola 1996, p. 1198, Fig. 4). The remaining fragments—a rim of the Dressel 20 type, which is clearly residual (see Fig. 14.7, 5), and the mouth of a possible mortar in common pottery with a Baetican fabric (see Fig. 14.7, 4)—do not allow for the chronology to be refined any further.

Concerning the rim of the Lusitanian amphora type Almagro 51c found in M-5 (see Fig. 14.7, 8), this type was in production for a long time, between ca. AD 175–450 for western Portuguese productions (Viegas et al. 2016) and ca. 200–500 for Algarve ones (Viegas 2016). The specimen belongs to an early variant, probably dating to the late third or early fourth-century AD. This ties in with the stratigraphy, which clearly indicates that M-5 postdates M-3/M-4 (the building techniques are also different, as will be seen shortly; the layout is neater and the lime mortar is applied more carefully) and also M-11, on which it rests.

Based on these results, we can contend that M-3/M-4 was built between the late second and early third centuries (late Antonine–early Severan period), that is, around AD 175–225, and that M-5 was built much later, in the late third or perhaps the fourth century and therefore belongs to our Phase III.

14.3.2 Building Techniques, Stratigraphic Relationships and Function of the Structures

In this section, we will describe the late Antique defensive features, which have been interpreted as a section and a corner of the city wall (M-3/M-4), internally reinforced with an older girth (M-11), which was later rebuilt (M-5) and equipped with a channel below (C-1); the exterior tower (M-6) was built abutting to it at a later date (see Fig. 14.8a).

The most important feature is M-3/M-4, which has been interpreted as a wall running from the east. In the excavated area the wall has a curved shape. Originally, this was probably a straight angle, but the western side collapsed

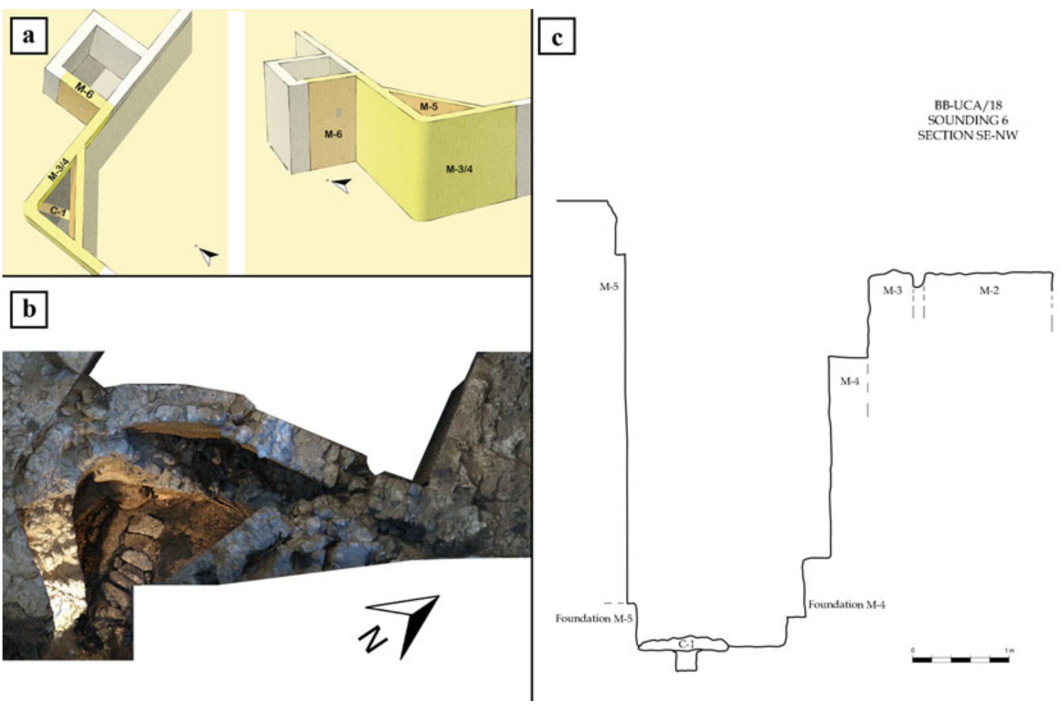

Fig. 14.8 Sketch of the structures (**a**), photogrammetric image of M-3/M-4 and Channel C-1 (**b**) and SE-NW section of the interior (**c**)

inwards, perhaps as a result of the earthquake and other taphonomic processes—e.g. the pressure exerted by the Portuguese bastion (see Fig. 14.8b). Although originally considered part of a tower, the length of the wall (nearly 13 m, projecting to the east) and this curved shape seem to suggest the corner of a fortified precinct. This interpretation is also supported by the height of the wall; the preserved height is 3.72 m, even though the top part is missing (see Fig. 14.8c). The wall is only moderately thick: ca. 60 cm at the top and just over 1 m at the bottom—although it is difficult to be sure owing to the structural damage that it suffered. Although this may seem too thin for an urban wall, various parallels exist. To mention but a couple of close examples, the wall of the *castellum* of *Tamuda*, in Tetouan, built when the province was created by Claudius, is between 80 cm and 1 m thick (Lenoir 2011, p. 254); in *Baelo Claudia*, in Spain, different sections of the 1200 m-long wall, built during the Augustan period and, after an earthquake, again in AD 50/60, are uneven in this regard: from 80 cm thick (or even less) in the southern sector to between 1 m and 1.3 m elsewhere (Sillières 1997, pp. 74 and 80).

The fact that M-3 and M-4 are often presented as two different units is due to the previous interpretation of Sounding G (BMR'16), in which M-4—the in situ bottom section of the wall (C013)—and M-3—the collapsed upper section—were recorded separately (Villada and Godoy 2017, p. 60, C006). After the 2018 season and the archaeoseismological study, it has become clear that both features were originally part of the same structure and can be thus presented as M-3/M-4. The collapse gives the false impression of two structures built at different levels, almost as a *chemin de ronde* (see Figs. 14.8c and 14.9b). The features display

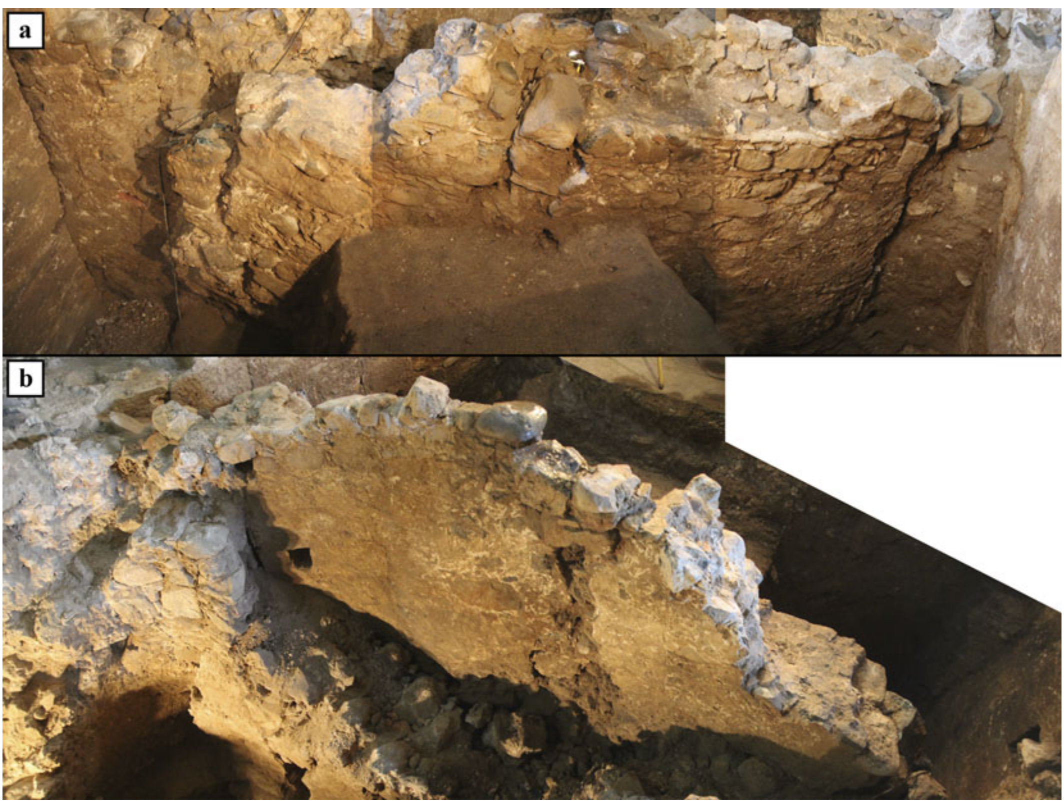

Fig. 14.9 M-3/M-4 from the outside (**a**) and the inside (**b**), illustrating the collapse of the top end of the structure northwards

unmistakable signs of a traumatic seismic event, as will be seen further on. This event explains the horizontal fracture that caused the collapse of the upper part, the elliptical shape of the bottom and the false impression of two separate structures. The wall follows a curved course, almost semi-circular; the original E-W orientation of the wall turns northwest-southeast beyond the bend.

The building technique used is a variation of *opus vittatum mixtum*, with a base of lime-rich mortar, dressed stone slabs and small and medium-sized pebbles arranged in false courses levelled with the aid of small pottery fragments, as previously noted (see Fig. 14.9a).

The inner face, which shows evidence of repairs, has at least two square openings approximately 30 × 30 × 40 cm in size, located at different heights. They may have had to do with the support of now lost interior features (see Fig. 14.9b): for example, wooden beams to support stairs or intermediate stories. The lower part of the M-4 also has a basal plate (see Fig. 14.8c).

The use of recycled material is also found in the foundations, where four earlier ashlar blocks were laid out. At least three of these belonged to pilasters with carved half-columns (see Fig. 14.10) (for details, see Bernal-Casasola et al.

Fig. 14.10 Detail of one of the ashlar blocks with carved half-columns (S-3) reused in the foundation of M-3/M-4

2020b). Because of their rigidity, these large block spoils reused in the wall became a weak point during the earthquake, causing cracks in the wall (see Sect. 14.3.3). At least four of them have been identified. They have been interpreted as originally belonging to the façade of a former monumental public building. The edges are quite sharp, which suggests that they were cannibalised from a nearby building when the urban wall was erected. The closest parallel is the monumental façade of the inner *tabernae* in *Baelo Claudia*'s *macellum*, built in the late first or early second-century AD and in use up until the third century. The stone blocks used in this façade are virtually identical to those found in the Baluarte de la Bandera in Ceuta (Didierjean et al. 1986). These elements have been mineralogical and petrographically characterised, confirming that they were carved from Cenozoic quartzitic arenites during the Aquitanian Age (Aljibe Flysch or Numidian, ca. 20 million years old): that is, they were not locally sourced, as this sort of rock does not exist in Ceuta or its hinterland. The closest sources are in the Cape Spartel area, near Tangier, at some points on the coastline between Tetouan and Ceuta (around the old Smir Lagoon), or in the vicinity of *Baelo Claudia*—Cabo/Sierra de la Plata and Bartolomé (Bernal-Casasola et al. 2020b). These are significant architectural pieces that suggest that substantial buildings, probably of a public nature, existed nearby. The urban layout of early Imperial *Septem Fratres* is poorly known as a result of continuous subsequent activity (Bernal-Casasola 2009).

We shall now deal with a series of features that have been associated with other elements of the fortification.

Channel C-1 runs diagonally in an N–S direction, beneath the foundations of the late Antonine–early Severan structures (see Fig. 14.11a). The inside of the channel is built in brick and regular stone blocks lined with mortar (ca. 3 cm thick). The channel was covered by a series of at least seven large irregular stone slabs, bound with a lime-rich mortar. The surviving visible section is 2.25 m long and ca. 65 cm wide (about the same width as the covering slabs) (see Figs. 14.11b, d). The actual channel was rectangular in section (20 × 20 cm), and was slightly bent at the north end (see Fig. 14.8c) to head towards the sea, where it must have evacuated.

In order to examine the structural relationship between the channel and the city wall and its other associated features, we opened a sounding at the channel's western end, where a level of clean clay was attested. This brownish silty layer (UE 6004) was overlain by another layer with similar characteristics (UE 6001/6002) but bearing a larger volume of inclusions in the form of small pebbles and brown, blackish and yellowish stone fragments. While layers 6001/6002 seem to correspond to the inner frequentation or abandonment levels of the walls, the clean clay of UE 6004 is more likely related to the waterproofing of the channel, as it is very compact and overlays the covering slabs at the channel's eastern and western ends.

The interior of the channel was completely filled with soil, and judging by the nature of the fill (UE 6003) this accumulation was the result of taphonomic processes that can provide us with no information, at least as far as chronology is concerned, although we are still waiting for the results of the micromorphological analysis to try to understand the channel's function. The sieving and triaging of the sediments have not yielded much data, apart from the presence of multiple land gastropods and micro-vertebrate remains, which are currently being studied.[2] Although it was initially thought that the channel might have belonged to an early Imperial fish processing facility similar to those that have been attested in the vicinity of the Puerta Califal (Villada et al. 2007), it seems more likely that its use was related to the defensive structures or that it might have been obliterated by their construction in the late second or early third-century AD. Its elevation also coincides with that of the structures; it runs exactly beneath the wall foundations (M-3/M-4, M-11 and M-5; see Fig. 14.11a, c, d).

[2] The malacological remains are being analysed by Juan Jesús Cantillo. The microfauna found is being analysed by Ángel C. Domínguez (UCM, Geodynamics, Stratigraphy and Palaeontology Department).

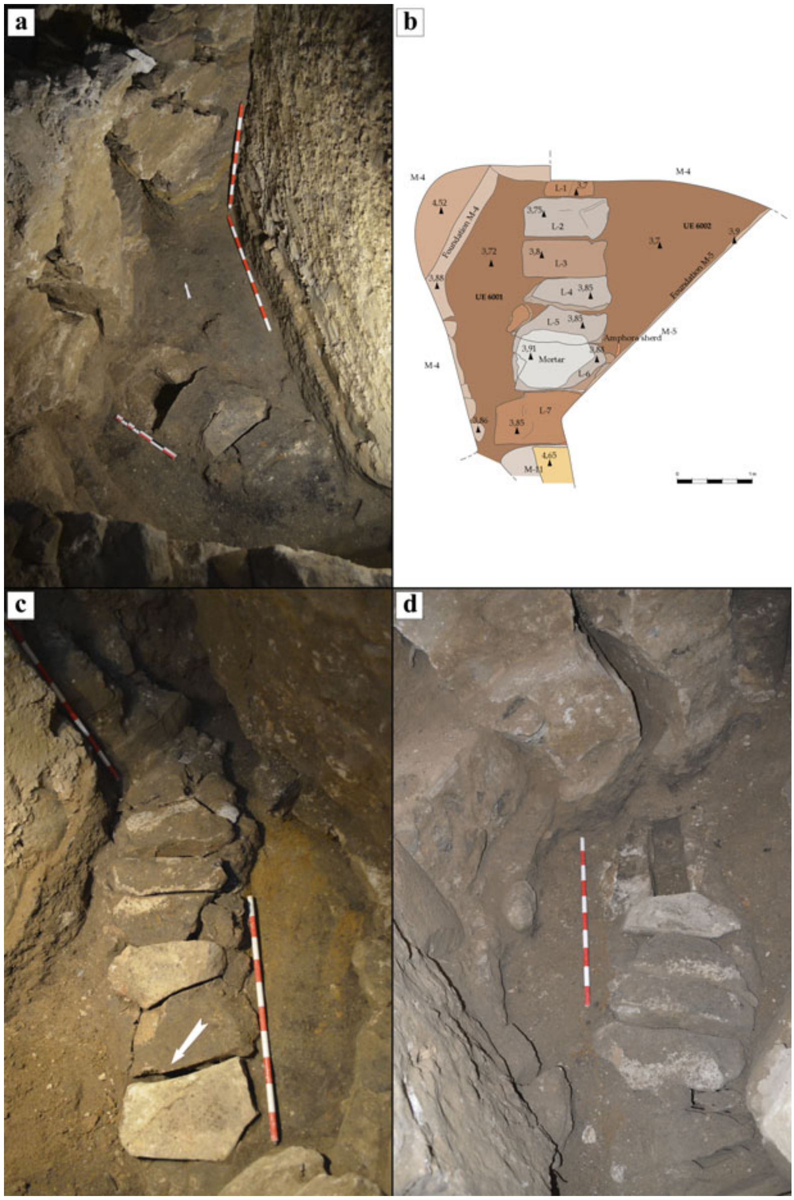

Fig. 14.11 Overview of Channel C-1 (**a**) and its associated structures (**b**) and details of the covering slabs (**c**, **d**)

Additionally, the excavation of the channel resulted in the identification of a layer of mortar that ran from C-1 to Section 1 of M-3/4 (beneath M-11), that is, mirroring the course of the channel. This seems to confirm the structural relationship with the defensive structures and, probably, also their coeval nature. The best parallel is found at the western gate of the *castellum* of *Tamuda*, under which ran an undulating channel, filled up in the second century AD, which was not aligned with the gate (Sáez et al. 2013, pp. 260–263, Figs. 16 and 17), an arrangement which is similar to that found in the Baluarte de la Bandera.

Two internal girths (the earlier M-11 and M-5 which were built on top it), reinforcing the structure of the internal face of the wall (see Fig. 14.12) were also discovered.

Built over the southern end of the channel, M-11 is a NE-SW wall, only 62 cm thick. It was

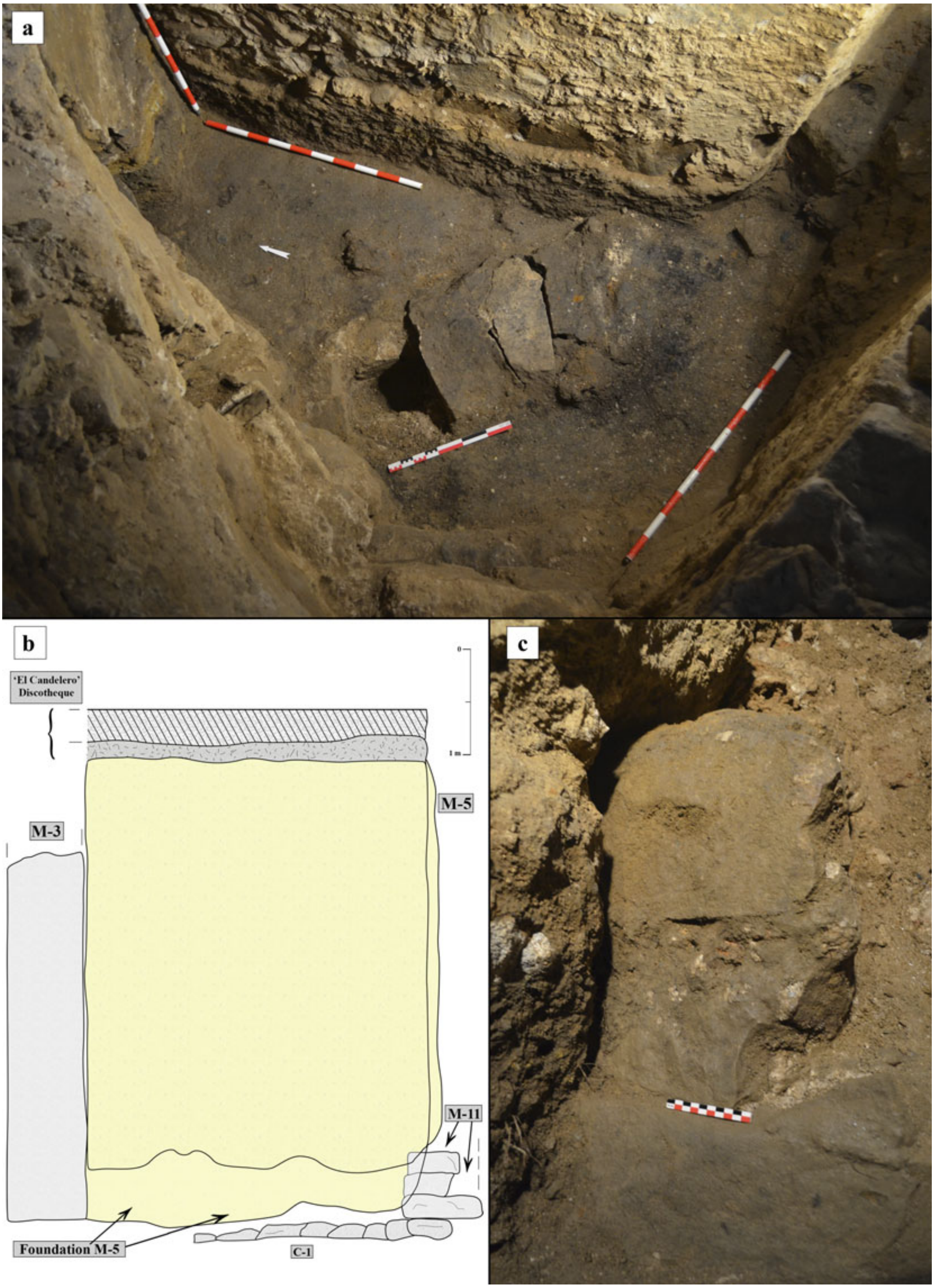

Fig. 14.12 Photograph (**a**) and section drawing (**b**) of M-5 and associated structures, with M-11 (arrow) embedded in its foundations (**c**)

built with irregular stone blocks bound with a thin layer of mortar. Only three blocks are preserved, so the length and thickness of the wall are unknown: however, another section of the wall can be seen to the southwest, beneath Wall M-5. We have associated it with M-3/M-4 based on its position and orientation, and have interpreted it as the remains of an early interior girth that was later affected by the construction of M-5.

As noted, Wall M-11 was affected by the construction of M-5 (see Fig. 14.12), a substantial wall (it is preserved to a height of 2.90 m, in addition to 40 cm of foundations) that runs in an N-S direction for 2.60 m; it is 60 cm thick. This imposing feature is built with small and medium-sized stone blocks bound with lime mortar, which was irregularly applied. Although the mortar is different, this building technique is similar to that found in M-3/M-4, including levelling courses laid out with pottery fragments. We have interpreted this as a reform of the original girth M-11; however, it should be noted that, although the interior face of M-3/4 is in contact with M-5 near its north-eastern end, this is not the case to the southwest, where M-5 exhibits no major signs of structural damage, but turns to the southeast (a section of wall, M-9, which has yet to be excavated, was identified and interpreted there as the possible prolongation of M-3/4).

It is worth remembering that a fragment corresponding to an Almagro 51c amphora (see Fig. 14.7, 8), dating from the late third or early fourth-century AD, was found within this feature. The northern face of M-3, the top of the interior face of M-4 and the middle and top sections of M-5 all have levelling courses laid out with pottery fragments, suggesting a similar technical know-how; these building techniques are absent from later structures (M-6 and M-2). It must be stressed that M-5 seems to be an interior reinforcement for the wall corner, and it occupies the same position where M-11 had once stood, so its construction may have been a response to some structural problem, Moreover, the fact that M-11 sat directly on top of one of the covering slabs of the channel (see Fig. 14.12b, slab L-7) supports the idea that all these structures (C-1, M-11 and M-3/M-4) formed part of a single construction programme. Finally, it should be recalled that M-5 was not apparently affected by the earthquake, which in our opinion is due to its different orientation, which must have made it more resilient to the seism.

The last feature to be dated to the Antonine–Severan period is Wall M-6, located to the east of the excavation area and originally documented in Sounding G in 2016 (BMR'16, C005; Villada and Godoy 2017, pp. 62–63); its northern and western sections were recorded during the excavation of Sounding 5.

The preserved height of this structure is 3.60 m (see Fig. 14.13a). The feature abuts the exterior face of the easternmost section of M-3/4 (see Fig. 14.9a). A length of 2.40 m has been recorded to date, but it is obvious that this wall, with an N–S orientation, continues further from the northern edge of the excavation area (see Fig. 14.13b). Its thickness is unknown, because the eastern face is covered by the interior fill laid out in the Emirate-Caliphate period (C041/UE 5007); the material found in association with this fill includes common glazed ware and kitchen ware, including a flat-bottomed, lip-rimmed cup and an early lamp; the deposit can probably be dated to between the eighth and the tenth centuries (Villada and Godoy 2017, pp. 33–35 and 75–77). The fills found in the gap between M-6 and the eastern section of M-3 (approximately 15–20 cm wide) (see Fig. 14.13c) is full of early medieval material. We think that the gap was created by the earthquake and filled up in the following centuries.

The building technique is similar to that found in the afore-mentioned structures, although in this case larger stone blocks were used and the lime-rich mortar was applied more systematically. Near the bottom, the mortar lining presents a series of finger marks applied when the mortar was fresh (see Fig. 14.13d). These marks form a wavy figure with some parallel strokes at the end, perhaps some sort of plant representation. This motif has no parallels in the repertoire of graffiti found in Ceuta's medieval and post-medieval fortifications, and only bears a vague resemblance to a series of incised lineal representations

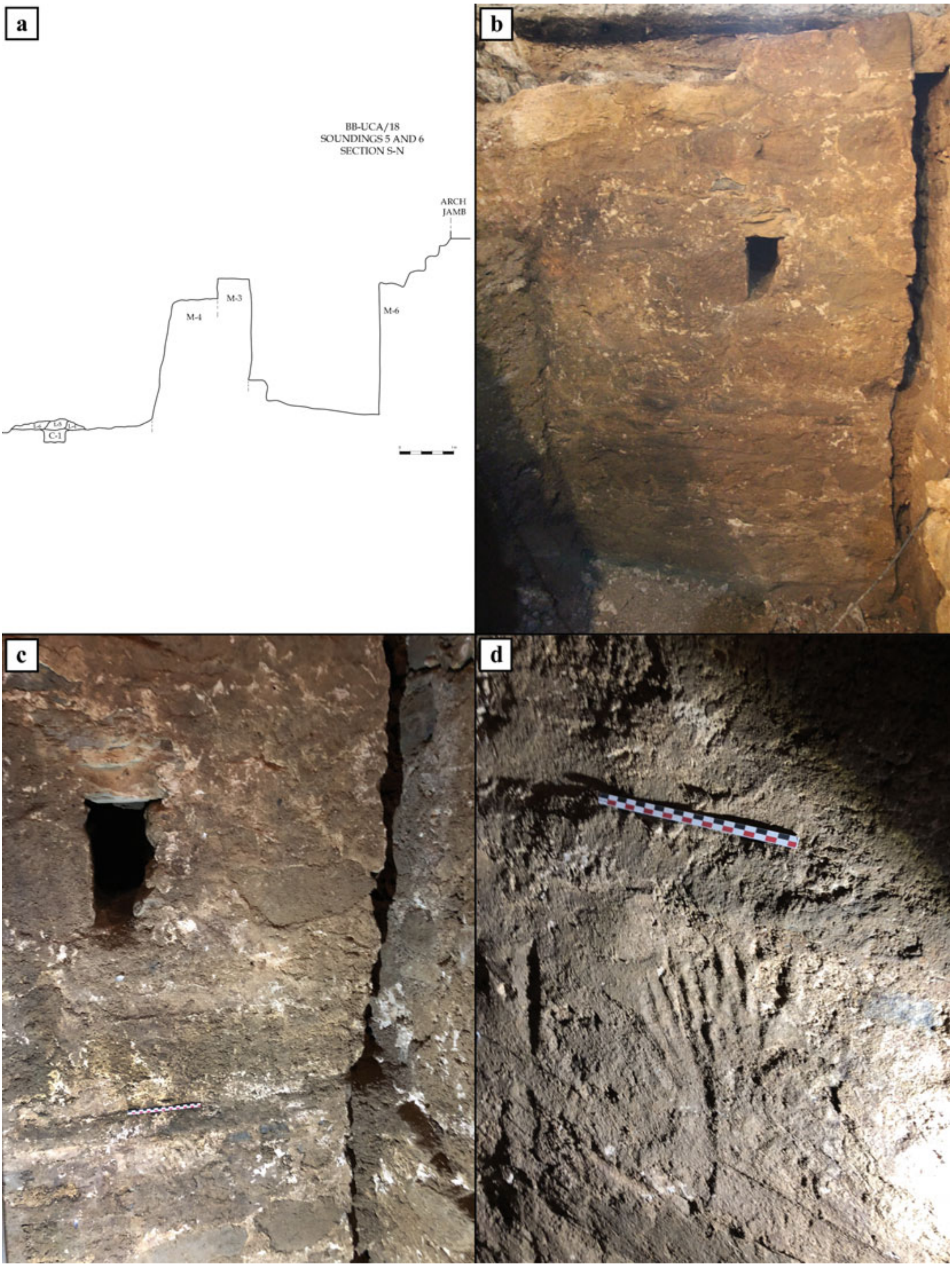

Fig. 14.13 S–N section of M-6 (**a**), and details of its western face (**b**), potential arrowslit (**c**) and graffiti (**d**)

(Fernández Ahumada and Villada 2017, no. 537, 541, 542, 555, among others). The presence of the graffiti confirms that this surface was exposed, as was a possible arrowslit (32 × 16 55 cm) opened in the western face (Villada and Godoy 2017, p. 25). The inside of this feature yielded Roman and Byzantine pottery—including an African Keay LXI fragment, dated to the seventh century—which bears witness to the taphonomic processes that the area underwent between late Antiquity and the period of the Caliphate (Villada and Godoy 2017, pp. 87–89).

The stratigraphy provides us with two clear chronological indications: it is later than the late Antonine–early Severan construction programme, as it abuts the exterior face of M-3/M-4—and the building techniques are different; and it is earlier than the seventh century, since at the westernmost end of the excavated area it is partially overlain by the in situ cremation burials (Villada and Bernal-Casasola 2019, pp. 204–207, Fig. 22). As already noted, the building techniques differ from those used in M-3/M-4 and M-5, so we are inclined to think that this structure was built late in Phase II, perhaps in the late fourth or even the fifth century; confirmation for this will have to wait until the excavation of the remaining deposits in Soundings 4 and 5. The structure was in use at least until the construction of the Caliphate period wall (M-1), as shown by the Emirate–Caliphate period ceramics found on its upper surface and at the point of union with M-3/M-4.

From a functional perspective, it seems likely that M-6 was part of a tower: on the one hand, because it was built next to the wall; and, on the other, because it has a projection to the north, the angle of which is not visible because the Baluarte de la Bandera was erected on top of it. Finally, its dimensions and the solid nature of its interior fill indicates that it was a sturdy construction. The external wall of the Baluarte embraces it, which makes it hard to explore some of its features, especially on the eastern side.[3] Since it was less than 100 m from the shoreline, it may have been used as a lighthouse, although this cannot be proven.

Concerning typology, in the Severan period the military camps of *Tingitana* had circular external towers, which were subsequently supplemented by "fanned" towers, for example in *Tamuda* (Villaverde 2001, pp. 502–507; Campos and Bermejo 2013) and Dhar Aseqfane, in the mountains of the strait area (El Khayari and Akerraz 2012). In any case, rectangular towers were much more common in the military camps of late Imperial *Mauritania Tingitana*, for example, Souk el-Arba du Gharb, El Benián and *Tabernae* (for a discussion, see Villaverde 2001, pp. 505–507 and 518, Plate 1; Lenoir 2011, pp. 263–266, Fig. 153–154). Square towers are also the most typical in urban contexts, as can be seen in *Baelo Claudia* which had nearly 40 such towers, built totally or partially abutting the external face of the walls (Sillières 1997, pp. 73–77); although we know much less about its walls, the system followed in *Carteia* is identical (see the plans published in Roldán et al. 1998, p. 145, Fig. 153).

14.3.3 Structural Pathologies in Defensive Wall M-3/M-4

The structure that displays the effect of the earthquake most clearly is M-3/M-4, which is also the only one with an E-W orientation. Its building technique would have also made it more vulnerable than the rest to this sort of effective structural stress.

The 1st INQUA-IGCP 568 International Workshop on Earthquake Archaeology and Palaeoseismology defined two types of earthquake archaeological effects (EAEs): penetrative fractures in masonry blocks or displaced/rotated and collapsed walls (Giner-Robles et al. 2009, pp. 28–29 and 35–36; and more comprehensively compiled in: Rodríguez-Pascua et al. 2011).

EAE 1. The head of M-3/M-4 is broken and displaced horizontally, so, as noted in previous

[3] Despite our attempts to locate its northwest corner in 2018, this was not possible owing to the presence of the Portuguese and modern structures.

sections only the western section of the wall remained structurally sound (see Fig. 14.14, blue). Therefore, we infer that a seismic shock (or an earthquake) split the wall into two parts, the bottom section, M-4, which remained more or less in situ (see Fig. 14.14, pink) and the upper section, M-3, which fell northwards (see Fig. 14.14, brown). Due to the damage and directivity of the displacements a near-source region of an earthquake, associated with strong ground motion, is evident. The epicentre of the earthquake was located either to the north(east) or south(west) of Ceuta, and had a magnitude larger than M 5.5; the wall section weighs several tonnes, but was displaced between 0.6 and 1 m from its original position. To the north of M-3/M-4 there was a substantial fill, nearly 2 m thick (see Fig. 14.15A), upon which M3 came to rest after the seismic event; this deposit prevented M3 from falling further and losing all structural connection with M-4. In fact, these fills have not been fully excavated to prevent the structure from collapsing. Two soundings were opened, one in 2017, between the western face of M-6 and the fills that were left in place for safety reasons; and one between these fills and the eastern face of M-2 (see Figs. 14.15b, c, and 14.16, left side). Our date for the earthquake is based on the sediments on which M-3/M-4 sits, dated to the second half of the seventh century. This is examined in detail in Sect. 14.5.

Furthermore, the earthquake opened multiple vertical cracks in both parts of the structure; we have highlighted the most severe of these and assigned them numbers from west to east (EAE 2 to EAE 6); they divided the wall into four numbered sections (see Fig. 14.16). These cracks match the joints between the reused blocks in the foundations of M-3/M-4. The combination of two different materials—very rigid quartz arenites and mortar-bound masonry, much more brittle—amplified the effect of the seismic shaking.

EAE 2 (see Figs. 14.17 and 14.18a, b). This crack is most clearly visible in the lower western section of M-4, especially inside the wall, although in the exterior it may connect with the eastern part of Section 2 of M-3/M-4. It stems from the joint between Blocks S-4 and S-2, near a step-like protrusion (this may form part of the foundations or a retaining girth to the outside of the curved feature, opposite S-4) on the interior face of the structure. The fracture runs in an NW–SE vertical direction, all the way from the foundations to the top of M-4. The crack seems to match the eastern joint of S-4. Unlike the rest, it is not strictly speaking a crack, since Section 2 of M-4 also shifted outwards; Section 1 remained in situ, apparently unaffected by the seismic deformation. The gap between Sections 1 and 2 is barely 15–25 cm wide. The fact that Section 1 was largely unaffected by the earthquake may have had to do with the extra support provided by M-8 and M-2 to the west. However, a change of orientation of a few degrees to the north can be attested in the north-eastern part of M-2, which suggests that the structure suffered the impact of Section 1 of M-4 which, especially towards the top, rests on M-8 and M-2. EAE 2 is approximately 2.5 m long, running along Section 1 of M-4 from top to bottom.

EAE 3 (see Figs. 14.17 and 14.18c). This crack is located to the east of S-2 which, like S-3 and S-4, may have contributed to the crack opening through M-4 and splitting Sections 2 and 3. The crack, which runs in an N-S vertical direction, is substantially wider than the previous one. It is between 25 and 35 cm wide at the bottom, for a stretch of 1.20 m measured from the foundations, and becomes much narrower (5–10 cm) towards the top. It runs through the whole breadth of S-2 (94 cm), which almost coincides with the whole width of the wall foundations (approximately 1 m). The role played by S-2 in opening the crack is clear, as this is much wider towards the bottom, closing in as it runs away from S-2. Finally, the western area of Section 3 displays the imprint of the half column of S-2 on the mortar, which allows us to reconstruct the original arrangement of the wall, and estimate how far Section 2 shifted away from Section 3.

EAE 4 (see Figs. 14.17 and 14.18d, e). This crack is located to the east of S-3 which, like in the previous examples, contributed to split the wall above it. S-3, unlike S-2 and S-4, sat in a

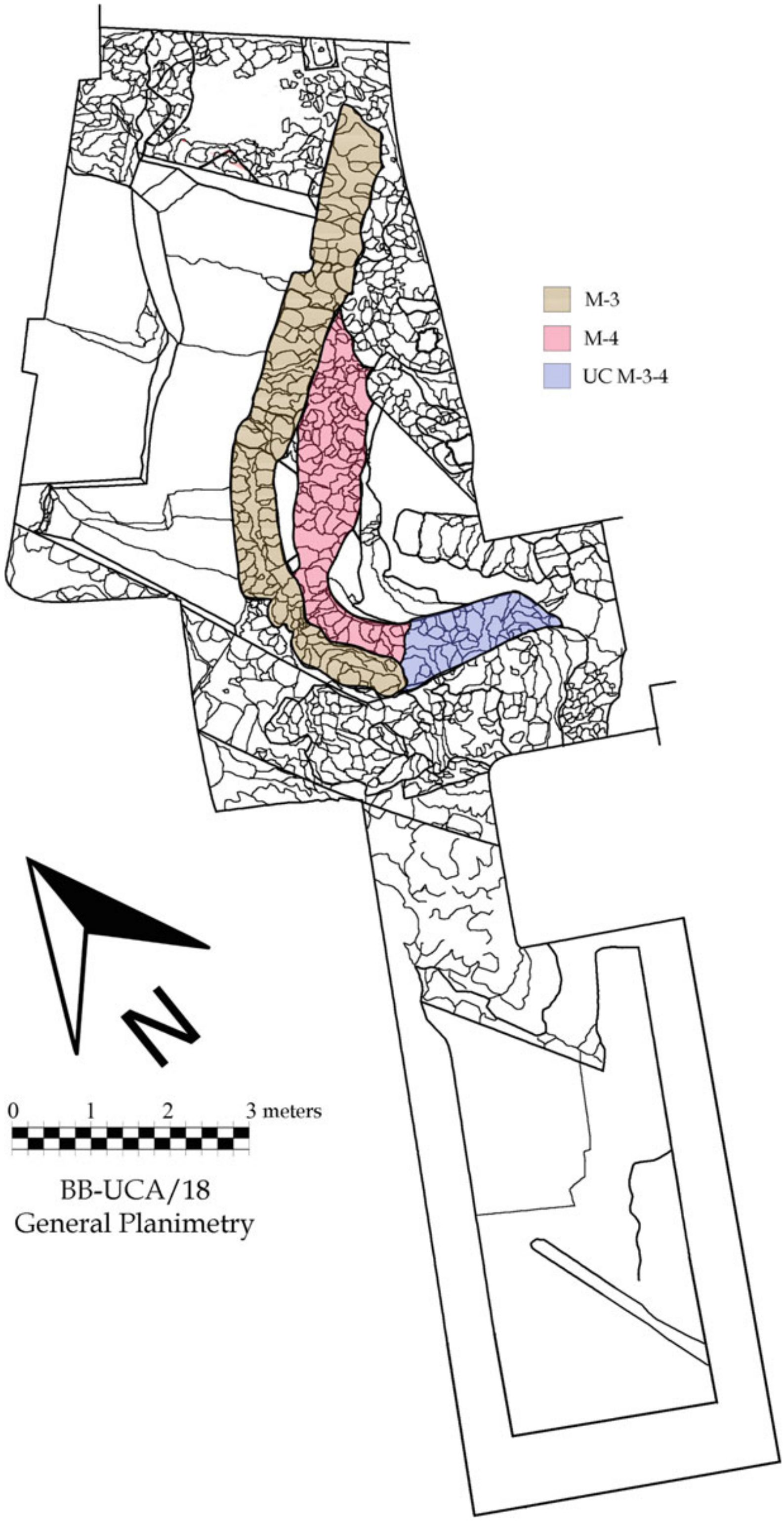

Fig. 14.14 Plan illustrating the displacement of the top section of M-3/M-4 northwards

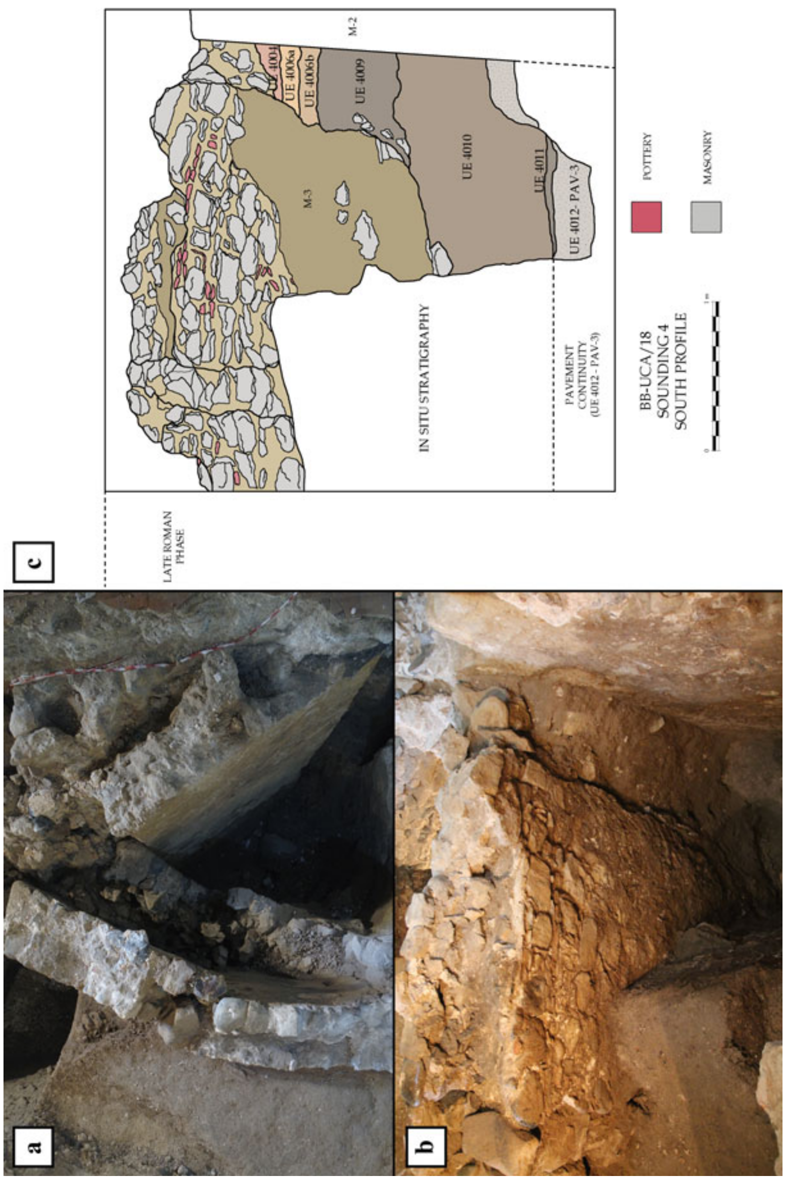

Fig. 14.15 Detailed top view of the section of M-3/M-4 that shifted the most (**a**), and view from the outside (**b**), with details of the stratigraphic layers on which it rests (**c**)

Fig. 14.16 Top-view of M-3/M-4, which illustrates the effects of the earthquake, including the horizontal displacement of the wall (EAE 1) and the main vertical cracks (EAE 2 and EAE 6) which split the wall into four sections (1–4)

vertical position, causing the crack to be much wider (50–60 cm) but much shallower too. For the most part, this crack also runs vertically, but its lower section is oriented obliquely. S-3 is less deep (ca. 50 cm) than S-2 and S-4 (94 cm), so the crack was wider but mostly affected the base of the wall, whereas in the other two cases the cracks ran through the whole structure. The trajectory followed by the crack is curved and irregular, like EAE 3, narrowing down to 5–10 cm from about 1 m from the bottom; the depth of this crack is unknown.

EAE 5 (see Figs. 14.17 and 14.18b). It is another crack in zigzag pattern on the upper interface of M-3, splitting Sections 2 and 3. Its width varies from 5 to 20 cm, and is partially obscured by fallen rubble. It runs through the wall (60 cm), on the inside face of which it is at least 2.2 m long, albeit with an irregular course. On the outside face of the wall only 60 cm are visible, because the area has not been fully excavated.

EAE 6 (see Fig. 14.18f). The last crack split Sections 3 and 4. It runs through the interior surface found during the excavation of Sounding G in 2016 (BMR'16). This substantial crack runs vertically in an N-S orientation from the foundations to the wall's crown. Unlike the others, this section of the wall does not rest on an ashlar block that may have contributed to the crack emerging. The crack detached Section 4 of M-3/M-4, which remains in situ, from Section 3, which shifted northwards. It is likely that M-6 offered Section 4 additional support despite the gap between them. Although similar to the rest, this crack is more even in terms of width and depth: it is approximately 1.40 cm long and 60 cm deep, running through the entire width of

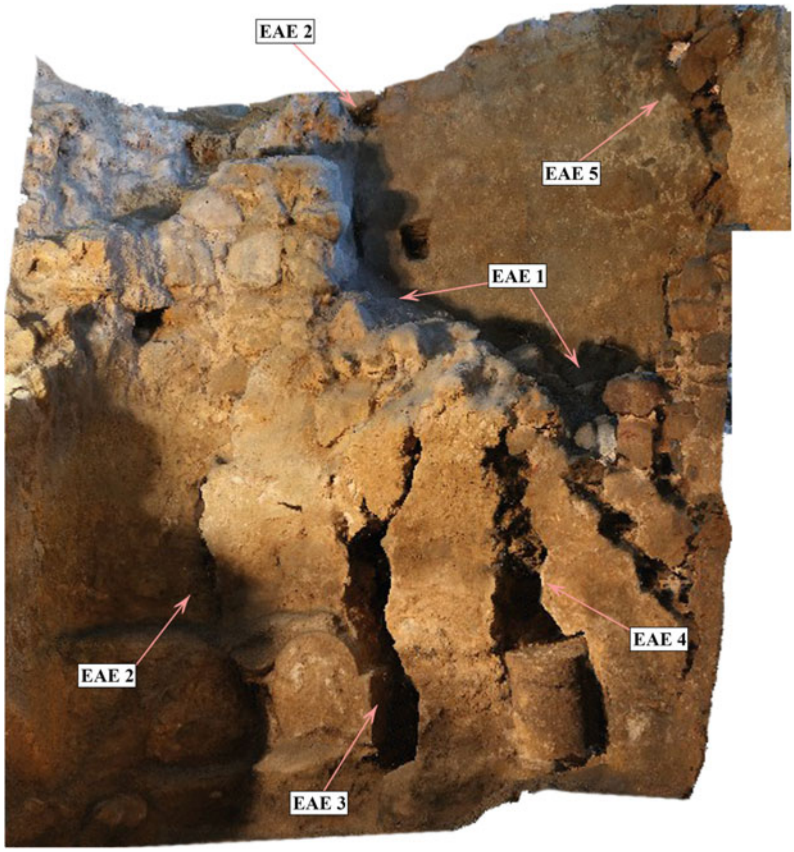

Fig. 14.17 Photogrammetric image of the interior face of M-3/M-4, with details of Cracks EAE 1 to EAE 5

the wall. The two sections display a difference in orientation of around 5–10 degrees, and the gap between them is 15–30 cm wide.

14.4 The Late Roman Wall of the Baluarte de la Bandera (Phase III)

The following phase comprises a wall, 1.28 m thick, that runs across Sounding 4 in an N–S direction (M-2). Its width and structural features clearly suggest a defensive function (see Fig. 14.19).

This wall is preserved to a height of 3.29 m, even though the top section was cut through by later constructions, and has a known length of 7.50 m. It was built with pebbles and dressed stone blocks bound with lime mortar. Two of the stone blocks on the eastern face have one opening apiece: one quadrangular (12 × 12 6 cm) and the other circular (4 cm in diameter and 2 cm deep). They are likely to have been used to attach lifting devices during the construction of the wall (see Fig. 14.19a).

At the deepest level reached by Sounding 4, near the base of Wall M-2, a compact lime-rich greyish level with no finds was attested (see Fig. 14.19c). This level was completely different from the archaeological layers above it, which were replete with material. This layer is raised near the base of the wall (see Fig. 14.19b), and it has been interpreted as a pavement (UE 4012 o Pav-3). The wall and pavement suggest that this was the interior frequentation level of the building.

At the southern end of the exposed section of M-2, a new wall was found abutting it. This wall (M-8) runs from northwest to southeast, forming a ca. 120° angle with M-2 (see Fig. 14.3). The

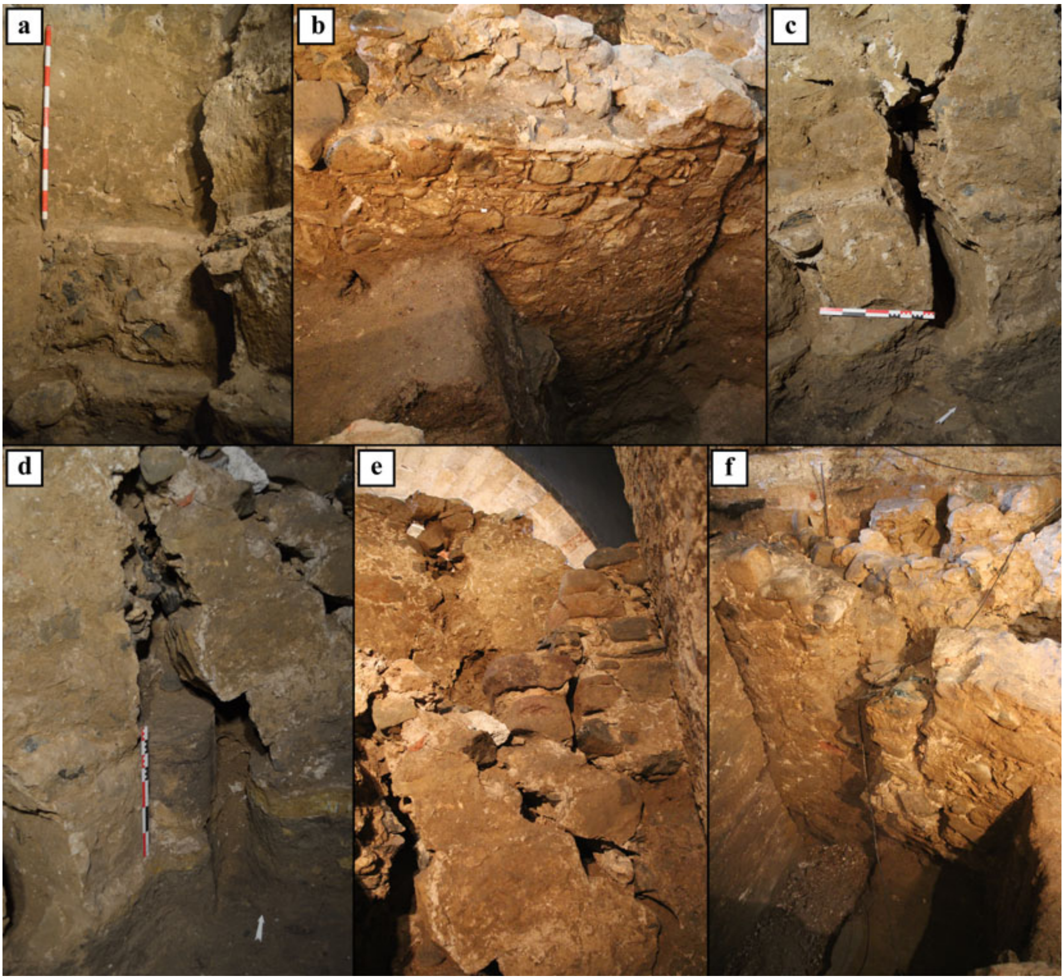

Fig. 14.18 Details of Crack EAE 2 (interior) (**a**) and EAE 2 and 5 (exteriors) (**b**), EAE 3 (interior) (**c**), EAE (bottom interior) (**d**) (and superior) (**e**) and EAE 6 (exterior) (**f**)

wall is 1.70 m wide and its preserved height is 2.56 m. The surviving length is merely 0.60 m. The building technique used is similar to M-2's, with pebbles and dressed stone blocks bound with lime mortar. The fact that M-2 and M-8 sit directly on the western face of M-3/M-4 clearly shows that both structures coexisted for some time: we believe that M-12 was an attempt to repair the fortification after the earthquake.

It is difficult to assign a date to these features, because we have not been able to excavate their foundation trenches; to the east, they are overlain by later structures (Sounding 4) and to the west by the Caliphate period defensive wall (M-1).

On the other hand, as with Tower Wall M-6, we are certain that the deposits that rest against the interior face of the wall accumulated well into the seventh century (as noted in Sect. 14.5; Bernal-Casasola et al. 2020c), which is our earliest *terminus ante quem* for this phase. That is, the wall was built sometime before AD 650, when sediments started accumulating against its external face and covering the frequentation level defined by the grey lime pavement (Pav-3). In approximately 50 years, these sediments reached a height of approximately 2 m, in a context of considerable activity including the processing of sea resources (there are multiple mussel shells). It

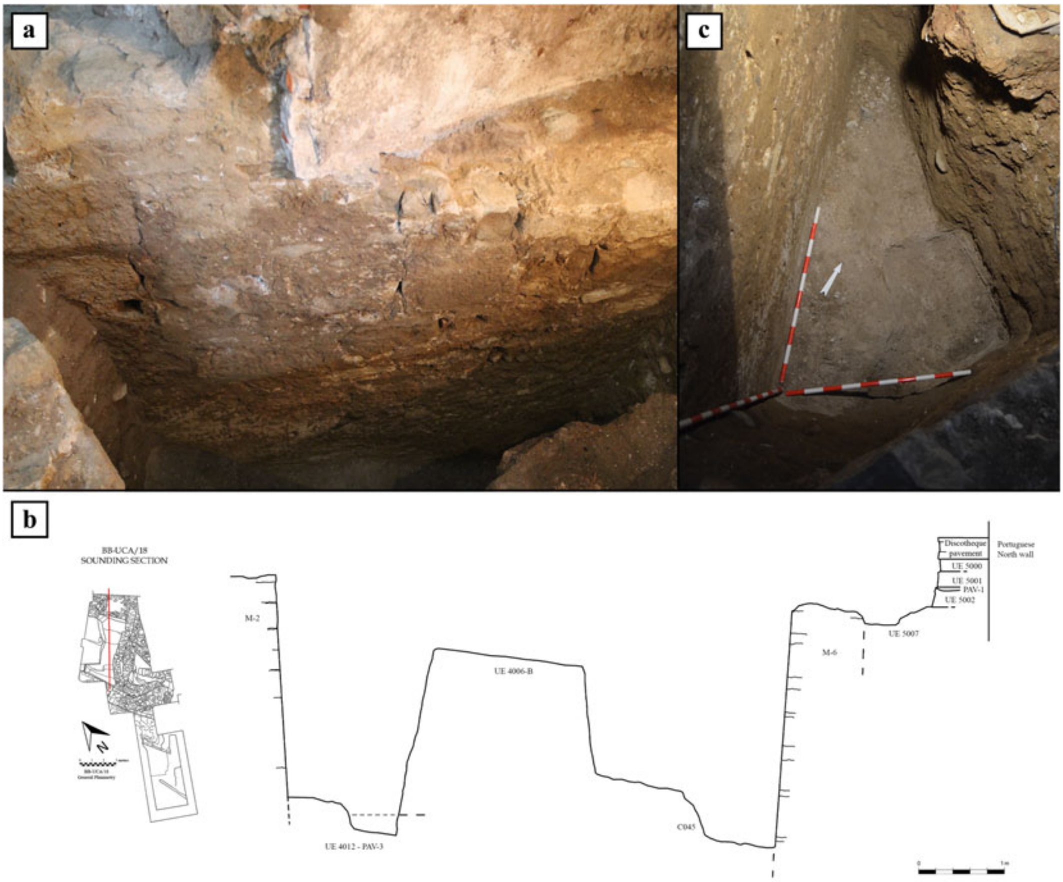

Fig. 14.19 View of M-2 from the east (**a**), with details of the possible pavement at its base (**c**), and E–W section (**b**)

is, however, almost certain that the wall remained in use until the third quarter of the tenth century, when the Caliphate period wall built by Abd al-Rahman III abutted it from the west.

The hypothesis on which we are currently working is that this is the wall built on Justinian's orders after the conquest of the city, as recounted by Procopius:

> *And at Gadira, at one side of the Pillars of Heracles, on the right side of the strait, there had been at one time a fortress on the Libyan shore named Septum; this was built by the Romans in early times, but being neglected by the Vandals, it had been destroyed by time. Our Emperor Justinian made it strong by means of a wall and strengthened its safety by means of a garrison. There too he consecrated to the Mother of God a noteworthy church, thus dedicating to her the threshold of the Empire, and making this fortress impregnable for the whole race of mankind* (Procop., *Aed,* VI, vii, 14-16; transl. H. Bronson Dewing, 1919).

However, although we know that this wall was built no later than the mid seventh century, when the city was still in Byzantine hands—as confirmed by Justinian II's famous *Iussio* (Vallejo 2012)—a much earlier date of construction cannot be ruled out.

It is important to bear in mind that two more sections of the Byzantine defensive precinct are known in *Septem*: in the Puerta Califal and the Baluarte de la Coraza (Villada and Bernal-Casasola 2019). Both run more or less north to south (Bernal-Casasola and Villada 2020, Fig. 5, see also our Fig. 14.22a); the orientation of M-2 is similar, which gives rise to a conundrum of sorts: either the northern Byzantine wall was located further north, which creates problems with the interpretation of Tower M-6 and the Severan wall, which was still in use until it collapsed as a result of the earthquake; or M-2 was a forward structure of the northern sector of the western side, which protected the harbour area. We know that the topography of this urban district was always peculiar, as illustrated by Braun's *Septa* in *Civitates Orbis Terrarum*, which represents the city prior to the construction of the navigable moat (see Fig. 14.22b). This illustration represents different types of towers and structures, including walls, erected at different levels and with different orientations (Fernández Ahumada and Villada 2017, p. 361). It is likely that the features excavated in the Baluarte de la Bandera form part of this architectural palimpsest.

14.5 The Date of the Seventh-Century Earthquake and the Byzantine Burials

Dating seismic events in man-made structures and buildings is a complex task (Silva et al. 2016). Concerning the Baluarte de la Bandera, the structures most seriously affected by the earthquake were M-3/M-4, which were built in the late Antonine–early Severan period, namely, long before the seismic event. Initially, and in light of the broader historical trajectory of the *Fretum Gaditanum*, we were first inclined to identify the seism with the one that partially destroyed the forum buildings in *Baelo Claudia* in the late third-century AD (Sillières 1997, pp. 57–63). In this interpretation, later fortifications would be dated to the Vandal and Byzantine periods. However, the excavations have painted a very different picture: the partial collapse of the Severan wall M-3/M-4 was partially arrested by a sedimentary sequence which has yielded a *terminus ante quem* in the second half of the seventh century.

The stratigraphic sequence framed by features M-2 (west), M-3/M-4 (south), M-6 (east) and the northern interior wall of the modern fortress (north) covers a surface area of approximately 12 m^2. This is the only sector of the whole excavation area that is free from structures, which to a certain extent confirms that this was used as a frequentation area. As illustrated by the aerial views (see Figs. 14.3 and 14.16), this sector can be divided into three parts: the eastern sector, excavated in 2016; the western sector, excavated in 2018; and the central sector, which has been left unexcavated to avoid the collapse of the top part of M-3/M-4. The stratigraphic sequence described below corresponds to the 2018 excavation season.

As will be seen in detail, we combined typological pottery analysis with radiocarbon dates, both of which yield dates in the second half of the seventh century (for further details, see Bernal-Casasola et al. 2020c).

Approximately 2 m deep (excluding modern layers) (see Figs. 14.20a, b), the stratigraphic sequence is divided into three phases.

The first phase comprises three layers (UE 4009, 4010 and, to a lesser extent 4011). These fills precede the seismic event. In addition to pottery, these contexts yielded remains of marine shells (patellidae, mytillidae and gastropods) which, along with some fragments of construction materials, such as *tegulae*, stone and lime and mortar fragments, indicate that the fills were intentional dumps. The sequence sits on the aforementioned layer of grey lime (Pav-3/UE 4012) relating to the construction of the late Roman wall (M-2). Immediately above it, there is a thin layer (UE 4011) with few finds and multiple lime nodules, interpreted as the result of the disaggregation of the pavement at its point of contact with the layer above it (UE 4010). The scarce material found within it—e.g. a residual Keay XIX amphora sherd—was part of the same piece found in the layer that overlaid it, which confirms that this context must be interpreted as little more than the interface between the pavement and UE 4010. The material found within the layer included miscellaneous finds belonging to different periods, including an early Imperial amphora (Beltrán IIA) and fragments of undefined late Republican ware (Italian amphorae of an uncertain type).

UE 4010 is a remarkably deep deposit—ca. 50 cm—constituted by a fine clayey-sandy material, similar in colour to the deposit that sits above it. The small excavated area yielded a large number of finds (384 NF, number of finds/16 MNI, minimum number of individuals), which increases the statistical reliability of the assemblage as a chronological marker. There were a few fragments of schist and hardly any bones or remains of malacofauna. The pottery assemblage included ARSW D tableware, amphorae, mostly African, but also eastern and Baetican types—the latter were likely to be residual—imported coarse ware, the occasional hand-built/slow wheel-made ware, and one *dolium.* The assemblage includes two rims belonging to very late African *sigillata* dishes. One of them has an almond-sectioned heavy rim (see Fig. 14.20c, 1) initially identified with Hayes Shape 105 but which, on closer scrutiny, was assigned to the earlier Hayes Shape 90 B, dating from the second half of the sixth or the early seventh century. The other rim, small and nearly circular in section (see Fig. 14.20c, 2), can

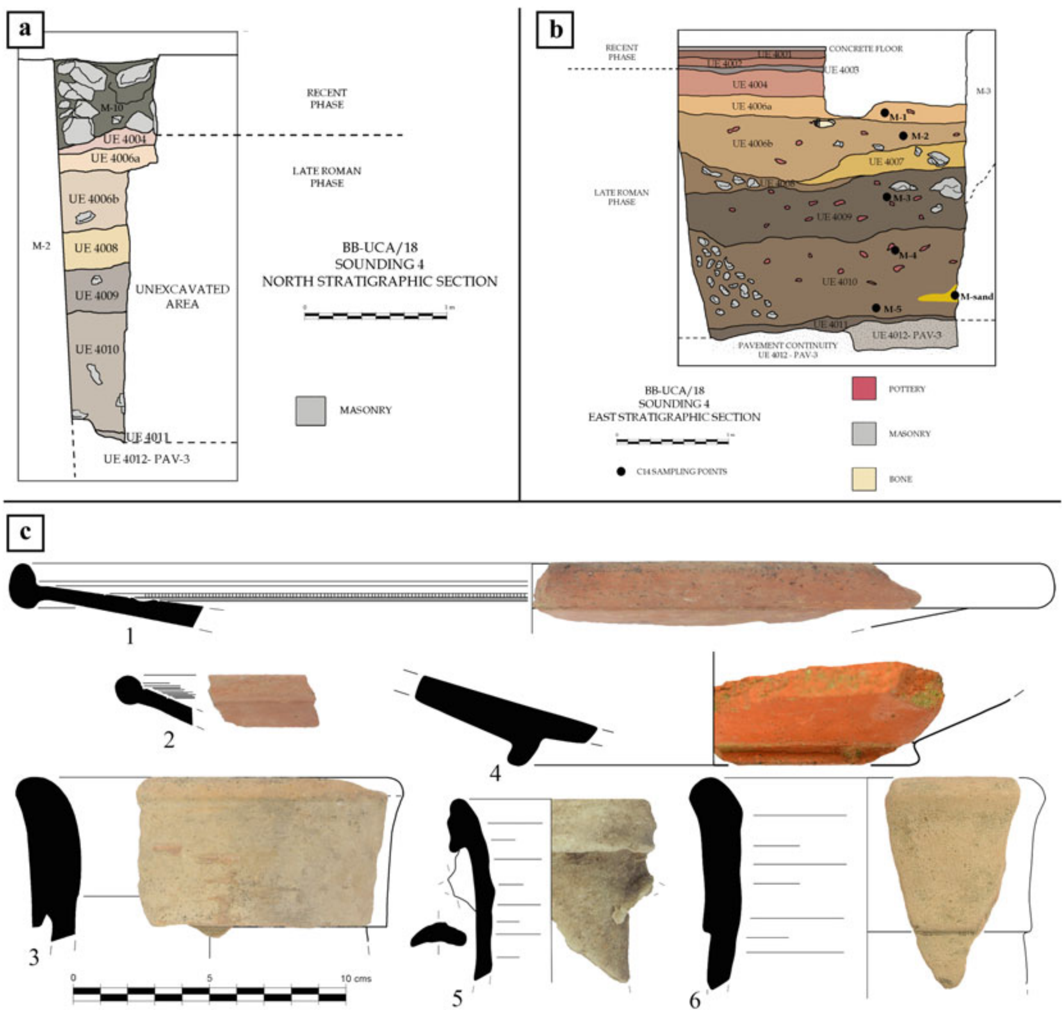

Fig. 14.20 North **a** and east **b** sections of the stratigraphic sequence built up against M-2, on top of which the collapsed section of M-3/M-4 came to rest, with a selection of chronological markers (C – 1–2. Rims of Hayes Shapes 90 B and 104 C in ARSW D, UE 4010; 3. Rim of African amphora Keay LXI, UE 4010; 4. Base of dish in ARSW D, UE 4009; 5. Rim of an African *spatheion* from the cleaning of the section; 6. Rim of a Keay 8A amphora)

be assigned to Shape 104c, dated between the mid-sixth and mid-seventh century, owing to the groove that runs around the inner wall (Bonifay 2004, p. 185, Fig. 98). Also noteworthy is the straight wall of a white-slipped African Keay LXI amphora (see Fig. 14.20c, 3). The straight wall, the considerable development of the rim and the absence of a moulding on the outside identifies it as belonging to the A variant, which is the latest, being dated to the mid- or late seventh century (Bonifay 2004, p. 141). One of the three samples sent for radiocarbon dating was taken from this deposit. The sample was collected near the bottom of the deposit (see Fig. 14.20b) and the results yielded a date of AD 545–645, with 95.4% probability (sample[4] Beta no. 526114). Given the presence in the assemblage of ceramic ware dating from the mid seventh century at the earliest (Keay LXI), other types that remained in circulation until the middle of that century (Hayes 104 c) and the radiocarbon dates, we are inclined to date the deposition of this fill to AD 640/650.

The layer above, UE 4009, had similar features; it was 56 cm thick, and the material found within it was also similar, but less abundant (105NF/8MNI). Of note is the base of a dish in ARSW D^2, which is hard to assign typologically, but which, based on its size, may be associated with Hayes Shapes 103, 104 or 105 (see Fig. 14.20c, 4), broadly dated to the seventh century. Also attested are coarse ware, hand-built ware, African amphorae and residual Baetican amphorae and African kitchen ware (Bernal-Casasola et al. 2020c). A pushed-in base found in this layer matched a fragment found in UE 4010, which strongly suggests that both deposits were contemporaneous.

Other significant finds were identified during the excavation of the northern section of the sounding, but this area was not excavated stratigraphically for logistical reasons (section cleaning UE 4006b/4009/4010/4011). For instance, the mouth and neck of an African *spatheion* with a white fabric, assigned to Bonifay's Type 3, Variant A (see Fig. 14.20c, 5), dated to the late sixth or first half of the seventh century, although some examples have been dated as late as to the second half of the seventh century (Bonifay 2004, 129, Fig. 69a). A radiocarbon sample collected from an intermediate level of the deposit (see Fig. 14.20b) yielded a date of AD 505–610, with a 65.6% probability (Beta no. 526113); this is certainly an earlier chronological interval than expected, but may be explained by the low accuracy of the result or the reworking of organic matter (charcoal).

A series of less substantial deposits, dated to the second half of the seventh century, followed the seismic event (although the data strongly suggest a date for the earthquake in the mid seventh century, we are deliberately placing it within a relatively broad time span). These deposits probably resulted from the collapse and subsequent disintegration of M-3/M-4. UE 4007 and UE 4008 largely consisted of stone fragments of various sizes and large pebbles (30 × 15 cm or larger), some of which had been worked to flatten their surfaces, similar to those used in the construction of M-3/M-4. The deposit also yielded remains of more or less disaggregated mortar and some heavily fragmented and non-diagnostic ceramic fragments, including construction materials (especially *tegulae*). Most of the pottery is heavily worn or covered in lime mortar, which suggests that it was also part of Wall M-3/M-4, in which, as already noted, ceramics were used as construction materials.

The top layers of the sequence (UE 4004, UE 4006a and UE 4006b) are similar in nature to the lower levels, in both terms of sediment and associated materials. UE 4006b is fairly complex. The associated materials include *tegulae*, coarse ware, tableware in ARSW D and amphorae, mostly African and eastern (late Roman 2 and other combed amphora productions); the deposit also contains remains of malacofauna and loose human bones, as well as one anatomically joined body, although the remains are poorly preserved as a result of the pressure caused by later activity, which has broken and splintered many of them. This body, together with the remains of over 10

[4] All radiocarbon samples were processed at the Beta Analytic Testing Laboratory (https://www.radiocarbon.com) in May/June 2019.

individuals, probably executed, cremated and buried in situ, found during the excavation of the nearby Sounding G in association with charred textile remains (Villada and Godoy 2017; Villada and Bernal-Casasola 2019; Bernal-Casasola et al. 2020a), suggests a radical change in the use of this area after the earthquake (we will not linger on this aspect owing to space constrains). A sample collected from this level yielded a radiocarbon date of AD 637–714, with an 88.4% probability (Beta no. 526112). Given the total absence of Islamic pottery and the continued presence of late Roman material, we are inclined to date the burials to the late seventh century, well after the seismic event.

The most recent units of the sequence are again similar. UE 4006a contains a substantial amount of pottery, including hand-built kitchen and coarse ware, a *dolium* fragment and non-diagnostic fragments of African and eastern amphorae, as well as bones of land animals and remains of mytillidae shells forming clusters, suggesting a consumption context. The most recent layer is UE 4004, which is also the richest in terms of ceramic fragments, including ARSW D, non-diagnostic combed eastern amphorae and residual fragments of Baetican amphorae. The presence in this context of African Keay 8A amphorae (see Fig. 14.20c, 6), dated to the second half of the seventh century (Bonifay 2004, p. 141), and the absence of Emirate period material, which is present in other areas of the site (e.g. near M-6), also seem to suggest a date for the burials in the very late seventh century.

No similar archaeological contexts have been found to date in the *Fretum Gaditanum*, with the exception of those on Alexander Henderson Street and the nearby San Nicolás Street, in *Iulia Traducta* (Jiménez-Camino et al. 2010; Bernal-Casasola et al. 2018). The most similar sequence is, however, found in the so-called Phase 3 of the *Alcazar* in Marseilles, which has a similar profile in terms of amphorae (Keay LXI—*spatheia*—and Keay L 8A (Bien 2007, pp. 264–265, Fig. 270–272).

14.6 Conclusions: New Perspectives on the Fortifications of *Septem* and a Late Antique Earthquake on the African Shores of the *Fretum Gaditanum*

The recent excavations undertaken in the Baluarte de la Bandera, Ceuta (2014–2018) have considerably increased our understanding of late Roman *Septem Fratres*, for two main reasons: the discovery of the first firm evidence for the city's fortifications, and the detection of a substantial earthquake in the late seventh-century AD, the first and oldest event of this nature to have been detected on the west coast of North Africa.

The late Roman fortifications of *Septem* have been paid little attention to date. It is important to highlight that the interpretation of their structural sequence is extremely complex because of the small size of the excavated area. The sequence of events that follows appears to us to be the most logical, but the reader must be aware of all its caveats. We have decided to give priority to stratigraphic criteria, rather than the organic nature of the architectural features and the written sources (especially Procopius). Trying to interpret archaeological sequences while rigidly following written accounts has caused endless interpretive problems—for instance with Polybius in the Iberian Peninsula (Morillo 2019). Archaeology must play first fiddle.

The archaeometric analysis of the mortars has not helped much to clarify the complex relationships between these features. So, the results yielded by different sections of M-5 are dissimilar, while Channel C-1 and Wall M-3, which seem to have been built simultaneously, have very similar compositions. M-4 and M-6, which were in all certainty built in different periods, have also yielded similar results.

Our interpretation of the construction sequence is as follows.

Phases II and III were built over an earlier horizon (Phase I), the nature of which is unclear.

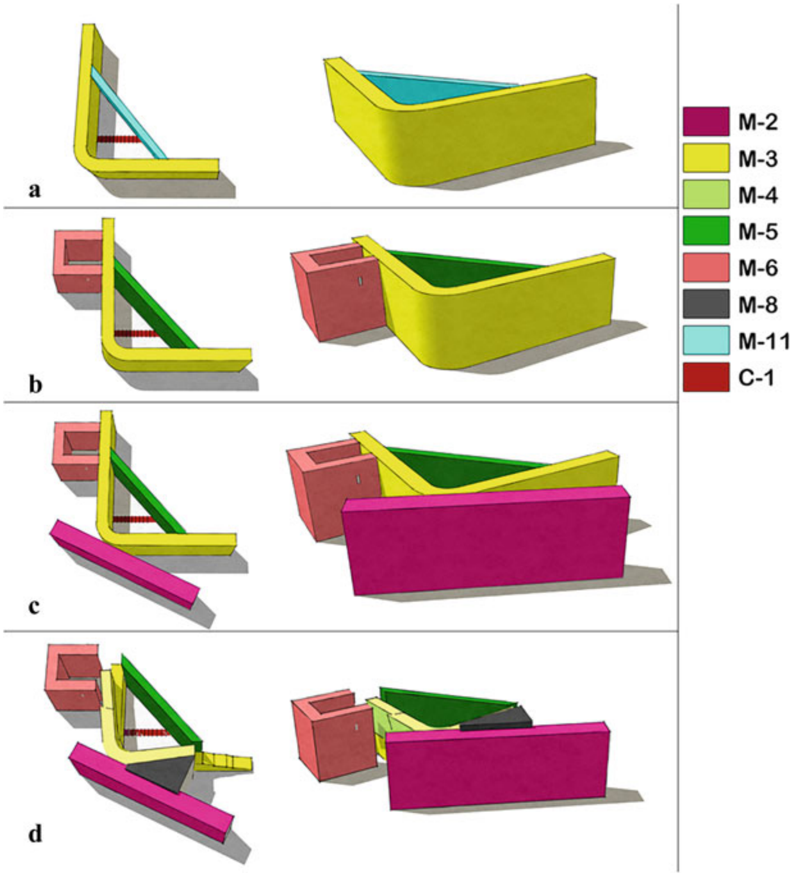

Fig. 14.21 Diagram with the sequence of the late Roman defensive structures found in the Baluarte de la Bandera (**a** building of wall; **b** addition of external tower; **c** construction of second wall; **d**. earthquake)

Phases II and III are marked by the construction of a series of defensive structures whose evolution is synthesised in Fig. 14.21.

First, there is the imposing Wall M-3/M-4, which was built in the late second or early third-century AD, based on the pottery reused in its construction. The preserved remains are over 10 m long and several metres high. The extant north-western corner was reinforced by two girths, M-11 and the later M-5, which were subsequently detached from it by the earthquake or other post-depositional processes (see Fig. 14.21a, b). The wall was equipped with a water drainage system (Channel C-1), which we think formed part of the same complex because of its association with (M-11) and because, should the channel have been earlier, it would have been affected by the construction of the wall. Parallels exist, for instance at the Western Gate of *Tamuda*'s *castellum*, which does not form a right angle with the defensive structures, like in the Baluarte de la Bandera. The inner face of Wall M-3/M-4 has various non-aligned openings, which should be associated with anchor points for wooden transit structures, rather than with supports for lifting devices during its construction or with upper stories.

At a later date, Feature M-6 was built abutting the earlier wall. Different building techniques were used. Only part of the western façade of this wall has been excavated to date. The presence of an arrowslit and the nature of the wall's associated fill suggest that this feature originally belonged to a tower (see Fig. 14.21b).

Its dimensions (between 60 and 100 cm thick and nearly 4 m high) and typology indicate that M-3/M-4 was a defensive feature (the corner of a perimeter wall, with square towers on the outside). The type of construction is reminiscent of those found in military camps—especially the thickness of the walls, which are characteristic of the early Imperial period but tend to become thicker in later periods, and the rounded corners. The dimensions are similar to those of *Tamuda*'s *castellum* (a wall thickness of between 0.80 and 1 m), and so is the floorplan: the earliest wall of the military camp, before the addition of the semi-circular towers (Lenoir 2011, 254). Tower M-6 was probably quadrangular, as is characteristic of the late Roman period. In *Tamuda*, the towers, which are earlier, are semi-circular.

It seems, however, more likely that these features formed part of *Septem*'s urban wall, rather than of a military camp. Other fortifications in the area of the strait present similar characteristics, in both urban (*Baelo Claudia*) and military camp settings (*Tamuda*).

The wall exhibits obvious pathologies caused by an earthquake: as already noted, it would be easy to argue for a seismic event in the late third-century AD, for similar events have already been attested in the region around this date (for instance, in *Baelo Claudia*). Moreover, the interpretation of the late Roman wall M-2 would not be difficult: M-2 would have been built to "clad" the obsolete defensive structures—as suggested by Procopius. However, the stratigraphy tells a different story, for the collapsed upper part of the earlier wall came to rest on a sedimentary deposit dated to the second half of the seventh century, which means that all these defensive structures (M-3/M-4, M-6 and M-2) had been simultaneously in use for some time.

These results have led to the reassessment of other archaeological sites in *Septem* (see Fig. 14.22a). The northern wall on Paseo de las Palmeras runs from east to west, like the wall built during the Caliphate period (Bernal-Casasola and Pérez 1999, p. 32, M-106 or UE 1058 and building techniques in p. 43). It is dated to the mid second century and is dozens of metres long. Both its thickness (90 cm), building technique and the use of dressed masonry over a lime-bound core are similar to those found in M-3/M-4 (Pérez and Bernal-Casasola 1995, p. 186). Another possible section of this wall was found on Queipo de Llano Street (Fernández Sotelo 2004, Figs. 68–69, Fig. 4). The wall built during the Caliphate period rested partially on this feature.

Traditionally, the walls on Paseo de las Palmeras and Queipo de Llano Street have been considered as the perimeter walls of the *cetariae* of the Roman city of *Septem,* but it can now be argued that they were, in fact, part of the city walls. Hopefully, future finds will confirm whether or not this hypothesis is correct (see Fig. 14.22a, 1, 4 and 5).

Returning to the Baluarte de la Bandera, we must again insist on the earthquake-induced structural pathologies that were described in detail above. As already observed, the natural approach would be to link this earthquake with similar events attested in the region (like the third-century AD seismic event in *Baelo Claudia*). This would provide an easy explanation for M-2, which would have "cladded" the former defensive structures. This also concurs with Procopius' account.

However, the stratigraphy is not compatible with this explanation, since M-3 collapsed on top of a sedimentary deposit dated to the second half of the seventh century, which implies that M-3/M-4, M-6 and M-2 coexisted as defensive structures. Therefore, M-2 was built for reasons that are unclear, but that had nothing to do with the earthquake.

Feature M-2 was built later, but still during the late Roman period. This has been interpreted as another defensive structure because of its thickness (1.28 m). Its exact construction date, however, is unknown, as its foundations have yet to be excavated (see Fig. 14.21c). In any case, it seems clear that it must have been built before the second half of the seventh century, because a sequence of deposits dated (based on ceramic deposits and radiocarbon dates) to AD 640/650–700 is known to have built up against it. That is, the wall was in use during the Byzantine period, And, although this cannot be proven with the evidence available, it seems plausible to interpret it as part of the wall built by Justinian I after the Byzantine conquest of Ceuta in 533. The wall was still visible at the time of the Islamic conquest, because the wall built in the tenth century (M-1) rested upon it. The chronology of M-1 is quite certain; wall sections that used the same building techniques (stretchers and double/triple headers), materials (marine calcarenite blocks cut to similar shapes) and thickness (between 1.5 and 2 m approximately) are found elsewhere in the city: Queipo de Llano Street, the Baluarte de la Bandera, the Baluarte de los Mallorquines, the northern flank of the medina, the Baluarte de la Coraza and the Puerta Califal (Hita, et al. 2008). Moreover, both in the Puerta Califal and the Baluarte de la Coraza, the Umayyad wall rests on late Roman walls—the Roman structure in the Puerta Califal has been dated by radiocarbon to AD 563–653.

In order to interpret M-2 correctly it is important to take into account the other two known sections of "Byzantine" wall—the Puerta Califal and the Baluarte de la Coraza—with which M-2 seems to be aligned—they all have an N–S orientation. However, the section in the Baluarte de la Bandera seems to have a "forward" position with regard to the rectangle that the other sections appear to outline (Fig. 14.22a, 1–3). This is also suggested by G. Braun plan of sixteenth-century Ceuta in *Civitates Orbis Terrarum*, in which this area of the city is labelled as *castrum*—heir to the late Antique *frourion*—and represented as a motley collection of fortifications of varying sizes and orientations (Fig. 14.22b, circle). In other words, the new wall section identified does not encircle the city's northern boundaries, but runs northwards towards the sea. At present, it is impossible to ascertain its function; it may be an isolated structure, albeit not too far from the walls, with which it might have been connected in some way, or it may be something else altogether—perhaps an inland projection of the port's structures? This possibility should be investigated further because, as the reconstruction plan illustrates, this area is located to the north of the fortifications in the area of the isthmus.

It is also important to clarify the relationship between the earliest Roman wall (M-3/M-4 and its later additions, such as M-6) and the Byzantine wall (M-2), because they were simultaneously in use for some time, although it is as yet impossible to be sure for how long. All the evidence suggests that M-2 is the interior face of *Septem*'s second late Roman wall; accordingly, the whole of the excavation area would be situated within the Byzantine defensive precinct, the course of which was later fossilised by the construction of the caliphate period wall: this would become the westernmost defensive line of the city, with the same orientation as the two walls in the Puerta Califal and the Baluarte de la Coraza (see Fig. 14.22a, 1–3). As already noted, this seems to have been a sort of forward fortification, sticking out of the rectangular plan of the city.

Fig. 14.22 Diagram of the defensive structures documented in *Septem*, in relation to the urban topography (**a**, based on a 1759 plan by Esteban de Panón, BNE—MR/42/381), with details of the area under study, after G. Braun's *Civitates Orbis Terrarum* (**b**)

The older Roman walls (M-3/M-4 and Tower M-6) protected the northern flank of the city, at least until they collapsed as a result of the earthquake.

Although Byzantine Africa immediately conjures up rectangular urban walls and fortresses (Pringle 1981), not all of them corresponded to this model, like for instance the kidney-shaped fortifications of *l'arx* in Cosa (Zanini 1998, p. 221, Figs. 58 and 59). Whereby it can be argued that the Byzantine fortifications did not encircle the pre-existing Roman fortification, but simply reinforced them wherever it was necessary, leading to a model of mixed walls, built-in different periods and, therefore, using different techniques. This is something common in late Roman cities, for instance in Mérida and Cartagena; the reuse of existing structures would have reduced somewhat the costliness of those projects. Perhaps these technical solutions were adopted by architects from Constantinople, who adapted the existing defensive structures to a rectangular layout, similar to the one followed later by Abd al-Rahman III's builders (Bernal-Casasola and Villada 2020, Fig. 5), but with a seaward projection on the north-western corner, towards the harbour and the city's entrance. It should be borne in mind that the fleet was of paramount importance for the Byzantine Empire —the *dromoi* that confronted the Visigoths first and the Umayyads later on (it is possible that Ceuta housed a naval base)—and the army's dependence on supplies brought in from elsewhere. This issue should be investigated further in the future.

The second key find of our excavations in the Baluarte de la Bandera is the evidence for a late Antique earthquake. The imposing cracks visible in the interior and exterior faces of the late Antonine-early Severan walls leave few doubts about this. For the sake of clarity, six of the EAEs have been described. EAE 1 was the fracture and displacement northwards of two sections of Wall M-3/M-4, which lost all structural connection with the wall, leaving it useless as a defensive feature. We do not know what happened with the top sections of the wall, but it is likely that they collapsed northwards into the nearby sea, although no archaeological evidence exists to substantiate this. The two displaced wall Sections (2 and 3, see Fig. 14.16), are both over 2 m long and weigh several tonnes, which gives some idea of the force of the seismic event. The remaining pathologies are vertical cracks (EAE 2–6) in both the exterior and interior face of the wall, some of which are over 3 m long. The reuse in the foundations of M-3/M-4 of a set of stone blocks cannibalised from a nearby public building exacerbated the effects of the earthquake, as shown by the much larger size of the cracks in this area (25–30 cm). It is important to recall that post-depositional phenomena may have contributed to increase the size of these cracks, especially the weight of the Portuguese fortification in 1541. On the other hand, the foundations were laid on relatively stiff or rigid basement rocks of the Sebtide—or Alpujárride—unit, which consist of high pressure-metamorphosed metapelites probably formed during the Permian–Triassic Age (Ruiz-Cruz and Sanz de Galdeano 2013). However, the official geological map of IGME (2002) indicates phyllites and deformed conglomerates of the Ordovician—Ghomaride complex. At any rate, the contact between the Sebtide and the Ghomaride complexes is close to the Baluarte de la Bandera, but the rocks are of comparable geotechnical quality. No unconsolidated sediments of the Pleistocene have been mapped here, which would have caused ground and site amplification of seismic waves.

It seems clear that, after sustaining this damage, this section of the wall lost all defensive value and was never rebuilt. This raises the question of how the defence of this flank of the city was organised after the seismic event. One possibility is that M-2 and M-6 were linked by another wall running to the north of the existing structures, but as this area is currently occupied by the Muralla Real this cannot be demonstrated.

It is equally important to determine why M-3/M-4 was the only feature to suffer the effects of the earthquake, as the other structures show little damage, with the possible exception of M-2, which exhibits some minor repairs (fill generated by M-12, see Fig. 3), and the gap opened between M-6 and the earliest Roman wall (see

Figs. 14.13b, c). In all likelihood, this had a lot to do with M-3/M-4's E-W orientation, as a possible N–S fault, i.e. the contact between Sebtide and Ghomaride complexes, which may have been responsible for the seismic event due to reactivation, has been mapped nearby (IGME 2002; Reicherter et al. 2019).

Establishing the chronology of the seismic event is an important step forward. It is clear that it occurred in the late Roman period, because it directly affected a structure built between the late second and the early third centuries. The date of the earthquake has been based on stratigraphic grounds: the collapse of the upper section of M-3/M-4 occurred when the nearby area was already full of sediment; otherwise the fractured section would have collapsed completely, losing all structural contact with the rest, when in reality it barely shifted 1 m. Therefore, the earthquake post-dated the formation of the sedimentary sequence excavated in Sounding 4 in 2018. The area was excavated with great care, and the chronology of the sequence has been examined in minute detail; the ceramic contexts (especially African *sigillatas* and amphorae) and the three radiocarbon dates clearly suggest a date in the seventh-century AD. As described in detail in Sect. 14.5, we think that the sequence began building up in ca. 640/650, and continued to do so until the late seventh century, when the area was used for a group of traumatic burials—in situ cremations and amputations included. This has led us to date the earthquake to the second half of the seventh century, during the reign of Heraclius II or Constans II, when the Byzantine Empire was already under pressure from Islamic expansion in the Eastern and Central Mediterranean, and Ceuta had become very vulnerable.

Chronology has played a key role in this research project; we are keenly aware of the problems that imprecise chronologies have had for the archaeology of the region around the Strait of Gibraltar. These problems have often stemmed from an excessive trust in radiocarbon dates, the best example of this being *Baelo Claudia*. To date, over 10 substantial discrepancies between radiocarbon dates and earthquake- and tsunami-related events, the so-called "anomalous episodes of abandonment", and other archaeological indicators, have been detected (Bernal-Casasola et al. 2015, p. 131, Table 2). Behind these issues lies a serious methodological problem: archaeologist have complete faith in palaeoseismologists, and palaeoseismologists sometimes have blind faith in unconfirmed and unpublished archaeological dates. It is for this reason that we have often limited ourselves to *ante quem* and *post quem* chronological thresholds. It is also important to consider the residual nature of many archaeological finds, which is more common than generally believed, especially concerning ceramics and coins during the Imperial period, during which the largest catalogue of identified earthquakes occurred. Another problem is an excessively rigid approach to the written sources. By and large, it is the mention of an earthquake in the written sources which sends archaeologists on its trail, in search of an archaeoseismological confirmation. A clear example of this is the earthquake documented for the Second Punic War (Rodríguez-Vidal et al. 2011). In recent years, a careful exegesis of references to tsunamis and earthquakes in the written sources has shown that most of them are inaccurate (Álvarez-Martí-Aguilar 2017, 2020).

There is no reference to seismic events in the seventh century in our region either in historical chronicles or in those catalogues published prior to the Second World War (Galbis 1932, 1940). Concerning the Iberian Peninsula, we know of an earthquake in 580 and another in 718, but none during our period (Martínez-Solares and Mezcua 2002, p. 23). Only in the comprehensive catalogue published by Emanuela Guidoboni (1994) is there a reference that may be of interest to the issue at hand. Of the 300 earthquakes recorded in the Mediterranean, 4% of them are dated to the seventh century (Guidoboni 1994, pp. 349–359, no. 231–242). Most of them were recorded in the Eastern Mediterranean—10 examples (AD 601–602, Hierapolis; AD 601–602, Cilicia; AD 602–603, Surb Karapet; AD 611, Constantinople; AD 634, Jerusalem; AD 634, Aleppo; AD 641–668, Byzantine Empire; AD 659, Palestine and Syria; AD 659, Jericho and AD 679, Batnan, Edessa, Mesopotamia)—plus a few in the Central Mediterranean (AD 618, Rome; second half of the seventh century, Sicily). Largely based on the written record, we know that there was seismic activity in the seventh-century AD, although very far away from Ceuta. Only the twelfth-century Byzantine historian Zonaras (2.88) records an earthquake during the reign of Constans II (641–668), which affected many regions controlled by the Romans, leading to the collapse of many buildings (Guidoboni 1994, pp. 356–357, no. 238 and 448). This could include Ceuta, which was still under Byzantine rule, although it is impossible to be sure owing to the generic nature of the reference. It is also significant that the only earthquake recorded in North Africa in Guidoboni's catalogue was the one dated from 16 May or 31 July 881, which was cited by two historians: al-Athīr (twelfth century) and Abī Zar' (thirteenth century). According to these authors, this seismic event affected different areas of the Mediterranean, including Syria, Egypt, Mesopotamia, North Africa and al-Andalus. Abī Zar' claims that the effects of this earthquake were particularly felt in the area between *Tanga* (Tangiers) and *Tilimsān* (Guidoboni 1994, p. 388, no. 275). The published maps clearly indicate that Tangiers is the only city associated with recorded seismic activity in western North Africa (Guidoboni 1994, pp. 414–421).

Therefore, in addition to pursuing the study of the effects of this earthquake in Ceuta,[5] we must try to track them also in other cities, in order to establish its magnitude—local, regional?—although it seems obvious that it did not have such devastating effects as the famous earthquake of AD 365, recorded by the Roman historian Ammianus Marcellinus. In the Strait of Gibraltar, recent research conducted by the University of Toulouse has attested the traumatic collapse of part of a Visigothic basilica in La Silla del Papa, in Bolonia Bay, Tarifa. The event has been dated to the seventh or early eighth century (see Figs. 14.23a, b). The excavations carried out between 2014 and 2016 have discovered a church which was originally rectangular, and to which various new elements were added over time. The ceramic material and radiocarbon dates indicate that the church was in use as of the very late sixth century and that it remained standing until the ninth century, by which time the building had lost its liturgical use and was being occupied by squatters; its heyday can be dated to the seventh century (Gutiérrez, Lefebvre and Moret 2017, pp. 206 and 212–213). The excavators have highlighted the collapse of the western end of the transept and main entrance (2 m high), which affected 13 masonry courses that appear to have fallen in one piece (Gutiérrez et al. 2017, Fig. 5; see our Figs. 14.23a, b, red rectangle). The excavators have offered two possible explanations for this: structural defects or an earthquake (Moret 2015, pp. 60–62, Figs. 6.7 and 6.8). The chronological coincidence is remarkable, but no firm evidence exists to prove that both collapses were caused by the same event.

Finally, it is worth mentioning that archaeoseismology is an incipient discipline in the region, with the exception of the pioneering studies performed in *Baelo Claudia* (Grützner et al. 2012; Silva et al. 2016). For this reason, the future may hold many surprises, such as the possible earthquake in Estepona (Malaga) in the ninth century, or the two seismic events detected in the Maritime Baths of *Baelo Claudia*: one dated to ca. 500, after the baths had been turned into an industrial facility; and the other to the fourteenth–fifteenth century, causing the traumatic collapse of the walls of the old Roman baths (see Fig. 14.23c), which by then still stood over 4 m high (Bernal-Casasola et al. 2015). The magnitude of this collapse can only be explained by an earthquake or an extreme wave event (e.g. Becker-Heidmann et al. 2007).

All considered, in the Strait of Gibraltar we are confronted by a paradox: on the one hand, some of the earthquakes that have been proposed may not be such or are not dated with sufficient accuracy; on the other hand, others have left practically no trace in the written, archaeological or sedimentary records. One possible example is

[5] For instance, through micromorphology analysis, currently being performed by Dr Mario Gutiérrez, University of Jaén.

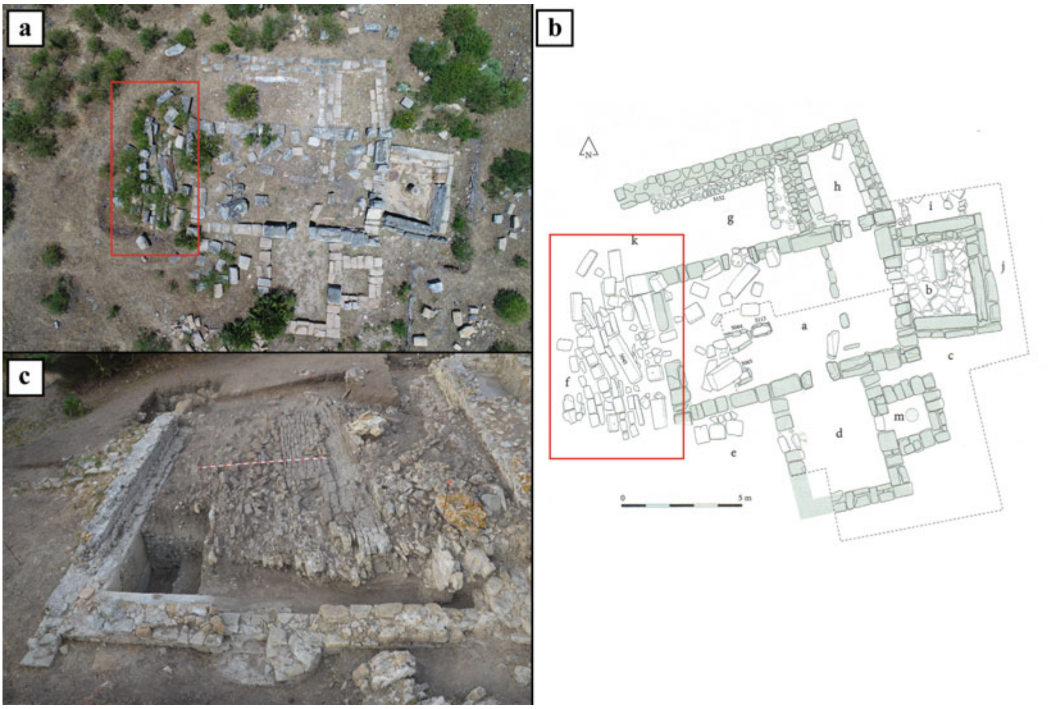

Fig. 14.23 Aerial photograph of Silla del Papa, with the Visigothic church and the collapse of the entrance (**a** Aerial photograph LABAP/UCA, 2019, courtesy of P. Moret), planimetry with the collapsed courses (**b** Gutiérrez, Lefebvre and Moret 2017, p. 203, Fig. 3f, rectangle); and traumatic collapses in the Maritime Baths in *Baelo Claudia*, dated to the late Middle Ages-early Modern Age, on top of another dated to ca. AD 500 (**c**)

the cracks on the Almohad vaults in Ceuta's Puerta Califal, which may have been the result of a yet undetected EAE. This new perspective may yield interesting results in the short, mid and long term.

Finally, we must stress that the sequence of pre-Islamic defensive structures excavated in the Baluarte de la Bandera is possibly one of the most challenging archaeological excavations ever conducted in Ceuta. Some of the questions that have remained open can only be answered with more research, which is also required to explore the earliest levels of the early Imperial occupation in *Septem*.

Acknowledgements This work has been conducted in the framework of the agreement signed by the autonomous city of Ceuta and the University of Cádiz concerning the archaeological projects at Benzú and *Septem*), and of projects GARVM III (PID2019-108948RB-I00) funded by the Spanish Government/FEDER; ARQUEOSTRA (FEDER-UCA18-104415), Programa Operativo FEDER Andalucía 2014–2020; ARQUEOFISH (P18-FR-1483) Programa de Ayudas a la I+D+i del Plan Andaluz de Investigación, Desarrollo e Innovación (PAIDI 2020); and GARVM-TRANSFER (PDC2021-121356-I00), Proof of Concept 2021 programme, Spanish Ministry of Science & Innovation. Reicherter was granted financial support by the Deutsche Forschungsgemeinschaft project RE1361/28-1. We wish to express our thanks to Michel Bonifay (CCJ, Aix-en-Provence) and Paul Reynolds (ERAAUB, Barcelona) for their useful comments about late Antique ceramics; to Angel Morillo (Complutense University, Madrid) for sharing his knowledge about the defensive architecture of Roman military camps and urban walls in Antiquity; to Pierre Moret (University of Toulouse) for sharing information about his excavations in Silla del Papa; and Manuel Álvarez-Martí-Aguilar for providing us with bibliography concerning catastrophic events.

References

Álvarez-Martí-Aguilar M (2017) La tradición historiográfica sobre catástrofes naturales en la Península Ibérica durante la Antigüedad y el supuesto tsunami del Golfo de Cádiz de 218–209 a.C. Dialogues d'histoire ancienne 43(2):117–145

Álvarez-Martí-Aguilar M (2020) The historicity of the earthquakes occurring in the Iberian Peninsula before A.D. 881 recorded in Spanish and Portuguese Seismic Catalogs. Seismol Res Lett 91(6):3585–3594

Becker-Heidmann P, Reicherter K, Silva PG (2007) 14C dated charcoal and sediment drilling cores as first evidence of Holocene tsunamis at the Southern Spanish coast. Radiocarbon 49(2):827–835

Bernal-Casasola D (1996) Le anfore tardo-romane attestate a Ceuta (Septem Fratres, Mauretania Tingitana). L'africa Romana 11:1191–1233

Bernal-Casasola D (2009) Ceuta en la Antigüedad Clásica. In: Villada Paredes F (coord) Historia de Ceuta: de los orígenes al año 2000, vol 1. Instituto de Estudios Ceutíes, Ceuta, pp 132–203

Bernal-Casasola D (2013) Septem Fratres, ciudad portuaria y comercial entre Juba II y Justiniano: del palimpsesto de su arqueología preislámica. In: Villada F (coord) Arqueología en las Columnas de Hércules: novedades y nuevas perspectivas de la investigación arqueológica en el Estrecho de Gibraltar. Instituto de Estudios Ceutíes, Ceuta, pp 9–50

Bernal-Casasola D (2016) Le Cercle du Détroit, une region géohistorique sur la longue durée: Karthago. Revue D'histoire Et D'archéologie Africaines 29:7–50

Bernal-Casasola D (2018) Continuidad y cesura en las ciudades tardorromanas del Estrecho de Gibraltar: el Fretum Gaditanum, un ámbito hispano-africano singular. In: Panzram S, Callegarin L (eds) Entre civitas y madīna: el mundo de las ciudades en la Península Ibérica y en el norte de África (siglos IV–IX). Casa de Velázquez, Madrid, pp 105–118

Bernal-Casasola D (2019) Ánforas tardorromanas en Hispania: claves de identificación. In: Fernández Ochoa C, Morillo Cerdán A, Zarzalejos Prieto M (eds) Manual de cerámica romana IV: producciones cerámicas de época medio-imperial y tardorromana. Comunidad de Madrid, Alcalá de Henares, pp 549–670

Bernal-Casasola D, Pérez Rivera JM (1999) Un viaje diacrónico por la Historia de Ceuta: resultados de las intervenciones arqueológicas en el Paseo de las Palmeras (Ceuta). Instituto de Estudios Ceutíes, Ceuta

Bernal-Casasola D, Pérez Rivera JM (2001) Las ánforas de Septem Fratres en los ss. II y III d.C.: un modelo de suministro de envases gaditanos a las factorías de salazones de la costa tingitana. In Chic García G (coord) Congreso Internacional Ex Baetica Amphorae: conservas, aceite y vino de la Bética en el imperio romano (Écija y Sevilla, 17 al 20 de diciembre de 1998), Actas 3. Editorial Gráficas, Écija, pp 861–885

Bernal-Casasola D, Villada Paredes F (2020) Acerca del *frourion* bizantino de *Septem*: entre Procopio, Gozalbes y la Arqueología. In: Pastor M, Perea S (eds) El Norte de África en época romana: Historia, sociedad, economía (Tributum in memoriam Enrique Gozalbes Cravioto). Universidad de Granada, Granada, pp 159–191

Bernal-Casasola D, Expósito JA, Lorenzo Martínez L (2018) Ocupación bizantina en Tradvcta tras el abandono de las cetariae. In: Bernal-Casasola D, Jiménez-Camino R (eds) Las cetariae de Ivlia Tradvcta: resultados de las excavaciones arqueológicas en la calle San Nicolás de Algeciras (2001–2006). Universidad de Cádiz, Cádiz, pp 251–273

Bernal-Casasola D, Jiménez-Camino Álvarez R (2018) De las cetariae a Tradvcta: contextualización atlántico-mediterránea y perspectivas. In: Bernal-Casasola D, Jiménez-Camino R (eds) Las cetariae de Ivlia Tradvcta. Resultados de las excavaciones arqueológicas en la calle San Nicolás de Algeciras (2001–2006). Universidad de Cádiz, Cádiz, pp 770–782

Bernal-Casasola D, Expósito JA, Díaz JJ et al (2015) Evidencias arqueológicas de desplomes paramentales traumáticos en las Termas Marítimas de Baelo Claudia: reflexiones arqueosismológicas. Cuaternario y Geomorfología 29(1–2):119–136

Bernal-Casasola D, Médard F, Villada Paredes F et al (2020a): Textiles tardorromanos en la norteafricana *Septem*: evidencias arqueológicas del Baluarte de la Bandera. VII International Symposium Purpureae Vestes (Granada, octubre 2019). Universidad de Granada, Granada, pp 119–127

Bernal-Casasola D, Villada Paredes F, Domínguez-Bella S et al (2020b) Spolia de la ciudad tingitana de Septem Fratres: de los elementos arquitectónicos reutilizados en el Baluarte de la Bandera. Actas del Congreso Internacional Exemplum et Spolia: la reutilización arquitectónica en la transformación del paisaje urbano de las ciudades históricas. Instituto de Arqueología de Mérida and CSIC, Madrid, pp 631–645

Bernal-Casasola D, Villada Paredes F, Retamosa Gámez JA et al (2019) Informe de Actividad Arqueológica: fase preislámica del Baluarte de la Bandera (Ceuta). Original inédito depositado en la Consejería de Educación y Cultura de la Ciudad Autónoma de Ceuta, Ceuta

Bernal-Casasola D, Villada Paredes F, Retamosa Gámez JA et al (2020c) Ceuta tardorromana: cerámicas severianas y bizantinas del Baluarte de la Bandera. International Conference LRCW 7. In: Late Roman Coarse Wares, Cooking Wares and Amphorae in the Mediterranean Archaeology and archaeometry: the ending of Late Roman pottery, the 8th century in the crossroads, València – Riba-Roja de Túria – Alacant, October 2019 (in press)

Bien S (2007) La vaisselle et les amphores en usage à Marseille au VII^{e} siècle et au début du VIIIè siècle: première ébauche de typologie évolutive. LRCW 2: archaeology and archaeometry, vol 1. Archaeopress, Oxford, pp 263–274

Bonifay M (2004) Études sur la céramique romaine tardive d'Afrique. Archaeopress, Oxford

Braga PD, Braga ID (2009) El dominio portugués hasta 1580. In: Villada Paredes (coord) Historia de Ceuta: de los orígenes al año 2000, vol. 1. Instituto de Estudios Ceutíes, Ceuta, pp 317–393
Brown P (2012) El mundo de la Antigüedad Tardía: de Marco Aurelio a Mahoma. Editorial Gredos, Madrid
Bustamante Álvarez M (2010) El comercio de terra sigillata altoimperial en el Círculo del Estrecho. Archaeopress, Oxford, Balance historiográfico y líneas de investigación
Campos Carrasco J, Bermejo Meléndez J (eds) (2013) La arquitectura militar del castellum de Tamuda: los sistemas defensivos. L'Erma di Bretschneider, Rome
Carmona Portillo A (2009) Ceuta bajo los Austrias. In: Villada Paredes F (coord) Historia de Ceuta. De los orígenes al año 2000, vol 2. Instituto de Estudios Ceutíes, Ceuta, pp 13–63
Contreras Garrido JJ (2010) La artillería de costa en Ceuta. Origen y evolución, Ceuta
Didierjean F, Ney C, Paillet J-L (1986) Belo III: le macellum. Casa de Velázquez, Madrid
El Khayari A, Akerraz A (2012) Al-Qsar Al-Awwal: nouvelles données archéologiques sur l'occupation de la base vallée de Ksar de la période tardo-antique au haut Moyen-Âge. In: El Boudjay A (ed) Ksar Seghir: 2500 ans d'échanges intercivilisationnels en Méditerranée. Institut des Etudes Hispano-Lusophones, Rabat, pp 11–34
Fernández Ahumada G, Villada Paredes F (2017) Scripta manent: inventario de los signos lapidarios de Ceuta I: La Ciudad. Ciudad Autónoma de Ceuta, Ceuta
Fernández Sotelo EA (2004) La muralla romana de Ceuta. Museo de Ceuta, Ceuta
Galbis J (1932) Catálogo sísmico de la zona comprendida entre los meridianos 5° E y 20° W de Greenwich y los paralelos 45° y 25° N, vol 1. Instituto Geográfico, Catastral y de Estadística, Madrid
Galbis J (1940) Catálogo sísmico de la zona comprendida entre los meridianos 5° E y 20° W de Greenwich y los paralelos 45° y 25° N, vol 2. Instituto Geográfico y Catastral, Madrid
García Vargas E, Bernal-Casasola D (2016) Puerto Real 2 (Costa Bética). In: Amphorae ex Hispania. Paisajes de producción y de consumo. http://amphorae.icac.cat/amphora/puerto-real-2-baetica-coast. Accessed 25 Apr 2020
Giner-Robles JL, Rodríguez-Pascua MA, Pérez-López R et al (2009) Structural analysis of Earthquake Archaeological Effects (EAE): Baelo Claudia examples (Cádiz, South Spain), Field Training Course Notebook. Instituto Geológico y Minero de España, Madrid
Gozalbes Cravioto E (1986) Los bizantinos en Ceuta (siglos VI-VII). Caja de Ahorros y Monte de Piedad de Ceuta, Ceuta
Gozalbes Cravioto E (1990) El nombre romano de Ceuta: de Septem Fratres a Ceuta. Concejalía de Cultura del Ayuntamiento de Ceuta, Ceuta
Grützner C, Reicherter K, Hübscher C, Silva PG (2012) Active faulting and neotectonics in the Baelo Claudia area, Campo de Gibraltar (southern Spain). Tectonophysics 554–557:127–142
Guidoboni E (ed) (1994) Catalogue of ancient earthquakes in the Mediterranean area up to the 10th century. Istituto Nazionale di Geofisica, Rome
Gutiérrez Lloret S, Lefebvre B, Moret P (2017) La iglesia altomedieval de la Silla del Papa (Tarifa, Cádiz). In: Brassous L, Lemaître S (coords) La ville Antique de Baelo, cent ans après Pierre Paris. Mélanges de la Casa de Velázquez 47(1):201–214
González Limón T, De Buergo Ballester MA (2002) The lime renderings from Plaza de la Corredera. Córdoba, Materiales De Construcción 52(267):19–30
Hita Ruiz JM, Villada Paredes F (2004) En torno a las murallas de Ceuta: reflexiones sobre el amurallamiento de Septem Fratres y la cerca omeya de Sabta. In: Actas de las I Jornadas de estudio sobre fortificaciones y Memoria Arqueológica del hallazgo de la muralla y Puerta Califal de Ceuta, 27–28 June 2002. Fundación Foro del Estrecho, Ceuta, pp 17–52
Hita Ruiz JM, Villada Paredes F (2009) Medina Sabta. In: Villada Paredes (coord) Historia de Ceuta. De los orígenes al año 2000, vol 1. Instituto de Estudios Ceutíes, Ceuta, pp 205–315
Hita Ruiz JM, Villada Paredes F, Suárez J (2008) Ceuta, puerta de Al-Andalus: una relectura de la Historia de Ceuta desde la conquista árabe hasta la fitna a partir de los datos arqueológicos. Cuadernos De Madinat Al-Zahra 6:11–52
IGME (2002) Mapa geológico de España, Ceuta 14–49, escala 1:25.000. Instituto Geológico y Minero de España, Madrid
Járrega Domínguez R (2019) La terra sigillata africana: centros de producción, caracterización y vías de difusión. In Fernández Ochoa C, Morillo Cerdán A, Zarzalejos Prieto M (eds) Manual de cerámica romana IV. Producciones cerámicas de época medio-imperial y tardorromana. Comunidad de Madrid, Alcalá de Henares, pp 135–188
Jiménez-Camino Álvarez R, Navarro Luengo I, Suárez Padilla J et al (2010) De Iulia Traducta a Al-Yazirat Al-Hadra: la Algeciras de los siglos VI al VIII a través de la excavación arqueológica de la calle Alexander Henderson, 19–21. In: García A, Izquierdo Benito R, Olmo Enciso L et al (eds) Espacios urbanos en el Occidente mediterráneo (s. VI–VIII). Toletvm Visigodo, Toledo, pp 143–152
Lagóstena Barrios L (2001) La producción de salsas y conservas de pescado en la Hispania romana (II a.C. – VI d.C.). Edicions Universitat Barcelona, Barcelona
Lenoir M (2011) Le camp romain: Proche Orient et Afrique du Nord. Bibliothèque des Écoles Françaises d'Athènes et de Rome, Rome
Martín Corrales E (2009) Ceuta en el siglo XVIII: de presidio a ciudad portuaria sin puerto. In: Villada Paredes F (ed) Historia de Ceuta. De los orígenes al año 2000, vol 2. Instituto de Estudios Ceutíes, Ceuta, pp 65–117
Martínez-Solares JM, Mezcua J (2002) Catálogo sísmico de la península Ibérica (880 a.C.–1900). Instituto Geográfico Nacional, Madrid

Moret P (coord) (2015) Proyecto General de Investigación La Silla del Papa (Tarifa, Cádiz), Primera fase de excavaciones (octubre 2014 – mayo de 2015). Informe inédito depositado en la Delegación Territorial de Cultura de la Junta de Andalucía en Cádiz

Morillo Cerdán A (2019) Arquitectura militar romana en Hispania. In: Sánchez López EH, Bustamante Álvarez M (eds) Arqueología romana en la Península Ibérica. Editorial Universidad de Granada, Granada, pp 385–407

Pérez Rivera JM, Bernal-Casasola D (1995) Reflexiones sobre la época romana y tardoantigua de Septem: los resultados de las excavaciones del Paseo de las Palmeras (Ceuta). CuPAUAM 22:181–198

Pringle D (1981) The defence of Byzantine Africa from Justinian to the Arab Conquest: an account of the military history and archaeology of the African provinces. British Archaeol Rep, Oxford

Reicherter K, Bernal-Casasola D, Villada Paredes F et al (2019) Archaeoseismic evidence for a Late Roman earthquake in Ceuta (Northern Africa). In: 20th congress of the international union for quaternary research (INQUA), Dublin, July 2019, P-4819, posters IV

Rodríguez-Pascua MA, Pérez-López R, Giner-Robles JL, Silva PG et al (2011) A comprehensive classification of earthquake archaeological effects (EAE) in archaeoseismology: application to ancient remains of Roman and Mesoamerican cultures. Quat Int 242:20–30

Rodríguez-Vidal J, Ruiz F, Cáceres LM et al (2011) Geomarkers of the 218–209 BC Atlantic tsunami in the Roman Lacus Ligustinus (SW Spain): a palaeogeographical approach. Quat Int 242:201–212

Roldán Gómez L, Bendala Galán M, Blánquez Pérez J et al (1998) Carteia. Consejería de Cultura de la Junta de Andalucía, Madrid

Ruiz-Cruz MD, Sanz de Galdeano C (2013) Coesite and diamond inclusions, exsolution microstructures and chemical patterns in ultrahigh pressure garnet from Ceuta (Northerm Rif, Spain). Lithos 177:184–206

Sáez AM, Bernal-Casasola D, Díaz JJ et al (2013) Del final de la ciudad mauritana a la construcción del campamento: el Sondeo 3 en la Puerta Occidental del campamento. Bernal-Casasola D (coord) Tamuda. Cronosecuencia de la ciudad mauritana y del castellum romano. Universidad de Cádiz, Cádiz, pp 235–290

Sánchez Moral S, García Guinea J, Luque Ripoll L et al (2004) Carbonation kinetics in roman-like mortar. Mater Constr 54(275):23–37

Sillières P (1997) Baelo Claudia. Una ciudad romana de Bética. Casa de Velázquez, Madrid

Silva PG, Giner-Robles JL, Reicherter K et al (2016) Los terremotos antiguos del Conjunto Arqueológico romano de Baelo Claudia (Cádiz, Sur de España): quince años de investigación arqueosismológica. Estud Geol 72(1):1–24

Vallejo Girvés M (1993) Bizancio y la España tardoantigua (ss. V-VIII): un capítulo de historia mediterránea. In: Memorias del Seminario de Historia Antigua, vol 4. Universidad de Alcalá de Henares, Madrid

Vallejo Girvés M (2012) Hispania y Bizancio. Una relación desconocida. Ediciones Akal, Madrid

Viegas C (2016) Almagro 51C (Lusitania Meridional). In: Amphorae ex Hispania: paisajes de producción y de consumo. http://amphorae.icac.cat/amphora/almagro-51c-meridional-lusitania. Accessed 25 Apr 2020

Viegas C, Raposo JMC, Pinto IV (2016) Almagro 51C (Lusitania Occidental). In: Amphorae ex Hispania: paisajes de producción y de consumo. http://amphorae.icac.cat/amphora/almagro-51c-western-lusitania. Accessed 25 Apr 2020

Villada Paredes F (2012) Excavaciones arqueológicas en la Muralla Real de Ceuta: persistencias y rupturas (1415–1668). Velhos e novos mundos: estudos de Arqueologia Moderna (Lisboa, 6–9 de abril de 2011), vol 1. Universidade Nova, Lisboa, pp 375–384

Villada Paredes F, Bernal-Casasola D (2019) Del istmo a las Murallas Reales: un desafío para la arqueología preislámica de Septem (ss. I-VII d.C.). Antiq Afr 55:183–210

Villada Paredes F, Godoy Ruiz D (2017) Memoria final, excavación arqueológica en las bóvedas adosadas a las Murallas Reales y al Baluarte de la Bandera de Ceuta. Ciudad Autónoma de Ceuta, Ceuta

Villada Paredes F, Gurriarán Daza P (2013) Recientes investigaciones sobre las fortificaciones del Califato Omeya en el estrecho de Gibraltar (Tarifa, Algeciras, Tánger, Ceuta). In: Ferreira Fernandez IC (coord) Fortificações e Território na Península Ibérica e no Magreb (Séculos VI a XVI). Edições Colibri, Lisboa-Mértola, pp 51–62

Villada Paredes F, Ortuño E (2014) Informe de la Actividad Arqueológica en el Baluarte del Torreón o de la Bandera. Ciudad Autónoma de Ceuta, Ceuta

Villada Paredes F, Navarrete Pendón V, Sepúlveda Toro E et al (2017) Memoria de la excavación arqueológica Baluarte del Torreón de la Muralla Real de Ceuta o Baluarte de la Bandera. Ciudad Autónoma de Ceuta, Ceuta

Villada F, Suárez J, Bravo S (2007) Nuevos datos sobre las factorías de salazones de Septem Fratres a raíz de los resultados de las excavaciones arqueológicas del Parador de Turismo La Muralla. In: Lagóstena L, Bernal-Casasola D, Arévalo A (eds) Cetariae: salsas y salazones de pescado en occidente en la Antigüedad. John and Erica Hedges Ltd., Oxford, pp 487–501

Villaverde Vega N (2001) Tingitana en la Antigüedad Tardía (siglos III – VII). Real Academia de la Historia, Madrid

VV. AA. (1981) Enciclopedia dell'Arte Antica, Classica e Orientale. Atlante delle forme ceramiche I: Ceramica fina romana nel bacino mediterraneo (medio e tardo imperio). Istituto della Enciclopedia italiana, Roma

Zanini E (1998) Le italie bizantine. Territorio, insediamenti ed economía nella provincia bizantina d'Italia (VI-VIII secolo). Edipuglia, Bari

15 Multi-proxy Analysis of the AD 1755 Lisbon Tsunami Deposits in El Palmar de Vejer, Spain

Mike Frenken, Christoph Cämmerer, Piero Bellanova, Lisa Feist, Max Chaumet, Kira Raith, Philipp Schulte, Frank Lehmkuhl, Jan Schwarzbauer, and Klaus Reicherter

Abstract

The study area, El Palmar de Vejer, located in the Gulf of Cadiz in southwestern Spain, was severely struck by the AD 1755 Lisbon tsunami. El Palmar de Vejer was chosen as the study area due to the topographical setting, characterized by the flat alluvial floodplain, which has good preconditions as a sedimentary archive for tsunami deposits in order to gain a better understanding of the effects of the Lisbon tsunami based on previous studies and historical descriptions. The sedimentological and geochemical features indicate the processes of successive tsunami wash-overs and subsequent backwash and ponding conditions. An analysis of the major elements revealed a distinction between marine and terrestrial depositional environments. Using organic geochemistry, several different natural compounds were detected (e.g., *n*-alkanes and *n*-aldehydes), as well as some anthropogenic compounds (polycyclic aromatic hydrocarbons). The results suggest a differentiation between the AD 1755 tsunami deposit and the lagoonal background sediments, thus making it possible to identify tsunami processes. The results of this study analyzing the sedimentary

M. Frenken (✉) · C. Cämmerer · P. Bellanova · L. Feist · M. Chaumet · K. Reicherter
Neotectonics and Natural Hazards Group, RWTH Aachen University, Lochnerstrasse 4-20, 52056 Aachen, Germany
e-mail: m.frenken@nug.rwth-aachen.de

C. Cämmerer
e-mail: c.cammerer@nug.rwth-aachen.de

P. Bellanova
e-mail: p.bellanova@nug.rwth-aachen.de

L. Feist
e-mail: l.feist@nug.rwth-aachen.de

M. Chaumet
e-mail: max.chaumet@rwth-aachen.de

K. Reicherter
e-mail: k.reicherter@nug.rwth-aachen.de

M. Frenken · P. Bellanova · J. Schwarzbauer
Institute for Geology and Geochemistry of Petroleum and Coal, RWTH Aachen University, Lochnerstrasse 4-20, 52056 Aachen, Germany
e-mail: jan.schwarzbauer@emr.rwth-aachen.de

L. Feist
Neotectonics and Natural Hazards, Department of Geosciences and Geography, RWTH Aachen University, Aachen, Germany

K. Raith
Human Origins and Paleoenvironments Research Group, Department of Social Sciences, Oxford Brookes University, Headington Campus, Oxford OX3 0BP, UK
e-mail: kira.raith-2017@brookes.ac.uk

P. Schulte · F. Lehmkuhl
Department of Geography, RWTH Aachen University, Wüllnerstrasse 5B, 52056 Aachen, Germany
e-mail: philipp.schulte@geo.rwth-aachen.de

F. Lehmkuhl
e-mail: FLehmkuhl@geo.rwth-aachen.de

M. Álvarez-Martí-Aguilar and F. Machuca Prieto (eds.), *Historical Earthquakes, Tsunamis and Archaeology in the Iberian Peninsula*, Natural Science in Archaeology,
https://doi.org/10.1007/978-981-19-1979-4_15

archive provide strong evidence that a multi-proxy approach, with the inclusion of geochemical applications, can confidently detect tsunami deposits, distinguish them from the surrounding background sediments and subsequently characterize their internal structure and composition.

Keywords

AD 1755 Lisbon tsunami · Gulf of Cadiz · Geochemical signatures · El Palmar de Vejer · Tsunami wave cycle · Multi-proxy analysis

15.1 Introduction

Tsunamis are high-energy events that can damage coastal infrastructures. By evaluation, reconstructing inundations and understanding historical tsunami deposits, it is possible to improve hazard maps and predict future events more accurately, as well as gaining a better knowledge of the magnitude, frequency and processes of these events. El Palmar de Vejer, located on the southwestern coast of the Gulf of Cadiz (Spain), has been frequently affected by tsunamis in the past. Historical records show that the Gulf of Cadiz coastline was hit by several earthquake-induced tsunamis, inter alia in c. 218/209 BC, 60 BC, c. AD 60, c. AD 382, AD 881/889, AD 1531, AD 1722, AD 1755, AD 1761, AD 1941, AD 1969 and AD 1975 (Baptista and Miranda 2009; Kaabouben et al. 2009; Lario et al. 2011; Ruiz et al. 2013; summary in Costa et al. this volume). However, some of the oldest mentioned events, for example, those occurring in c. 218/209 BC, 60 BC and c. AD 382, have yet to be confirmed by reliable sources due to the absence of contemporary reports. Historical accounts of these events were only mentioned by Spanish and Portuguese historians (e.g., Ocampo 1543) in the sixteenth and seventeenth centuries, more than 1000 years after they had occurred, for which reason their historicity is a moot point (Udías 2015, 2020; Andrade et al. 2016; Álvarez-Martí-Aguilar 2020, this volume). Furthermore, the coastline has been frequently struck by other extreme events, including storms and surges (Del Río et al. 2012). For some of these extreme wave events (hereinafter EWEs), either geological evidence has yet to be identified or they did not produce waves large enough to leave an imprint in the geological archives, whereby they have received little or no attention to date (e.g., Andrade et al. 2016).

In addition to the historically documented events, some paleotsunami records were discovered in the Gulf of Cadiz and dated to 6000–7000 BP (Scheffers and Kelletat 2005), 5300–5500 BP (Ruiz et al. 2005; Vizcaino et al. 2006; Baptista and Miranda 2009), approximately 4000 BP (Ruiz et al. 2005; Koster and Reicherter 2014), 3700 BP (Reicherter et al. 2019), 3600 BP (Ruiz et al. 2005; Vizcaino et al. 2006), 2400–2700 BP (Lario 1996), and 2200–2300 BP (Luque et al. 2002; Vizcaino et al. 2006). The relatively high-risk potential of earthquakes and subsequent tsunamis in this area apparently has to do with its proximity to the Azores-Gibraltar fault zone (hereinafter AGFZ), which is a major active fracture zone in and along the Gulf of Cadiz (Duarte et al. 2013; Bezzeghoud et al. 2014), and with subduction within the Gibraltar Arc area (Gutscher et al. 2002, 2006). The sea level has not changed much in the Gulf of Cadiz since approximately 8000 BP (Zazo et al. 2008).

One of the best described EWEs is the AD 1755 Lisbon tsunami induced by the eponymous earthquake (e.g., Martínez Solares et al. 1979; Gracia et al. 2006; Rodríguez-Vidal et al. 2011; Costa et al. 2016). Although it's precise epicenter has yet to be established and, consequently, is still a matter of much debate (e.g., Baptista et al. 1998; Mader 2001; Zitellini et al. 2001; Lario et al. 2011), it may have been located in the AGFZ (Baptista et al. 1998; Lario et al. 2011; Duarte et al. 2013). Both the earthquake and tsunami had devastating effects along the Moroccan and Iberian Atlantic seaboards, especially on the Algarve coast and on our study area, the southwestern Spanish coast (Campos 1991). Many studies have been performed on the impact of the AD 1755 tsunami on the Spanish coastline, especially in the vicinity of Cape Trafalgar. Well-located along the Spanish section of the Gulf of Cadiz, between El Palmar de Vejer and Conil de la Frontera (province of Cadiz, Andalusia), is the low lying back-barrier floodplain of the Conilete creek (*Arroyo de Conilete*) with favorable settings due to its flat and open geomorphology, sparse vegetation and a former lagoon (Costa et al. 2012; Dawson et al. 2020; Spiske 2020). It serves as an excellent sediment archive for paleoenvironmental changes, especially EWE deposits like those of tsunamis.

A new field study was conducted with the aim of (1) identifying and characterizing the AD 1755 Lisbon tsunami; (2) inquiring deeper into its effect on the flood plain; (3) reconstructing the tsunami processes in El Palmar de Vejer; and (4) detecting possible additional EWE deposits. To achieve these goals a multi-proxy analysis was performed to paint a comprehensive picture of the sedimentological setting and the possible EWE deposits in El Palmar de Vejer. The application of ground-penetrating radar (hereinafter GPR) and sedimentology contributes to gain a better understanding of sedimentary processes, erosion, sediment transport and depositional conditions during a tsunami and, above all, in combination with geochemistry to provide deeper insights into the tsunami processes (e.g., Cuven et al. 2013; Chagué-Goff et al. 2017; Bellanova et al. 2020).

The field studies performed by Luque et al. (2004), Lario et al. (2009) and Gutiérrez-Mas et al. (2016), based on historical descriptions of this area and focusing on the sedimentological, geophysical and geoarchaeological properties of the respective tsunami layers, notably discovered AD 1755 Lisbon tsunami deposits in the vicinity of El Palmar de Vejer. Their Conil de la Frontera field site was located further north on the floodplain of the Salado River. Based on their descriptions and findings of tsunami deposits, we started our fieldwork further south to explore the floodplain of the Conilete creek and to reconstruct the effects of the tsunami on the entire floodplain between Conil de la Frontera and El Palmar de Vejer.

15.2 Research Area

15.2.1 Study Area

El Palmar de Vejer is located in the Gulf of Cadiz, in southwestern Spain, where the climate is characterized by rainy winter months and dry summers (Moreno et al. 2010). The low-energy semidiurnal mesotidal coast (Borrego et al. 1993) is exposed to prevailing winds from the west-northwest (*poniente*) or from the east-southeast (*levante*), the former being responsible for the littoral drift along the Spanish Atlantic coast, mainly flowing to the SE (Alonso et al. 2016). These conditions influence the sedimentology and hydrogeology in the area, because the littoral drift is closing estuaries during dry periods (Zazo et al. 2008). Deposited sediments are supplied by the area's main rivers (Lario et al. 2002), which are supplemented by drift sediments from the more northern coastlines (Gutiérrez-Mas et al. 1996). The study area can be divided into two sections: the beach and dune area close to the shoreline; and the alluvial flat adjacent to the dunes (Gutiérrez-Mas et al. 2016). The floodplain occasionally has a flooded shallow lagoon (Luque et al. 2004; Lario et al. 2009), fed by the Conilete creek and smaller tributaries during the wet winters (Fig. 15.1). Furthermore, the coastal lagoon is embedded in the flat backshore topography, which was formed after the post-glacial sea level rise (Zazo et al. 2008). The backshore area is associated with the Holocene filling of former marshland, and the catchment area is located in the Campo Gibraltar Unit of the Lower Miocene, and post-orogenic calcarenites of the Late Miocene and Pliocene (Piedra/roca ostionera; González-Acebrón et al. 2016; Gutiérrez-Mas et al. 2016). It is characterized by the presence of abandoned meanders, which bear witness to the recent migration of the Conilete creek (Luque et al. 2004), but the main river course has remained stable over the past 100 years as visible on the historical map of Conil 1873 (López 1873). The hinterland is separated from the Atlantic Ocean by 6–10 m-high coastal dunes (Gutiérrez-Mas et al. 2016). Therefore, major inundations in the creek and the coastal lagoon mainly take place during EWEs, like tsunamis and storm surges, breaching the dunes or breaking through the blocked river estuary (Lario et al. 2009). Even though episodic storm flooding only affects the first 100 m of the floodplain, the AD 1755 tsunami was reported to have penetrated at least 300 m further inland

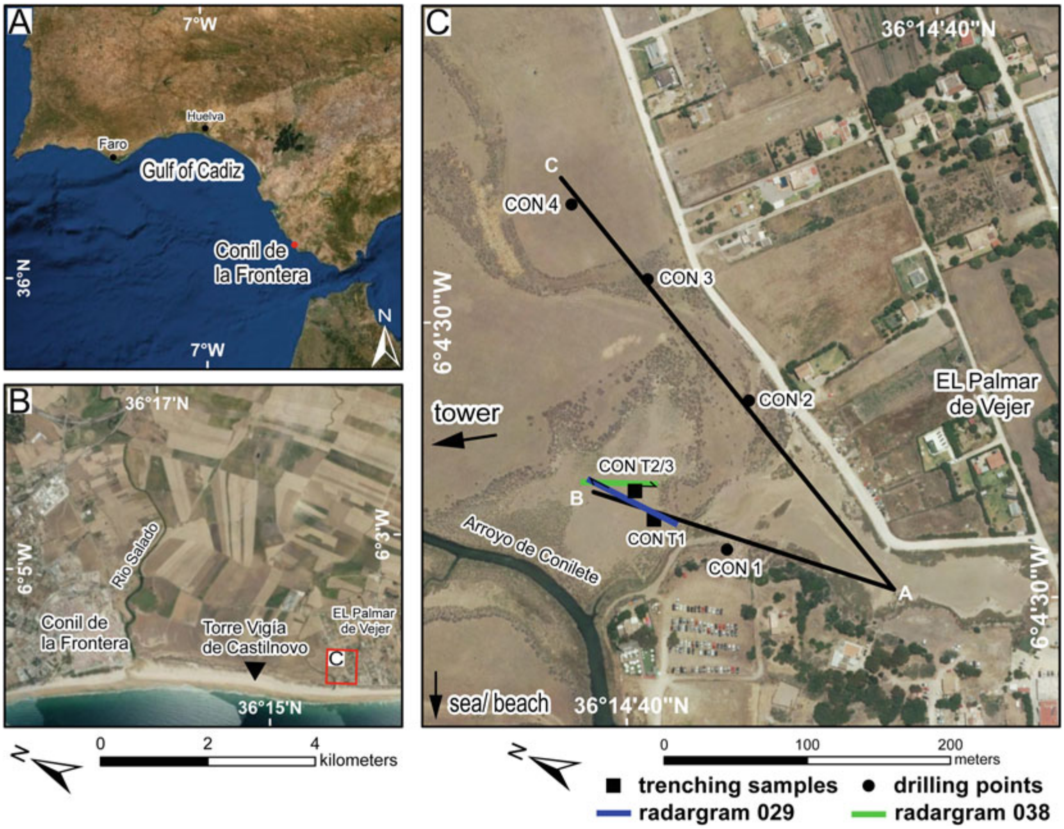

Fig. 15.1 Study site overview. **a** Study site location in the Iberian Peninsula. **b** Sampling site south of Conil de la Frontera. **c** Field site overview with sampling locations and GPR profiles in El Palmar de Vejer

(Lario et al. 2009). The normal tidal range in El Palmar de Vejer is around 2.4 m to a maximum of 4 m (Instituto Geográfico Nacional 1991; Luque et al. 2004).

Historically, the area was mainly given over to agriculture and, above all, fishing and stock-breeding (Luque et al. 2004; Santos and Koshimura 2015). In addition, the Castilnovo watchtower (*Torre Vigía de Castilnovo*) built in the sixteenth century to defend the area from naval invasions and to monitor tuna fish migration, and the Conilete settlement, which was located close to the watchtower, are anthropogenic influences in the backshore area (Rodríguez de la Torre 2005; Campese Gallego et al. 2009). Furthermore, the "La Chança" tuna factory was located ca. 3 km to the north, close to the Salado, the floodplain's major river (Gutiérrez-Mas et al. 2016).

Nowadays, the area between Conil de la Frontera and El Palmar de Vejer is still used for agriculture, but the research site has been declared a natural reserve, leaving it undisturbed by activities such as plowing. The steadily growing town of Vejer de la Frontera is also close to the study area.

Four cores (CON 1–CON 4), a smaller trench (CON T1) and a larger trench (CON T), with two sampling profiles (CON T2 and CON T3), were sampled for this study (Fig. 15.1). CON 1, with a drilling depth of 4.9 m, is the closest core to the coast (Table 15.1) behind the dune system next to an occasional tributary of the Conilete creek. With a depth of 0.65 m, CON T1, the second sampling point closest to the ocean, is located in the floodplain's branch in the depression (Table 15.1). CON T2/3, situated in the lagoonal depression, runs parallel to the coastline with a

Table 15.1 Coordinates of the cores and trenches, distance from the ocean and elevation

Cores/trenches	Coordinates	Distance from coast (m)	Elevation (m.a.s.l)
CON 1	36°14.660′ N 06°04.542′ W	340	2.2
CON T1	36°14.410′ N 06°04.320′ W	360	2.2
CON T2	36°14.700′ N 06°04.532′ W	380	2.2
CON T3	36°14.699′ N 06°04.529′ W	380	2.2
CON 2	36°14.673′ N 06°04.472′ W	440	2.6
CON 3	36°14.723′ N 06°04.440′ W	530	2.9
CON 4	36°14.764′ N 06°04.423′ W	580	3.6
Reference samples			
Dune 1	36°14.628′ N 06°4.670′ W		
Dune 2	36°14.628′ N 06°4.670′ W		
Dune 3	36°14.610′ N 06°4.634′ W		
River (Conilete creek)	36°14.660′ N 06°4.654′ W		
Beach 1	36°14.606′ N 06°4.703′ W		
Beach 2	36°14.617′ N 06°4.709′ W		
Intertidal 1	36°14.635′ N 06°4.745′ W		
Intertidal 2	36°14.588′ N 06°4.750′ W		
Nearshore	36°14.580′ N 06°4.788′ W		

depth of around 0.9 m (Table 15.1). CON 2 and CON 3 are located on higher elevations on the outer margin of the floodplain with drilling depths of 3 m (Fig. 15.2; Table 15.1). CON 4, the most distal sediment core, has a drilling depth of 3 m and is more elevated than the other sediment cores and trenches (Fig. 15.2; Table 15.1).

15.2.2 AD 1755 Lisbon Tsunami

On November 1, AD 1755, the Lisbon tsunami flooded the coastal lowland of El Palmar de Vejer (Real Academia de la Historia 1756). Blanc (2008, 2011) reported six waves approximately 37 km northwest of the city of Cadiz, Cuven et al. (2013) discussed multiple waves some 49 km southeast of Los Lances Bay and witnesses reported three main waves hit the Cadiz coast (Aparicio 2017). According to Luque et al. (2004) and Lario et al. (2009), more than one wave reached the Spanish coast in the Gulf of Cadiz. Several waves are realistic (Santos and Koshimura 2015), but eyewitness reports are the only evidence. Historical reports documented that the sea first withdrew, followed by the tsunami wave striking the beach (Luque et al. 2004). As to damage, the sources mainly refer to the severe damage to the Castilnovo watchtower and the complete destruction of the Conilete settlement (Rodríguez de la Torre 2005; Campese Gallego et al. 2009; Lario et al. 2009), supported by archaeological evidence within the tsunami layer in the immediate vicinity of the former settlement (Gutiérrez-Mas et al. 2016). The former Conilete settlement is located approximately 1 km northwest of the field site close to the Castilnovo watchtower. Other effects of the tsunami included the overflowing of the Conilete creek and Salado River, as well as the destruction of the “La Chança” tuna factory to the north of the backshore (Gutiérrez-Mas et al. 2016). Furthermore, historical documents mention several casualties in the tuna factory and the destruction of fishing boats and other materials (Gutiérrez-Mas et al. 2016). During the tsunami, the high

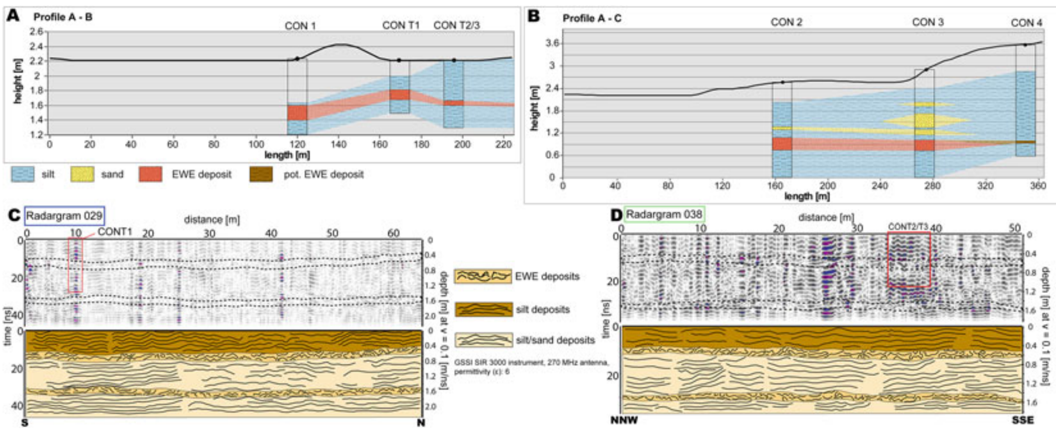

Fig. 15.2 Elevation model and ground-penetrating radargrams reflecting the possible tsunami extension. **a** Elevation transect of CON 1, CON T1 and CON T2/3 with the thicknesses and extension of the EWE deposits. **b** Elevation transect of CON 2, CON 3 and CON 4 with the thicknesses and extension of the EWE deposits. **c**, **d** Ground-penetrating radargrams to identify the EWE layer of AD 1755 Lisbon tsunami at ca. 0.5 m (location in Fig. 15.1c)

tide had a special impact on the coast, as most fishing activities were performed at that moment (Luque et al. 2001). In addition, the increased sea level intensified the tsunami wash-over in this area. A serious consequence was the inundation of the open and flat areas (Luque et al. 2004), with a loss of 599 head of cattle (Santos and Koshimura 2015). The tsunami waves were channeled by the Salado river in the northern sector and the inundation reached several kilometers inland (Martínez Solares 2001; Campese Gallego et al. 2009; 8.25 km after Luque et al. 2004; Lario et al. 2009), whereas the area surrounding the Conilete creek was inundated approximately 2–3 km inland (Luque et al. 2004; Lario et al. 2009). According to historical data (Real Academia de la Historia 1756; Luque et al. 2004), the inundation height on the floodplain between Conil de la Frontera and El Palmar de Vejer was estimated at 8 m a.s.l., albeit taking into account the high tide. Furthermore, eyewitnesses reported that water was brown, indicating that it contained a high level of sediment (Luque et al. 2004). According to Santos and Koshimura (2015), the effects of the tsunami on the sea level lasted for about 10 h.

15.3 Methods

The samples originate from several field studies (April 2016, September 2017 and September 2019) performed on the floodplain between Conil de la Frontera and El Palmar de Vejer in southwestern Spain (Fig. 15.1). For identifying the tsunami deposits, the following five approaches were applied: (1) GPR, (2) grain size analysis, (3) magnetic susceptibility (hereinafter MSM), (4) X-ray fluorescence (hereinafter XRF) and (5) organic geochemistry. In the current state of tsunami research, grain size and XRF analyses are the predominant techniques. However, for determining and characterizing tsunami deposits, other approaches, such as organic geochemistry, have shown potential (e.g., Bellanova et al. 2019, 2020) and may be considered for multi-proxy applications.

15.3.1 GPR

Non-destructive ground-penetrating measurements were taken to scan the floodplain of El

Palmar de Vejer for stratigraphic differences. The measurements were taken using the SIR 3000 instrument coupled to a 270 MHz antenna (Geophysical Survey Systems Inc.). The frequency of the antenna and the adjusted permittivity (ε) of 6 allows for high-resolution measurements to be taken in dry sand conditions from the surface to a depth of 2–4 m (Neal 2004). For GPS-based measurements (based on distance mode), a calibrated survey wheel was used, and GPS coordinates of the start and finish points were collected. Data processing was performed using the ReflexW software version 7.0 (Sandmeier Scientific Software 2019), including the following six processing steps: move-start-time, background-removal, remove-header-gain, energy-decay, average xy-filter and a band-pass Butterworth filter. A topographic correction was not needed, as the area is flat.

15.3.2 Sample Material

Soil samples of 10–100 g were collected from four sediment cores (CON 1–CON 4) of a transect perpendicular to the coastline with a focus on possible EWEs. Additionally, two trenches were excavated (CON T1 and CON T with two sampling profiles CON T2 and T3). Table 15.2 shows the sample depth and quantity. Sampling was implemented for sedimentological, inorganic and organic geochemical analyses. The organic geochemical samples were conserved in aluminum containers and stored at 4–7 °C to avoid contamination and microbial alterations, while the sedimentological and inorganic samples were stored in plastic bags. In addition, nine reference samples (50–100 g) from the river, dune, beach, intertidal and nearshore settings were collected (Table 15.1).

15.3.3 Grain Size Analysis

The grain size samples from CON 1, CON 2, CON 3, CON 4 and CON T1 were measured with the same method, while CON T2 was measured in another way. Prior to the grain size analysis, all samples were dried at 35–40 °C, homogenized and passed through a 2 mm sieve. Furthermore, the organic matter was removed with hydrogen peroxide (H_2O_2, 15%), while sodium pyrophosphate ($Na_4P_2O_7$) was used to avoid coagulation (Gee and Or 2002; Pye and Blott 2004). Treatment with hydrochloric acid (HCl) was not considered as the carbonates could be a primarily component of the transported sediments. Grain size measurements were performed with a Laser Diffraction Particle Size Analyzer (Beckman CoulterTM LS13 320 with additional PIDS technology, Beckman Coulter GmbH, Germany) described by Schulte and Lehmkuhl (2017). The measurement results ranged from 0.04 to 2000 µm with an error of 2%. Each sample was measured twice to reduce the error and to ensure the measurement of all the particles. The final results are the mean values of both measurements. In addition, a smaller grain size dataset from CON T2 was measured by sieving.

The granulometric parameters were calculated based on Folk and Ward (1957) by using the GRADISTAT V8 software (Blott and Pye 2001). Likewise, the software assured a comparability of the results, as sieving measurements were in weight percentage and Laser Diffraction Particle Size Analyzer measurements in volume percentage. The statistical parameters of mean, sorting, kurtosis, skewness, median and the percentiles were used to make bivariate plots emphasizing differences. Bivariate plots of median versus C (D99)-percentile, after Passega (1964) and Passega and Byramjee (1969), and mean grain size versus sorting, after Tanner (1991a, b), extended with the deposition energy by Lario et al. (2002), are especially important for identifying different mechanisms and energy conditions during deposition. For comparability, the values of CON T2 are not plotted in the bivariate diagrams.

15.3.4 XRF

Two methods were used for inorganic geochemistry: on the one hand, XRF measurements

Table 15.2 Granulometric results of all six analyzed sampling profiles

		Sample	Depth [m]	Mean [Φ]	Sorting [Φ]	Kurtosis [Φ]	Skewness [Φ]	Median (D50) [μm]	C/D99 [μm]	Clay [%]	Silt [%]	Sand [%]
CON 1	Post-tsunami	CON 1–1	0.60–0.64	4.54	3.05	0.77	0.56	101	640	13	30.7	56.3
	Tsunami (EWE 1)	CON 1–2	0.64–0.68	3.18	2.30	1.98	0.73	217	590	6.4	16.2	77.4
		CON 1–3	0.68–0.70	2.18	1.19	3.30	0.46	237	600	2.8	7.8	89.4
		CON 1–4	0.70–0.71	2.06	0.58	1.62	0.16	240	600	1.5	3	95.5
		CON 1–5	0.71–0.80	2.00	0.84	2.57	0.27	250	620	1.8	3.8	94.4
		CON 1–6	0.80–0.84	1.72	0.50	1.03	−0.10	297	700	0	0	100
	Pre-tsunami	CON 1–7	0.85–0.90	4.23	3.13	0.74	0.65	150	630	12.5	26.1	61.4
		CON 1–8	1.25–1.30	7.20	2.88	0.99	−0.19	5.06	225	29.8	53.7	16.5
		CON 1–9	1.35–1.45	6.40	3.00	0.68	−0.09	9.45	275	22	48.7	29.3
		CON 1–10	1.65–1.72	8.25	2.00	0.98	0.03	3.48	50	36.3	63.2	0.5
		CON 1–11	2.30–2.40	7.90	2.17	0.88	0.07	4.53	75	31.9	66.2	1.9
		CON 1–12	2.60–2.70	7.87	2.27	0.89	0.00	4.33	100	32.8	63.3	3.9
		CON 1–13	3.15–3.20	8.44	2.05	0.91	−0.02	2.92	52	40.4	59.3	0.3
		CON 1–14	3.60–3.70	8.14	2.18	0.86	0.06	3.89	90	35.9	62.3	1.8
	Possible EWE 2	CON 1–15	4.55–4.62	4.13	3.17	0.79	0.75	199	590	13.2	20.4	66.4
		CON 1–16	4.62–4.75	3.04	2.78	2.19	0.53	229	1910	7.4	14.9	77.7
	Pre-tsunami	CON 1–17	4.77–4.83	6.27	3.15	0.67	−0.12	9.20	270	21.9	47.8	30.3
		CON 1–18	4.83–4.90	7.86	2.20	0.86	0.01	4.33	56	32.3	67.5	0.2
CON 2	Post-tsunami	CON 2–1	0.51–0.55	5.57	2.84	0.73	0.12	22.8	300	13.9	48.7	37.4
		CON 2–2	0.55–0.59	6.30	2.84	0.74	−0.01	11.6	200	19.1	53	27.9
		CON 2–3	0.60–0.67	5.02	2.58	0.79	0.55	60.2	230	11.3	39.3	49.4
		CON 2–4	0.68–0.72	6.32	2.35	1.03	0.05	12.2	180	13.8	69.3	16.9
		CON 2–5	0.75–0.78	5.87	2.81	0.72	0.13	18.7	230	16.1	48.9	35
		CON 2–6	1.15–1.20	5.21	3.21	0.75	0.32	45.8	680	16.6	36.9	46.5
		CON 2–7	1.20–1.25	3.84	3.26	0.83	0.63	199	1480	11.4	21.5	67.1
		CON 2–8	1.25–1.30	4.03	3.70	0.67	0.46	146	1500	14.5	30.2	55.3
		CON 2–9	1.30–1.35	6.51	3.33	0.87	−0.21	7.35	580	25.1	51.2	23.7
		CON 2–10	1.35–1.41	5.15	3.80	0.63	−0.04	23.5	1120	18.5	37	44.5
	Tsunami (EWE 1)	CON 2–11	1.50–1.55	2.11	1.32	3.53	0.37	240	630	3.1	6.2	90.7
		CON 2–12	1.70–1.75	2.04	1.66	3.71	0.41	255	1040	4.5	8.9	86.6
	Pre-tsunami	CON 2–13	1.85–1.90	5.32	3.40	0.81	−0.06	21.0	1200	14.7	40.8	44.5
		CON 2–14	2.20–2.25	6.98	3.39	0.84	−0.36	3.70	290	36.1	43.3	20.6
		CON 2–15	2.80–2.85	7.96	2.18	0.87	0.05	4.00	90	32.9	65.2	1.9
CON 3	Post-tsunami	CON 3–1	0.50–0.65	3.50	2.76	1.34	0.77	247	660	7.5	18.1	74.4
		CON 3–2	0.65–0.70	4.39	3.37	0.77	0.42	96.3	1180	13.2	29.8	57
		CON 3–3	0.75–0.80	5.92	3.25	0.75	−0.20	10.9	700	17.3	50.1	32.6
		CON 3–4	0.85–0.90	3.08	3.24	0.95	0.71	369	1375	8.9	18.8	72.3
		CON 3–5	1.10–1.15	3.56	3.51	0.77	0.55	224	1700	11.2	24.3	64.5
		CON 3–6	1.20–1.25	6.01	3.34	0.66	−0.09	12.2	700	21.4	41.6	37
		CON 3–7	1.25–1.30	3.50	3.05	1.68	0.67	233	900	9.1	15.4	75.5
		CON 3–8	1.30–1.35	3.85	3.17	0.87	0.69	209	910	11	18.7	70.3
		CON 3–9	1.45–1.50	5.48	3.35	0.68	0.07	24.3	725	17.9	38.6	43.5
	Tsunami (EWE 1)	CON 3–10	1.55–1.60	3.40	2.44	3.79	0.79	222	565	7	12.1	80.9
		CON 3–11	1.75–1.80	3.05	2.12	2.56	0.73	220	590	5.4	15.6	79
	Pre-tsunami	CON 3–12	1.85–1.90	5.62	3.27	0.66	0.10	22.0	610	18.5	42.8	38.7
		CON 3–13	2.20–2.25	6.97	2.86	0.89	−0.07	7.45	290	25.4	58.2	16.4
		CON 3–14	2.45–2.50	5.86	2.97	0.69	0.34	28.4	250	20.4	41.9	37.7
		CON 3–15	2.80–2.85	7.23	2.65	0.86	−0.05	6.25	185	27.3	59.8	12.9

(continued)

Table 15.2 (continued)

		Sample	Depth [m]	Mean [Φ]	Sorting [Φ]	Kurtosis [Φ]	Skewness [Φ]	Median (D50) [μm]	C/D99 [μm]	Clay [%]	Silt [%]	Sand [%]
CON 4	Post-tsunami	CON 4–1	0.70–0.75	7.38	2.45	0.91	−0.01	5.91	111	27	64	9
		CON 4–2	1.45–1.50	6.75	3.17	0.76	−0.15	6.80	274	28.2	49.1	22.7
		CON 4–3	1.76–1.82	4.83	3.01	0.69	0.54	78.4	345	14.3	33.5	52.2
		CON 4–4	2.20–2.25	8.55	1.86	0.85	0.01	2.72	38	41.5	58.5	0
		CON 4–5	2.40–2.45	6.19	3.14	0.69	−0.05	11.6	590	21.2	45.6	33.2
		CON 4–6	2.48–2.54	7.46	2.46	0.94	−0.05	5.39	113	28.1	62.3	9.6
	Post-tsunami	CON 4–7	2.54–2.60	4.34	3.19	0.72	0.72	162	598	14.2	26.1	59.7
	Pre-tsunami	CON 4–8	2.65–2.70	6.26	3.14	0.64	−0.05	10.8	253	23	45.1	31.9
		CON 4–9	2.70–2.76	6.38	2.91	0.69	0.05	12.0	193	21.9	49.3	28.8
		CON 4–10	2.76–2.85	6.98	2.58	0.81	0.06	8.25	138	23.7	63.2	13.1
CON T1	Post-tsunami	CON T1–1	0.20–0.22	8.12	2.68	0.78	0.05	3.88	131	38.7	57.0	4.2
		CON T1–2	0.22–0.24	8.26	2.60	0.79	0.02	3.42	119	40.3	56.2	3.5
		CON T1–3	0.24–0.26	7.85	3.00	0.86	−0.03	4.50	289	36.7	52.8	10.4
		CON T1–4	0.26–0.28	6.72	3.75	0.70	−0.12	7.08	659	31.4	40.9	27.7
		CON T1–5	0.28–0.30	5.68	3.75	0.68	0.16	26.1	1043	23.5	34.3	42.2
		CON T1–6	0.30–0.32	5.24	3.61	0.72	0.37	51.5	736	20.4	31.5	48.1
		CON T1–7	0.32–0.34	5.24	3.82	0.74	0.30	48.6	1187	21.2	31.1	47.8
		CON T1–8	0.34–0.36	5.25	3.66	0.72	0.35	50.1	944	20.7	31.4	47.9
		CON T1–9	0.36–0.38	4.97	3.57	0.74	0.50	80.1	781	19.2	28.2	52.6
		CON T1–10	0.38–0.40	4.37	3.37	0.92	0.61	135	1031	14.5	23.8	61.7
	Tsunami (EWE 1)	CON T1–11	0.40–0.42	3.87	3.17	1.14	0.60	167	1388	11.1	21.2	67.7
		CON T1–12	0.42–0.44	3.24	2.90	1.47	0.61	222	1147	8.4	17.4	74.2
		CON T1–13	0.44–0.46	1.76	1.70	2.65	0.32	304	1406	3.8	8.3	87.9
		CON T1–14	0.46–0.48	1.97	1.69	3.07	0.35	268	1384	4.1	8.1	87.9
		CON T1–15	0.48–0.50	3.21	2.79	1.88	0.63	226	1529	7.8	15.9	76.3
		CON T1–16	0.50–0.52	3.66	3.57	0.89	0.55	202	1594	12.5	23.7	63.7
	Pre-tsunami	CON T1–17	0.52–0.54	5.87	3.85	0.73	0.05	18.5	1093	23.5	36.1	40.3
		CON T1–18	0.54–0.56	4.06	3.68	0.86	0.52	156	1421	14.6	23.6	61.8
		CON T1–19	0.56–0.58	4.18	3.25	0.95	0.63	151	929	13.0	23.3	63.7
		CON T1–20	0.58–0.61	5.70	3.61	0.73	0.22	28.9	1023	22.0	34.5	43.5
CON T2	Post-tsunami	CON T2–1	0.06–0.10	5.86	1.33	0.76	−0.02	n.d	n.d	0	93.4	6.6
		CON T2–2	0.36–0.40	5.13	1.61	0.75	0.09	n.d	n.d	0	69.8	30.2
	Tsunami (EWE 1)	CON T2–3	0.52–0.54	4.54	1.96	0.73	0.08	n.d	n.d	0	57.9	42.1
		CON T2–4	0.59–0.61	3.68	1.64	1.21	0.34	n.d	n.d	0	29.9	70.1
		CON T2–5	0.63–0.65	5.57	1.55	0.81	−0.04	n.d	n.d	0	82.4	17.6
		CON T2–6	0.66–0.70	5.22	1.62	0.76	0.05	n.d	n.d	0	71.9	28.1
	Pre-tsunami	CON T2–7	0.80–0.84	4.32	1.92	0.69	0.17	n.d	n.d	0	54.4	45.6
Reference	River			2.29	0.67	2.15	0.31	207	549	2.3	3	94.7
	Dune 1			2.03	0.40	0.98	−0.03	244	535	0	0	100
	Dune 2			2.02	0.41	0.98	−0.04	245	588	0	0	100
	Dune 3			2.05	0.43	0.97	−0.07	240	630	0.1	0.4	99.5
	Beach 1			0.95	0.79	0.98	0.04	527	1740	0.3	0.2	99.5
	Beach 2			1.51	0.72	1.08	−0.23	332	1657	0	0	100
	Intertidal 1			1.91	0.58	1.17	−0.21	258	1482	0	0	100
	Intertidal 2			1.57	0.69	1.04	−0.21	317	1120	0	0	100
	Nearshore			1.51	0.92	0.92	−0.28	311	1740	0.2	0.2	99.6

with a spectrometer for the samples from CON T1; and, on the other, a portable XRF device for measuring the bulk samples from CON 1 to CON 4.

Preparation for the XRF analysis involved sieving the samples to a grain size of ≥ 63 mm. Afterwards, this grain fraction was ground with a planetary mill (Pulverisette 7 classic device, Fritsch) and all samples were dried overnight at 105 °C to ensure the residual moisture was removed. Subsequently, 8 g of the samples was pressed with 2 g of wax (Fluxana CEREOX®) into tablets, so to increase binding without affecting the measurements. These tablets were measured with a Spectro XEPOS X-ray fluorescence spectrometer (SPECTRO Analytical Instruments GmbH, Germany), as described by Krauß et al. (2016). This method enables the detection of 52 elements, of which five (Ca, Fe, Sr, Ti and K) were selected for further analysis of the deposits (due to their differentiation potential). CON T1 was measured at an interval of 2 cm and at visually detected variations in sedimentation between a depth of 0.2–0.8 m.

Furthermore, the bulk samples of the sediment cores (CON 1–CON 4) were analyzed with a portable XRF device (Niton XLt 792Y 7329, Analyticon Instruments GmbH, Germany) at RWTH Aachen University. The portable scanner was directed at the bulk sample for 90 s. This time was sufficient for obtaining reliable results (Kalnicky and Singhvi 2001), yielding a possible spectrum of 22 elements, from which the same five elements were selected for a better comparability with the method described above. Both methods obtain element concentrations in ppm for comparability.

In light of the results, different element ratios were calculated, which can provide insights into the origin and composition of the sediments, as well as the identification of potential EWE deposits (Chagué-Goff et al. 2017).

15.3.5 MSM

For the sediment samples, MSM was measured with a Bartington MS2-system with a MS2K sensor (Bartington Instruments Ltd., United Kingdom). With this device, the response volume of the samples is in the range of 3 cm^3. The measurements are all given in the dimensionless (m^3/m^{-3}) SI unit. All bulk samples from CON 1–CON 4 and CON T1 were measured in plastic containers at RWTH Aachen University laboratory.

15.3.6 Total Carbon

The measurement of total carbon (hereinafter TC), total organic carbon (hereinafter TOC) and total inorganic carbon (hereinafter TIC) was performed with the Elementar Elemental Analyzer Vario EL Cube (Elementar Analysensysteme GmbH, Germany) on CON 1 to CON 4. For preparation, the samples were homogenized and, for the TOC measurements, pretreated with HCl (5%) and heated on a plate to remove inorganic carbon. TIC was calculated subtracting TOC from TC.

For the organic geochemical analysis of the samples from CON T1, T2 and T3, TOC values were calculated for normalization of sample results to the unit ng/g_{TOC}, providing comparability across samples of a different composition and grain size, according to Bellanova et al. (2019). Pretreatment included drying and homogenizing the samples, before 0.1 g of ground sample material was combusted at 550 °C for 30 min, using the Elementar Liqui TOC III (Elementar Analysensysteme GmbH, Germany).

15.3.7 Organic Geochemistry

15.3.7.1 Extraction and Measurement

For the extraction of biomarkers and anthropogenic markers, solid–liquid extraction via overhead shaking with different solvents (acetone and *n*-hexane), followed by fractionation, was performed according to the protocol proposed by Bellanova et al. (2019; and references therein). To each sample fraction, 50 µl internal surrogate standard solution (5.8 ng/µl fluoroacetophenone, 6.28 ng/µl d_{10}-benzophenone and 6.03 ng/µl

d_{34}-hexadecane) was added before GC–MS measurements were taken. The concentration of sample fractions was determined by GC-FID measurements according to the measurement protocol proposed by Bellanova et al. (2020; and references therein), performed on a Fisons GC8000 series 8060 (Fison Instruments Ltd, United Kingdom) equipped with a 30 m × 0.25 mm i.d. × 0.25 µm film ZB-5 fused silica capillary column (Zebron capillary GC column, Chrompack) and a flame ionization detector (FID). For quantification, a GC–MS analysis using a quadrupole, benchtop GC–MS instrument (Thermo Finnigan Trace GC–MS, Thermo Finnigan LLC, USA) in full scan mode (EI+) was conducted following the measurement protocol of Dsikowitzky et al. (2004) and Bellanova et al. (2020).

For interpreting and identifying organic compounds, mass spectra were compared with the spectral libraries of the NIST database (National Institute of Standards and Technology—U.S. Department of Commerce) using the Amdis 32 software (Automated Mass Spectral Deconvolution and Identification System). Furthermore, the quantification of the detected organic compounds was performed using the software Xcalibur™ by Thermo Scientific™ with the integration of specific ion chromatograms and an external four-point calibration with reference material. Calculations of quantified results (ng/g_{TOC}) were carried out according to Bellanova et al. (2019) for all the organic geochemical markers.

15.3.7.2 Data Presentation

The organic geochemical processing revealed a total of 50 biomarkers in three sampling profiles (CON T1, CON T2 and CON T3). The biological compounds can be divided into two compound groups, *n*-alkanes (C_{12} to C_{35}) and *n*-aldehydes (C_9 to C_{32}) (Tables 15.3 and 15.4). In addition, 33 anthropogenic markers were detected, which can be attributed to polycyclic aromatic hydrocarbons (hereinafter PAHs) (25 compounds) with their alkylated homolgs (eight compounds) (Table 15.5). Aromatic components are classified mainly as modern anthropogenic markers, increasing especially with the advent of industrialization. However, Pontevedra-Pombal et al. (2012) detected concentrations of aromatic compounds before industrialization, because these compounds emerge in detectable concentrations as soon as human activity is present (Bellanova et al. 2019).

The obtained results were presented with different indices and ratios.

N-alkanes were illustrated with:

(1) Terrigenous/aquatic ratio (hereinafter TAR), after Peters et al. (2005)

$$TAR = \frac{n-C_{27}+n-C_{29}+n-C_{31}}{n-C_{15}+n-C_{17}+n-C_{19}} \quad (15.1)$$

TAR clarifies the relative amount of terrigenous, predominantly *n*-alkanes of higher plants (C_{27}, n-C_{29} and n-C_{31}) (Rieley et al. 1991) versus the aquatic/marine *n*-alkanes, mainly n-C_{15}, n-C_{17} and n-C_{19} (Jaffé et al. 2001). TAR values in this study were divided by 10 for a better interpretation.

(2) Carbon preference index (hereinafter CPI), after Gogou et al. (1996)

$$CPI = \frac{(\sum odd\, n-C_{13}-n-C_{33})+(\sum odd\, n-C_{15}-n-C_{35})}{2x\sum even\, n-C_{12}-n-C_{34}} \quad (15.2)$$

CPI is an index for distinguishing between the petrogenic and biogenic origin of aliphatic compounds. While higher values indicate a dominance of odd-numbered *n*-alkanes, which are primarily biogenic, a lower CPI points to a shift towards even-numbered *n*-alkanes of petrogenic origin (Simoneit and Mazurek 1982; Schwarzbauer et al. 2017).

15.4 Results

15.4.1 GPR Profiles

Two GPR profiles were selected as being representative of the floodplain and lagoon transect in this study. The first GPR profile has a length of

Table 15.3 *n*-Alkane results with the most important ratios and indices

n-alkane		Sample	Depth [m]	Short-chain [ng/gTOC]	Medium-chain [ng/gTOC]	Long-chain [ng/gTOC]	Total concentration [ng/gTOC]	C_{max}	Odd over even
CON T1	Tsunami	CON T1–1B	0.39–0.42	28,697	64,866	437,289	530,852	C_{31}	4.39
		CON T1–2B	0.43–0.45	32,503	70,516	293,868	396,887	C_{31}	2.97
		CON T1–3B	0.46–0.49	124,169	102,107	824,244	1,050,520	C_{31}	3.71
	Pre-tsunami	CON T1–4B	0.61–0.65	22,411	34,459	559,446	616,316	C_{31}	5.78
CON T2	Post-tsunami	CON T2–1	0.06–0.10	88,551	11,664	526,892	732,087	C_{29}	2.84
		CON T2–2	0.36–0.40	76,585	21,401	34,100	132,086	C_{12}	1.30
	Tsunami	CON T2–3	0.52–0.54	51,969	87,025	396,080	535,074	C_{29}	2.74
		CON T2–4	0.59–0.61	39,609	53,345	286,003	378,957	C_{31}	3.62
		CON T2–5	0.63–0.65	118,017	328,799	1,856,896	2,303,712	C_{28}	1.17
		CON T2–6	0.66–0.70	53,964	67,856	350,202	472,023	C_{31}	2.31
	Pre-tsunami	CON T2–7	0.80–0.84	44,561	61,892	383,374	489,827	C_{31}	2.54
CON T3	Post-tsunami	CON T3–1	0.06–0.10	43,665	71,286	439,978	554,929	C_{29}	3.37
		CON T3–2	0.35–0.39	33,957	52,378	251,591	337,926	C_{29}	3.11
	Tsunami	CON T3–3	0.50–0.53	101,753	214,654	1,402,135	1,718,542	C_{31}	3.29
		CON T3–4	0.54–0.56	134,384	106,193	713,061	953,638	C_{31}	2.22
		CON T3–5	0.59–0.61	151,841	169,356	766,502	1,087,698	C_{29}	2.64
		CON T3–6	0.63–0.64	81,674	7869	583,666	743,709	C_{33}	2.90

65 m and runs from south to north in the lagoon (Fig. 15.2c). The uppermost layer is characterized by parallel internal layering to a depth of 0.4 m. It is followed by anomalies up to a depth of between 0.4–0.6 m, showing different "parabolic" reflections in relation to the uppermost deposits (Fig. 15.2c). This area displays an irregular "zig-zag" pattern (by hyperbolae originating from pebbles) and a nonplanar erosional base. Further down, the GPR profile is characterized by parallel patterns comparable to the top layer at a depth between 0.6 and 1.5 m. Another layer at a depth between 1.5 and 1.6 m also displays irregular reflections like the "zig-zag" pattern. The last identifiable layer exhibits parallel layering comparable to the top layer and diminishes with the resolution at a depth of 2.2 m.

The second GPR profile, with a length of c. 51 m, was recorded parallel to the coastline (NNW–SSE) and, as before, four layers are identifiable (Fig. 15.2d). The top layer is characterized by parallel and internal reflectors at a depth of around 0–0.5 m. Between 0.5 and 0.7 m reflections with "zig-zag" patterns and discontinuous reflectors, as well as an unconformable (erosional) base, are visible. This is followed by mostly parallel internal layering, comparable to the top layer, at a depth between 0.7 and 1.5 m. These radargram images also indicate a second layer with irregular reflections ("zig-zag") at a depth between 1.5 and 1.7 m. This is followed by a layer with parallel internal layering ending at a depth of 1.85 m due to resolution.

In both radargrams, two layers can be clearly distinguished from the parallel layered

Table 15.4 *n*-Aldehyde results with the total concentration and calculated indices

n-aldehyde								
		Sample	Depth [m]	Short-chain [ng/gTOC]	Long-chain [ng/gTOC]	Total concentration [ng/gTOC]	C_{max}	Odd over even
CON T1	Tsunami	CON T1–1B	0.39–0.42	1040	200	1240	C_{30}/C_{14}	0.05
		CON T1–2B	0.43–0.45	2083	392	2430	C_{26}/C_{14}	0.05
		CON T1–3B	0.46–0.49	3875	63,005	66,880	C_{29}	3.71
	Pre-tsunami	CON T1–4B	0.61–0.65	1409	845	2254	C_{30}/C_{14}	0.15
CON T2	Post-tsunami	CON T2–1	0.06–0.10	1035	2994	4030	C_{26}	0.51
		CON T2–2	0.36–0.40	7207	16,627	23,834	C_{29}	1.16
	Tsunami	CON T2–3	0.52–0.54	1240	31,025	32,266	C_{22}	0.23
		CON T2–4	0.59–0.61	1295	3042	4337	C_{22}	0.22
		CON T2–5	0.63–0.65	1256	3253	4509	C_{30}	0.25
		CON T2–6	0.66–0.70					
	Pre-tsunami	CON T2–7	0.80–0.84	1611	12,253	1364	C_{30}	0.29
CON T3	Post-tsunami	CON T3–1	0.06–0.10	368	5924	6292	C_{28}	0.12
		CON T3–2	0.35–0.39	56	3417	3473	C_{28}	0.22
	Tsunami	CON T3–3	0.50–0.53	1062	5843	6905	C_{26}	0.25
		CON T3–4	0.54–0.56	82	2203	2285	C_{30}	0.22
		CON T3–5	0.59–0.61	33.6	3719	3753	C_{26}	0.26
		CON T3–6	0.63–0.64	42.5	7402	7445	C_{26}	0.22

background sediment. Their thicknesses are identical, as is the structure of their reflectors and erosional base. The internal zig-zag pattern of these layers, which contrasts with the laminated layers, has been interpreted as coarse-grained material and shell layers, along with other internal sedimentary structures (e.g., scours).

15.4.2 *Granulometric, Inorganic and Organic Geochemistry—Stratigraphic Units*

The cores and trenches obtained from the floodplain of the Conilete creek indicate comparable depositional units with almost identical sedimentological and geochemical properties, although their depth and thickness vary slightly. These can be divided into three units. Unit I forms the base, while Unit III reflects the uppermost unit, namely, the modern sediments. There is a clear interruption in the silty sedimentation between Unit I and Unit III, represented by Unit II, which is mainly composed of sand, along with an erosional base. Table 15.2 contains all the granulometric properties, and Figs. 15.3, 15.4, 15.5, 15.6, 15.7, 15.8 and 15.9 show the grain-size, inorganic and organic parameters of all the profiles and samples.

15.4.2.1 Unit I

All the cores and trenches show similar patterns in sedimentary Unit I. The lower unit is

Table 15.5 Anthropogenic geochemical marker results (parent and alkylated PAHs) with the concentration of predominant compounds

Polycyclic aromatic hydrocarbons

		Sample	Depth [m]	Parent PAHs [ng/gTOC]	Alkylated PAHs [ng/gTOC]	Total concentration [ng/gTOC]	Phenanthrene [ng/gTOC]	Fluoranthene [ng/gTOC]	Pyrene [ng/gTOC]	Benz[a] anthracene [ng/gTOC]	Chrysene [ng/gTOC]
CON T1	Tsunami	CON T1–1B	0.39–0.42	496	n.d	496	5.14	37.8	41.4	11.6	15.1
		CON T1–2B	0.43–0.45	306	n.d	306	3.93	29.0	23.7	0.62	1.46
		CON T1–3B	0.46–0.49	1054	n.d	1054	9.07	108	94.8	17.7	38.9
	Pre-tsunami	CON T1–4B	0.61–0.65	483	n.d	483	0.06	0.14	0.5	12.2	10.5
CON T2	Post-tsunami	CON T2–1	0.06–0.10	534	195	730	5.40	70.9	71.2	12.0	39.5
		CON T2–2	0.36–0.40	941	132	1073	23.3	27.3	97.3	35.5	78.3
	Tsunami	CON T2–3	0.52–0.54	21,608	3487	25,095	2668	3677	2952	1169	3267
		CON T2–4	0.59–0.61	5991	604	6595	1016	678	436	195	527
		CON T2–5	0.63–0.65	33,084	6793	39,877	4118	8938	4010	5334	5732
		CON T2–6	0.66–0.70	16,513	2708	19,221	1374	4239	1328	1877	2304
	Pre-tsunami	CON T2–7	0.80–0.84	34,767	4816	39,583	2211	8540	6068	2386	3626
CON T3	Post-tsunami	CON T3–1	0.06–0.10	1730	210	1940	310	321	195	19.3	175
		CON T3–2	0.35–0.39	5368	628	5996	35	949	699	267	705
	Tsunami	CON T3–3	0.50–0.53	8626	1013	9639	740	1025	762	223	1231
		CON T3–4	0.54–0.56	3627	111	3738	1133	125	83.5	43.6	91.0
		CON T3–5	0.59–0.61	4490	171	4661	1026	160	116	17.1	172
		CON T3–6	0.63–0.64	2641	150	2791	578	88.3	70.2	48.2	88.9

characterized as very poorly sorted silts (4.06 Φ–8.44 Φ) with a greyish to brownish color (Table 15.1; Figs. 15.3, 15.4, 15.5, 15.6, 15.7, 15.8 and 15.9). All the samples show a very platykurtic kurtosis (0.67 Φ–0.99 Φ) and symmetrical to fine skewed grains (−0.36 Φ–0.65 Φ). Their characteristics include a high MSM, a high-to-medium range TOC and a low TIC. Furthermore, Unit I is characterized by high K, Fe, Ti and low Ca and Sr concentrations, as well as low ratios of Ca/Ti and Ca/K. CON 1 has a peculiarity at a depth between 4.62 and 4.75 m, where the silty layer is interrupted by a very fine sand layer (3.04 Φ) with a very poor sorting (2.78 Φ).

N-alkane distribution illustrates a low total concentration, with the maximum in long-chain *n*-alkanes. The highest enrichment (C_{max}) is shown by *n*-C_{31} in all the samples (Table 15.3). By and large, the odd-chain *n*-alkanes predominate over the even-chain *n*-alkanes in the silty layer. Furthermore, CPI values in the base unit are between 2.53 (CON T2) and 5.7 (CON T1), whereas TAR values are 3.3 (CON T2) and 21.3 (CON T1) and thus below the highest values of the respective trenches. *N*-aldehyde distribution is higher in Unit I with an even over odd predominance. The aromatic hydrocarbons were identified with an increased concentration of total PAHs, with a predominance of fluoranthene, pyrene, benz[a]anthracene and chrysene.

15.4.2.2 *Unit II—Sand Layer*

Unit II differs from the background sedimentation in its coarser grain size and other geochemical parameters. All the cores and trenches show similar trends, but the granulometric values vary depending on the location, for which reason each core/trench is described below individually.

Light brown sand is a special feature of the sand layer in CON 1 located at a depth of 0.64–0.84 cm (Table 15.2; Fig. 15.3). A fining upward sequence is detectable in the entire Unit II, whereby the sand content decreases from 100 to 77%. Furthermore, the layer has an erosional base to the underlying deposits. The sand layer shows varied sorting, kurtosis and skewness in the upper four samples (CON 1–5 to CON 1–2). Sample CON 1–6 consists of symmetrical (−0.1 Φ), well-sorted (0.5 Φ), medium sand (1.73 Φ), which becomes poorly sorted and finer at a greater depth.

The sediment unit in CON T1 is characterized by light brown sand at a depth between 0.40 and 0.52 cm (Table 15.2; Fig. 15.7). The sedimentological features are muddy and organic-rich rip-up clasts, erosional contact and a distinct fining upward sequence in the upper part of the sand layer (CON T1–13 to CON T1–11). Samples CON T1–15, CON T1–12, CON T1–11 and CON T1–16, the latter two are those in contact with the surrounding layer, contain a very poorly sorted (2.79–3.85 Φ), fine skewed (0.55–0.63 Φ) and very fine sand (3.21–3.86 Φ), whereas the other two samples (CON T1–14 and CON T1–13) are characterized by poorly sorted (1.69–1.70 Φ), symmetrical (0.32–0.35 Φ) and medium sand (1.76–1.97 Φ).

Unit II sediments in CON T2 and T3 (CON T2:0.52–0.7 cm; CON T3:0.49–0.65 cm), which are from the same trench, but 1 m apart, are composed of light brown, fine sand and coarse silt (Table 15.2; Fig. 15.8). CON T2 features poorly sorted (1.55–1.96 Φ), symmetrical (0.04–0.08 Φ) coarse silt (4.54–5.22 Φ) on the top and at the base (CON T2–3, CON T2–5 and CON T2–6), and the middle sample (CON T2–4) is characterized by poorly sorted (1.64 Φ), symmetrical (0.34 Φ) and fine sand (3.68 Φ). Furthermore, mud and organic-rich rip-up clasts were identified in the sand layer. In addition, some sand lenses in the coarser silt layer were detected.

In CON 2 and CON 3, Unit II sediments are at a depth of around 1.40 m–1.75 m (CON 2) and 1.55–1.80 m (CON 3) (Table 15.2; Figs. 15.4 and 15.5) and consist of poorly sorted (1.32–2.44 Φ), fine to very fine sand (2.04 Φ and 3.40 Φ). CON 3 has multiple sand layers, but only the lowest sand layer (1.55–1.80 cm) was assigned to Unit II, due to similar kurtosis as the other layers of Unit II (mesokurtic, 2.56–3.79 Φ), but also due to the correlation of depth, as it is comparable in depth to Unit II in CON 2. While the sand content is 88% in CON 2, this amounts to 80% in CON 3 (Table 15.2). An

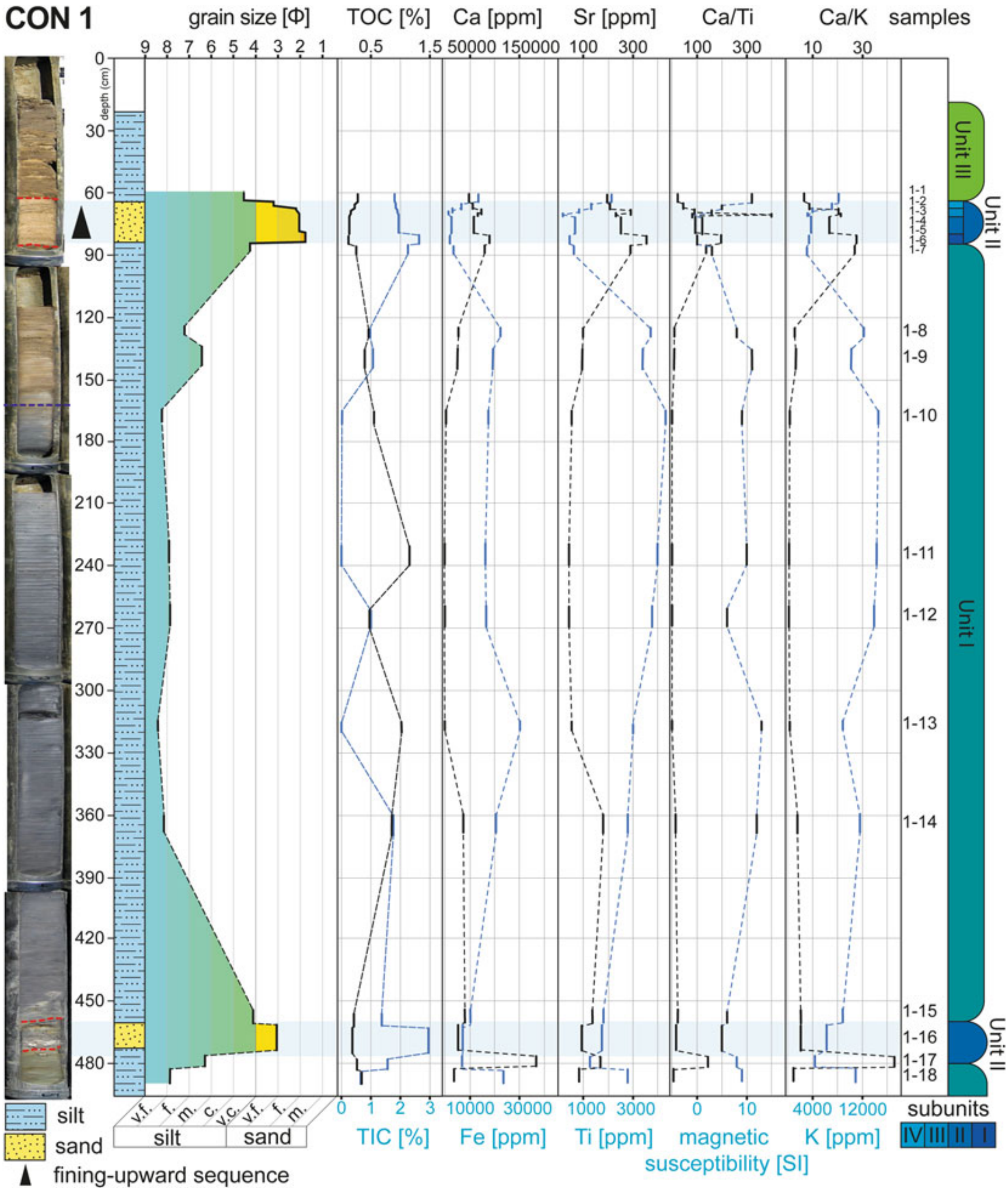

Fig. 15.3 Sedimentological features, grain size, MSM and inorganic geochemical results of the samples from CON 1 (location in Fig. 15.1c)

erosional contact with the underlying layer was detected in CON 2. Notably, an interesting layer in CON 4 was found at a depth of 2.54 m, consisting of coarser silt (4.34 Φ) and increased, fine skewness (0.72 Φ) (Table 15.2; Fig. 15.6).

In general, all the cores and trenches show increased Ca, Sr, Ca/Ti, Ca/K, TIC and decreased K, Ti, Fe, MSM and TOC values in relation to the surrounding material (Figs. 15.3, 15.4, 15.5, 15.6, 15.7, 15.8 and 15.9). However,

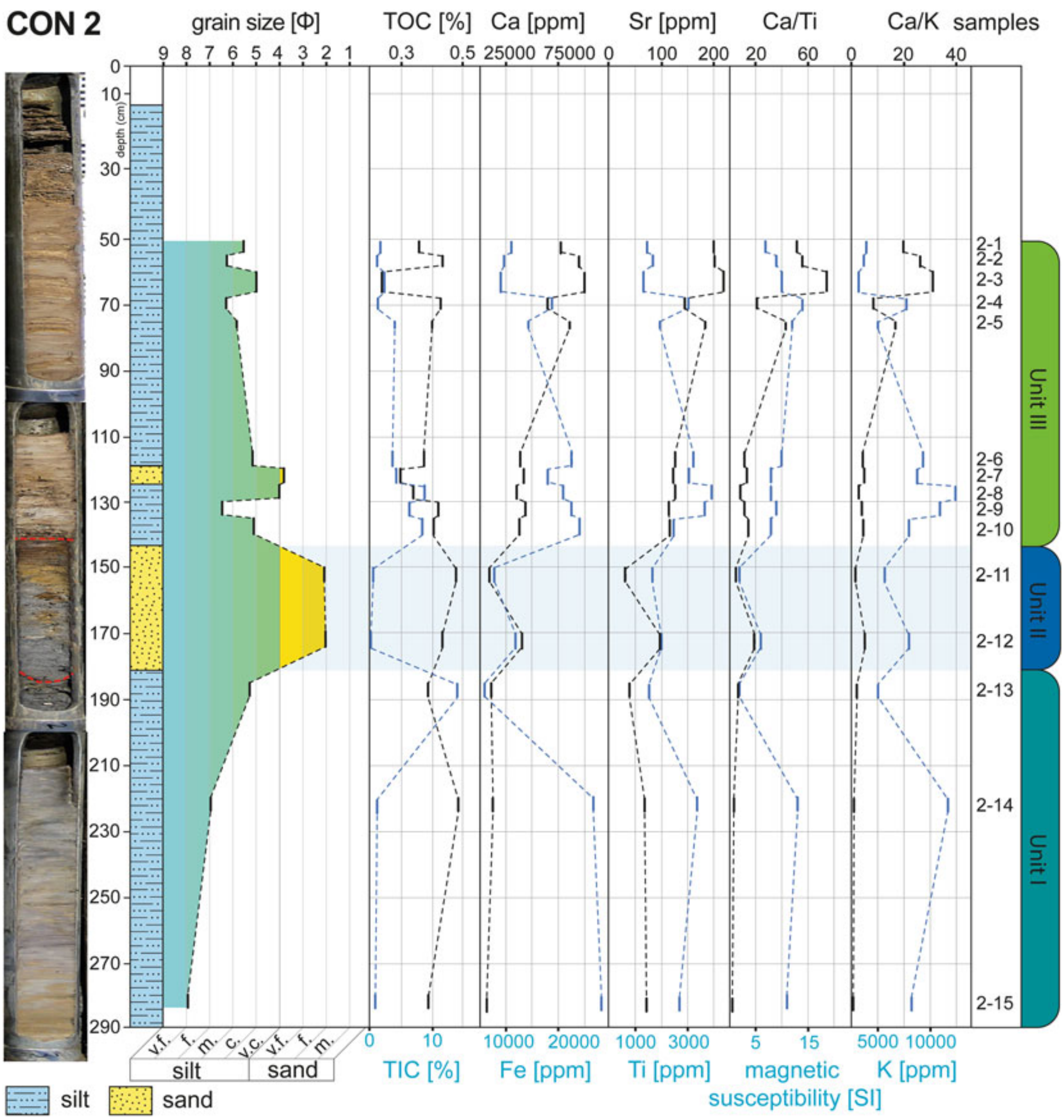

Fig. 15.4 Sedimentological features, grain size, MSM and inorganic geochemical results of the samples from CON 2 (location in Fig. 15.1c)

the marine signal decreases, and the terrestrial signal increases further inland. The organic geochemistry indicates a predominance of odd over even-chain *n*-alkanes in the sand unit as a whole. Maximum enrichment (C_{max}) is mostly at a chain length of *n*-C_{29} and *n*-C_{31} (Table 15.3). Furthermore, some organic geochemical parameters (TAR, *n*-alkane distribution according to chain length, CPI, PAHs) fluctuate through the entire sand layer (Fig. 15.9). Therefore, the sand unit can be divided into four distinct subunits. This subdivision is based on specific, sedimentological, inorganic and organic geochemical results obtained from CON 1, CON T1 and CON T2/T3. The other three cores have an insufficient sample density in Unit II.

The specific characteristics of the four sand subunits are as follows (Figs. 15.3, 15.4, 15.5, 15.6, 15.7, 15.8 and 15.9):

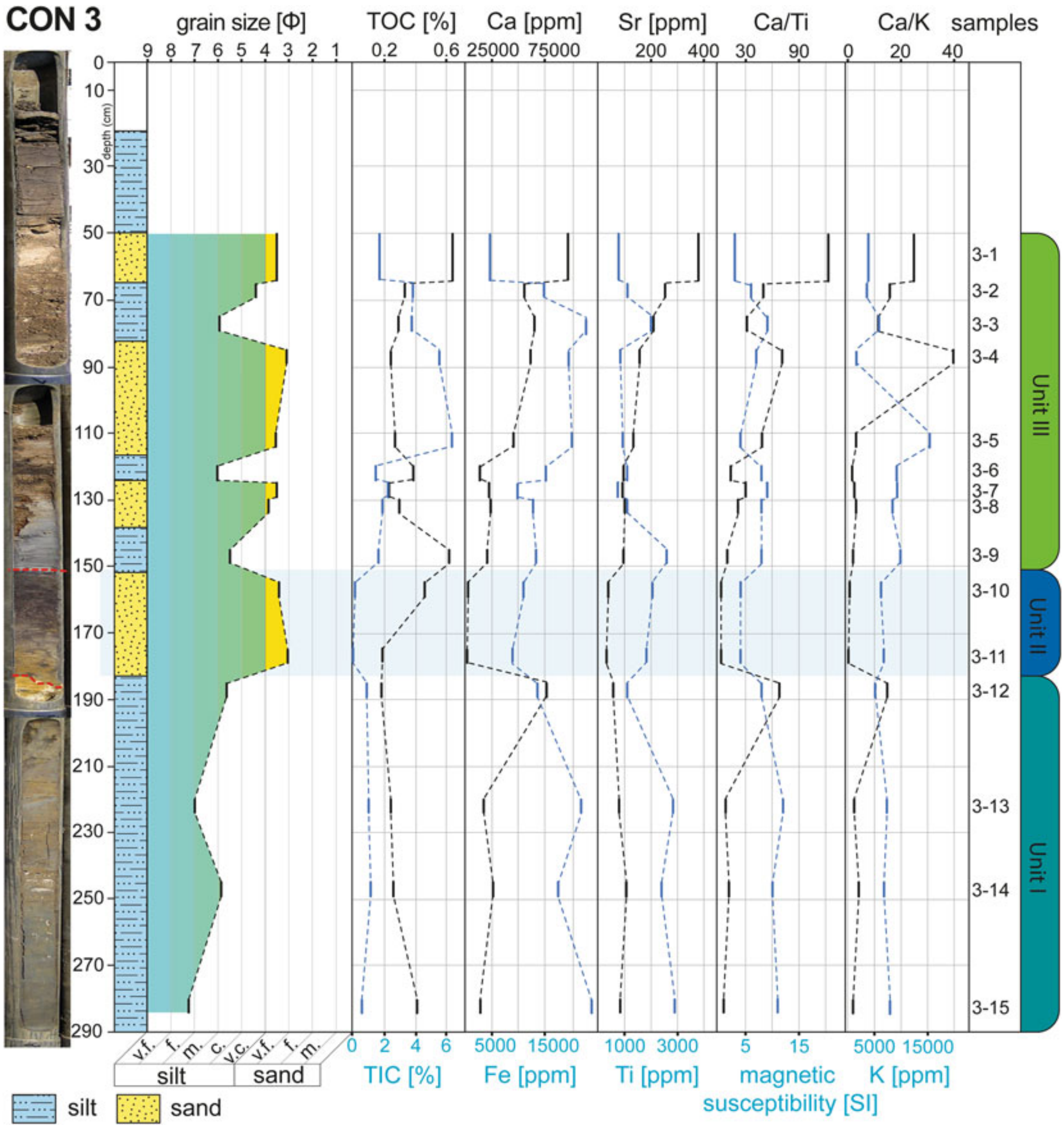

Fig. 15.5 Sedimentological features, grain size, MSM and inorganic geochemical results of the samples from CON 3 (location in Fig. 15.1c)

1. Subunit I. Indicates a sudden transition from Unit I, especially in CON 1. Ca, Sr, Ca/Ti and Ca/K increase, while K, Ti, Fe and MS decrease. Other features are as follows: increased total concentration of *n*-aldehydes and short-chain *n*-alkanes (*n*-C_{19}, *n*-C_{18}, *n*-C_{17}), decreased medium- and long-chain *n*-alkanes, and lower TAR (2.1–2.2) and CPI values (2.3–2.9) in contrast to the underlying unit. Furthermore, there is a lower total concentration of PAHs in comparison to Unit I with a predominance of fluoranthene, pyrene and chrysene. The differences in the cores are mainly the coarser grain size of CON 1 in contrast to the very fine sands and coarser silts of CON T1, T2 and T3. Organic rip-up clasts can also be found in the trenches.
2. Subunit II. Ca, Sr, Ca/Ti and Ca/K indicate a depletion and K, Ti, Fe and MS an enrichment in contrast to Subunit I. The total

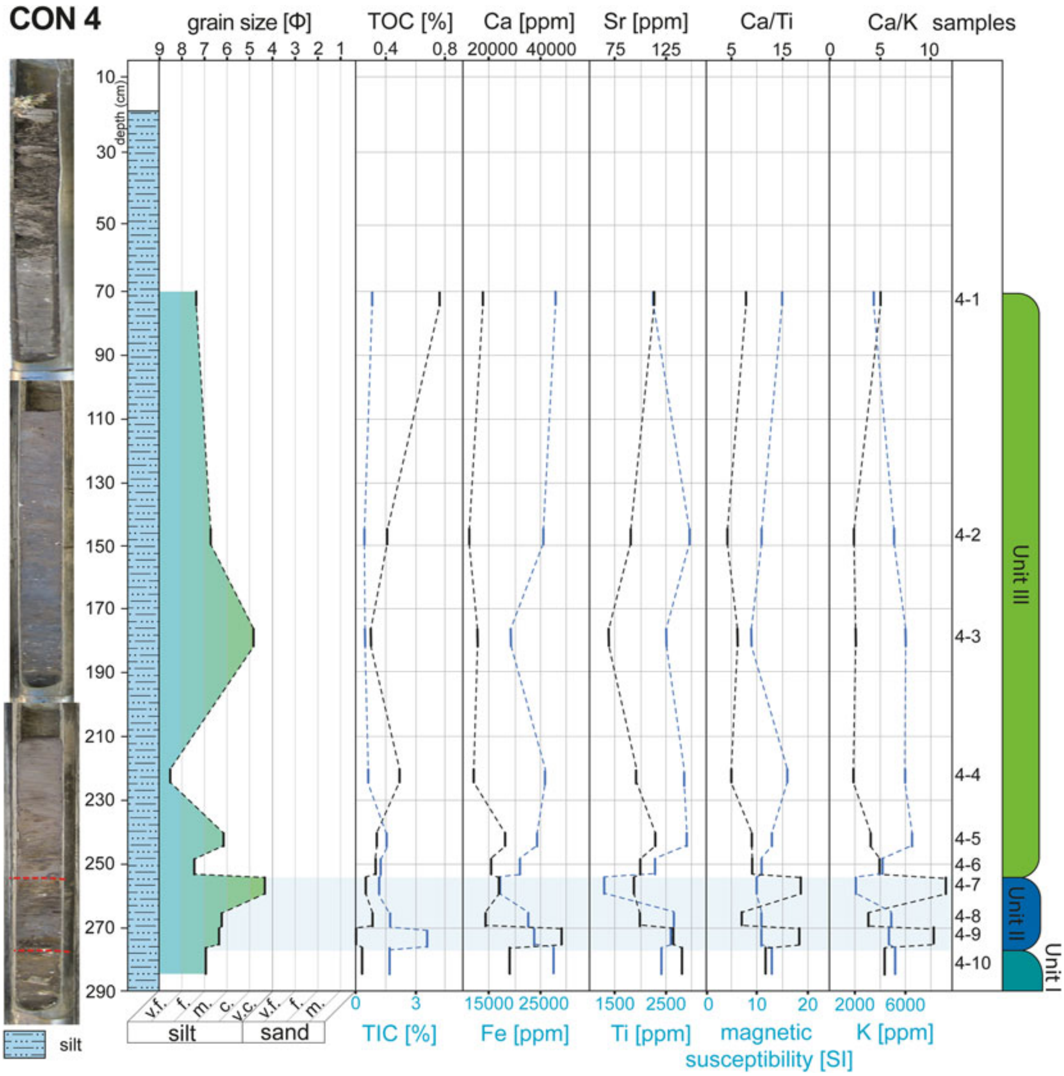

Fig. 15.6 Sedimentological features, grain size, MSM and inorganic geochemical results of the samples from CON 4 (location in Fig. 15.1c)

concentration of *n*-alkanes and TAR values (6.9–7.1) increase, except in CON T3 with 1.6, while CPI values decrease further (1.1, 2.6, 3.7). There is also a significant increase in total PAHs with a predominance of fluoranthene, benz[a]anthracene, chrysene and phenanthrene, and a lower *n*-aldehyde concentration.

3. Subunit III. This has the same inorganic features as Subunit I. However, there are slight changes in the organic geochemical properties in contrast to Subunit I, with a lower concentration of total *n*-alkanes, lower TAR (1.2, 2.5, 6.4) and CPI values in CON T1/T3 (2.2, 3.0), with the exception of CON T2 with an increased CPI (3.6). PAHs have a similar distribution as in Subunit I, with a lower concentration of all compounds. It also has the lowest *n*-aldehyde concentration of all four subunits.
4. Subunit IV. With the same inorganic features as Subunit II, it has a higher total

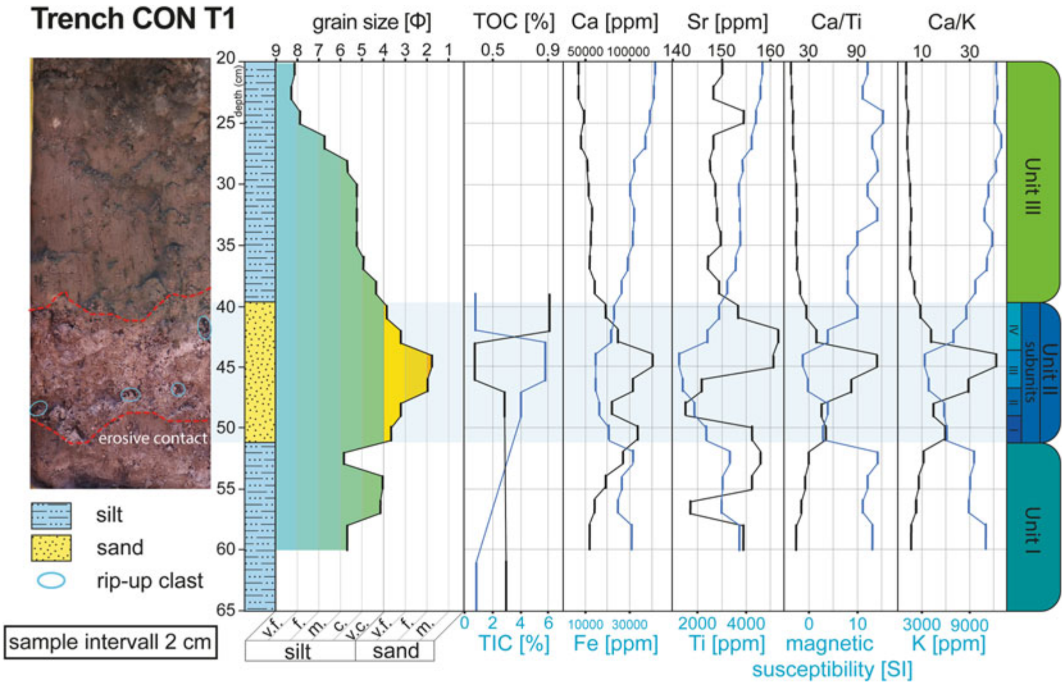

Fig. 15.7 Sedimentological features, grain size, MSM and inorganic geochemical results of the samples from CON T1 (location in Fig. 15.1c)

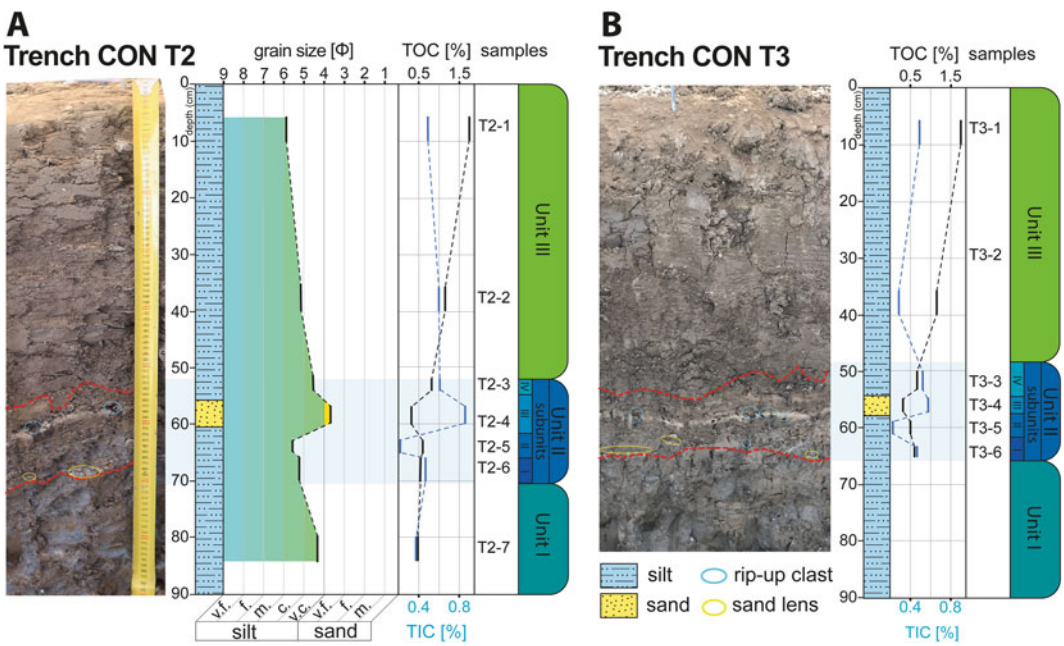

Fig. 15.8 **a** Sedimentological features, grain size and TC results of the samples from CON T2. **b** Sedimentological features and TC results of the samples from CON T2 and CON T3 (locations in Fig. 15.1c)

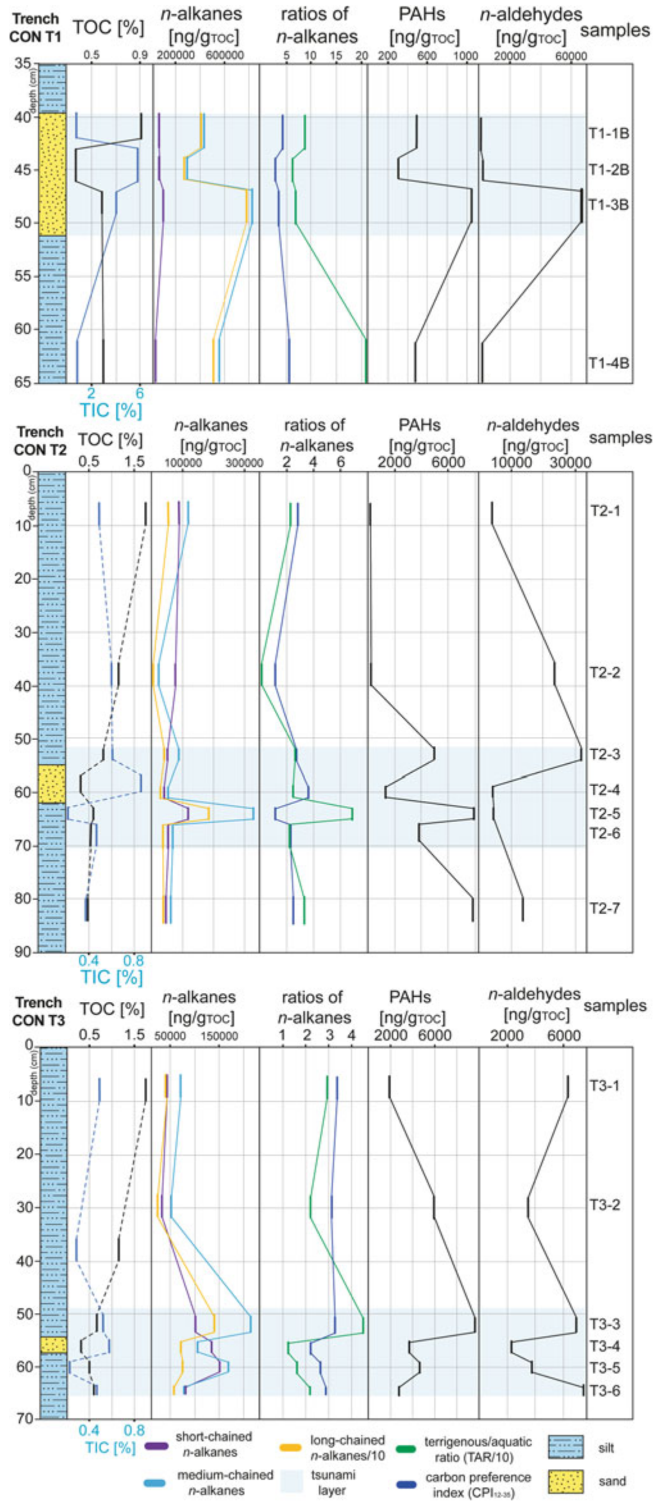

Fig. 15.9 Organic geochemical data (*n*-alkanes, *n*-aldehydes and PAHs) of the samples from the trenches (locations in Fig. 15.1c)

concentration of especially long-chained *n*-alkanes, as well as higher TAR values (2.6, 4.5, 8.9). CON T2 has lower CPI values (2.4), while in CON T1/T3, these are higher (3.3, 4.4). Although PAHs have a similar distribution as in Subunit II, that of *n*-aldehydes is remarkably higher. The grain size in all the cores shows a fining upward cycle with respect to Subunit III and a similar mud-cap subunit in the trenches.

15.4.2.3 Unit III

Unit III has comparable properties in all sample locations (Table 15.2; Figs. 15.3, 15.4, 15.5, 15.6, 15.7, 15.8 and 15.9). The uppermost unit consists mainly of brownish, alternating, laminated silts (4.39–8.26 Φ), with embedded sand lenses in CON 2 and CON 3 (CON 2: 3.8 Φ, CON 3: 3.08–3.85 Φ). The kurtosis is mainly very platykurtic (0.66 Φ–1.34 Φ), and the skewness is fine skewed to symmetrical (−0.21 Φ–0.77 Φ). The uppermost part of this unit indicates bioturbation, roots (CON 2, CON 3 and CON 4) and salt inclusions (CON T2/3). The inorganic geochemical features of Unit III include low Ca and high K, Ti and Fe values. MSM is greater, TIC content is low, and TOC values are moderate to high concentrated. In addition, there is a slight peak in Ca and Sr and in Ca/K and Ca/Ti ratios in some parts of this unit, which can be correlated to the embedded sand layers (CON 2: 1.20–1.25 m, CON 3: 0.5–0.65 m, 0.8–1.15 m and 1.25–1.35 m). The upper sand layers in CON 3 differ, from the lowest sand layer (assigned to Unit II), mainly by the very platykurtic kurtosis of the samples.

Unit III exhibits a lower total concentration of *n*-alkanes. There is a greater distribution of long-chain *n*-alkanes versus their medium- and short-chain counterparts. N-C_{29}-alkanes are the most abundant aliphatic hydrocarbon in this unit (C_{max}). Comparable to Unit I, odd-chain *n*-alkanes are more abundant than their even-chain counterparts. Two other indicators are the TAR and CPI values, which are practically the same as in Unit I. The *n*-aldehyde concentration generally increases in the silt unit, with only the uppermost sample of CON T2 showing a depletion. The even-chain *n*-aldehydes increase in contrast to their odd-chain counterparts. PAHs have a lower concentration of compounds at a lower depth, whereby the unit has the lowest concentration of all the sampling profiles. The predominant aromatic substances are phenanthrene and fluoranthene.

15.4.2.4 Reference Samples

Reference samples were collected from the river, dune, beach, intertidal and nearshore settings (depth of ca. 2 m) (Table 15.2). The river sample contains moderately well-sorted (0.67 Φ) fine sand (2.29 Φ), symmetrically skewed (0.31 Φ) with a platykurtic kurtosis (2.15 Φ). The dune samples have nearly the same grain size properties (2.02–2.05 Φ), except for a good sorting (0.4–0.42 Φ) and a very platykurtic kurtosis (0.97–0.98 Φ). The beach sample consists of moderately well-sorted (0.72–0.79 Φ), symmetrically skewed (−0.23–0.04 Φ), coarse to medium sand (0.95–1.51 Φ), whereas the intertidal sample consists of moderately well-sorted (0.58–0.69 Φ), medium grained sand (1.57–1.91 Φ) with a symmetrical skewness (−0.21 Φ). The nearshore sample is characterized by moderately sorted (0.92 Φ), medium sand (1.51 Φ) with the same properties of skewness (−0.28 Φ) and kurtosis (0.92 Φ) as the other reference samples. The XRF analysis, which was only performed on the dune and intertidal reference samples, shows increased Ca, Sr and TIC content, while the values of K, TOC, MSM and Fe are lower.

15.5 Discussion

15.5.1 Interpretation of the Sedimentological Units

Based on the sedimentological and granulometric features, as well as the inorganic and organic geochemical properties of the sediments, three units were defined with different deposition processes and characteristics.

15.5.1.1 *Unit I—Floodplain, Backshore Lagoon Deposits*

The poorly sorted silts of Unit I probably reflect the environmental conditions during deposition. The origin of these deposits is interpreted as floodplain and backshore lagoon in a low energy regime. The greyish color in the lower parts of the unit is caused by anoxic conditions during warmer summer months (Cioffi et al. 1995), and the silt deposits are typical features of freshwater lagoonal sediments (Peng and Zhang 2007). MSM indicates the enrichment of ferro- and paramagnetic minerals in the sediments (Reicherter et al. 2010). The clay and silt may have been formed further inland by the weathering and erosion of the Campo Gibraltar Unit (Early Miocene), calcarenites (Late Miocene) and the Pleistocene/Holocene deposits of the floodplain (González-Acebrón et al. 2016; Gutiérrez-Mas et al. 2016). Deposition takes place from the hinterland mainly through the sedimentary input of the Conilete creek into the lagoon, especially in the winter when it is rainy in the hinterland. The increasing grain size and change in color (grey to light brown) in the upper part of this unit indicate oxygenation processes within the lagoon (Fig. 15.3). Luque et al. (2004) and Lario et al. (2009) described a change from a freshwater to a saltwater lagoon, which indicates episodes of desiccation. A period of drought in the early eighteenth century, described in historical sources (Archivo de la Hermandad de la Virgen de la Merced 1722), might have led to a silty sequence (silt-up) due to lower water inflow through the Conilete creek and its occasional tributaries. Furthermore, the temporarily blocked outlet of the Conilete creek into the Gulf of Cadiz may have been opened due to changing climatic conditions, which might have caused seawater ingression into the creek.

Medium- and long-chain *n*-alkanes, which are the most prominent ones, can be attributed to an aquatic and terrestrial origin (Ficken et al. 2000; Alpar et al. 2012). The slight accumulation of medium-chain *n*-alkanes serves as an index of aquatic input through the Conilete creek or other hydrological activities (e.g., the lagoon). The highly enriched terrestrial *n*-alkanes can be attributed to organic input, like plants and other vegetation (Alpar et al. 2012). The maximum concentration of n-C_{27} and n-C_{29}-alkanes could be an indicator for river-transported terrestrial material due to an input of vascular land plants upstream (e.g. Mathes-Schmidt et al. 2013; Schwarzbauer et al. 2017). As water erosion, sediment production and terrigenous input are strong in this area (Faust and Herkommer 1995), the terrestrial influence exceeds the marine influence (see TAR values) (Peters et al. 2005).

The proximity of different settlements (e.g., Vejer de la Frontera and Conilete) in the past to the study area may explain the accumulated PAH concentration (Gordo et al. 2008; Gutiérrez-Mas et al. 2016). Settlements are mostly an indication of human activities and release of PAHs, such as agriculture (especially fishing), the combustion of organic material and historical industry (e.g., “La Chança” tuna factory) (Pontevedra-Pombal et al. 2012). The historically documented fishing structures and stockbreeding areas (Luque et al. 2004; Lario et al. 2009; Santos and Koshimura 2015) may point to other small historical industries. The primary origin of PAHs with a greater number of rings (fluoranthene, pyrene and benz[a]anthracene) was the result of burning wood and other organic material (Ravindra et al. 2008; Guillon et al. 2013). Winds, especially easterlies (from Vejer de la Frontera) and westerlies (from coastal settlements), might have transported these pollutants dissolved in smoke to the alluvial areas. Similarly, precipitation and wastewater discharge into the river from settlements, as well as natural processes such as historical forest- and wildfires in the area (López-Sáez et al. 2002; Vallejo-Villalta et al. 2019), might have introduced PAHs into the study area.

15.5.1.2 *Unit II—EWE Layer*

The distinct discontinuity in the sedimentation between Unit I and III indicated by sandy Unit II suggests a possible EWE. The sand layer can be subdivided into four different sections in which the higher grain size reflects a high energy process. Due to the high energy currents during the EWE, suspended sediments might have been transported to the floodplain and might have generated a deposit differing from the surrounding materials. The distinction between this unit and the background sedimentation (Units I and III) can be observed in the granulometric features as a better sorting and a higher kurtosis. The mean grain size is characterized by sand, with the grain size decreasing further inland.

Sedimentological characteristics help to distinguish between EWE deposits, such as those generated by tsunamis and storms. Erosional base contacts, an indicator of tsunami deposits (Dawson et al. 1988; Fujiwara et al. 2000; Srinivasalu et al. 2009), are visible in most of the cores (CON 1, CON 2, CON T1), as are the fining upward sequences found in CON 1, CON T1 (upper part) and CON T2 (Foster et al. 1991; Dawson 1994; Fujiwara et al. 2000; Chagué-Goff et al. 2002). Rip-up clasts are present in the cores of the depression (CON T1, CON T2 and CON T3), which are indicators of eroded substratum material, being rounded during tsunami transport (Dawson 1994; Goff et al. 2001, Szczuciński et al. 2006; Spiske 2020). Another feature that may indicate tsunami sediment deposition is the landward fining sequence described by Foster et al. (1991), which can be applied to the floodplain of El Palmar de Vejer (Table 15.2). However, some of these features are not exclusive to tsunamis but can also be characteristic of storm deposits (Morton et al. 2007; Horton et al. 2009). Thus, the combination of several features indicates that the deposits are more likely to be the result of a tsunami.

The bivariate plots illustrate some properties that help to distinguish between Unit II and Unit I, respectively, III. In the sorting-versus-mean diagram of Lario et al. (2002), after Tanner (1991a, b) (Fig. 15.10), the tsunami samples are plotted in the area of fluvial to high-energy episodes, and in the CM diagram, after Passega (1964) and Passega and Byramjee (1969), they are plotted in the area of rolling and suspension, which are typical processes during the wash-over of tsunamis (El Talibi et al. 2016; Yoshii et al. 2018) (Fig. 15.11). Furthermore, the bivariate plot of mean versus sorting, after Stewart (1958), illustrates river and wave processes as transport mechanism of the tsunami sediments (Fig. 15.10). The sand samples from CON 1, CON T1 and CON 2 are still within the range of the reference samples, with a coarser grain size and good to moderate sorting, whereas CON 3 has already a worse sorting and finer grain size (Figs. 15.10 and 15.11).

As a method supplementing the sedimentological properties, GPR was used to identify the layer between Unit I and Unit III. By evaluating the two processed high-resolution radargrams, it is possible to clearly distinguish the tsunami layer from the embedding sediment layers (Fig. 15.2). With a varying thickness, Unit II indicates continuous irregular reflectors in contrast to the other units, which have mostly parallel reflectors. This correlates with the results of the grain size analysis. The internal zig-zag pattern of Unit II indicates coarser-grained material and an erosional base at the bottom and sharp contact to the uppermost layer resulting from a high energy event (Koster et al. 2013). The reflectors become more irregular (hyperbolae) as the grain size increases (Neal 2004).

According to the inorganic geochemical review performed by Chagué-Goff et al. (2017), some elements and ratios were chosen to identify the sand layer as a tsunami deposit. Thereafter, increased Ca and Sr values are good indicators for an input of marine material, such as carbonate shell hash, biogenic carbonates and coral sands (Chagué-Goff et al. 2017; and references therein) (Figs. 15.3, 15.4, 15.5, 15.6, 15.7, 15.8 and 15.9). The high levels of Sr are an indication of increased salinity (Martín-Puertas et al. 2010) and marine sedimentation processes. Additionally, the elements Fe, K and Ti show decreased concentrations in most of the tsunami deposits, thus excluding terrestrial influence (Chagué-Goff et al. 2017; and references therein). Furthermore, increasing ratios, such as Ca/Ti and Ca/K, illustrate the marine influence on the deposited sediment (Chagué-Goff et al. 2012 and references therein). Accumulated Ca/Ti in the samples indicates fossil shells in the possible sediment source (Donnelly et al. 2016; Yu et al. 2016).

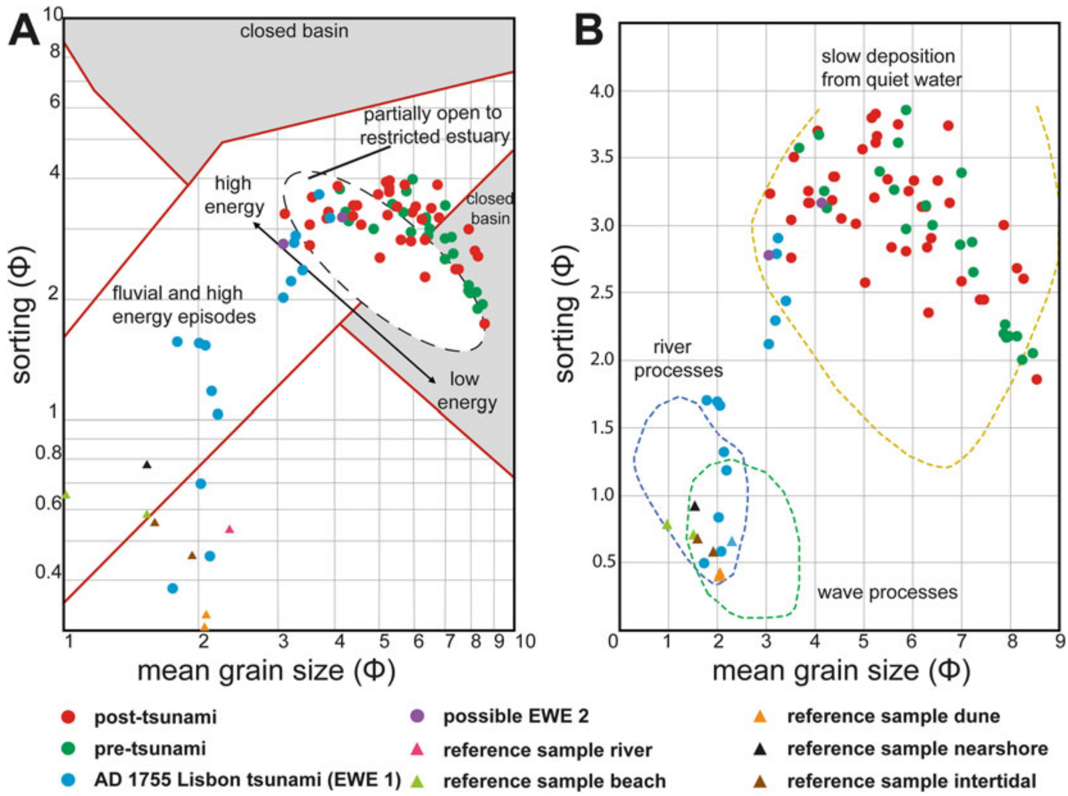

Fig. 15.10 Bivariate plots of the granulometric features of the EWE samples in contrast to the surrounding (post- and pre-tsunami) and reference samples. **a** Logarithmic scale of mean grain size versus sorting with defined areas of deposition conditions (after Lario et al. 2002; Tanner 1991a, b). **b** Mean grain size versus sorting, after Stewart (1958)

Increased Ca/K points reveal a marine signal in the sandy samples (May et al. 2012). Low MSM in the tsunami deposits indicates the presence of diamagnetic and carbonate minerals in the sand (Figs. 15.3, 15.4, 15.5, 15.6, 15.7, 15.8 and 15.9) due to the absence of ferro- and paramagnetic clay minerals, as well as iron-bearing minerals (Reicherter et al. 2010; Wassmer et al. 2020). Typically, a decreased TOC, like in all the sandy samples, is an indicator of marine sediments as organic carbon mostly enriched in the terrestrial geosphere.

The tsunami layer most likely originated from the AD 1755 Lisbon tsunami. North of the study area, Gutiérrez-Mas et al. (2016) detected deposits of the AD 1755 tsunami at a depth of approximately 0.6–0.7 m, with similar characteristics as regards sorting, grain size and higher sand content. Luque et al. (2004) identified AD 1755 Lisbon tsunami deposits at a depth of around 0.5 m, which is consistent with the findings of this study. Lario et al. (2009) described a tsunami layer at a depth of up to 0.5 m as an area (300 m long) with high-energy sedimentation containing fragments of the buildings of the Conilete settlement. Because of the similar depth and the detection of several waves, a correlation with the results of this study is possible. Based on the results of Gutiérrez-Mas et al. (2016), Lario et al. (2009) and Luque et al. (2004), in this study, Unit II can be described as high-energy sediment clearly linked to the AD 1755 Lisbon tsunami. According to the historical records, the AD 1755 tsunami was the last major one in this region (Lario et al. 2011; Luque et al. 2002, 2004) and it is the only EWE

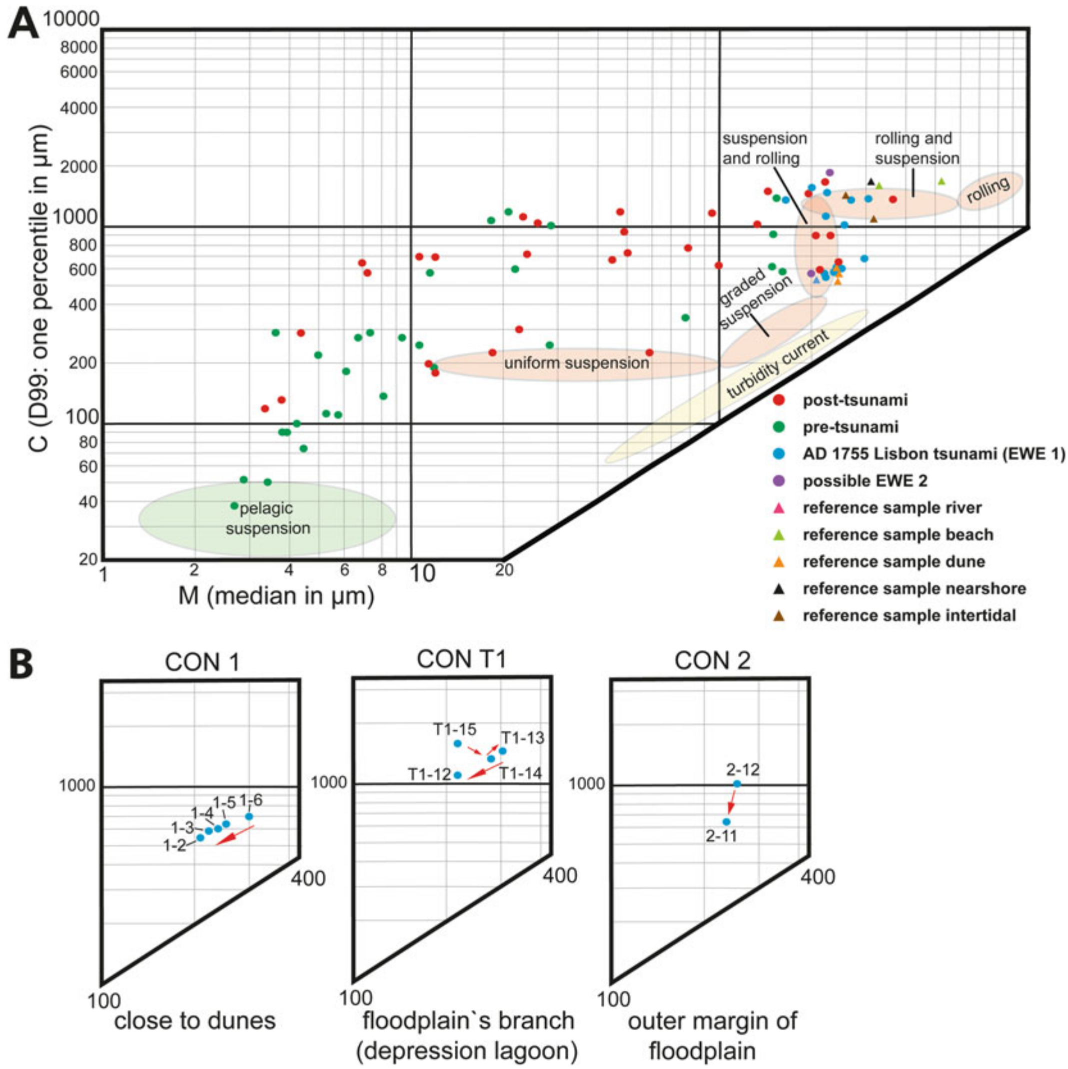

Fig. 15.11 **a** CM diagram of median grain size (µm) and the C-percentile (D99) of all the samples (after Passega and Byramjee 1969). **b** Tsunami samples from different locations in CON 1, CON 2 and CON T2 (Fig. 15.1c), with changing transport mechanisms during the tsunami (arrows indicating the samples from the base to the top)

evidence in the uppermost 1.5 m of lagoonal/floodplain deposits, representing more than 1,500 years.

Not only the sedimentological and inorganic geochemical features point to an EWE, but the organic geochemical characteristics of the sand layer also show that its origin and properties differ from those of the surrounding material. Shorter-chain *n*-alkanes present ubiquitous biomass production with potential marine signature of the most abundant markers (*n*-C_{15}, *n*-C_{17}, *n*-C_{18} and *n*-C_{19}) in these EWE layers (Gelpi et al. 1970; Mackie et al. 1974; Jaffé et al. 2001; Alpar et al. 2012). *N*-C_{17} and *n*-C_{19} most probably originated from algae and marine microorganisms transported by the extreme wave inundation (Gelpi et al. 1970; Shinozaki et al. 2015). While *n*-C_{18} could be an indicator of fish remains (Mackie et al. 1974; Shinozaki et al. 2015), which could be introduced by the tsunami washover affecting the lost Conilete settlement with smaller fish factories, as they were common along the Atlantic coast of Spain (Luque et al. 2001).

All *n*-alkanes higher than *n*-C_{23} usually derive from higher land plants and their epicuticular waxes (Eglinton and Hamilton 1963; Alpar et al. 2012; Schwarzbauer et al. 2017) with a predominance of *n*-C_{29} (tree waxes) and *n*-C_{31} (grass waxes) in the tsunami (Jeng and Huh 2006). Furthermore, long-chain *n*-alkanes are produced in warmer regions and at lower latitudes (Poynter and Eglinton 1990). The most abundant long-chain *n*-alkane in the samples is *n*-C_{31}, indicating the material input of grasslands (Table 15.3). During the field survey and compared with Gutiérrez-Mas et al. (2016), the vegetation in the alluvial flat is made up of herbaceous vegetation and crop plants, which correspond to the substances deposited in the sediments. Strikingly, plants containing *n*-C_{31} alkanes peak in the layers of the tsunami phases, especially in CON T2 and CON T3, while they prevail throughout CON T1. Input of these *n*-alkanes during the tsunami occurred mainly through vegetation destruction and reworking of the backshore material. However, the shorter numbered terrestrial-derived *n*-alkanes from macrophytes (*n*-C_{23}, *n*-C_{24} and *n*-C_{25}) were separated from the long-chain ones (Ficken et al. 2000; Bellanova et al. 2020) and occurred in the study area due to the overflowing of Conilete creek and the lagoon during the inundation.

TAR values are well above 1 in all the samples, thus indicating a predominant terrestrial influence (Peters et al. 2005). However, even slight variations in TAR values are indicative of changes in input of terrestrial material, which could explain decreased terrestrial and increased marine material (Mathes-Schmidt et al. 2013) and therefore may be interpreted as evidence of a tsunami origin. CPI values also vary slightly in the tsunami deposits. In the main, these have lower CPI values than the surrounding material and thus an indication of a decreased input of biogenic sources, mainly vascular land plants (Peters et al. 2005; Schwarzbauer et al. 2017). The difference in the values of the respective trenches can be attributed to the discontinuity of tsunami deposits in relation to the micro-topography of the alluvial floodplain. The almost complete absence of long-chain *n*-aldehydes (*n*-C_{19}–*n*-C_{32}) in the sand units is mainly an indicator of non-terrestrial organic matter (Prahl and Pinto 1987; Schwarzbauer et al. 2000; Schwarzbauer 2006).

The presence of PAHs in the sand layer may indicate possible human activity in southwestern Spain. First and foremost, parent and unsubstituted PAHs predominate over associated alkylated PAHs in all the sand samples, which indicates a pyrogenic source (Stogiannidis and Laane 2015) (Table 15.5). Pyrogenic sources have different origins, such as car exhaust and industrial processes, but also combustion. The first two possibilities are not applicable to the sand samples from El Palmar de Vejer because it is assumed that the tsunami layers were deposited by the AD 1755 Lisbon tsunami, when cars, machines and industrial processes had not yet been invented (Pontevedra-Pombal et al. 2012). In all likelihood, they were mainly pollutants present in smoke produced by the burning of organic material. Page et al. (1999) described the compounds fluoranthene, pyrene and phenanthrene as prominent markers for pyrogenic sources, particularly fluoranthene and pyrene are predominant in wood combustion (Guillon et al. 2013). All three substances are always among the compounds with the highest concentration in the sand samples. Furthermore, higher concentrations of benz[a]anthracene and chrysene (Stark et al. 2003) have been detected in the fireplaces of settlements and are also the compounds with a greater presence in these sand deposits (Table 15.5). The EWE may have caused a higher input of PAHs (Alpar et al. 2012; Bellanova et al. 2019), which could have been due not only to substances from combustion dissolved in the sea but also to the remobilization of the pollutants from the underlying silt. During the tsunami event, these pollutants were presumably transported to the floodplain. These considerations are consistent with most of the tsunami samples from El Palmar de Vejer (Table 15.5).

15.5.1.3 Unit III

This sediment unit can be divided into silty and sandy deposits (CON 2 and CON 3) (Figs. 15.4 and 15.5). The lagoon is only occasionally flooded during the winter due to precipitation and occasional overwash, while during dry season, its outflow into the ocean is blocked by littoral drift deposits (Moreno et al. 2010).

The laminated silts are indicative of the occasional flooding of the lagoon, as they have similarities to Unit I (grain size, inorganic and organic geochemistry). Furthermore, the described salt inclusions of the trenches found in this unit might have been caused not only by the combination of freshwater and saltwater (Lario et al. 2009) but also by wind-induced salt spray (Craft et al. 2008). The silt samples in the sorting-versus-mean diagram of Lario et al. (2002), after Tanner (1991a, b), indicate a periodically blocked depositional milieu (Fig. 15.10), as the Conilete creek is (Zazo et al. 2008). Furthermore, the bivariate plot, after Stewart (1958), indicates that the sediments were deposited in still waters (Fig. 15.10).

Quartz-rich sand layers with a low carbonate content intercalated in silty deposits indicate changes in the depositional scenario. Due to the low sampling density, it is currently impossible to determine the precise origin of the sands. Be that as it may, the first possibility is that these deposits were formed during periods of higher rainfall, thus causing wider flooding of the lagoon. According to Rodrigo et al. (1999), there was abundant rainfall in 1797, 1800 and 1804 and, consequently, the sands are of terrestrial origin. The second possibility would be the deposition of marine sands during storm events, which indeed occur in El Palmar de Vejer (Lario et al. 2009). Although for Lario et al. (2009), storm deposits only occur in the area close to the coastline (only 100 m inland), in this study, the deposits were located further inland. The input of sand during strong wind phases is the third possibility for the origin of the sand layers (Collinson 1978). The sand layers have been protected from erosion because, with the occasional low-energy inundation of the floodplain, they were subsequently overlaid by finer-grained silt.

An indicator of the different deposition processes is the CM diagram, after Passega (1964) and Passega and Byramjee (1969) (Fig. 15.11), in which the sand samples are plotted in the area of rolling, while the silt samples indicate a deposition in suspension. Typical characteristics of EWEs can be excluded by the mean-versus-sorting diagram of Lario et al. (2002), after Tanner (1991a, b), in which the sand and silt samples are plotted in the range of lower energy and the periodically blocked estuary (Fig. 15.10).

n-Alkanes are valuable indicators, with a clear prevalence of terrestrial ones, as in Unit I. However, the total concentration is lower in contrast to the tsunami deposits. Aquatic *n*-alkanes also prevail over marine *n*-alkanes, except in CON T2–2, where the former is more enriched. This suggests the occasional flooding of the lagoon within a brackish environment. The presence of PAHs can be explained by the proximity of the study area to El Palmar de Vejer, Conil de la Frontera and Vejer de la Frontera. However, lower PAH inputs may be owing to the designation of the area where the samples were collected as a nature reserve. With regard to the origin of PAHs, there is a greater number of petrogenic PAH sources, which increased significantly after industrialization (Pontevedra-Pombal et al. 2012). Indicators include enriched alkylated PAHs, in contrast to parent PAHs, in some samples (Stogiannidis and Laane 2015). By and large, the lower concentration in the most modern deposits can be explained by the presence of petrogenic compounds, as they are more sensitive to biodegradation than their pyrogenic counterparts (Stogiannidis and Laane 2015). However, the main source of the (combination of pyrogenic and petrogenic) PAHs can be explained by transport, industry, tourism and the settlements in the vicinity.

15.5.2 Hydrodynamic Characteristics of the Tsunami Deposits in El Palmar de Vejer

A more detailed analysis of the grain size, as well as the marine and terrestrial signals, reveals different influences on the tsunami layer the further inland the cores are located. The distance from the coastline played an important role as regards the characteristics of the tsunami deposits on/in the Conilete floodplain/lagoon. Due to the energy reduction of the tsunami, the marine signals thin out and the grain size diminishes, the further inland the wave penetrated (e.g., Dawson 1994; Minoura et al. 1996). Increased friction between the wash-over flow and the subsurface of the floodplain led to a loss in transport capacity. Conversely, the terrestrial signals in the sediment increase further inland due to the sediment uptake and incorporation of the substratum (Chagué Goff et al. 2012; May et al. 2012; Chagué Goff et al. 2015) (Fig. 15.12). Topographically controlled backflows have little effect on distal deposits, but deposition of backflow material and erosion can occur in coastal deposits (Spiske 2020), whereas in the depressed areas ponding is predominant, in which mainly suspended, fine-grained material is deposited in the water (Wassmer et al. 2010; May et al. 2012). CON 4, which does not have a distinct tsunami sand layer, strengthens the interpretation of finer-grained sediment deposition during ponding, as it has a larger grain size in comparison to the background sediment at a depth of between 2.54 and 2.70 m. The inorganic parameters show that finer-grained material with increased marine inorganics was transported further inland than coarser-grained material (Chagué-Goff et al. 2012; Bartzke et al. 2018). Suspended silt in ponded water is deposited under low energy conditions (May et al. 2012), especially in coastal depressions, where ponding is stronger than on topographic highs (Paris et al. 2010; Wassmer et al. 2010). Therefore, the silty layer of CON 4 is most likely the finer-grained portion of the tsunami deposit. In general, the flat topography favored the deposition of tsunami deposits in terms of thickness and preservation (Dawson et al. 2020; Spiske 2020).

Several studies describe multiple tsunami waves for the Atlantic coast of Spain. The precise number of waves is difficult to determine, as some factors, such as bathymetry, topography, tsunami deposit erosion and the lack of sediment evidence for some of the wave cycles all play an important role. According to Luque et al. (2004) and Lario et al. (2009), at least two tsunami waves reached the floodplain between Conil de la Frontera and El Palmar de Vejer, close to the study area. As to the deposits in the southern alluvial flat near El Palmar de Vejer, there is possible evidence of at least two successive waves. The grain-size distribution from base to top is indicative of floodplain inundation caused by successive waves (Wassmer et al. 2010; Cuven et al. 2013; El Talibi et al. 2016). CON 1 has an erosional contact with the underlying substratum, which indicates a change in the depositional environment (Fig. 15.12). Furthermore, the normal grading and distinct marine signal are indicators of the first wash-over (Wassmer et al. 2010; May et al. 2012; Koster and Reicherter 2014). The sediment source most likely had an onshore origin, as the granulometric features have similarities to the coastal sediments. Topographically controlled backflows then transported the sediment back towards the coast (Nanayama et al. 2000). The location of CON 1 close to a tributary of the Conilete creek and the dunes did not offer good conditions for ponding but was rather influenced by the weak backflow, resulting in heterogeneous backwash depositions. In contrast to the wash-over deposition, differences include poorer sorting, mesocurtic kurtosis and terrestrial inorganic signals, which are indicators of a mixture of sediments. The second tsunami wave cycle is reflected in the analogous properties in CON 1, namely, a marine signal during wash-over and a heterogeneous signal of inorganic substances, along with a fining upward sequence, during weak backwash.

CON T1, CON T2 and CON T3 display analogous properties, but the deposits should be interpreted slightly differently. The depression of the lagoon, most likely filled during the AD 1755 Lisbon Tsunami, had an influence on the

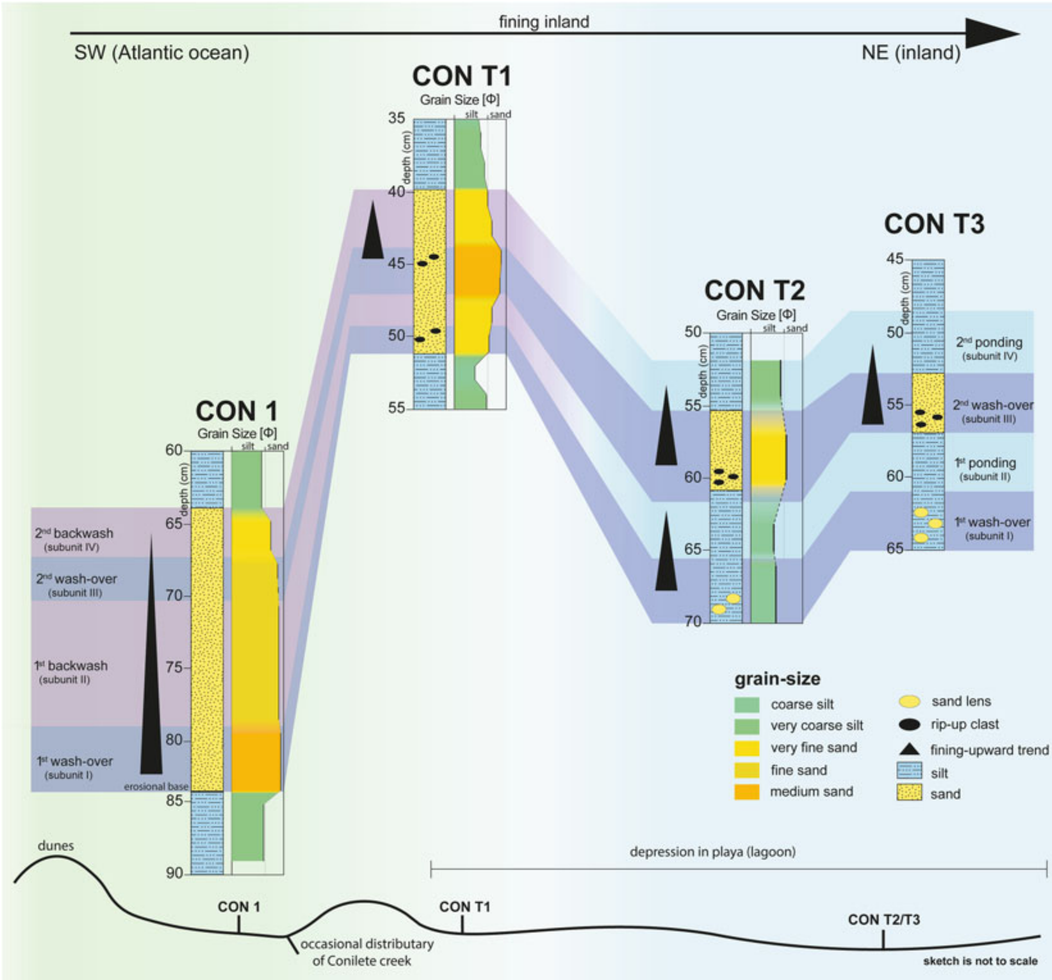

Fig. 15.12 Distinctive features of CON 1, CON T1, CON T2 and CON for clarifying the four different phases during the two wave cycles of the AD 1755 Lisbon tsunami. Profile in Fig. 15.2b

energetic conditions of the tsunami wash-over. One assumption is that the wash-over created turbulent high-energy currents, causing the underlying lagoon material to be eroded, reworked and mixed, while there was a minor sediment input from the floodwaters. Whereas CON T1, closer to the coast, has a very fine sandy layer with a high content of silt, the first wash-over deposits of CON T2 and CON T3 consist solely of reworked and redeposited lagoon material with sand lenses. Indicators for the first wash-over with high turbulences are the organic-rich rip-up clasts in CON T1 and the sand lenses in CON T2/T3 (Fig. 15.12). The dissimilarities (e.g., grain size) in the first tsunami wash-over deposition might have been caused by the different energetic conditions, CON T1, located at the edge of the depression, being more affected than CON T2/T3 in the basin (Fig. 15.12). Further evidence not only includes the smaller grain size with markedly coarser grains than the underlying material but also the lower marine and higher terrestrial signature due to the reworked underlying material (May et al. 2012). Furthermore, the accumulation of *n*-aldehydes and the depletion in *n*-alkanes and PAHs indicate a mixture of marine and terrestrial signals, as described by Chagué-Goff et al. (2012) for inorganic parameters.

Subunit II of CON T1 indicates backwash deposits, with very fine sand, coarser than the wash-over deposit, a marked decrease in the inorganic marine signal and a slight increase in the inorganic terrestrial signal, comparable to the deposits from CON 1, as well as a higher level of terrestrial and aquatic *n*-alkanes. On the contrary, the deposits from CON T2 and CON T3 did not originate from the backwash-induced currents but from the subsequent ponding. The floodwaters with suspended material retreated with little force and the ponded water remained in the lagoon with fine material in suspension. The suspended finer-grained sediments as silt (Subunit II of T2 and T3), which might have been deposited during the ponding stage, are characterized by a mixture of elements and compounds (Figs. 15.3, 15.4, 15.5, 15.6, 15.7, 15.8 and 15.9). Marine compounds were enriched chiefly by seawater and mixed with the finer formerly lagoon sediments. Also, the aquatic *n*-alkanes were enriched due to the overflowing of rivers during the previous tsunami wash-over (Fig. 15.9). Furthermore, the higher level of terrestrial aliphatic compounds of a predominantly forest and grass origin did not only result from the reworking of terrestrial sediments but also from the destruction of plants and vegetation during the wash-over and backwash. The accumulated concentrations of PAHs could also be indicative of ponding because the conditions during this phase possibly facilitated the deposition of pollutants in the sediment. Terrestrial signals predominate in all the samples.

The second ponding phase was limited in time for, after a short period, it is possible that a second tsunami wash-over occurred. This second wave might have eroded and transported material, mainly dune and beach sand and material deposited by the first wave, to a greater extent owing to lower ground roughness, resulting in the transport of a higher sediment load inland. Hence, the second tsunami-induced wash-over would have led to an increased sediment input and, accordingly, coarser event deposits in the geological record of the depression, as seen in CON T1, T2 and T3. The wash-over phase is again characterized by an input of marine material. There are event similarities to the proxies of different marine signals of the first run-up, which may indicate an analogous process. This was presumably followed by minor backwash-induced currents, draining the floodplain through the Conilete creek and instable dunes, with the subsequent ponding of floodwaters.

The tsunami deposits generated by ponding after the second wave cycle are identical to the ones described for the first wave cycle. However, this ponding phase was more intense and might have taken place over a longer period.

Two fining upward sequences in the tsunami deposits were detected in CON T2/T3, as well as one fining upward sequence in CON T1 associated with the second wave cycle. These two cycles led to a certain layering of the tsunami deposits (Fig. 15.12). Distinctive layering in tsunami deposits was reported in the lagoonal milieu by May et al. (2012) and Wassmer et al. (2010) and in several other tsunami sediments (e.g., 2004 Indian Ocean tsunami by Richmond et al. 2006; Szczuciński et al. 2006). For their part, Shinozaki et al. (2015) reported an alternation of mud and sand deposited by the 2011 Tohoku-oki tsunami but could not clearly classify it as one event. Finally, the sedimentological and geochemical analyses have potentially divided the AD 1755 Lisbon tsunami deposits in El Palmar de Vejer into four periods originating from two waves.

15.5.3 Overview of the Hydrodynamic Characteristics of the AD 1755 Lisbon Tsunami in El Palmar de Vejer

The first wave cycle of the AD 1755 Lisbon tsunami was the wash-over, which affected the coastline of El Palmar de Vejer at 9.30 am on 1 November (Luque et al. 2004; Lario et al. 2009). The inundation phase ensured the transport of marine compounds, suspended in the seawater, to the floodplain (Fig. 15.13), the erosion of terrestrial material, and the transport and redepositing of local and onshore material, especially the silty substratum of the floodplain. Once the wash-over had reached the maximum inundation distance, namely, the point of almost zero energy, the material transported in suspension was deposited with a heterogeneous (marine and terrestrial) signal. The landward extent of the tsunami wash-over depended on several factors, above all the local topography and possibly the change in direction of the backwash towards the sea. Due to the low inclination in the study area (Fig. 15.13), the backwash had rather less impact on the distal cores because it was primarily weak and topographically controlled. However, not only the topography is a crucial factor of backflow but also the evolution of water, flow depth and discharge possibilities (May et al. 2012; El Talibi et al. 2016). In the main, the backwash followed the path of least resistance, which resulted in both a channeled discharge along the riverbed of the Conilete creek and through unstable points in the foreshore dune ridge. Furthermore, the weak topographically controlled backwash transported not only terrestrial but also marine material towards the coastline and left a heterogeneous signal in the proximal cores. The transport of terrestrial material seaward during the backwash has been reported for the 2004 Indian Ocean tsunami (Pongpiachan et al. 2013) and several other tsunami deposits (Nanayama et al. 2000; Bony et al. 2011). In this case, the flat topography of the floodplain favored the ponding of eroded and reworked sediments, especially in the depression of the lagoon (Fig. 15.13). The deposits generated by ponding are characterized by finer-grained sediments, as fine sand and silt remain in suspension in the water column of the tsunami wave and are only deposited during lower energy conditions such as ponding (Dawson and Stewart 2007; Wassmer et al. 2010; Chagué-Goff et al. 2012).

15.5.4 Tsunami Propagation

The geochemical analyses provide important information about the extent of the inundation and the origin of the deposited sediments. Most studies of the Portuguese Algarve and the Spanish coast of the Gulf of Cadiz refer to sedimentological tsunami sand deposits, microfossils, XRF, GPR and MagSus measurements. Geochemistry has an advantage in that marine (bio-)markers can be identified beyond sand, thus supplementing the other study method. Especially, the marine markers in CON 4 indicate a high-energy origin, namely, a tsunami wave, and suggest a greater maximum inundation distance.

The AD 1755 tsunami transported a great deal of sediment to the flat, open area between Conil de la Frontera and El Palmar de Vejer, whereby it can be claimed that its impact greatly altered the coast. Furthermore, historical data (Real Academia de la Historia 1756) may only be used as a benchmark to a certain extent, as the written sources may also have transmitted incorrect or over- or underestimated data. Therefore, the 8 m inundation height should only be taken as a conjecture—despite the fact that it is evinced by the impact marks on the Castilnovo watchtower at the same height (Lario et al. 2009). At present, it is difficult to calculate the exact inundation distance, inasmuch as the only visible evidence of the tsunamis are the sand deposits, as can be seen from most of the cores in this study. However, the sand deposits only cover a small proportion of the area inundated by the tsunami. Further inland, the tsunami deposits are composed of muddy and silty sediments (Chagué-Goff et al. 2012), as in CON 4, which represent a larger proportion of the tsunami-induced wash-over fan and can mainly be detected with geochemistry. Regarding the 2011 Tohoku-oki tsunami deposits in Japan, in their study, Chagué-Goff et al. (2012) found that the maximum extent of tsunami sand and tsunami mud and silt was only 60 and 95% of the total inundation limit, respectively. Findings of the silty tsunami deposit in CON 4 suggest similar characteristics of tsunami deposits in our study area. Sand and mud limits depend principally on the tsunami wave energy, as well as the topography of the coast. The importance of the topography can be anticipated from the differences in the floodplain between Conil de la Frontera and El Palmar de

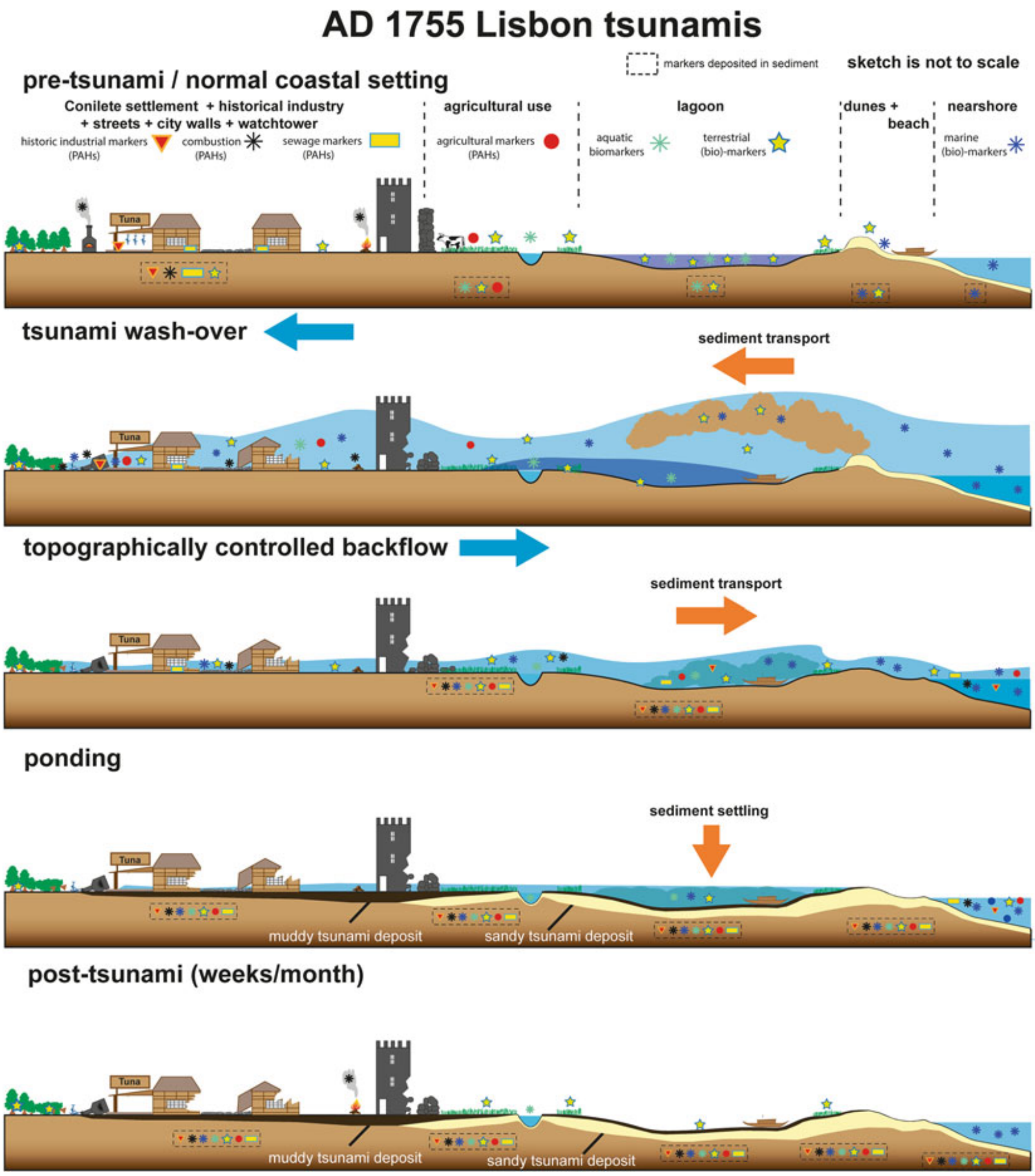

Fig. 15.13 Conceptual model for the distribution of geochemical markers and sediment transport in the normal coastal setting, during the tsunami inundation and the topographically controlled backflow, during ponding and in a post-tsunami setting with regard to the floodplain of El Palmar de Vejer (Conilete settlement). Model is not to scale

Vejer. While in the north of the area, a greater inundation distance was reached (several km) owing to the fact that the Salado river acted as a channel for the tsunami, the Conilete creek did not do so to the same extent due to topographical differences (Fig. 15.12). Further field studies should focus on the extension of silty and fine-grained tsunami deposits in this area to investigate the propagation of the AD 1755 Lisbon tsunami.

15.5.5 Other Evidence for an EWE in the Study Area

CON 1 shows a peculiarity in its sedimentological archive in that an interbedded very fine sand layer is recognizable at a depth between 4.55 and 4.75 m. The intercalated layer exhibits properties, especially with regard to grain size and inorganic parameters, which differ from those of the surrounding material. The sand content ranges from 78 to 66%, while the upper and lower contact samples have a sand content of 30 and 2%, respectively. TOC content decreases and TIC content increases significantly in contrast to the surrounding material. Ca, Sr Ca/Ti and Ca/K peak slightly in this layer (Table 15.2; Fig. 15.3). The aforementioned findings are all consistent with an EWE, but the layer was only detected in one core as the rest were not drilled as deep. To confirm this possible second EWE layer, further field campaigns, involving the drilling of deeper cores (up to a depth of 5 m) would be required to obtain more samples. Based on the historical records, the coast of the Gulf of Cadiz was hit by different tsunamis in the past and the presence of other EWE layers is possible in this study area.

15.6 Conclusions

Our study bears out that a multi-proxy approach has many advantages for research on tsunami deposits. Not only the sedimentological properties but also the geochemical characteristics of the tsunami layers offer deep insights into EWE processes and deposits on the floodplain of El Palmar de Vejer. The advantages offered by our study area mainly include its flat topography and its good sedimentary record of a tsunami deposit.

All our analyses have provided further evidence of and insights into the impact of the AD 1755 Lisbon tsunami on the coast of El Palmar de Vejer. Our geochemical analyses offer indications of the effect of at least two tsunami wave cycles. After the two waves, ponding mainly caused by the area's flat topography occurred. Both sedimentology and geochemistry hint at different conditions during the tsunami phases. During the first wash-over, reworked materials of the pre-tsunami sediments were likely to have been deposited, with heterogeneous mixed marine and terrestrial signals in the lagoonal tsunami deposits and a distinct marine signal in those outside the lagoon. During ponding, deposits of a terrestrial origin (K, terrestrial *n*-alkanes and *n*-aldehydes) predominated, with minor marine influences on the sediments also being detectable. The second wash-over, with suspended material in the floodwaters, reached an already inundated area. The features of the second ponding phase are similar to those of the first, but probably with longer periods of ponding. Ponding resulted in the increased deposition of fine-grained sediments in suspension and, consequently, a higher input of terrestrial material. Both the elements and the organic geochemical biomarkers are good indicators of the different processes. Even though it is possible to use anthropogenic markers in rural areas and apply them to historical tsunamis, as we have shown here, it should be noted that they are difficult to interpret due to the fact that the sources from which PAHs originate were either thin on the ground or non-existent back then. Indeed, at the time of the AD 1755 Lisbon tsunami, the only sources from which PAHs could have originated were human activities like fishing and farming, plus natural phenomena like wildfires, for it occurred before industrialization.

The floodplain, especially the depressions of the lagoon and the low inclination, is a good location for the sedimentological analysis of tsunami deposits due to the high preservation potential. Organic geochemical biomarkers are a useful tool for the identification and determination of inundation areas in relation to tsunamis, but anthropogenic markers are not the most ideal for performing analyses in this study area due to their lack of substance.

Acknowledgements This study was granted by German Research Foundation (DFG, RE 1361/28-1). We would like to thank Yvonne Esser and Miriam Birx for their support during the organic geochemical sample processing and Annette Schneiderwind for her technical support during the GC-MS analysis. Our thanks also go to the Institute of Geographic of the University of Cologne (Dr.

Simon Matthias May, Dr. Stephan Opitz and Dr. Anna Pint) and the Department of Geography of RWTH Aachen University (Marianne Dohms) for their help with the sedimentological and inorganic geochemical preparation and the sample measurements. Furthermore, we are indebted to Dr. Nicole Höbig, Dr. Margret Mathes-Schmidt and the BA and MA students, Simone Aschenbrenner, Adrienne Gäb, Natalie Driessen, Gina Querrengässer, Oskar Bastian, Franciska Radić, Yareli Stäglich and Viktoria Vorbusch, who were involved in the field and lab work.

References

Archivo de la Hermandad de la Virgen de la Merced (1722) Rogativas a la Virgen de la Merced, Jerez de la Frontera

Alonso B, Ercilla G, Casas D et al (2016) Contourite vs gravity-flow deposits of the Pleistocene Faro Drift (Gulf of Cádiz): sedimentological and mineralogical approaches. Mar Geol 377:77–94

Alpar B, Ünlü S, Altınok Y et al (2012) New approaches in assessment of tsunami deposits in Dalaman (SW Turkey). Nat Hazards 60(1):27–41

Álvarez-Martí-Aguilar M (2020) The Historicity of the earthquakes occurring in the Iberian Peninsula before A.D. 881 Recorded in Spanish and Portuguese seismic catalogs. Seism Res Lett 91(6):3585–3594. https://doi.org/10.1785/0220200168

Andrade C, Freitas MC, Oliveira MA et al (2016) On the sedimentological and historical evidences of seismic triggered tsunamis on the Algarve Coast of Portugal. In: Duarte JC, Schellart WP (eds) Plate boundaries and natural hazards. American Geophysical Union, Washington, pp 219–232

Aparicio JA (2017) 1755 El maremoto que viene. Q-book, Cádiz

Baptista MA, Miranda JM (2009) Revision of the Portuguese catalog of tsunamis. Nat Hazard 9(1):25–42

Baptista MA, Miranda PMA, Miranda JM, Victor LM (1998) Constrains on the source of the 1755 Lisbon tsunami inferred from numerical modelling of historical data on the source of the 1755 Lisbon tsunami. J Geodyn 25(1):159–174

Bartzke G, Schmeeckle MW, Huhn K (2018) Understanding heavy mineral enrichment using a three-dimensional numerical model. Sedimentology 65:561–581

Bellanova P, Frenken M, Richmond B et al (2019) Organic geochemical investigation of far-field tsunami deposits of the Kahana Valley, O'ahu, Hawai'i. Sedimentology 67(3):1230–1248

Bellanova P, Frenken M, Reicherter K et al (2020) Anthropogenic pollutants and biomarkers for the identification of 2011 Tohoku-oki tsunami deposits (Japan). Mar Geol 422:106–117

Bezzeghoud M, Adam C, Buforn E et al (2014) Seismicity along the Azores Gibraltar region and global plate kinematics. J Seism 18(2):205–220

Blanc PL (2008) The tsunami in Cadiz on 1 November 1755: a critical analysis of reports by Antonio de Ulloa and by Louis Godin. Comptes Rendus Geosci 340 (4):251–261

Blanc PL (2011) The Atlantic tsunami on November 1st, 1755: world range and amplitude according to primary documentary sources. In: Mörner NA (ed) The tsunami threat-research and technology. IntechOpen, Rijeka, pp 423–446

Blott SJ, Pye K (2001) GRADISTAT: a grain size distribution and statistics package for the analysis of unconsolidated sediments. Earth Surf Proc Land 26 (11):1237–1248

Bony G, Marriner N, Morhange C, Kaniewski D, Perinçekc D (2011) A high-energy deposit in the Byzantine harbour of Yenikapi, Istanbul (Turkey). Quatern Int 266:117–130

Borrego J, Morales JA, Pendón JG (1993) Holocene filling of an Estuarine Lagoon along the Mesotidal Coast of Huelva (SW Spain). J Coastal Res 9(1):242–254

Campese Gallego F, Gamero Rojas M, González Polvillo A et al (2009) Los efectos del maremoto de 1755 sobre las costas andaluzas. In: Bravo Caro JJ, Sanz Sampelayo J (eds) Población y grupos sociales en el Antiguo Régimen, vol. 1. Fundación Española de Historia Moderna, Málaga, pp 363–377

Campos ML (1991) Tsunami hazard on the Spanish coasts of the Iberian Peninsula. Sci Tsunami Hazard 9 (1):83–90

Chagué-Goff C, Dawson S, Goff JR et al (2002) A tsunami (ca. 6300 year BP) and other Holocene environmental changes, northern Hawke's Bay, New Zealand. Sediment Geol 150(1–2):89–102

Chagué-Goff C, Andrew A, Szczuciński W et al (2012) Geochemical signatures up to the maximum inundation of the 2011Tohoku-oki tsunami—implications for the 869 AD Jogan and other palaeotsunamis. Sed Geol 282:65–77

Chagué-Goff C, Goff J, Wong HKY, Cisternas M (2015) Insights from geochemistry and diatoms to characterise a tsunami's deposit and maximum inundation limit. Mar Geol 359:22–34

Chagué-Goff C, Szczuciński W, Shinozaki T (2017) Applications of geochemistry in tsunami research: a review. Earth Sci Rev 165:203–244

Cioffi F, Di Eugenio A, Gallerano F (1995) A new representation of anoxic crises in hypertrophic lagoons. Appl Math Model 19(11):685–695

Collinson JD (1978) Alluvial sediments. In: Reading HG (ed) Sedimentary environments and facies. Wiley, Oxford, pp 15–60

Costa PJM, Andrade C, Freitas MC et al (2012) A tsunami record in the sedimentary archive of the central Algarve coast, Portugal: characterizing sediment, reconstructing sources and inundation paths. Holocene 22(8):899–914

Costa PJM, Costas S, González-Villanueva R et al (2016) How did the AD 1755 tsunami impact on sand barriers across the southern coast of Portugal? Geomorphology 268:296–311

Craft CB, Bertram J, Broome S (2008) Coastal zone restoration. In: Encyclopedia of ecology, vol 1. Elsevier, pp 637–644

Cuven S, Paris R, Falvard S et al (2013) High-resolution analysis of a tsunami deposit: case-study from the 1755 Lisbon tsunami in southwestern Spain. Mar Geol 337:98–111

Dawson A (1994) Geomorphological effects of tsunami run-up and backwash. Geomorphology 10(1–4):83–94

Dawson A, Long D, Smith D (1988) The Storegga slides: evidence from eastern Scotland for a possible tsunami. Mar Geol 82(3–4):271–276

Dawson AG, Stewart I (2007) Tsunami deposits in the geological record. Sed Geol 200(3–4):166–183

Dawson S, Costa PJM, Dawson A, Engel M (2020) Onshore archives of tsunami deposits. In: Engel M, Pilarczyk J, May SM et al (eds) Geological records of tsunamis and other extreme wave. Elsevier, Amsterdam, pp 95–111

Del Rio L, Plomaritis TA, Benavente J et al (2012) Establishing storm thresholds for the Spanisch Gulf of Cádiz coast. Geomorphology 143–144:13–23

Donnelly J, Goff J, Chagué-Goff C (2016) A record of local storms and trans-Pacific tsunamis, eastern Banks Peninsula, New Zealand. Holocene 27(4):496–508

Dsikowitzky L, Schwarzbauer J, Kronimus A, Littke R (2004) The anthropogenic contribution to the organic load of the Lippe river (Germany). Part 2: Quantification of specific organic contaminants. Chemosphere 57:1288–1293

Duarte JC, Rosas FM, Terrinha P et al (2013) Are subduction zones invading the Atlantic? Evidence from the southwest Iberia margin. Geology 41(8):839–842

Eglinton G, Hamilton RJ (1963) The distributions of alkanes. In: Swan T (ed) Chemical plant taxonomy. Academic Press, New York, pp 187–217

El Talibi H, El Moussaoui S, Zaghloul MN et al (2016) New sedimentary and geomorphic evidence of tsunami flooding related to an older events along the Tangier-Asilah coastal plain, Morocco. Geoenviron Disasters 3(14):1–21

Faust D, Herkommer M (1995) Rillerosion in lower Andalusia: a statistical evaluation of rills. Zeitschrift Für Geomorphologie Supplement Volumes 99:17–28

Ficken KJ, Li B, Swain DL, Eglinton G (2000) An n-alkane proxy for the sedimentary input of submerged/floating freshwater aquatic macrophytes. Org Geochem 31(7–8):745–749

Folk RL, Ward WC (1957) Brazos River bar [Texas]; a study in the significance of grain size parameters. J Sediment Res 27(1):3–26

Foster IDL, Albon AJ, Bardell KM et al (1991) High energy coastal sedimentary deposits; an evaluation of depositional processes in Southwest England. Earth Surf Proc Land 16(4):341–356

Fujiwara O, Masuda F, Sakai T et al (2000) Tsunami deposits in Holocene bay mud in southern Kanto region, Pacific coast of central Japan. Sed Geol 135(1–4):219–230

Gee GW, Or D (2002) Particle-size analysis. In: Dane JH, Topp GC (eds) Methods of soil analysis. Part 4—Physical methods. Soil science society of America Book Series 5. Madison, Wisconsin, pp 255–293

Gelpi E, Schneider H, Mann J, Oró J (1970) Hydrocarbons of geochemical significance in microscopic algae. Phytochemistry 9:603–612

Goff J, Chagué-Goff C, Nichol S (2001) Palaeotsunami deposits: a New Zealand perspective. Sed Geol 143(1–2):1–6

Gogou A, Stratigakisi N, Kanakidou M, Stephanou EG (1996) Organic aerosols in Eastern Mediterranean: components source reconciliation by using molecular markers and atmospheric back trajectories. Org Geochem 25(1–2):79–96

González-Acebrón L, Mas R, Arribas J et al (2016) Very coarse-grained beaches as a response to generalized sea level drops in a complex active tectonic setting: Pleistocene marine terraces at the Cádiz coast, SW Spain. Mar Geol 382:92–110

Gordo AG, Laurent J, Rodríguez AM (2008) J. Laurent's photographs of Vejer (1867–1879): a critical study. Sociedad Vejeriega de Amigos del País, Vejer de la Frontera

Gracia FJ, Alonso C, Javier B et al (2006) The different coastal records of the 1755 tsunami waves along the south Atlantic Spanish coast. Z Geomorphol 146:195–220

Guillon A, Le Menach K, Flaud PM et al (2013) Chemical characterization and stable carbon isotopic composition of particulate polycyclic aromatic hydrocarbons issued from combustion of 10 Mediterranean woods. Atmos Chem Phys 13(5):2703–2719

Gutiérrez-Mas JM, Hernandez-Molina FJ, Lopez-Aguayo F (1996) Holocene sedimentary dynamics on the Iberian continental shelf of the Gulf of Cádiz (SW Spain). Cont Shelf Res 16(13):1635–1653

Gutiérrez-Mas JM, Fernández VG, García-López S et al (2016) Comparative analysis of the deposits left by the tsunami that followed to the Lisbon Earthquake (1755 AD), on the Castilnovo beach and the Old Tuna Factory of La Chança (Conil de la Frontera, SW Spain). Revista de la Sociedad Geológica de España 29:21–33

Gutscher M-A, Malod J, Rehault JP et al (2002) Evidence for active subduction beneath Gibraltar. Geology 30(12):1071–1074

Gutscher M-A, Baptista MA, Miranda JM (2006) The Gibraltar Arc seismogenic zone (part 2): constraints on a shallow east dipping fault plane source for the 1755 Lisbon earthquake provided by tsunami modeling and seismic intensity. Tectonophysics 426(1–2):153–166

Horton BP, Rossi V, Hawkes AD (2009) The sedimentary record of the 2005 hurricane season from the Mississippi and Alabama coastlines. Quatern Int 195(1–2):15–30

Instituto Geográfico Nacional (1991) Atlas Nacional de España: el medio marino, sección III, grupo 13. Instituto Geográfico Nacional, Madrid

Jaffé R, Mead R, Hernandez ME et al (2001) Origin and transport of sedimentary organic matter in two subtropical estuaries: a comparative, biomarker-based study. Org Geochem 32(4):507–526

Jeng WL, Huh CA (2006) A comparison of sedimentary aliphatic hydrocarbon distribution between the southern Okinawa Trough and a nearby river with high sediment discharge. Estuar Coast Shelf Sci 66(1):217–224

Kaabouben F, Baptista MA, Iben Brahim A et al (2009) On the moroccan tsunami catalogue. Nat Hazard 9 (4):1227–1236

Kalnicky DJ, Singhvi R (2001) Field portable XRF analysis of environmental samples. J Hazard Mater 83 (1–2):93–122

Koster B, Reicherter K (2014) Sedimentological and geophysical properties of a ca. 4000 year old tsunami deposit in southern Spain. Sed Geol 314:1–16

Koster B, Hadler H, Vött A, Reicherter K (2013) Application of GPR for visualising spatial distribution and internal structures of tsunami deposits—case studies from Spain and Greece. Z Geomorphol 57 (4):29–45

Krauß L, Zens J, Zeeden C et al (2016) A multi-proxy analysis of two Loess-Paleosol sequences in the Northern Harz Foreland, Germany. Palaeogeogr Palaeoclimatol Palaeoecol 461:401–417

Lario J (1996) Último y presente Interglacial en el área de conexión Atlántico-Mediterráneo: Variaciones del nivel del mar, paleoclima y paleoambientes. Dissertation, Universidad Complutense de Madrid

Lario J, Zazo C, Goy JL et al (2002) Changes in sedimentation trends in SW Iberia Holocene estuaries (Spain). Quatern Int 93–94:171–176

Lario J, Luque L, Zazo C et al (2009) Tsunami deposits at Torre de Castilnovo, Conil de la Frontera. In: Lario et al (eds) Palaeoseismicity and active tectonics during the Quaternary in the Gibraltar Strait (Betic Cordillera, South Spain). IGME, Madrid, pp 85–96

Lario J, Zazo C, Goy JL et al (2011) Holocene palaeotsunami catalogue of SW Iberia. Quatern Int 242(1):196–200

López L (1873) Trabajos Topograficos—Provincia de Cadiz—Ayuntamiento de Conil (Sheet 14, 1/25000). Instituto Geográfico Nacional, Madrid

López Sáez JA, López García P, Martín Sánchez M (2002) Palaeoecology and Holocene environmental change from a saline lake in South-West Spain: protohistorical and prehistorical vegetation in Cádiz Bay. Quatern Int 93–94:197–206

Luque L, Lario J, Zazo C et al (2001) Tsunami deposits as palaeoseismic indicators: examples from the Spanish coast. Acta Geol Hisp 36(3–4):197–211

Luque L, Lario J, Civis J et al (2002) Sedimentary record of a tsunami during Roman times, Bay of Cádiz, Spain. J Quatern Sci 17(5–6):623–631

Luque L, Zazo C, Lario J (2004) El efecto del tsunami de 1755 en el litoral de Conil de la Frontera (Cádiz). In: Baquedano E, Rubio S (eds) Miscelánea en Homenaje a Emiliano Aguirre, vol I. Geología. Museo Arqueológico Regional, Alcalá de Henares, pp 72–82

Mackie PR, Whittle KJ, Hardy R (1974) Hydrocarbons in the marine environment: I. *n*-Alkanes in the firth of clyde. Estuar Coast Mar Sci 2(4):359–374

Mader CL (2001) Modeling the 1755 Lisbon tsunami. Sci Tsunami Hazards 19(2):93–98

Martín-Puertas C, Jiménez-Espejo F, Martínez-Ruiz F et al (2010) Late Holocene climate variability in the southwestern Mediterranean region: an integrated marine and terrestrial geochemical approach. Clim Past 6(6):807–816

Martínez Solares JM (2001) Los efectos en España del terremoto de Lisboa (1 de noviembre de 1755). Instituto Geográfico Nacional, Madrid

Martínez Solares JM, López Arroyo A, Mezcua J (1979) Isoseismal map of the 1755 Lisbon earthquake obtained from spanish data. Tectonophysics 53:301–313

Mathes-Schmidt M, Schwarzbauer J, Papanikolaou I et al (2013) Geochemical and micropaleontological investigations of tsunamigenic layers along the Thracian Coast (Northern Aegean Sea, Greece). Zeitschrift für Geomorphologie 57(4):5–27

May SM, Vött A, Brückner H, Smedile A (2012) The Gyra washover fan in the Lefkada Lagoon, NW Greece—possible evidence of the 365 AD Crete earthquake and tsunami. Earth Planets Space 64 (10):859–874

Minoura K, Gusiakov VG, Kurbatov A et al (1996) Tsunami sedimentation associated with the 1923 Kamchatka earthquake. Sed Geol 106(1–2):145–154

Moreno IM, Ávila A, Losada MÁ (2010) Morphodynamics of intermittent coastal lagoons in Southern Spain: Zahara de los Atunes. Geomorphology 121:305–316

Morton RA, Gelfenbaum G, Jaffe BE (2007) Physical criteria for distinguishing sandy tsunami and storm deposits using modern examples. Sed Geol 200:184–207

Nanayama F, Shigeno K, Satake K et al (2000) Sedimentary differences between the 1993 Hokkaido nansei-oki tsunami and the 1959 Miyakojima typhoon at Taisei, southwestern Hokkaido, northern Japan. Sed Geol 135(1–4):255–264

Neal A (2004) Ground-penetrating radar and its use in sedimentology: principles, problems and progress. Earth Sci Rev 66(3–4):261–330

Ocampo F (1543) Los quatro libros primeros de la Cronica general de España que recopila el maestro Florian do Campo criado y cronista del Emperador Rey nuestro señor por mandado de su magestad Çesarea. Juan Picardo, Zamora

Page DS, Boehm PD, Douglas GS et al (1999) Pyrogenic polycyclic aromatic hydrocarbons in sediments record past human activity: a case study in Prince William Sound, Alaska. Mar Pollut Bull 38(4):247–260

Paris R, Cachão M, Fournier J, Voldoire O (2010) Nannoliths abundance and distribution in tsunami deposits: example from the December 26, 2004 tsunami in Lhok Nga (northwest Sumatra, Indonesia). Géomorphologie Relief, Processus, Environnement 1:109–118

Passega R (1964) Grain size representation by CM patterns as a geologic tool. J Sediment Res 34 (4):830–847

Passega R, Byramjee R (1969) Grain-Size Image of clastic deposits. Sedimentology 13(3–4):233–252

Peng S, Zhang J (2007) Sedimentary environments and geologic structures. Engineering geology for underground rocks. Springer, Berlin, pp 27–44

Peters KE, Walters CC, Moldowan JM (2005) The biomarker guide: biomarkers and isotopes in petroleum systems and earth, vol 2. Cambridge University Press, Cambridge

Pongpiachan S, Thumanu K, Tanthanuch W et al (2013) Sedimentary features of tsunami backwash deposits as assessed by micro-beam synchrotron x-ray fluorescence (μ-SXRF) at the Siam photon laboratory. J Tsunami Soc Int 32(2):96–115

Pontevedra-Pombal X, Rey-Salgueiro L, García-Falcón MS et al (2012) Pre-industrial accumulation of anthropogenic polycyclic aromatic hydrocarbons found in a blanket bog of the Iberian Peninsula. Environ Res 116:36–43

Poynter JG, Eglinton G (1990) Molecular composition of three sediments from hole 717C: the Bengal Fan. In: Cochran JR, Stow DAV et al (eds) Proceedings of the ocean drilling program scientific results, vol 116, pp 155–161

Prahl FG, Pinto LA (1987) A geochemical study of long-chain n-aldehydes in Washington coastal sediments. Geochim Cosmochim Acta 51(6):1573–1582

Pye K, Blott SJ (2004) Particle size analysis of sediments, soils and related particulate materials for forensic purposes using laser granulometry. Forensic Sci Int 144:19–27

Ravindra K, Sokhi R, Van Grieken R (2008) Atmospheric polycyclic aromatic hydrocarbons: source attribution, emission factors and regulation. Atmos Environ 42 (13):2895–2921

Real Academia de la Historia (1756) Noticia individual que da la Academia de la Historia del Terremoto de 1º de noviembre de 1755 por orden del Rey Nuestro Señor a quien la dedica. Real Academia de la Historia, Madrid

Reicherter K, Vonberg D, Koster B et al (2010) The sedimentary inventory of tsunamis along the southern Gulf of Cádiz (southwestern Spain). Zeitschrift für Geomorphologie 54(3):147–173

Reicherter K, Vött A, Feist L et al (2019) Lisbon 1755, Cruise No. M152/1, 02.11.–14.11.2018, Funchal (Portugal)—Hamburg (Germany). Leitstelle Deutsche Forschungsschiffe 11. https://doi.org/10.2312/cr_m152

Richmond BM, Jaffe BE, Gelfenbaum G, Morton RA (2006) Geologic Impacts of the 2004 Indian Ocean Tsunami on Indonesia, Sri Lanka, and the Maldives. Zeitschrift für Geomorphologie 146:235–251

Rieley G, Collier RJ, Jones DM, Eglinton G (1991) The biogeochemistry of Ellesmere Lake, UK I: source correlation of leaf wax inputs to the sedimentary record. Org Geochem 17(6):901–912

Rodríguez de la Torre F (2005) Documentos en el Archivo Histórico Nacional (Madrid) sobre el terremoto del 1 de Noviembre de 1755. Cuadernos Dieciochistas 6:79–116

Rodríguez-Vidal J, Cáceres LM, Abad M et al (2011) The recorded evidence of AD 1755 Atlantic tsunami on the Gibraltar coast. J Iber Geol 37(2):177–193

Rodrigo FS, Esteban-Parra MJ, Pozo-Vázquez D, Castro-Díez Y (1999) A 500-year precipitation record in Southern Spain. Int J Climatol 19:1233–1253

Ruiz F, Rodríguez-Ramírez A, Cáceres LM et al (2005) Evidence of high-energy events in the geological record: Mid-Holocene evolution of the southwestern Doñana National Park (SW Spain). Palaeogeogr Palaeoclimatol Palaeoecol 229(3):212–229

Ruiz F, Rodríguez-Vidal J, Abad M et al (2013) Sedimentological and geomorphological imprints of Holocene tsunamis in southwestern Spain: an approach to establish the recurrence period. Geomorphology 203:97–104

Santos A, Koshimura S (2015) The historical review of the 1755 Lisbon tsunami. J Geod Geomat Eng 1:38–52

Scheffers A, Kelletat D (2005) Tsunami relics on the coastal landscape west of Lisbon, Portugal. Sci Tsunami Hazards 23(1):3–16

Schulte P, Lehmkuhl F (2017) The difference of two laser diffraction patterns as an indicator for post-depositional grain size reduction in loess-paleosol sequences. Palaeogeogr Palaeoclimatol Palaeoecol 509:126–136

Schwarzbauer J (2006) organic contaminants in riverine and groundwater systems—aspects of the anthropogenic contribution. Springer, Berlin, Heidelberg

Schwarzbauer J, Littke R, Weigelt V (2000) Identification of specific organic contaminants for estimating the contribution of the Elbe river to the pollution of the German Bight. Org Geochem 31(12):1713–1731

Schwarzbauer J, Stock F, Brückner H et al (2017) Molecular organic indicators for human activities in the Roman harbor of Ephesus, Turkey. Geoarchaeology 33(4):498–509

Shinozaki T, Fujino S, Ikehara M et al (2015) Marine biomarkers deposited on coastal land by the 2011 Tohoku-oki tsunami. Nat Hazards 77(1):445–460

Simoneit BRT, Mazurek MA (1982) Organic matter of the troposphere—II* natural background of biogenic lipid matter in aerosols over the rural Western United States. Atmos Environ 16(9):2139–2159

Spiske M (2020) The sedimentology and geometry of fine-grained tsunami deposits from onshore environments. In: Engel M, Pilarczyk J, May SM et al (eds) Geological records of tsunamis and other extreme wave. Elsevier, Amsterdam, pp 213–238

Srinivasalu S, Rajeshwara Rao N, Thangadurai N et al (2009) Characteristics of 2004 tsunami deposits of the northern Tamil Nadu coast, southeastern India. Boletín de la Sociedad Geológica Mexicana 61 (1):111–118

Stark A, Abrajano T, Hellou J, Metcalf-Smith JL (2003) Molecular and isotopic characterization of polycyclic aromatic hydrocarbon distribution and sources at the international segment of the St. Lawrence River. Org Geochem 34(2):225–237

Stewart JHB (1958) Sedimentary reflections of depositional environment in San Miguel lagoon, Baja California, México. Am Assoc Petrol Geol Bull 42:2567–2618

Stogiannidis E, Laane R (2015) Source characterization of polycyclic aromatic hydrocarbons by using their molecular indices: an overview of possibilities. In: Whitacre DM (ed) Reviews of environmental contamination and toxicology, vol 234, pp 49–133

Szczuciński W, Chaimanee N, Niedzielski P et al (2006) Environmental and geological impacts of the 26 December 2004 tsunami in coastal zone of Thailand —overview of short and long-term effects. Pol J Environ Stud 15(5):793–810

Tanner WF (1991a) Suite statistics: the hydrodynamic evolution of the sediment pool. In: Syvitski JPM (ed) Principles, methods and applications of particle size analysis. Cambridge University Press, Cambridge, pp 225–236

Tanner WF (1991b) Application of suite statistics to stratigraphy and sea-level changes. In: Syvitski JPM (ed) Principles, methods and applications of particle size analysis. Cambridge University Press, Cambridge, pp 283–292

Udías A (2015) Historical earthquakes (before 1755) of the Iberian Peninsula in early catalogs (electronic supplement: critical revision of earthquakes in the Iberian Peninsula before year 1000). Seismol Res Lett 86(3):999–1005

Udías A (2020) Large earthquakes and tsunamis at Saint Vincent Cape before the Lisbon 1755 earthquake: a historical review. Pure Appl Geophys 177:1739–1745

Vallejo-Villalta I, Rodríguez-Navas E, Márquez-Pérez J (2019) Mapping forest fire risk at a local scale—a case study in Andalusia (Spain). Environments 6(3):1–22

Vizcaino A, Gracia E, Escutia C et al (2006) Characterizing Holocene Paleoseismic record in the SW Portuguese margin. European Geoscience Union 2006 geophysical research abstracts 8:EGU06-A-08469

Wassmer P, Schneider J-L, Fonfrège A-V et al (2010) Use of anisotropy of magnetic susceptibility (AMS) in the study of tsunami deposits: application to the 2004 deposits on the eastern coast of Banda Aceh, North Sumatra Indonesia. Mar Geol 275(1–4):255–272

Wassmer P, Font E, Gomez C, Iskandarsyah YWM (2020) Magnetic susceptibility and anisotropy of magnetic susceptibility: versatile tools to decipher hydrodynamic characteristics of past tsunamis. In: Engel M, Pilarczyk J, May SM et al (eds) Geological records of tsunamis and other extreme wave. Elsevier, Amsterdam, pp 343–363

Yoshii T, Tanaka S, Matsuyama M (2018) Tsunami inundation, sediment transport, and deposition process of tsunami deposits on coastal lowland inferred from the Tsunami Sand Transport Laboratory Experiment (TSTLE). Mar Geol 400:107–118

Yu N-T, Yen J-Y, Chen W-S et al (2016) Geological records of western Pacific tsunamis in northern Taiwan: AD 1867 and earlier event deposits. Mar Geol 372:1–16

Zazo C, Dabrio CJ, Goy JL et al (2008) The coastal archives of the last 15 ka in the Atlantic-Mediterranean Spanish linkage area: sea level and climate changes. Quatern Int 181:72–87

Zitellini N, Mendes LA, Córdoba D et al (2001) Source of 1755 Lisbon earthquake and tsunami investigated. Eos Trans Am Geophys Union 82(26):285–291